U.S.
$20

LABORATORY INVESTIGATIONS IN NUCLEAR SCIENCE

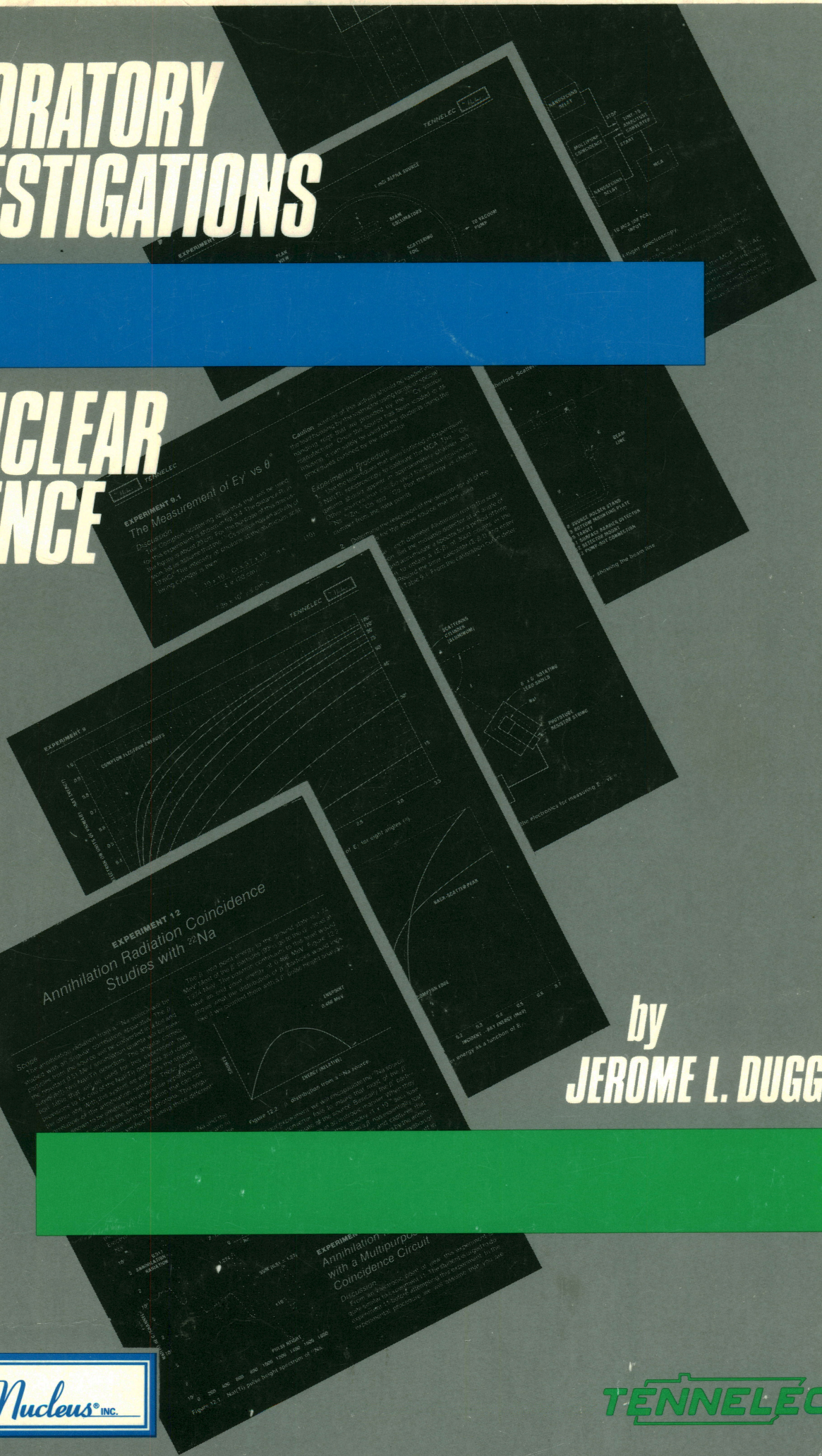

by
JEROME L. DUGGAN

the Nucleus® INC.

TENNELEC

TN-2000

LABORATORY INVESTIGATIONS IN NUCLEAR SCIENCE

by

JEROME L. DUGGAN

Department of Physics
University of North Texas
Denton, Texas 76203 USA

Published By

the Nucleus INC.

TENNELEC

Oak Ridge, TN USA

COPYRIGHT © 1988: THE NUCLEUS, INC.

Safe Use of Radioactive Sources

In general, the experiments that are to be performed in a radioisotope class should be done in a specified area. Never eat, drink, or smoke in the specified area where the experiments are being done. After you have finished with the class, it is a good idea to wash your hands. Most of the weak gamma sources are manufactured in a disk geometry. These sealed sources are usually less than 5 μCi activity. These low activity sealed sources can safely be handled with your hands. When handling these sources, hold them by the outer edge. Try to minimize the exposure time to your hands.

Some of the alpha sources that are used in the alpha spectroscopy, de/dx, and Rutherford scattering experiments are unsealed sources and hence, special precautions should be taken. If you will look carefully, you can see where the radioactive source spot has been deposited in the center of the disk. Never touch this area with your hands because you might inadvertently wipe some of the radioactive material away. These sources should be carefully handled at the outer edge of the disk.

The Am-Be neutron source, x-ray fluorescence sources and Compton scattering gamma source should only be handled by the instructor after he or she has carefully read the instructions provided by the source manufacturer. The students can safely use these sources after they have been transferred from storage containers to their respective chambers.

The x-ray fluorescence sources used in experiments 8, 17, and 18 usually range from 25-100mCi (see Table 8.1) and should be carefully transferred from their cylindrical lead storage containers to the fluorescence chamber. This can safely be done with a pair of tongs (about 30 cm long). The instructor should make this transfer, following the instructions of the source manufacturer. Once the fluorescence source has been transferred, the students can safely use the chamber for the indicated experiments.

The ^{137}Cs source used for the Compton Scattering experiment is usually from 10-30mCi and as in the above case, should only be handled with tongs or the special rods provided by the manufacturer. Once the source is loaded into the Compton Scattering lead shield, the experiment can easily be performed.

The alpha source used in Experiment 10, Rutherford Scattering has an activity of from 250 μCi to 1 mCi. It should be handled with tongs. These sources are sealed under a thin titanium foil but it is always wise to use tongs or forceps. The neutron sources used in experiment 15 (Neutron Activation Analyses) are usually 1Ci Am-Be. These sources are shipped in a large steel drum that is filled with a moderator. Instructions are always supplied with the source in regard to removal from the storage container. Once the source has been transferred to the Neutron Activation Chamber, it can safely be used by the students.

All of the experiments in this manual have been done safely for at least 20 years by many universities throughout the world. It is the responsibility of the instructor to maintain good health physics procedures during the laboratory period.

Preface

The experiments in this manual are composed of basic and some rather advanced experiments in Nuclear Science. These experiments, where appropriate, can be used in nuclear courses in physics, chemistry, nuclear engineering, nuclear technology, health physics, and biology. The choice of which experiments should be used for a given discipline depends on the course syllabus, and the equipment that is available in the department. Most of the experiments require either a multichannel analyzer or a personal computer with a Nucleus Personal Computer Analyzer (PCA) card. Since most academic units now possess personal computers, it is a simple matter to add a PCA card and have a "state-of-the-art" multichannel analyzer for use with these experiments. Very little can go wrong with the PCA card, and if a problem does occur, it is a simple matter to pull the card out and send it back to The Nucleus in a mailing envelope. These PCA cards have opened up the world of rather sophisticated nuclear experiments to schools, that a few years ago, would not dream of being able to do these experiments.

Many of the spectra that have been generously used in this manual were taken from the Department of Energy publications. We have taken NaI(Tℓ) spectra from the original Department of Energy bible on this work by Dr. R. L. Heath, *Scintillation Spectrometry, Gamma Ray Spectrum Catalogue*. Many of the high resolution germanium spectra were taken from Dr. Heath's compilation of *Germanium Gamma Ray Spectrum Catalogue*. Some of the high resolution alpha spectra were taken from the *Surface Barrier Alpha Catalogue* developed by the Idaho Falls Department of Energy Laboratory. Some of the spectra on X-ray Fluorescence were taken from work that was done at Lawrence Berkeley Laboratory. We have also taken some figures and tables from experiments that were developed by the Manpower Education Research and Training (MERT) division of Oak Ridge Associated Universities. In particular, we have called heavily upon the experiments in Neutron Activation Analysis and X-Ray Fluorescence that were developed by Geoffrey I. Gleason, whom, by almost any measure, is the grand Dean in the field of nuclear education and training. Finally, thanks are due the thousands of professors and students who have critiqued the experiments that have been written by the author over the least 20 years. This feed-back is greatly appreciated and helps us to produce material that is appropriate to the needs of universities.

J. L. D.
Denton, Texas

CONTENTS

EXPERIMENT 1	**The Geiger Counter**	**1**
1.1	Determining the Operating Plateau for the Geiger Tube	1
1.2	Resolving Time Corrections	2
1.3	Half-Life Measurement	3
1.4	Linear Absorption Coefficient	3
1.5	The Inverse Square Law	4
1.6	Statistical Variation of Data	5
EXPERIMENT 2	**Gamma-Ray Spectroscopy Using NaI(Tℓ)**	**7**
2.1	Gamma Energy Calibration	10
2.2	Identification of Unknown Gamma Emitters	12
2.3	Gamma Analysis of the .835 MeV Spectrum of ^{54}Mn	14
2.4	Energy Resolution of ^{137}Cs	14
2.5	Determining the Activity of a Gamma Source (Relative Method)	16
2.6	Determining the Activity of a Gamma Emitter by the Absolute Method	16
2.7	Analysis of the Sum Peak in NaI(Tℓ) Spectroscopy	18
2.8	The Linear Absorption Coefficient of Lead Gammas	19
EXPERIMENT 3	**Alpha Particle Measurements with Surface Barrier Detectors**	**21**
3.1	Energy Calibration with a Pulser for Alpha Spectroscopy	22
3.2	Using the Calibration Curve to Determine the Energy of the Unknown Alpha Source	24
3.3	Determination of the Activity of an Unknown Alpha Source by the Relative Method	26
3.4	The Absolute Method of Determining an Unknown Alpha Activity	27
3.5	A Study of the Decay Scheme of ^{230}Th by Alpha Emission Spectroscopy	27
EXPERIMENT 4	**A Study of the Energy Loss of Alpha Particles in Matter**	**29**
4.1	Energy Loss of Alpha Particles in Thin Metallic Foils	32
4.2	Alpha Particle Energy Loss in Helium Gas	34
4.3	Alpha Particle Range in Air	35
EXPERIMENT 5	**Beta and Conversion Electron Measurements with Solid State Detectors**	**37**
5.1	Energy Calibration for Beta Spectroscopy	38
5.2	Beta End Point Energy of ^{204}Tl	40
5.3	Measurement of the Internal Conversion Coefficients for ^{137}Cs and ^{137}Ba	41
EXPERIMENT 6	**High Resolution Gamma Ray Spectroscopy**	**43**
6.1	Energy Calibration and Resolution of a HpGe Spectrometer	45
6.2	The Efficiency of a HpGe Detector	47
6.3	Determination of an Unknown Gamma Activity by the Absolute Method	47
6.4	Determination of an Unknown Activity by the Relative Method	48
6.5	The Study of a Complex Decay Scheme by High Resolution HpGe Spectroscopy	48
6.6	A Study of Pair Production Escape Peaks in ^{228}Th	50
EXPERIMENT 7	**High Resolution X-Ray Spectroscopy**	**51**
7.1	Energy Calibration and Detector Resolution	53
7.2	Efficiency Measurements for a Si(Li) Detector	54
7.3	Intensity Ratios for Daughter X-Rays from Radioactive Sources	55
7.4	X-Ray Absorption in Thin Foils	56
EXPERIMENT 8	**X-Ray Fluorescence with High Resolution Silicon and Germanium Detectors**	**59**
8.1	Calibration of the Si(Li) Detector by Fluorescing Known Elements	63
8.2	The Analysis of Unknown K and L Shell Samples by XRF with a ^{109}Cd Source	64
8.3	Analysis of Environmental, Biological, and Geological Samples by XRF with ^{109}Cd	65
8.4	X-Ray Fluorescence Studies with an ^{55}Fe Source	67
8.5	XRF with High Resolution Germanium Detectors (^{57}Co Excitation Source)	68
EXPERIMENT 9	**Compton Scattering**	**69**
9.1	The Measurement of $E\gamma'$ vs θ	71
9.2	The Differential Cross Section for Comptons Scattering	73
9.3	Measurement of the Electron Recoil Energy in Compton Scattering	74
EXPERIMENT 10	**Rutherford Scattering**	**77**
10.1	Determination of I_0, the Alpha Particle Intensity at the Target	77
10.2	The $1/\sin^4 \theta/2$ Dependence of the Rutherford Scattering Cross Section	80
10.3	The Absolute Rutherford Differential Cross Section for Au (α, α) Au	81
10.4	The Z^2 Dependence of the Rutherford Scattering Cross Section	82
10.5	The $1/E^2$ Dependence of the Rutherford Differential Cross Section	82

EXPERIMENT 11 **Coincidence Measurements in Nuclear Spectroscopy and Absolute Activity Determination by β, γ Coincidence Studies** **85**
11.1 A Simple Coincidence Experiment with a Multipurpose Coincidence Module 85
11.2 Coincidence Measurements with a Linear Gate 87
11.3 Coincidence Measurements with a Time-to-Amplitude Converter (TAC) 89
11.4 A β,γ Coincidence Experiment Which Yields the Absolute Activity of a Source 91

EXPERIMENT 12 **Annihilation Radiation Coincidence Studies with ^{22}Na** **95**
12.1 Annihilation Measurements with a Multipurpose Coincidence Circuit 95
12.2 (γ-γ) Annihilation Measurements with a Linear Gate 98
12.3 (γ-γ) Annihilation Measurements with a Time-to-Amplitude Converter (TAC) 99

EXPERIMENT 13 **Nuclear Lifetimes of ^{181}Ta and ^{57}Fe by Coincidence Spectroscopy** **101**
13.1 Measurement of the Nuclear Lifetime of the 615 keV State in ^{181}Ta by β,γ Coincidence with a Surface Barrier Detector and a NaI(Tℓ) Detector 103
13.2 Measurement of the Nuclear Lifetime of the 615 keV State in ^{181}Ta by β,γ Coincidence Using a Surface Barrier Detector and a High Resolution Germanium Gamma Detector 104
13.3 Mean Lifetime Measurement of the 14 keV State in ^{57}Fe with Two NaI(Tℓ) Detectors and a Time-to-Amplitude Converter (TAC) 105
13.4 Mean Lifetime Measurement of the 14 keV State in ^{57}Fe, Measured with Germanium and Si(Li) Detectors and a TAC 107

EXPERIMENT 14 **Angular Correlation** **109**
14.1 Verification of the Gamma-Gamma Coincidence for ^{60}Co Using a Multipurpose Coincidence Circuit 110
14.2 Verification of the γ-γ Cascade in the Decay of ^{60}Co (Linear Gate Method) 112
14.3 Gamma-Gamma Angular Correlation of ^{60}Co with Two NaI(Tℓ) Detectors Using [Time-to-Amplitude Converter (TAC) Method] 113
14.4 Gamma-Gamma Angular Correlation of ^{60}Co with Two Germanium Detectors [Time-to-Amplitude Converter (TAC) Method] 115

EXPERIMENT 15 **Neutron Activation Analysis** **117**
15.1 Measurement of the Saturation Factor for Thermal Neutron Activation Analysis 119
15.2 Measurement of the Thermal Neutron Flux (ϕ) in the Activation Chamber 120
15.3 Determination of the Thermal Neutron Cross Section for the ^{74}Ge(n,γ)^{75}Ge [NaI(Tℓ) Spectroscopy] 121
15.4 Determination of the Thermal Neutron Cross Section for ^{51}V(n,γ)^{52}V by High Resolution Gamma Spectroscopy (Germanium Detector) 122
15.5 Fast Neutron Activation Analysis 124

EXPERIMENT 16 **Time-of-Flight Measurements in Nuclear Spectroscopy** **127**
16.1 Alpha Particle Time-of-Flight Spectroscopy: Setting up the System and Measuring the Sum of E Plus ΔE for ^{231}Pa Alphas 127
16.2 Time-of-Flight Measurement of the 7.36 MeV Alpha Group in ^{231}Pa 129
16.3 (dE/dx) Measurement of Alphas in Copper by Time-of-Flight Spectroscopy 131
16.4 Gamma Ray Time-of-Flight Spectroscopy 132

EXPERIMENT 17 **X-Ray Measurements and X-Ray Fluorescence Using a Gas Filled Proportional Counter** **135**
17.1 Energy Calibration of the Proportional Counter 136
17.2 Mass Absorption Coefficient Measurement for 8.04 keV Photons in Copper 136
17.3 Mass Absorption Coefficient Measurement for 22.1 keV Photons in Silver 139
17.4 X-Ray Fluorescence Using a Gas Filled Proportional Counter and a Specially Designed Fluorescence Chamber 140

EXPERIMENT 18 **Trace Element Measurements Using X-Ray Fluorescence and Neutron Activation Analysis: Applications in Environmental, Biological, and Geological Studies** **143**
18.1 Source Excited X-Ray Fluorescence in Environmental, Biological, and Geological Samples ... 146
18.2 Tube Excited X-Ray Fluorescence Analysis 147
18.3 Trace Element Studies by Neutron Activation Analysis 148

EXPERIMENT 19 **Experiments in Health Physics and Radiation Protection** **151**
19.1 A Study of the Efficiency of a GM Counter for Gammas and Betas 152
19.2 Beta Backscattering as a Function of Atomic Number 153
19.3 The $1/R^2$ Relationship for An Intense Gamma Source 154
19.4 The Analysis of Gamma Shielding Material 157
19.5 Radon Counting 159
19.6 Low Level Alpha, Beta, and Gamma Counting 161

EXPERIMENT 20 **Fundamental Nuclear Electronics** **165**
20.1 The Pulse Generator 166
20.2 A Study of Basic Amplifier Parameters 167
20.3 The Integral Mode of the Single Channel Analyzer 168
20.4 The Differential or Window Mode of the Single Channel Analyzer 169

APPENDIX A **Gamma Spectra and Nuclide Identification Catalog** **171**
I. Nuclide Index 175
II. Search Gamma for Nuclide Identification 181

APPENDIX B **X-Ray Critical-Absorption and Emission Energies in keV** **207**

EXPERIMENT 1
The Geiger Counter

Discussion

In the study of radioactivity there are usually three parameters associated with an unknown source that are necessary to know. These are: 1) What kinds of particles is the source emitting, 2) What are the energies of these particles, and 3) How many particles per unit time is the source emitting. In this experiment, the Geiger-Mueller counter (called GM) will be used to help answer the third question. In subsequent experiments, the other two questions will be studied in great detail.

The GM tube is one of a variety of radiation detectors that take advantage of the fact that charged particles lose energy in a gas by creating electron-ion pairs. In air for example, an alpha particle will ionize from 50,000 to 100,000 molecules per cm of its path. The Geiger tube is simply a metal cylinder that is filled with some kind of counting gas. A thin window at one end of the cylinder allows the radiation to enter the counting region. The ion-pairs that are produced by the radiation are swept out and collected by an electric field that is maintained between a thin wire on the axis of the tube (anode) and the metal cylinder (cathode). The electric field between these two electrodes is high enough that the ions produced by the initial radiation are accelerated and produce secondary ions. This phenomena is called an avalanche.

In this experiment β's, & γ's will be measured with one of these end-window Geiger tubes. In order to detect gammas with these detectors, a two step process must occur. The gamma must first make a photoelectric or Compton interaction in the gas. The recoil electrons from these interactions then produce the ion-pairs that cause the avalanche. In the experiment, it will be seen that the GM tube is quite efficient for detecting beta particles, and the voltage gradient across the tube will be set such that any of these ionizing particles that enter the sensitive region will cause an avalanche. The output pulse is usually greater than one volt. The GM tube does not differentiate between kinds of particles or energies; it simply gives an output pulse when any ionizing particle triggers this avalanche. These output pulses are then recorded in a scaler which acts as an electronic adding machine.

Scope

In this experiment, the properties of the GM tube and some important counting parameters will be studied. These include the GM operating voltage plateau and the resolving time of the GM tube. After these introductory measurements, the GM counter will be used to study absorption, the inverse square law, half-life, and counting statistics.

EXPERIMENT 1.1
Determining the Operating Plateau for the Geiger Tube

Experimental Procedure

Figure 1.1 shows a typical voltage plateau curve for a GM tube. At low voltages, there is no output. As the voltage is increased, a few counts will be recorded at the "starting voltage." As the voltage is further increased, the counting rate will change rapidly until the "knee" or threshold of the plateau is reached. From this point on, the counting rate is fairly constant for approximately 200 volts. This is called the plateau region. Shortly after the plateau region, the tube breaks down and goes into a continuous discharge. The operating voltage for the measurements in this experiment will be 25% of the plateau above the knee or threshold. Halogen quenched geiger tubes, such as the Model PK-2 used in this experiment, are NOT harmed by a continuous discharge. Lower the voltage to the plateau level, and the GM tube will again operate normally.

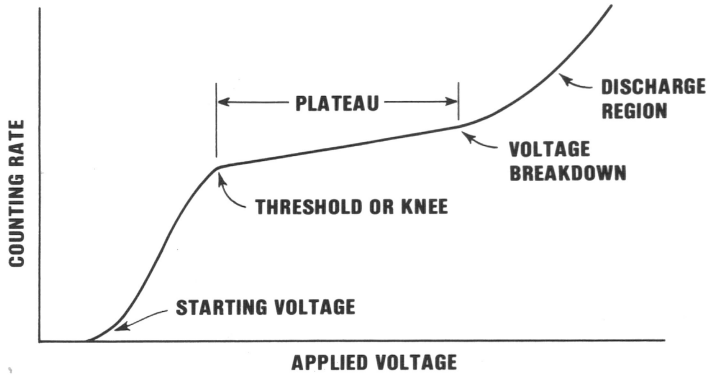

Figure 1.1. Typical Geiger-Mueller Characteristic Curve.

1. Set up the electronics as shown in Figure 1.2

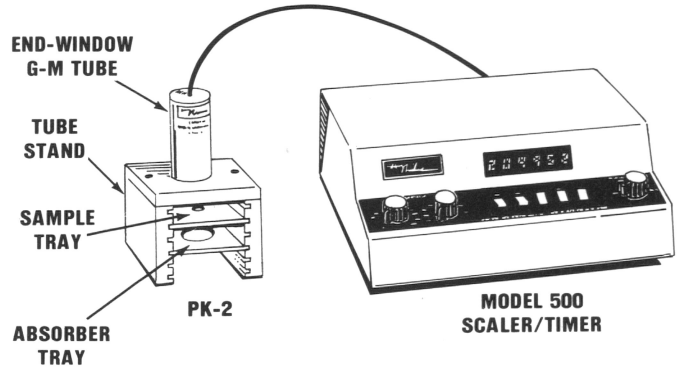

Figure 1.2. Electronics for GM Counting.

2. Place the ^{204}Tl beta source on the second shelf of the GM stand. Set the timer on "manual" so that the voltage on the tube can be slowly raised and the student can observe all of the features of figure 1.1. Slowly raise the voltage until the starting voltage is reached. Record this value. Continue to increase the voltage until the counting rate levels off. This is the knee of the plateau. Record this value. Continue increasing the voltage until the voltage breakdown region is reached. Record this value. This concludes the visual inspection of the curve.

3. Now we will take data so that the plateau curve can be plotted and the operating voltage for the GM tube established. Go back to the value of the starting voltage and take 60 sec. counts in 50V increments until the breakdown point is reached. Fill in Table 1.1.

Table 1.1 Data for Constructing a Plateau Curve

Run No.	Voltage	Counts	Time Sec	Counting Rate Cts/s
1				
2				
3				
4				
5				
6				
7				
8				
9				
10				
11				
12				

Exercise A Plot a curve of counting rate versus voltage and determine the position of the knee and the voltage breakdown region. Record the operating point, which is 25% of the Plateau, starting from the knee.

Exercise B The plateau region rises with a gentle slope. Calculate the value of the slope. It should be slightly less than 10%.

EXPERIMENT 1.2
Resolving Time Corrections

Discussion

In the earlier discussion it was mentioned that the Beta particle enters the GM tube through the window and loses its energy by creating electron-ion pairs. The electrons that are produced in the resulting avalanche are accelerated to the anode and collected in a short period of time. The positive ions, however, are more massive and make their way slowly to the cylindrical cathode. If their average transient time is called Δt_1, the GM tube is busy, so to speak, during Δt_1. If another ionizing particle enters the GM tube during Δt_1, it will not be counted. This time Δt_1, is called the "dead time" of the tube. In this experiment the resolving time of the GM tube will be determined and the correction factor which can account for these lost events will be shown.

Experimental Procedure

1. Set the GM counter at its operating voltage. Obtain the split source from the instructor. This source is designed such that each half of the source can be counted separately without too many losses, but when both parts are counted at the same time, substantial losses occur. Count the first half of the source on shelf one for 60 sec. Calculate the counting rate and call this rate R_a. Repeat the exact measurement for the second half of the source and call this rate R_b. Now count both halves together for 60 sec. and call this rate R_{a+b}.

Exercise Calculate the resolving time of the GM tube which is given by:

$$T_R = \frac{R_a + R_b - R_{a+b}}{2 R_a R_b} \qquad (1)$$

The true counting rate R_1 can be calculated from the observed counting rate (R_2) by the following:

$$R_1 = \frac{R_2}{1 - R_2 T_R} \text{ counts/sec} \qquad (2)$$

Note: Because of the solid state electronics used in the circuitry of modern instrumentation such as the scaler, the resolving time of these instruments is normally one microsecond or less. Therefore, only the resolving time of the GM tube affects the true count rate.

For the rest of the data taken in the experiment with the GM tube, eq. (2) should be used to correct the resulting counting rate. Also, the radioactive sources should be moved away and a 60 sec background taken. This background rate should be subtracted from all measurements.

In the experiments to follow, this background rate will be referred to as $\frac{\Sigma - B}{t}$.

EXPERIMENT 1.3
Half-Life Measurement

Discussion

The intensity of a radioactive source changes with time in accordance to the relation:

$$I = I_o e^{-\lambda t} \quad (3)$$

where λ is the decay constant in reciprocal seconds. I=the intensity at time(t)

I_o = the initial intensity

The half-life, by definition, is the time required for the intensity to fall to one half of its initial value. From eq. (3):

$$\frac{I}{I_o} = 0.5 = e^{-\lambda T_{1/2}} \quad (4)$$

where $T_{1/2}$ is the half-life. Equation (4) reduces to:

$$\text{Ln } 0.5 = -0.693 = -\lambda T_{1/2} \quad (5)$$

or

$$T_{1/2} = \frac{.693}{\lambda} \quad (6)$$

In this experiment the $T_{1/2}$ value will be measured for a short half-life isotope.

Experimental Procedure

1. Set the GM counter at its operating voltage. Take a 300 sec background count and determine the background rate. Obtain the short half-life sample from the instructor. These samples are obtained from a minigenerator or produced with a neutron source by activation. The instructor will usually give a hint as to the value of $T_{1/2}$. This hint will tell how often you must take counts. For example, if the half life is approximately 2 hours, take 5 minute counts every 20 minutes for 3 hours. Other parts of this experiment can be done in between half-life measurements. For each half-life measurement, be sure to place the source at exactly the same distance from the window of the detector. If a minigenerator is used to produce a short $T_{1/2}$ nuclide, place the liquid source in the center of the ringed planchette, and do NOT remove the planchette for the sample tray while obtaining count rate data.

Exercise Subtract the background counting rate from each of the measured rates. Correct each of the rates for resolving time after they have been corrected for background. On semilog paper make a plot of intensity vs elapsed time. This should give a straight line graph similar to figure 1.3. From the graph determine the half-life and λ.

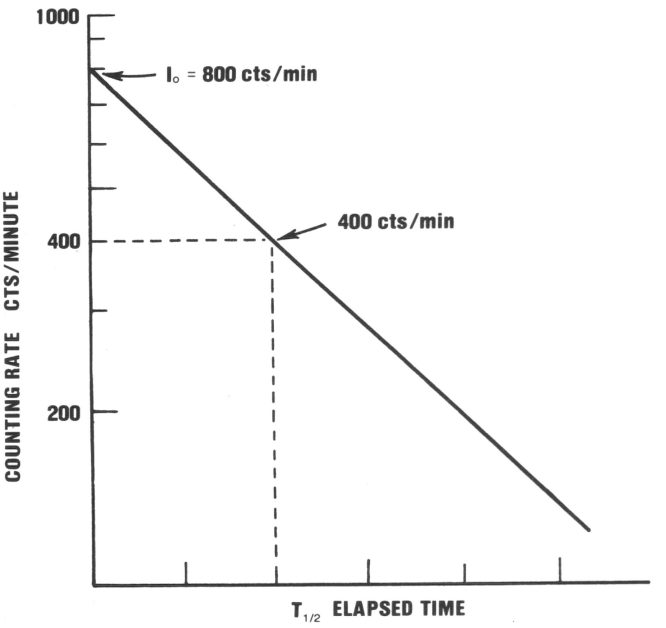

Figure 1.3. Typical Half-Life Curve.

EXPERIMENT 1.4
Linear Absorption Coefficient

Discussion

When gamma rays pass through matter, the intensity (I) after having gone through X thickness of the material is given by:

$$I = I_o e^{-\mu x} \quad (7)$$

where

I_o = the measured intensity without an absorber
μ = linear absorption coefficient

From equation (7) we can write:

$$\mu = \frac{.693}{x_{1/2}} \quad (8)$$

where

$x_{1/2}$ = the half value thickness

This experiment is quite similar to the half life experiment. The fall off in intensity of gammas as they pass through absorbers of increasing thickness will be measured. From the data, a plot of Intensity vs Absorber thickness will be made on semilog paper and the $x_{1/2}$ and μ values calculated from the data.

Experimental Procedure

1. Set the voltage of the GM tube at its operating value. Obtain a 5 minute background count and determine the background counting rate. Obtain the ^{137}Cs source from the instructor and place it on shelf 3.

2. Take a two minute count, calculate the counting rate, subtract the background and record this I_o value in your data table. Remove the thinnest lead absorber from the kit and place it between the source and the window of the detector. Determine the corrected counting rate for this absorber. Repeat for enough absorbers to reduce the initial intensity to 20% of its original value.

Exercise On semilog paper, make a plot of corrected intensity vs absorber thickness. Figure 1.4 shows a typical absorption curve that was made for this experiment. How does the measured value of μ compare with the accepted value of $\frac{0.105\ cm^2}{g}$ for the 0.662 MeV gammas from ^{137}Cs in lead?

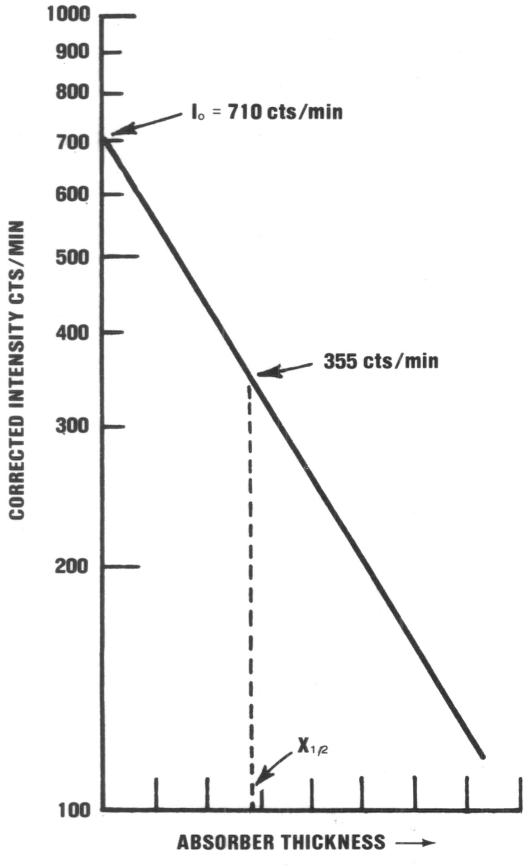

Figure 1.4. Typical Data for the Linear Absorption Coefficient Measurement.

EXPERIMENT 1.5

The Inverse Square Law

Discussion

Most radioactive sources are isotropic in nature. This means that gammas (for a gamma source) are given off equally in all directions. There are some sources, however, where there is a correlation of one gamma relative to the other that is not isotropic. It will be seen in a later experiment that this angular correlation will allow us to predict some properties of the nuclear states that are involved in the decay of these isotopes. In the case of an isotropic source, it is a well known fact that the intensity of the source falls off as $1/R^2$. In this experiment, this $1/R^2$ relationship for a ^{137}Cs source will be verified.

Experimental Procedure

1. Set the voltage of the GM counter at its operating value. Determine the background counting rate.

2. For this experiment, use a ^{137}Cs source. The betas from the source must be attenuated out, since air absorption of the betas will modify the results. This can be done by placing a thin piece ($^1/_{16}$") of almost any material between the source and the window. Place the ^{137}Cs source 1 cm from the window and count for a long enough period of time to get good statistics. Record this uncorrected counting rate in Table 1.2.

Table 1.2 Data for $1/R^2$ Determination

Run No.	Distance	Counting Rate Uncorrected	Background Rate	Counting Rate Correction for Background & Resolving Time
1	1 cm			
2	2 cm			
3	3 cm			
4	4 cm			
5	5 cm			
6	6 cm			
7	7 cm			
8	8 cm			

3. Move the source to the 2 cm position and count for a period of time long enough to get reasonable statistics. Record the uncorrected counting rate in Table 1.2. Continue for the other distances in the table. It should be obvious that the counting time will have to be increased for the longer distances, to get good statistics.

Exercise A On linear graph paper, plot the corrected intensity vs distance. From the 3 cm data point, obtain the constant K as follows:

$$I = \frac{K}{R^2} \qquad (9)$$

Exercise B On the same curve, plot eq. (9) with the other values of R. Use the value of K that was found above. What we have done is normalize the data to the 3 cm measurement. How do the two curves compare?

EXPERIMENT 1.6

Statistical Variation of Data

Discussion

There is no way to predict when a person will have an automobile accident that does $1000 worth of damage to his car. However, if a very large number of drivers are considered it is possible for an insurance company to predict with reasonable accuracy, how many accidents, costing $1000, will occur this year. Insurance companies use large computers to store mounds of statistical data so they can accurately predict these probabilities from random events.

The radioactive decay of a nucleus is also a random event. There is no way to determine when a particular nucleus will decay. However, as we have seen, the half-life can accurately be determined. If two identical counts are taken in sequence on a long lived radioisotope, the counts will almost always differ. If a large number of these individual counts are taken, the average count N can be determined. From this data, a predictable deviation of each count from this average can be calculated. The standard deviation

$$\sigma = \sqrt{\bar{N}}$$

For this experiment, 35 independent measurements will be taken on the long lived isotope $^{137}Cs(T_{1/2} = 30y)$ and with this data, the predictable behavior of the measurements will be shown.

Experimental Procedure

1. Set the operating voltage of the GM counter to its recommended value. Place the ^{137}Cs source at a distance such that 2000 counts can be obtained in 0.5 min.

2. Take 35 sequential 0.5 minute counts and record these uncorrected events (N) in a Table similar to Table 1.3.

Table 1.3 Counting Statistics Data Table

Run No.	N	$N-\bar{N}$	$\frac{N-\bar{N}}{\sigma}$	$\frac{N-\bar{N}}{\sigma}$ (Rounded)
1				
2				
3				
4				
5				
6				
7				
8				

Exercise A Calculate the average of these 35 counts $\bar{N}$. Tabulate $N-\bar{N}$ in the table. Note, the number $N-\bar{N}$ can be positive or negative. If you will add up all of the $(N-\bar{N})$ in the table, the answer should be zero. If it is not, a mistake has been made. Calculate σ which is $\sqrt{\bar{N}}$. This is called the standard deviation. Sixty-eight (68) percent of the observed data should lie within the range $\bar{N} + \sigma$ to $\bar{N} - \sigma$.

In the above case, 24 of these measurements should fall within this range. Does the data fit?

Exercise B Calculate $\frac{N-\bar{N}}{\sigma}$ and tabulate it in the data table. Now round off the value for each entry to the nearest 0.5. For example, if $\frac{N-\bar{N}}{\sigma} = +1.11$, the rounded off figure would be +1 . etc. Plot the frequency of rounded off events versus σ and a normal distribution curve should be seen.

Figure 1.5 shows a normal distribution curve that should be similar to your calculations.

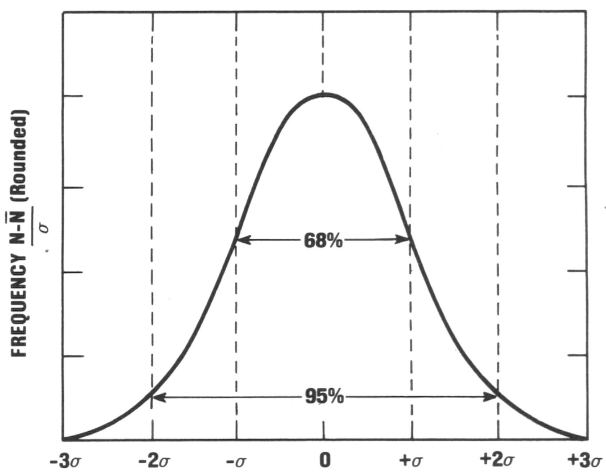

Figure 1.5. Typical Gaussian, Generated from an Extensive Set of Data.

REFERENCES FOR *EXPERIMENT 1*

1. Chase, G., Rituper, S., & Sulcoski, J. W., *Experiments in Nuclear Science*, Burgess Press 1964 (Available from the Nucleus).

2. G. D. Chase and J. L. Rabinowitz, *Principles of Radioisotope Methodology*, 3rd Edition, Burgess Publishing Co., Minnesota (1967).

3. C. M. Lederer and V. S. Shirley, Eds., *Table of Isotopes*, 7th Edition, John Wiley and Sons, Inc., New York (1978).

4. *Radiological Health Handbook*, U.S. Dept. of Health, Education, and Welfare, PHS Publication 2016. Available from National Technical Information Service, U. S. Dept. of Commerce, Springfield, Virginia.

5. E. W. Emergy, *Geiger-Mueller and Procurement Counters in Radiation Dosimetry*, II, F. H. Attix and W. C. Roesch, Eds., Academic Press, New York (1966).

6. G. F. Knoll, *Radiation Detection and Measurement*, John Wiley and Sons, New York (1979).

7. H. L. Andrews, *Radiation Biophysics*, Prentice-Hall, New Jersey (1974).

8. V. Arena, *Ionizing Radiation and Life*, The C. V. Mosby Co., Missouri (1971).

9. C. E. Crouthamel, *Applied Gamma Ray Spectrometry*, Pergamon Press, New York (1960).

EXPERIMENT 2

Gamma-Ray Spectroscopy Using NaI(Tℓ)

Objective

This experiment is designed to familiarize the student with the basic concepts of Scintillation Spectroscopy. It is written for spectroscopy with multichannel analysis. In doing this set of experiments, the experimenter becomes familiar with the basic science associated with gamma decay and interaction. The student is also afforded the privilege of using "state of the art" nuclear instrumentation.

This set of experiments is quite comprehensive in that it covers most of the different types of measurements that can be done with NaI(Tℓ) detectors. It may very well be that the instructor wishes to have the student do only selected experiments in keeping with the theory part of the course, as it is taught. The estimated time for each experiment is listed, following the title of the experiment. The laboratory instructor can decide which experiments are to be done within the existing time frame for the lab. This complete set of scintillation spectroscopy experiments can easily be done in (3) two hour laboratory periods.

Scintillation Spectroscopy and Gamma Interactions with Matter (Theory and Practical Considerations)

When a gamma from a radioactive source interacts with matter, there are three primary methods by which it is absorbed. These are: 1) The Photoelectric Effect, 2) Compton Interaction, and 3) Pair Production. In this experiment, we will carefully study these interactions. Figure 2.1 shows the special case where a gamma source is being counted by a Sodium Iodide NaI(Tℓ) detector. The detector is surrounded by a lead shield similar to that which is used in experiment #2. For the time being, we will ignore all of the events shown in figure 2.1 except the photoelectric effect, Compton interaction, and pair production.

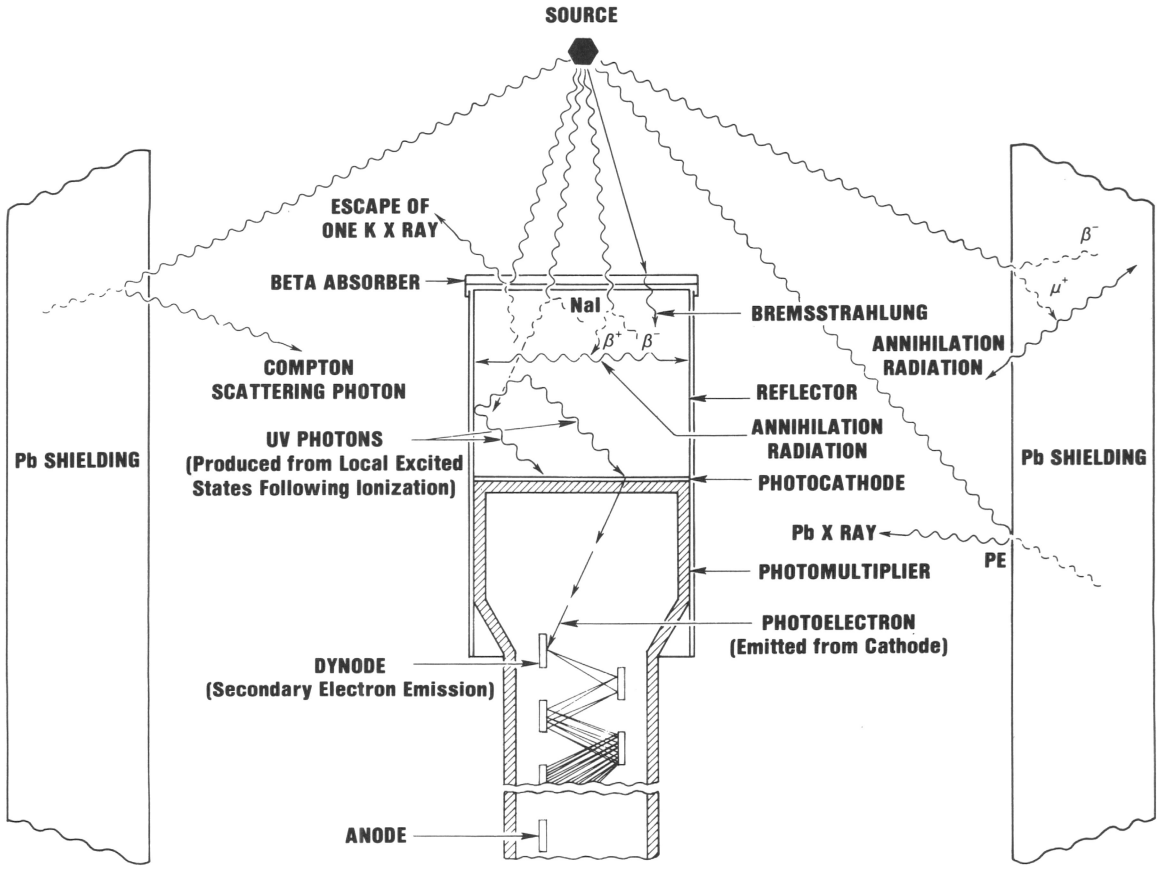

Figure 2.1. Gamma Source, NaI(Tℓ) Detector, Photomultiplier Tube, and Lead Shield, showing various types of Interactions. (Courtesy of Idaho Operations Office, DOE)

The Photoelectric Effect

The Photoelectric Effect gives us a well defined peak in our measured spectrum and, hence, we will discuss it first. Gamma rays enter the NaI(Tℓ) crystal and interact primarily with the bound K or L shell electrons from the Iodine in the crystal. Essentially, the gamma gives all of its energy to the bound electron and knocks it out of the atom with an energy (E_e) given by:

$$E_e = E\gamma - B$$

where B is the binding energy of the electron. Since B is only 33 keV for the Iodine K shell, we can see that the recoiling electron has most of the energy of the incident gamma ray which is usually of the order of 1 MeV or greater. As this recoiling electron goes through the NaI(Tℓ) crystal, it loses its energy by ionization, excitation, and the production of thermal energy. Some fixed fraction of the electron energy will be converted to light photons which then impinge on the photocathode of the photomultiplier tube shown in figure 2.1. These photons will produce photoelectrons from the photocathode surface of the photomultiplier. Only one is shown in the figure. These photoelectrons are attracted to the first dynode of the phototube by a positive voltage which is provided by the voltage divider resistor string attached to the photocathode and dynodes of the phototube. Secondary electrons emitted by the first dynode are attracted to the second dynode and so forth. The final avalanche of electrons arrive at the anode and produce an electrical pulse which is proportional to the energy of the incident gamma ray. Pulses from the anode are fed through the preamplifier, amplifier and into the multichannel analyzer for analysis. Figure 2.2 shows the electronic block diagram that will be used for all parts of the experiment.

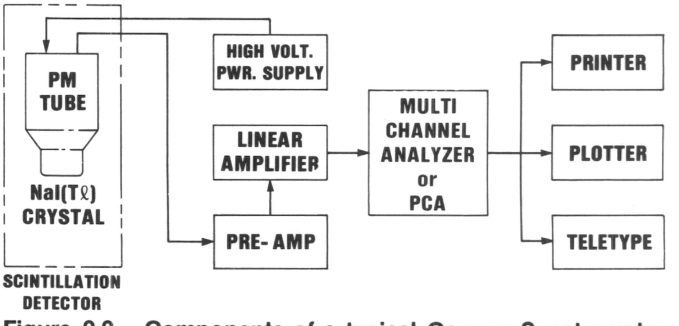

Figure 2.2. Components of a typical Gamma Spectrometry System (Printer, Plotter and Teletype are optional).

Figure 2.3 shows a typical pulse height spectrum that is observed in the MCA of figure 2.2 The pronounced photopeak is clearly seen in channel 100 of this 256 channel spectrum. The position of this peak channel (100) is proportional to the gamma ray energy from ^{137}Cs (0.662 MeV). Since the system is linear, a gamma ray source with energy 1.32 MeV (twice the ^{137}Cs gamma energy) would occur in channel 200 etc. Shown also in the spectrum, is the broad distribution of pulses from the Compton edge down to the electronic cut-off. This distribution of pulses is produced by Compton interactions in the NaI(Tℓ) crystal.

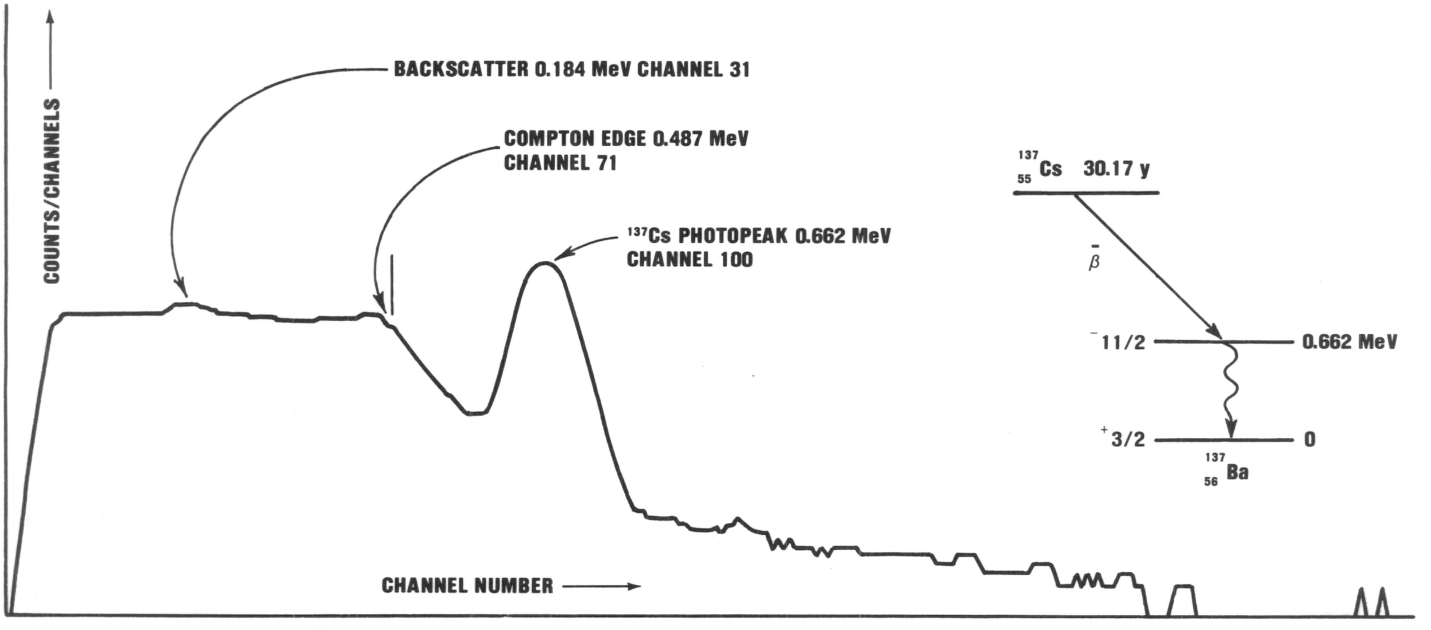

Figure 2.3. Pulse Height Spectrum for ^{137}Cs taken with a Nucleus Spectrum 88 MCA, 1μCi source on shelf 3 and the electronics shown in figure 2.2.

The Compton Interaction is purely a kinematic collision between the incident gamma photon and an electron in the crystal that is either free or loosely bound.

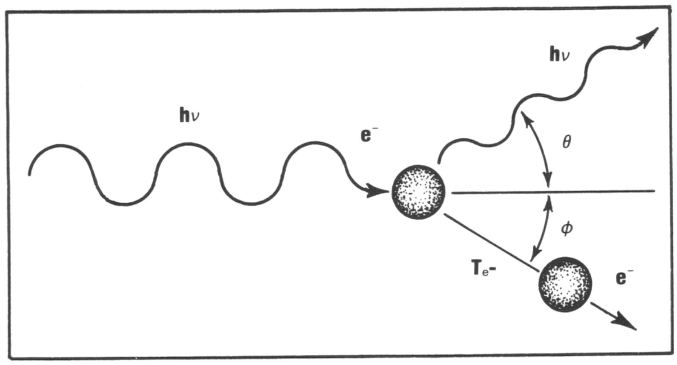

Figure 2.4. Shows a kinematic picture of the reaction.

The incident gamma ray has an energy E = hν. This energy is shared between the Compton scattered photon and the recoiling Compton electron. The scattered photon has an energy E = hν′ and the electron has an energy T_e. Since the total energy is conserved in the interaction, we can write:

$$h\nu = h\nu' + T_e \qquad (1)$$

Momentum is also conserved in the interaction and from a consideration of conservation of momentum we can write the two expressions below:

$$\frac{h\nu}{c} = \frac{h\nu'}{c}\cos\theta + P\cos\theta$$

(x component momentum) (2)

$$o = \frac{h\nu'}{c}\sin\theta - P\sin\theta$$

(y component momentum) (3)

where P represents the momentum of the electron.

From a simultaneous solution of these three equations, we can derive Compton's well known formula for the energy of the scattered photon in terms of the initial energy, hν and scattering angle θ, (remember, m_oc^2 = 0.511 MeV for an electron).

$$h\nu' = \frac{h\nu}{1 + (1-\cos\theta)\, h\nu/m_oc^2} \qquad (4)$$

The kinetic energy of the Compton electron can be written as:

$$T_e = h\nu - h\nu' \qquad (5)$$

An examination of the last two eq's. (4 and 5) indicates that the scattered photon, hν′, may go in any direction with respect to the incident gamma ray; whereas, the electron can be scattered only in a forward direction. By using the eq's. (4 and 5) for scattered photon and electron energies and by substituting different values of scattering angle θ and different incident gamma energies, Table 2.1 is obtained.

Table 2.1

θ	hν = 1022 keV hν′	T_e	hν = 662 keV hν′	T_e	hν = 323 keV hν′	T_e
0	1022	0	662	0	323	0
30	806	216	564	98	298	25
60	511	511	402	260	245	78
90	341	681	288	374	198	125
120	256	766	225	437	166	157
150	216	806	194	468	148	175
180	204	818	184	478	143	180

An inspection of the data shown in Table 2.1 reveals that the electron receives the maximum kinetic energy when it is projected forward and the Compton photon is scattered backward (θ = 180°).

The probability of a Compton interaction varies as the ratio of atomic number to mass number (Z/A) of the absorber material and is less dependent on the photon energy than is the photoelectric effect.

From figure 2.4 and the fact that all angles θ for hν′ are about equally probable, the recoiling electron energies T_e are equally probable (see Table 2.1 for ^{137}Cs) from zero up to the maximum Compton recoil energy for ^{137}Cs which is 0.478 MeV. This value corresponds to the Compton edge in figure 2.3.

Pair Production

For incident gammas that have energies greater than 5 MeV, the most pronounced interaction in the NaI(Tℓ) crystal is pair production (see figure 2.6). In this process, a photon of sufficient energy gives up all of its energy and forms two particles, an electron and a positron. This process is pictured (see figure 2.5) as occurring near the nucleus of an atom, for it is only in this way that momentum can be conserved. The minimum energy needed for pair production is given $E = 2m_oc^2$, where m_o is the rest mass of an electron or positron. Since the rest mass of an electron is equivalent to 0.511 MeV, the photon must have an energy ≧1.02 MeV for pair production to occur.

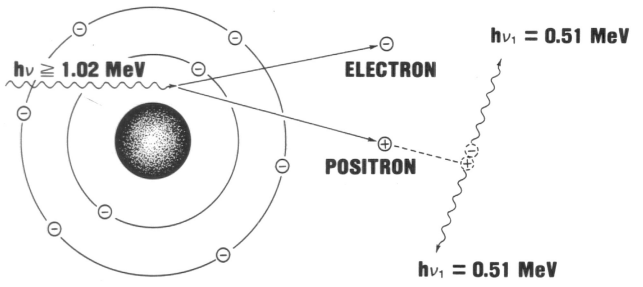

Figure 2.5. Pair Production: The gamma photon enters from the left and forms an electron-positron pair near the Iodine nucleus. A few nanoseconds later, the positron will annihilate in the crystal giving two photons of energy 0.511 MeV.

When this process occurs, energy of the photon beyond 1.02 MeV is imparted as kinetic energy to the electron-positron pair and a portion to the nucleus in order to conserve momentum. Both electron and positron lose kinetic energy through ionization of atoms in the crystal. In a few nanoseconds the positron interacts with an electron in the detector in a process called annihilation. In this process, the mass of the particles is changed into two photons of 0.511 MeV each, emitted in nearly opposite directions. They may interact further in the crystal through the photoelectric or Compton effects.

Since this process does not occur at all, unless the gamma energy is ≧1.02 MeV, pair production is important only for gammas of high energy. The process is also proportional to Z^2 of the absorber. Thus, pair production predominates for substances of high Z and gamma energies greater than 5.0 MeV.

We will discuss the other interactions shown in figure 2.1, as well as their probabilities in later sections of this experiment. Figure 2.6 shows cross sections for Photoelectric, Compton, Pair Production, and Total Photon Interaction for a NaI(Tℓ) detector.

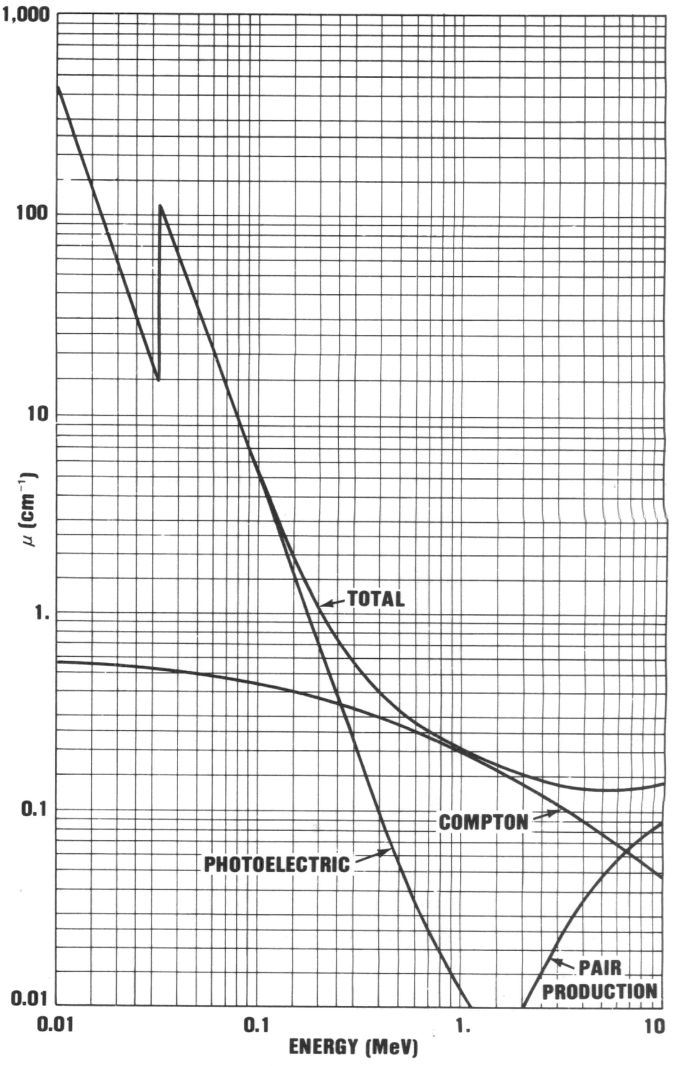

Figure 2.6. Photoelectric, Compton, Pair Production, and Total Photon Interaction for a NaI(Tℓ) Detector Versus Photon Energy (taken from NBS Circular No. 583).

EXPERIMENT 2.1

Gamma Energy Calibration

(Time for completion 1 hr.)

Experimental Procedure

Electronics Set Up: Figure 2.2 shows the electronics arrangement that will be used for all parts of this experiment. Be sure to read the instruction manuals for all components before setting up the electronics, and that all power is off before making interconnections. All of the cable connections are made with RG58U or RG62U except the SHV cable that connects the High Voltage power supply to the HV input of the phototube (for most of the NaI(Tℓ) experiments, 256 channels on the MCA is adequate). When all of the electrical connections are made, you are ready to start the calibration experiment.

1. Position the 1μCi ^{137}Cs source on shelf No. 4 of the P-2000/2 sample stand. This shelf gives a detector the source distance of 3.3 cm.

2. Turn on and slowly increase the high voltage to a positive value of 1000V.

3. The output cable from the pre-amp should be connected to the negative input of the amp. Use the bipolar output of the amp to the MCA or PCA. Adjust the coarse and fine gain of the amplifier so that the photopeak (see figure 2.3) from ^{137}Cs is in channel 66 of the multichannel analyzer. Acquire a spectrum for a counting time of 100 seconds. The spectrum observed should be similar to figure 2.3. With the geometry used, there will be approximately 4000 counts in the photopeak height. The total number of counts under the photopeak should be approximately 20,000 events. The energy of the photopeak from ^{137}Cs is 662 keV, therefore, the energy per channel number is 662 keV/66 channels or approximately 10 keV/ch.

Readout the spectrum, or use the cursor from the MCA or PCA and determine the exact peak location of the 662 keV photopeak. Record the channel number of the peak location in Table 2.2.

Table 2.2

Event	Energy (MeV)	Channel Number
1 ^{137}Cs Photopeak	0.662	
2 ^{60}Co Photopeak	1.17	
3 ^{60}Co Photopeak	1.33	
4 ^{57}Co Photopeak	0.122	

4. Replace the ^{137}Cs source with ^{60}Co (shelf 4) and accumulate for 100 seconds. Record the positions of the two photopeaks from ^{60}Co in Table 2.2 as in step **3** above. Figure 2.7 shows a screen dump of ^{60}Co that was taken on a Nucleus Spectrum 88 analyzer.

5. Replace the ^{60}Co source with ^{57}Co and record the position of the 0.122 MeV photopeak in Table 2.2

Exercise A From the data shown in Table 2.2, make a plot on linear graph paper of the energy of the photopeak versus the channel number of the centroid of the photopeak. Figure 2.8 shows a typical calibration curve for the above data.

Exercise B *(optional)* Table 2.3 shows a complete tabulation of the gamma sources and their photopeak energies for the S-13 gamma source set.

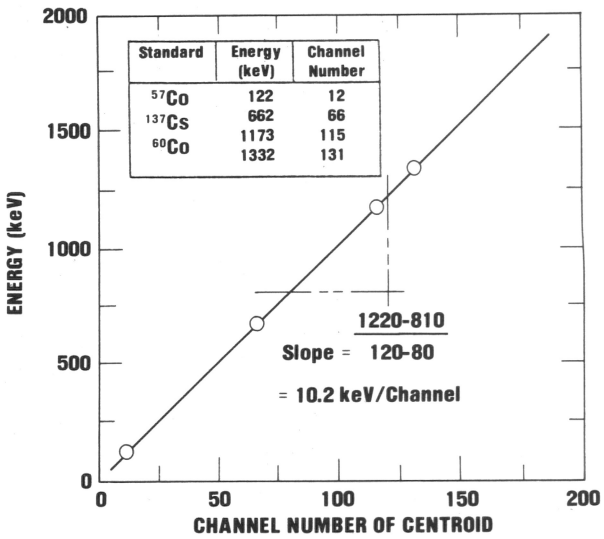

Figure 2.8. Typical Energy Calibration Curve for ^{57}Co, ^{137}Cs, and ^{60}Co.

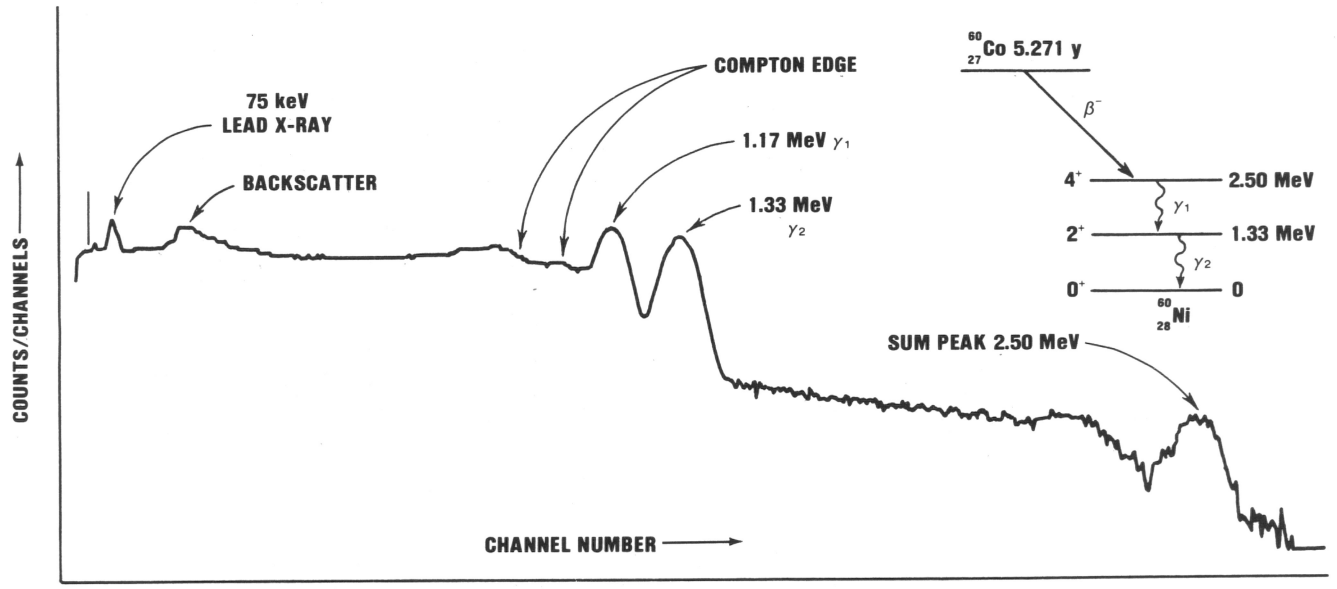

Figure 2.7. Pulse height spectrum of ^{60}Co taken with a Nucleus Model Spectrum 88 Analyzer.

Accumulate spectra for ^{22}Na and ^{54}Mn and include these points in your data table and calibration curve.

Table 2.3 Gamma Emitters from Student Laboratory Source Set S-13

Isotope	Half Life	f_g (Fraction of γ's per decay)	Gamma Peaks of Interest
^{60}Co	5.62 years	0.99	1.173, 1.332
^{22}Na	2.62 years	.999	0.511, 1.275
^{54}Mn	303 days	1.00	0.835
^{137}Cs	30 years	0.92	0.662
^{133}Ba	7.2 years	see Ref. 1	.080, 0.276, 0.302 0.356, 0.382
^{109}Cd	453 days	see Ref. 1	0.088
^{57}Co	270 days	see Ref. 1	0.014, 0.122, 0.136

EXPERIMENT 2.2

Identification of Unknown Gamma Emitters

(Time for completion 0.5 hr.)

Objective

We will use the calibration curve that was generated in experiment 2.1 to identify the gamma lines of several unknown sources that the instructor will supply. The student will identify the photopeaks of each unknown source and then go to the tabulation (Appendix A of this manual) of Selected Gamma Rays by Decreasing Energy and thus determine the unknown isotope.

Experimental Procedure

1. Obtain the first unknown gamma source from the instructor. Accumulate a spectrum for a time period long enough to clearly be able to identify the peaks in the spectrum. Assign a centroid peak position to each of these peaks. From your calibration curve determine the energy of each peak.

2. Repeat procedure #1 for the rest of the unknowns provided by the instructor.

Exercise Determine the unknown isotope or isotopes by consulting Appendix A or references 1 and 2 at the end of this experiment.

Gamma Spectrum Analysis

Objective

To carefully analyze the effects of the various types of interactions shown in figures 2.1 and illustrate their effect on the pulse height spectrum that is being measured. These interactions include the Compton edge, backscatter from the lead shield, x-ray fluorescence from the lead, giving the 75 keV lead Kα x-ray, the annihilation process giving escape peaks or additional 0.511 MeV peaks that apparently should not be in the spectrum.

Discussion

A Backscatter Figure 2.3 shows a spectrum of ^{137}Cs which has, for the most part, a pronounced photopeak and a Compton distribution. A small backscatter peak can be observed at an energy of 184 keV (Channel 31). Where did it come from? The answer can be easily seen by analyzing the energy of a ^{137}Cs photon that Compton scatters from the lead shield and then the scattered photon goes into the NaI(Tl) detector and is absorbed by the photoelectric process. Since most of these photons scatter at approximately 180°, they are called backscatter photons. From the kinematic analysis of the Compton interaction (see Table 2.1) the scattered energy of these backscattered photons is 184 keV. One such event is shown in figure 2.1. The photon on the left backscatters into the crystal as described above.

Backscatter will also occur from the table, detector housing, supports, etc. Most of these backscatter photons come from the lead shield that surrounds the detector. The shield, however, is necessary to reduce the room background which is by far a larger problem than the backscatter peak produced by the shield. It is easy to calculate the position of the backscatter peak. Equation 4 can be written: (since m_oc^2 = 0.511 MeV, θ = 180° for backscatter)

$$E\gamma' \cong \frac{E\gamma}{1 + 3.91\ E\gamma} \qquad (6)$$

Figure 2.7 shows a pulse height spectrum of ^{60}Co. The backscatter peak is clearly seen in the figure. Eq. (6) will show the energy of this peak if you substitute $E\gamma$ = 1.33 MeV into it and solve for $E\gamma'$.

B Lead X-Ray Photons that strike the lead shield can also produce a fluorescent 74.96 keV Kα x-ray. Some of these x-rays will interact with the NaI(Tl) detector and produce a 74.96 keV x-ray peak in the spectrum. The lead x-ray is produced by the initial photon from the source interacting with the lead by the photoelectric process. Remember, from our earlier discussion, in the photoelectric process the gamma gives all of its energy to a bound K or L shell electron, thus knocking it out of its orbit. If it is

a K-shell lead electron that is removed, the vacancy will be filled by an L-shell electron falling into the vacancy giving the Pb Kα x-ray which is 74.96 keV. This process can be seen in figure 2.1 as the lower photon on the right hand side strikes the lead shield. The 74.96 keV lead Kα x-ray can be seen clearly in figure 2.7. In order to accentuate this lead x-ray, we have placed a thick sheet of lead behind the source, thus inducing more lead x-ray fluorescence to illustrate the effect.

C Annihilation Radiation This process can produce peaks in the spectrum, depending on whether the annihilation, which results from pair production, occurs in the lead or in the NaI(Tℓ) detector. Both of these possibilities are shown in figure 2.1. If the annihilation occurs in the lead and one of the 0.511 MeV gamma pairs interact in the detector, then an extra 0.511 MeV peak will appear in the spectrum that is being measured. It should be remembered that this process can only occur for radioactive sources that have gammas in their decay scheme greater than 1.02 MeV. (See figure 2.6)

In the second case, where the incident photon annihilates in the detector (see figure 2.1), there are, in general, three peaks that can be produced. If the initial gamma has an energy Eγ, the first peak seen in the spectrum corresponds to Eγ. In this case, Eγ annihilates in the detector and both annihilation quanta interact by the photoelectric process before escaping from the detector. We have thus totally absorbed the energy of the incident gamma. A second peak will be seen at Eγ - 0.511 MeV. This peak is produced when one of the annihilation quanta is absorbed and the other escapes. In the spectra, this is called the first escape peak. The third peak of energy Eγ - 1.02 MeV is observed when both annihilation quanta escape from the detector before being absorbed. This peak is called the second escape peak. The probability of seeing the total absorption peak and the two escape peaks depends on the incident gamma energy and the size of the detector. Figure 2.9 shows a NaI(Tℓ) spectrum of ^{228}Th and its daughters. In this case Eγ is 2.615 MeV from ^{208}Tl. The single escape peak is 2.104 MeV and double escape occurs at

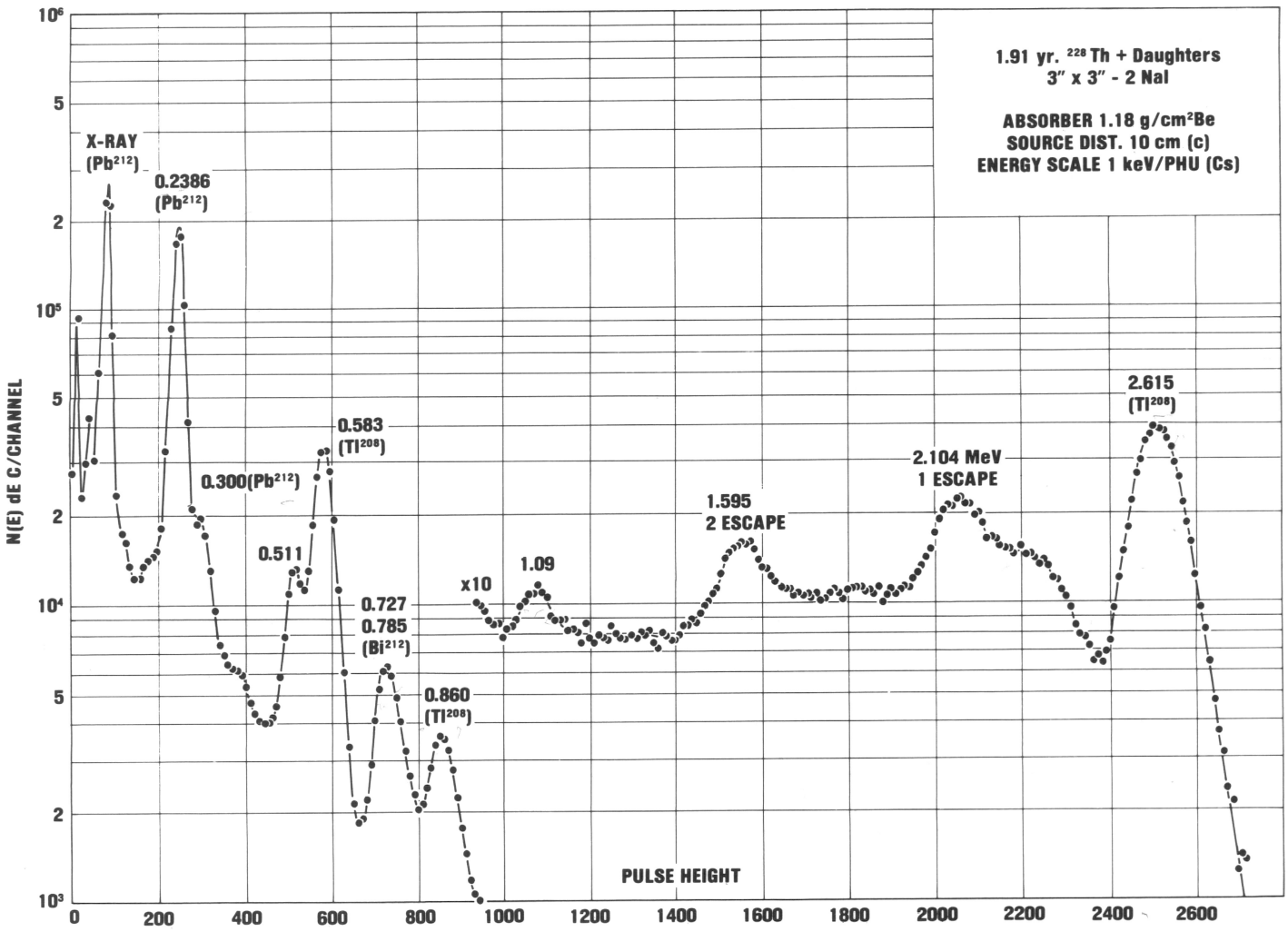

Figure 2.9. Gamma Ray Pulse Height Spectrum of a ^{228}Th Source. This spectrum shows the single and double Escape Peaks from the 2.615 MeV ^{208}Tl Line.

1.595 MeV. Figure 2.9 was taken from reference 2, *Scintillation Spectrometry Gamma-Ray Spectrum Catalogue* by R. L. Heath. This reference contains scintillation spectra from most of the commonly used isotopes. It makes a valuable addition to the library that should be assembled to accompany these scintillation experiments.

The Sum Peak

Figure 2.7 shows a pulse height spectrum of the gammas from ^{60}Co. This isotope is neutron rich and will β decay to the 2.50 MeV level in ^{60}Ni. In order to de-excite to the ground state, a gamma (γ_1) is emitted leaving ^{60}Ni in its 1.33 MeV state of excitation. This state decays to the ground state in a mean time of 7×10^{-13} seconds by the emission of a 1.33 MeV photon (γ_2). The normal spectrum thus contains the 1.33 MeV and 1.17 MeV gammas as shown in figure 2.7. These gammas are given off in equal numbers because of the sequential nature of the decay scheme. The 1.17 MeV peak will have a larger sum in the measured spectrum because the NaI(Tℓ) detector has a slightly higher efficiency for this lower energy gamma. For the purpose of analyzing the sum peak, we can assume that γ_1 and γ_2 are given off in an isotropic manner (later we will see that the angular correlation is isotropic within 16%). From the standpoint of the analysis, if γ_1 is given off in the direction of the detector, then γ_2 can be given off in any direction. Therefore, it is possible for γ_1 and γ_2 to simultaneously go into the detector. As far as the detector is concerned, if both γ's were totally absorbed, we would observe a sum peak whose magnitude is γ_1 plus γ_2. This sum peak, 2.50 MeV is easily seen in figure 2.7. Later we will analyze the probability of this peak compared to γ_1 and γ_2.

EXPERIMENT 2.3

Gamma Analysis of the .835 MeV Spectrum of ^{54}Mn

Experimental Procedure

1. Use the same electronics and energy calibration as for experiments 2.1 and 2.2.

2. Place the ^{54}Mn source from the source kit on shelf No. 3.

3. Place the lead absorbers No's. A, B, and C from Kit No. A15, behind the source in order to enhance backscattering and the production of the Pb Kα x-ray. This is approximately one-inch of lead.

4. Accumulate a spectrum for a time long enough to clearly see the backscatter peak and lead Kα x-ray. Figure 2.10 shows a screen dump for ^{54}Mn from a Nucleus Spectrum 88 MCA.

5. Read out the spectrum or use the cursor function to determine the channel numbers for: The Compton edge, the backscatter peak, and the Pb x-ray.

Exercise A Fill in Table 2.4, from the information collected above and the calibration curve. Note: The theoretical value for the Compton edge can be found by substituting 0.835 MeV into eq. (5). The backscatter energy is found by solving eq. (4) for $h\nu = 0.835$ MeV and $\theta = 180°$.

Exercise B *(optional)* Make a table similar to Table 2.4 for the Compton edges and backscatter peaks from ^{60}Co and ^{137}Cs. Collect the necessary data from these sources and fill in the table.

EXPERIMENT 2.4

Energy Resolution of ^{137}Cs

(Time for completion 0.5 hr.)

Discussion

Figure 2.7 shows the decay scheme and pulse height spectrum of ^{60}Co. In the spectrum the 1.17 and 1.33 MeV peaks are clearly resolved. These two peaks are about 13% different in energy and the detector used in this experiment clearly resolves these two gammas. The ability of a NaI(Tℓ) detector to resolve two gammas that are close together in energy is called the resolution of the detector. For a NaI(Tℓ) detector the resolution can easily

Table 2.4 Spectrum Analysis of ^{54}Mn

Event	Channel No.	Energy (Measured) MeV	Energy Theory MeV
1 ^{54}Mn (photopeak)			0.835
2 ^{54}Mn Compton Edge			
3 ^{54}Mn Backscatter			
4 Pb-Kα, x-ray			0.0749

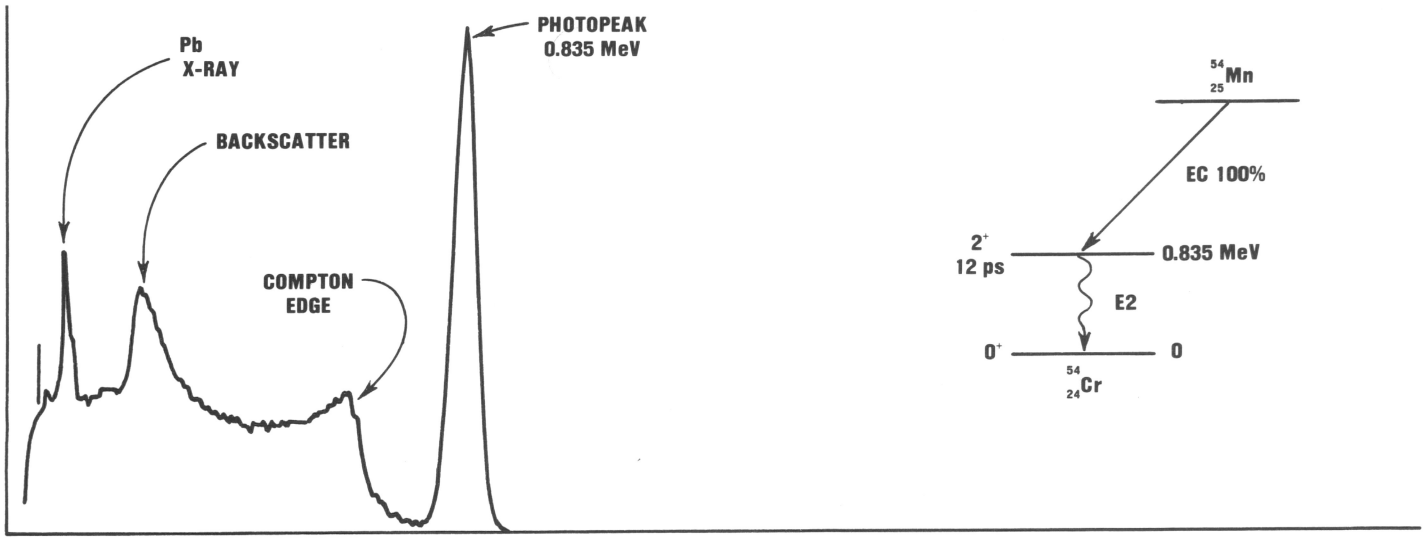

Figure 2.10. Screen dump from a Spectrum 88 MCA for a ^{54}Mn source with lead behind the source to enhance backscattering and the lead Kα x-ray (shelf No. 3 of the P-2000/2 Scintillation Probe).

be obtained from the pulse height spectrum by solving the following equation:

$$R = \frac{\Delta C}{C_o} \times 100\% \qquad (7)$$

where

R = the resolution in percent

ΔC = the number of channels in the full width at half maximum of the photopeak (FWHM). This is the measured spread of the peak at one half the maximum peak height

C_o = the channel number of the centroid of the photopeak.

Figure 2.11 shows an expanded spectrum of the ^{137}Cs photopeak. The numbers used to calculate the resolution are shown in the insert. In this experiment we will calculate the resolution of the ^{137}Cs photopeak from the gamma source set.

Experimental Procedure

1. Place the ^{137}Cs source on shelf three and accumulate a spectrum for a time period long enough to obtain about 5000 counts in the maximum photopeak channel.

2. Readout the spectrum or use the cursor function of the MCA to obtain C_o and ΔC.

Exercise A Use eq. (7) to calculate the resolution for the detector.

Exercise B *(optional)* Repeat the above experiment for the 0.835 photopeak of ^{54}Mn. (See figure 2.10)

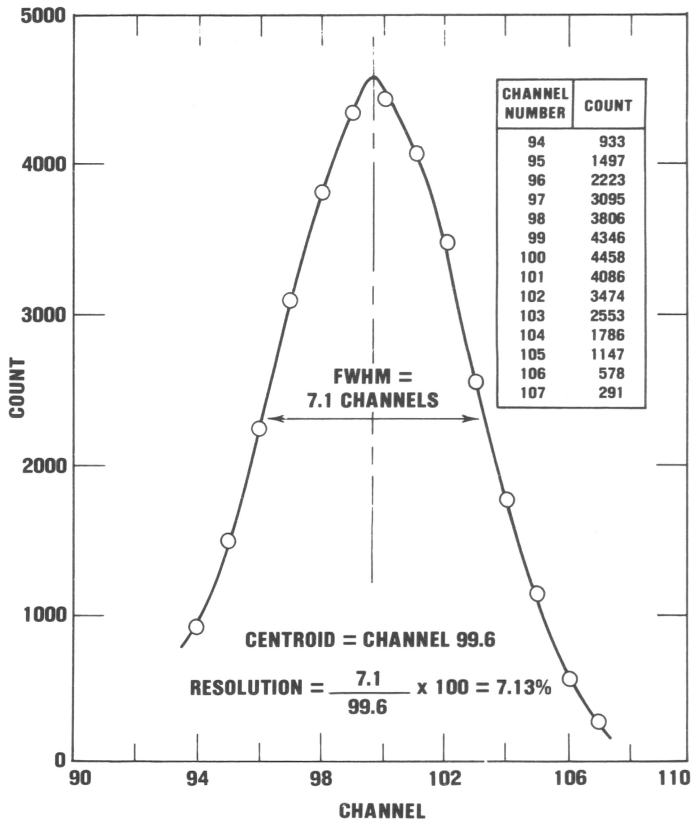

Figure 2.11. Expanded Spectrum of the 0.662 MeV Photopeak from ^{137}Cs showing the FWHM of the peak and the resolution of the NaI(Tℓ) detector.

EXPERIMENT 2.5

Determining the Activity of a Gamma Source (Relative Method)

(Time for completion 0.5 hr.)

Discussion

Figure 2.12 shows a plot of the absolute peak efficiency (ε_1) of the P-2000/2 NaI(Tℓ) detector for different gamma energies from the 3rd shelf. The absolute peak efficiency ε_1 is the ratio of counts under the photopeak to the total number of gammas that leave the source. For a given gamma energy, the efficiency is a constant. The ratio of two source activities is, therefore, determined easily by taking the ratio of the sums under their respective photopeaks. The activity of an unknown (A_x) is, therefore, given by:

$$A_x = \frac{R_x}{R_s} A_s \qquad (8)$$

where

R_x = counts/sec under the photopeak of the unknown source.

R_s = counts/sec under the photopeak of the known activity source

A_s = the known activity of the standard source

Experimental Procedure

1. The electronics and calibration are the same that have been used for experiments 2.1 through 2.5.

2. Obtain a calibrated ^{137}Cs source from the instructor and use the half life (30.174 yr.) to calculate its activity today. (A_s)

3. Count this ^{137}Cs calibrated source (shelf 3) for a period of time long enough to obtain approximately 7000 counts under the photopeak. Calculate the counts/second under the photopeak.

4. Place the unknown activity ^{137}Cs source on shelf 3 and count it for a time period long enough to obtain approximately 7000 counts under the photopeak. Calculate the counts/second under the photopeak.

5. Remove all sources and obtain a background count for 200 seconds. Calculate the background counting rate under the same channels that were used in summing the ^{137}Cs photopeaks. Define this quantity to be R_b.

Exercise A Subtract the background counting rate from the ^{137}Cs photopeaks for both the standard and unknown sources. Therefore:

R_x = Counting rate under the unknown ^{137}Cs photopeak minus R_b.

R_s = Counting rate under the standard ^{137}Cs photopeak minus R_b.

From the data above, and eq. (8), calculate A_x the activity of the unknown.

Exercise B *(optional)* The instructor will supply you with two ^{54}Mn sources, a known and an unknown activity. Use the above procedure to determine the unknown ^{54}Mn activity.

Note to the Student: The above relative method of determining the unknown activity of a source is the best *and* most widely used source strength calibration procedure. There is really very little room for error. Standard calibrated sources can be purchased with virtually any accuracy that is desired. The United States National Bureau of Standards has taken a leading role in providing, at a reasonable price, accurately known calibration standards for radioisotope measurements.

EXPERIMENT 2.6

Determining the Activity of a Gamma Emitter by the Absolute Method

(Time for completion 1.0 hr.)

Discussion

The same data taken in experiment 2.5 can be used to determine the unknown source activity by the absolute method. The activity of an unknown source can be written:

$$A = \frac{R_x}{\varepsilon_1 f_g} \qquad (9)$$

where

ε_1 = the value read from figure 2.12 for the gamma in question (remember this is for shelf 3 of the P-2000/2 NaI(Tℓ) detector).

f_g = the gamma decay fraction of the unknown activity. This is the fraction of decays in which the gamma of interest is being emitted. (See Table 2.3 for some of the most common isotopes, also reference 1).

Experimental Procedure

1. You may use all the data collected in experiment 2.5 for this experiment.

Exercise A Use eq. (9) to calculate the activity of the unknown and standard sources and compare your values to the answers obtained in experiment 2.5. Figure 2.13 shows an integrated screen dump for a 1μCi ^{137}Cs source. The region of interest has been set to bracket the photopeak. The sample calculation shown on this figure indicates an 8.8% error which is well within the accuracy of the standard source activity from the source set.

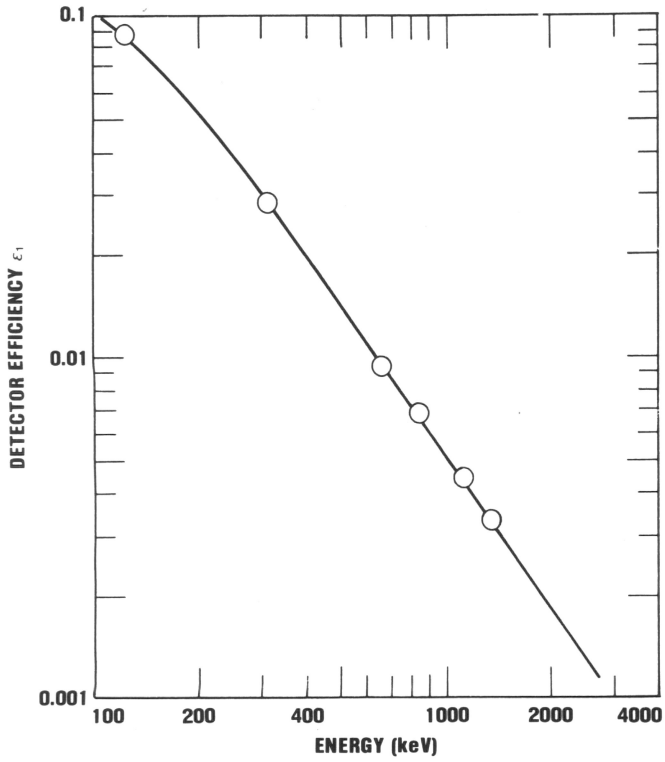

Figure 2.12. The absolute peak efficiency (ε_1) of the P-2000/2 NaI(Tℓ) detector as a function of gamma energy (shelf No. 3).

Exercise B *optional for NaI(Tℓ) crystals of different size.* Figure 2.14 shows the intrinsic peak efficiency ε_a for six different crystal sizes. The plotted values for ε_a are for a source to crystal distance of 9.3 cm. If your laboratory has a NaI(Tℓ) detector that is included in this figure, you can determine the source activity of an unknown source by using eq. (10):

$$A = \frac{R_x}{\varepsilon_a G f_g} \qquad (10)$$

where

$$G = \frac{\text{Face area of the detector}}{4\,\pi\,S^2} \quad (cm^2)$$

$s = 9.3$ cm

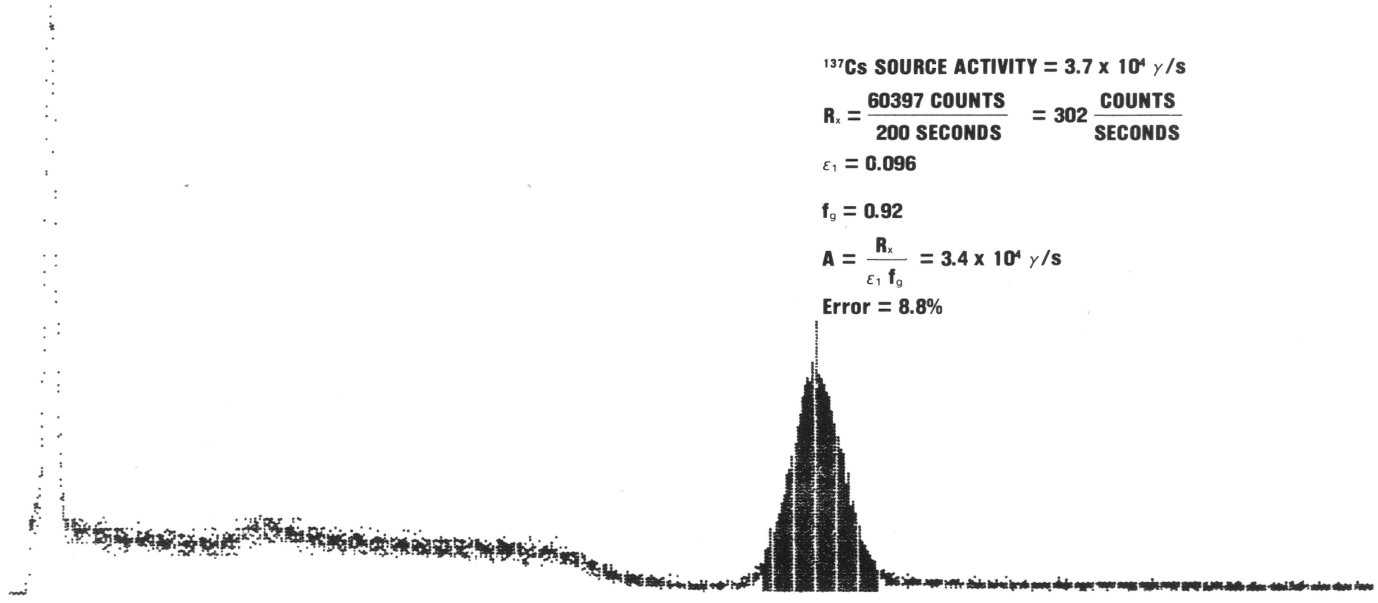
^{137}Cs SOURCE ACTIVITY = 3.7 x 10^4 γ/s
$R_x = \frac{60397 \text{ COUNTS}}{200 \text{ SECONDS}} = 302 \frac{\text{COUNTS}}{\text{SECONDS}}$
$\varepsilon_1 = 0.096$
$f_g = 0.92$
$A = \frac{R_x}{\varepsilon_1 f_g} = 3.4 \times 10^4\ \gamma/s$
Error = 8.8%

Figure 2.13. ^{137}Cs pulse height spectrum for the absolute efficiency measurement, shelf three of the P-2000/2 NaI(Tℓ) detector, 200 seconds, showing the Region of Interest (ROI). Measured on a (Nucleus) Spectrum 88 MCA.

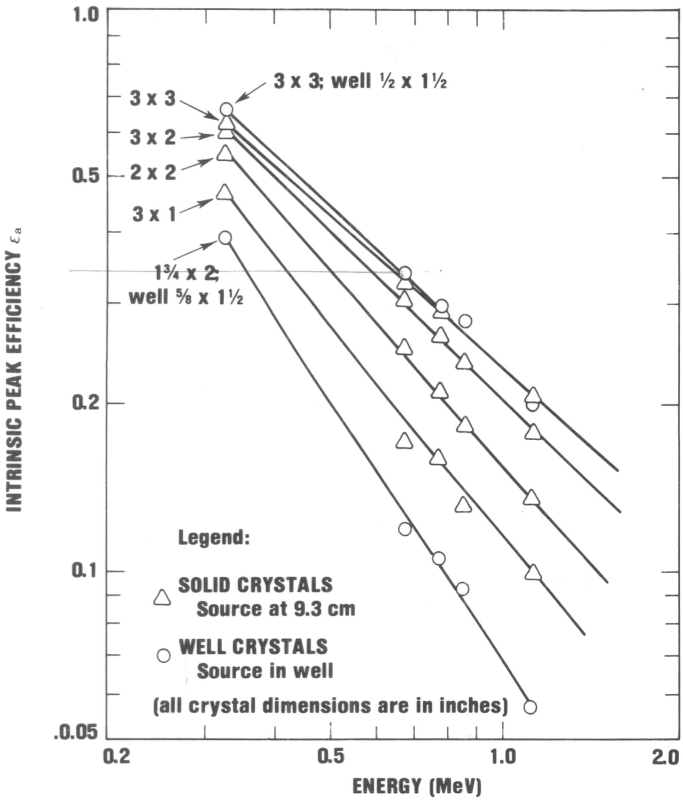

Figure 2.14. Intrinsic peak efficiency (ε_a) for a wide variety of NaI(Tℓ) crystals. The source to detector distance is 9.3 cm (Courtesy of Idaho Operations Office DOE).

Of course the relative method of determining an unknown source activity can also be used for the detectors in figure 2.14. The procedure is the same as for experiment 2.5.

EXPERIMENT 2.7

Analysis of the Sum Peak in NaI(Tℓ) Spectroscopy

(Time for completion 0.5 hr.)

Discussion

Figure 2.7 shows a pulse height spectrum of the two gammas from ^{60}Co and their sum peak at 2.50 MeV. In our above discussion of sum peak analysis, it was indicated that there was a finite probability of γ_1 and γ_2 entering the detector simultaneously. The word simultaneously as used here means that γ_1 and γ_2 interact in the detector within a time period Δt which is shorter than the resolving time of the system (1 microsecond). When this occurs, the light pulse out of the detector will be γ_1 plus γ_2. In figure 2.7 the integrated sum under γ_1 (the 1.17 MeV photopeak) is given by:

$$\Sigma_1 = \varepsilon_1 f_g A t \qquad (11)$$

where

A = the activity of the ^{60}Co source in counts/sec

f_g = 1 for ^{60}Co (see Table 2.3)

ε_1 = the efficiency from figure 2.12 for γ_1

likewise the theoretical sum under γ_2 can be written:

$$\Sigma_2 = \varepsilon_2 A t \qquad (12)$$

since f_g is also equal to unity

The number of counts under the sum peak can be determined by combining eq's. (11 and 12):

$$\Sigma_s = \varepsilon_1 \varepsilon_2 A t \{W(0°)\} \qquad (13)$$

where $\{W(0°)\} \cong 1$ for ^{60}Co.

Experimental Procedure

1. Use the same energy calibration as in the previous experiment.

2. Place the standardized ^{60}Co source at a distance from the detector that is compatible with the efficiency curve that is being used. (See figure 2.12 for the P-2000/2 detector)

3. Accumulate a spectrum for a period of time long enough to obtain 2000 counts in the sum peak. (See figure 2.7). Calculate $\left(\frac{\Sigma_s}{t}\right)$

Exercise A Use eq. (13) and the values of ε_1 and ε_2 from figure 2.12 to calculate $\Sigma_{s/t}$ for your standardized ^{60}Co source. How do your experimental values compare to eq. (13)?

Exercise B The above exercise is for the 1.5"x1" detector in the P-2000/2 assembly. If your detector is one of the sizes shown in figure 2.14 you may take the data with the indicated geometry in the figure. Each efficiency is then given by eq. (10). The $\left(\frac{\Sigma_s}{t}\right)$ is then given by:

$$\left(\frac{\Sigma_s}{t}\right) = \varepsilon_1 \varepsilon_2 G^2 A$$

where ε_1 and ε_2 are the intrinsic peak efficiencies for γ_1 and γ_2 from figure 2.14.

EXPERIMENT 2.8

The Linear Absorption Coefficient of Lead Gammas

(Time for completion 1.0 hr.)

Discussion

Figure 2.6 shows a plot of the cross-sections of the Photoelectric, Compton, and Pair Production processes as a function of gamma energy for a NaI(Tℓ) detector. Shown also on this plot, is the total cross-section for all three processes. Since the gamma sources used in this experiment are lower in energy than 1.5 MeV, we are primarily interested in the Photoelectric and Compton interactions. From figure 2.6 it can be seen that at an energy of 0.260 MeV the Photoelectric and Compton cross-sections are about equal. At this point μ, the linear absorption coefficient, has a value of approximately 0.35 cm^{-1}. In terms of our measured spectrum, this would theoretically mean that the area under the photopeak for a 0.260 MeV gamma source would exactly equal the area under the Compton distribution. Experimentally, we would find that at this energy, the Photopeak sum is larger than the Compton distribution. The reason for this is that even for small NaI(Tℓ) detectors, some of the scattered photons from the Compton interaction will make photoelectric interactions before escaping from the crystal and thus be totally absorbed. These pulses would show up under the photopeak. There are many ways that these multiple interactions can give total absorption and hence a better name for the photopeak is the total absorption peak.

A plot of the linear absorption coefficient for lead would be similar in shape to figure 2.6. The major difference would be that the magnitude of the linear absorption coefficient for lead is higher than the values in figure 2.6 since the atomic number of lead is higher. Likewise, the values for aluminum would be lower. In order to study the attenuation of gammas through material, it is necessary to consider Lambert's Law (see reference 3). The decrease in intensity of gammas as they pass through an absorber is given by:

$$I = I_o e^{-\mu x} \qquad (14)$$

I = intensity after the absorber

I_o = initial intensity

μ = total mass absorption coefficient in $\frac{cm^2}{g}$

x = density thickness in g/cm_2 (density thickness is the density of the absorber foil multiplied by its thickness).

Table 2.5 gives the total mass attenuation coefficient in lead for four of the isotopes that are found in source kit S-13.

Experimental Procedure

(Linear Absorption Coefficient for Lead and ^{137}Cs Gammas)

1. The same gains and calibration curve that have been used in the previous experiments will be employed for this experiment.

Table 2.5 Mass Absorption Coefficient for ^{60}Co, ^{54}Mn, ^{137}Cs, and ^{57}Co in Lead Absorbers

Isotope	Energy (MeV)	μ (Lead) $\frac{cm^2}{g}$
^{60}Co	1.17, 1.33 (average 1.25)	0.063
^{54}Mn	0.835	0.083
^{137}Cs	0.662	0.105
^{57}Co	0.122	3.10

2. Place the 1μCi ^{137}Cs source on shelf No. 5 and the absorber holder card on shelf 4. Accumulate a spectrum for 100 seconds. Readout the spectrum or use the cursor and ROI functions of the MCA to determine the sum of the total photopeak. Clear the MCA.

3. Place the first lead absorber (900×10^{-3} g/cm^2) on the absorber card shelf 5 and accumulate a spectrum for 100 seconds. Sum the total spectrum as in step **2**.

4. Repeat step **3** for the rest of the lead absorbers and combinations of same to give a total thickness of at least 13 g/cm^2. This will give a total of about 8 data points.

Exercise A Make a plot on one cycle semilog graph paper of the sum collected versus absorber thickness. From this straight line, determine the half value layer (HVL). The HVL is defined to be the thickness of lead that will decrease the gamma sum to one-half of its value with no absorber. From eq. (14) for the (HVL), $I/I_o = 0.5$. We can, therefore, determine μ from the following equation:

$$\mu = \frac{0.693}{(HVL)} \frac{cm^2}{g} \qquad (15)$$

The accepted value for μ from Table 2.5 for ^{137}Cs is 0.105 cm^2/g. Your measured value should be within 10% of this value.

Exercise B *(optional)* Repeat the linear absorption coefficient measurement for any of the other isotopes listed in Table 2.5 that the instructor may wish you to study.

REFERENCES FOR *EXPERIMENT 2*

1. C. M. Lederer and V. S. Shirley, Eds. *Table of the Isotopes,* 7th Edition, John Wiley and Sons, Inc., New York (1978).

2. R. L. Heath, *Scintillation Spectrometry, Gamma Ray Spectrum Catalogue 1 and 2.* Report No. IDO-16880. Available from National Technical Information Center, U.S. Department of Commerce, Springfield, Virginia.

3. K. Siegbahn, Ed. *Alpha, Beta, and Gamma Spectroscopy*, North Holland Publishing Co., Amsterdam (1968).

4. *W. Mann and S. Garfinkel,* Radioactivity and its Measurement, Van Nostrand-Reinhold Publishing Co. N.Y. (1966).

6. G. F. Knoll, *Radiation Detection and Measurement*, John Wiley and Sons, New York (1979).

5. P. Quittner, *Gamma Ray Spectroscopy,* Halsted Press, New York (1972).

7. *Spectrometry Experiments with Multichannel Analyzers,* Available from The Nucleus, P.O. Box 2561, Oak Ridge, Tennessee 37831

8. G. I. Gleason and Barbara H. Reed, *Gamma Spectra and Nuclide Identification Catalogue.* Available from Oak Ridge Associated Universities, Oak Ridge, Tennessee 37830.

EXPERIMENT 3

Alpha Particle Measurements with Surface Barrier Detectors

Discussion

This experiment is designed to show the student how to use surface barrier detectors to study the properties of alpha emitting isotopes. In Experiment #4 which follows this experiment, the energy loss of alphas in thin foils will be studied. The electronic configuration for the two experiments is the same.

Silicon Surface Barrier Charged Particle Detectors

The first thing that the student will realize is that these detectors are extremely easy to use. Tennelec makes detectors that range in size from 25 mm^2 to 2000 mm^2 active area. These detectors are 100% efficient over their active area and can be used to measure a wide range of charged particles. This range includes protons and electrons as low as 20 keV up to fission fragments of energy over 100 MeV. Figure 3.1 shows a pulse height spectrum of scattered protons at 150 keV. On the other hand, fig. 3.2 shows a fission fragment spectrum from ^{252}Cf. The light fission fragment group (the one on the right) has an energy of 103 MeV while the heavy group is 70 MeV. The data analysis with these detectors is extremely simple since they are 100% efficient. For example, in fig. 3.1, if one wished to know the number of scattered protons for the data in the figure, it would only be necessary to integrate under the peak and subtract the estimated background from the sum. These detectors can be thought of as a solid state ionization detector. When a charged particle enters the depletion region of the detector, it loses its energy primarily by making electron hole pairs in the silicon.

For each electron hole pair that is made, the initial charged particle must lose 3.6 eV. In this experiment we will be measuring alpha particles that have an energy of 5.486 MeV. When these alphas enter the detector, 1.52 x 10^6 electron-hole pairs will be produced. The detector is reverse biased and these electron-hole pairs are collected to produce the output pulse of the detector. Since there are a large number of charge carriers produced, the statistical variation in the number collected is small and hence very good resolution is possible. Tennelec can provide detectors with resolutions as low as 12 keV for alphas for the PP series premium partially depleted detectors. The detector recommended for this experiment is a PD series Partially Depleted Detector with 15 keV resolution. This detector is cheaper and is quite adequate for the experiment.

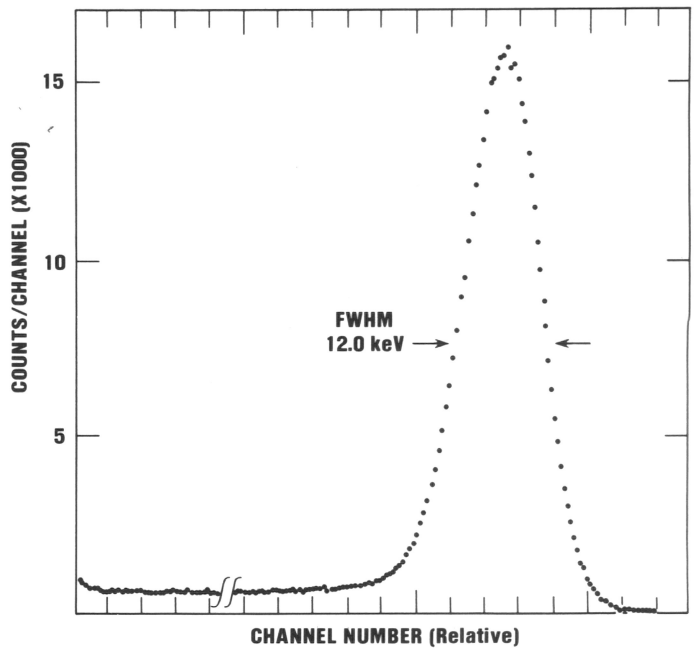

Figure 3.1. Silicon Surface Barrier Detector pulse height spectrum of 150 keV scattered protons from the ^{12}C (p,p) ^{12}C reaction at 30°.

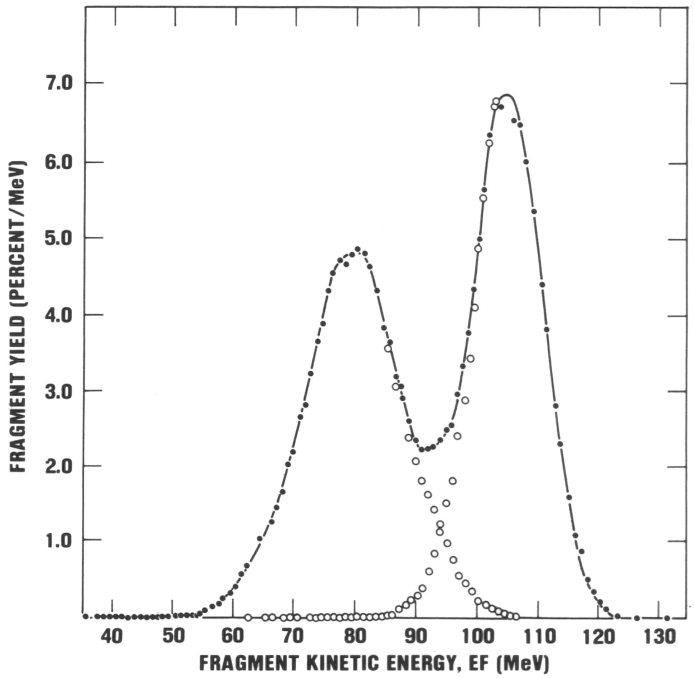

Figure 3.2. Surface Barrier Detector Fission Fragment Spectra from ^{252}Cf (courtesy of Stan Whetstone and the Physical Review Reference 1).

The final parameter necessary to evaluate in selecting a detector is the depletion depth of the detector. In the next experiment, we will study the energy loss and range of charged particles in matter. Alpha particles from radioactive sources have a range of energies from 1.83 MeV for $^{144}N_d$ to 11.65 MeV for ^{212m}Po. Most of the alpha sources that are convenient to use for this experiment have energies around 5.0 MeV. Figure 3.3 shows the theoretical range of five different charged particles in Silicon. From the figure, it can be seen that the 5 MeV alphas that we use for this experiment have a range of approximately 20 microns (μ). These alphas can easily be stopped in any of the partially depleted detectors that Tennelec manufactures since the minimum depletion region of all of these detectors is at least 100 μ. The detector recommended for this experiment is Tennelec model PD-050-100-014-CM. Figure 3.4 explains the significance of this number.

In summary, the detectors are small, easy to use, relatively inexpensive, have excellent resolution, and can be used to measure virtually any charged particle.

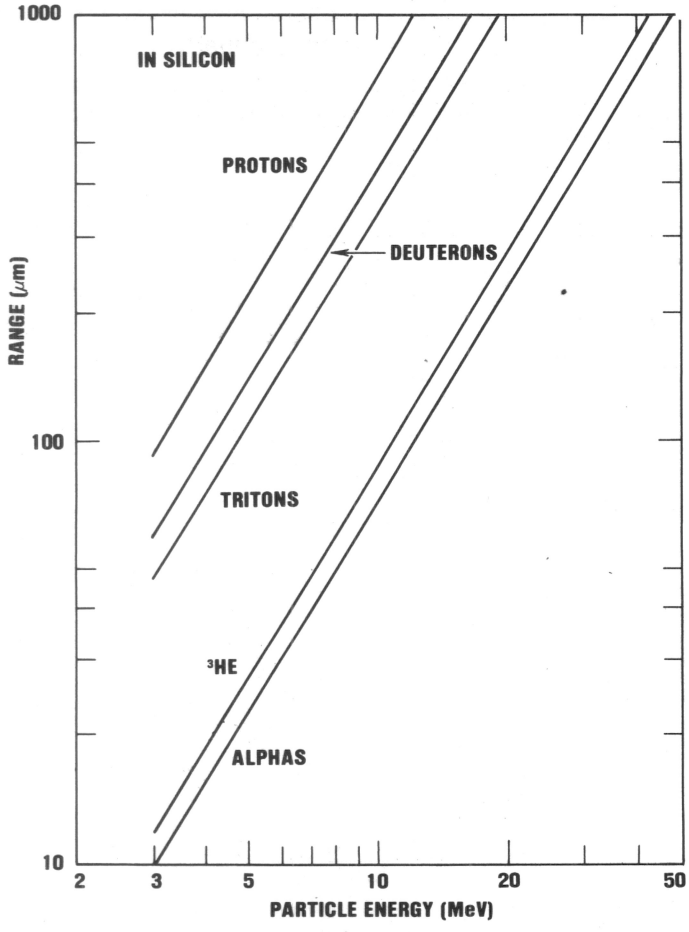

Figure 3.3. Calculations of range vs energy curves for different charged particles in Silicon (from D. J. Skyrme, Ref 2).

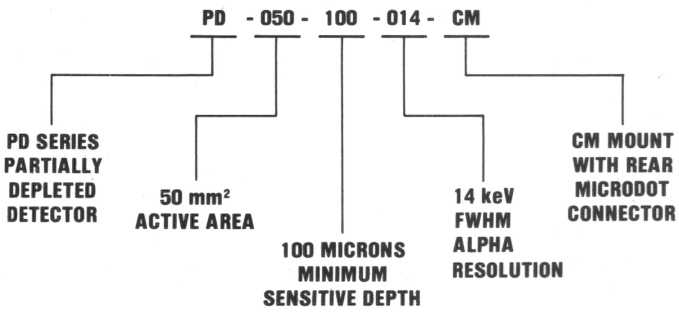
PD - 050 - 100 - 014 - CM
PD SERIES PARTIALLY DEPLETED DETECTOR
50 mm² ACTIVE AREA
100 MICRONS MINIMUM SENSITIVE DEPTH
14 keV FWHM ALPHA RESOLUTION
CM MOUNT WITH REAR MICRODOT CONNECTOR

Figure 3.4. Explanation of the nomenclature used to define the model numbers of Tennelec Surface Barrier Detectors.

Health Physics Considerations for Alpha Sources

The alpha sources that are used for this experiment have been either electrodeposited or evaporated onto a metal disk. If you look very carefully, the deposited spot, which is usually about 1 mm in diameter, can be seen in the center of the disk. The spot should never be touched with the fingers because some of the evaporated material might break loose and contaminate your hand and/or the work area. Always handle these sources by holding the edge of the disk. In the case of the ^{210}Po source, the radioactive material is evaporated onto a silver disk. The disk is then completely encapsulated with plastic, except for a small hole on the front surface to emit the 5.31 MeV alphas from the source.

EXPERIMENT 3.1

Energy Calibration with a Pulser for Alpha Spectroscopy

Scope

The electronics shown in fig. 3.5 will be calibrated. An energy versus pulse height curve will be be constructed with the aid of the Pulse generator. The resolution of the system will be determined for alphas from ^{210}Po.

Experimental Procedure

1. Set up the equipment as shown in fig. 3.5. Place the ^{210}Po source in the vacuum chamber approximately 1 cm from the face of the detector. Evacuate the chamber for about 2 minutes. If there are no leaks, the fore pump will run very quietly after this period of time.

2. Set the Bias Supply to positive and adjust its value to the recommended value for the Silicon Surface Barrier Detector, correcting for the voltage drop on the series

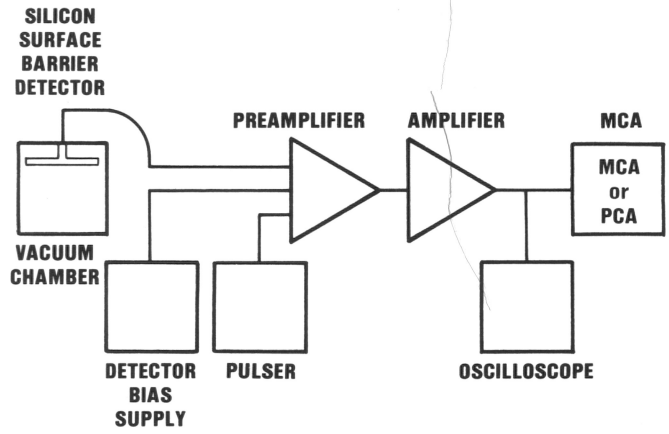

Figure 3.5. Alpha Spectroscopy System with Multichannel Analyzer (MCA).

resistor of the preamplifier as a result of detector leakage current.

Note, whenever you pump down or let the chamber up to air, it is imperative that the Bias supply be turned off. It can be turned on only when the system is under vacuum or at atmospheric pressure. If these procedures are not followed, the detector and the preamp could be damaged.

3. Set the input polarity of the amplifier to positive. The baseline restorer should be set to AUTO. The output from the amplifier to the MCA should be unipolar. Use 1000 channels for the MCA.

4. Adjust the coarse and fine gain of the amplifier so that the output pulses are about 4V in amplitude. The alphas from ^{210}Po have a discrete energy of 5.31 MeV. The output of the amplifier will be a single isolated pulse height and easy to observe with the scope.

5. Turn on the MCA or PCA and you will see a single peak that comes in around mid scale. Adjust the gain of the amp such that the ^{210}Po alphas fall approximately in channel 800.

6. Accumulate a spectrum for a time period long enough to have 500 counts in the peak channel. This should take only a few minutes. Use the cursor of the MCA to determine the centroid channel of the peak. If your MCA has a centroid finding program, the centroid can easily and accurately be found by using this program. Once this centroid channel is found, it should be labeled C_1.

7. Turn on the relay of the pulse generator. Set its polarity to negative. The (C) output of the pulser should be fed into the preamp. Set the pulse height dial at $^{531}/_{1000}$. The pulse height dial is a ten-turn potentiometer. Each turn corresponds to 100 divisions. Full scale on the dial is therefore 1000 divisions. $^{531}/_{1000}$ is 53% of full scale. Now adjust the attenuation switches and the CAL screwdriver adjustment until the pulser peak falls at exactly C_1 in the MCA. You have now calibrated the pulser pulse height dial so that $^{531}/_{1000}$ divisions is equal to 5.31 MeV or 5310 keV. Each division is then 10 keV. It is now quite easy to generate a 4 MeV pulse by setting the pulse height dial at $^{400}/_{1000}$, etc.

8. Erase the MCA and set the pulse height dial on the pulser at $^{100}/_{1000}$ (1 MeV) and accumulate for a period of time (about 1.5 minutes) long enough to determine the centroid of the peak. Repeat for the other pulse height settings in Table 3.1. Fill in the rest of Table 3.1.

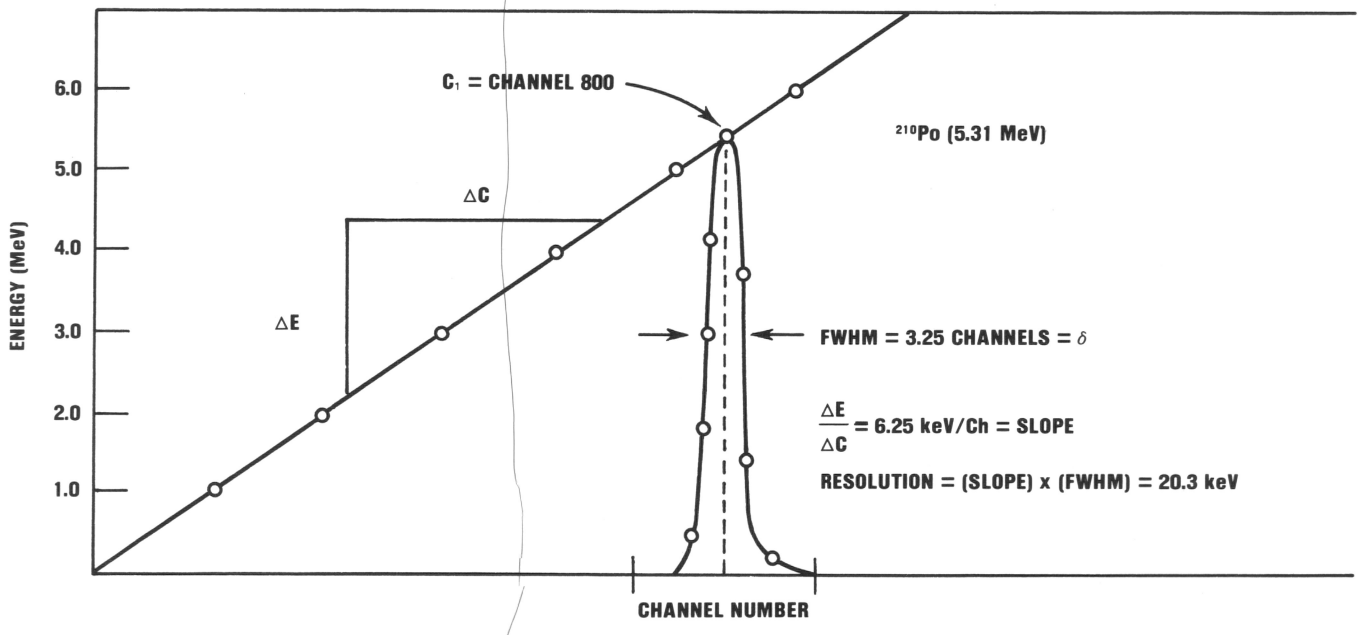

Figure 3.6. Calibration curve for the Pulse Generator showing a ^{210}Po spectra and the Resolution of the detector.

Table 3.1 Pulser Calibration Data

Pulse Height Dial Setting	Energy	Channel Number (Centroid)
$^{100}/_{1000}$	1.0	
$^{200}/_{1000}$	2.0	
$^{300}/_{1000}$	3.0	
$^{400}/_{1000}$	4.0	
$^{500}/_{1000}$	5.0	
$^{600}/_{1000}$	6.0	

Exercise A From the data in Table 3.1, make a plot of energy versus channel number. Figure 3.6 shows a typical calibration curve for this experiment.

Exercise B From the calibration curve that was plotted from Table 3.1, determine the slope in $^{keV}/_{channel}$. CALCULATE the resolution of the system by multiplying the slope of the calibration curve by the Full Width at Half Maximum (FWHM) of the ^{210}Po peak. Note the FWHM is the spread δ of the peak at half maximum. It takes N + 1 channels to give a spread of N channels.

$$\text{Resolution} = \frac{\Delta E}{\Delta C} \times \delta \text{ (channels spread at FWHM)} \quad (1)$$

It should be noted that some of the programs in the more advanced MCA's and PCA's will give you δ directly if you use the cursors to identify the peak. These advanced features make it possible to determine the resolution quite accurately.

EXPERIMENT 3.2

Using the Calibration Curve to Determine the Energy of the Unknown Alpha Source

Scope

The calibration obtained in Experiment 3.1 will be used to accurately determine the alpha energies of one or more unknown sources.

Experimental Procedure

1. Turn off the Bias voltage and slowly leak the vacuum chamber up to atmospheric pressure. This should take about 1 minute. Replace the ^{210}Po source with the unknown source that is supplied by the instructor. Pump the system back down and then turn on the Bias supply to its recommended value.

2. Accumulate a spectrum in the MCA until reasonable statistics are acquired in all of the peaks of interest for the unknown.

3. Use the cursor of the MCA or one of the programs stored in the MCA to find the centroid and the number of channels across the FWHM for the unknown source.

4. Repeat steps 1-3 for the other unknowns that the instructor may wish to have analyzed.

Exercise A Determine the energy or energies of the alpha peaks in your unknown spectrum from the calibration curve. Figure 3.7 and 3.8 shows pulse height spectrum of ^{241}Am and ^{238}Pu. These might well have been the unknowns given to you by the instructor. Table 3.2 shows some of the more common alpha emitting radioisotopes, their half lives and abundances of the more pronounced groups. Please note that if these had been the unknowns two of the groups from ^{241}Am ($E\alpha$ = 5.443 and 5.486 MeV) two groups from ^{238}Pu ($E\alpha$ = 5.456 and 5.499 MeV) are listed in Table 3.2. With the profound resolution capabilities of these solid state detectors, the alpha energies of unknown sources can easily be determined as shown in the above example.

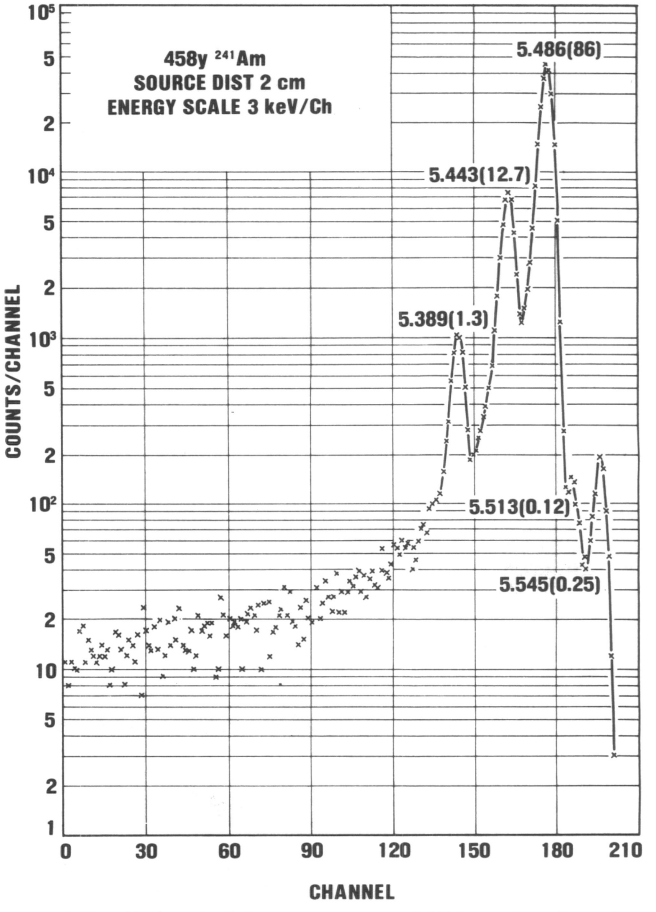

Figure 3.7. Pulse height spectrum of ^{241}Am showing the major peaks. The overall resolution for this spectrum is 15 keV (taken from Reference 3).

Table 3.2 Selected Alpha Sources with Half Lives Greater Than 100 Days

Energy (MeV)	Nuclide	Half-Life	Abundance* (%)	Energy (MeV)	Nuclide	Half-Life	Abundance* (%)
11.65	^{212m}Po	45s	97	5.490	^{222}Rn	3.823d	100
8.88	^{211m}Po	25s	7	5.486	^{241}Am	458y	86
8.785	^{212}Po	0.30μs	100	5.456	^{218}Pu	86y	28
8.377	^{213}Po	4.2μs	100	5.448	^{214}Bi	19.7m	0.012
7.687	^{214}Po	164μs	100	5.447	^{224}Ra	3.64d	6
7.448	^{211}Po	0.52s	99	5.443	^{241}Am	458y	13
7.384	^{215}Po	1.78ms	100	5.427	^{228}Th	1.910y	71
7.28	^{211m}Po	25s	91	5.386	^{246}Cm	5.5x10^{3}y	81
7.200	^{254}Fm	3.24h	85	5.362	^{245}Cm	9.3x10^{3}y	80
7.158	^{254}Fm	3.24h	14	5.344	^{228}Th	1.910y	28
7.14	^{218}Rn	35ms	100	5.342	^{246}Cm	5.5x10^{3}y	19
7.07	^{217}At	32ms	100	5.324	^{232}U	72y	68
7.027	^{255}Fm	20.1h	93	5.306	^{245}Cm	9.3x10^{3}y	7
6.818	^{219}Rn	40s	81	5.305	^{210}Po	138.4d	100
6.777	^{216}Po	0.15s	100	5.276	^{243}Am	7.95x10^{3}y	88
6.70	^{218}At	2s	94	5.267	^{232}U	72y	32
6.65	^{218}At	2s	6	5.234	^{243}Am	7.95x10^{3}y	11
6.640	^{253}Es	20.47d	90	5.168	^{240}Pu	6580y	76
6.622	^{211}Bi	2.15m	84	5.156	^{239}Pu	24,400y	73
6.56	^{222}Ra	38s	96	5.143	^{239}Pu	24,400y	15
6.551	^{219}Rn	4.0s	11	5.123	^{240}Pu	6580y	24
6.437	^{254}Es	276d	93	5.105	^{239}Pu	24,400y	12
6.424	^{219}Rn	4.0s	8	5.058	^{231}Pa	3.25x10^{4}y	11
6.340	^{221}Fr	4.8m	82	5.054	^{229}Th	7340y	7
6.34	^{226}Th	30.9m	79	5.028	^{231}Pa	3.25x10^{4}y	23
6.287	^{220}Rn	55s	100	5.013	^{231}Pa	3.25x10^{4}y	24
6.28	^{219}At	0.9m	97	4.967	^{229}Th	7340y	6
6.278	^{211}Bi	2.15m	16	4.96	^{210m}Bi	3x10^{4}y	58
6.22	^{226}Th	30.9m	19	4.951	^{231}Pa	3.25x10^{4}y	22
6.126	^{221}Fr	4.8m	15	4.95	^{227}Ac	21.6y	1.2
6.119	^{252}Cf	2.65y	84	4.92	^{210m}Bi	3x10^{6}y	36
6.115	^{242}Cm	163d	74	4.903	^{242}Pu	3.79x10^{5}y	76
6.090	^{212}Bi	60.6m	10	4.899	^{229}Th	7340y	11
6.076	^{252}Cf	2.65y	15	4.863	^{242}Pu	3.79x10^{5}y	24
6.071	^{242}Cm	163d	26	4.842	^{229}Th	7340y	58
6.061	^{243}Cm	32y	6	4.821	^{233}U	1.62x10^{5}y	83
6.051	^{212}Bi	60.6m	25	4.811	^{229}Th	7340y	11
6.037	^{227}Th	18.2d	24	4.787	^{237}Np	2.14x10^{6}y	51
6.031	^{250}Cf	13y	83	4.782	^{226}Ra	1602y	95
6.002	^{218}Po	3.05m	100	4.778	^{233}U	1.62x10^{5}y	15
5.994	^{243}Cm	32y	6	4.773	^{234}U	2.47x10^{5}y	72
5.987	^{250}Cf	13y	17	4.770	^{237}Np	2.14x10^{6}y	19
5.976	^{227}Th	18.2d	23	4.765	^{237}Np	2.14x10^{6}y	17
5.887	^{230}U	20.8d	68	4.733	^{231}Pa	3.25x10^{4}y	11
5.87	^{213}Bi	47m	2	4.722	^{234}U	2.47x10^{5}y	28
5.868	^{211}At	7.21h	41	4.684	^{230}Th	8.0x10^{4}y	76
5.846	^{251}Cf	800y	45	4.617	^{230}Th	8.0x10^{4}y	24
5.83	^{225}Ac	10.0d	54	4.599	^{226}Ra	1602y	6
5.816	^{230}U	20.8d	32	4.597	^{235}U	7.1x10^{8}y	5
5.812	^{249}Cf	360y	84	4.57	^{210m}Bi	3x10^{6}y	6
5.806	^{244}Cm	17.6y	77	4.556	^{235}U	7.1x10^{8}y	4
5.79	^{225}Ac	10.0d	28	4.493	^{236}U	2.39x10^{7}y	74
5.786	^{243}Cm	32y	73	4.44	^{236}U	2.39x10^{7}y	26
5.763	^{244}Cm	17.6y	23	4.415	^{235}U	7.1x10^{8}y	4
5.755	^{227}Th	18.2d	20	4.396	^{235}U	7.1x10^{8}y	57
5.745	^{223}Ra	11.43d	9	4.366	^{235}U	7.1x10^{8}y	18
5.742	^{243}Cm	32y	12	4.200	^{238}U	4.51x10^{9}y	77
5.73	^{225}Ac	10.0d	10	4.15	^{238}U	4.51x10^{9}y	23
5.714	^{223}Ra	11.43d	54	4.011	^{232}Th	1.41x10^{10}y	77
5.707	^{227}Th	18.2d	8	3.95	^{232}Th	1.41x10^{10}y	23
5.684	^{224}Ra	3.64d	94	3.18	^{190}Pt	6x10^{11}y	100
5.68	^{247}Bk	1.4x10^{3}y	37	3.18	^{148}Gd	84y	100
5.666	^{251}Cf	800y	55	2.73	^{150}Gd	2.1x10^{6}y	100
5.605	^{223}Ra	11.43d	26	2.50	^{174}Hf	2x10^{15}y	100
5.537	^{223}Ra	11.43d	9	2.46	^{146}Sm	7x10^{7}y	100
5.52	^{247}Bk	1.4x10^{3}y	58	2.23	^{147}Sm	1.05x10^{11}y	100
5.512	^{214}Bi	19.7m	0.008	2.14	^{152}Gd	1.1x10^{14}y	100
5.499	^{238}Pu	86y	72	1.83	^{144}Nd	2.4x10^{15}y	100

* Percentage of the total decay events.

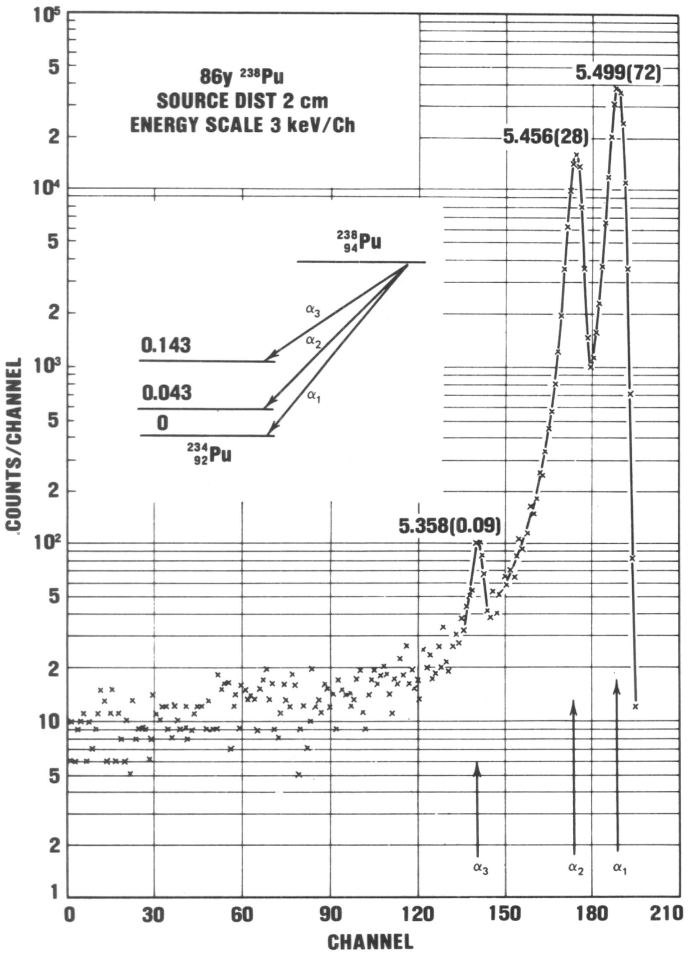

Figure 3.8. Pulse height spectrum of ^{238}Pu showing the three alpha groups present in the decay scheme (taken from Reference 3).

EXPERIMENT 3.3

Determination of the Activity of an Unknown Alpha Source by the Relative Method

Scope

The instructor will provide the student with a calibrated ^{241}Am source and one or more uncalibrated sources. The student will determine the activity of the unknown sources by comparing them directly with the standard.

Experimental Procedure

1. Obtain the standard ^{241}Am source from the instructor. Place the source 1 cm from the detector, pump down, and then return the bias to its recommended value.

2. Accumulate a spectrum for a period of time long enough to have at least 4000 counts under the combined 5.486, 5.443, and 5.389 MeV peaks. See fig. 3.7. Note with the gain settings that have been set for this experiment and the detector being used, these peaks will all be fairly close together and hence easy to integrate. The background will be insignificant or very low. Record the analysis time and subtract the estimated background.

3. Remove the ^{241}Am source and replace it with the first unknown. The source to detector distance should again be 1 cm. Accumulate for a period of time long enough to obtain about 4000 counts under the peaks of interest. Sum the peaks and subtract the estimated background.

4. Repeat for the other unknown alpha activity sources that the instructor provides.

Exercise It was pointed out at the beginning of this series of experiments that solid state detectors were 100% efficient for alpha detection. This fact allows us to compare a standard and unknown directly with each other. It does not matter that the sources have different alpha energies. Remember in Experiment #2, the situation was quite different for γ's where the efficiency of the detector was a strong function of the energy of the gamma source.

The analysis of the alpha data is therefore quite simple. The activity of the unknown source can be found as follows:

$$A_1 = \text{The activity of the unknown } \left(\frac{\text{disintegrations}}{\text{sec}}\right)$$

$$A_0 = \text{The activity of the standard } \left(\frac{\text{disintegrations}}{\text{sec}}\right)$$

$$\left(\frac{\Sigma-\beta}{t}\right)_{uk} = \text{The sum for the unknown minus background divided by the analyzer live time.}$$

$$\left(\frac{\Sigma-\beta}{t}\right)_{STD} = \text{The sum for the standard minus background divided by its analyzer live time.}$$

$$\therefore A_1 = A_0 \frac{\frac{(\Sigma-\beta)_{uk}}{t}}{\frac{(\Sigma-\beta)}{t}_{STD}} \text{(counts sec)}$$

Note: The instructor will probably give you the activity of the standard at the time it was purchased. You will have to correct it for today's activity in disintegrations/sec.

EXPERIMENT 3.4

The Absolute Method of Determining an Unknown Alpha Activity

Scope

The student will determine the activity of an unknown alpha source by carefully measuring the geometry of the system and calculating the activity directly from these parameters.

Experimental Procedure

1. Obtain the ^{210}Po source from the instructor that has an unknown activity. Place the source in the chamber exactly 4 cm from the face of the detector. From the data sheet provided for the detector, find its active area. Pump the system down and then adjust the bias to its proper operating value.

2. Accumulate a spectrum for a time period long enough to obtain 3000 counts under the alpha peak. Sum the peak and subtract the estimated background. Record the live time for the measurement.

3. Repeat this experiment for other unknown alpha isotopes that the instructor may wish to provide.

Exercise Determine the activity of the source from the following:

$$G_1 = \frac{\text{Area of the detector (cm}^2\text{)}}{4\ \Pi\ R_1^2} \qquad (2)$$

$$R_1 = 4 \text{ cm}$$

$$A_1 = \left(\frac{\Sigma - \beta}{t}\right)_{uk} \frac{1}{G_1} \qquad (3)$$

EXPERIMENT 3.5

A Study of the Decay Scheme of $^{230}_{90}$Th by Alpha Emission Spectroscopy

Scope

The student will measure the ratio of alpha decay to ground, first and second excited states of $^{226}_{88}$Ra from $^{230}_{90}$Th. From this data the energies of the first and second excited states will be determined and their decay ratios relative to the ground state will be established.

Discussion

Figure 3.9 shows the measured alpha spectra from a

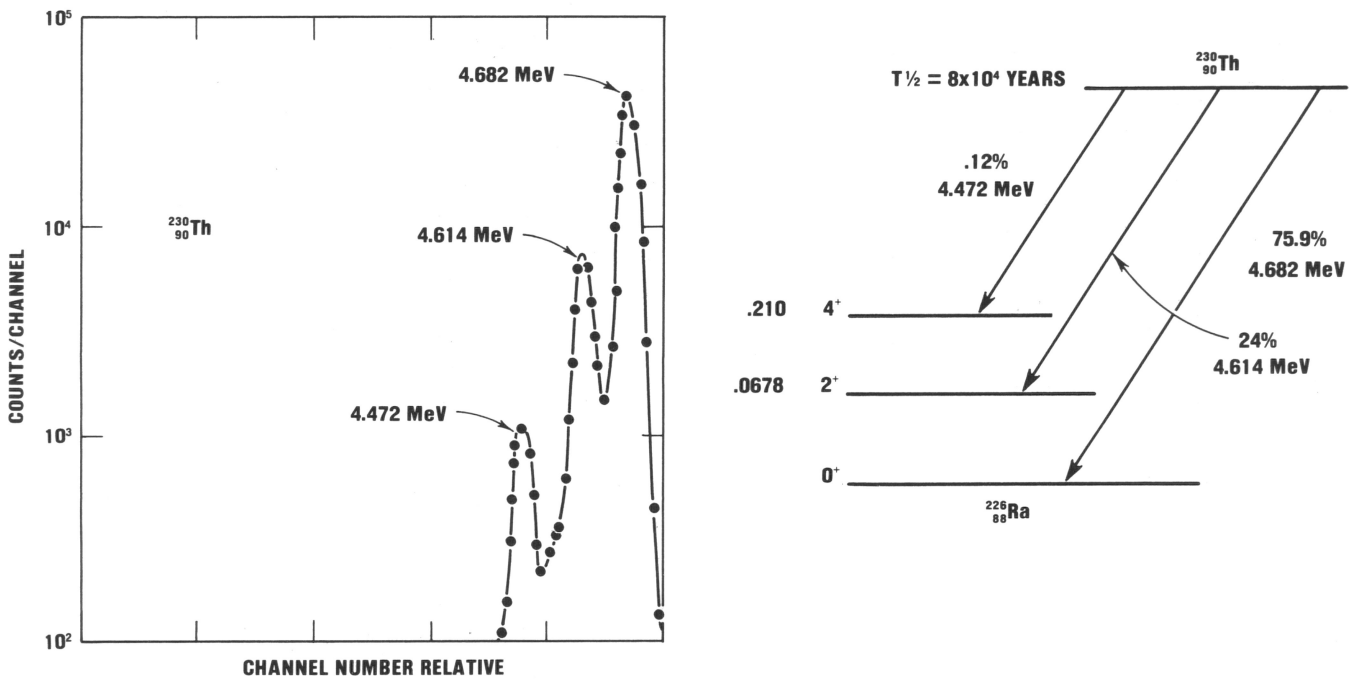

Figure 3.9. Pulse height spectrum and decay scheme for $^{230}_{90}$Th.

$^{230}_{90}$Th alpha source. The corresponding decay scheme for $^{230}_{90}$Th to $^{226}_{88}$Ra is also shown in the figure. From the decay scheme, it can be seen that most of the decay occurs to the ground state (about 76%). Decay to the $^{+}2$, 0.0678 MeV state occurs 24% of the time with a small (0.12%) fraction decaying to the 4^{+}, 0.210 MeV state. From the measured pulse height spectrum, it is possible to verify that the decay ratios are in the correct proportion and that the alpha energies are correct.

The energy available to the ground state alphas for this decay, can be determined in the following manner:

$$\Delta M = M_{Th\ (230)} - M\alpha - M_{Ra\ (225)} \qquad (4)$$

where

$M_{Th\ (230)}$ = Mass of Th-230

$M\alpha$ = Mass of the α particle

$M_{Ra\ 226}$ = Mass of Ra 226

Energy available to the ground state = Q_0

$$Q_0 = \Delta Mc^2 \qquad (5)$$

The alpha, however, does not get all of the energy because conservation of momentum will give the recoiling ^{226}Ra a small part of the energy. The solution to the kinematic equations will show:

$$E(\alpha_0) = \left(\frac{226}{230}\right) Q_0 \qquad (6)$$

The energy available for decay to the first excited state is Q_1.

$$Q_1 = Q_0 - \varepsilon_1 \qquad (7)$$

Where ε_1 = .0678 MeV, the energy of the first excited state is given by:

$$E\alpha_1 = \left(\frac{226}{230}\right) Q_1 \qquad (8)$$

If the first excited state decayed directly to the ground state by γ emission, a coincidence measurement between the α's and the 0.0678 MeV γ's would show that only the first excited state group was in coincidence. However, most low lying levels in heavy nuclei will lose their energy of excitation by Internal Conversion. X-rays from the electron vacancy, therefore, would be in coincidence with the alphas.

In this experiment we are going to determine the sums under the various alpha groups and their energies. From this data we will verify the energies of the first and second excited states and the decay rations relative to the ground state.

Experimental Procedure

1. Obtain the ^{230}Th source from the instructor. Place it 2 cm from the face of the detector, evacuate, and apply the recommended bias for the detector.

2. It will be necessary to accumulate a spectrum for one hour or longer. After the spectrum has been taken, determine the energies of $E\alpha_0$, $E\alpha_1$, and $E\alpha_2$ (see fig. 3.9). Also find the sums under these groups minus the estimated backgrounds.

Exercise A *(Decay Ratios)* Define the Sums as follows:

Sum under the 4.682 MeV group = $(\Sigma\text{-}\beta)_0$

Sum under the 4.614 MeV group = $(\Sigma\text{-}\beta)_1$

Sum under the 4.472 MeV group = $(\Sigma\text{-}\beta)_2$

Use the absolute technique established in Experiment 3.4 to determine the true number of alphas per second in these three groups. From the given activity of the source, verify that the decay ratios are the same as those shown in fig. 3.9.

Exercise B In this exercise we will determine the energies of the first and second excited states of $^{226}_{88}$Ra.

Use the measured energies of $E\alpha_0$ and $E\alpha_1$ to determine ε_1 (the energy of the first excited state in $^{226}_{88}$Ra. This is quite easy since eqs.1 through 5 will show $E\alpha_0 - E\alpha_1 = \varepsilon_1$. Repeat this exercise and find ε_2 the energy of the second excited state.

REFERENCES FOR *EXPERIMENT 3*

1. S. L. Whetstone, *Phys. Rev.* **131**, 1232 (1963).

2. D. J. Skyrme, *Nuc. Instr. & Methods* **57**, 61 (1967).

3. R. N. Chandra & R. A. Deal "Catalogue of Semiconductor Alpha Particle Spectra", Idaho Falls, DOE report No. IN-1261 (1970).

4. G. F. Knoll, *Radiation Detection and Measurement*, John Wiley and Sons, New York (1979).

5. G. Dearnaley, "Nuclear Radiation Detection by Solid State Devices," *J. Sci. Instrum.* **43**, 869 (1966).

6. J. L. Duggan, W. D. Adams, R. J. Scroggs, and L. S. Anthony, "Charged-Particle Detector Experiment for the Modern Physics Laboratory," *Am. J. Phys.* **35**(7), 631 (1967).

7. C. M. Lederer and V. S. Shirley, Eds., *Table of Isotopes*, 7th Edition, John Wiley and Sons, Inc., New York (1978).

8. G. T. Ewan, "Semiconductor Spectrometers" (in progress), *Nucl. Tech. and Instrum.* **3**, F. M. Farley, Ed. Elsevier, North Holland, New York (1968).

EXPERIMENT 4

A Study of the Energy Loss of Alpha Particles in Matter

Scope

The same electronic arrangement used in Experiment 3 will be used in this experiment. First, the system will be calibrated and then the energy of the alpha particles before and after they pass through thin foils will be measured. The measured values will then be compared with those obtained from theoretical predictions.

Discussion

When an alpha particle passes through matter, it loses energy by ionization and excitation of the medium through which it is passing. In the ionization process, the alpha particle imparts enough energy to the orbiting electron to completely remove it from the atom. In this process, an ion pair is formed. The average energy required to create an ion pair is called the Ionization potential (W). This value depends on the average binding energy of the electrons that are being removed. Bohr's theory tells that the binding energy of an electron is dependent on the electrostatic potential energy and the kinetic energy of the electron. Further restrictions dictate that the orbital angular momentum must be quantized such that:

$$MvR = \frac{nh}{2\pi} \qquad (1)$$

In gases, these ionization potentials range from 22 ev/ion pair in ^{131}Xe to 46 ev/ion pair in ^{4}He. In air, the value is 35 ev/ion pair. For copper, the value is 10.8 ev/ion pair.

Because of the double positive charge and its large mass, an α particle forms a rather high number of ion pairs per unit path length. The specific ionization is defined as the number of ion pairs formed per cm of path. The actual value of the specific ionization for α particles is not a constant. The specific ionization depends upon the velocity of the alpha particle, as well as the atomic number and mean ionization potential of the absorbing substance. The range of specific ionization in air extends from about 10,000 to 70,000 ip/cm. If the ionization produced by an alpha particle is plotted against the distance of penetration in a substance, the specific ionization gradually increases as the particle loses energy (see fig. 4.1). Finally, the ionization reaches a peak value and drops to zero as all the alpha energy is lost. An alpha, whose energy is entirely lost in a substance, will pick up two electrons and become a neutral helium atom.

The exact behavior of an ion traveling through matter depends on a number of factors. Figure 4.2 shows a plot of dE/dx versus energy for protons in aluminum.

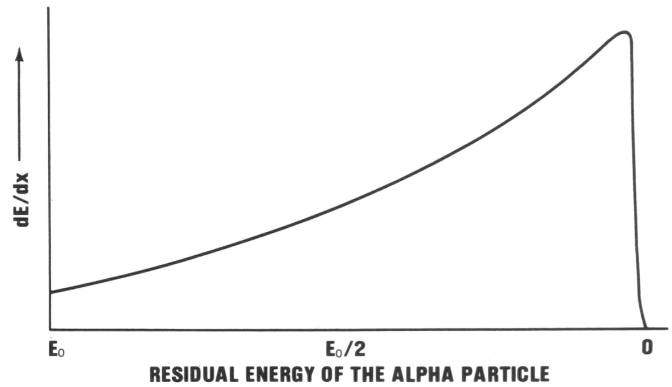

Figure 4.1. A plot of (dE/dx) versus residual range. This is the so called Bragg Curve. It is valid for most charged particles in matter.

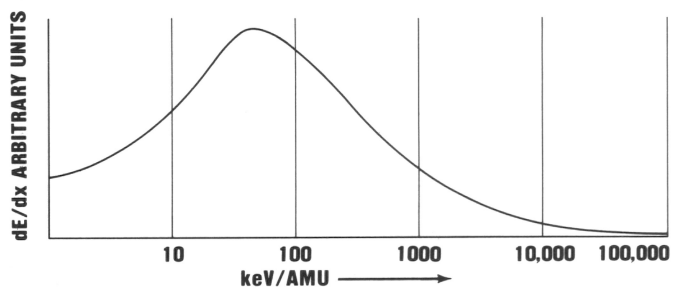

Figure 4.2. Plot of dE/dx versus Energy for Protons in Aluminum.

In the low energy region (less than 10 keV) of fig. 4.2 the dE/dx is evaluated using the theory of the Thomas-Fermi statistical model. (See for example ref. 1-3.) For the experiments in this manual, the nuclear stopping power can be ignored since it contributes almost nothing to the stopping power cross section for energies above 10 keV. Experimentally, it is not possible for us to measure alpha particles in this low energy region. In the energy realm of interest, the stopping power is in the so called electronic realm which was treated in the first part of this discussion. The theory for this region has been fairly well established by Lindhard and Scharff (see ref. 4). This theory has been very successfully used to describe a wealth of experimental dE/dx measurements. J. F. Ziegler and H. H. Anderson have published a sequence of dE/dx volumes that compares the theory with a vast number of experimental measurements (see ref. 5).

For the measurements outlined in this experiment the dE/dx of alphas can be written as follows[6]:

$$\frac{dE}{dx} = \frac{2\pi Z_i^2 e^4 N Z}{M_o^2} \ln\left(\frac{2M_o^2 Q_{max} - 2\beta^2}{I^2 (1-\beta^2)}\right) \qquad (1)$$

where

Z_1 The atomic number of the alpha
e The electronic charge (esu)
M_0 = rest mass of the electron (g)
v = velocity of the alpha cm/s
β = v/c
NZ = number of electrons/cm^3
Q_{max} = maximum kinematic transfer from an electron to an alpha particle (ergs)
I = mean ionization potential (ergs)
E = energy of the incident particle

The logarithmic term in eq. (1) varies slowly with energy and hence it is approximately correct to write:

$$dE/dx = \frac{\text{constant}}{E} \qquad (2)$$

For a thin foil:

$$E = \left(\frac{dE}{dx}\right) \Delta X \qquad (3)$$

However, from fig. 4.2 it is obvious that for a fairly thick foil there is need to integrate the dE/dx expression over the thickness of the foil since the dE/dx upon entry will be different than its value for the last row of atoms in the foil, the true energy loss can be found as follows:

$$\Delta E = \int \left(\frac{dE}{dx}\right) dx \qquad (4)$$

In eq. (4), the analytic expression for dE/dx is used. It is seen from the experiment that the range curves are perhaps the easiest and best way to get the theoretical value for energy loss. Rearranging eq. (4) and integrating from the incident alpha energy E_0 to zero gives:

$$\text{Range} = \int_{E0}^{0} \frac{dE}{\left(\frac{dE}{dx}\right)} \qquad (5)$$

In this experiment, both the (dE/dx) and range method of calculating the energy loss of alphas in a variety of materials will be used.

Table 4.1 shows the integrated ranges for the foils that will be studied in this report. These semiempherical values were taken from ref. 7.

Table 4.1 Range of Alpha Particles Versus Energy For Al, Ni, Cu, Ag, Ag and Mylar (Taken from Reference 7)

Range in Units of mg/cm^2

Energy (MeV)	Al	Ag	Au	Cu	N	O	Ne	Mylar	He
.050	.142	.371	.746	.479	.123	.132	.149	.097	.081
.080	.190	.487	.976	.525	.170	.181	.204	.133	.113
.128	.252	.634	1.269	.605	.232	.247	.277	.180	.158
.201	.327	.812	1.620	.726	.312	.330	.367	.238	.219
.400	.497	1.199	2.362	.968	.490	.513	.560	.366	.364
.500	.574	1.369	2.675	1.085	.563	.588	.639	.421	.425
.640	.680	1.597	3.086	1.300	.654	.684	.739	.493	.500
.800	.802	1.854	3.539	1.440	.750	.783	.844	.570	.579
1.000	.959	2.178	4.099	1.688	.863	.900	.969	.665	.671
1.60	1.475	3.209	5.825	2.503	1.193	1.246	1.346	.959	.937
2.00	1.86	3.955	7.039	3.107	1.428	1.493	1.620	1.174	1.121
2.401	2.283	4.758	8.323	3.758	1.687	1.765	1.925	1.412	1.320
2.80	2.745	5.622	9.687	4.455	1.979	2.073	2.269	1.678	1.538
3.20	3.244	6.544	11.126	5.196	2.308	2.418	2.655	1.973	1.778
4.000	4.349	8.549	14.205	6.808	3.079	3.227	3.564	2.658	2.331
5.00	5.920	11.339	18.411	9.057	4.236	4.444	4.931	3.682	3.156
6.40	8.460	15.759	24.929	12.610	6.189	6.487	7.222	5.422	4.556
8.00	11.835	21.512	33.237	17.280	8.851	9.277	10.321	7.829	6.504

Table 4.2 shows the stopping power of alpha particles as a function of energy for various foils.

Table 4.2 dE/dx in MeV/mg/cm² for Various Materials (Taken from Reference 7)

Energy (MeV)	Al	Ag	Au	Cu	N	O	Ne	Mylar	He
.050	.532	.223	.112	.311	.564	.530	.471	.713	.851
.080	.673	.282	.141	.401	.684	.644	.576	.889	.989
.128	.852	.358	.180	.670	.817	.777	.710	1.107	1.102
.201	1.040	.444	.226	.643	.956	.930	.865	1.346	1.211
.400	1.28	.575	.307	.764	1.303	1.262	1.201	1.757	1.572
.500	1.317	.604	.331	.780	1.442	1.389	1.327	1.888	1.745
.640	1.323	.622	.349	.781	1.604	1.546	1.466	2.021	1.955
.800	1.299	.622	.357	.770	1.734	1.665	1.574	2.096	2.117
1.000	1.248	.610	.357	.740	1.816	1.748	1.632	2.114	2.239
1.60	1.086	.555	.338	.660	1.776	1.688	1.529	1.947	2.237
2.00	.996	.520	.322	.630	1.640	1.561	1.396	1.786	2.112
2.401	.904	.480	.302	.580	1.458	1.385	1.238	1.593	1.926
2.80	.832	.448	.285	.550	1.292	1.227	1.098	1.427	1.756
3.20	.773	.422	.271	.520	1.152	1.098	.982	1.287	1.593
4.00	.682	.380	.250	.460	.949	.900	.802	1.073	1.329
5.00	.598	.340	.228	.410	.792	.756	.672	.895	1.113
6.40	.512	.297	.204	.360	.655	.626	.561	.730	.907
8.00	.442	.262	.183	.320	.556	.530	.479	.610	.750

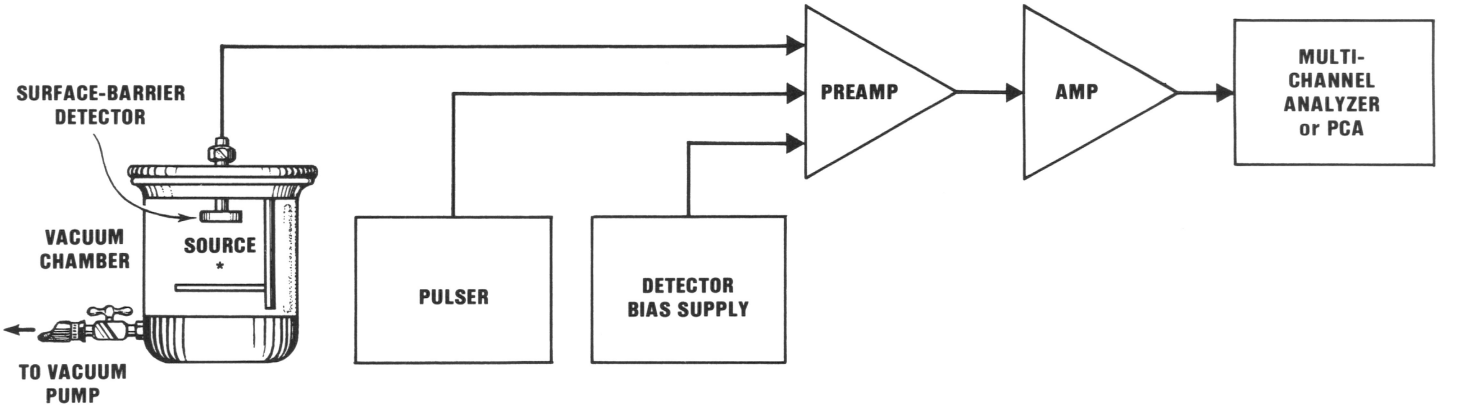

Figure 4.3. Electronics for dE/dx Experiment.

EXPERIMENT 4.1

Energy Loss of Alpha Particles in Thin Metallic Foils

Experimental Procedure

(dE/dx for Copper)

1. Set up the equipment as shown in fig. 4.3. Use the ^{210}Po source and the pulse generator to construct an energy versus channel calibration curve. The gain of the amplifier should be set such that the 5.31 MeV alphas from ^{210}Po are approximately in channel 800. Calculate the slope of the calibration curve in keV/channel.

2. Turn off the bias and vent the system to air. Place the thinnest copper foil between the ^{210}Po source and the detector, and pump the system back down. Return the bias to its recommended value and determine the position of the alpha peak. From the calibration curve, determine its energy (E_f) and record this value in Table 4.3.

3. Turn off the bias and slowly let the system up to air. Remove the copper foil and replace it at the same position with the next thickest foil. Determine the energy of the ^{210}Po alphas through this foil and record the measured value in Table 4.3.

4. Repeat for the rest of the copper foils in the set. Figure 4.4 shows a typical superposition of several of the above measurements on the same graph.

5. This experiment may also be done for any of the other foils that the instructor may provide (see Tables 4.1 and 4.2 or ref. 7). Figure 4.4 shows a typical pulse height spectrum of the ^{210}Po alphas before going through a foil. This experiment could have been done with any of the alpha sources that were shown in Experiment 3. Figure 4.5 shows a spectrum of another alpha source which is suitable for this experiment ^{234}U.

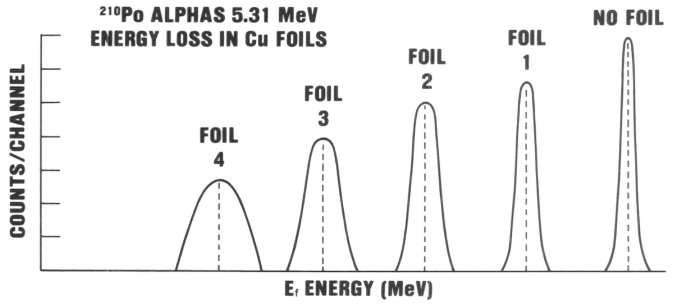

Figure 4.4. Composite Spectra of the Energy Loss of ^{210}Po Alphas in Thin Copper Foils.

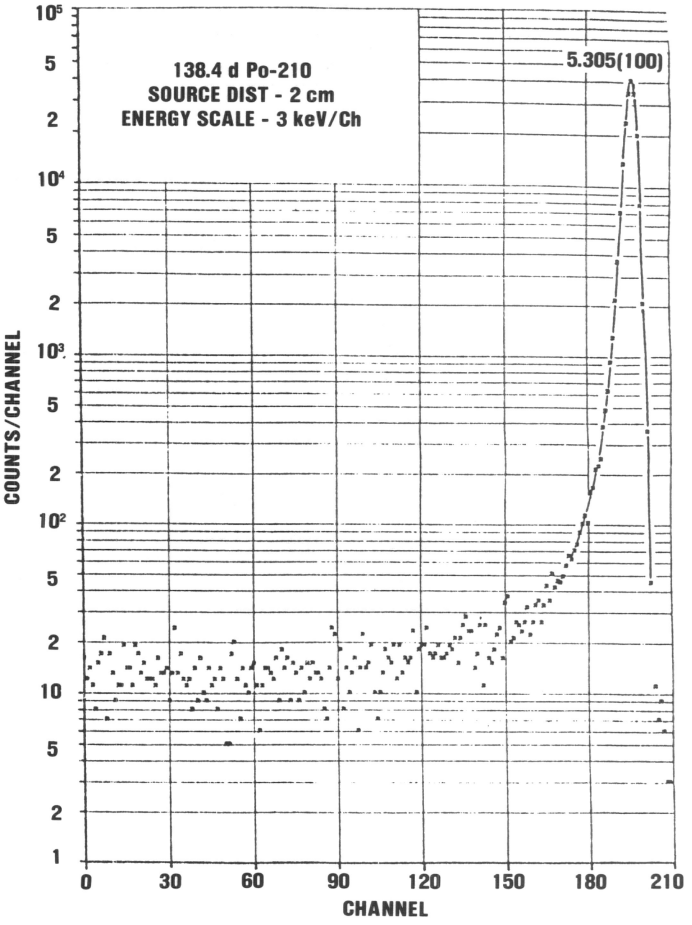

Figure 4.5. Alpha Particle Pulse Height Spectrum of ^{210}Po (No Foil).

Table 4.3 Comparison of the Experimental and Theoretical Value of Energy Loss of ^{210}Po Alphas in Thin Copper Foils

No.	Foil Thickness mg/cm^2	Channel No.	Final Energy E_f MeV	ΔE_m Measured MeV	ΔE Theory Range Method	ΔE Theory (dE/dx) Method	% Difference $\frac{\Delta E_m - \Delta E \text{ Range}}{\Delta E \text{ Range}}$
1							
2							
3							
4							
5							

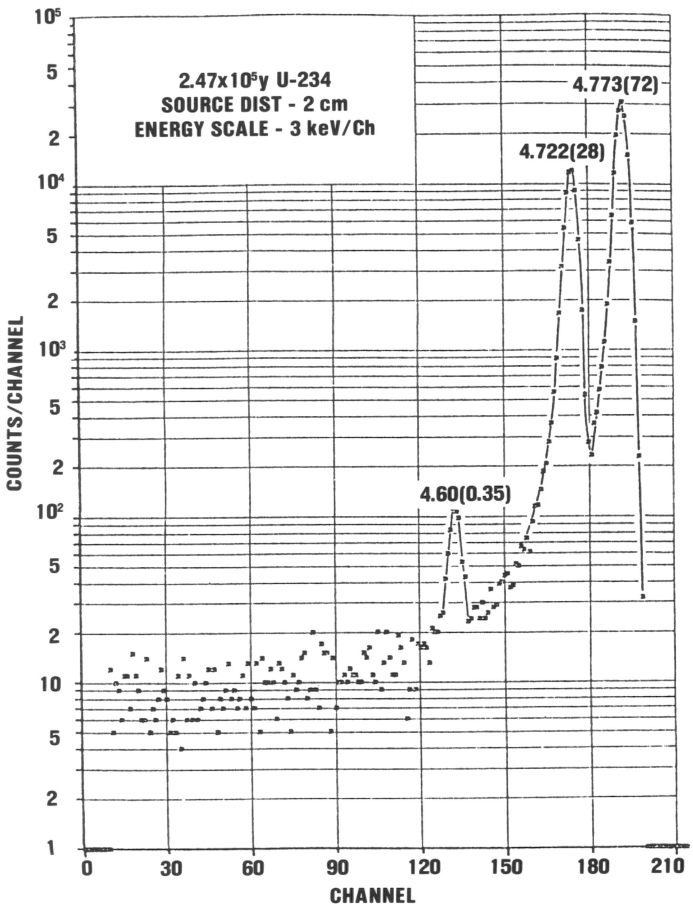

Figure 4.6. Alpha Particle Pulse Height Spectrum of ^{234}U (No Foil).

Exercise A Calculation of the theoretical value for the energy loss E_{Th} can be done by two methods. These are the range method (Exercise a) and the $(dE/dx)_{av}$ method (Exercise b).

As mentioned in the preliminary discussion eq. (5), the range of an alpha particle can be determined by integrating the (dE/dx) of the alpha over its path length from E_0, the initial energy, to zero, the final energy. Figure 4.7 shows the range that results from this integral for incident alphas between 0.10 and 6 MeV. From this curve it can be seen that the range of an alpha from ^{210}Po that has an energy of 5.31 MeV corresponds to a range in copper of 9.3 mg/cm^2. Assume that the first copper foil used was 2.0 mg/cm^2. Figure 4.7 can be used to find the final energy E_f of the alpha after it has passed through the foil. This is done by subtracting the foil thickness from the 9.3 mg/cm^2 and then reading the energy E_f of the alpha from fig. 4.7. Example:

$$R_f = (9.3 - 2.0)\ mg/cm^2 = 7.3\ mg/cm^2 \qquad (6)$$

From fig. 4.7, the energy E_f of an alpha whose range is 7.3 mg/cm^2 is 4.2 MeV. Therefore, E_f, the energy that the alpha gives ΔE_{Th} = 5.30 MeV — 4.2 MeV = 1.1 MeV. This value would then be entered into Table 4.3 as ΔE for that foil.

Compute ΔE_{Th} for all of the copper foils that the instructor provides. Repeat these calculations for any other foils that the instructor may provide.

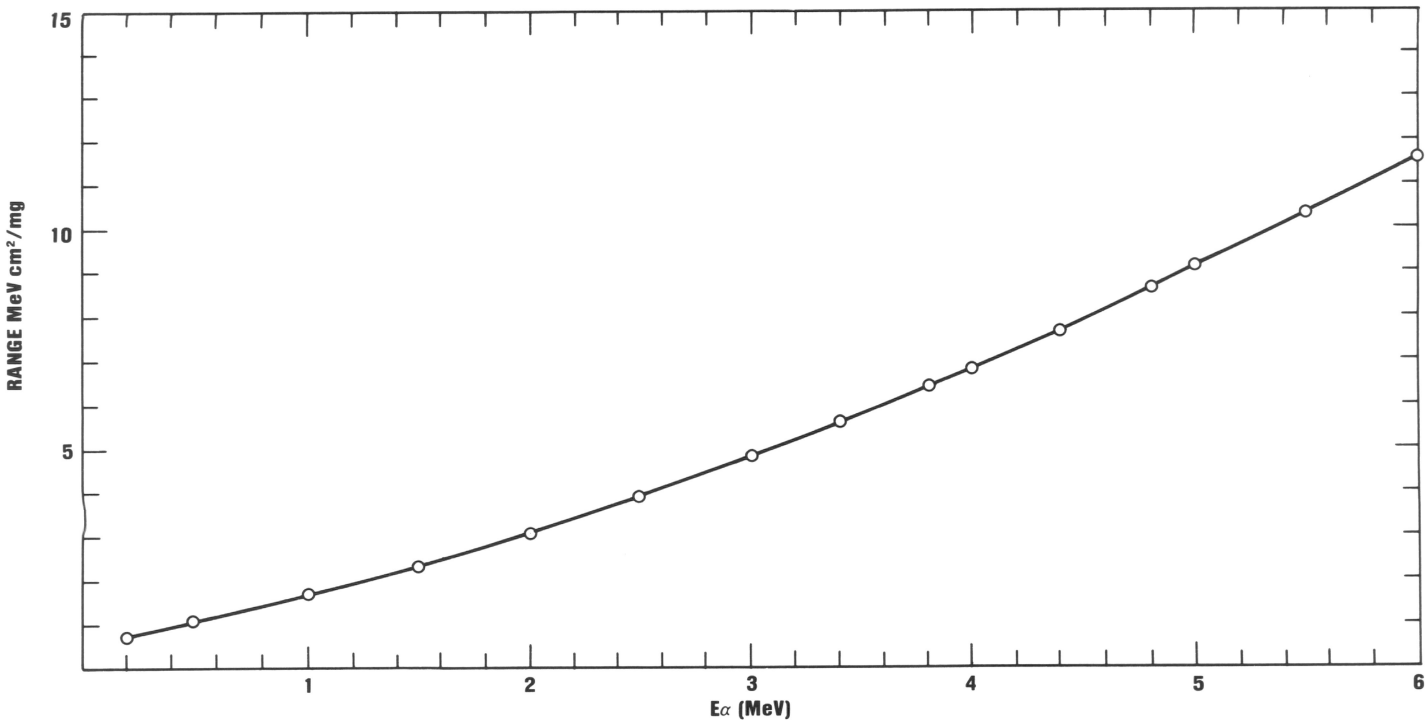

Figure 4.7. Energy vs Range for Alphas in Copper (taken from ref. 7). Note, the student should plot this range curve on graph paper from the data in Table 4.1 The range numbers can then be accurately read from the graph.

Exercise B The theoretical (dE/dx) may also be determined by using the average (dE/dx) method.

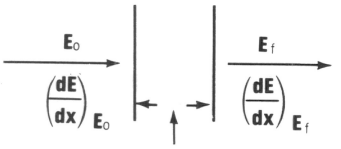

Figure 4.8. Illustration showing an alpha of energy E_0 entering a foil and leaving with an energy E_f.

The value of $(dE/dx)_{E0}$ at the incident energy can be found from Table 4.2. When the alpha leaves the foil, its energy is E_f and the $(dE/dx)_{Ef}$ can also be found from Table 4.2. Since the foil is fairly thin, it can be assumed the (dE/dx) change across the foils is approximately linear. It is thus possible to write:

$$\left(\frac{dE}{dx}\right)_{Av} = \frac{\left(\frac{dE}{dx}\right)_{E0} + \left(\frac{dE}{dx}\right)_{Ef}}{2} \qquad (7)$$

The theoretical energy loss using $(dE/dx)_{Av}$ is then given by:

$$(\Delta E)_{Th} = \left(\frac{dE}{dx}\right)_{Av} \cdot \Delta X \qquad (8)$$

Note, that since the units of dE/dx are in MeV/mg/cm^2 and the foil thickness ΔX is in mg/cm^2, the resultant product in eq. (8) has units of MeV.

Use eq. (8) to calculate $(\Delta E)_{Th}$ for all of the foils that are provided for this experiment. Record these values in Table 4.3.

Exercise C The last column in Table 4.3 is the % difference. Since the ΔE_{Th} obtained by the range method (exercise a) should be more accurate, use it as the accepted value. If the student is very careful with the measurements and accurately reads the graphs, tables, and calibration curves, these % differences should be less than 10%.

EXPERIMENT 4.2

Alpha Particle Energy Loss in Helium Gas

Discussion

The energy loss of alpha particles in helium gas can be measured very accurately. The reason for this accuracy is the fact that the effective thickness of the helium target in mg/cm^2 can easily be determined. Helium behaves, for this experiment, like an ideal gas. Therefore, the ideal gas law can be used to determine the density of the gas at a given pressure and temperature. The pressure in the chamber can be accurately determined by placing a mercury manometer in the system. The temperature of the chamber can be measured with an ordinary labora-

Table 4.4 Comparison of the Experimental and Theoretical Values of Energy Loss of ^{210}Po Alphas in Helium Gas

Run No.	Helium Pressure cm of H_g	Helium Thickness mg/cm^2	Peak Channel Number	Final Alpha Energy E_f	ΔE_M Measured	ΔE_{Th} Range Method	ΔE_{Th} $\left(\frac{dE}{dx}\right)_{Av}$ Method	% Difference $\frac{\Delta E_m - \Delta E_{Range}}{\Delta E \text{ Range}}$
1	0.0							
2	4.0							
3	10.0							
4	20.0							
5	30.0							
6	40.00							
7	50.00							
8	60.00							
9	70.00							
10	76.00							

tory thermometer that is taped to the side of the chamber.

Experimental Procedure

1. Place the ^{210}Po source 2 cm from the face of the detector. Evacuate the chamber to 76 cm of mercury. Turn on the bias voltage to its recommended value and collect a spectrum for ^{210}Po. The amplifier gain should be set such that the 5.31 MeV alphas are around channel 800 as in the previous experiment. Record the channel number in Table 4.4.

2. Lower the bias to zero and backfill the chamber (Helium) to 4 cm of Hg pressure. Return the bias to its operating value and accumulate a spectrum. Record the position of the alpha peak in Table 4.4. Repeat for the other manometer pressure settings in Table 4.4. The bias level can be left at its operating value for all of these measurements.

Exercise For the pressure values recorded in Table 4.4, use the ideal gas law to calculate the helium path thickness in mg/cm^2. Record these values in the Table. From the energy calibration curve, determine E_f for all of the gas thicknesses. Calculate ΔE_m, E_{Th} (range method), and ΔE_{Th} (dE/dx average method) and fill in the rest of the Table. Calculate the % differences. These numbers should be within 8%.

EXPERIMENT 4.3
Alpha Particle Range in Air

Discussion

In this experiment the effective range in air of the 5.3 MeV alphas from ^{210}Po will be measured. A general rule of thumb for alphas in air at atmospheric pressure is: Eα = range (cm) + 1.5 cm.

The experiment is quite simple but it shows excellent results. Since air is a mixture, for the most part, of nitrogen and oxygen, the combined range for these two gases is being measured. From ref. 7 the range of a 5 MeV alpha particle in nitrogen is 4.236 mg/cm^2 and for oxygen it is 4.444 mg/cm^2. When calculating the results for this experiment, the range measured will be close to these values.

Experimental Procedure

1. Place the ^{210}Po source 1 cm from the detector. Close the chamber and raise the bias to its recommended value. The detector will not be damaged by operating it at atmospheric pressure. The gain of the system should be set such that the 5.3 MeV alphas in vacuum are stored around channel 800 as in all of the experiments in this section.

2. Record a spectrum for a time period long enough to obtain a (Σ-β) of at least 3000 counts. Calculate the number of alphas per second, the energy, and the resolution of the peak. Record the results in Table 4.5

Table 4.5 Alpha Particle Range in Air

Run No.	Distance cm	Thickness mg/cm^2 of Air	Alpha Channel Centroid	Measured Energy	ΔE_m Energy Loss	Peak Resolution keV	Measured counts/sec	Corrected counts/sec for $1/R^2$
1	1 cm	0.00			0.00			
2	1 cm							
3	2 cm							
4	3							
5	4							
6	4.1							
7	4.2							
8	4.3							
9	4.4							
10	4.5							
11	4.6							
12	4.7							

3. Turn down the bias voltage, lift the lid from the chamber and adjust the source to detector distance to 2 cm. Return the bias voltage to its operating value. Accumulate a spectrum, and calculate the counting rate as in number 2. Record the position and resolution of the peak.

4. Repeat for distances of 3, 3.2, 3.4, 3.6, etc. until the range of the alphas has been exceeded. As the source is moved farther away, the counting time will have to be increased in order to get reasonable statistics in the peak. When the range in air has been exceeded, only background counts will be observed.

Exercise A Record all of the measured values in Table 4.5. For runs 2, 3, 4, etc., use the ideal gas law (PV = NRT) and the recorded values of atmospheric pressure and temperature to calculate the path length in mg/cm^2. Use the calibration curve to determine the alpha energies, $(\Delta E)_M$, and the resolution for all measurements. Record these values in the data table.

Exercise B Run number 2 in Table 4.5 was made at atmospheric pressure and a distance of 1 cm. Assume that the counting rate is N_1. Normalize all subsequent measurements to this run. Since the $1/R^2$ law applies, the correction factor for the next run, which is 2 cm, should be $(2\ cm)^2 = 4$. The next run would have a correction factor of 9 and so forth.

Correct all of the measured counting rates in this manner and make a plot of corrected counting rate versus distance. Figure 4.9 shows approximately how this data should look. From this figure, the range of alphas in air can easily be determined.

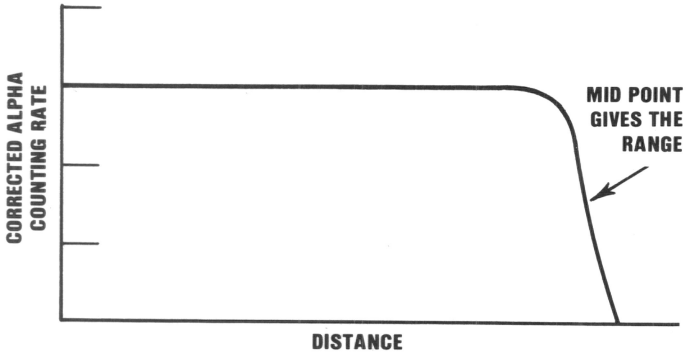

Figure 4.9. Plotted Data to Show Alpha Particle Range in Air at Atmospheric Pressure.

REFERENCES FOR *EXPERIMENT 4*

1. U Fano, *Annual Review of Nuclear Science*, Vol. 13, 1 (1963).

2. W. Whaling, *Handbuch der Physik*, Vol. 34, p202, Springer, Berlin (1958).

3. J. F. Ziegler & W. K. Chu, *Atomic Data & Nuclear Data Tables*, Vol. 13, p463 (1974).

4. J. Lindhard & M. Scharff, *Physical Review*, Vol. 124, p128 (1961).

5. H. H. Anderson & J. F. Ziegler, *The Stopping and Ranges of Ions in Matter*, (5 Volume Set) Pergamon Press, NY.
Vol. 1. The Theory of the Stopping of Ions in Matter
Vol. 2. Bibliography (1907-1976) with comments containing 922 References.
Vol. 3. Hydrogen Stopping Power & Ranges
Vol. 4. Helium Stopping Power & Ranges
Vol. 5. Heavy Ions Stopping Power & Ranges

6. C. F. Williamson, J. P. Boujot, and J. Picard, *Tables of Range and Stopping Power of Chemical Elements for Charged Particles of Energy 0.5 to 500 MeV*, **CEQ-R-3042** (1966). Available from Clearinghouse for Federal Scientific and Technical Information, Springfield, Virginia.

7. L. C. Northcliffe and R. F. Schilling, *Nuclear Data Tables A7*, 233 (1970).

8. G. F. Knoll, *Radiation Detection and Measurement*, John Wiley and Sons, New York (1979).

9. J. B. Marion and F. C. Young, *Nuclear Reaction Analysis*, John Wiley and Sons, New York (1968).

10. J. L. Duggan, W. D. Adams, and L. S. Anthony, "Charged-Particle Detector Experiments for the Modern Physics Laboratory," *Am. J. Phys.* **35**(7), 631 (1967).

11. J. F. Janni, *Calculations of Energy Loss, Range, Pathlength, Straggling, Multiple Scattering, and the Probability of Inelastic Nuclear Collisions for 0.1- to 100-MeV Protons*, **AFWL-TR-65-150** (AD-643837), (1966). Available from Clearinghouse for Federal Scientific and Technical Information, Springfield, Virginia.

12. S. Matteson, E. K. L. Chau, and D. Powers, *Phys. Rev. A* **14**, 169 (1976).

13. G. Dearnaley and D. C. Northrop, *Semiconductor Counters for Nuclear Radiations*, 2nd Ed., John Wiley and Sons, New York (1966).

EXPERIMENT 5

Beta and Conversion Electron Measurements with Solid State Detectors

Scope

In this experiment, calibration of a surface barrier detector with the known energies of the conversion electrons from ^{207}Bi will be done. This calibration will be done with a precision pulse generator that is normalized to the 976 keV line from ^{207}Bi. The next part of the experiment will be to determine the precise energies of the conversion lines from several other isotopes. The beta end point energy of ^{204}Tl will then be determined with this calibration and a Kurie plot. The final measurements deal with the study of the ratio of internal conversion from the K and L shell electrons and the ratio for K and L conversion to gamma ray emission.

Discussion

Beta emission is perhaps one of the most important decay mechanisms that will be studied in this manual. It has been through the measurement of Beta end point energies that many of the nuclear levels listed in the Table of the Isotopes have been determined. One of the main reasons for this, is that many of the isotopes that can be studied are produced in a reactor by the so called (n, γ) reaction. These reactions will be studied in detail in a later experiment. In producing these isotopes, the material to be studied is placed in the thermal neutron flux of the reactor. The material that is to be irradiated will produce the following reactions:

$$ {}^{m}_{z}A_1 + n \rightarrow {}^{m+1}_{z}A_1^* + \gamma \qquad (1) $$

The γ is prompt and will leave the sample in a time of the order of 10^{-15} seconds. The remaining nucleus ${}^{m+1}_{z}A_1^*$ is, in general, radioactive and will decay to an energetically more stable nucleus. A typical decay scheme for ${}^{m+1}_{z+1}A_1^*$ is shown in fig. 5.1.

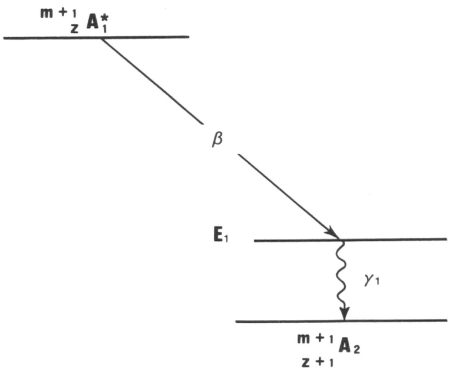

Figure 5.1. Typical Decay Scheme for a Beta Emitting Isotope.

The nucleus ${}^{m+1}_{z}A_1^*$ is neutron rich. In other words, the absorption of the neutron in eq. (1) has produced an excess of neutrons in the nucleus for stability. In order to reach a more stable configuration, one of the neutrons in the nucleus is converted to a proton by the following reaction:

$$ n \rightarrow p + \beta^- + \text{neutrino} \qquad (2) $$

Neither the proton, β^-, or neutrino from (2) can exist in the nucleus prior to the decay. The energy from the decay will be kinematically shared between the three products on the right of eq. (2).

From these Kinematic laws of conservation of energy and momentum, it can be shown that the proton receives very little of the energy that is available. The energy is therefore shared by the β^- and the neutrino. Since the neutrino can't be detected with this laboratory equipment, only the β^-'s can be measured. There are three nuclear particles on the right hand side of eq. (2) and therefore the β's that are measured will not have discrete energy. If the energy available during the decay is E_1, any combination of sharing this energy between the β's and the neutrino is possible. Figure 5.2 shows a picture of what the β spectrum for the decay of ${}^{m+1}_{z}A_1^*$ might show:

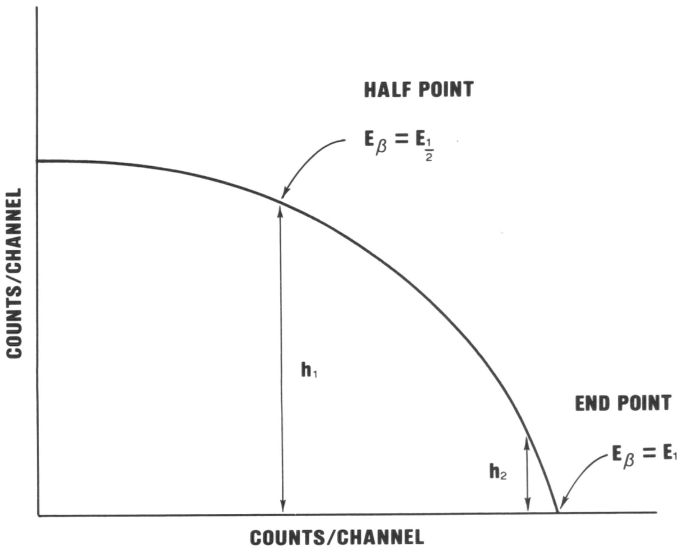

Figure 5.2. Typical Beta Spectrum showing the Continuous Distribution of Beta Energies up to the $E\beta_{max}$ End Point Energy.

Consider what nuclear information can be determined from the decay scheme in fig. 5.1 and the measured β spectrum in fig. 5.2. From the calibration and measured end point energy in fig. 5.2, the energy difference between ${}^{m+1}_{z}A_1$ and E_1 the first excited state can be determined. As mentioned in Experiment #2, the energy of level E_1 can be established by simply measuring γ_1. Furthermore, if ${}^{m+1}_{z}A_1$ also decayed directly to the ground state of ${}^{m+1}_{z+1}A_2$ that β^- end point energy could be measured and directly establish the energy difference between the ground state of ${}^{m+1}_{z+1}A_2$ and ${}^{m+1}_{z}A_1$. In a later experiment, the principle of coincidence measurements will be illustrated. In the example, γ_1 would be in coincidence with the β particle shown in fig. 5.1.

Before leaving this discussion, the topic of Internal Conversion electrons should be discussed since these discrete lines for energy calibration will be used.

Internal electron conversion is a decay process that is in direct competition with gamma emission. In fig. 5.1, ${}^{m+1}_{z}A_1$ decays by β^- emission to the first excited state E_1 of the nucleus ${}^{m+1}_{z+1}A_2$. In an earlier example, the state E_1 decayed to the ground state by the emission of γ_1. For some nuclei, it is possible for this energy of excitation to be given directly to an orbiting electron in the daughter nucleus ${}^{m+1}_{z+1}A_2$. This usually happens to the K, L, or M electrons. If this energy of excitation is large enough to remove the K shell electron, it will be knocked out of its orbit with an energy given by:

$$(E_0) = E_1 - K_{ab} \qquad (3)$$

where K_{ab} is the binding energy of the K shell electron of the daughter nucleus. Some smaller fraction of these conversions will occur to the L shell electrons. When this happens, the energy of L conversion electron is given by:

$$(E_0) + E_1 - L_{ab} \qquad (4)$$

Since eq. (3) and (4) give discrete energies, they can be used to calibrate the system. Figure 5.3 shows a spectrum of conversion lines from the decay of ^{133}Ba to ^{133}Cs.

Thus, by the use of conversion electron spectra, the system can be accurately calibrated and the β end point energy for an isotope can be measured. As pointed out earlier, β spectroscopy has given much of the valuable nuclear information that is tabulated in the Table of the Isotopes. This is, therefore, one of the most important experiments in this manual.

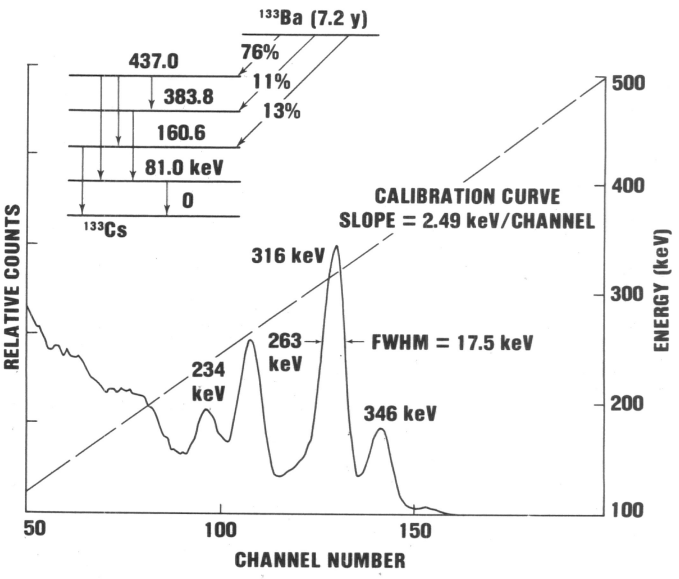

Figure 5.3. Electron Conversion Spectra for a 7.2 yr half life ^{133}Ba source.

EXPERIMENT 5.1

Energy Calibration for Beta Spectroscopy

Experimental Procedure

1. Set up the electronics as shown in fig. 5.4. Note this is exactly the same arrangement used for the last two experiments. Please take all of the precautions that were used in these earlier experiments. Place the ^{207}Bi source 2 cm from the face of the detector. Pump the system down and set the bias voltage for the surface barrier detector.

2. Adjust the gain of the amplifier so that the 976 keV conversion line from ^{207}Bi is at approximately channel 300. Figure 5.5 shows the spectrum of conversion electrons from a thin ^{207}Bi source.

3. Record the exact channel of the 976 keV line. Remember, for some analyzers and PCA's, a centroid finding program can be used to determine this value. Turn on the pulser and adjust the pulse height dial to 976/1000. Use the attenuation switches and the calibrate adjustment to set the pulser peak in the same channel as the 976 keV conversion electron line. The pulser is now calibrated so that each division on it corresponds to 1 keV. Set the pulser at 1000/1000 and record the position of the peak. Fill in the rest of the calibration data points in Table 5.1. Plot a calibration curve, and calculate the slope of the curve in keV/ch. From the slope of the calibration curve, calculate the resolution of all of the lines from the pulser and the ^{207}Bi Conversion Spectrum.

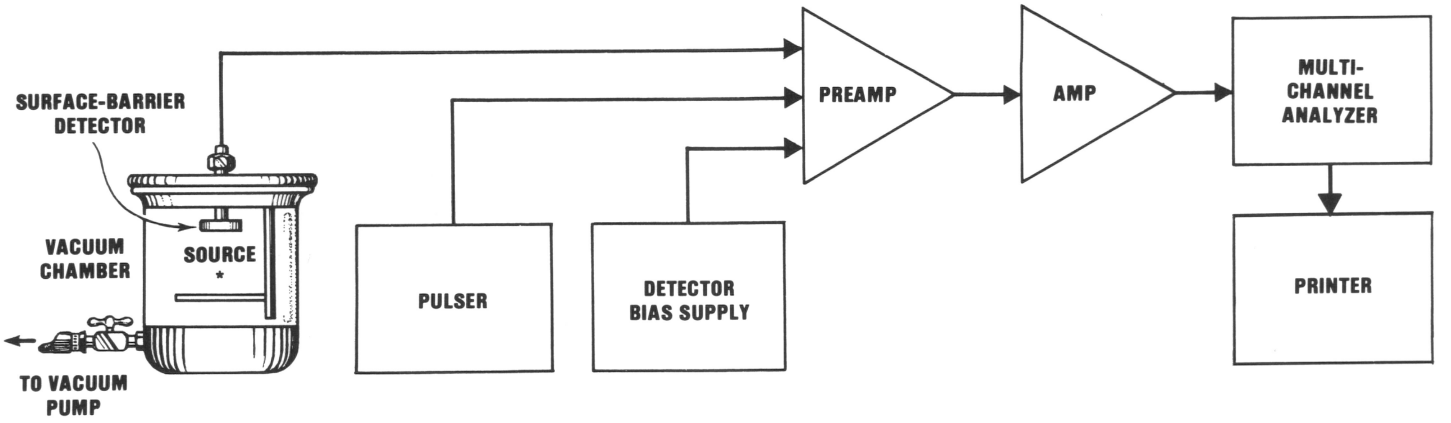

Figure 5.4.

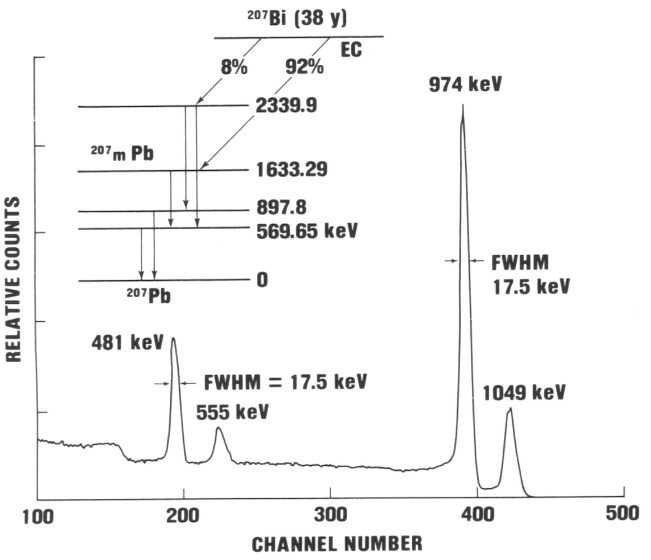

Figure 5.5. Conversion Electron Spectra from ^{207}Bi.

Figure 5.3 shows a spectrum of ^{133}Ba. Superimposed on this pulse height spectrum is a calibration curve similar to the one that will be done in this experiment.

Table 5.1 Calibration Data from ^{207}Bi Conversion Electron Lines

Run No.	Pulse Setting	Energy keV	Channel Number	Resolution keV
1	1000/1000	1000		
2	800/1000	800		
3	600/1000	600		
4	400/1000	400		
5	200/100	200		
6	482 keV line	554		
7	554 keV line	976		
8	1048 keV line	1048		

EXPERIMENT 5.2

Beta End Point Energy of ^{204}Tl

Experimental Procedure

1. Remove the ^{207}Bi source and replace it with the ^{204}Tl source. Accumulate a spectrum for ^{204}Tl for a period of time that is long enough to get reasonable statistics in the spectrum. The ^{204}Tl spectrum will resemble fig. 5.2 which is a pure β emitter. The number of counts/ch at the height h_1 in the spectrum should be approximately 500.

2. From the spectrum select ten points that are evenly spaced between h_1 and h_2 in your ^{204}Tl spectrum (see fig. 5.2). Record in Table 5.2, the channel numbers and the number of counts in these channels. From the calibration curve determine the energy of each point that was taken.

Discussion

The shape of the β distribution for ^{204}Tl will be fitted to a Kurie plot and the end point energy can accurately be determined from this plot.

For an allowed β transition, the pulse height distribution for a given β can be written:

$$\frac{1}{W}\left(\frac{N(E)}{G(Z,W)}\right)^{1/2} = K\,(E_0 - E) \qquad (5)$$

where

N(E) = the number of counts at energy E
W = E + 1; E is the energy of the point in MeV divided by 0.511
G(Z,W) = The modified Fermi function (see ref. 5).

For this experiment G(Z,W) can be obtained from Table 5.3. In these dimensionless units, $P = (W^2 - 1)^{1/2}$. This is the momentum of the electron. For example, assume that the energy of one of the points N(E) is 0.50 MeV. Therefore W = .5/.511 + 1 or 1.978. This would give the momentum a value $p = [(1.978)^2 - 1]^{1/2} = 1.71$. The corresponding value of G(Z,W) from Table 5.3 would be 20.8.

Table 5.3 Modified Fermi Function G(Z,W) for the β Decay of ^{204}Tl (See Reference 5)

P	G(Z,W)	P	G(Z,W)
0.0	28.26	0.9	24.33
0.1	28.19	1.0	23.98
0.2	27.99	1.2	22.95
0.3	27.67	1.4	22.01
0.4	27.25	1.6	21.17
0.5	26.76	1.8	20.41
0.6	26.23	2.0	19.72
0.7	25.66	2.2	19.10
0.8	25.09	2.4	18.54

Exercise On linear graph paper, make a plot of P vs G(Z,W). Calculate the dimensionless momentum P for each Energy in Table 5.2. Record these (P) values in the table. From the curve of P vs G(Z,W) read off G(Z,W) for each of the momentum values and record them in Table 5.2. Calculate $1/W\,[N(E)/G(Z,W)]^{1/2}$ for each point and record in the table. Make a plot of $1/W\,[N(E)/G(Z,W)]^{1/2}$ versus the energy of the point in MeV. Figure 5.6 shows

Table 5.2 Data Table for the Kurie Plot of ^{204}Tl

Channel Number	Energy MeV	N(E)	W	P	G(Z,W)	$\frac{1}{W}\left(\frac{N(E)}{G(Z,W)}\right)^{1/2}$

this typical Kurie plot for ^{204}Tl. Look up the accepted value in ref. 1 or ask the instructor. The results should be within 7% of the accepted value.

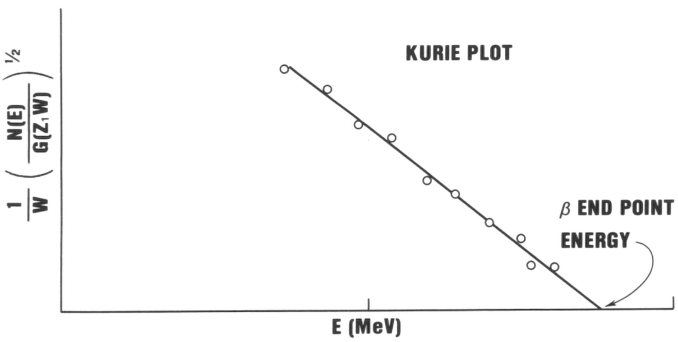

Figure 5.6. Typical Kurie Plot for the Allowed Beta Transitions from ^{204}Tl.

EXPERIMENT 5.3

Measurement of the Internal Conversion Coefficients for ^{137}Cs and ^{137}Ba

Discussion

Figure 5.7 shows the ^{137}Cs gamma spectrum that was measured in Experiment number 2.

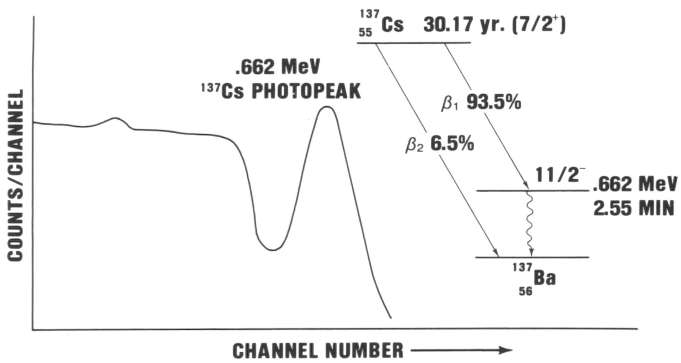

Figure 5.7. NaI Spectrum of ^{137}Cs.

The .662 MeV state gamma decays directly to the ground state 86% of the time. The other 14% of the time this energy of excitation 662 keV is directly transferred to the K, L, or M orbiting electrons in ^{137}Ba. Figure 5.8 shows a Conversion Electron Spectrum from the ^{137}Cs source.

In this experiment, the E_K/γ ratio will be measured. These ratios are referred to as the Internal Conversion coefficients a_K and a_L for the source. The energy of the K and L electrons for ^{137}Ba will also be determined.

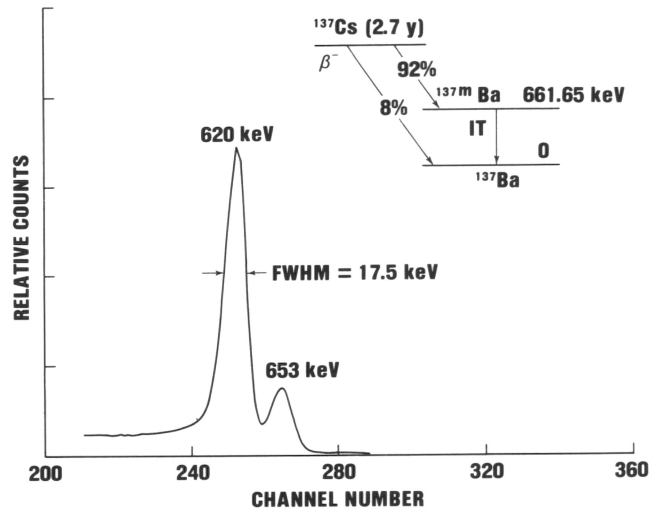

Figure 5.8. Internal Conversion Spectrum for ^{137}Cs.

Experimental Procedure

1. The instructor will provide a ^{137}Cs source that has been calibrated. (**Note:** This must be a thin window source for electron conversion measurements.) If it hasn't been calibrated, set up the electronics in experiment number 2 and determine its activity by measuring the gammas by either the relative or absolute method. For the Internal Conversion measurement, place the source 4 cm from the solid state detector, evacuate the vacuum chamber and store a spectrum for a time period long enough to have 2000 counts under the E_K peak. The energy calibration, etc. that was determined for the last experiment will be used for these measurements.

2. Record the time and determine $(\Sigma\text{-}\beta)_K$ and $(\Sigma\text{-}\beta)_L$. It can be seen from fig. 5.8 that this should be easy to do since there are no interferences in the spectrum. There is now enough data to calculate the internal conversion coefficients for ^{137}Cs.

Exercise A From experiment 3, the geometry of the measurement is given by:

$$G_1 = \frac{\text{Area of the detector cm}^2}{4\,\pi\,R_1^2} \qquad (6)$$

$$R_1 = 4 \text{ cm}$$

The corrected activity for $(\Sigma\text{-}\beta)_K$ and $(\Sigma\text{-}\beta)_L$ is given by:

$$A_K = \frac{(\Sigma\text{-}\beta)_K}{t}\,\frac{1}{G_1} \qquad (7)$$

Use eq. (7) to correct the measurements made above.

Now the corrected activities for the K and L shell conversions are defined to be A_K and A_L. The units are

counts/sec. If the corrected gamma activity is defined to be I_γ for the 0.662 MeV level then:

$$a_K = \frac{A_K}{I_\gamma} \text{ and } a_L = \frac{A_L}{I_\gamma} \qquad (8)$$

Determine the coefficients a_K and a_L from the data. How do these compare to the accepted values from the Table of Isotopes:

$$a_K = 0.093 \text{ and } a_L = 0.014$$

Exercise B The absolute values of the binding energies for the K and L orbiting electrons in ^{133}Ba can be determined from the calibration curve and your figure which is equivalent to fig. 5.8. Remember from the introductory discussion, the energy of the conversion electrons to the K and L shell are given by:

$$(E_e)_K = E_{ex} - K_{ab} \text{ and } (E_e)_L = E_{ex} - L_{ab} \qquad (9)$$

In eq. (9), E_{ex} = 662 keV and $(E_e)_K$ and $(E_e)_L$ can be determined directly from the conversion spectrum and the calibration curve. How do the measured values for K_{ab} and L_{ab} compare to those that are listed in the Appendix (See Critical Absorption and Emission Energies in the Appendix).

REFERENCES FOR *EXPERIMENT 5*

1. C. M. Lederer and V. S. Shirley, Eds., *Table of Isotopes*, 7th Edition, John Wiley and Sons, Inc., New York (1978).

2. G. F. Knoll, *Radiation Detection and Measurement*, John Wiley and Sons, New York (1979).

3. J. B. Marion and F. C. Young, *Nuclear Reaction Analysis*, John Wiley and Sons, New York (1968).

4. G. Bertolini and A. Coche, eds., *Semiconductor Detectors*, American Elsevier Publishing Co., Inc. (1968).

5. K. Siegbahn, ed., *Alpha-, Beta-, and Gamma-Ray Spectroscopy*, **1** and **2**, Chapters VIII and XXIII, North Holland Publishing Co., Amsterdam (1965).

6. E. Segre, *Nuclei and Particles*, The Benjamin-Cummings Publishing Co., Reading, Massachusetts (1977).

7. G. Dearnaley and D. C. Northrop, *Semiconductor Counters for Nuclear Radiations*, 2nd Ed., John Wiley and Sons, New York (1966).

8. J. L. Duggan, W. D. Adams, and L. S. Anthony, "Charged-Particle Detector Experiments for the Modern Physics Laboratory," *Am. J. Phys.* **35**(7), 631 (1967).

EXPERIMENT 6

High Resolution Gamma Ray Spectroscopy

Scope

In this experiment the HpGe detector will be used to study gammas and their interactions in the detector. It will be seen that the superior resolution of these detectors has allowed us to measure gamma lines from nuclear levels that were simply not observed with NaI(Tℓ) detectors. In the experiment, a calibration curve will be constructed with known gamma lines from standard radioactive sources. The resolution of the detector for the 1.33 MeV gamma from ^{60}Co will be measured and compared to the specified value for the detector. From the calibration curve, the gamma energies of several unknowns will be determined with a high degree of accuracy. The efficiency and response function of the detector will be measured by both the relative and the absolute methods. High energy gamma sources will be used to study pair production in the detector by observing the single and double escape peaks in the spectra.

Discussion

In experiment number 2, the NaI(Tℓ) detector was used to study gamma from radioactive sources. It was found that the energy resolution of a good 3" x 3" NaI(Tℓ) detector was about 7% for the 662 keV line from ^{137}Cs. If this is converted to keV, the value is 46 keV. It should be recalled that the resolution of a detector is its ability to distinguish between two gammas that are ΔE apart in energy. It will be shown in this experiment that these HpGe detectors have energy resolution capabilities of less than 2 keV. It is therefore possible to distinguish individual lines in many cases where the NaI(Tℓ) detector showed a single peak.

Figure 6.1 shows a 3" x 3" NaI(Tℓ) spectrum of ^{57}Co. The region of interest for this discussion is the photopeak at 122 keV. From the decay scheme (see fig. 6.2) it can be seen that there is also a 136 keV line that should be present. The NaI(Tℓ) detector shows the 136 keV gamma as a distortion on the side of the stronger 122 keV line.

Figure 6.2 shows a Germanium spectrum of ^{57}Co with the 122 and 136 keV lines well resolved.

The resolution capabilities of these detectors has greatly facilitated the study of nuclear science. These detectors are usually specified in terms of the FWHM for the 1330 keV line of ^{60}Co. A good detector will show better than 2 keV for this gamma transition. This is approximately 40 times better than would be seen with a NaI(Tℓ) detector for the same gamma.

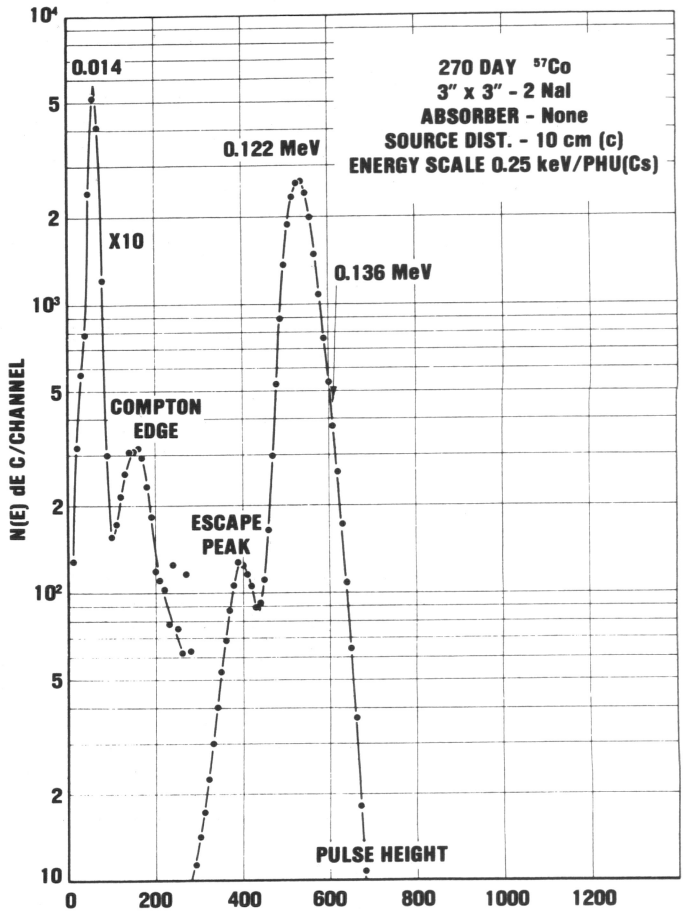

Figure 6.1 NaI(Tℓ) pulse height spectrum of ^{57}Co showing the 122 keV gamma as a peak with the 136 keV line as distortion on the high energy side of the peak.

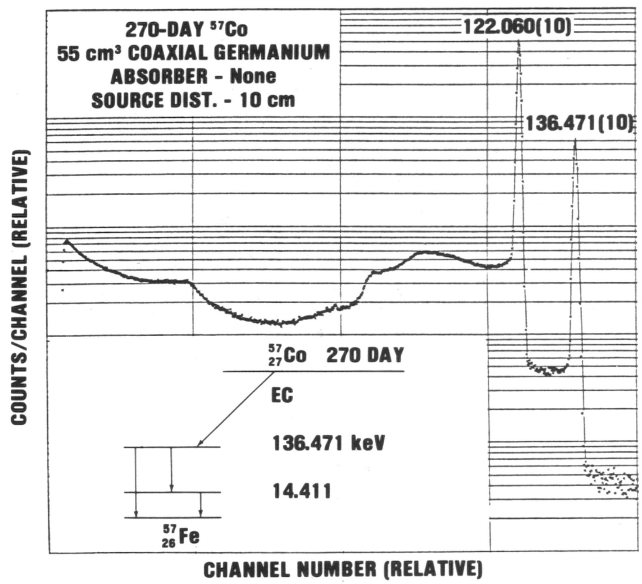

Figure 6.2. Germanium pulse height spectrum of ^{57}Co showing the resolved 122 and 136 keV lines.

Efficiency, however, is another matter. If one considers only the photoelectric interaction, Iodine ($_{53}$I) should be much more efficient than $_{32}$Ge as a detector. In an earlier discussion, it was pointed out that the photoelectric cross section varied as Z^5. This fact alone would indicate that for the same volume detector NaI(Tℓ) should be twelve times as efficient as HpGe. Most manufacturers specify the efficiency of germanium detectors relative to a 3″ x 3″ NaI(Tℓ). The largest HpGe detectors manufactured to date have efficiencies of approximately 50% of the 3″ x 3″ NaI(Tℓ) detectors. Figure 6.3 shows the linear absorption coefficient for germanium as a function of gamma ray energy. Shown on the graph are the contributions from photoelectric, Compton, and Pair Production. It can be seen from fig. 6.3 that the photoelectric process is by far the dominant mechanism below 150 keV. For example, at 20 keV the photoelectric cross section is approximately 200 times the Compton interaction. We will see in the next experiment that the Compton interaction is almost nonexistent in the Si(Li) spectra of these low energy photons. For germanium, the photoelectric and Compton cross-sections are approximately equal at 150 keV. If multiple interactions could not occur in the germanium crystal, the sum under the photopeak would be equal to the sum of the Compton distribution at 150 keV. Figure 6.4 shows a Germanium pulse height spectrum of ^{47}Sc which illustrates this point. In this figure, Σ-β for the Compton is approximately 50,000 counts while Σ-β for the total absorption peak is of the order of 70,000 counts for this 159.3 keV photon. Multiple interactions in the crystal will always tend to make the total absorption peak larger than the photoelectric cross section would predict.

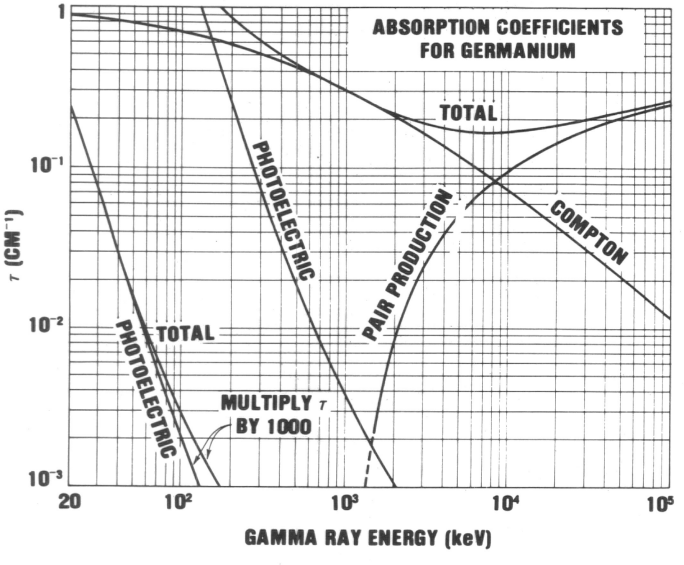

Figure 6.3. Linear absorption coefficients for a HpGe detector showing photoelectric, Compton, and pair production.

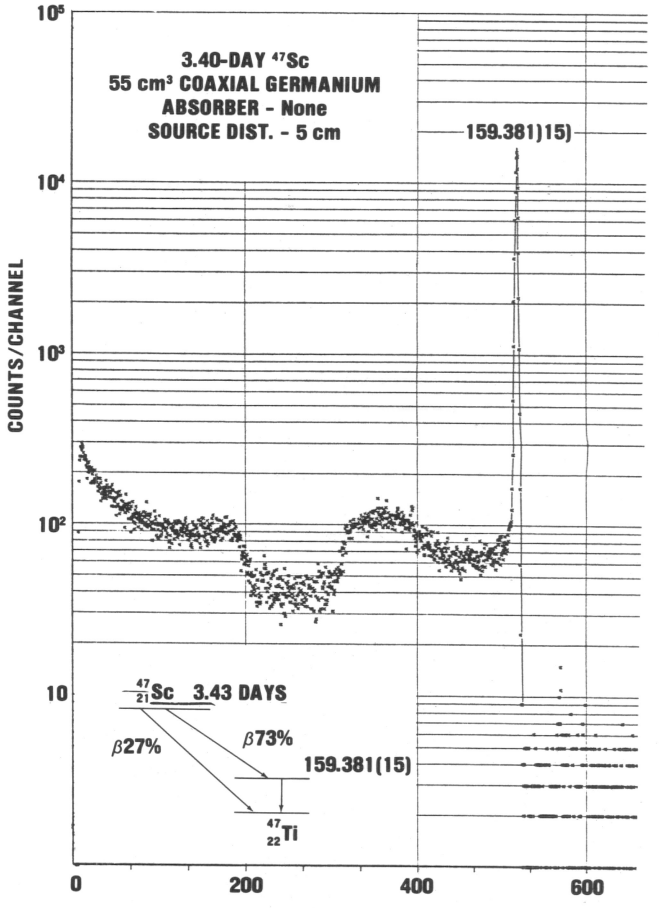

Figure 6.4. Germanium pulse height spectrum of the 159 keV photon from ^{47}Sc. NOTE, at this energy, the photoelectric cross section is approximately equal to the Compton cross section.

At higher photon energies, the Compton distribution becomes more important. At 300 keV, the Compton cross section is five times larger than the photoelectric absorption. By the time 1000 keV is reached, the Compton cross section is 75 times as large as the photoelectric effect. Nevertheless, multiple interactions, primarily Compton scattering, followed by a photoelectric effect will still produce a significant total absorption peak at these higher energies. Figure 6.5 shows a spectrum of ^{54}Mn (834 keV). In the figure, it can be seen that the toal absorption peak is still a dominant feature of the pulse height distribution. In general, these HpGe detectors can be used for incident gamma energies up to 4 MeV or higher, if necessary. Most of the nuclear decay gamma rays, however, are less than 2 MeV and HpGe detectors, therefore, are ideally suited for decay scheme studies.

As in the case of the NaI(Tℓ) detectors studied in experiment number 2, *Pair Production* is theoretically possible at energies greater than 1.02 MeV which is the threshold energy for the process. At 2 MeV the pair production process is at least a factor of 20 greater than the Photoelectric effect. The Compton effect is the dominant mechanism at this energy since it is 6 times the Pair

Production Cross Section. At energies greater than 3 or 4 MeV, it can be seen from fig. 6.3 that Pair Production is becoming the most important reaction mechanism.

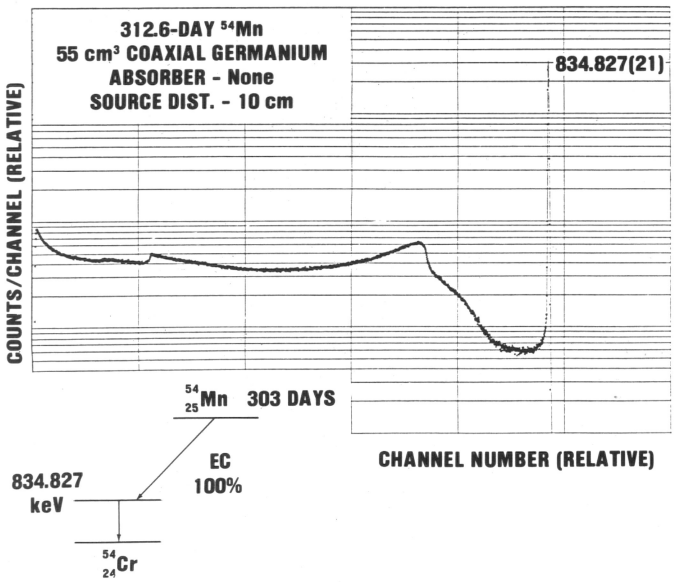

Figure 6.5. Germanium pulse height spectrum of the 834 keV gamma from the decay of ^{54}Mn.

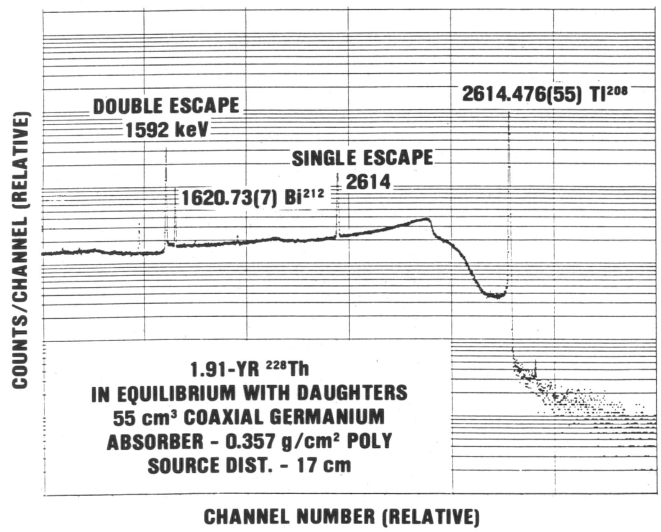

Figure 6.6. Germanium pulse height spectrum of the 1.91 ^{228}Th activity showing the primary 2614 keV gamma and single (2614 keV) and double (1592 keV) escape peaks.

Of course, when the Pair Production process occurs, the single and double escape peaks will be seen in the spectrum at E_0-511 keV and E_0-1020 keV. Figure 6.6 shows the high energy portion of a spectrum from the 1.91 year ^{228}Th Decay. The primary gamma is 2614 keV. The single escape peak (SE) can be seen at 2614 keV and the double escape (DE) group is at 1592 keV.

EXPERIMENT 6.1

Energy Calibration and Resolution of a HpGe Spectrometer

Experimental Procedure

1. Set up the electronics as shown in fig. 6.7. The instructor will provide information in regard to the proper bias voltage and other data for the HpGe detector. The MCA that is used in fig. 7.3 should have at least 2000 channels in order to take advantage of the inherent resolution capabilities of the detector. If a 2000 channel analyzer is not available, the digital offset feature of the MCA or a Biased Amplifier can be used.

2. Place a ^{60}Co source 1 cm from the detector and adjust the gain of the amplifier so that the 1332 keV line falls in approximately channel 1800. Figure 6.8 shows a pulse height spectrum similar to that which should be observed. Record the positions of the 1332 keV and 1173 keV peaks. Store the pulse generator in approximately channel 1900, record the FWHM of the groups. As was mentioned before, many of the modern MCA's or Personal Computer Analyzers (PCA's) have peak search routines that will automatically determine the centroids and FWHM's of the peaks. If these routines are available, use them.

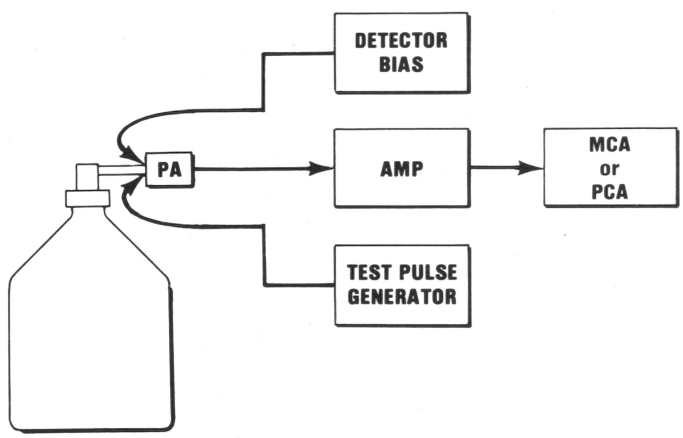

Figure 6.7. Electronics for high resolution gamma experiment with a HpGe detector.

3. Fill in Table 6.1 for the other standard sources that the instructor provides.

4. Obtain the unknown sources and collect spectra for a period of time long enough to clearly determine the peaks of interest.

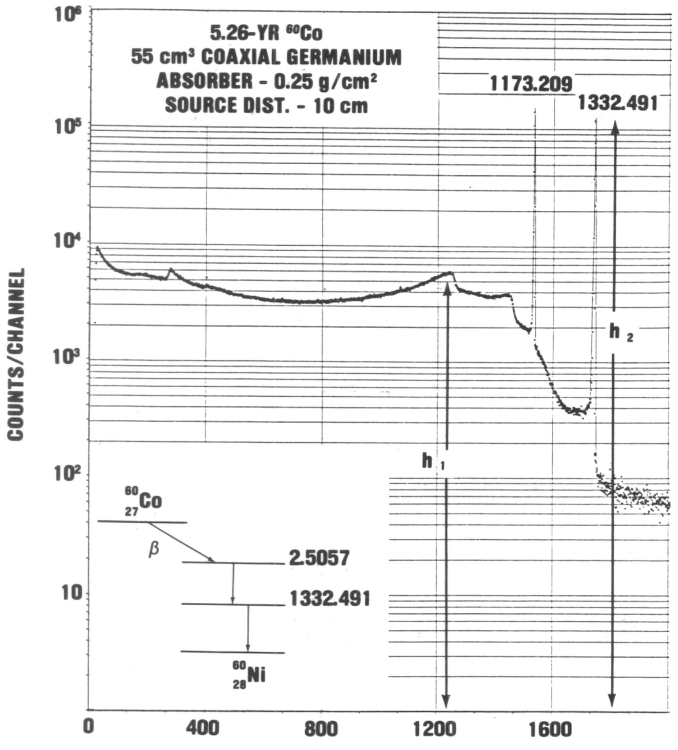

Figure 6.8. Germanium pulse height spectrum of ^{60}Co.

Exercise A From the data collected in Table 6.1, plot a calibration curve for the HpGe detector. From the slope of the calibration curve and the pulser peak, determine the FWHM in keV of each of the peaks in the table. **Note:** A linear least squares fit routine should be used on the calibration data to obtain the best calibration curve for the detector. This is the only method by which a high degree of accuracy can be obtained in the assignment of the unknown energies.

Exercise B Determine the energies of the total absorption peaks of the unknowns. Use Appendix A and ref. 1 and 2 to identify the unknowns.

Exercise C The FWHM of the peaks (keV) recorded in Table 6.1 are a measure of the system resolution R_s. The major components of R_s are given by:

$$R_s = R_d + R_E \qquad (1)$$

where R_d is the resolution of the HpGe detector and R_E is the system Electronic resolution.

The value of R_E can be determined by the FWHM value of the pulse generator that was recorded for the detector in Experimental Procedure 1. From the R_s for the 1332 keV peak from ^{60}Co, determine R_d the true resolution of the detector. How does this value compare to the specified value for the detector?

Table 6.1 Energy Calibration Standards for HpGe Detectors

Isotope	Gamma Energy keV	Intensity of Source γ/s A_1	Peak Channel	$\left(\frac{\Sigma-\beta}{t}\right)$ Photopeak A_3	FWHM keV	Effi-ciency
^{60}Co	1332.491					
^{60}Co	1173.209					
^{65}Zn	1115.518					
^{65}Zn	511.00					
^{54}Mn	834.827					
^{22}Na	1274.511					
^{22}Na	511					
^{137}Cs	661.638					
^{133}Ba	386.851					
^{133}Ba	356.005					
^{133}Ba	302.851					
^{133}Ba	276.397					
^{133}Ba	80.998					
^{57}Co	136.471					
^{57}Co	122.060					

EXPERIMENT 6.2

The Efficiency of a HpGe Detector

Note: All measurements that will be made in experiment number 6.2, will use the same electronic configuration and the same electronic gains, etc. The calibration curve that was determined in experiment 6.1 is therefore valid for all parts of experiment 6.2.

Discussion

This experiment is very similar to the absolute efficiency measurements that were made for the NaI(Tℓ) detector in experiment number 2. Standard sources of the isotopes listed in Table 6.1 will be provided by the instructor. The student will use the activity of the source and ref. 1 to fill in the number of γ/s for each line in the source. The total absorption efficiency of the detector will be determined for each of the sources and an efficiency curve plotted for energies between 81 and 1332 keV. These measurements will be made for a source to detector distance of 25 cm which is the standard geometry for the industry. The efficiency of the HpGe detector for the 1332 keV line from ^{60}Co will be compared to the quoted value for the detector.

Experimental Procedure

1. As stated above, the same energy calibration, etc. that was used in experiment 6.1 will be used in this experiment. Place the standard ^{60}Co source at a distance of 25 cm from the face of the detector. Accumulate a spectrum for a period of time long enough to obtain a (Σ-β) for each peak of at least 4000 counts. Determine (Σ-β) for both gamma groups. Record these values in Table 6.1. Repeat this exact experiment for the other standard sources in Table 6.1.

Exercise A Define:

A_1 = γ/s emitted from the source from Table 6.1
A_2 = γ/s that strike the face of the HpGe detector
A_3 = γ/s that are recorded as total absorption events from the measured spectra
$A_3 = \frac{\Sigma\text{-}\beta}{t}$ from Table 6.1

therefore,

$$A_2 = \frac{A_1}{G_1} \qquad (2)$$

where

$$G_1 = \frac{\text{Area of the detector face (cm}^2\text{)}}{4\,\pi\,S_1^2}$$

S_1 = 25 cm

The total absorption efficiency ε_{TA} is given by:

$$\varepsilon_{TA} = \frac{A_3}{A_1} \qquad (3)$$

Calculate ε_{TA} for all of the energies recorded in Table 6.1. Plot the efficiency curve of ε_{TA} vs Eγ. How does the value of ε_{TA} at 1332 keV compare to the quoted value for the detector? From the definitions above, ε_{TA} is the ratio of photons counted as total absorption to those that leave the source.

EXPERIMENT 6.3

Determination of an Unknown Gamma Activity by the Absolute Method

Experimental Procedure

1. For this experiment the instructor will provide ^{137}Cs and ^{60}Co sources of unknown activity. Place the ^{137}Cs source exactly 25 cm from the face of the HpGe detector. Count for a period of time long enough to obtain 4000 counts in the 662 keV line. Determine (Σ-β/t)

2. Count the ^{60}Co source for a time long enough to get 3000 counts in the 1332 keV peak. Determine Σ-β/t

Exercise A From the plot of ε_{TA} vs Eγ in experiment 6.2 determine ε_{TA} for the 662 keV line in ^{137}Cs and also for the 1332 and 1173 keV gammas in ^{60}Co. Please note from **exercise a** experiment 6.2, A_3 has been determined from the above measurements. Use eq. (3) to find A_1.

Note: In the case of ^{60}Co, the activity of the source can be determined independently by both gamma groups. The answers should agree within 6%. Of course, in all three measurements, ref. 1 will have to be used to determine the activity of the sources since the fraction of gammas per decay is needed for this calculation. Figure 6.9 shows a typical pulse height spectrum for ^{137}Cs.

Exercise B Figure 6.8 shows a Germanium spectrum for ^{60}Co. A figure of merit that is often quoted for these detectors is the peak to Compton ratio. From the readout, determine h_2 and h_1 in fig. 6.8 and calculate h_2/h_1. How does this compare to the accepted value that the instructor has given to the class?

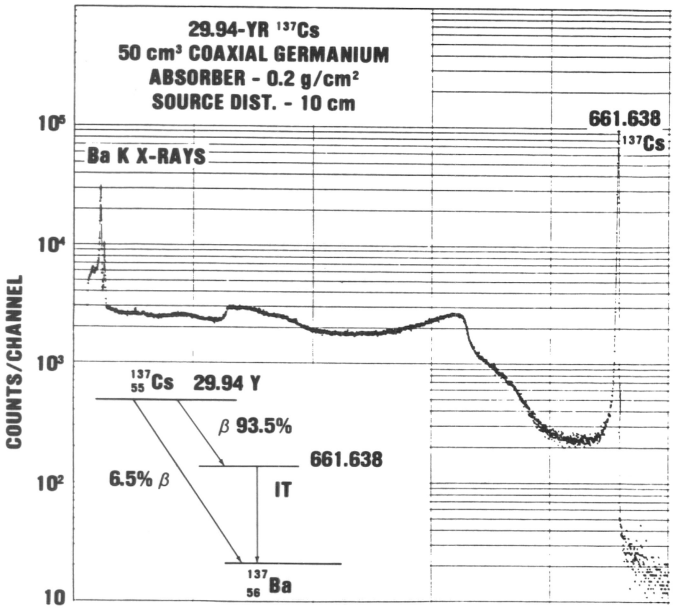

Figure 6.9. Germanium pulse height spectrum for the 662 keV line of ^{137}Cs. NOTE, for this spectrum Σ-β can easily be determined either by hand, or, if available, one of the computer fitting programs.

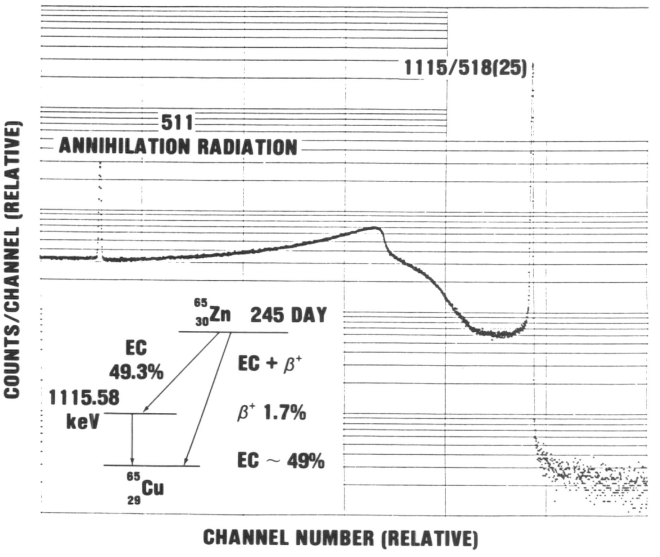

Figure 6.10. Germanium pulse height spectrum of ^{65}Zn. NOTE, the low energy portion of this spectrum has been cut off to emphasize the high energy region.

EXPERIMENT 6.4

Determination of an Unknown Activity by the Relative Method

Discussion

Figure 6.10 shows a pulse height spectrum of the 245 day ^{65}Zn activity. The instructor will provide a ^{65}Zn source of known activity and one of unknown activity. The simplest way to accurately determine the activity of the unknown ^{65}Zn source is to compare the unknown to the known under identical geometric conditions. This ratio method is of course valid for any isotope if a known and unknown are available for that isotope.

Experimental Procedure

1. Obtain the known activity ^{65}Zn source from the instructor. Place it 25 cm from the face of the HpGe and count for a period of time long enough to obtain $(\Sigma\text{-}\beta)_k$ in the photopeak of 4000 counts. Determine $(\Sigma\text{-}\beta/t)_k$ for the known source.

2. Repeat this measurement for the unknown activity ^{65}Zn source.

Calculate $(\Sigma\text{-}\beta/t)$ for this source.

Exercise A

$$\frac{A_{uk}}{A_k} = \frac{\left(\frac{\Sigma\text{-}\beta}{t}\right)_{uk}}{\left(\frac{\Sigma\text{-}\beta}{t}\right)_k} \qquad (4)$$

where A_{uk} is the activity of the unknown.

Calculate A_{uk} from eq. (4).

Exercise B The same results should be obtained if the ratios of the 511 keV peaks are used instead of the 1115.518 keV lines. Repeat the calculation for the 511 keV groups. Are the answers the same?

EXPERIMENT 6.5

The Study of a Complex Decay Scheme by High Resolution HpGe Spectroscopy

Discussion

Most of the decay schemes that have been studied in this manual have been rather simple. It is possible with the HpGe detector to study a more complex isotope. The gamma spectrum of ^{133}Ba is shown in fig. 6.11. The nine major gammas that constitute the decay of this isotope are shown on the figure. The decay scheme with these gammas and their intensities, relative to the 356.005 keV transition (γ_8), are shown in fig. 6.12. All of the numbers

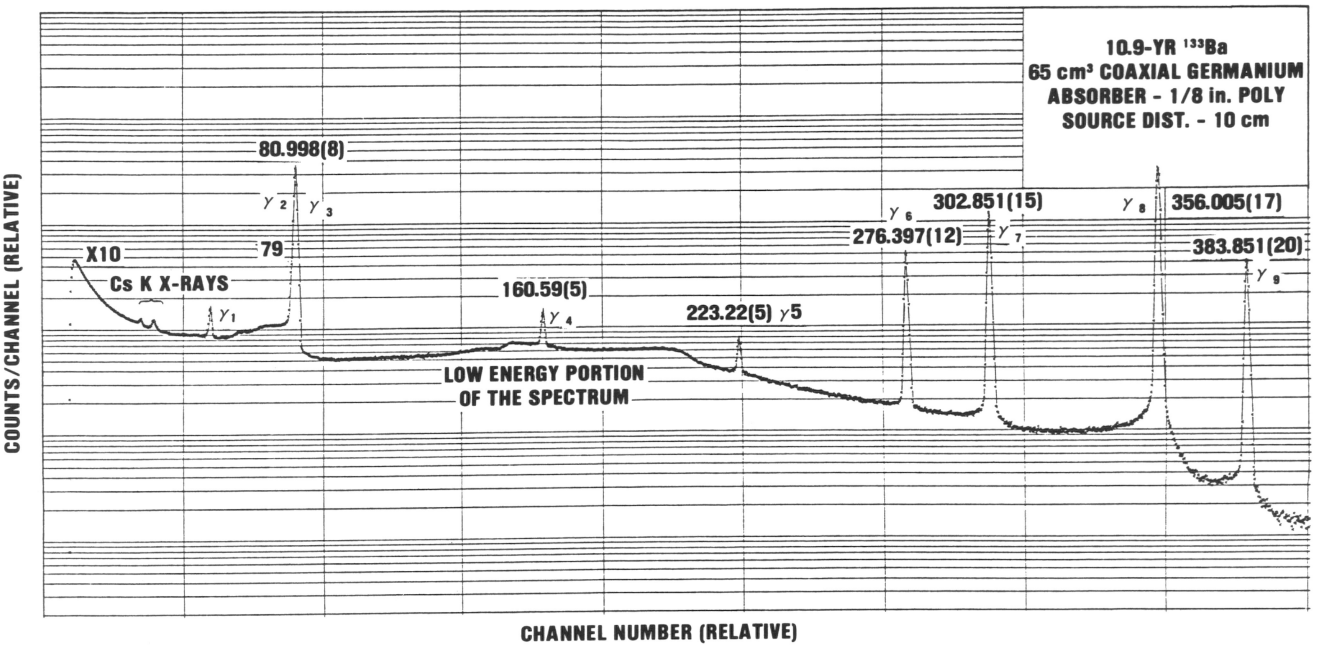

Figure 6.11. Germanium spectrum of $^{133}_{56}$Ba showing the nine major gamma lines that are tabulated in fig. 6.12.

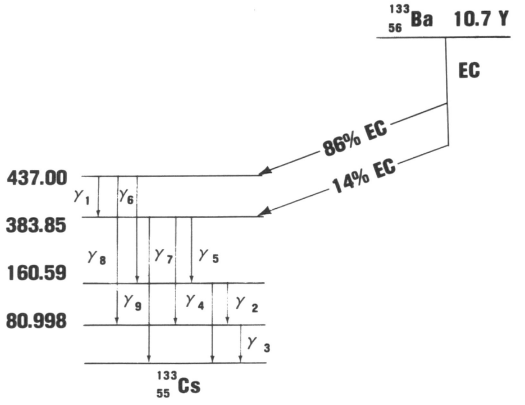

that appear in fig. 6.12 were taken from the most recent tabulation which is given in ref. 1. In this experiment, the absolute efficiency curve that was constructed in experiment 6.2 will be used to verify the *Intensity Ratios* that are listed in fig. 6.12.

Experimental Procedure

1. Obtain the ^{133}Ba source from the instructor and position it 25 cm from the face of the detector (on axis). Count for a period of time long enough to obtain Σ-β of 1000 counts in γ_5 (223.22 keV). Determine (Σ-β/t) for the nine gamma groups shown in fig. 6.11. Record these values on the Table in fig. 6.12.

Gamma Designation	Eγ	Intensity Relative to γ_8 from Reference No. 1	Measured (Σ-β/t)	Σ_{TA} From Expt. 6.2	Measured Relative Intensity Normalized to 356.005 keV
γ_1	53.15	3.78			
γ_2	79.63	4.5			
γ_3	80.998	55.3			
γ_4	160.590	1.16			
γ_5	223.22	0.74			
γ_6	276.397	11.43			
γ_7	302.851	29.29			100.00
γ_8	356.005	100.00			
γ_9	383.851	14.47			

Figure 6.12. Decay scheme for $^{133}_{56}$Ba showing the designation gamma lines that are present in the Germanium spectrum.

2. From the efficiency curve plotted in experiment 6.2 for ε_{TA} vs $E\gamma$, read off the ε_{TA} values for each of the gamma energies listed in fig. 6.12. Record these values in the Table.

Exercise Divide each of the $(\Sigma\text{-}\beta/t)^5$ by the corresponding ε_{TA} to obtain the absolute counting rates for the gamma groups. In order to normalize these activities to the 356.005 keV gamma, it is necessary to divide all of the absolute counting rates by the absolute counting rate for the 356.005 keV group. How do the answers compare to those listed in fig. 6.12. They should be within $\pm 8\%$.

EXPERIMENT 6.6

A Study of Pair Production Escape Peaks in ^{228}Th

Discussion

Figure 6.6 shows a portion of the high energy gamma spectrum from ^{228}Th. Shown in the spectrum are the 2614 keV gamma transition and its single (2614 keV) and double (1592 keV) escape peaks. In this experiment, the probability of single and double escape will be studied.

Experimental Procedure

1. Obtain the ^{228}Th source from the instructor and place it 3 cm away from the detector (on axis).

2. Record a spectrum in the MCA for a period of time long enough to obtain 2000 counts in the single escape peak. Record the time and calculate $\Sigma\text{-}\beta/t$ for each of the three groups.

Exercise The ratio of the $(\Sigma\text{-}\beta/t)$ for each of the groups is proportional to the efficiency for that process. Therefore,

$$\varepsilon_{FE} = K \frac{(\Sigma\text{-}\beta)}{t} \quad \text{full energy} \qquad (5)$$

$$\varepsilon_{SE} = K \frac{(\Sigma\text{-}\beta)}{t} \quad \text{single escape} \qquad (6)$$

$$\varepsilon_{DE} = K \frac{(\Sigma\text{-}\beta)}{t} \quad \text{double escape} \qquad (7)$$

Now calculate

$$\frac{\varepsilon_{SE}}{\varepsilon_{FE}} \quad \& \; ; \quad \frac{\varepsilon_{DE}}{\varepsilon_{FE}}$$

For the detector that was used, these values give an indication of the probabilities of single and double escape for a 2614 keV gamma interaction.

REFERENCES FOR *EXPERIMENT 6*

1. C. M. Lederer and V. S. Shirley, Eds., *Table of Isotopes*, 7th Edition, John Wiley and Sons, Inc., New York (1978).

2. R. L. Heath, "Scintillation Spectrometry," *Gamma-Ray Spectrum Catalog*, **1** and **2**, Report No. IDO-16880. Available from the National Technical Information Service, U.S. Dept. of Commerce, Springfield, Virginia. (All of the Germanium gamma spectra in this manual were taken from the reference.)

3. G. F. Knoll, *Radiation Detection and Measurement*, John Wiley and Sons, New York (1979).

4. K. Siegbahn, Ed., *Alpha-, Beta-, and Gamma-Spectroscopy*, North Holland Publishing Co., Amsterdam (1968).

5. S. M. Shafroth, Ed., *Scintillation Spectroscopy of Gamma Radiation*, Gordon and Breach, London (1967).

6. *Radiological Health Handbook*, U.S. Dept. of Health, Education, and Welfare, PHS Publ. 2016. Available from National Technical Information Service, U.S. Dept. of Commerce Springfield, Virginia.

7. A. Coche and P. Siffert, *Lithium Drifted Silicon and Germanium Detectors in Semiconductor Detectors*, G. Bertolini and A. Coche Eds., Elsevier-North Holland, Amsterdam (1968).

8. F. Adams and R. Dams, *Applied Gamma Ray Spectrometry*, 2nd Edition, Pergammon Press, Ltd. (1970).

9. D. M. Walker and J. M. Palms, *IEEE Trans. Nucl. Sci.* **NS-17**(3). 296 (1970).

EXPERIMENT 7

High Resolution X-Ray Spectroscopy

Discussion

In experiment number 2, the resolution of a NaI(Tℓ) detector for ^{137}Cs was measured. It was found that, for a good detector, the resolution was about 7%. If this is converted to keV, the results are 46 keV. In the present experiment, it will be found that these High Resolution X-Ray detectors Si(Li) have resolutions as low as 148 eV for the 5.9 keV Kα x-ray from ^{54}Mn. This excellent resolution will allow the researcher to distinguish x-rays from adjacent elements for most of the periodic chart. In the experiment on x-ray fluorescence (Experiment 8) it will be seen that this resolution allows us to characterize materials and easily identify the elements in an unknown alloy. These Si(Li) detectors are nearly 100% efficient for photons in the range from 4 keV to 25 keV. Below 4 keV the entrance beryllium window of the detector and other effects associated with x-ray attenuation cause the efficiency to decrease significantly. They can still be used at energies lower than 4 keV, but the efficiency drops off significantly. It is also quite difficult to measure the absolute efficiency of these Si(Li) detectors below 3 keV because suitable radioactive sources are not available in this low energy realm. One of the problems is that the sources themselves have so much self absorption that the absolute disintegration rate is hard to determine. Nevertheless, Si(Li) detectors have been used (see ref. 1) to measure Kα x-rays from ^{19}F which have an energy of only 677 eV. With the development of new entrance windows, it is now possible to see Boron Kα x-rays at 185 eV. To give an appreciation for the window problem, this sheet of paper would attenuate nearly all of the 185 eV x-rays that tried to pass through.

In this experiment, the Si(Li) detector will be used to study the x-rays that are given off during radioactive decay. Since the detector has excellent resolution capabilities, it will be possible to determine with high precision the x-ray energies present and hence the unknown radioisotope. The two most pronounced decay mechanisms that have x-rays in their decay scheme are Electron Capture (EC) and Internal Conversion (IC). Figure 7.1 shows the decay schemes of ^{57}Co, ^{54}Mn, ^{55}Fe, and ^{65}Zn which are four of the more common isotopes that are used to calibrate these Si(Li) detectors. All of these isotopes will produce x-rays characteristic of the daughter nuclide. For example, the ^{55}Fe source from fig. 7.1 would show characteristic Kα and Kβ x-rays from ^{55}Mn. In Appendix B of this manual, we have printed the x-ray critical Absorption and Emission Energies for all elements. If one looks at this chart, Mn Kα = 5.98 keV and Kβ = 6.49 keV. Figure 7.2 shows a spectrum that was measured for an ^{55}Fe source showing the ^{55}Mn Kα and Kβ x-rays. It is very important that the student remembers that the x-rays from a radioactive source are characteristic of the *daughter* and not the parent. If this fact is not remembered, every calibration curve that is drawn will be in error.

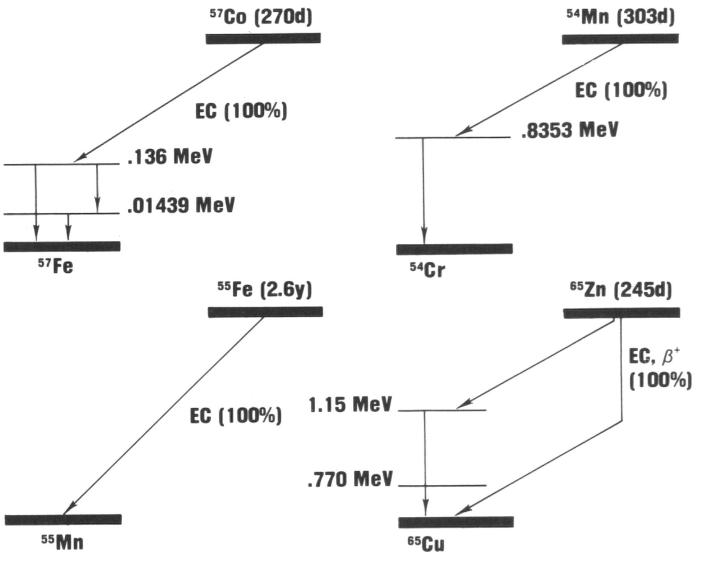

Figure 7.1. Decay schemes of ^{57}Co, ^{55}Fe, ^{54}Mn and ^{65}Zn.

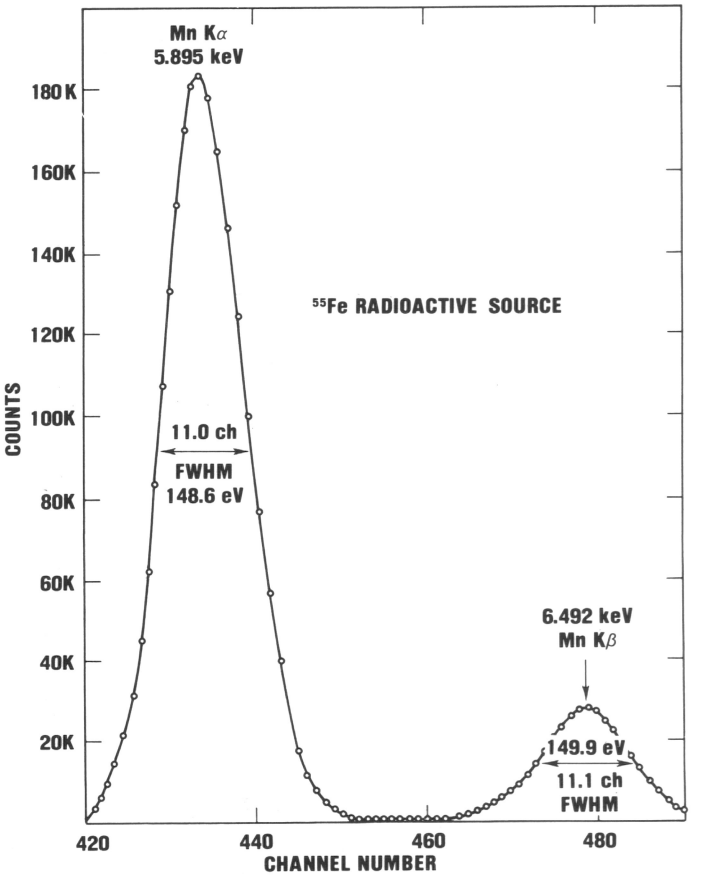

Figure 7.2. Pulse height spectrum of an ^{55}Fe source, showing the daughter ^{55}Mn Kα and Kβ x-rays. (Courtesy of C. D. Moak, Oak Ridge National Laboratory.)

Table 7.1 shows a listing of some of the more common isotopes that are used in calibrating Si(Li) detectors or in efficiency measurements.

Table 7.1 Calibration Sources for Si(Li) Detectors

Nuclide	Energy of X-Rays and Low-Energy Gamma (keV)	Energy of High-Energy Gamma (keV)	Intensity Ratio X/γ
^{54}Mn	5.414 (Kα) 5.946 (Kβ)	834.8	0.2514 (±0.5%) Kα + Kβ
^{57}Co	6.40 (Kα) 7.06 (Kβ) 14.43 (γ)	122.1	0.5727 (±2.0%) 0.7861 (±2.9%) 0.112 (±1.8%)
^{65}Zn	8.04 (Kα) 8.9 (Kβ)	1115.5	0.6596 (±0.8%) 0.0911 (±2.0%)
^{241}Am	11.89 N_pL_l 13.90 $N_pL\alpha$ 17.9 $N_pL\beta$ 20.8 $N_pL\gamma$ 26.35 γ	59.5	0.022 0.375 0.512 0.138 0.07
^{85}Sr	13.38 (Kα) 15.0 (Kβ)	514.0	0.5020 (±0.65%) 0.0880 (±1.4%)
^{88}Y	14.12 (Kα) 15.85 (Kβ)	898.0	0.5491 (±1.2%) 0.0989 (±1.9%)
^{109}Cd	22.10 (Kα) 25.0 (Kβ)	88.0	22.02 (±4.9%) 4.68 (±5.0%)
^{113}Sn	24.14 (Kα) 27.4 (Kβ)	391.7	1.219 (±3.5%) 0.267 (±3.6%)
^{137}Cs	32.1 (Kα) 36.6 (Kβ)	661.6	0.0666 (±3.0%) 0.0159 (±3.1%)
^{139}Ce	33.29 (Kα) 38.0 (Kβ)	165.9	0.808 (±11%) 0.195 (±11%)
^{198}Au	70.15 (Kα) 80.7 (Kβ)	411.8	0.0229 (±2.3%) 0.00635 (±2.4%)
^{203}Hg	72.11 (Kα) 83.0 (Kβ)	279.2	0.1247 (±2.1%) 0.0348 (±2.3%)

In the electron capture process, for example ^{55}Fe, the ^{55}Fe nucleus captures a K or L shell orbiting electron. The daughter nucleus that is immediately formed is ^{55}Mn since there are now only 25 protons in the nucleus. If a K shell electron was captured, then there is a vacancy in the K shell for the daughter ^{55}Mn. In general, this vacancy will be filled by an L shell electron falling into the vacancy. The result is the Kα x-rays from ^{55}Mn. This is why the daughter x-rays are always seen.

Figure 7.3 is a diagram showing the atomic energy levels that are involved in x-ray emission. The Kα ^{55}Mn x-ray shown in fig. 7.2 results when an L_{III} electron falls into the vacancy that is produced in the K shell of Mn resulting from Electron Capture.

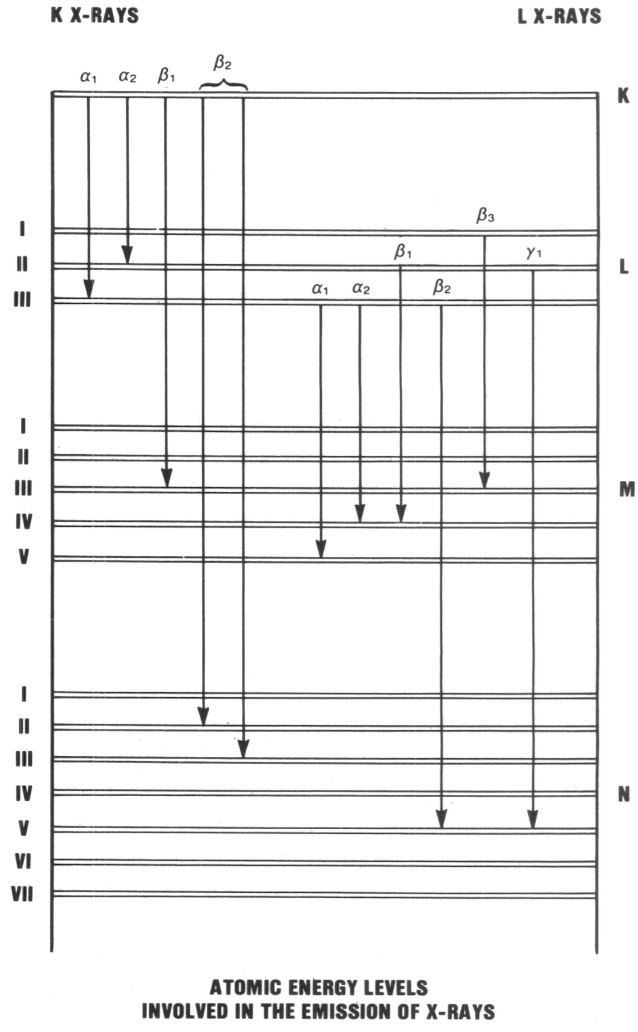

Figure 7.3. Atomic energy levels involved in the emission of x-rays.

The L_{II} and L_{III} electron binding energies are too close together to resolve Kα_1 and Kα_2 and hence in using the X-ray Emission Chart in Appendix B, the Kα_1 energy is usually recorded.

Likewise, the Kβ energy is the only x-ray that will be observed when the initial K shell vacancy is filled with an M electron falling into the vacancy. For elements lighter than $_{40}$Zr, the K shell spectrum will always look similar to the $_{55}$Mn, Kα and Kβ peaks shown in fig. 7.2. The intensity ratios of the Kα and Kβ will also look like they do in the figure for most elements below $_{40}$Zr. When an L shell electron falls into a K shell vacancy, K x-rays are observed, but there now also exists a vacancy in the L shell. From fig. 7.3, we would expect to see an Lα_1 x-ray

when an M_v electron falls into an L vacancy. This in fact happens, but in the case of ^{55}Mn, the L x-rays are only 600 eV and they do not have enough energy to penetrate the window of the detector and hence are not measured with the Si(Li) detector used in this experiment. L-x-rays from $_{51}Sb$ (3.60 keV) are just high enough to be seen with the detector. Hence, the L x-rays for anything heavier than $_{51}Sb$ will show up if they are present in the decay scheme of the source. For example, fig. 7.4 shows the Lα and Lβ, and Lγ lines from Au.

Scope

In this experiment a Si(Li) detector will be calibrated with a pulse generator and radioactive sources. Next, the energies of x-rays from several unknown isotopes will be

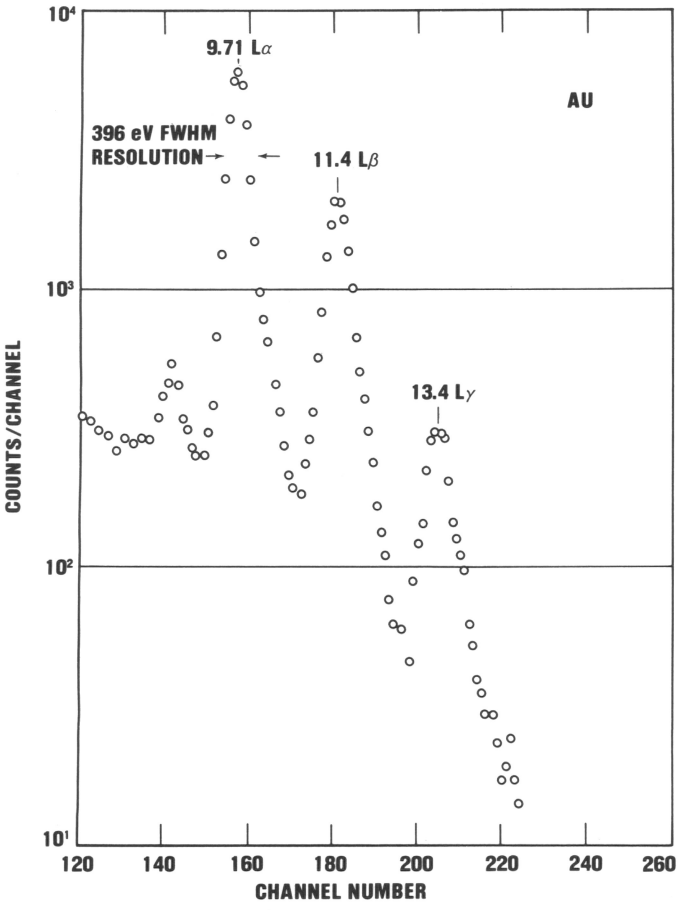

Figure 7.4. L x-rays from gold showing the characteristic Lα and Lβ, and Lγ lines.

determined and hence identify these unknown by the daughter x-rays. The absolute efficiency of the detector will be determined using standard x-ray sources. Entrance window effects will be studied. The next section of this experiment deals with the probability of L and M shell x-rays filling a K vacancy as shown in fig. 7.3. Finally, the attenuation of x-rays in thin foils will be studied and the linear absorption coefficient measured for low energy x-rays.

EXPERIMENT 7.1

Energy Calibration and Detector Resolution

Experimental Procedure

1. Set up the electronics as shown in fig. 7.5. Adjust the detector bias voltage to its recommended value. Place the ^{55}Fe source about 1 cm from the window of the detector. **Caution:** Never touch the beryllium window of these detectors with anything. The beryllium window is very fragile and will certainly break if it is touched. Use 1000 channels of the MCA.

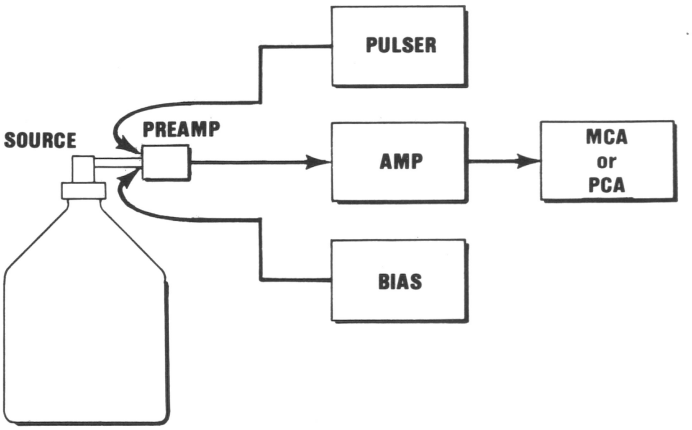

Figure 7.5. Electronics for high resolution Si(Li) x-ray measurements.

2. Adjust the gain of the amplifier so that the 5.898 keV peak from the ^{55}Fe source falls roughly in channel 250. The spectrum that is observed should be similar to fig. 7.2. Record the exact channel C_0 where this 5.898 keV peak occurs. Remove the source.

3. Turn on the pulse generator and set the pulse height dial to 58.9/1000. Adjust the calibrate control on the pulser until the pulser peak is exactly in channel C_0. The pulser is now calibrated such that 5.89 keV corresponds to 58.9 divisions, therefore, 100 divisions = 10 keV, etc. In order to make the indicated energy calibration, the pulse readings should be stored in the MCA for all of the values shown in Table 7.2.

Table 7.2 Pulse Generator Calibration Data

Run No.	Pulser Pulse Height	Energy keV	Channel No.
1	250/1000	25.0	
2	200/1000	20.0	
3	150/1000	15.0	
4	100/1000	10.0	
5	75/1000	7.5	
6	50/1000	5.0	
7	25/1000	2.5	

4. Obtain the unknown x-ray sources from the instructor and measure each of them for a time period long enough to clearly identify the centroids of the peaks of interest. Use the cursor or the MCA programs to find the centroids of the peaks of interest. Record the centroids and FWHM's of the pronounced peaks.

Exercise From the pulser calibration curve, determine the energies and resolutions of the x-ray peaks from the unknowns. Use the x-ray table in Appendix B to find the daughter isotope and hence the unknown. Figure 7.6 shows a rather complicated unknown, ^{241}Am. Figure 7.7 shows the alpha decay of ^{241}Am to low lying levels in ^{237}Np.

In fig. 7.6, the 26.36 keV gamma originates from gamma decay. This decay is seen on fig. 7.7 as decay from the 2nd excited state (60 keV) to the first excited state (33 keV). The Pt L x-rays are produced by the alpha particles from the source fluorescing the Pt blank. This process of x-ray fluorescence will be discussed in the next experiment. The Np L x-rays are produced by the Internal Conversion of the low lying levels of ^{237}Np.

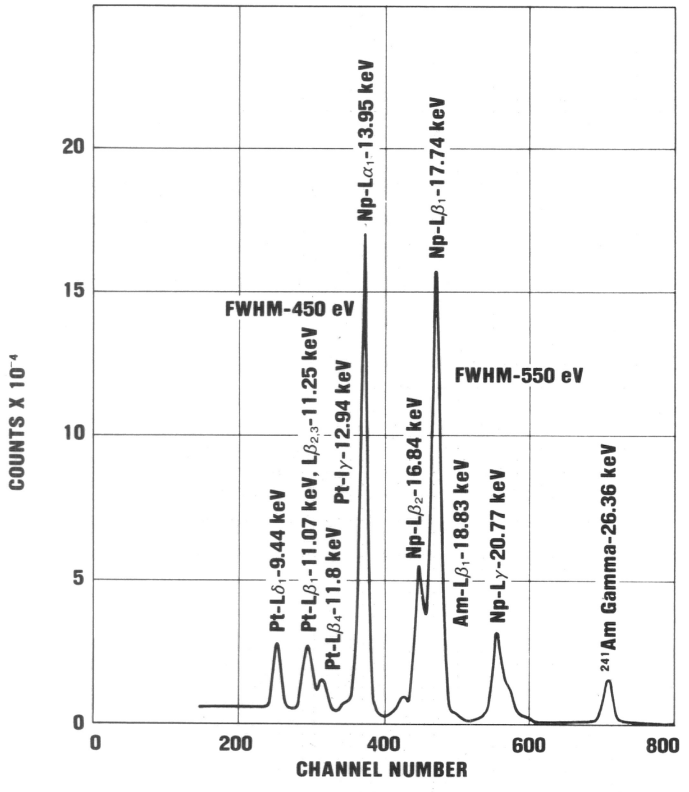

Figure 7.6. X-ray spectrum from a ^{241}Am source which has been electrodeposited on a Pt blank.

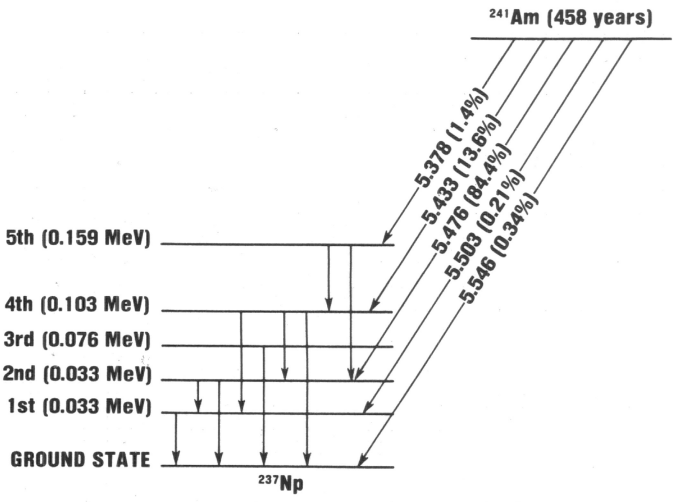

Figure 7.7. Decay scheme for ^{241}Am to levels in ^{237}Np.

EXPERIMENT 7.2

Efficiency Measurements for a Si(Li) Detector

Discussion

It was mentioned in our earlier discussion that these detectors are nearly 100% efficient for x-rays from 4 to 25 keV. Figure 7.8 shows a typical efficiency curve. It will be seen when the experiment is done that there is a great deal of theory and experimental technique associated with producing and understanding fig. 7.8. For a detailed description of both the theory and techniques, the student is referred to the wealth of papers in the literature on this subject. See for example, refs. 2-4. The main features of the efficiency curve are governed both at the high and low energy ends by:

$$I = I_o e^{-\mu x} \qquad (1)$$

For the energies that will be considered in this report, μ is almost all photoelectric absorption.

On the high energy end of the efficiency curve, the Silicon crystal thickness (from 3 to 5 mm) starts to become a limiting factor. Therefore, as we go to higher energies, μ_{PE} in eq. (1) decreases and hence the efficiency continues to decrease. For energies below 4 keV, another attenuation phenomena enters the picture. If the Si(Li) detector didn't have a window, silicon dead layer, or gold electrode layer, it would be 100% efficient for all x-rays below 4 keV. The construction of these detectors, however, requires that all of these components be there and hence, the low energy x-rays are severely attenuated

before they actually reach the crystal. Therefore, at energies below 4 keV, μ_{PE} in eq. (1) is given by the following photoelectric linear absorption coefficients:

$$\mu_{PE} = \mu_{BE} + \mu_{AU} = \mu_{Si} \qquad (2)$$

By using calibrated x-ray standard sources of various energies, it is possible to measure the absolute efficiency of the detector. From the efficiency curve, the x-ray activity of an unknown source can be determined.

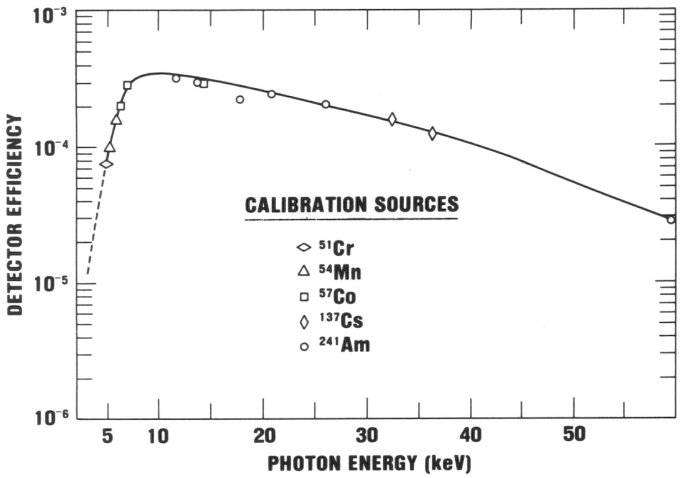

Figure 7.8. Typical efficiency curve for a Si(Li) x-ray detector.

Experimental Procedure

1. Use the same energy calibration that was determined in Experiment 7.1. Obtain the standard x-ray sources from the instructor. Table 7.1 shows some of the more commonly used isotopes for efficiency measurements. **Note:** The number of x-rays per second is needed from each of the sources that are used. In Table 7.1, the last column shows X/γ which is the ratio of x-rays to gammas for that source. To get the number of x-rays per second for the source, the student will have to go to the decay scheme for that isotope in the Table of Isotopes (ref. 7). Once the number of x-rays/sec is established for each source, the efficiency calibration is quite easy.

2. Place the first calibrated source at a distance of 5 cm from the center of the detector and accumulate a spectrum for a time period long enough to get reasonable statistics in the peaks of interest. Repeat this 5 cm measurement for the other standard sources that are supplied by the instructor.

Exercise From the information that is provided by the instructor and the Table of Isotopes, calculate the number of x-rays/sec for each source. **Note:** In this calculation, the half life of the isotope will also have to be considered. The efficiency is given by:

$$\varepsilon = \frac{A_1}{A_0} \quad \frac{4\pi S^2}{A_d}$$

where

A_1 = The number of x-rays/s that are measured for a given source
A_0 = The activity of that source in x-rays/s
A_d = The area of the Si(Li) detector in mm^2
S = 50 mm

Calculate ε for each source and plot an efficiency curve similar to fig. 7.8.

EXPERIMENT 7.3

Intensity Ratios for Daughter X-Rays from Radioactive Sources

Discussion

Figure 7.2 shows a pulse height spectrum of the daughter ^{55}Mn, Kα and Kβ x-rays from an ^{55}Fe source. It was pointed out in an earlier discussion that the Kα and Kβ x-rays (see fig. 7.3) are too close together to resolve with these Si(Li) detectors. They are therefore seen as one group in fig. 7.2. The Kβ_1, Kβ_2 and Kβ_3 x-rays also appear as one group for the same reason. For heavier elements, the Bohr theory predicts that the individual energy levels will become farther apart and hence, the separation of the fine structure x-ray groups might be possible. Figure 7.9 shows the well resolved Kα_1 and Kα_2 lines from $_{80}Hg$. From Appendix B it can be seen that the K shell binding energy (K_{ab}) for $_{80}Hg$ is 83.106 keV. The L_{II} binding energy is 14.212 keV and L_{III} is 12.285 keV. From fig. 7.3:

$$K\alpha_1 = K_{ab} - L_{III} = (83.106\text{-}12.285)\ \text{keV} \qquad (4)$$
$$= \underline{70.821\ \text{keV}}$$

and

$$K\alpha_2 = K_{ab} - L_{II} = (83.106\text{-}14.212)\ \text{keV} \qquad (5)$$
$$= \underline{68.894\ \text{keV}}$$

Therefore, the energies of Kα_1 and Kα_2 are easily resolvable for these heavy elements. A similar argument can be made for Kβ_1 and Kβ_2 that are seen in fig. 7.9. Figure 7.10

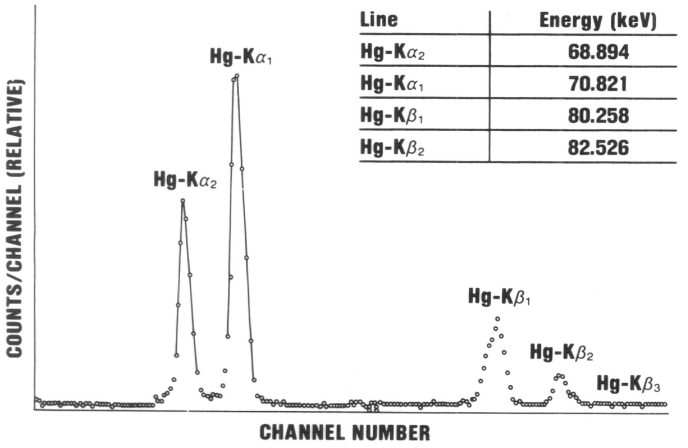

Line	Energy (keV)
Hg-Kα2	68.894
Hg-Kα1	70.821
Hg-Kβ1	80.258
Hg-Kβ2	82.526

Figure 7.9. High resolution germanium spectrum of $_{80}$Hg x-rays showing the resolved (Kα_1, Kα_2) and (Kβ_1, Kβ_2) groups.

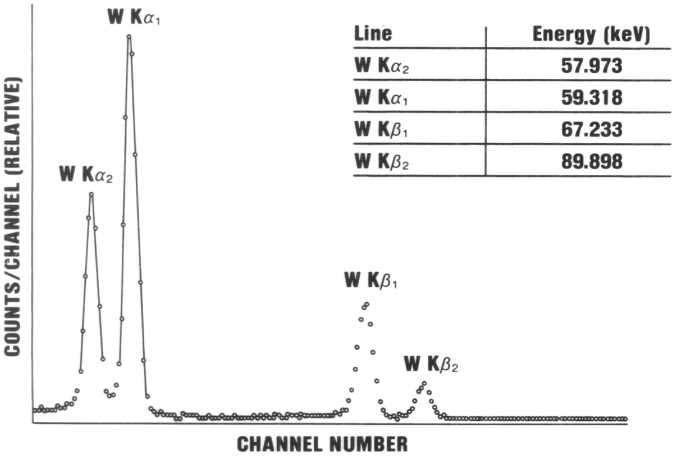

Line	Energy (keV)
W Kα2	57.973
W Kα1	59.318
W Kβ1	67.233
W Kβ2	89.898

Figure 7.10. High resolution germanium spectrum of $_{74}$W x-rays showing the resolved (Kα_1, Kα_2) and (Kβ_1, Kβ_2) groups.

Table 7.3 Kα/Kβ Ratios for Some Common Nuclei

Element	Kα/Kβ	Element	Kα/Kβ
$_{24}$Cr	7.40	$_{38}$Sr	5.05
$_{26}$Fe	7.40	$_{42}$Mo	5.07
$_{28}$Ni	7.40	$_{44}$Ru	4.90
$_{30}$Zn	7.24	$_{46}$Pd	4.76
$_{32}$Ge	6.80	$_{48}$Cd	4.69
$_{34}$Se	6.37	$_{50}$Sn	4.54
$_{36}$Kr	5.81	$_{56}$Ba	4.22
$_{40}$Br	5.26		

shows that for $_{74}$W these groups are still resolved. Figure 7.4 illustrates a similar behavior for Lα, Lβ, Lγ from $_{79}$Au.

Scope

In this experiment the Kα to Kβ ratios for ^{57}Co, ^{55}Fe, ^{65}Zn and ^{54}Mn will be measured. The results will be compared to the tabulated results that are found in the literature. From fig. 7.3 the Kα x-rays occurs when L_{II} and L_{III} electrons fall into the K vacancy. The Lβ_1 x-rays occur when a K vacancy is filled by an M_{III} electron. The ratio of Kα to Kβ therefore gives an indication of the probability ratio of either an L or M shell electron falling into a given K vacancy. Experimentally (see fig. 7.2), it amounts to the sum under the Kα peak divided by the sum under the Kβ peak.

Experimental Procedure

1. Use the same energy calibration that was determined in Experiment 7.1. Count the ^{57}Co source for a period of time long enough to obtain at least 2000 counts in the Kβ group. Determine (Σ-β) for the Kα and Kβ groups. Record these sums.

2. Repeat the above measurement for the ^{55}Fe, ^{65}Zn, and ^{54}Mn sources. Determine (Σ-β) for the Kα and Kβ groups for these sources.

Exercise From the data, determine $(\Sigma-\beta)_K\alpha/(\Sigma-\beta)_K\beta$. How do the results compare with the tabulated ratios in Table 7.3? Figure 7.11 shows pulse height spectra from ^{57}Co and ^{67}Zn sources that were taken simultaneously with the same detector.

EXPERIMENT 7.4

X-Ray Absorption in Thin Foils

Discussion

In experiment 7.2, eq. (1) shows:

$$I = I_o e^{-\mu_{PE} x} \qquad (1)$$

where μ_{PE} is the photoelectric cross section for the element being considered. Table 7.4 shows the photoelectric cross sections in cm^2/g for six elements. These cross sections are tabulated for x-rays that come from commonly available sources. This experiment is quite similar to the gamma attenuation measurement that was done in experiment number 2. The only difference is that in this experiment, low energy photons are being used and the attenuation foils are quite thin.

Scope

The half value layer for the 8.04 keV x-rays from a ^{65}Zn source will be measured in copper and aluminum. From this data the x-ray cross section in cm^2/g will be determined. These values will then be compared to the accepted values in Table 7.4.

Experimental Procedure

1. Use the same energy calibration that has been implemented in the other parts of this experiment. Place the ^{65}Zn source far enough away from the Si(Li) detector so that the absorber foils can easily be placed between the source and the detector.

2. Store a spectrum in the MCA for a time period long enough to obtain 5000 counts under the 8.047 keV Kα peak. Calculate Σ-β/t for the peak.

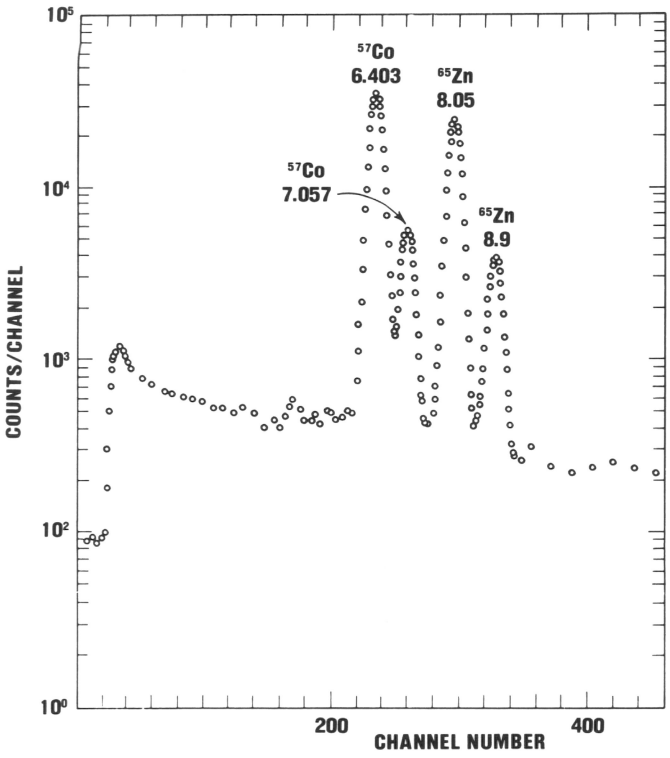

Figure 7.11. Si(Li) spectra from ^{57}Co and ^{65}Zn.

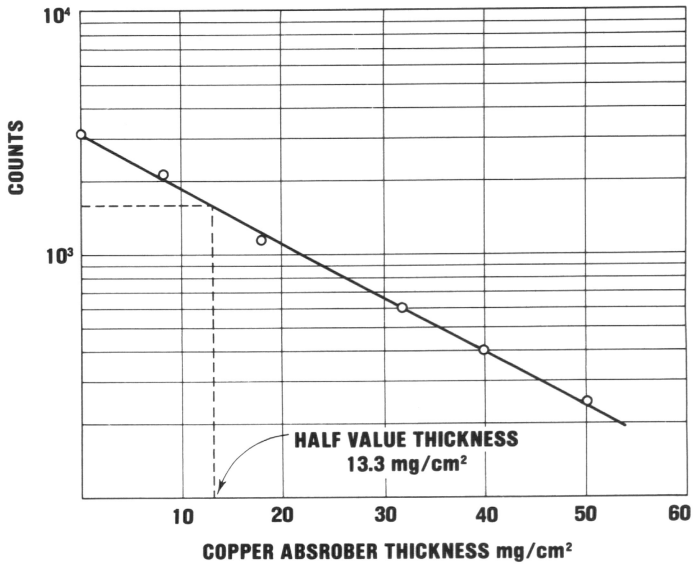

Figure 7.11. Measurement of the mass attenuation coefficient for 8.047 keV x-rays in copper.

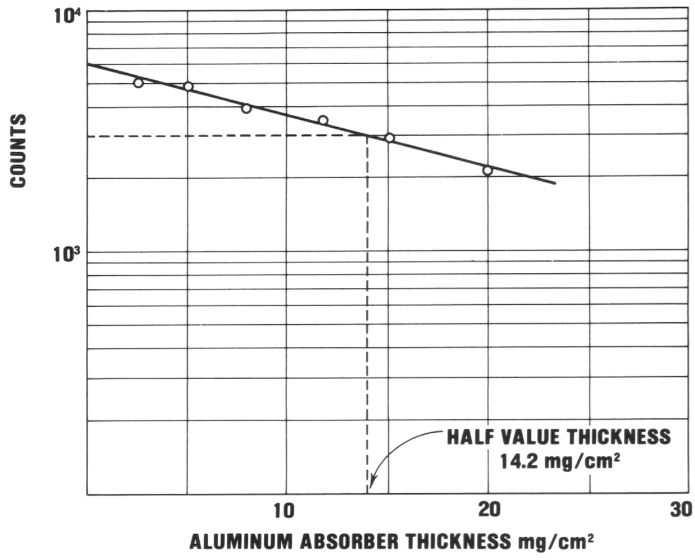

Figure 7.12. Measurement of the mass attenuation coefficient for 8.047 keV x-rays in aluminum.

Table 7.4 X-Ray Cross Sections in cm^2/g for Foils That Are Commonly Available

Source	(keV)	Al	X-Ray Energy Fe	Ni	Cu	Ag	Au
^{55}Fe	5.89	124	88.9	115	123	495	457
^{57}Co	6.40	97.5	70.4	91.8	97.4	398	371
^{65}Zn	8.04	50.2	304	48.8	51.5	218	208
^{109}Cd	22.1	2.54	19.3	24.3	25.5	13.7	60.2
^{109}Cd	25.0	1.81	13.7	17.3	18.2	97.8	43.9

3. Place the thinnest copper foil between the source and the detector and again count for a long enough period of time to get reasonable statistics under the K peak. Calculate Σ-β/t. Repeat for enough copper thicknesses to plot a mass attenuation curve similar to fig. 7.11.

4. Repeat this same set of measurements for the ^{65}Zn source and the aluminum foils. Figure 7.12 shows a set of experimental data for similar measurements.

5. *(Optional)* Table 7.4 shows the x-ray cross sections for a variety of elements and x-ray energies. Half value thickness can be determined for any of these source, element combinations.

Exercise From the above data, plot Σ-β/t vs absorber thickness. Determine the half value thickness and μ the x-ray cross section. Your answers should agree with those in Table 7.4.

REFERENCES FOR *EXPERIMENT 7*

1. J. Price, J. L. Duggan, F. D. McDaniel, et al, *Phys. Rev.* **32**, 2088, 1986.

2. W. J. Gallagher and S. Cipolla, *Nuc. Inst. and Meth.*, **122**, 405, 1974.

3. J. L. Campbell and L. A. McNelles, "An Intercomparison of Efficiency Calibration Techniques for Semiconductor X-Ray Detectors," *Nucl. Instrum. Methods* **125**, 205-223 (1975).

4. R. J. Gehrke and R. A. Lokken, *Nuc. Inst. and Meth.* **97**, 219 (1971).

5. G. F. Knoll, *Radiation Detection and Measurement*, John Wiley and Sons, New York (1979).

6. K. Siegbahn, Ed., *Alpha-, Beta-, and Gamma-Spectroscopy*, North Holland Publishing Co., Amsterdam (1968).

7. C. M. Lederer and V. S. Shirley, Eds., *Table of Isotopes*, 7th Edition, John Wiley and Sons, New York (1978).

EXPERIMENT 8

X-Ray Fluorescence with High Resolution Silicon and Germanium Detectors

Scope

This experiment will overview the use of High Resolution Si(Li) and Germanium detectors for x-ray fluorescence. The Si(Li) detector will be calibrated by fluorescing known samples with photons from a ^{109}Cd source. The x-ray energies from these standards will be used to construct a calibration curve of energy vs channel number. The elements present in several unknown samples will then be determined from this calibration curve. The elements which exist on thin environmental samples will also be determined from this calibration. A quantitative analysis calibration curve will be constructed by drying known concentrations of standard solutions onto filter paper. The filter paper will then be fluoresced by the ^{109}Cd source and the $(\Sigma-\beta)$ for K x-rays will be plotted as a function of % concentration of the known elements. This curve will then be used to quantify the elements that were found on environmental samples. Finally a high resolution germanium detector will be used to study K x-rays from heavy elements ($K\alpha > 25$ keV). An energy calibration curve will be constructed by fluorescing known heavy elements. This calibration will then be used to identify high Z unknown samples.

Discussion

The advent of high resolution silicon and germanium detectors has revolutionized the older science of X-ray Fluorescence (XRF) Analysis. The basic ideas behind XRF are quite simple. A sample is bombarded with photons from a radioactive source or an x-ray tube and the photoelectric effect occurs in the sample producing a vacancy in the K or L shell of the sample. The x-rays that are produced in filling these levels by the outer electrons are then measured by a high resolution detector. Si(Li) detectors are commonly used to detect these x-rays when the energy range is less than 25 keV. Since the photoelectric cross-section varies at Z^5, higher energy x-rays are perhaps best measured with high resolution germanium detectors. In this laboratory experiment, examples of both kinds of detectors will be shown. It will be seen in this experiment that XRF is one of the best nuclear techniques that can be studied in a university. The technique has wide research application in industry, research, medicine, and environmental studies. A few examples include such diverse studies as: analysis of impurities in semiconductors, air and water pollution studies, and the analysis of trace elements in blood or certain organs to determine the relation of these elements to disease. Aside from the educational experiments outlined in this report, it is quite easy to set up a research program in this area. The costs are certainly not prohibitive and many university science departments have already proved that it is a productive research area.

XRF EXCITATION SOURCES

Table 8.1 shows a listing of the most common radioactive sources that are used in XRF. Shown also on the table are the photons that produce the excitation and the range of elements that can be excited with the source. The recommended activity of the excitation source is also shown. A word of **caution**, these sources should be used in keeping with the health physics procedures that are given by the instructor for your laboratory. The recommended sources all have activities of the order of millicuries and therefore should never be touched by

Table 8.1 XRF Excitation Sources

Source	Major Photons for Excitation	Source Activity	Recommended Elements that can be excited with Source	Theoretical Yield % (Per Disintegration) or x/γ
^{55}Fe	5.896 keV Mn Kα	25-100 mCi	$Z < 23$	26%
^{57}Co	122 keV γ	25-100 mCi	$Z > 50$	~89%
^{109}Cd	22.16 keV Ag Kα	25-50 mCi	$45 > Z > 20$	x/γ = 4.9%
^{241}Am	60 keV γ	25-50 mCi	$66 > Z > 30$	~
^{153}Gd	103 keV; gamma 97 keV; gamma 70 keV; gamma 41 keV; Eu K x-rays	25-50 mCi	$Z > 20$	20.0% 30.0% 2.6% 110.0%
^{238}Pu	12-17 keV; U-L x-rays	25-50 mCi	$20 < Z < 37$	10

hand. Tongs or forceps should be used to move the source from its storage container to the fluorescence chamber. Once the source is in the chamber, it can be used safely for the experiment.

In order to understand the excitation mechanism, let us assume that the K x-rays of lead are to be excited for the experiment. The excitation source should have a photon energy high enough to remove the K-shell electron from Lead (88.001 keV, see Appendix B) by the photoelectric process. Figure 8.1 shows the photoelectric attenuation of lead as a function of photon energy. Notice that the highest probability of a photoelectric interaction is at the binding energy of the K shell electron (K_{ab}). In practice, it is best to have an excitation source that is at least 2 keV higher in energy than K_{ab} for the element. For the lead example, the cross-section is 8 cm^2/gm at the absorption edge and falls to a value of 1.0 cm^2/gm at 200 keV. To give a specific example, let us assume that two sources are available to fluoresce the lead in some paint samples that are being studied for lead content. These fluorescence sources are ^{57}Co and ^{137}Cs. From fig. 8.1, it can be seen that the cross section for K excitation for the 122 keV photons from ^{57}Co is 3 cm^2/g while the 662 keV photons from ^{137}Cs have a photoelectric cross section of only 0.12 cm^2/gm. From this consideration, it would therefore be 25 times better to use ^{57}Co. In summary, for XRF, it is wise to choose an excitation source which is close to (~ 2 keV above) the K_{ab} for the highest atomic number (Z) that is being studied. For multiple elements, it is sometimes necessary to use several different excitation sources. As was mentioned earlier the K_{ab} values and the L shell binding energies are listed in Appendix B (x-ray critical absorption and emission energies in keV). These can also be seen in fig. 8.2 which is a plot of the *average* K x-ray energy versus atomic number. It is interesting to note from the figure that the highest x-ray energy for the last element

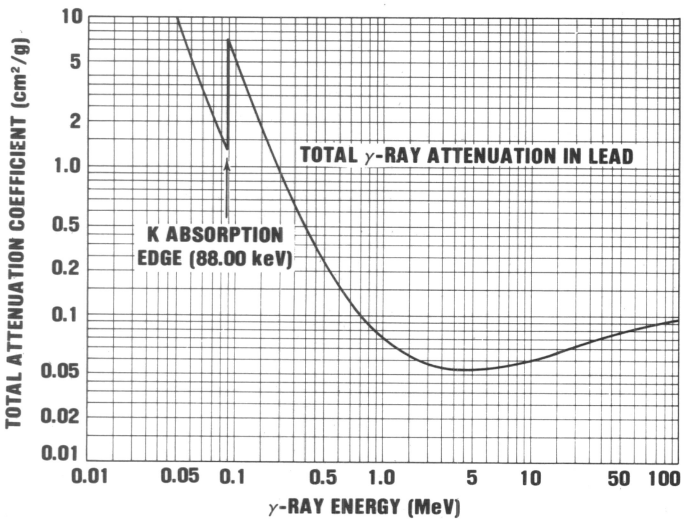

Figure 8.1. Total gamma ray attenuation in lead versus incident gamma energy.

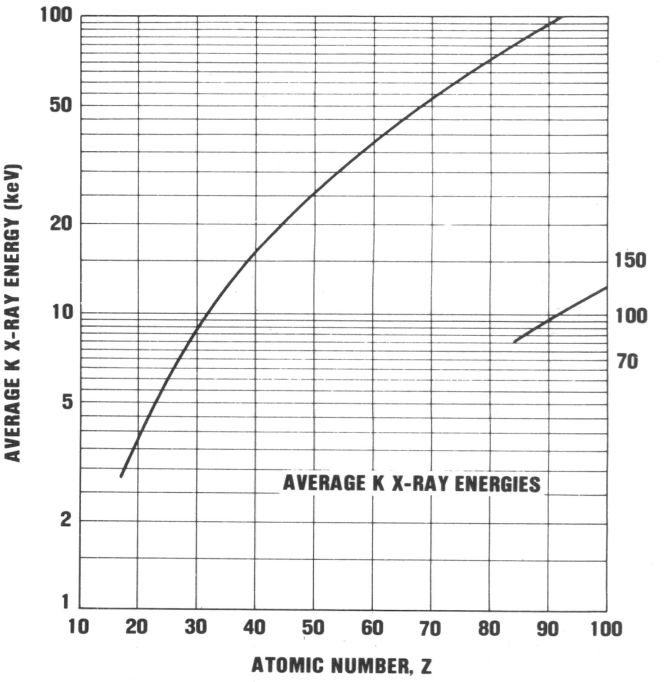

Figure 8.2. Average x-ray energies induced in shielding material as a function of atomic number.

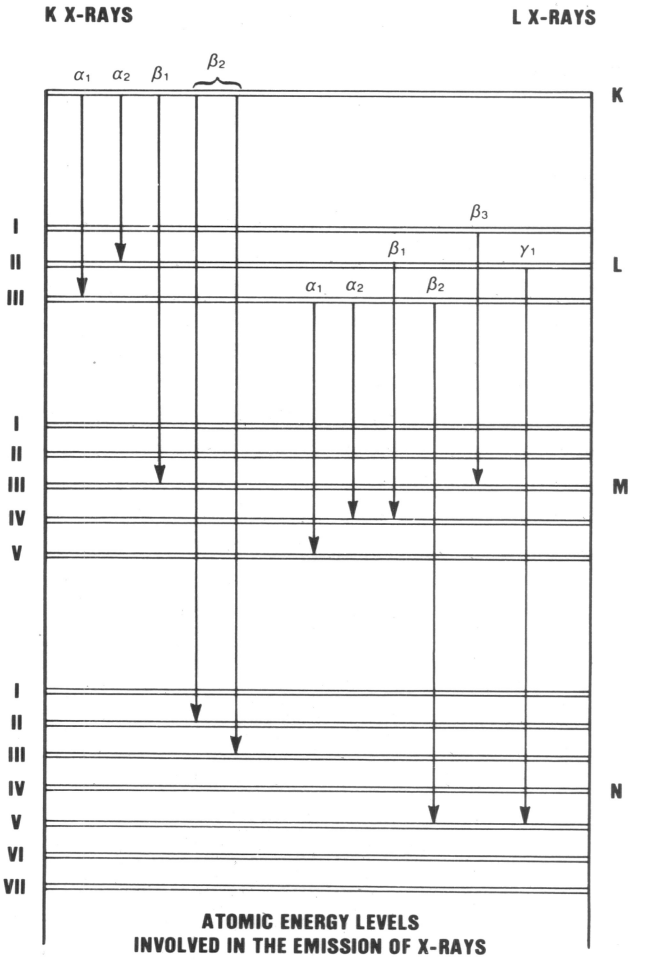

Figure 8.3. Atomic energy levels involved in the emission of x-rays.

Table 8.2 X-Ray Lines Most Commonly Seen in X-Ray Fluorescence

$K\alpha_1 = K_{ab}\text{-}L_3$	$L\alpha_1 = L_3\text{-}M_5$
$K\alpha_2 = K_{ab}\text{-}L_2$	$L\alpha_2 = L_3\text{-}M_4$
$K\alpha_3 = K_{ab}\text{-}L_1$	$L\alpha = L\alpha_1\text{-}L\alpha_2$
$K\alpha = K\alpha_1 + K\alpha_2 + K\alpha_3$	$L\beta_1 = L_2\text{-}M_4$
$K\beta_1 = K_{ab}\text{-}M_3$	$L\beta_{2,15} = (L_3\text{-}N_5) + (L_3\text{-}N_4)$
$K\beta_2 = (K_{ab}\text{-}N_3) + (K\alpha\beta\text{-}N_2)$	$L\beta_3 = L_1\text{-}M_3$
$K\beta_3 = K_{ab}\text{-}M_2$	$L\beta_4 = L_1\text{-}M_2$
$K\beta_4 = (K_{ab}\text{-}N_4) + (K\alpha\beta\text{-}N_5)$	$L\beta_5 = (L_3\text{-}O_4) + (L_3\text{-}O_5)$
$K\beta_5 = (K_{ab}\text{-}M_4) + (K\alpha\beta\text{-}M_5)$	$L\beta_6 = L_3\text{-}N_1$
$K\beta_1^1 = K\beta_1 + K\beta_3 + K\beta_5$	$L\gamma_1 = L_2\text{-}N_4$
$K\beta_2^1 = K\beta_2 + K\beta + \ldots$	$L\gamma_2 = L_1\text{-}N_2$
$K\beta = K\beta_1 + K\beta_2 + K\beta_3 + K\beta_4 + K\beta_5 + \ldots$	$L\gamma_3 = L_1\text{-}N_3$
	$L\gamma_6 = L_2\text{-}O_4$
	$L\eta = L_2\text{-}M_1$
	$L\alpha = L_3\text{-}M_1$

Note in using this table L_3 is the same as L_{IIIab} from the Table of Critical Absorption and Emission Energies in Appendix B, $L_2 = L_{IIab}$ etc.

plotted is 141.5 keV. The element is Fermium (^{253}Fm). This also means that characteristic x-rays from the highest atomic number elements can't be any higher than this number.

Table 8.2 shows the most probable x-rays that will be seen in XRF. Figure 8.3 shows these same lines in a level diagram notation. Figure 8.4 shows a XRF spectrum that contained Manganese metal evaporated onto a thin copper foil. The Mn Kα energy can be easily calculated by using Table 8.2 for $K\alpha_1$ and recording the proper values of the binding energies of the levels from the *Critical Absorption and Emission Values in Appendix B*. It should be remembered from experiment 7 that for light elements, $K\alpha_1$ and $K\alpha_2$ are so close together in energy that they will be seen as a single peak which is labeled Kα in fig. 8.4. All of the Kβ groups in Table 8.2 are unresolved and fall under the peak labeled Kβ in fig. 8.4. From experiment 7, it was learned that the best resolution of these Si(Li) detectors is about 150 eV. Therefore, if two x-ray groups are closer together in energy than this value, they will show up as one group in the spectrum. The resolution of the detector shows the Kα and Kβ x-rays as a single group for light elements. Figure 8.5 (top figure) shows a spectrum of Potassium Chloride (KCL) where the Kα and Kβ from chlorine are seen as one group. The Kβ group for potassium shows up as a shoulder on the side of the Kα group. In the lower spec-

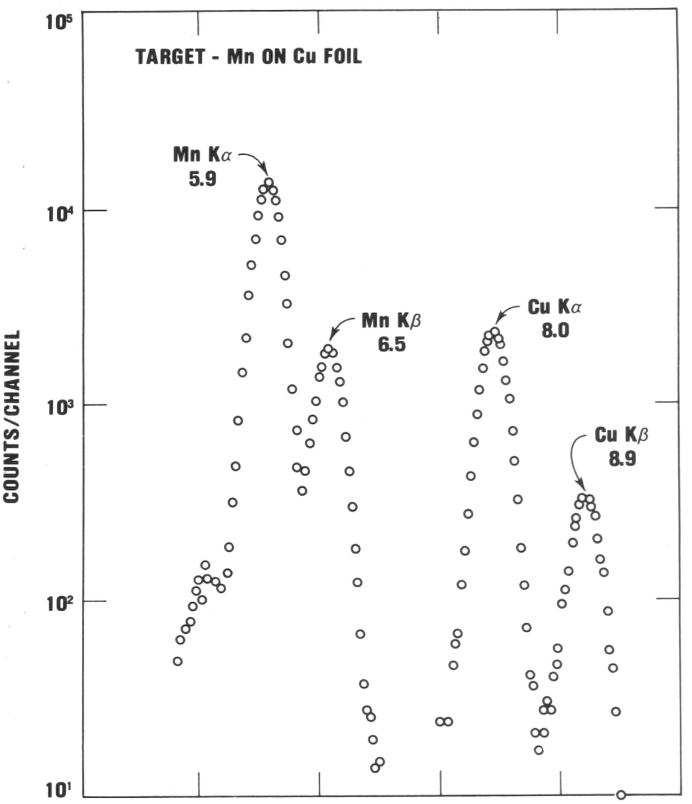

Figure 8.4. Typical XRF spectrum taken with a Si(Li) detector. The target was manganese metal which was evaporated onto a thin copper foil.

trum in fig. 8.5, the scandium Kα and Kβ are just far enough apart in energy that they are resolved into two groups.

IDENTIFICATION OF UNKNOWNS

There are, in general, two questions that should be answered in regard to an unknown sample. For example, let us assume that an air pollution filter sample is being studied. The questions are: what are the elements present on the sample, and how many $\mu g/cm^2$ of the various elements are present. The first question is at least an order of magnitude easier to answer than the second. To determine what elements are present, an energy calibration curve is constructed. This curve can be constructed by fluorescing known samples with the XRF source or by using radioactive sources as in experiment 7. It will be seen that if the calibration is done carefully, it is possible to assign the unknown x-ray energy within ± 15 eV. With this kind of accuracy, it is virtually impossible to miss assign an unknown element if the peaks are clearly seen. One of the most difficult problems in x-ray analysis is resolving between adjacent elements in the periodic chart for light elements. Figure 8.5 (top) shows that Chlorine (Z=17) and potassium (Z=19) are clearly resolved by these Si(Li) detectors. The problem of determining what elements are present gets much easier for higher Z elements since the levels are farther apart. Hence, the Kα and Kβ x-rays are clearly seen as distinct groups. Figure 8.6 shows a Si(Li) K spectrum from palladium and L spectrum from holmium which clearly illustrates this point.

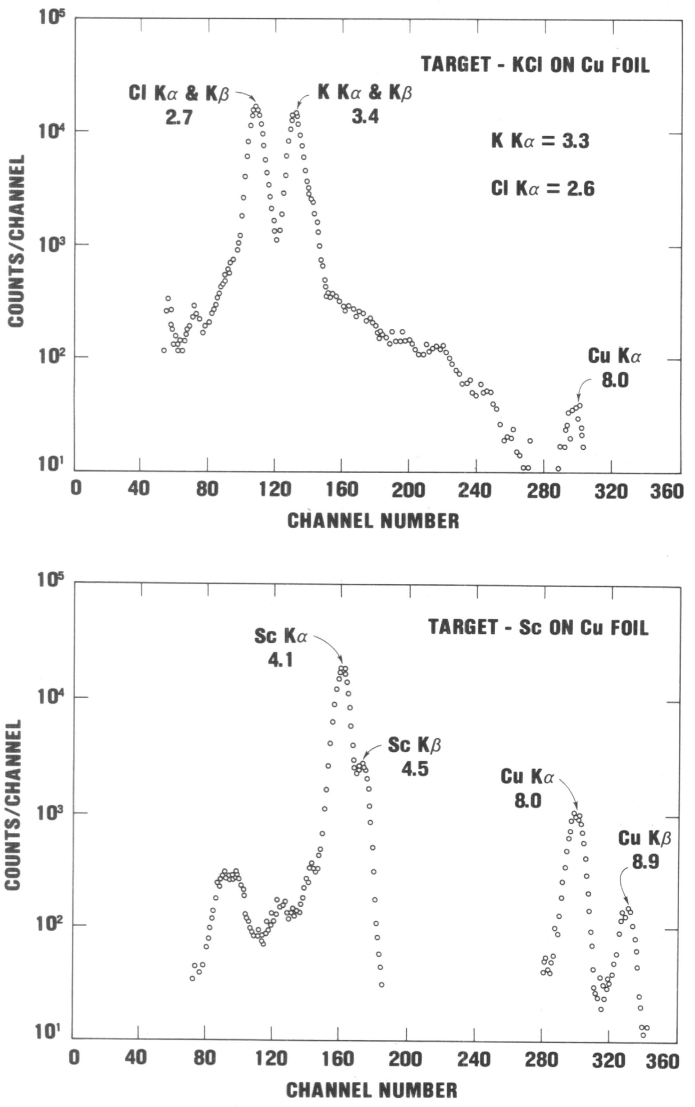

Figure 8.5. Si(Li) x-ray spectra of (top) KCl which has been evaporated on a Cu blank and (bottom) scandium metal deposited on a copper foil. (Note, the Sc Kα and Kβ are barely resolved).

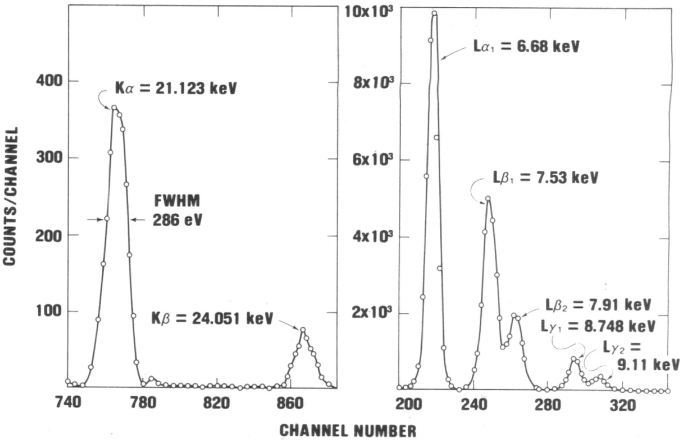

Figure 8.6. K spectra of palladium (left) and L spectra of holmium (right). Taken with a Si(Li) detector.

Determining how much of an element is present on a sample is much more difficult. For thin samples, the problem is somewhat easier since the matrix attenuation effects are minimal. Examples of thin samples might be air pollution filter samples, dried blood samples, dried water samples, or thin slices of tissue. For these samples, it is sometimes possible to prepare known concentration standards for the elements present in the sample. Figure 8.7 shows a *quantitative analysis* graph that was made by depositing known concentrations of certain elements onto filter paper. Those standards were studied under the same geometry as the unknown specimens. The counts per minute for the K x-rays were then determined and normalized to concentration in %. The concentration of the unknown elements can be determined by comparing their counting rates to those for the corresponding elements from fig. 8.7.

For thick samples, the problem becomes much more difficult. For example, let us assume that a piece of pottery is being studied for archaeological purposes. This is a thick sample and therefore the excitation photons are attenuated upon entering the sample. If a photoelectric interaction does occur at a depth X, the x-rays photons that are produced will also be attenuated in their path back to the detector. Quite often these linear absorption

coefficients are not known for the particular matrix which is being studied. It can be seen that the problem is quite difficult. Extensive computer programs have been written for a variety of experimental arrangements, sources, and samples, but it is beyond the scope of this study to discuss them.

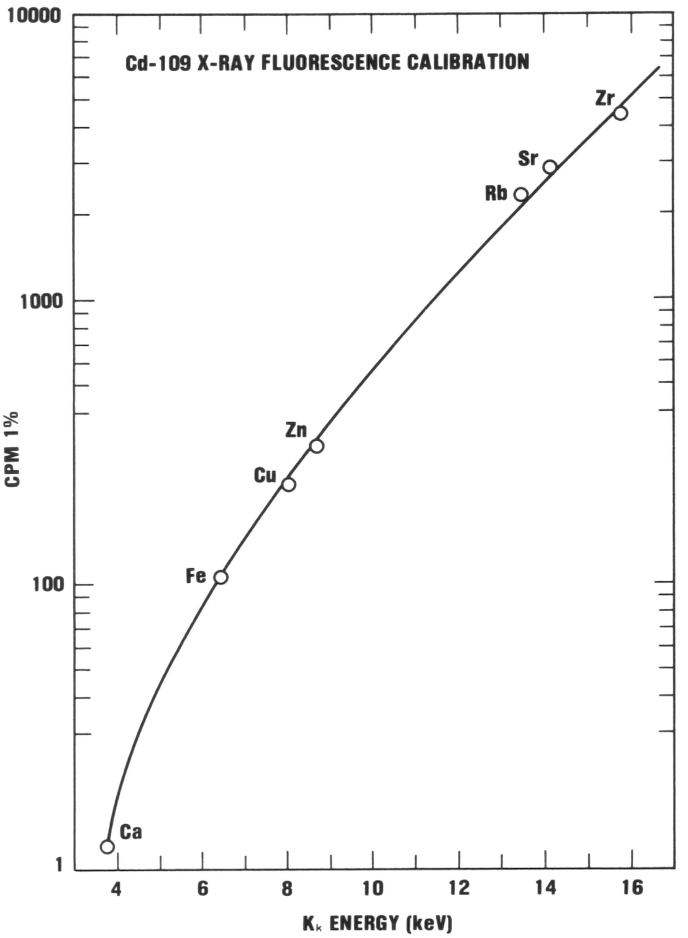

Figure 8.7. Qualitative analysis graph of thin samples made by evaporating standard solutions of the element desired onto filter paper.

EXPERIMENT 8.1

Calibration of the Si(Li) Detector by Fluorescing Known Elements

1. Set up the electronics as shown in fig. 8.8. The instructor will place the ^{109}Cd excitation source in the chamber. The chamber is designed so that it can be evacuated, but it is not necessary for this portion of the experiment. Adjust the detector bias voltage to its recommended value.

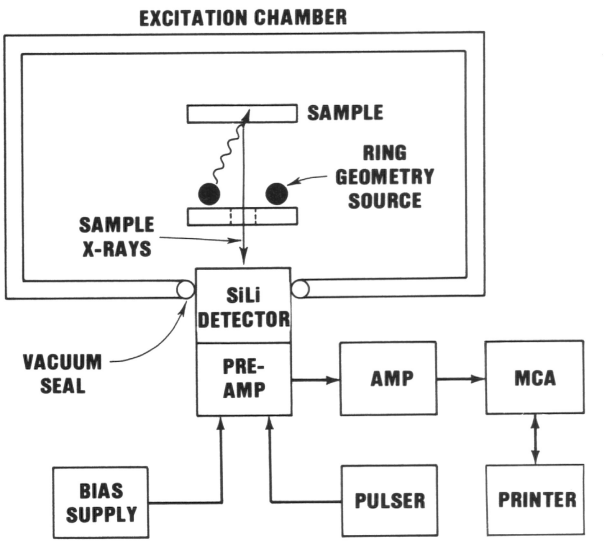

Figure 8.8. Electronic arrangement for x-ray fluorescence with a high resolution Si(Li) detector.

2. Use 1024 channels of the MCA. Place the Titanium sample in the chamber and adjust the gain of the amplifier so that the 4.510 keV Kα peak falls in channel 280. This will give a slope to the calibration curve of approximately 16 eV/ch.

3. Record the Ti-Kα and Kβ x-ray data in Table 8.3. Repeat for the other samples in Table 8.3. As in all of the previous experiments, the data should be taken for a

Table 8.3 Data Table for XRF Calibration Si(Li) With a ^{109}Cd Source

Run No.	Sample	Energy keV	Channel Number	FWHM eV
1	Titanium	Kα 4.510 Kβ 4.931		
2	Iron	Kα 6.403 Kβ 7.057		
3	Copper	Kα 8.047 Kβ 8.904		
4	Germanium	Kα 9.885 Kβ 10.981		
5	Potassium Bromide	Kα 11.923 Kβ 13.290		
6	Zirchonium	Kα 15.774 Kβ 17.666		
7	Tungsten	Lα 8.396 Lβ 9.670 Lγ 11.283		
8	Lead	Lα 10.549 Lβ 12.611 Lγ 14.762		

period of time long enough to obtain reasonable statistics in the peaks of interest. If a peak fitting routine is available on the MCA or PCA that is being used, be sure to use it for the measured channel numbers that are to be recorded in Table 8.3.

Exercise A Plot a calibration curve from the data in Table 8.3. Calculate the slope of the curve in eV/ch and determine the FWHM of all peak in (eV). Record the FWHM values in Table 8.3. Figure 8.9 shows a typical calibration curve for a Si(Li) detector. The gain used for our data was about three times higher than that in fig. 8.9.

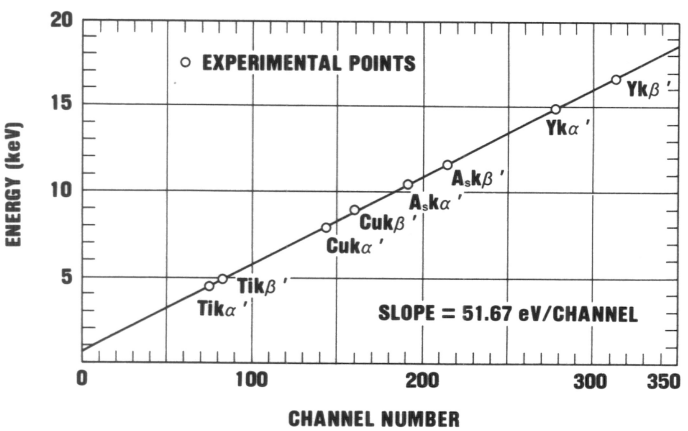

Figure 8.9. Typical XRF calibration curve for a Si(Li) detector.

essence, tells how good the guess was. If the data was taken carefully enough, ΔE should be no worse than ±15 eV. Figure 8.10 is an L pulse height spectrum of Dysprosium which is an unusual unknown.

Table 8.4 Data Table for Unknown K and L Shell Elements by XRF with a ^{109}Cd Excitation Source

Run No.	Measured Peaks from Unknown	Unknown Element (Guess)	X-Ray Energies from Appendix	ΔE in eV
1 (K Shell)	Kα Kβ		Kα Kβ	
2 (K Shell)	Kα Kβ		Kα Kβ	
3 (K Shell)	Kα Kβ		Kα Kβ	
4 (L Shell)	Lα Lβ Lγ		Lα Lβ Lγ	
5 (L Shell)	Lα Lβ Lγ		Lα Lβ Lγ	
6 (L Shell)	Lα Lβ Lγ		Lα Lβ Lγ	

EXPERIMENT 8.2

The Analysis of Unknown K and L Shell Samples by XRF with a ^{109}Cd Source

1. The same calibration curve will be used for this experiment as for experiment 8.1. Obtain the first K shell unknown from the instructor. Run a spectrum for a time period long enough to clearly establish the Kα and Kβ peaks. From the calibration, record the energies of those peaks in Table 8.4. From the listings in Appendix B, guess what the element is and record this in Table 8.4.

2. Repeat for the rest of the K and L shell samples that are provided by the instructor. Record all values in Table 8.4.

Exercise From your guess as to the unknown, record the theoretical values for the x-ray lines in column 4 of Table 8.4. Subtract the theoretical lines from the measured values and thus determine ΔE in (eV). This, in

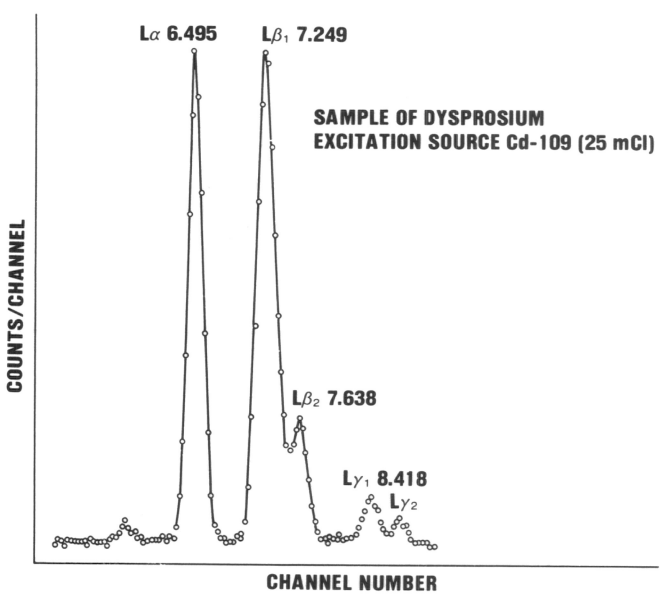

Figure 8.10. L x-ray spectrum of dysprosium.

EXPERIMENT 8.3

Analysis of Environmental, Biological, and Geological Samples by XRF with ^{109}Cd

Discussion

It was mentioned in the discussion at the beginning of Experiment 8, that XRF could be used for a wide variety of measurements. Water and blood samples are usually dried before analysis; however, liquids can be fluoresced under the proper conditions. Many other biological samples are freeze dried before they are studied. Some samples can be powdered and then uniformly spread on a piece of filter paper before use. Certainly the easiest samples to obtain are the air pollution filter samples. In most cases, it is best to prepare thin samples if possible. It is a simple matter to identify the major elements that are present on a sample, but, as mentioned earlier, quantifying the results is not always easy. Thin samples can be compared to standards, but, for thick samples, matrix effects make the problem much more difficult.

Experimental Procedure

1. The same calibration will be used on this experiment as in the previous measurements. Obtain the first pollution, biological, etc. sample from the instructor. Place it in the chamber and count for a period of time long enough to obtain reasonable statistics in the major peaks. Use the MCA or PCA programs to determine (Σ-β) for all the major peaks. Record these values in an appropriate data table.

2. Repeat these measurements for the other samples that the instructor has provided. If quantitative analysis is to be performed, the instructor will provide standard samples for these measurements. For example, let us assume that fig. 8.11 is an air pollution sample that was measured in the first part of this experiment. Our problem is to determine the number of $\mu g/cm^2$ of Zn on the sample. The instructor will provide a sample that, for example, has 10 $\mu g/cm^2$ of Zn on it. The fluorescence measurement on this standard would yield approximately 6000 cpm/μg of the Zn K x-rays. The thickness of the Zn on the pollution sample can then be determined by comparing it directly with the standard. Figure 8.12 was constructed by analyzing a number of these standard samples.

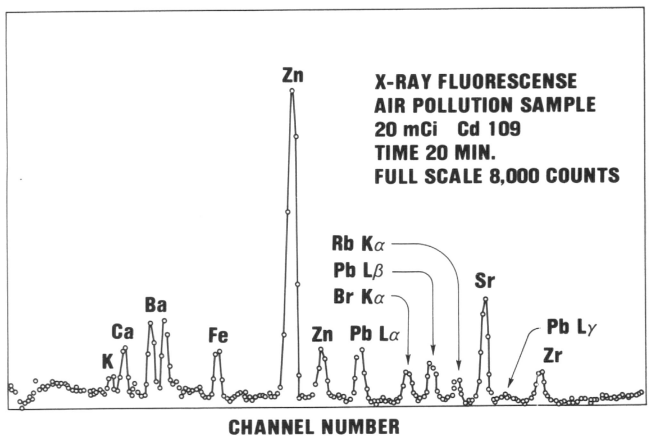

Figure 8.11. Si(Li) spectrum of an air pollution sample that was fluoresced with ^{109}Cd.

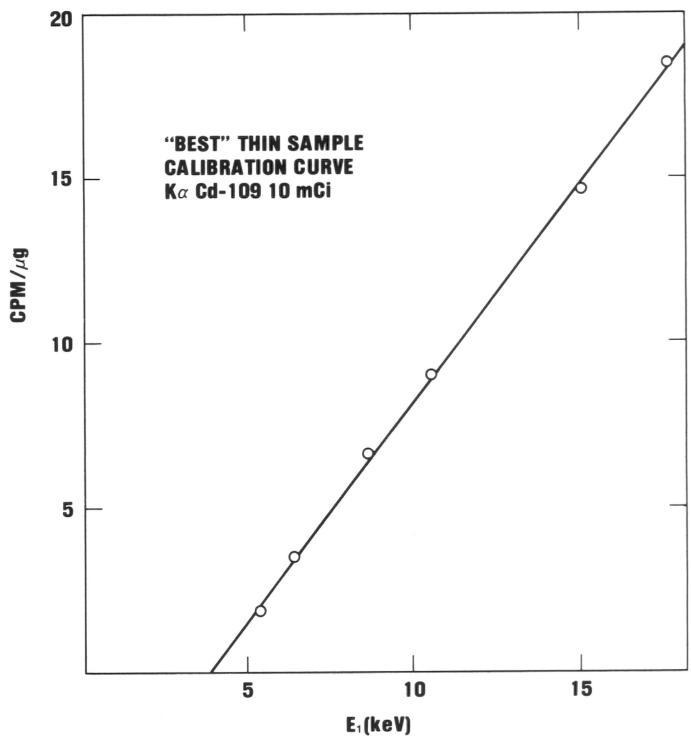

Figure 8.12. XRF quantitative analysis calibration curve. This curve was obtained by fluorescing thin sample standards which were prepared from standard solutions.

Exercise From the calibration curve assign energies to all of the major peaks that are seen on the samples. Use fig. 8.12 to quantify the results. Figures 8.13 through 8.17 show typical examples of the wide variety of measurements that can be made with this fluorescence technique.

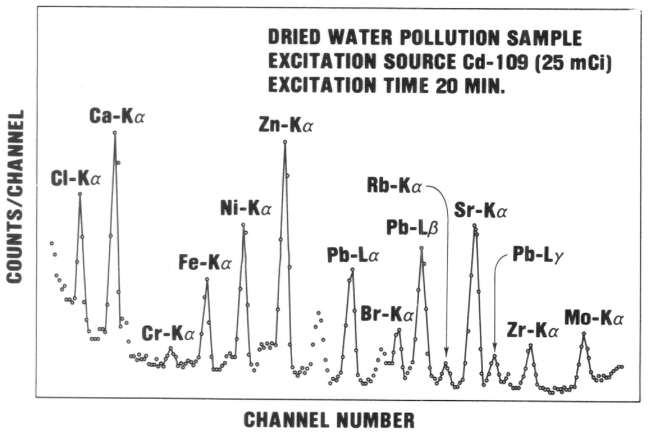

Figure 8.13. Si(Li) spectrum of a dried water pollution sample (^{109}Cd excitation).

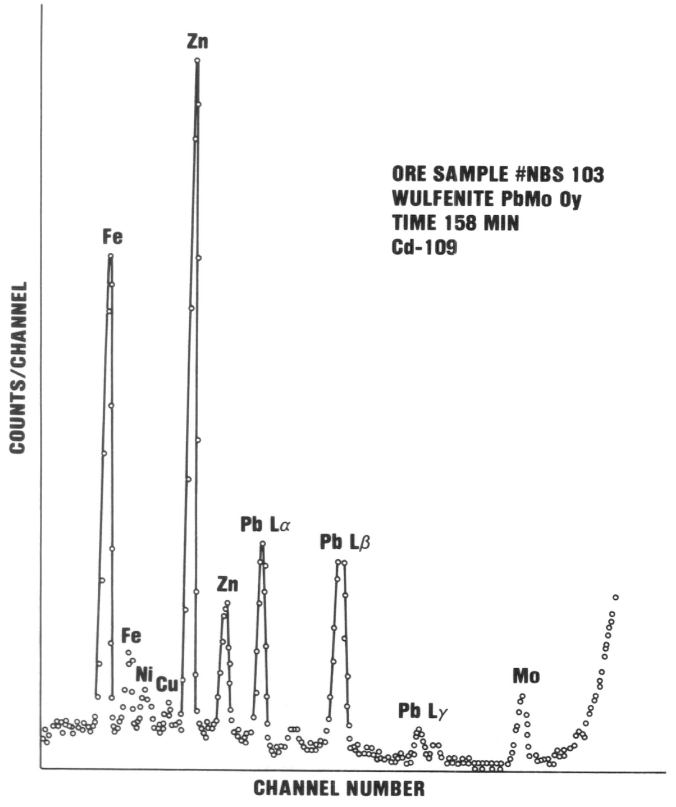

Figure 8.14. Si(Li) spectrum of an NBS ore sample (^{109}Cd excitation).

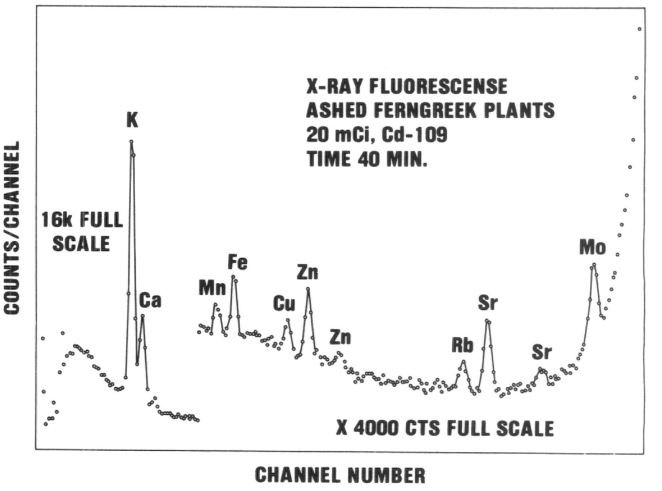

Figure 8.15. Si(Li) spectrum of ferngreek plants (^{109}Cd excitation).

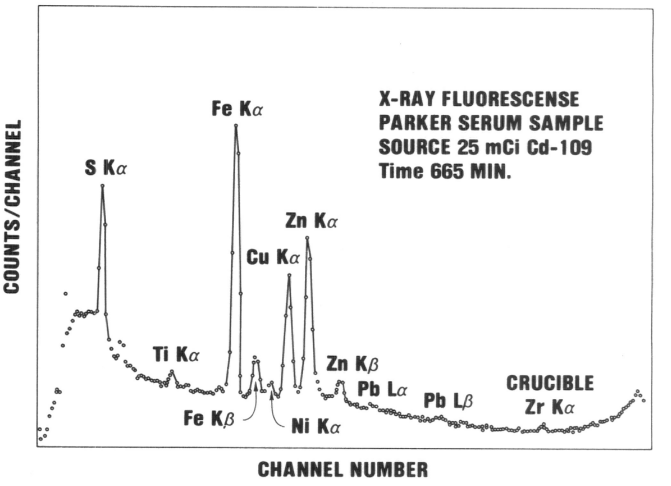

Figure 8.16. Si(Li) spectrum of a blood serum sample (^{109}Cd excitation).

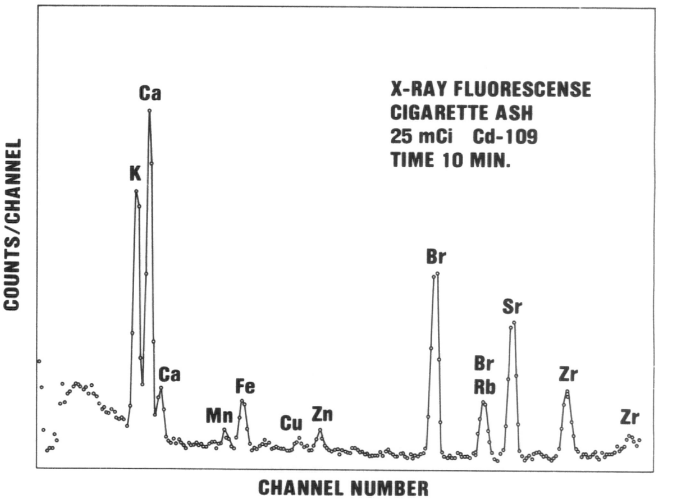

Figure 8.17. Si(Li) spectrum of cigarette ash (^{109}Cd excitation).

EXPERIMENT 8.4

X-Ray Fluorescence Studies with an ^{55}Fe Source

Discussion

Figure 8.1 shows the photoelectric cross section in lead as a function of energy. It was pointed out earlier that if a certain element is to be studied, the best excitation source would be one that is slightly higher than the K binding energy for that element. ^{55}Fe decays to ^{55}Mn by the electron capture process. For an ^{55}Fe excitation source, the photons doing the fluorescence are therefore the 5.898 Kα and 6.490 Kβ x-rays. ^{55}Fe is therefore the best excitation source for looking at elements lower than $_{24}Cr$ in the periodic chart.

Experimental Procedure

1. The instructor will load the ^{55}Fe excitation source in the chamber. For this experiment, the chamber will be evacuated for each measurement. The instructor will provide standard samples of vanadium, titanium, calcium, chlorine, and aluminum for the calibration procedure. Place the vanadium sample in the chamber and evacuate until the vacuum pump is quiet. Adjust the gain so that the $_{23}V$ Kα (4.952 keV) x-ray is in channel 300.

2. Accumulate a spectrum for a long enough period of time to obtain 3000 counts in the Kα peak. Record the peak channels for the V Kα and Kβ in a data table. Repeat this measurement for the titanium, calcium, chlorine, and aluminum samples. Record all peak channels in the data table.

3. Obtain the unknown elemental or environmental samples from the instructor and fluoresce them under vacuum conditions for a period of time long enough to obtain reasonable statistics in the peaks of interest.

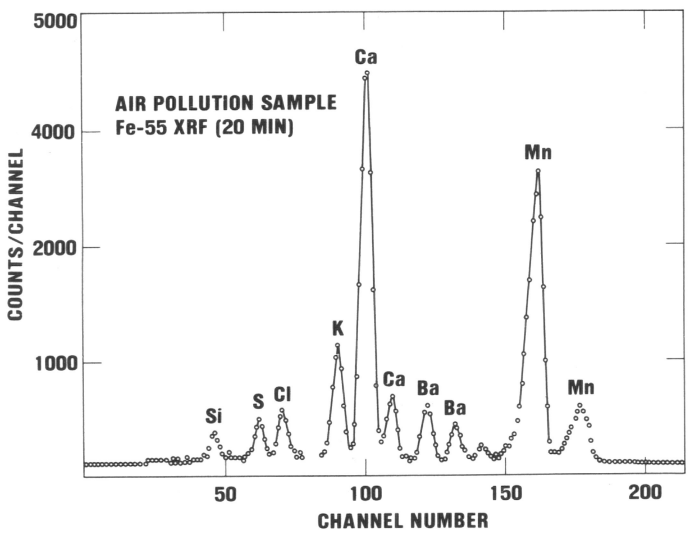

Figure 8.18. Si(Li) x-ray spectrum of an air pollution sample excited by an ^{55}Fe source.

Exercise A Plot the calibration curve from the data table and obtain its slope as in experiment 8.1. Determine the resolution (FWHM) of each peak in (eV) and record these values in the data table. Identify all peaks in the unknown elemental or environmental samples.

Exercise B If the instructor wants quantitative results of the thin samples, standards will be provided to make a cpm/μg curve similar to fig. 8.12. Figure 8.18 shows an air pollution sample that was fluoresced with an ^{55}Fe source. The Mn peaks shown in the spectrum are the Kα and Kβ x-ray lines that are Rayleigh scattered from the source into the detector. Figure 8.19 shows a cigarette ash sample which contains Ca, K, and Cl. The Ar peak in the spectrum comes from the air.

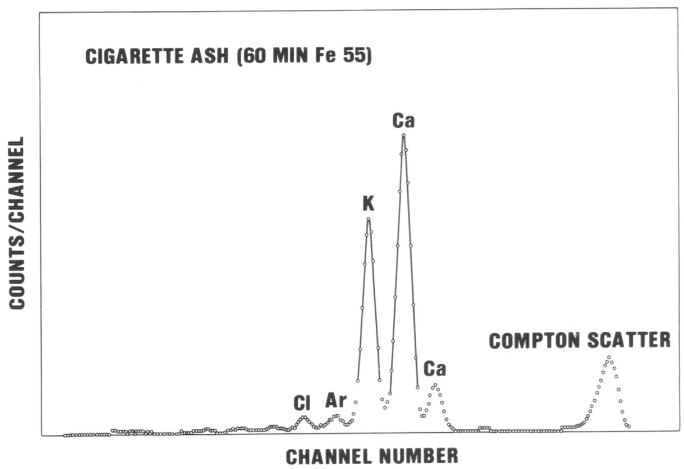

Figure 8.19. Si(Li) x-ray spectrum of cigarette ash excited by an ^{55}Fe source.

Figure 8.20 shows an aluminum sample that was fluoresced with an ^{55}Fe source. The aluminum Kα x-rays are 1.487 keV. This spectrum shows a 10 minute run with and without evacuating the chamber. Under vacuum conditions the Al peak is about 5 times as large as it is under the same counting conditions in air. This shows that air attenuates these 1.487 keV x-rays by about 80%. **Note:** Also in the spectrum, the Ar peak is present when air is in the chamber. The Ar Kα peak has an energy of 2.957 keV.

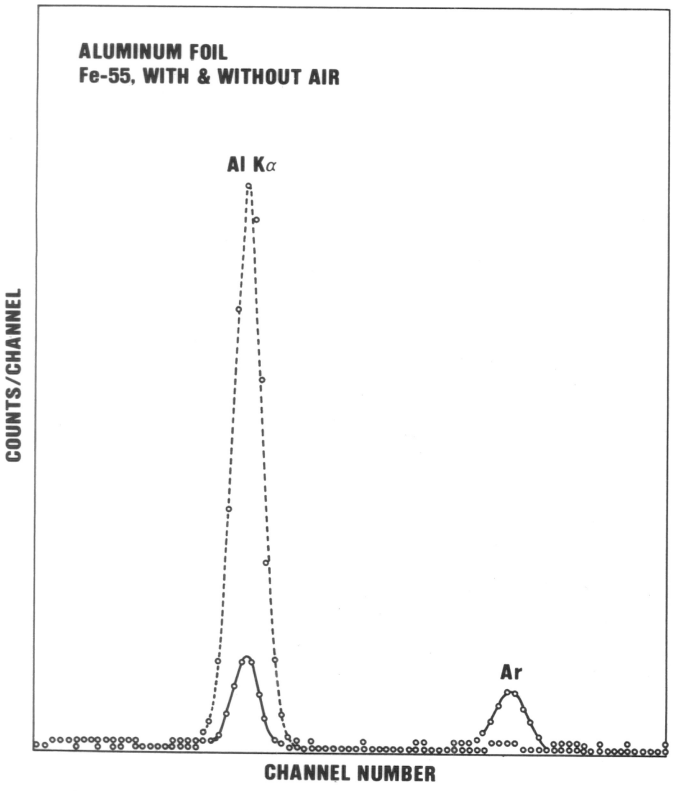

Figure 8.20. Si(Li) x-ray spectrum of an aluminum sample with and without air in the chamber (^{55}Fe excitation source).

EXPERIMENT 8.5

XRF with High Resolution Germanium Detectors (^{57}Co Excitation Source)

1. Set up the electronics as shown in fig. 8.8. The detector in this case will, however, be a High Resolution Germanium Detector. Adjust the bias level to that which is recommended for the detector. The instructor will transport the ^{57}Co excitation source from its storage container to the chamber.

2. In this experiment, high energy x-rays are being studied so the calibration standards are foils of high Z material. The samples to be used for the calibration curve are $_{82}$Pb, $_{79}$Au, $_{74}$W, $_{67}$Ho, and $_{50}$Sn. The highest energy K x-rays in this group are the Pb Kα and Kβ photons at 74.957 and 84.922 keV. Place the Pb sample in the chamber and adjust the gain of the amplifier so that the 74.957 keV Kα peak falls in channel 800. Record the channel numbers for the Kα and Kβ peaks in a data table along with the energies. Repeat this measurement for the Au, W, Ho, and Sn samples. For each peak, record the FWHM.

3. Obtain the unknown samples from the instructor and accumulate a spectrum for each of them for a period of time long enough to obtain reasonable statistics in the peaks of interest.

Exercise Construct a calibration curve from the data for the standards. Calculate the slope and the FWHM (in eV) for each peak. From the calibration curve, assign energies to the peaks in the unknown samples. Determine what elements are present on the unknowns and calculate ΔE for each peak. Remember ΔE is how many (eV) you were over or under the unknown Kα, Kβ, Lα, Lβ, Lγ energies from Appendix B. In experiment 7, fig. 7.9 shows the mercury K and L lines that would have been measured, if one of the unknowns had been Hg.

EXPERIMENT 9

Compton Scattering

Scope

In this experiment the Compton kinematic equations will be studied. The scattered gamma from the interaction will be measured as a function of the scattering angle. A plot of $1/E\gamma$ vs $(1-\cos\theta)$ will be made to verify the theory. The variation of the Compton cross section will be studied as a function of the atomic number (Z) of the scattering material. Finally, coincidence techniques will be used to show that the recoiling electron in a Compton interaction also satisfies the laws of conservation of energy and momentum.

Discussion

In Experiment 2, the NaI(Tℓ) spectra that were measured showed photoelectric, Compton, and Pair Production interactions. It was seen in the experiment that for gamma energies in the range from 150 keV to 3 MeV, the Compton interaction was by far the most pronounced effect. The reaction was also seen to depend on the Atomic number (Z) of the scattering material.

When photons scatter from electrons by the Compton reaction, the electrons are usually free electrons or loosely bound. This is to be contrasted to the Photoelectric interaction in which the incident photon almost always reacts with a tightly bound K, L or M electron. In the case of the Photoelectric reaction, the energy of the photoelectron E_e is given by:

$$E_e = E\gamma - BE \qquad (1)$$

where BE is the binding energy of the K, L, M, etc. electron in the material being studied.

In this experiment the kinematic equations that govern the Compton reaction will be studied in detail. These equations which simply conserve energy and momentum for the collision of a photon with a free electron can be written: (see fig. 9.1)

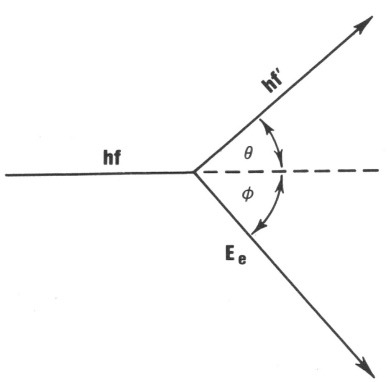

Figure 9.1. Kinematics of Compton scattering.

$$hf = hf' + E_e \text{ (conservation of Energy)} \qquad (2$$

$$\frac{hf}{c} = \frac{hf'}{c}\cos\theta + P_e\cos\phi \qquad (3$$

(conservation of momentum in the x direction)

$$O = \frac{hf'}{c}\sin\theta - P_e\sin\phi \qquad (4$$

(conservation of momentum in the y direction)

where

$hf = E\gamma$, $hf' = E\gamma'$ and

E_e = the energy of the recoil Compton Electron (MeV) (5

$= mc^2 - m_oc^2$

$$m = m_o\sqrt{1 - \frac{v_e^2}{c^2}} \qquad (6$$

$P_e = mv_e$; (v_e is the velocity of the electron) (7

Equations (2), (3), and (4) represent three independer equations. Since we are normally interested in $E\gamma'$, th three equations can be solved to eliminate parameter associated with the recoil electrons. If this is done, th following can be written:

$$E\gamma' = \frac{E\gamma}{1 + \frac{E\gamma}{m_oc^2}(1-\cos\theta)} \qquad (8$$

Define $(E\gamma/m_oc^2) = \alpha$; $m_oc^2 = 0.511$ MeV (for the elec tron)

then

$$\frac{E_e}{E\gamma} = \frac{\alpha(1-\cos\theta)}{[1 + \alpha(1-\cos\theta)]} \qquad (9$$

Figure 9.2 shows the solution of eq. (9) for eight angle (θ) as a function of $E\gamma$.

Figure 9.3 shows the solutions of eqs. (9) and (2) whe $\theta = 180$ degrees (backscatter). The Compton edge is als shown on the figure. It should be remembered that th Compton edge is the maximum energy that can be give to a recoil electron by the Compton scattering proces

In eqs. (2) through (9), the relativistic expression used for the momentum and energy of the recoil Comp ton electrons. This is necessary since in this experime the recoil electrons will reach velocities where the ter v_e^2/c^2 can not be ignored. In any case, the energies either the scattered gamma $E\gamma'$ or the recoil electron can be found at a particular angle (θ) by either solving e (8) or reading the required value from figs. 9.2 or 9.3

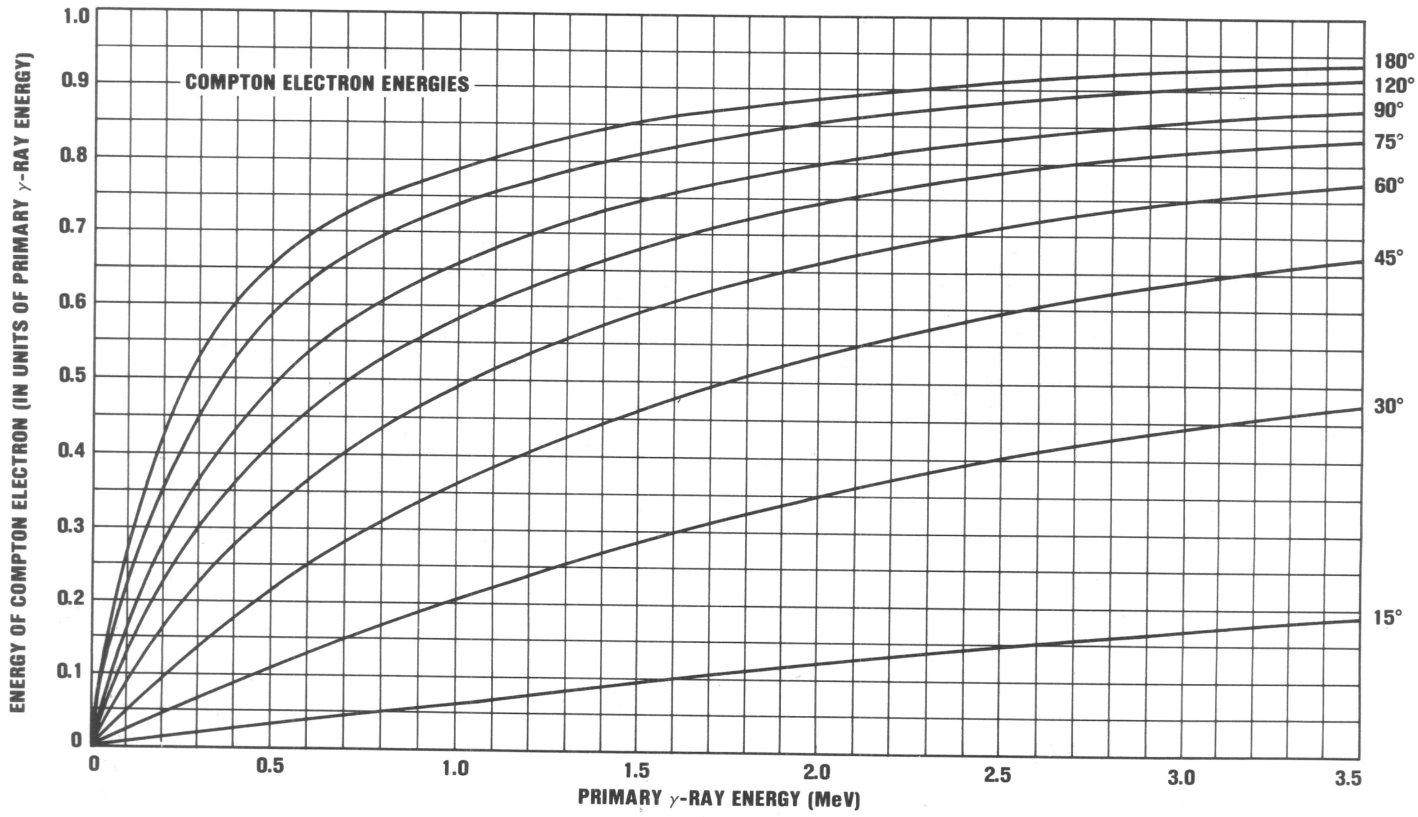

Figure 9.2. Energy of Compton electrons as a function of Eγ for eight angles (θ).

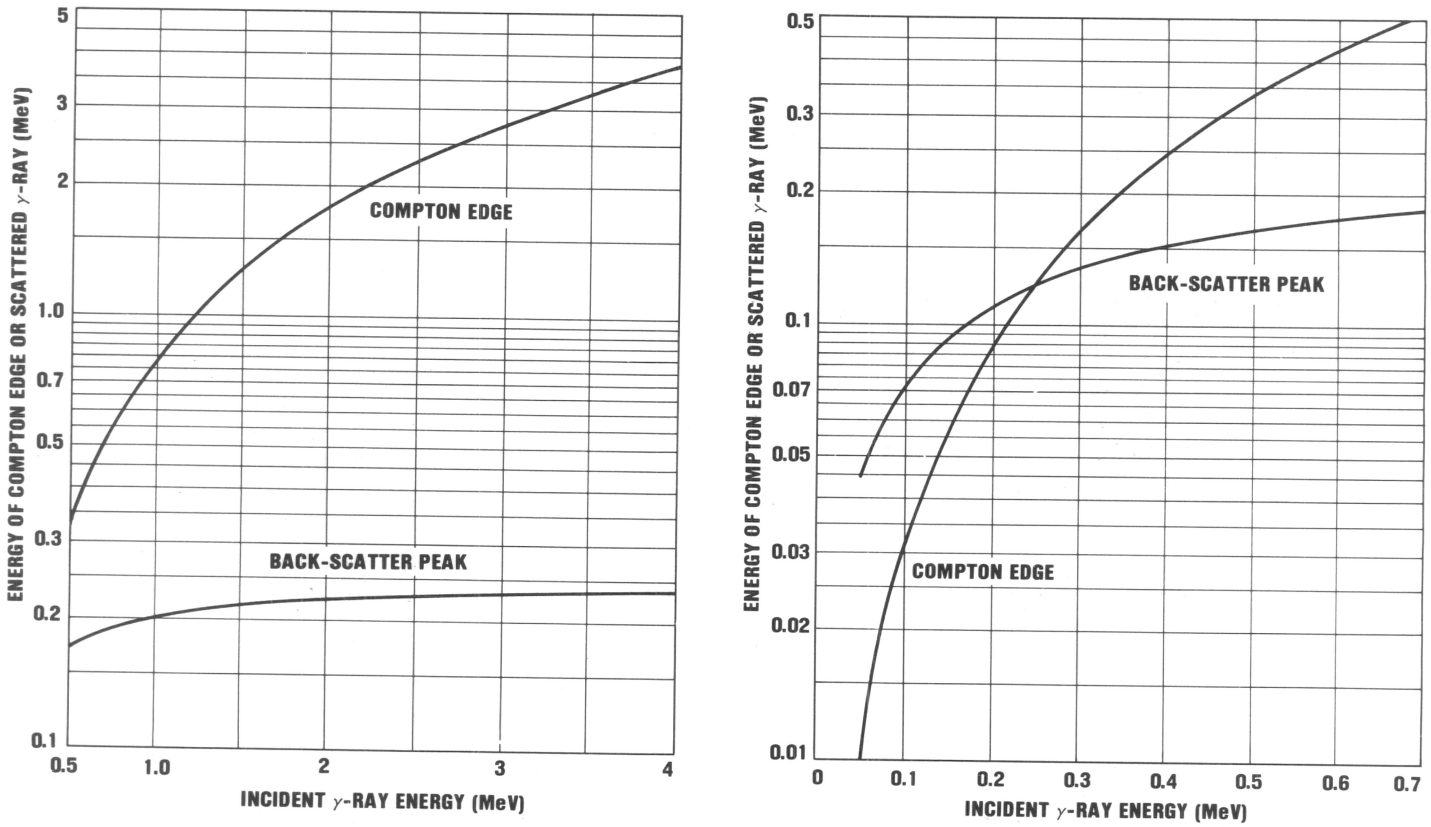

Figure 9.3. Energy of the Compton edge and the backscatter energy as a function of Eγ.

EXPERIMENT 9.1

The Measurement of Eγ' vs θ

Discussion

The Compton Scattering apparatus that will be used for this experiment is shown in fig. 9.4. The distance R_1 in the figure is about 20 cm. For the purpose of this discussion, let us assume that the ^{137}Cs source has an activity of 10 mCi. The intensity (I) of photons at the aluminum scattering cylinder is then:

$$I = \frac{10 \times 10^{-3}}{4\pi\ (20\ cm)^2} \frac{Ci \times 3.7 \times 10^{10}}{} d/s \qquad (10)$$

$$= 7.36 \times 10^4\ \gamma's/cm^2s$$

As we will see, this intensity of γ's at the scattering sample will give a γ' counting rate in the movable detector that is barely adequate to measure a pulse height spectrum in a time of 5 minutes. The point here is that the ^{137}Cs needs to have an activity of from 10 to 30 mCi for us to be able to complete this experiment in a two hour laboratory period.

Caution: Sources of this activity should be loaded into the lead housing by the instructor using tongs, or special handling rods, that are provided by the ^{137}Cs source manufacturer. Once the source has been loaded in its housing, it can safely be used by the students following the procedures outlined by the instructor.

Experimental Procedure

1. Use the techniques that were outlined in Experiment 2 NaI(Tℓ) spectroscopy to calibrate the MCA. The ^{137}Cs gamma should appear in approximately channel 350. Other sources that can be used for this calibration are ^{22}Na, ^{65}Zn, ^{60}Co and ^{57}Co. Plot the energy vs channel number from the data points.

2. Determine the resolution of the detector for all of the gamma lines for the above source that is used.

3. Place the ½ inch diameter Aluminum Scattering Rod in the scattering position. Set the movable detector at an angle of 20 degrees and accumulate a spectra for a period of time long enough to obtain a (Σ-β) of 3000 counts in the photopeak. Record the time, calculate (Σ-β/t) and enter this figure in Table 9.1. From the calibra-

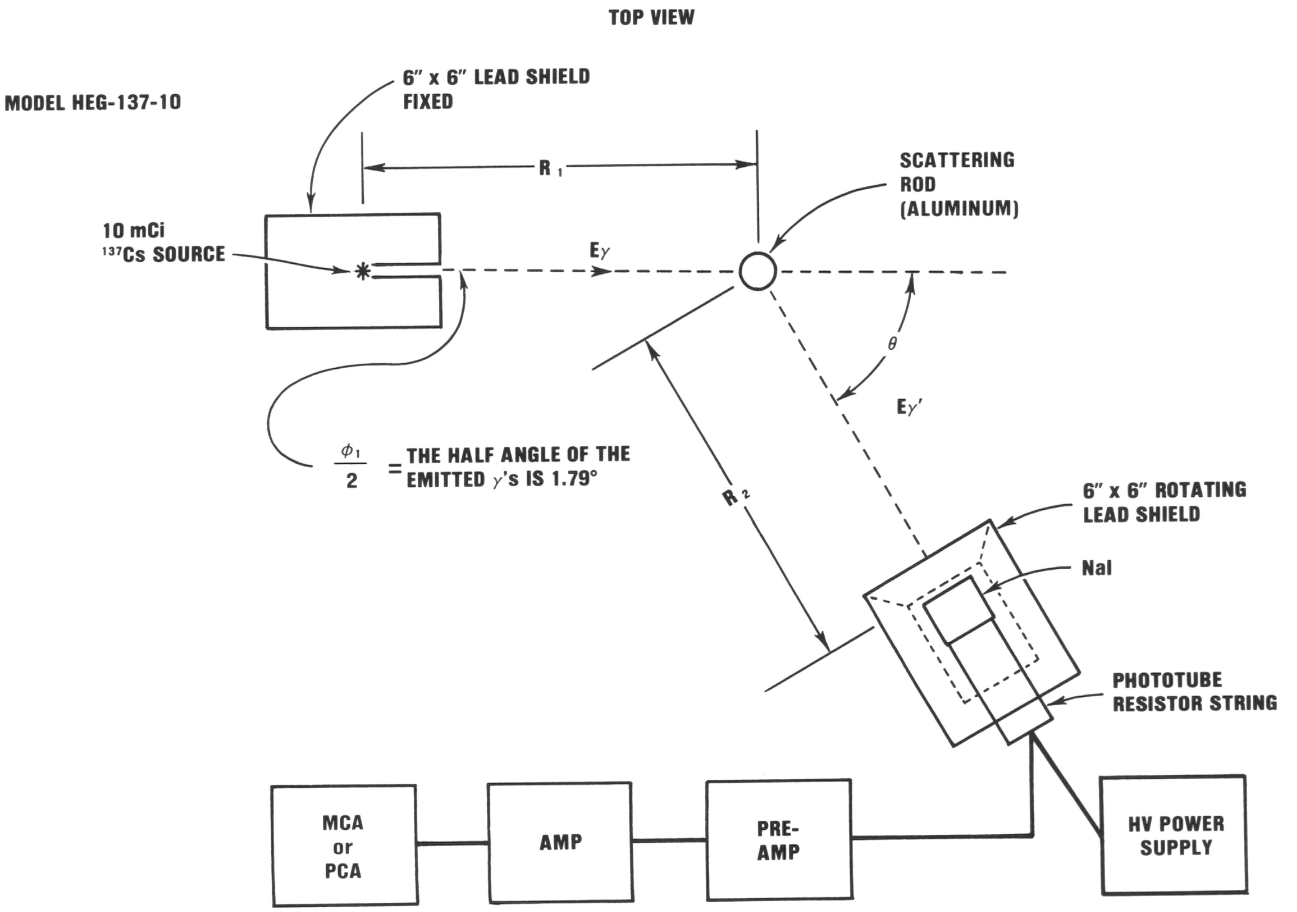

Figure 9.4. Plan view of Compton scattering apparatus showing the electronics for measuring Eγ' vs θ.

tion curve determine $E\gamma'$ and record it in the table. Repeat the measurement for the rest of the angles in the data table.

Exercise A From eq. (8), calculate $E\gamma'$ for all of the angles listed in Table 9.1. Fill in $1/E\gamma'$ (theory) and the $(1-\cos\theta)$ entry in the table. On a piece of linear graph paper, plot $1/E\gamma'$ (theory) y axis vs $(1-\cos\theta)$. From eq. (8), it can be seen:

$$\frac{1}{E\gamma'} = \frac{1}{E\gamma} + \frac{1}{m_o c^2}(1-\cos\theta) \qquad (10)$$

This equation is of the form:

$$y = mx + b \qquad (11)$$

where

$$y = \frac{1}{E\gamma'}$$

$$m = \frac{1}{m_o c^2} = \frac{1}{0.511\ \text{MeV}} = 1.96\ \text{MeV}^{-1}$$

$$b = \frac{1}{E\gamma} = 1.51\ \text{MeV}^{-1}$$

The "theory" plot of $1/E\gamma'$ vs $(1-\cos\theta)$ should therefore be a straight line.

Exercise B Plot the measured $(1/E\gamma')$ points on the theory curve with the estimated error bars for $1/E\gamma'$. Figure 9.5 shows typical experimental results.

It should be noticed from the experimental data (on fig. 9.5) that the fundamental rest mass (m_o) can be determined from the graph. Instead of plotting the straight line theory on the figure, fit a straight line to your experimental points. The experimental slope thus obtained is $(1/m_o c^2)$. This simple experiment thus yields one of the most fundamental quantities in nuclear science "the rest mass of the electron."

Table 9.1 Data Table for Compton Scattering: $E\gamma'$ vs θ, and $(d\sigma/d\Omega)_{Compton}$

Run No.	Peak Channel	θ Degrees	$E\gamma'$ (Calculated)	$E\gamma'$ (Measured)	$\left(\frac{\Sigma-\beta}{t}\right)$	$\left(\frac{d\sigma}{d\Omega}\right)$ Measured	$\left(\frac{d\sigma}{d\Omega}\right)$ Theory	$\frac{1}{E\gamma'}$ MeV^{-1} Theory	$(1-\cos\theta)$
1		20							
2		40							
3		60							
4		80							
5		100							
6		120							
7		140							
8		160							

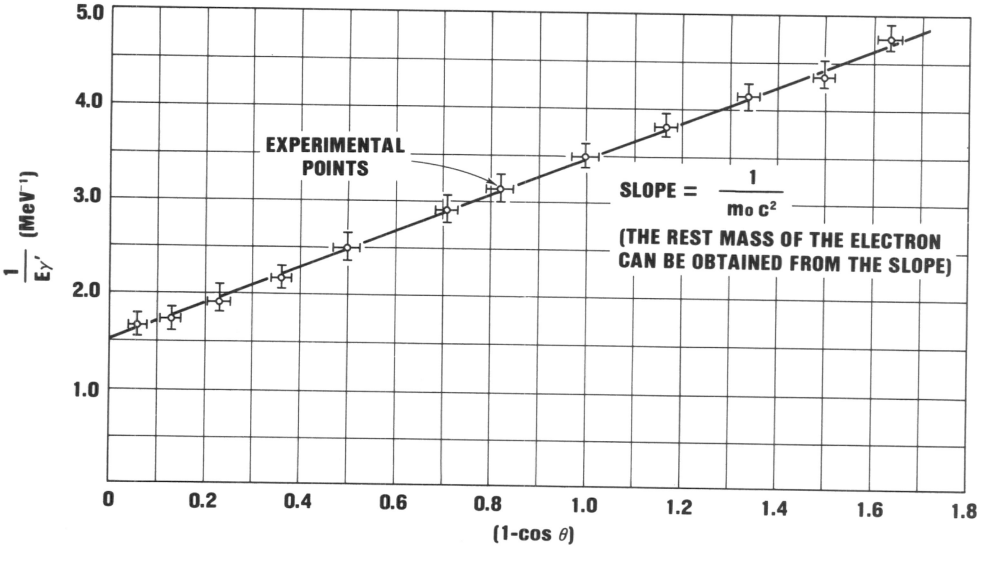

Figure 9.5. Experimental verification of the Compton scattering equations (see eq. 10).

EXPERIMENT 9.2

The Differential Cross Section for Comptons Scattering

Discussion

The theoretical scattering cross-section for the Compton Interaction can be written (see refs. 2 and 3):

$$\left(\frac{d\sigma}{d\Omega}\right) = \frac{r_o^2}{2}\left[\frac{1+\cos^2\theta}{[1+\gamma\,(1-\cos\theta)]^2}\right] \times \left[1+\frac{\gamma^2\,(1-\cos\theta)^2}{(1+\cos^2\theta)\,[1+\gamma(1-\cos\theta)]}\right]\frac{cm^2}{Sr} \qquad (12)$$

where

$$\gamma = \frac{E\gamma}{m_o c^2} = 1.29 \text{ for the } 0.662\ E\gamma \text{ from } {}^{137}Cs$$

and

$$r_o = 2.82 \times 10^{-13} cm \text{ (classical electron radius)}$$

Figure 9.6 shows a plot of eq. (12) as a function of θ. In this experiment, the measured data points from Table 9.1 will be compared to this theoretical expression.

Exercise A The data for this experiment was collected in experiment 9.1. It was recorded in Table 9.1 as $(\Sigma\text{-}\beta/t)$ for $E\gamma'$.

Figure 9.7 shows $E\gamma'$ at $\theta = 60$ degrees. At larger angles $E\gamma'$ decreases in accordance with eq. (10). At 130 degrees $E\gamma'$ would be 211 keV. The values of $(\Sigma\text{-}\beta)$ recorded in Table 9.1 have to be corrected for the intrinsic peak efficiency of the detector. The student should review Experiment 2 for this procedure. The corrected sum is given by:

$$\left(\frac{\Sigma-\beta}{t}\right)_{corrected} = \frac{1}{\varepsilon_p}\left(\frac{\Sigma-\beta}{t}\right) \qquad (13)$$

where ε_p is the intrinsic peak efficiency for $E\gamma'$.

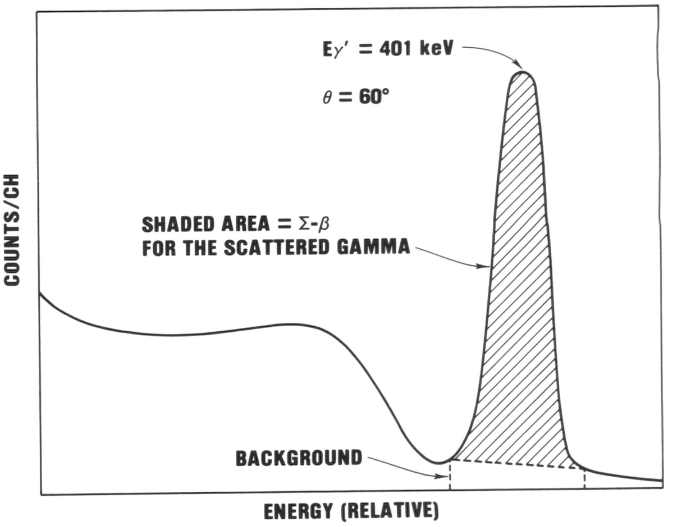

Figure 9.7. NaI(Tℓ) pulse height spectrum of Compton scattered gammas at θ= 60 degrees from ^{137}Cs. (Note: At θ = 0 degrees, the scattered peak would have the full energy of the ^{137}Cs source 662 keV).

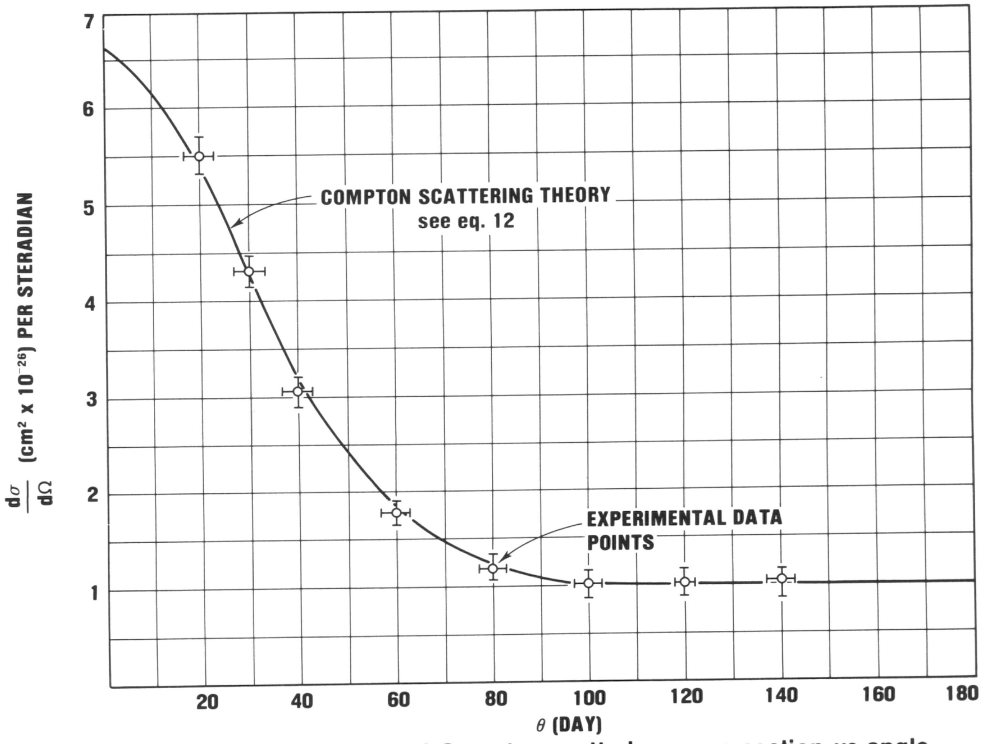

Figure 9.6. Theoretical Compton scattering cross-section vs angle.

For example, the (Σ-β) shown in fig. 9.7 would be divided by the appropriate ε_p for an energy of 401 keV. The measured Compton cross section is then given by:

$$\left(\frac{d\sigma}{d\Omega}\right)_m = \frac{\left(\frac{\Sigma-\beta}{t}\right)_{corrected}}{n\,\Delta\,\Omega\,I_o} \qquad (14)$$

where

n = the number of electrons in the scattering volume.

$$= \frac{(\text{volume})\ (\text{density of Al})\ (\text{Avogadros No})}{(\text{Atomic Weight})} \qquad (15)$$

$\Delta\Omega$ = Solid angle of the NaI(Tℓ) in steradians

$$= \frac{\text{Area of the detector (cm}^2\text{)}}{R_2^2\ (\text{cm}^2)} \qquad (16)$$

I_o = The number of incident γ's on the Aluminum scatterer per cm^2 per S.

= The number of γ's from the source divided by

$$\frac{1}{4\,\pi\,R_1^2} \text{ (see fig. 9.4)} \qquad (17)$$

Note, in eq. (15), the volume of the aluminum scatterer is given by:

$$V = \pi\,R_o^2\,h \qquad (18)$$

where

R_o = .635 cm

h = $R_1 \sin \phi_1$ (see fig. 9.4)

ϕ_1 = 3.58 degrees

From your experimental data (Σ-β/t) in Table 9.1 calculate $(d\sigma/d\Omega)_{measure}$ eq. (14). Enter these experimental points on the theoretical curve 9.6 as shown in the figure. The results should show that the Klein-Nishina theory (eq. 12) does a good job of predicting the scattered Compton differential cross-section.

EXPERIMENT 9.3

Measurement of the Electron Recoil Energy in Compton Scattering

Discussion

In order to complete our study of the Compton kinematic equations, the recoil electron energy (E_e) will be measured as a function of angle. From eq. (2), it is a simple matter to calculate E_e since, in the previous experiments, we have calculated hf′ as a function of angle. Calculate these E_e values and record them in Table 9.2 as E_e (calculated). In order to measure the recoil electrons, the aluminum scatterer in fig. 9.4 will be replaced with an organic scintillator (½″ in diameter) which is coupled to a phototube. When photons from the ^{137}Cs source scatter from the organic scintillator, the recoil electrons will be observed as individual flashes in the scintillator. The coincidence electronics shown in fig. 9.6 will be used to assure us that the recoiling electron that is observed, comes from the corresponding Eγ′ that is measured with the phototube.

Table 9.2 Calculated and Measured Values of the Energies of Compton Recoil Electrons

(degrees)	Peak Channel Number	E_e Measured	E_e Calculated	$\left(\frac{1}{E\gamma-E_e}\right)$ Calculated
20				
40				
60				
80				
100				
120				
140				
160				

Experimental Procedure

1. Set up the electronics as shown in fig. 9.8. Place a lead brick between the ^{137}Cs source and the plastic scintillator scatterer. The purpose of this shielding is to cut out all incident photons from the source while the plastic scintillator is being calibrated.

2. For the calibration, we wish to observe pulses from the plastic scintillator. Take the output of the amplifier from the plastic scintillator and feed it directly into the MCA. Obtain a ^{207}Bi source from the instructor and place it in contact with the plastic scintillator.

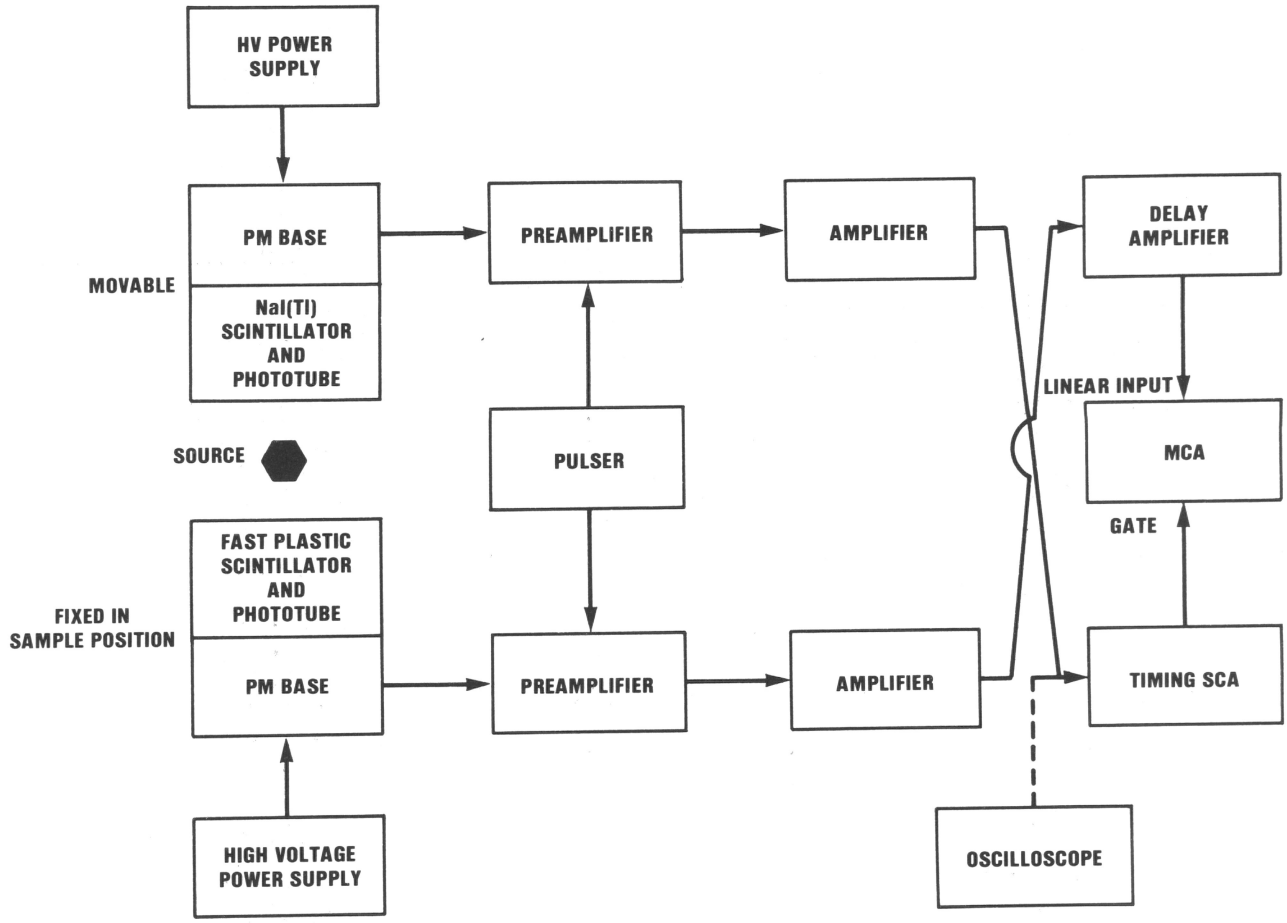

Figure 9.8. Electronic arrangement for measuring the electron recoil energy in Compton scattering.

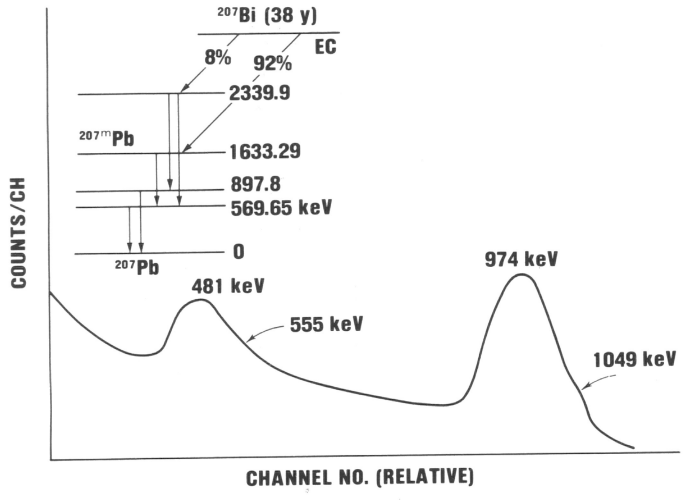

Figure 9.10. Pulse height spectrum of the conversion electrons of ^{207}Bi with a plastic scintillator.

Adjust the gain of the amplifier such that the 974 keV peak is in approximately channel 500. (See fig. 9.10). Record the positions of the the 974 and 481 keV peaks.

3. Remove the ^{207}Bi source and place a 2 μci ^{137}Cs source directly against the plastic scintillator. Figure 9.11 shows what the Compton distribution will look like for a ^{137}Cs source. Notice, this distribution looks almost like the case of the NaI(Tℓ) detector response except there is no photopeak. As you will recall, the photoelectric cross-section varies as Z^5. Since the average Z for an organic scintillator is low, very few photoelectric interactions will be observed.

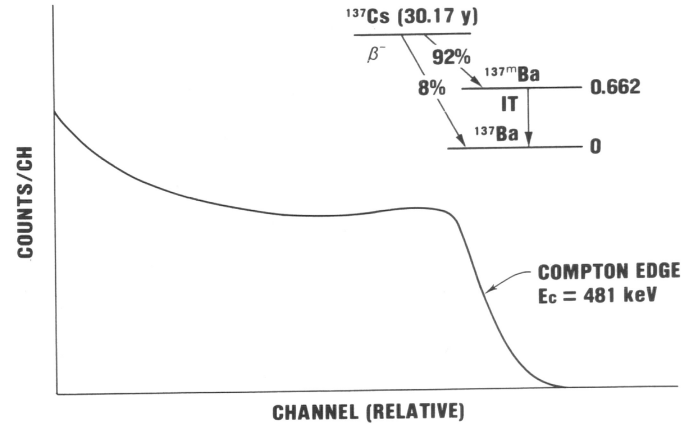

Figure 9.11. Pulse height spectrum of the Compton distribution for an organic scintillator (^{137}Cs source).

4. Record the position of the 481 keV Compton edge in the data table. Plot a calibration curve from the 974 and 481 keV points.

5. Remove all calibration sources and the lead shield that was used to block the 0.662 γ's from the ^{137}Cs scattering source. Connect the electronics back as shown in fig. 9.7. The NaI(Tℓ) calibration should be the same that was used in Experiment 9.2. Set the timing SCA in the integral mode with the E dial at 100/1000.

6. Set the MCA in the coincidence gate mode and feed the +5V logic output from the timing SCA into the gate input of the MCA. Set the NaI(Tℓ) detector at θ = 20 degrees and record a spectrum for a period of time long enough to clearly see the recoil electron peak in the MCA. Record the peak channel number in Table 9.2. Repeat this measurement for the other angles in Table 9.2. Figure 9.12 shows a typical recoil Compton electron (E_e) spectrum.

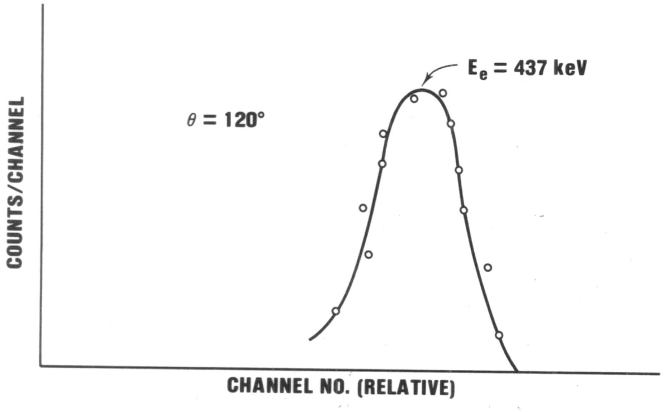

Figure 9.12. Recoil Compton electron spectrum at θ = 120 degrees for ^{137}Cs (see fig. 9.4 for a plan view of the experimental arrangement).

Exercise Plot $(1/E\gamma - E_e)$ calculated versus $(1-\cos\theta)$. Enter your points E_e (measured) onto this graph. Since, from eq. (2) $E\gamma' = E\gamma - E_e$ this new curve plus the data should show exactly the same results as fig. 9.5. It is the same curve. We have therefore, verified the kinematic equations for Compton scattering by two independent methods.

REFERENCES FOR *EXPERIMENT 9*

1. W. Heitler, *The Quantum Theory of Radiation*, 3rd ed., Oxford Univ. Press 1957.

2. R. D. Evans, *The Atomic Nucleus,* McGraw-Hill, New York (1955) pp 674-676.

3. A. C. Melissinos, *Experiments in Modern Physics,* Academic Press, New York (1966).

4. G. F. Knoll, *Radiation Detection and Measurement*, John Wiley and Sons, New York (1979).

5. P. Quittner, *Gamma Ray Spectroscopy*, Halsted Press, New York (1972).

6. R. L. Heath, "Scintillation Spectrometry," *Gamma-Ray Spectrum Catalog*, 2nd Edition **1** and **2**, IDO 16880, August (1964). Available from Clearinghouse for Federal Scientific and Technical Information, Springfield, Virginia.

7. C. M. Lederer and V. S. Shirley, Eds., *Table of Isotopes,* 7th Edition, John Wiley and Sons, New York (1978).

8. K. Siegbahn, Ed., *Alpha-, Beta-, and Gamma-Ray Spectroscopy,* **1**, North Holland Publishing Co., Amsterdam (1965).

9. A. W. Mann and S. Garfinkel, *Radioactivity and its Measurement*, Van Nostrand-Reinhold, New York (1966).

10. J. B. Marion and P. C. Young, *Tables of Nuclear Reaction Graphs*, John Wiley, New York (1968).

EXPERIMENT 10

Rutherford Scattering

Introduction

Clearly one of the most profound experiments ever performed in nuclear science was the scattering of alpha particles from a thin hammered gold foil. This experiment was performed in 1911 by Lord Ernest Rutherford in the Cavendish Laboratory in England. At the time of this experiment, the approximate size of the atom was known from the properties of gases and kinetic theory. Sir J. J. Thompson had proposed a model of the atom in which the electrons and other nucleons were mixed up in an ordered fashion in the atom. In this model the electrons maintained an equilibrium position in this matrix and variations in this average position, by excitation would yield emission of light. When Rutherford tried to use this model to understand the scattering of alpha particles from gold, he found that it was not possible to explain the large back angle scattering cross-section that was observed in the experiments. In the Thompson model the positive charges were distributed throughout the atom and hence the electric field was not large enough in any location within the atom to produce the necessary force on the alpha for observed backscattering. Rutherford knew from his experiments that the positive charges had to be clustered more closely to explain his results. Through his tremendous insight into physical phenomena, Rutherford finally developed a model in which all of the positive charge of the atom was concentrated in a hard core called the nucleus and the electrons rotated about the nucleus in a planetary fashion. This hard core nucleus had a radius of approximately 10^{-13} cm which was 1/100,000 the known diameter of atoms. Rutherford's calculations from the Coulomb field for this atomic model gave the necessary forces to explain the relatively large back angle scattering for the experiment. Later experiments would also prove that this new model would give the correct frequencies of light from Bohr theory. This simple alpha particle scattering experiment gave us a correct picture of the atom and certainly formed a foundation upon which modern nuclear science is based.

Scope

An alpha source and a specially designed chamber will be used to study the Rutherford scattering of alphas from thin foils. The Au (α, α) Au cross-section will be measured as a function of laboratory angle to verify the strong $1/\sin^4 \theta/2$ dependence. The $1/E^2$ dependence will be studied by reducing the energy of the incident alphas with thin foils similar to what was done in the (dE/dx) experiment. Finally the Z^2 dependence of $(d\sigma/d\Omega)$ will be investigated by using a variety of different atomic number scattering targets.

EXPERIMENT 10.1

Determination of I_0, the Alpha Particle Intensity at the Target

Discussion

Figure 10.1 shows a plan view of the experimental arrangement that will be used for the *Rutherford Scattering* experiment. The electronics that will be used for this experiment are identical to the set up for **Experiment 3 (Alpha Particle Spectroscopy).** Figure 10.2 shows a side view of the chamber with the beam line. The first part of this experiment will be to calibrate the surface barrier detector and measure the flux of alphas (I_0) that impinge on the gold foil. The Rutherford differential scattering cross section is given by:

$$\left(\frac{d\sigma}{d\Omega}\right)_m = \frac{I_1}{I_0 \, \Delta\Omega \, \eta_0} \quad \frac{cm^2}{sr} \qquad (1)$$

where

I_1 = the number of alphas per second that impinge on the scattering foil. (2)

$\Delta\Omega$ = the solid angle of the detector (steradians) (3)

$= \frac{A_d}{R_1^2}$; A_d = area of the detector

η_0 = number of nuclei per cm^2 (4)

$$= \frac{(g/cm^2 \text{ of the target}) \text{ (Avogaros No.)}}{\text{(Atomic wt. of the target)}}$$

In this part of the experiment I_0 will be experimentally measured.

Experimental Procedure

1. Set up the electronics as shown in fig. 10.1. For this part of the experiment, the gold scattering foil has been removed but the alpha source is in the chamber. Set the angle θ at 120 degrees so that not many alphas from the 1 mCi alpha source will scatter into the detector. Obtain a weak ^{210}Po source from the instructor. This source will be used to calibrate the system. Place this source 1 cm from the detector. Evacuate the chamber and adjust the bias voltage of the detector to its recommended value.

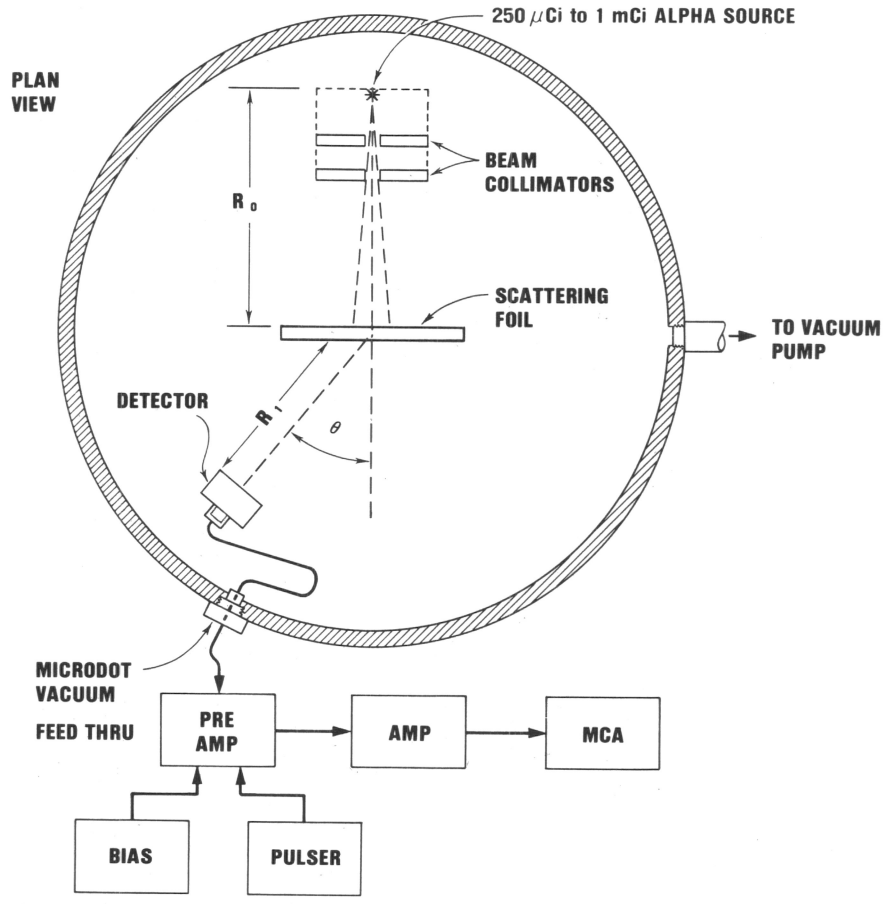

Figure 10.1. Experimental arrangement for Rutherford Scattering.

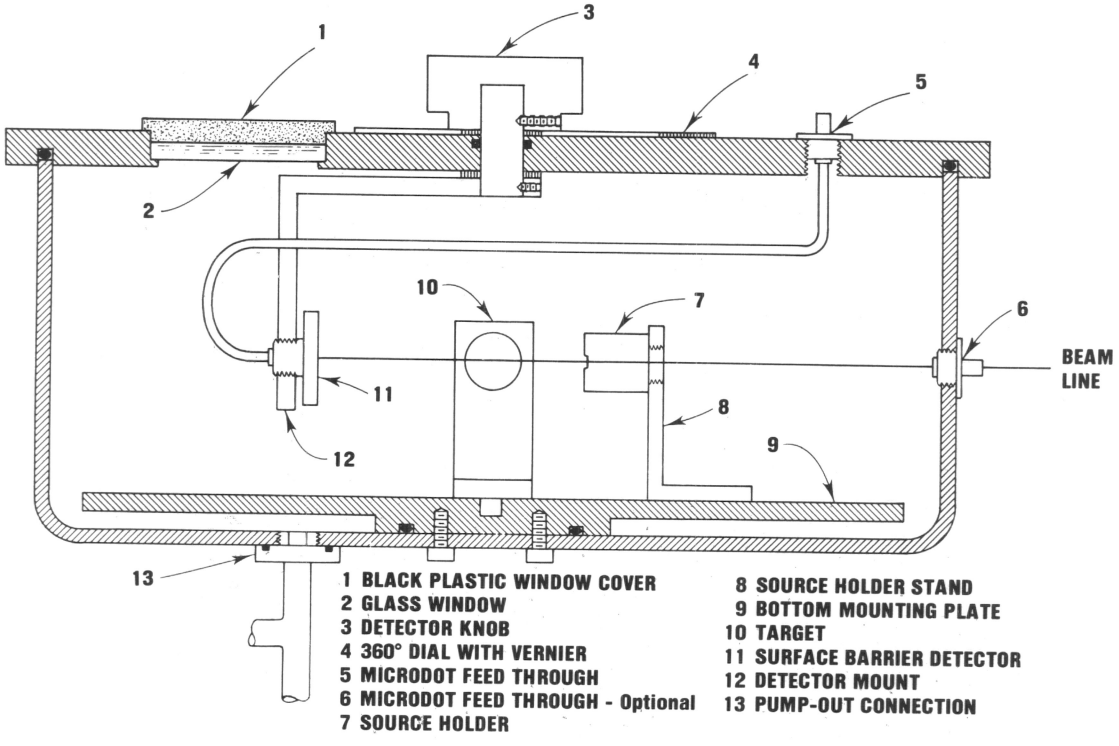

Figure 10.2. Side view of Rutherford Scattering chamber showing the beam line.

2. Adjust the gain of the system so that the 5.305 MeV alphas from the source fall in channel 200. Figure 10.3 shows a pulse height spectrum of the 138 day ^{210}Po alphas.

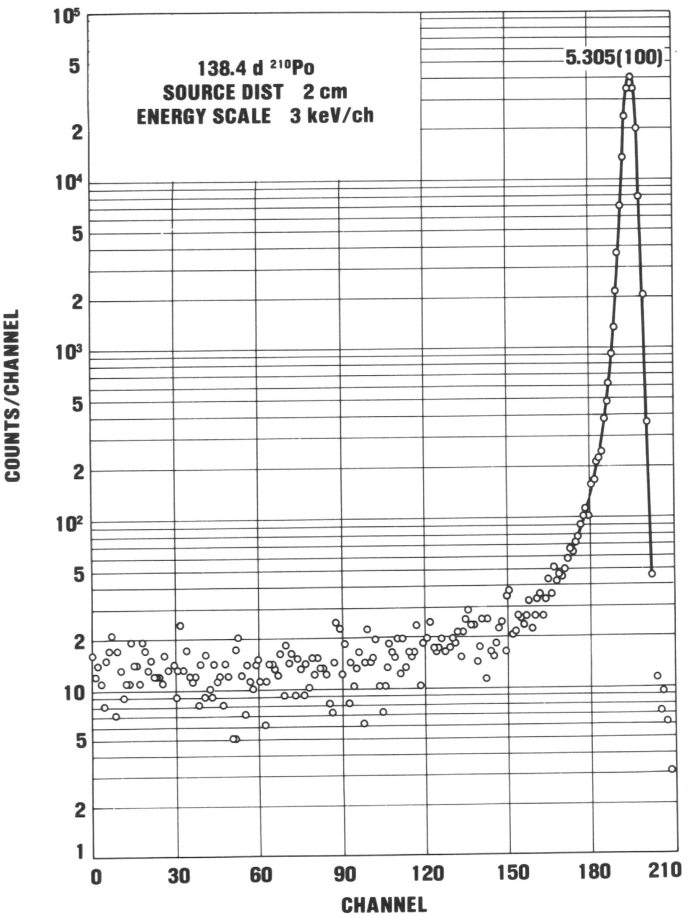

Figure 10.3. Silicon surface barrier detector pulse height spectrum of the alphas from ^{210}Po.

3. Turn on the pulse generator and set the pulse height dial at 530/1000. Adjust the calibrate potentiometer until the pulser peak is also stored in channel 200. The pulser is now calibrated so that 530/1000 = 5.30 MeV, etc. Set the pulse height dial setting at 100/1000 and accumulate a spectrum for a long enough period of time to determine its channel number. Record this vaue in Table 10.1. Repeat for the other pulser values in the table. The system is now calibrated. Plot a calibration curve, measure its slope in keV/ch and determine the resolution of the ^{210}Po alphas. This procedure was outlined in **Experiments 3 and 4**.

4. Turn off the bias voltage, and let the chamber slowly up to air. Remove the ^{210}Po source and rotate the detector to θ = 0 degree. Evacuate the chamber and return the bias voltage to its proper value. We are now in a position to see alphas coming directly from the scattering alpha source. The most common two alpha sources for Rutherford Scattering are ^{241}Am and ^{244}Cm. For the purpose of this discussion, let us assume that the source is ^{241}Am. The primary alpha energy from ^{241}Am is 5.486 MeV. (**See Experiment 3**). The energy that we will measure, however, will not be this value. The energy that reaches the detector will be degraded primarily because of energy loss in the source itself and the cover that must be manufactured over the source to eliminate contamination. Accumulate a spectrum for a period of time long enough to determine (E_1) the measured energy of the source without a scattering foil. Also determine (Σ-β/t) for the source. Record these values.

Table 10.1 Pulser Calibration Data for Rutherford Scattering

Pulse-Height Dial Setting	Energy (MeV)	Channel Number of MCA Peak
100/1000	1.0	
200/1000	2.0	
300/1000	3.0	
400/1000	4.0	
500/1000	5.0	
600/1000	6.0	
700/1000	7.0	

Exercise When the detector is at θ = 0 degree, its distance from the source (**See Fig. 10.1**) is (R_0 + R_1). The intensity at the scattering foil is therefore:

$$I_0 = \left[\frac{(R_0 + R_1)^2}{R_0^2}\right] I_1 \qquad (5)$$

$$I_1 = \left(\frac{\Sigma\text{-}\beta}{t}\right) \qquad (6)$$

Calculate I_1 and I_0 and record them in a data table.

EXPERIMENT 10.2

The $1/\sin^4 \theta/2$ Dependence of the Rutherford Scattering Cross Section

Discussion

The theoretical expression for the Rutherford cross section is given by:

$$\left(\frac{d\sigma}{d\Omega}\right)\frac{mb}{sr} = 1.296\left(\frac{Z_1 Z_2}{E_1}\right)^2\left[\frac{1}{\sin^4 \theta/2} - 2\left(\frac{M_1}{M_2}\right)^2\right] \quad (6)$$

where

Z_1 = the atomic number of the projectile (2 for α's)

Z_2 = the atomic number of the target (79 for Au)

E_1 = energy of the alpha particle in MeV, M_1 and M_2 are mass numbers for the projectile and target (4 and 197 for the above reaction).

Equation (6) should be calculated and entered in Table 10.2 as $(d\sigma/d\Omega)$ calculated, column (6).

Figure 10.4 shows a plot of eq. (6) for E_1 = 5.1 MeV. Keep in mind, the energy of the alphas from ^{241}Am are 5.48 MeV, however, energy loss in the source and the gold foil has given an effective energy of 5.1 MeV. We will use this number throughout the experiment.

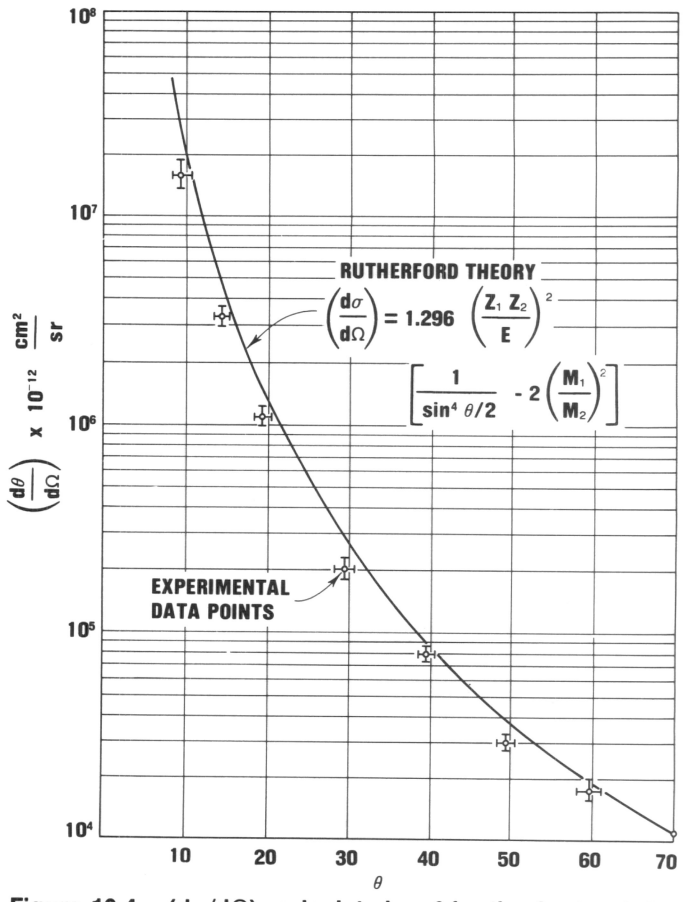

Figure 10.4. $(d\sigma/d\Omega)_c$ calculated vs θ for the Au (α, α) Au reaction. Note this was calculated for E^1 = 5.1 MeV for eq. (6).

Table 10.2 Data for Rutherford Scattering Experiment (Gold Foil)

Run No. (1)	Theta (deg) (2)	$\left(\frac{\Sigma-\beta}{t}\right)$ Measured (3)	$\left(\frac{\Sigma-\beta}{t}\right)$ Frame Scatter (4)	$\left(\frac{\Sigma-\beta}{t}\right)_c$ Corrected (5)	$\left(\frac{d\sigma}{d\Omega}\right)_c$ Calculated (6)	$\left(\frac{d\sigma}{d\Omega}\right)_m$ Measured (7)
1	10					
2	15					
3	20					
4	25					
5	30					
6	40					
7	50					
8	60					
9	70					
10	80					
11	90					
12	100					

In this experiment, we will collect all of the data that is needed to fill in Table 10.2. Only part of the data will be used to show the $1/\sin^4\theta/2$ dependence.

Experimental Procedure

1. The first measurement that will be made is a determination of the number of alphas that scatter from the frame that holds the gold foil. This is column (4) in Table 10.2. Mount the blank frame in the chamber. This frame is identical to the frame that holds the gold foil, only there is no foil on it. Evacuate the chamber, adjust the Bias voltage to its recommended value. Set θ = 10 degrees and accumulate a spectrum for a time period of 300 seconds. Record this $(\Sigma\text{-}\beta/t)$ in Table 10.2 column (4). Repeat for the other angles in the table.

2. Remove the blank frame and replace it with the gold foil. Set the detector back to θ = 10 degrees and accumulate a spectrum for a period of time long enough to obtain reasonable statistics in the scattered alpha group. Determine $(\Sigma\text{-}\beta/t)$ and record it in column (3) of Table 10.2.

3. Repeat this measurement for the other angles in Table. 10.2.

Exercise A The value of $(\Sigma\text{-}\beta/t)_c$ corrected (column 5) will now be calculated. This value is determined by subtracting column (4) from column (3). Make this subtraction and fill in column (5).

Exercise B The $1/\sin^4\theta/2$ dependence will be established by normalizing $(\Sigma\text{-}\beta/t)_c$ corrected to the theoretical $(d\sigma/d\Omega)_c$ at θ = 30 degrees.

Therefore:

$$K_1\left(\frac{\Sigma\text{-}\beta}{t}\right)_c = \left(\frac{d\sigma}{d\Omega}\right)_c \qquad (7)$$

Find K_1 from eq. (7) and multiply all values of $(\Sigma\text{-}\beta/t)_c$ by K_1. Plot these values on your theoretical curve (fig. 10.4). The experimental numbers should agree at all angles, thus showing the $1/\sin^4\theta/2$ dependence.

EXPERIMENT 10.3

The Absolute Rutherford Differential Cross Section for Au (α, α) Au

Discussion

The value of I_1 in eq. (1) is the same as column (5) in Table 10.2. We have previously determined the value of I_0 (Experiment 10.1).

Exercise Equation (1) will be used to determine $(d\sigma/d\Omega)_m$ the measured differential cross section. Calculate $\Delta\Omega$ from eq. (3) and η_0 from the quoted thickness of the gold foil. Fill in the value of the measured cross sections (column 7) in Table 10.2. Plot these values on the theoretical curve (see fig. 10.4). The $1/\sin^4\theta/2$ dependence can be seen if $(d\sigma/d\Omega)_m$ is plotted versus $1/\sin^4\theta/2$. From eq. (6), this is of the form Y = mx + b, and it should yield a straight line. Figure 10.5 shows a typical plot of $(d\sigma/d\Omega)_m$ versus $1/\sin^4\theta/2$. Experimental points are also shown on the curve.

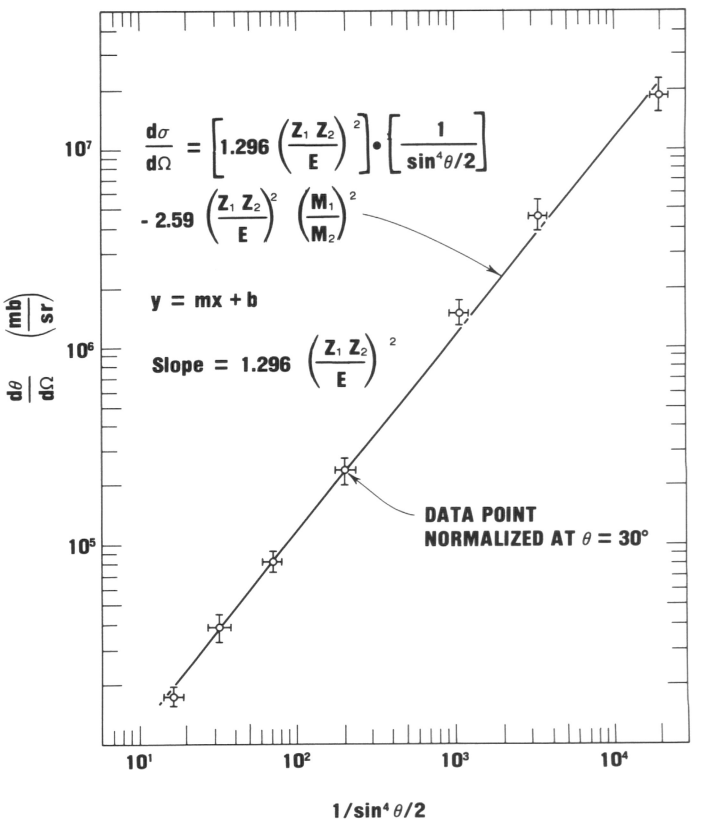

Figure 10.5. Experimentally measured Rutherford differential cross section versus $1/\sin^4\theta$ for Au (α, α) Au.

EXPERIMENT 10.4

The Z^2 Dependence of the Rutherford Scattering Cross Section

Discussion

The Z^2 dependence of the Rutherford Cross Section can be determined by performing the $(d\sigma/d\Omega)_m$ experiment for a variety of different scattering foils. In this experiment $(d\sigma/d\Omega)_m$ at 30 degrees will be determined for scattering foils of $_{79}$Au, $_{47}$Ag, $_{29}$Cu, and $_{13}$Al. The data for $_{79}$Au has already been taken in Experiment 10.2.

Experimental Procedure

1. Remove the $_{79}$Au foil and replace it with a $_{47}$Ag foil. Repeat all of the above measurements that are necessary to measure $(d\sigma/d\Omega)_m$ for $_{47}$Ag at θ = 30 degrees.

2. Repeat the above measurement for the $_{29}$Cu and $_{13}$Al targets at only θ = 30 degrees as above. Record all of these values in an appropriate data table.

Exercise For all of the scattering foils, plot $(d\sigma/d\Omega)_m$ versus Z^2.

Figure 10.6 shows a typical plot of this data.

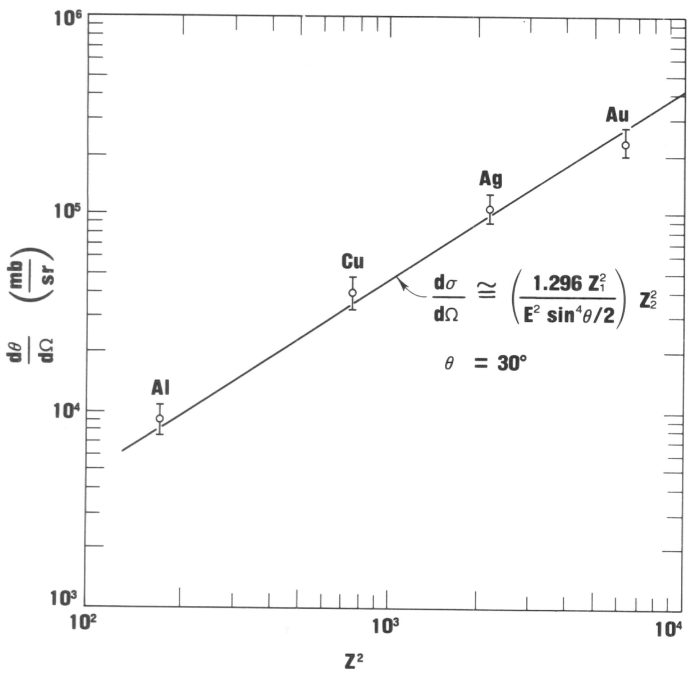

Figure 10.6. $(d\sigma/d\Omega)_m$ versus Z^2 for ^{79}Au, ^{47}Ag, ^{29}Cu, and ^{13}Al scattering foils at θ = 30 degrees.

EXPERIMENT 10.5

The $1/E^2$ Dependence of the Rutherford Differential Cross Section

Discussion

In this experiment we will measure the Au (α, α) Au scattering cross section at θ = 30 degrees for a variety of different incident alpha particle energies. The energy of the alpha particles will be varied by placing appropriate copper foils between the source and gold scattering foil. The student should review **Experiment 4** before attempting this experiment.

Experimental Procedure

1. Set the detector at 30 degrees and re-run the data that was taken in Table 10.2. Record this value of $(d\sigma/d\Omega)_m$ as Run No. 1 in Table 10.3.

2. Open the chamber and place the first copper foil between the source and the gold scattering foil. The thickness of the Cu should be adequate to reduce the transmitted alpha energy to approximately 4.5 MeV (see Experiment 4). Measure $(d\sigma/d\Omega)_m$ for this new alpha energy. Record the measured differential cross section in Table 10.3.

3. Remove the copper foil and replace it with one thick enough to reduce the alpha energy to approximately 4.0 MeV. Determine $(d\sigma/d\Omega)_m$ and record in Table 10.3. Repeat for other Cu foil thickness to complete the Table.

Exercise Calculate $(d\sigma/d\Omega)_c$ for each of the measurements made in Table 10.3 and record these values in column (5). Plot $(d\sigma/d\Omega)_m$ versus $1/E^2$ from the data. Figure 10.7 shows such a plot with the experimental data.

Table 10.3 The $1/E^2$ Dependence of the Rutherford Differential Scattering Cross Section at θ = 30 Degrees

Run No. (1)	Copper Foil Thickness (2)	Eα Incident Alpha Energy (3)	$\left(\frac{d\sigma}{d\Omega}\right)_m$ Measured (4)	$\left(\frac{d\sigma}{d\Omega}\right)_c$ Calculated (5)
1	0.00	5.1		
2		4.5		
3		4.0		
4		3.5		
5		3.0		
6		2.5		

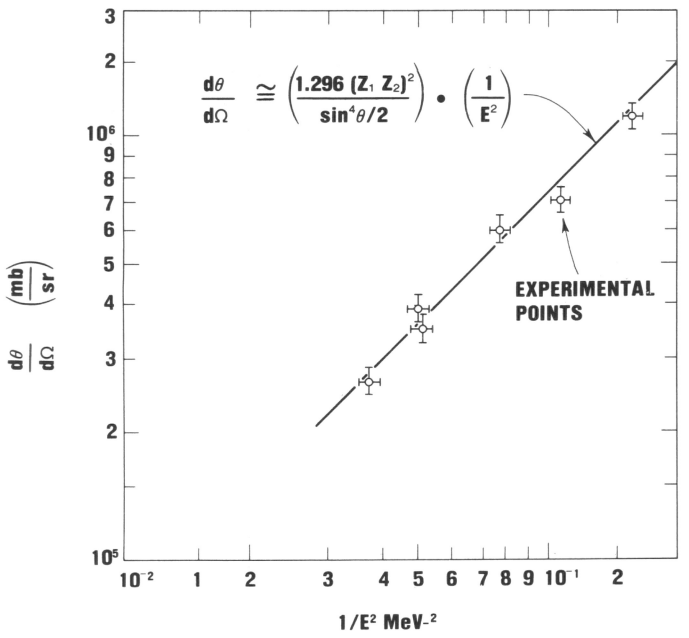

Figure 10.7. Measured Rutherford differential cross-section versus $1/E^2$ for Au (α, α) Au at θ = 30 degrees.

REFERENCES FOR *EXPERIMENT 10*

1. J. W. Mayer and E. Remini, *Ion Beam Handbook for Material Analysis*, Academic Press, New York 1977.

2. A. C. Melissinos, *Experiments in Modern Physics*, Academic Press, New York (1966).

3. J. L. Duggan and J. F. Yegge, "A Rutherford Scattering Experiment," *J. Chem. Ed.*, **45** 85 (1968).

4. J. L. Duggan, et.al., *Am. J. Phys.* **35**, 631 (1967).

5. H. A. Enge, *Introduction to Nuclear Physics*, Addison-Wesley Publishing Co., Massachusetts (1966).

6. R. D. Evans, *The Atomic Nucleus*, McGraw-Hill, New York (1955).

7. B. L. Cohen, *Concepts of Nuclear Physics*, McGraw-Hill, New York (1971).

8. G. Marion and P. C. Young, *Tables of Nuclear Reaction Graphs*, John Wiley and Sons, New York (1968).

9. C. M. Lederer and V. S. Shirley, Eds., *Table of Isotopes*, 7th Edition, John Wiley and Sons, Inc., New York (1978).

EXPERIMENT 11

Coincidence Measurements in Nuclear Spectroscopy and Absolute Activity Determination by β,γ Coincidence Studies

Scope

In this experiment several experimental configurations will be used to study coincidence events in nuclear spectroscopy. In the first experiment, a multipurpose coincidence circuit will be used with a pulse generator to determine an overlap coincidence spectrum. This will be followed by a study of the Linear Gate and the Time-to-Amplitude Converter (TAC) in coincidence spectroscopy. Finally, the absolute activity of ^{60}Co will be determined by a β,γ coincidence experiment.

Discussion

Figure 11.10 shows the decay scheme of ^{60}Co. In the figure ^{60}Co decays by β emission of the 2.507 MeV 4+ level in ^{60}Ni. The 2.507 MeV state decays by two cascading gammas to the 1.3325 MeV 2+ level and then to the ground state of ^{60}Ni. Without coincidence spectroscopy, it is impossible to tell very much about the decay scheme. For example, let's assume that we measure the β spectrum from ^{60}Co. It is not shown in fig. 11.13 but there are βs to a 2.158 MeV state in ^{60}Ni. There are also βs to the 1.3325 MeV state. The β continuum that we measure would therefore be composed of three β particle energies and it would be difficult to tell much about the decay scheme with just the β spectrum from the isotope. However, if we do a β,γ coincidence between the 2.507 MeV state and the 1.17 MeV γs, we would then measure only βs to that state.

In experiment number 3, **Alpha Spectroscopy**, we saw that most of the isotopes that were studied had numerous branches to their decay. Typically, the parent isotope would decay by alpha emission to seven or eight different levels in the daughter nucleus. Some of these levels would gamma cascade to the ground state while internal conversion would be very important for low lying levels in the daughter nucleus. The only way that these decay schemes can be unraveled is by coincidence experiments of the type (α,γ), (α,e), or (α,x). Coincidence spectroscopy has therefore given us the electronic tool to study in detail the fine points of nuclear structure.

EXPERIMENT 11.1

A Simple Coincidence Experiment with a Multipurpose Coincidence Module

Discussion

The electronics for this experiment are shown in fig. 11.1. The attenuated output of the pulser is fed simul-

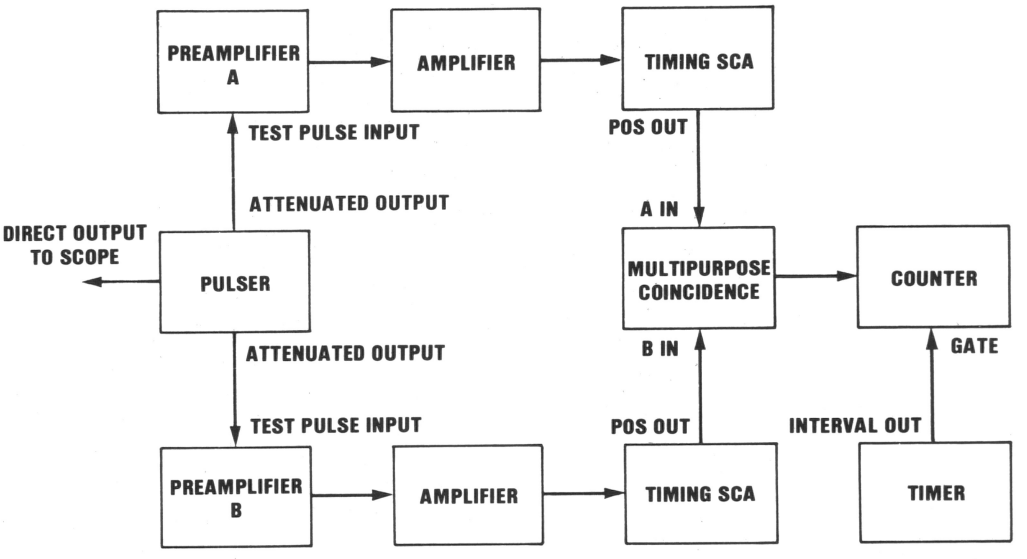

Figure 11.1. Electronics for a simple coincidence experiment with a multipurpose coincidence module.

taneously into the two preamps by a BNC Tee connector on the output of the pulser. Since output pulses of the preamps are negative, the polarity of the pulser should be set to match the preamp output. The preamp outputs should be fed into the negative input of each amplifier. The gain of the amplifiers should be set such that the biopolar output pulses have an amplitude of approximately 3.7 volts (V).

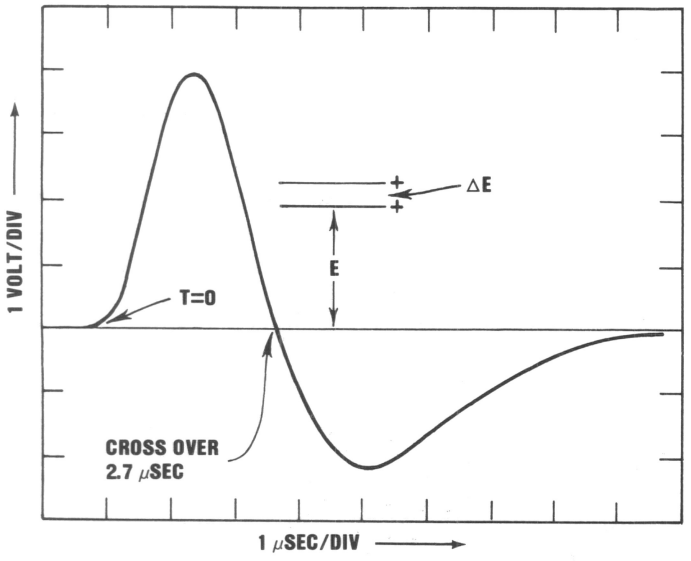

Figure 11.2. Typical bipolar amplifier output observed with an oscilloscope.

Figure 11.2 shows a typical amplifier output pulse with a pulse generator input. **Note:** From T = O until the positive portion of the pulse reaches the baseline is approximately 2.7 μsec. This cross-over time is adjusted with the peaking time control on the amplifier. For fig. 11.2, the peaking time (rise time) was set at 1 μsec. The output pulses from each amplifier in fig. 11.1 are fed into the input of a constant fraction timing Single Channel Analyzer (SCA). The SCA should be set in the ASYMmetrical window mode. In this mode of operation, the SCA inspects the output pulses of the amplifier (see fig. 11.2). If the output pulse is greater than E but less than E + ΔE, the SCA will generate a +5V, 500 nanosecond (nsec) wide logic pulse which in effect says the input criterion of the SCA have been met. In other words, the output pulses must fall within the ΔE window of the SCA to produce a corresponding SCA output. In fig. 11.2, the E dial (lower level) is set at 2.00 volts and ΔE (window) is set at 0.3 volts width. Therefore, before the SCA in fig. 11.2 will give an output pulse, the pulses out of the amplifier must be between 2.0 and 2.3 volts. In the figure the output pulses from the amplifier are approximately 3.7 volts high and therefore, the SCA will not give output pulses. If we slowly raise the lower level (E dial) on the SCA, output pulses will be observed from it when the lower level is at 3.4 volts. We would continue to see these output pulses until the E level reaches 3.7 volts at which time the SCA pulses will stop.

For a timing SCA the output pulse is generated at the time of cross-over (see fig. 11.2). These pulses are then fed into the A and B inputs (fig. 11.1) of the multipurpose coincidence circuit. The coincidence module is a circuit that will generate a +5V logic pulse into the counter if the A and B input pulses fall within the resolving time of the circuit. This resolving time can be adjusted to a large number of values between 50 nsec and 6.5 μsec. This resolving time range is adjusted by a multiposition switch on the front of the module. The particular coincidence circuit that will be used can have up to five inputs but we will just use the A and B inputs for this experiment. The timer in fig. 11.1 turns off the counter after the preset time. Both may be contained in the same module called a counter and timer.

Experimental Procedure

1. Set up the electronics as shown in fig. 11.1. Take the attenuated output of the pulser and feed it simultaneously into preamps A and B. This is done by placing a BNC Tee connector on the attenuated output of the pulser. For this discussion, it is assumed that we are using a non-inverting preamp. The pulser should be set for negative output. The preamp outputs will therefore be negative. Turn on the pulse generator and adjust the pulse height dial and the attenuation switches so that the amplitude of the attenuated output is 0.1V. See fig. 11.3.

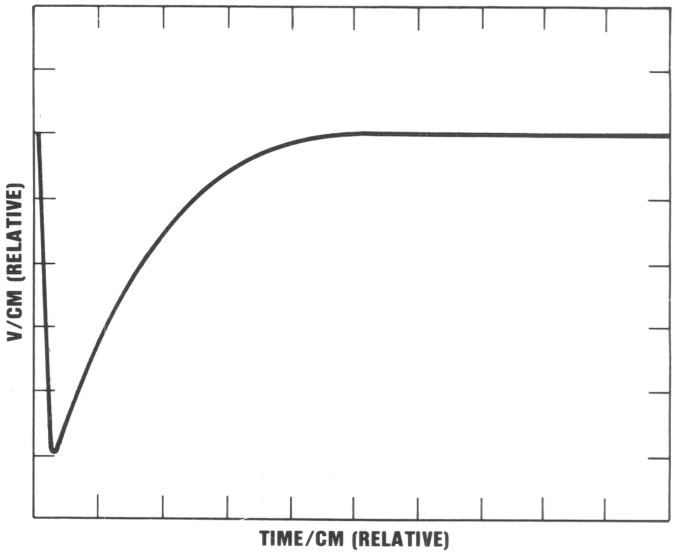

Figure 11.3. Typical pulser output: 0.10 volts negative.

2. The outputs of the preamps are fed into the negative input of the amplifiers. Set the peaking time of the amplifiers at 1 μsec. The bipolar output of the amplifiers should be fed into the inputs of the constant fraction timing SCAs.

3. Set the SCAs on the ASYMmetrical window mode (delay = minimum). In this mode the window width ΔE can be varied from (0 to +1.0V). This is done with the 10

turn upper level or window potentiometer on the SCA. Set the window width (ΔE) at 200/1000. This corresponds to two complete turns on the 10 turn ΔE potentiometer. Remember, most of the potentiometers that we will be using are 10 turn devices. Each turn corresponds to 100 divisions on the dial setting. Full scale is therefore (1000/1000) divisions or 10 turns. Our setting of 200/1000 corresponds to 0.2 volts.

4. Set the lower level potentiometer at 360/1000 or 3.6 volts. The SCAs are now set in such a manner that they will give an output anytime an input pulse is greater than 3.6 volts but not greater than 3.8 volts. Set the delay on the SCA for the 0.1 to 1.1 μsec range. This is a 10 turn potentiometer so 1000 nsec = 1000 div on this range. Set the delay potentiometer to minimum or 100 nsec.

5. Set the gain of each amplifier (A and B) so that the positive portion of the bipolar pulse is 3.7 volts. See fig. 11.2. Since the SCAs are set to accept pulses between 3.6 and 3.8 volts, they should now give output pulses. If you look at the positive logic output pulses from the SCAs, a +5V pulse should be produced for each input pulser pulse. Therefore, the counting rate out of each SCA should be 60 Hz.

6. Set the A and B switches on the coincidence unit to COINC. and the C, D and E switches to OUT. Set the resolving time at 1000 nsec and the coincidence requirements switch at 2. The F or G outputs of the coincidence circuit should show +5V logic pulses at a 60 Hz rate. This indicates that both branches of the circuit are set properly. If there is no output at these points, the timing on one of the SCAs is probably off. Observe the output of the coincidence circuit while changing the delay on either the A or B side of the circuit. When the overlap is proper, the coincidence circuit will start registering pulses.

7. Now set the coincidence resolving time at 250 nsec and adjust the delays on the SCAs until the +5V pulses are again observed at the output of the coincidence unit. Turn one of the delays (A) until the coincidence output stops. Record this value in nsec. Remember 1 div = 1 nsec.

8. The +5V output pulses of the coincidence circuit should now be fed into the input of the counter-timer. Set the discriminator level of the counter-timer to 0.1V. Set the dwell to off. Set the time for 10 sec and record the number of coincidence events from the counter (this value should be zero). Read the counter-timer; change the delay time on SCA no. A to 25 nsec and count for 10 sec. Record the number of counts in a data table and reset the counter. Increase the delay in SCA no. A by 25 nsec and count for 10 sec. Continue until the overlap coincidence no longer occurs. Figure 11.4 shows a plot of a typical overlap coincidence spectrum for these measurements.

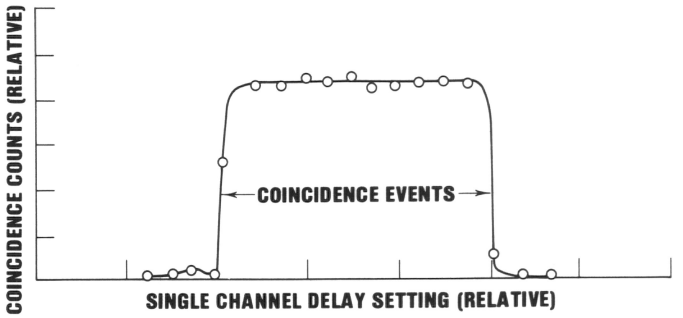

Figure 11.4. Typical delay versus coincidence counting rate measurement for the electronics in fig. 11.4.

Exercise From your fig. 11.4, determine the overlap coincidence resolving time.

EXPERIMENT 11.2

Coincidence Measurements with a Linear Gate

Discussion

In this discussion, it will be assumed that the student has already done experiment 11.1 or, at least, has carefully read the complete experiment. Figure 11.5 shows the electronic schematic that will be used for this experiment.

We are familiar with all of the modules in fig. 11.5 except the Delay Amplifier and the Linear Gate. The delay amplifier is perhaps the simplest module that we will use in this manual. Normally an amplifier output is fed into the input of the delay amp. The output of the delay amp looks just like the input except it is delayed by the sum of the delay switches on the front of the module. If you so desire, +5V logic pulses can also be delayed with this module. Delay amplifiers are used to provide certain timing requirements in coincidence experiments.

The Linear Gate is a linear device that will pass an amplifier pulse through to be analyzed provided that a properly timed logic pulse opens the gate. In time sequence what happens is the following: 1.) A gate pulse arrives at the gate input of the linear gate, 2.) The gate pulse opens the linear gate for a period of time ΔT_1, 3.) If a linear pulse from an amplifier arrives at the input while the gate is open, it will pass through and be analyzed. Amplifier pulses that arrive while the gate is closed will be rejected.

The gate input on most multichannel analyzers operates in the same manner.

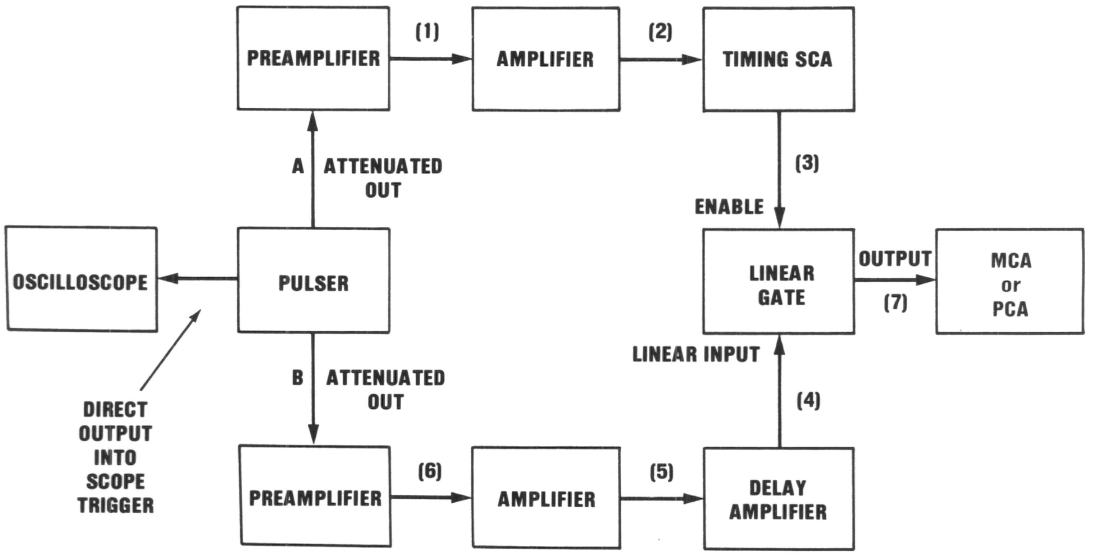

Figure 11.5. Coincidence spectroscopy with a pulse generator and a linear gate.

Timing Measurements with the Scope

In fig. 11.5, we have shown the direct output of the pulse generator going into the trigger input of the scope. For timing measurements, this establishes a true T = 0 reference. If we now look at the output of either preamp, (1) or (6) in fig. 11.5, the time delay in these devices is automatically shown on the face of the scope. Since the preamps are the same, very little time difference will be observed in the pulses at (1) and (6). This same reasoning will show the timing at position (2) and (5) are also about the same. The timing at position (3) however, is another matter. From fig. 11.2 we observed that the timing SCA generates its logic pulse at the cross over point, which, for our example, was 2.7 μsec after the amplifier pulse enters the SCA. Therefore, if we look at position (3) with a scope that is being triggered with the direct output from the pulser, the logic pulse would be delayed by: (1) The transient time in the preamp (~200 nsec), and (2) the 2.7 μsec that the timing SCA uses to generate its logic pulse. Figure 11.6 gives what the scope would show for the SCA at position (3) in fig. 11.5.

From what we said earlier about the linear gate, the logic pulse (3) should arrive at the gate just prior to the amplifier pulse that is to be processed into the MCA. This can be accomplished in fig. 11.5 by setting the delay amplifier on 3 μsec. Under these conditions, the gate pulse would arrive 0.1 μsec before the linear pulse from the delay amplifier. In this experiment, we will simply set the timing on these units such that the linear gate will process the pulser pulses in the MCA at 60 Hz and with the proper amplitude.

Experimental Procedure

1. Set up the electronics as shown in fig. 11.5. Adjust the attenuated output of the pulse generator and the gain of each amplifier so that the amplifier outputs are about

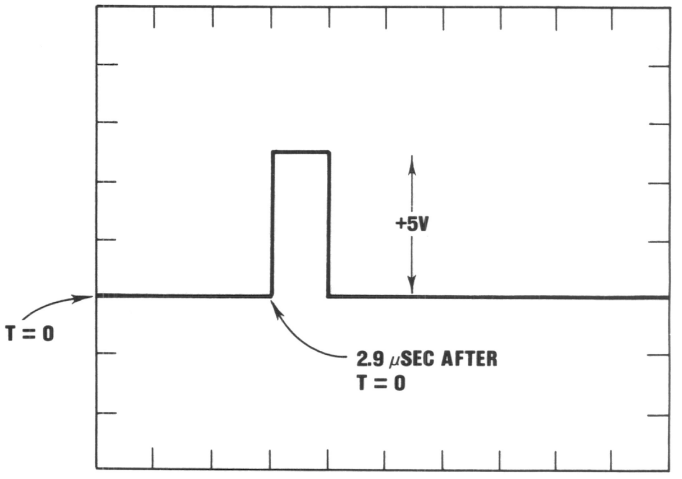

Figure 11.6. Scope trace of the SCA logic output in fig. 11.5. The scope is being triggered with the direct output of the pulse generator which gives the T=0 reference.

3.7 volts as shown in fig. 11.2. **Note:** The peaking time of the amplifier should be set at 1 μsec as in experiment 11.1. Use the bipolar output of the amplifiers.

2. Set the timing SCA on ASYMmetrical (delay = minimum) with the window set at 0.20 volts. Trigger the scope with the direct output of the pulser and observe the logic output pulses of the SCA. Raise the lower level of the SCA until logic pulses appear. These should occur at a lower level setting of approximately 3.5 volts (350/1000 divisions on the dial). Continue raising the lower level dial until the ΔE window clearly brackets the amplifier output pulses. If everything is correct, this should be about (360/1000) divisions. The logic output of the SCA should be similar to fig. 11.6.

3. Disconnect the output of the delay amplifier from the linear input of the linear gate and feed it directly into the

input of the MCA. Set the MCA on 1000 channels full scale. Record the channel number of the peak positions. Count for 100 seconds and determine (Σ-β/t). This number should be 60 Hz. Now, connect the delay amplifier back up to the linear gate as shown in fig. 11.5.

4. Set the delay amplifier at 3 μsec and observe the output of the linear gate with the scope. If the timing is correct, you should see the amplifier pulses as shown at position (5) only delayed by about 3 μsec. If for some reason the timing is not correct, the delay switches on the delay amplifier can be adjusted until the amplifier pulses are correct at the output of the linear gate.

5. Set the MCA at 100 sec and analyze the output pulses from the linear gate. Record the peak centroid in the MCA and determine (Σ-β/t) which again should be 60 Hz. The position of the peak should be approximately where it was when we analyzed the direct output of the linear gate in step 3. It may not be exactly in the same channel since the gain of the delay amplifier is probably not exactly (x1). In this experiment, we have studied the timing requirements for the linear gate with a pulse generator. As was mentioned above, most MCA's have a linear gate for coincidence requirements. If you understand this experiment, you should understand coincidence spectroscopy with an MCA.

EXPERIMENT 11.3

Coincidence Measurements with a Time-to-Amplitude Converter (TAC)

Discussion

Figure 11.7 shows the electronics that will be used for this experiment. We have discussed all of the modules in this block diagram except the Nanosecond Delay Module and the Time-to-Amplitude Converter (TAC). The nanosecond delay module is exactly what its name implies. It is designed to delay the fast negative logic pulses from the SCA. This delay can be changed from 1.0 to 63 nsec by actuating toggle switches on the front of the nanosecond delay module. The timing SCA puts out both a +5V slow pulse and a -0.8V fast pulse each time the SCA records an event. For timing experiments with a TAC, the fast negative pulse is always used. Furthermore, 50Ω cable should be used for connections (3), (4), and (5) in fig. 11.7.

The TAC is essentially a fast electronic stop watch. We provide it with a start pulse to start its timing sequence and a stop pulse to stop its sequence. The time difference between the start and stop pulses is ΔT. The TAC gives us an output that is proportional to ΔT. In other words, if ΔT = 1 μsec, the output of the TAC might be a 1V pulse. If ΔT = 2 μsec, the TAC would give a 2V pulse, etc. If we then consider what the TAC does, it not only says that two events are in coincidence, but it also tells us how these coincidences are distributed with respect to time. The full scale range of the TAC can be set from 25 nsec to 3 milliseconds from the front panel. As we will see, for

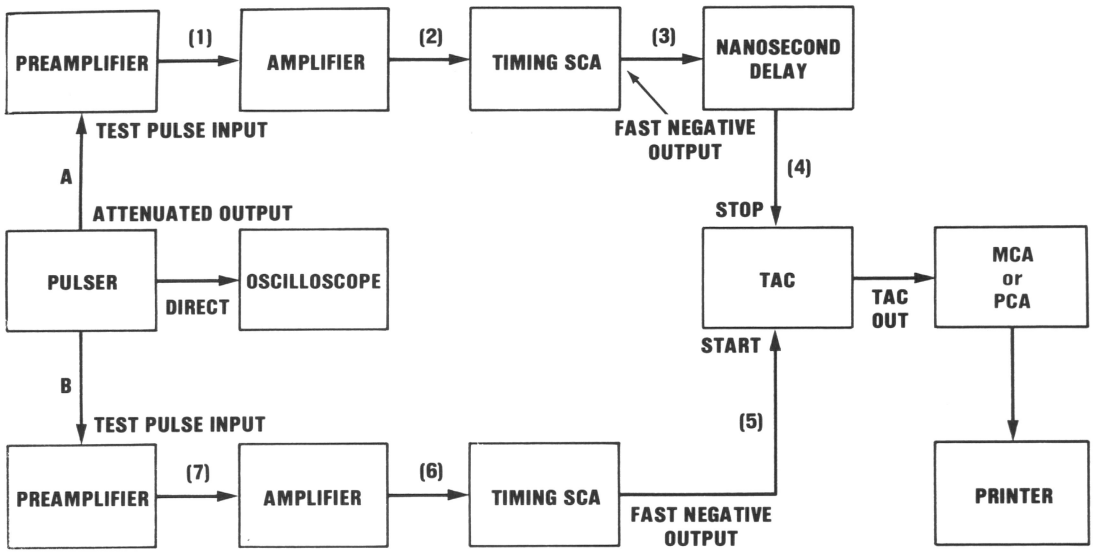

Figure 11.7. Coincidence spectrometry with a Time-to-Amplitude Converter (TAC).

many applications, it is the best way to do coincidence spectroscopy.

Experimental Procedure

1. Set up the electronics as shown in fig. 11.7. All electronic connections should be made with 50Ω cable. Turn on the pulser and adjust its height and the gain of each amplifier so that the output (bipolar) pulses are about 3.7 volts high (see fig. 11.2).

2. Set each SCA in the ASYMmetrical mode with the lower level at 3.6 volts (360/1000 div) and the window at 0.2V (200/1000 div). Look at the +5V logic output of each SCA as we did in the last experiment. We should see +5V logic pulses similar to fig. 11.6. So far we haven't done anything different than we did for experiment 11.1.

3. Set the delay on each of the SCA's to minimum. Cable (3) (fig. 11.7) should be connected to the fast negative logic output of the SCA and the input of the nanosecond delay module. Set all of the toggle switches on the delay module to the right. This corresponds to a total delay of 63 nsec. Feed the output of the nanosecond delay module into the stop side of the TAC. On the bottom part of the circuit, the negative logic signal is fed directly into the START side of the TAC with a short piece of 50Ω cable.

4. Set the TAC at a full scale time range of 100 nsec. The gate should be in anticoincidence. The output width can be set at 0.5 μsec (minimum).

5. Connect the scope to the TAC output. You should observe a pulse which is about 5V in amplitude and 0.5 μsec wide. It is possible that the pulses will not be there because of the differences in delays throughout the A and B paths to the TAC.

If This is the case, adjust the delay on the stop SCA until the output pulses from the TAC are 6 volts. When this is set, record the channel number of the peak and determine (Σ-β/t) for a 100 sec run. Remember (Σ-β/t) should be 60 Hz.

6. Repeat this measurement for the other delay values in Table 11.1 and fill in the table.

Exercise On linear graph paper, make a plot of delay (y axis) versus the channel number from Table 11.1. Figure 11.8 shows a typical delay versus pulse height curve for the TAC. **Note:** The slope of the curve is the number of nsec/ch for the TAC settings. In order to measure the time resolution of the pulser peak multiply the FWHM of the peak by the slope of the delay vs pulse height curve. See fig. 11.8 (upper left hand corner). This calculation should be done for each pulser peak that is observed in Table 11.1. Record these values in column (4) of the Table.

Table 11.1 Calibration Data for the TAC

Run No.	(1) Delay nsec	(2) Channel No.	(3) $\frac{\Sigma-\beta}{t}$	(4) FWHM ΔT
1	63			
2	55			
3	47			
4	32			
5	24			
6	18			
7	10			
8	4			

In fig. 11.8 the FWHM shows a time resolution (ΔT) of 5.07 x 10^{-10} sec. This, in effect, means that we have the ability to resolve between two events that are ΔT apart in time. If one carefully considers this capability, it is amazing what modern day electronics can do.

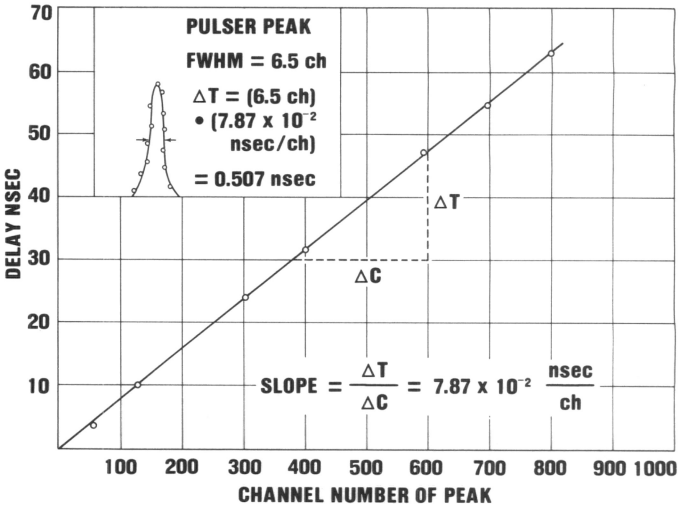

Figure 11.8. Time-to-Pulse Height (TAC). Delay vs pulse height calibration. The time resolution of one of the pulser peaks is shown in the upper left hand corner.

EXPERIMENT 11.4

A β,γ Coincidence Experiment Which Yields the Absolute Activity of a Source

Discussion

In this experiment we are going to measure the absolute source activity of a ^{60}Co source. In experiment number 2, this was done by the *relative* and *absolute* methods. The student should review experiment number 2 before attempting this experiment. The electronics that will be used for this experiment are shown in fig. 11.9. This measurement is quite similar to experiment 11.3 and the electronics arrangement is approximately the same. In this experiment, the start pulse for the TAC will come from a surface barrier detector that counts βs from the source. The stop pulse will be derived from a NaI(Tℓ) detector that is set to count the 1.17 and 1.33 MeV gammas from the source. Figure 11.10 shows a NaI(Tℓ) spectrum of the decay scheme of ^{60}Co, and the suggested lower level threshold setting for the experiment. We will independently use the electronics arrangement in fig. 11.11 to set this threshold. The β spectrum from the solid state surface barrier detector in fig. 11.9 will be similar to the spectrum shown in Experiment 5 (see fig. 5.2). The electronics in fig. 11.11 will also be used to set an SC threshold at about 10% β max in the spectrum. **Note:** I the electronics for this experiment (fig. 11.9), we a counting independently Iγ (the γ intensity), Iβ (the intensity), and I_c (the coincidence events). From ref. the intensity of the source I_s, is given by:

$$I_s = \frac{I\gamma\ I\beta}{I_c} \qquad (1$$

The units in the equation will come out counts/sec.

This experiment will give us a good practical overvie of the coincidence techniques that have been outline up to this point.

Experimental Procedure

1. The first task that we have is to set the threshold fo the ^{60}Co spectrum (see fig. 11.10). Set up the electronic as shown in fig. 11.11. Set the high voltage supply at th value recommended for the NaI(Tℓ) detector. The peak ing time of the amplifier should be set at 1 μsec. Place 1 μCi ^{60}Co source 1 cm from the face of the NaI(Tℓ) detec tor. Use the bipolar output. Adjust the coarse and fin gains of the amplifier so that the scope shows an outpu of approximately 5V for the 1.33 MeV gamma line.

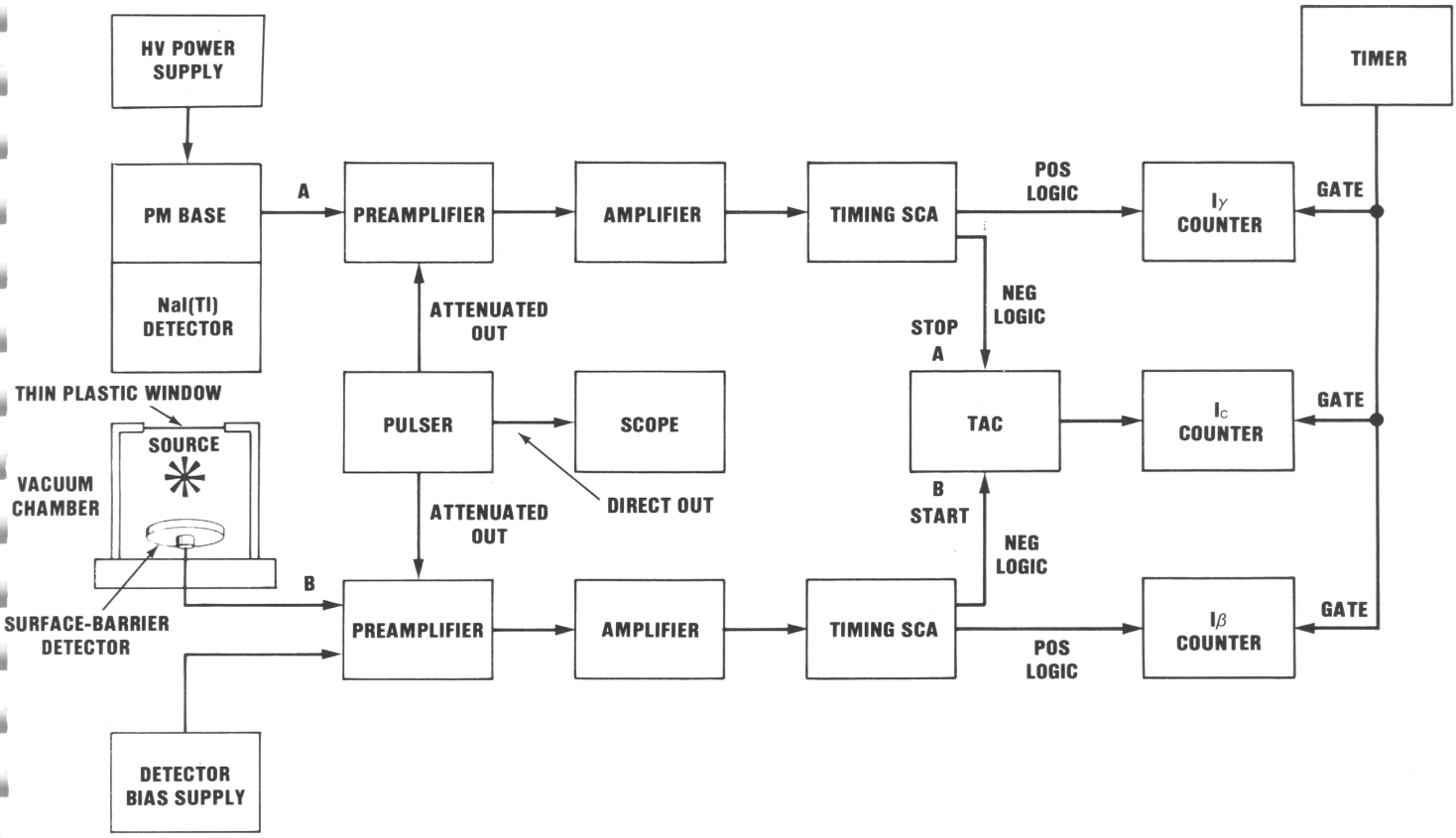

Figure 11.9. Electronics for the absolute activity measurement of a (β,γ) source.

2. Set the NaI(Tℓ) SCA in the INTG MODE and the lower level at (40/1000). Feed the +5V logic pulse into the gate input of the MCA. Set the delay on the SCA at minimum (0.1 μsec).

3. Set the delay on the NaI(Tℓ) delay amplifier at 3 μsec. Use 512 channels. Start the MCA and a spectrum similar to fig. 11.10 should be observed. If the analyzer does not show a spectrum for ^{60}Co that is proper, it is probably due to the timing. If the spectrum does not look similar to fig. 11.10, either increase or decrease the setting of the delay amp while the analyzer is counting. Let us assume that the spectrum is now OK. The threshold of the SCA can now be slowly raised while the MCA is counting. When the proper threshold is set, there will be very few counts below the dashed line in fig. 11.10. It is almost like magic, but the electronics are just functioning properly. The amplifier and SCA in the top portion of fig. 11.9 are now set.

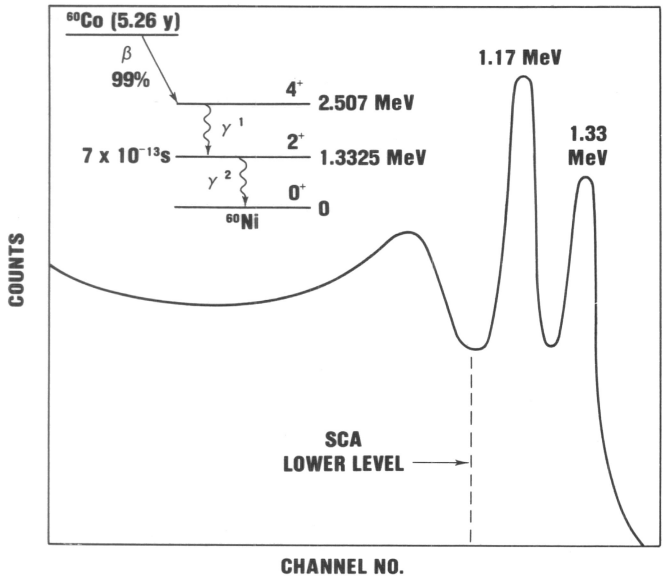

Figure 11.10. NaI(Tℓ) pulse height spectrum of ^{60}Co showing the decay scheme and the timing SCA lower level threshold setting.

4. We will now use a similar technique to set the amplifier and SCA on the B portion of fig. 11.9. Connect the electronics again as shown in fig. 11.11, only this time the solid state surface barrier detector will be used in the circuit instead of the NaI(Tℓ) detector.

5. Place the 1 μCi ^{60}Co source in the chamber and evacuate the chamber. Raise the detector bias voltage to its recommended value. Adjust the amplifier to 1 μsec peaking time and set the gain so that the β continuum from ^{60}Co reaches out to 4 volts as observed with the oscilloscope. Set the SCA in the INTG mode, delay at minimum, and the lower level at (30/1000). Feed the +5V logic pulse into the GATE of the MCA.

6. Set the delay of the delay amp at 3 μsec. Start the MCA. You should see a β continuum similar to fig. 5.2 of Experiment 5. Now raise the lower level on the SCA until 10% of the spectrum is gated out. We now have the surface barrier amplifier and SCA set for the β,γ coincidence experiment.

7. Set up the electronics as shown in fig. 11.9. Obtain the ^{60}Co source to be analyzed from the instructor and place it in the vacuum chamber. Evacuate the chamber, put bias voltage on the surface barrier detector and high voltage on the NaI(Tℓ) detector. The settings for both amplifiers and SCA's have already been made. With the oscilloscope, make sure that the positive logic pulses from both SCAs are there. Now set the full scale time range of the TAC at 200 nsec. Feed the output pulses from the TAC into the I_c (intensity coincident) counter. Look at the output of the TAC with the scope while increasing the delay of the NaI(Tℓ) SCA. Continue doing this until the TAC output pulses are at least +5 volts.

8. Set the timer so that it will simultaneously start all three counters. Count for 300 seconds and record Iγ, Iβ, and I_c. We can now use this data to quite accurately determine the activity of this unknown ^{60}Co source.

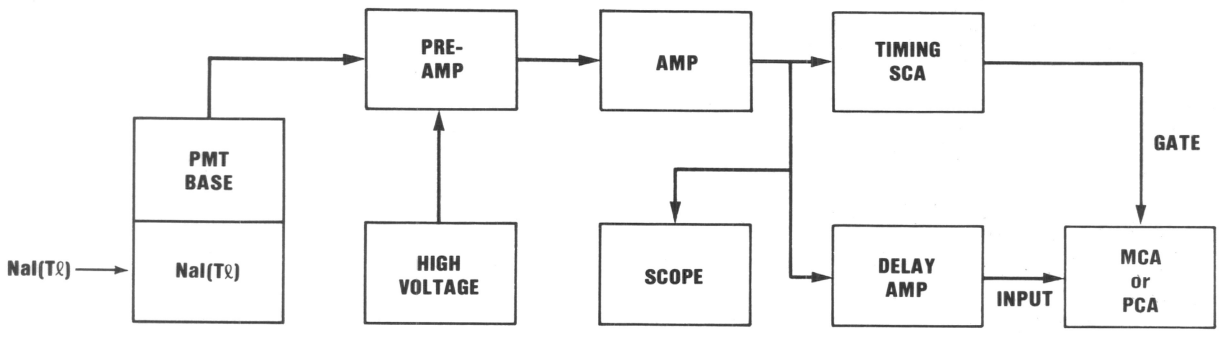

Figure 11.11. Electronics for setting the lower level threshold and ΔE windows for a single channel analyzer.

Exercise Use eq. (1) to calculate the number of disintegrations/sec from the unknown source. How do your answers compare to the value that the instructor has for the source?

Summary

The coincidence techniques that were learned in this series of experiments are very important and indeed will be used in many subsequent experiments. If you do not understand a certain section, please see the instructor and carefully go back over that section. It has been through experiments similar to these that decay schemes, spins, angular correlations, mean lives, internal conversion coefficients, and a host of other nuclear parameters have been determined. Coincidence techniques are very important in Nuclear Spectroscopy.

REFERENCES FOR *EXPERIMENT 11*

1. K. Siegbahn, Ed., *Alpha-, Beta-, and Gamma-Ray Spectroscopy* **1** and **2**, North Holland Publishing Co., Amsterdam (1965).

2. *Radiological Health Handbook*, U.S. Dept. of Health, Education, and Welfare, PHS Publication 2016. Available from National Technical Information Service, U.S. Dept. of Commerce, Springfield, Virginia.

3. G. F. Knoll, *Radiation Detection and Measurement*, John Wiley and Sons, New York (1979).

4. V. Arena, *Ionizing Radiation and Life*, The C. V. Mosby Co., St. Louis, Missouri (1971).

5. P. Quittner, *Gamma Ray Spectroscopy*, Halsted Press, New York (1972).

6. A. C. Melissinos, *Experiments in Modern Physics*, Academic Press, New York (1966).

7. W. Mann and S. Garfinkel, *Radioactivity and Its Measurement*, Van Nostrand-Reinhold, New York (1966).

8. H. L. Andrews, *Radiation Biophysics*, Prentice-Hall, Englewood Cliffs, New Jersey (1974).

9. V. Acosta, C. L. Cowan, and B. J. Graham, *Essentials of Modern Physics*, Harper and Row, New York (1973).

10. A. H. Wapstra, et al., *Nuclear Spectroscopy Tables*, North Holland Publishing Co., Amsterdam (1959).

EXPERIMENT 12

Annihilation Radiation Coincidence Studies with ^{22}Na

Scope

The annihilation radiation from a ^{22}Na source will be studied with an angular correlation apparatus. The β^+ particles from the source will be converted in a foil and the resultant .511 MeV annihilation quanta will be measured with two NaI(Tℓ) detectors. The angular correlation table that will be used for this experiment has provisions to fix one of the NaI(Tℓ) detectors and rotate the other one. With this system, we will verify the angular correlation of the annihilation radiation. These quanta will be shown to be emitted with an angular separation of 180 degrees, which is the only correlation that can conserve linear momentum for the two photons. This angular correlation will be verified by using three different coincidence arrangements.

Discussion

Figure 12.1 shows the decay scheme of ^{22}Na and the resultant NaI(Tℓ) spectrum. **Note:** The positrons are in coincidence with γ's from the 1.274 MeV (2+) state. The mean life of the 1.274 MeV state is 3×10^{-12} sec and therefore, from our timing situation, decay is immediate. A small fraction of the positrons (0.05%) decay directly to the ground state of ^{22}Na. The Q_{EC} = 2.843 MeV shown in the figure is the excess energy that would be available if Electron Capture (EC) occurred to the ground state of ^{22}Na.

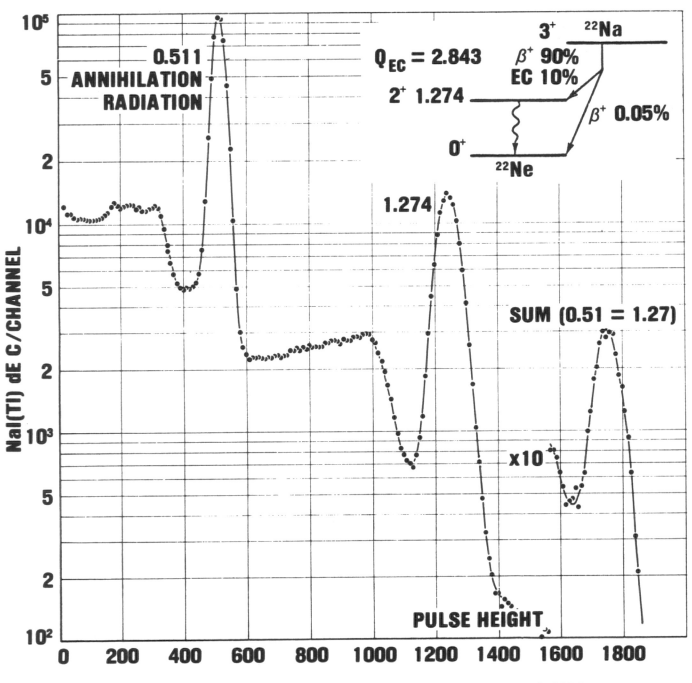

Figure 12.1. NaI(Tℓ) pulse height spectrum of ^{22}Na.

The β^+ end point energy to the ground state is 1.7 MeV. Most of the β^+ particles (90%) go to the (2^+) level a 1.274 MeV. The positron continuum to this level woul have an end point energy of 0.466 MeV. Figure 12.2 shows what the distribution of β^+ particles would loo like if we counted them with a β^+ pulse height analyzer

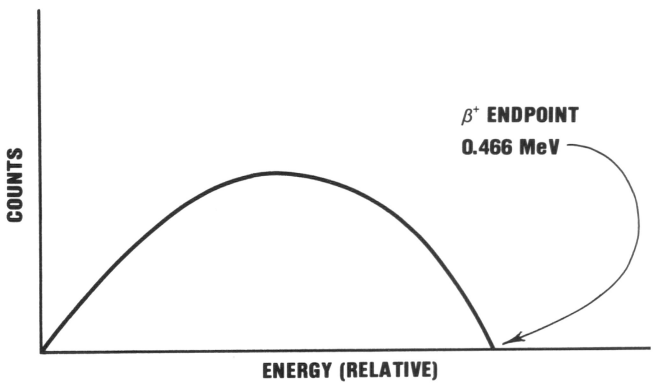

Figure 12.2. β^+ distribution from a ^{22}Na source.

In our experiment, we will encapsulate the ^{22}Na sourc with two converter foils to insure that most of the β particles annihilate at the source. Basically the β^+ parti cles leave the source in an isotropic manner. When the enter the converter foil, they quickly (1×10^{-9} sec) los energy by dE/dx in the foil. When a β^+ has essentially los all of its energy, it finds an electron and captures tha electron to form positronium which decays by the ann hilation of the e^+ and e^- into two gammas. Conservatio of momentum tells us that these gammas have to go o in opposite directions. This gives an angular separatio of the gammas of 180 degrees. In this experiment, we wi verify these conservation principles.

EXPERIMENT 12.1

Annihilation Measurements with a Multipurpose Coincidence Circuit

Discussion

From an electronic point of view, this experiment quite similar to experiment 11. The student is urged to c experiment 11 before attempting this experiment. In th experimental procedure, we will assume that you a

familiar with all of the techniques discussed in experiment 11. The only real difference is that we will use two NaI(Tℓ) detectors for the two input channels instead of the pulse generator used in experiment 11.

Figure 12.3 shows a plan view of the angular correlation table that will be used for this experiment. After the timing has been set for the electronics that will be used (fig. 12.4), it is a simple matter to fix one of the detectors and then record coincidence events as a function of $\pm\theta$. Since the annihilation radiation $\gamma_1 + \gamma_2$ leave the source with an angular separation of 180 degrees, our maximum counting rate will be observed at $\theta = 0$ in fig. 12.3. For the experiment, we will record coincidence events for the angles listed in Table 12.1. We will also make a similar table for angles on the other side of zero ($-\theta$). When we have finished with the experimental data, a plot of the data similar to fig. 12.5 will be made for the data.

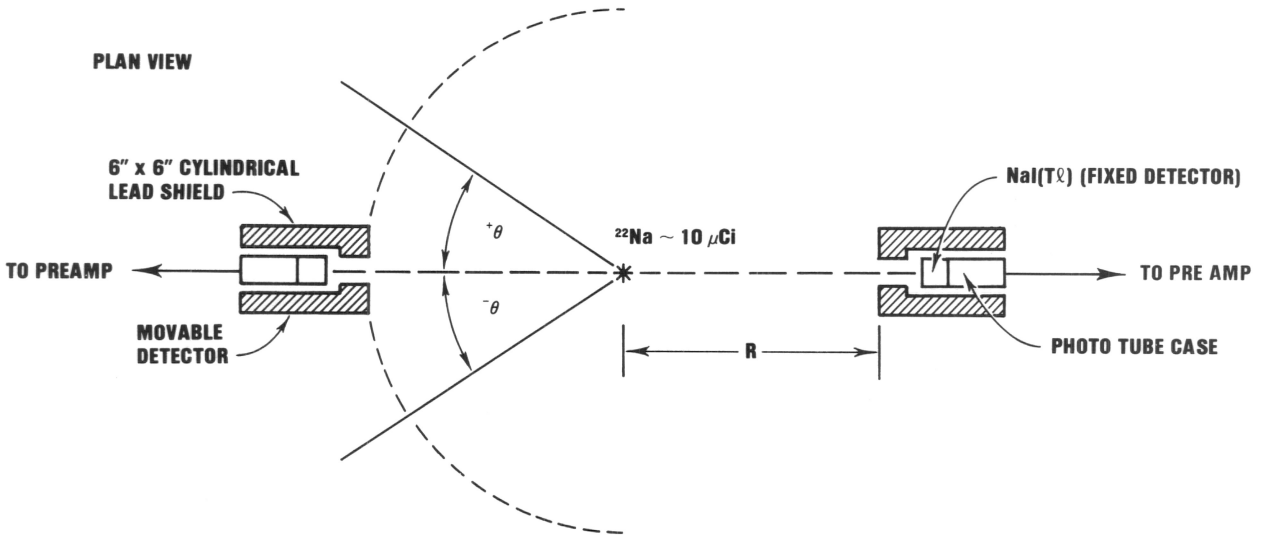

Figure 12.3. Angular correlation table with heavy rotating lead shields for the NaI(Tℓ) detectors.

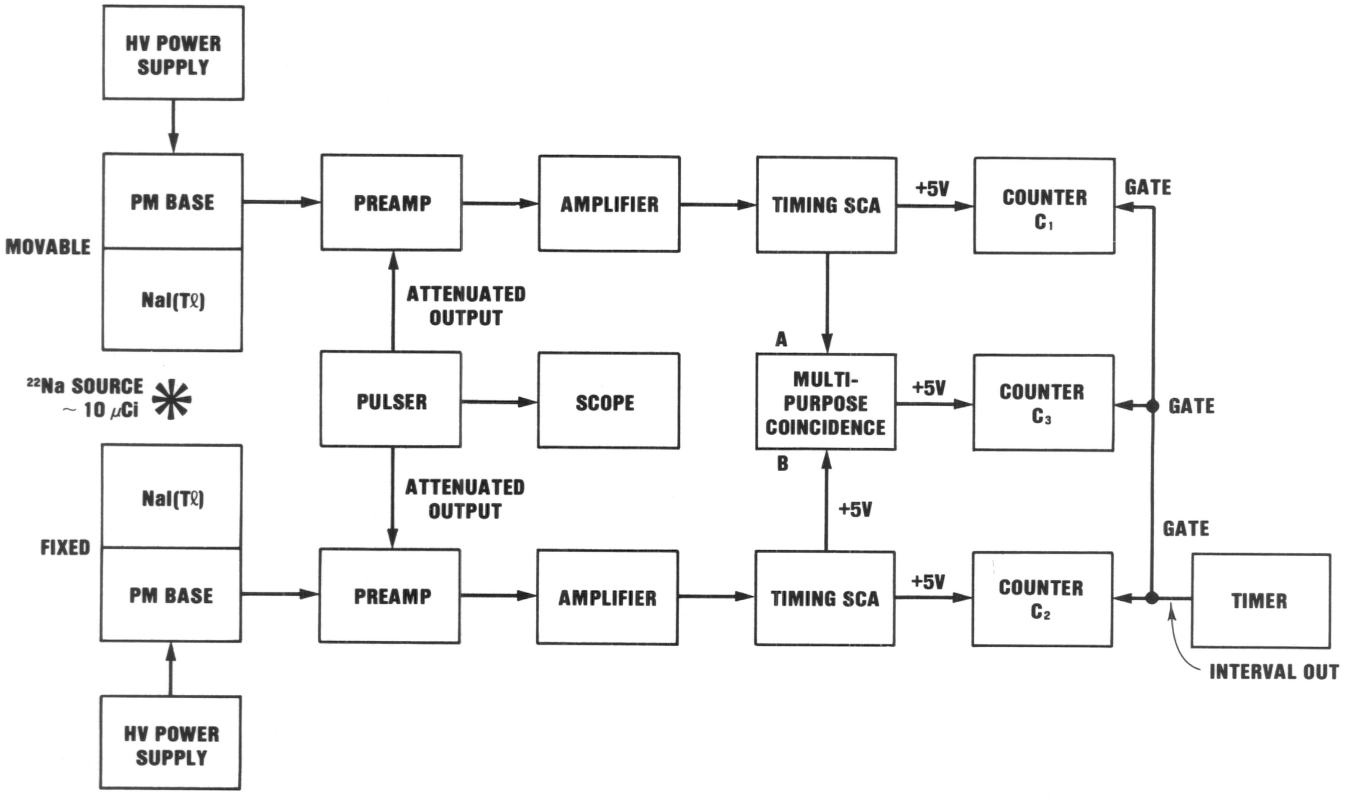

Figure 12.4. Electronics for annihilation measurements with a multipurpose coincidence circuit.

Table 12.1 Coincidence Data for the Annihilation Experiment

Run No.	+ degrees	C_1 counts/s	C_2 counts/sec	C_3 counts/sec
1	0			
2	1			
3	2			
4	3			
5	4			
6	5			
7	6			
8	7			
9	8			
10	9			
11	10			
12	12			
13	15			
14	20			

Experimental Procedure

1. Place the copper converter foils on either side of the 10 μCi ^{22}Na source and secure the foils with tape. Place the source in the center pivot of the angular correlation table. Adjust the high voltage on each NaI(Tl) detector to its recommended value. Set each amplifier on 1 μsec peaking time. Use the bipolar output of each amplifier into the SCAs. Adjust the gain of each amplifier so that the 1.274 MeV gammas are about 5 volts in amplitude.

2. Remove the source and turn on the pulse generator. Adjust the pulser so that the output pulses from each amplifier are about 3.5 volts. Set each timing SCA in the integral mode with the lower level set at 50/1000. Set the delays at minimum. Use a BNC Tee on the +5 volt logic pulse from each SCA. For each SCA, one output logic pulse goes into the multipurpose coincidence input and the other goes into the counter as shown in fig. 12.4.

3. For the coincidence circuit, set the resolving time at 250 nsec, 2 coincidence requirements, use A and B inputs, and route the F output into counter C_3.

4. Set the timer for 300 sec and start all counters. If the timing is correct, C_1, C_2, and C_3 should all give Σ/t = 60 Hz. If this is not the case, adjust the delays on the SCAs until the timing is correct.

5. Turn off the pulse generator and place the ^{22}Na source in its position on the angular correlation table. Set the angle at 0 degrees and the timer at 300 sec. For each counter, determine Σ/t in counts/sec and fill in the first entry in Table 12.1. Continue for the other angular settings in the table. Repeat this whole data table for negative angles ($-\theta$) with the same absolute values as the positive angles in Table 12.1. Of course, the counting time will have to be increased for the larger angles to get reasonable statistics. If the system is lined up properly, the counting rates in counters C_1 and C_2 should remain about the same because, without the coincident requirement, we are simply looking at an isotropic source of gammas.

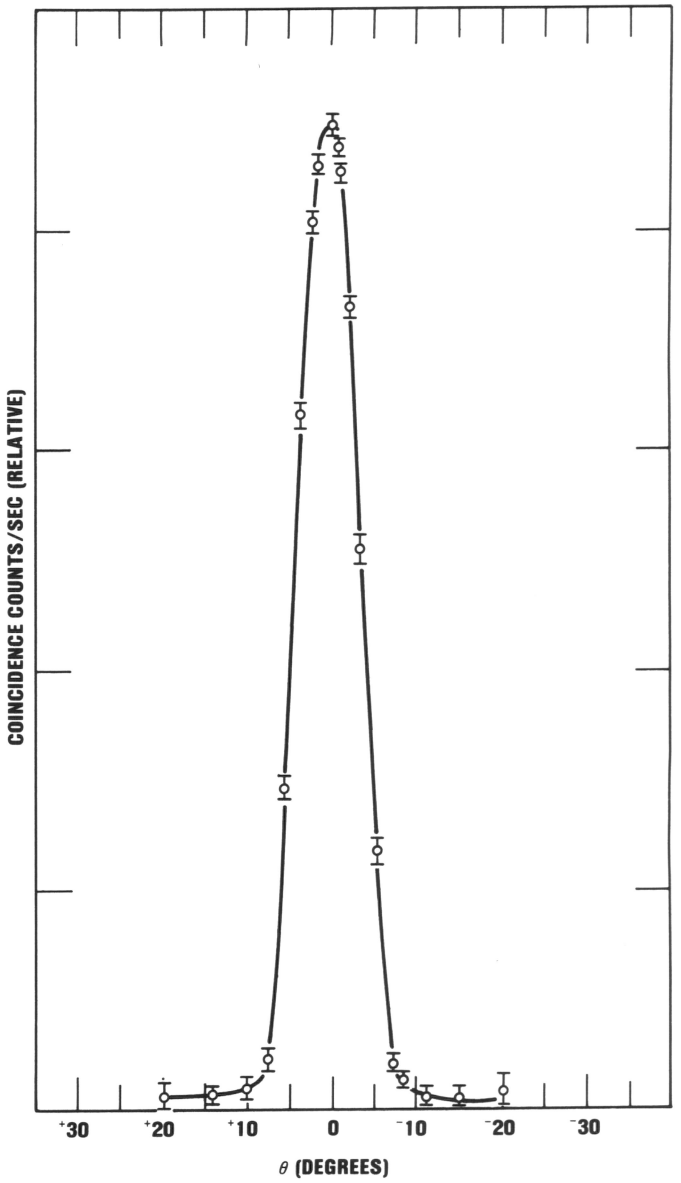

Figure 12.5. Angular correlation data for ^{22}Na.

Exercise Plot the number of coincidence counts/sec vs θ from your data. Your angular distribution should be similar to fig. 12.5.

EXPERIMENT 12.2

(γ-γ) Annihilation Measurements with a Linear Gate

Experimental Procedure

1. Place the ^{22}Na source at its position on the angular correlation tables. Set both amplifiers at 1 μsec time constant. Adjust both amplifier gains so that the 1.274 MeV gamma pulses are about 5 volts at the bipolar outputs.

2. Remove the ^{22}Na source and turn on the pulse generator. Increase the amplitude of the pulser until the output of each amplifier is 5 volts. Set SCA #1 as follows: Integral mode, lower level 50/1000, minimum delay. Put a BNC Tee on the positive output of SCA #1 and feed the pulses into counter C_1 and the enable input to the linear gate as shown in fig. 12.6.

2. Set the delay/amplifier on 3 μsec. Put a BNC Tee on its output and feed one cable into the input of the linear gate and the other into timing SCA #2 as shown in fig. 12.6. Set SCA's #2 and #3 as follows: Integral mode, lower level 50/1000, minimum delay, +5 logic out into the counters.

3. Set the timer for 100 sec and record the counting rates C_1, C_2 and C_3. They should all read 60 Hz.

4. Turn off the pulse generator and place the ^{22}Na source on the angular correlation table.

5. Set the angle at 0 degrees, the timer at 300 sec and run. Fill in the data table as we did for Experiment 12.1.

Exercise Plot your data in the manner shown in fig. 12.5.

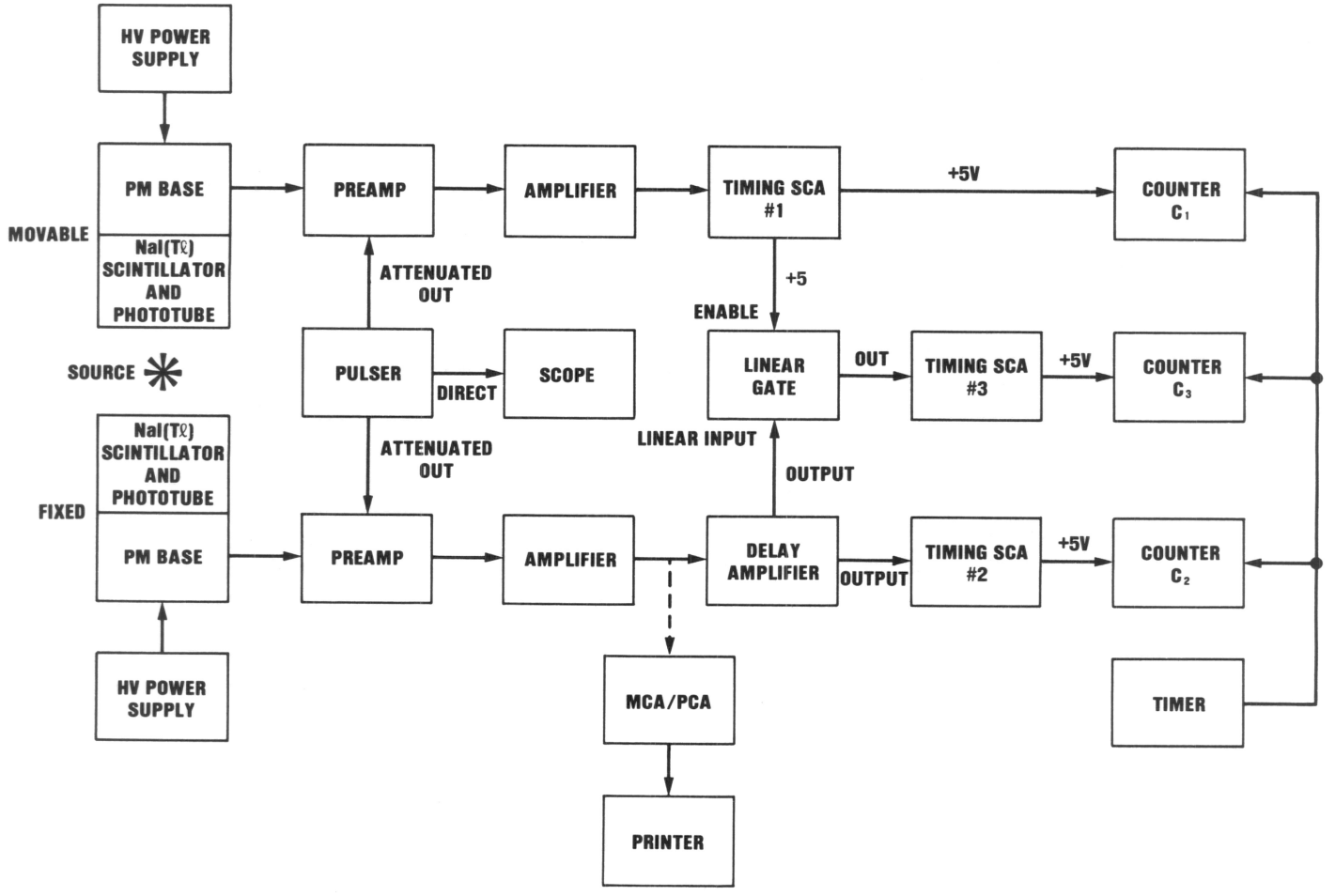

Figure 12.6. Electronics for annihilation measurements using a linear gate.

EXPERIMENT 12.3

(γ-γ) Annihilation Measurements with a Time-to-Amplitude Converter (TAC)

Experimental Procedure

1. Set up the electronics as shown in fig. 12.7. Place the ^{22}Na source in its holder on the angular correlation table. Adjust the gains of both amplifiers so that the output of the 1.274 MeV gammas is approximately 5 volts as in the previous experiment.

2. Remove the ^{22}Na source and turn on the pulse generator. Adjust the pulser pulse height until the output of each amplifier is 5 volts. Set SCA's #1 and #2 as follows: Integral mode, lower level 50/1000. The delay should be minimum on SCA #1 and 50 nsec on SCA #2.

3. Set the TAC on the 200 nsec full scale time range. Feed the output into a 100 ch MCA or PCA.

4. The timer is connected so that it automatically starts and stops counters C_1, C_2 and the MCA. Set the timer for a long time and start counting. C_1 and C_2 should count at a rate of 60 Hz. The MCA should show a single isolated peak if the timing is correct. If no peak is observed in the MCA, increase the delay on SCA #2 until the peak is being recorded about mid-scale on the MCA. Stop the timer; clear everything and count for 100 sec. The MCA, C_1, and C_2 should all show Σ/t = 60 Hz.

5. Turn off the pulser; place the source on its holder, and set θ = 0 degrees. Set the timer for 300 sec and start counting. The MCA should show a strong group accumulating about mid-scale. If this does not happen, you may have to change the delay on SCA #2 or #1. It is usually pretty easy to find the proper delay setting to put the TAC peak at mid-scale. Clear everything; set the timer at 300 sec and record the first data point. Continue for all of the $\pm\theta$ values in the table and plot a curve similar to fig. 12.5.

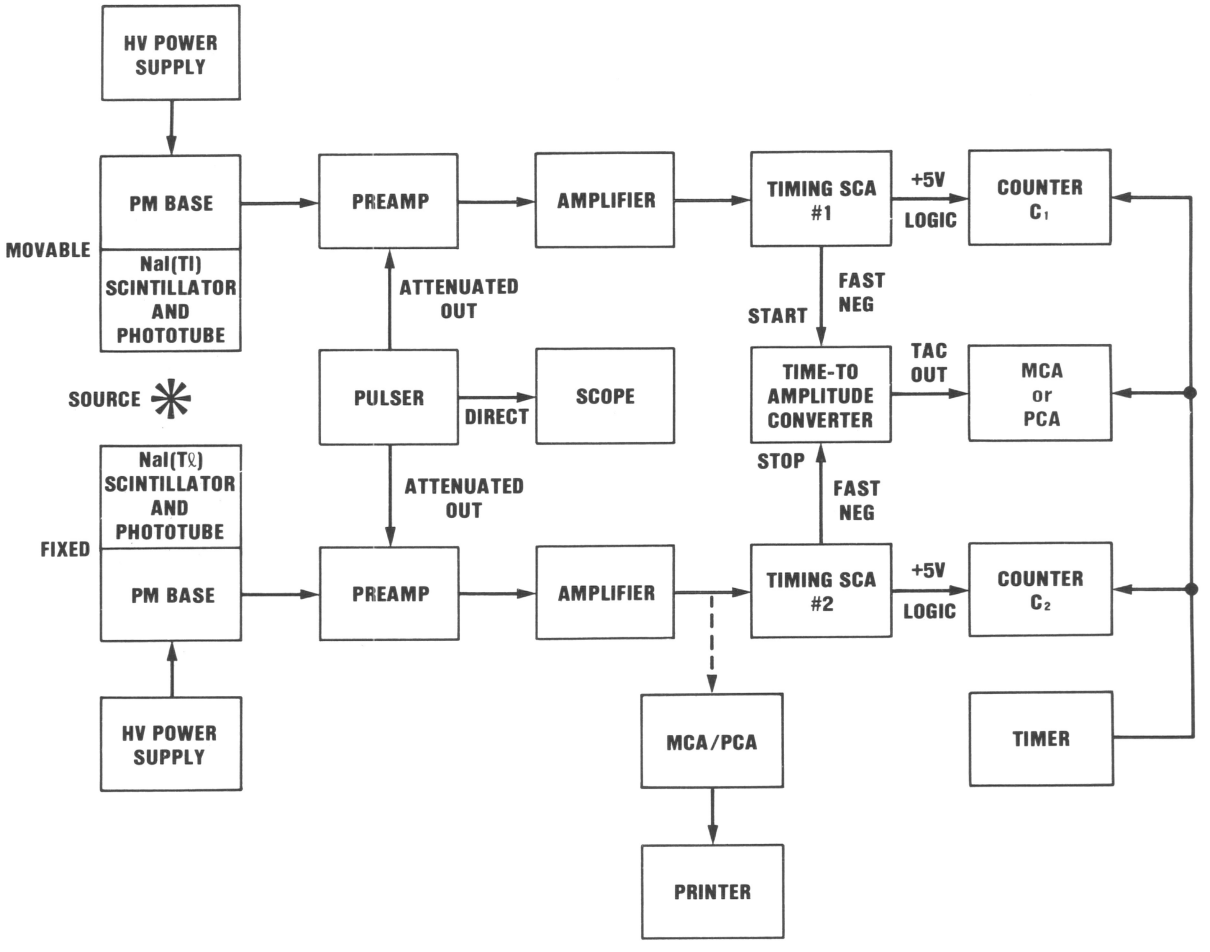

Figure 12.7. Electronics for annihilation measurements with a Time-to-Amplitude Converter (TAC).

REFERENCES FOR *EXPERIMENT 12*

1. A. C. Melissinos, *Experiments in Modern Physics,* Academic Press, New York (1966).

2. R. D. Evans, *The Atomic Nucleus*, McGraw-Hill, New York (1955).

3. H. A. Enge, *Introduction to Nuclear Physics,* Addison-Wesley (1966).

4. K. Seigbahn, *Alpha, Beta, and Gamma Spectroscopy*, North Holland Publishing Co., Amsterdam.

5. L. C. Biedenharn and M. E. Rose, *Rev. Mod. Phys.* **25**, 729 (1953).

6. B. L. Cohen, *Concepts of Nuclear Physics*, McGraw-Hill, New York (1971).

7. C. E. Crouthamel, *Applied Gamma-Ray Spectrometry*, Pergammon, New York (1960).

8. C. M. Lederer and V. S. Shirley, Eds., *Table of Isotopes,* 7th Edition, John Wiley and Sons, Inc., New York (1978).

9. F. Adams and R. Dams, *Applied Gamma Ray Spectrometry*, 2nd Edition, Pergammon Press, Ltd. (1970).

10. G. F. Knoll, *Radiation Detection and Measurement*, Wiley, New York (1979).

11. *Nuclear Data Sheets*, Edited by the Nuclear Data Project, Academic Press, New York and London.

12. E. Segre, *Nuclei and Particles*, The Benjamin-Cummings Publishing Co., Reading, Massachusetts (1977).

13. J. B. Marion and F. C. Young, *Nuclear Reaction Analysis*, John Wiley and Sons, New York (1968).

EXPERIMENT 13

Nuclear Lifetimes of ^{181}Ta and ^{57}Fe by Coincidence Spectroscopy

Scope

The **Nuclear Lifetimes** of the 615 keV state in ^{181}Ta and the 14.39 keV level in ^{57}Fe will be measured with a Time-to-Amplitude Converter (TAC). In the case of ^{181}Ta, the start pulse for the TAC will come from a Surface Barrier Detector which measures the prompt β's in the decay. The stop pulse will be provided by a NaI(Tℓ) (Experiment 13.1) or a germanium detector (Experiment 13.2). In the case of ^{57}Fe, the 122 keV gamma will be used to start the TAC and the 14 keV gamma will stop the timing sequence. In Experiment 13.3 a standard NaI(Tℓ) detector will be used to start the TAC and a Thin Window NaI(Tℓ) will stop the time sequence. In Experiment 13.4, the 122 keV start pulse will be provided by a germanium detector and the 14 keV stop pulses will be provided by a Si(Li) detector.

Discussion

The lifetimes of most nuclear states are quite short ($\sim 10^{-12}$ sec or shorter). There are, however, many isotopes that have states whose lifetimes can be measured with the electronics used in this course. As we will see, the measurement of nuclear lifetimes constitutes one of *the best experimental* techniques to verify the Heisenberg uncertainty principle.

Heisenberg suggested that it is not possible to know the exact values of the dynamic variables of a system at all times. In our example, the following can be written:

$$\Delta E \bullet \Delta T = \hbar = 1.048 \times 10^{-22} \text{ MeV} \bullet \text{sec} \qquad (1)$$

In other words, the uncertainty of the width of a nuclear level ΔE multiplied by the mean decay time of the level ΔT is of the order $\hbar$. In most cases, it is difficult for us to measure ΔE, the width of the level. These values are of the order of 10^{-12} MeV which is much too small to be observed with even the best detectors. In some cases, we can measure the mean life time of the state. This allows us to assign the width of the level (ΔE) from the uncertainty principle. In this experiment, we have chosen two isotopes and a variety of experimental techniques to measure these lifetimes. Figure 13.1 shows the partial decay scheme of the ^{181}Hf source.

There are actually eight levels involved in the total decay. We have shown the ones that represent most of the activity of the decay and certainly the only levels that are of importance to us in this experiment. Basically what happens in the decay is as follows: ^{181}Hf decays by the emission of 408 keV β to the 615 keV level in ^{181}Ta. This state has a mean life of 17.8 μsec. It is this mean life that we will measure in the experiment. The state decays by the emission of a 133 keV gamma to the 482 keV level which decays 81% of the time directly to the ground state of ^{181}Ta. In the experiment, we will start the TAC with the 408 keV β's and stop it with the 482 keV gamma.

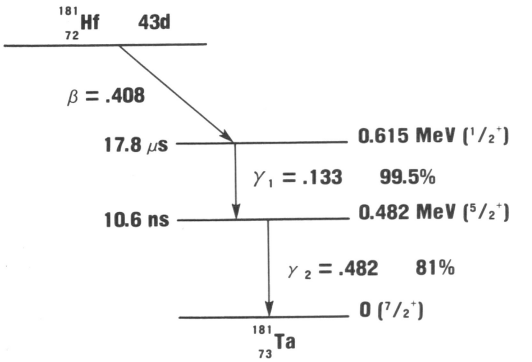

Figure 13.1. Decay scheme of ^{181}Hf showing the levels of importance to the nuclear lifetime of the 651 keV state.

Figure 13.2 shows a 3" x 3" NaI(Tℓ) spectrum for the gamma decay of ^{181}Hf. **Note:** The 482 keV and 133 keV peaks are the most pronounced gammas in the decay as indicated in the decay scheme (fig. 13.1).

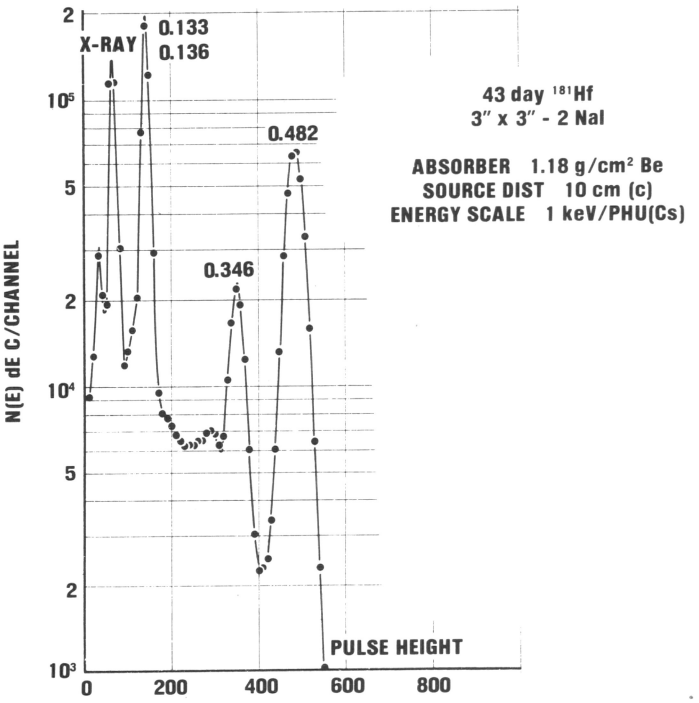

Figure 13.2. NaI(Tℓ) spectrum of ^{181}Hf.

As mentioned earlier, a germanium detector will be used in Experiment 13.2 to measure the 482 keV gammas. Figure 13.3 shows a pulse height spectrum of the gammas from ^{181}Hf with a germanium detector.

The β spectrum that provides the start pulse for the measurement will be similar to fig. 5.2 in Experiment 5. The β end point energy is 408 keV. Figure 13.4 shows a schematic of the electronics that will be used for Experi-

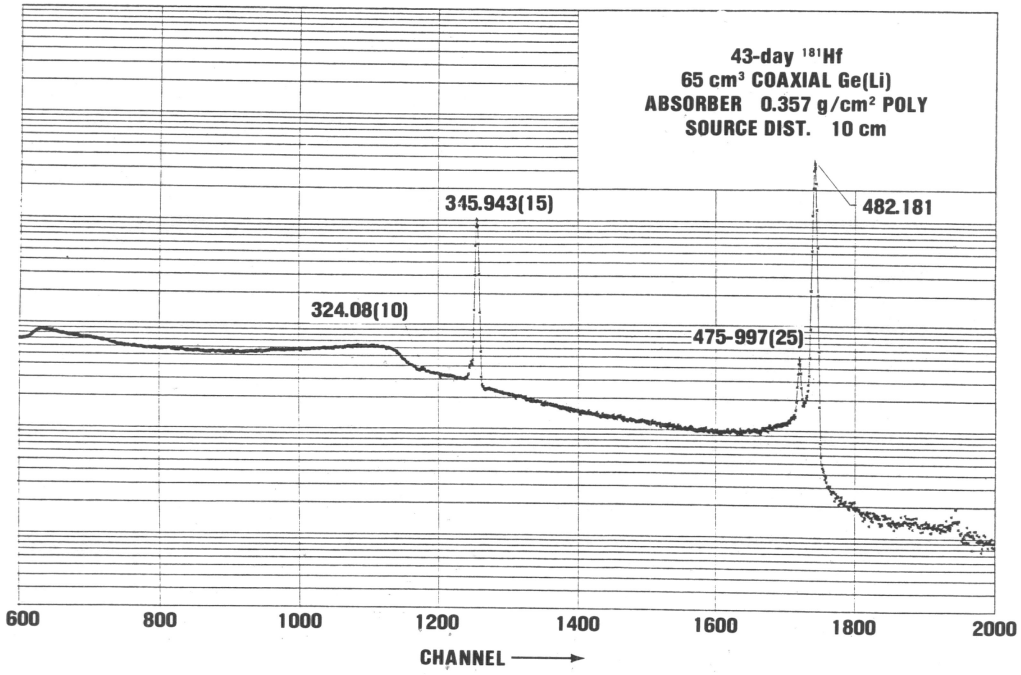

Figure 13.3. Germanium spectrum of the gammas from ^{181}Hf.

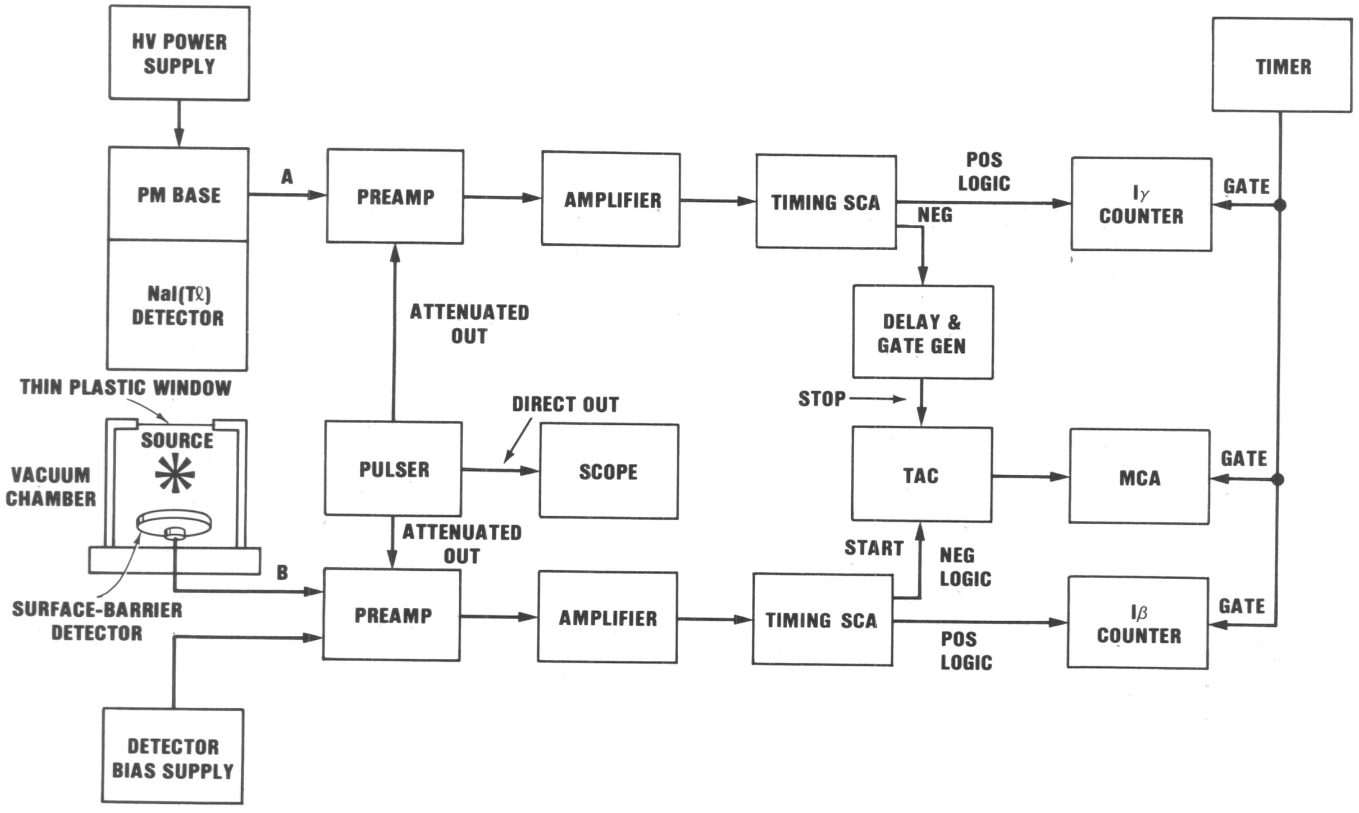

Figure 13.4. Electronics used (Experiment 13.1) to measure the mean life of the 615 keV state in ^{181}Ta. [NaI(Tℓ) and surface barrier method].

ment 13.1. As we mentioned above, the start pulses come from β in the Surface Barrier Detector and stop pulses are derived from the NaI(Tℓ) detector. In Experiment 13.2, we will measure the 482 keV gammas with a germanium detector.

The electronics will be exactly like fig. 13.4 except the NaI(Tℓ) detector will be replaced in the schematic with a High Resolution germanium detector. Experiments 13.3 and 13.4 are two experiments to measure the mean life of the 14 keV state in ^{57}Fe. We will discuss these experiments in detail after we finish Experiment 13.1 and 13.2.

EXPERIMENT 13.1

Measurement of the Nuclear Lifetime of the 615 keV State in ^{181}Ta by β,γ Coincidence with a Surface Barrier Detector and a NaI(Tℓ) Detector

Experimental Procedure

In this discussion, it will be assumed that the student has done Experiments 11 and 12 or, at least, is familiar with the coincidence techniques covered in these experiments.

1. Set up the electronics as shown in fig. 13.4. Place the ^{181}Hf source inside the Thin Window vacuum chamber and pump down the chamber. Apply voltage to both detectors. Adjust the gain of the NaI(Tℓ) amplifier so that the 482 keV gammas are about 4 volts in amplitude. In a similar manner, adjust the gain of the Surface Barrier amplifier so that the β continuum is distributed to a maximum pulse height of 4V. The amplifier gains are now set for the experiment.

2. Turn off the voltages and remove the source from the chamber. Turn on the pulse generator and adjust the delays of the SCA's so that the two counters and the MCA all show 60 Hz. This technique was discussed in Experiments 11 and 12. Set the TAC on a full scale time range of 50 μsec. Adjust the delay and gate generator for a delay period of 40 μsec. Store a spectrum in the MCA; record the channel. Repeat for enough delay values to determine a delay vs pulse height curve from 40 μsec down to 5 μsec (see fig. 11.8). After this has been done, turn off the pulse generator and place the source in the chamber. Place voltage on both detectors.

3. Use the techniques discussed in Experiments 11 and 12 to set the NaI(Tℓ) SCA in the differential mode with the window bracketing the 482 keV peak (see fig. 13.2).

4. On the β channel, set the SCA in the integral mode with the lower level adjusted so that ¾ of the β spectrum is being counted.

5. Set the delay and gate generator for a delay of 0.1 μsec. Set the timer for a time of 600 sec and accumulate a TAC spectrum in the MCA.

Exercise From the delay and gate generator data obtained in (**2**), plot a delay vs pulse height curve and obtain the time per channel for the TAC settings used. From this data, convert the channels to time for the spectrum measured in (**5**) and plot your curve which is similar to fig. 13.5. From the curve, calculate the mean life of the 615 keV state. The accepted value is 17.8 μsec.

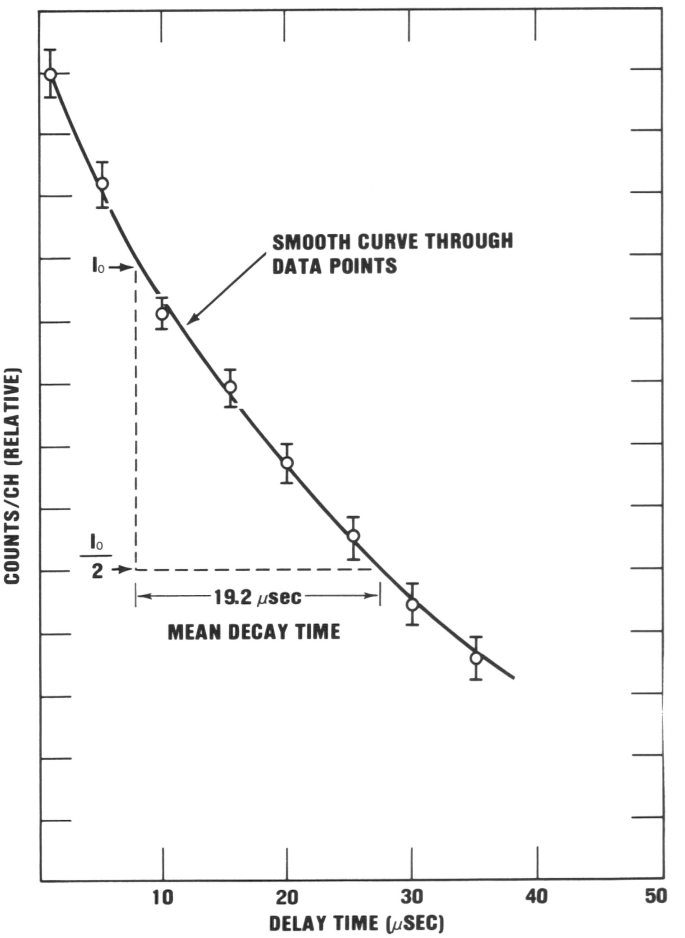

Figure 13.5. Experimental data for measuring the mean life of the 615 keV ($^1/_2^+$) state in ^{181}Ta.

EXPERIMENT 13.2

Measurement of the Nuclear Lifetime of the 615 keV State in ^{181}Ta by β,γ Coincidence Using a Surface Barrier Detector and a High Resolution Germanium Gamma Detector

Figure 13.6 shows the electronics that will be used for this experiment. It should be noted that the experimental arrangement is identical to that of the last experiment except we are using a germanium gamma detector instead of the NaI(Tℓ) detector. Figure 13.3 shows a pulse height spectrum of a ^{181}Hf source as observed with a germanium detector. **Note:** The 482 keV state that shows up as one state in the NaI(Tℓ) spectrum fig. 13.2 is actually composed of a 482.181 keV state for our experiment and a weak 475.99 keV line from the decay of the 482.18 keV level to the low lying 6.3 keV ($^9/_2^-$) state in ^{181}Ta. Since both 482.18 and 475.9 keV lines come from the state we are measuring, we can set the ΔE window to bracket both lines for our stop pulse.

Experimental Procedure

1. Set up the electronics as shown in fig. 13.6. Place the ^{181}Hf source in the Thin Window vacuum chamber and evacuate. Apply bias voltage to both detectors.

2. Adjust the gain of the germanium amplifier so that the 482.18 keV line (fig. 13.3) is approximately 4 volts in amplitude. The SCA can be set to bracket the 482.181 and 475.99 keV peaks by using the electronic arrangement in fig. 11.11. **Note:** When this is set up, the only difference between your arrangement and fig. 11.11 is the fact that you have a HpGe detector instead of the NaI(Tℓ) shown in the figure.

3. The lower level of the SCA on the surface barrier side can also be set by using the electronics shown in fig. 11.11. These techniques were outlined in Experiment 11.

4. After both SCA's have been set, turn off both bias supplies and remove the source. Connect the circuit back as shown in fig. 13.4. Turn on the pulse generator. As in the last experiment, use the **Delay and Gate Generator** to make a delay vs pulse height calibration for the TAC. Plot a curve of delay vs channel number. Turn off the pulser.

5. Put the source back in the chamber, evacuate and apply the necessary bias voltages. Set the timer for a long enough time period to get reasonable statistics in the TAC output and accumulate a spectrum.

Exercise Plot a Mean Life Curve similar to fig. 13.5.

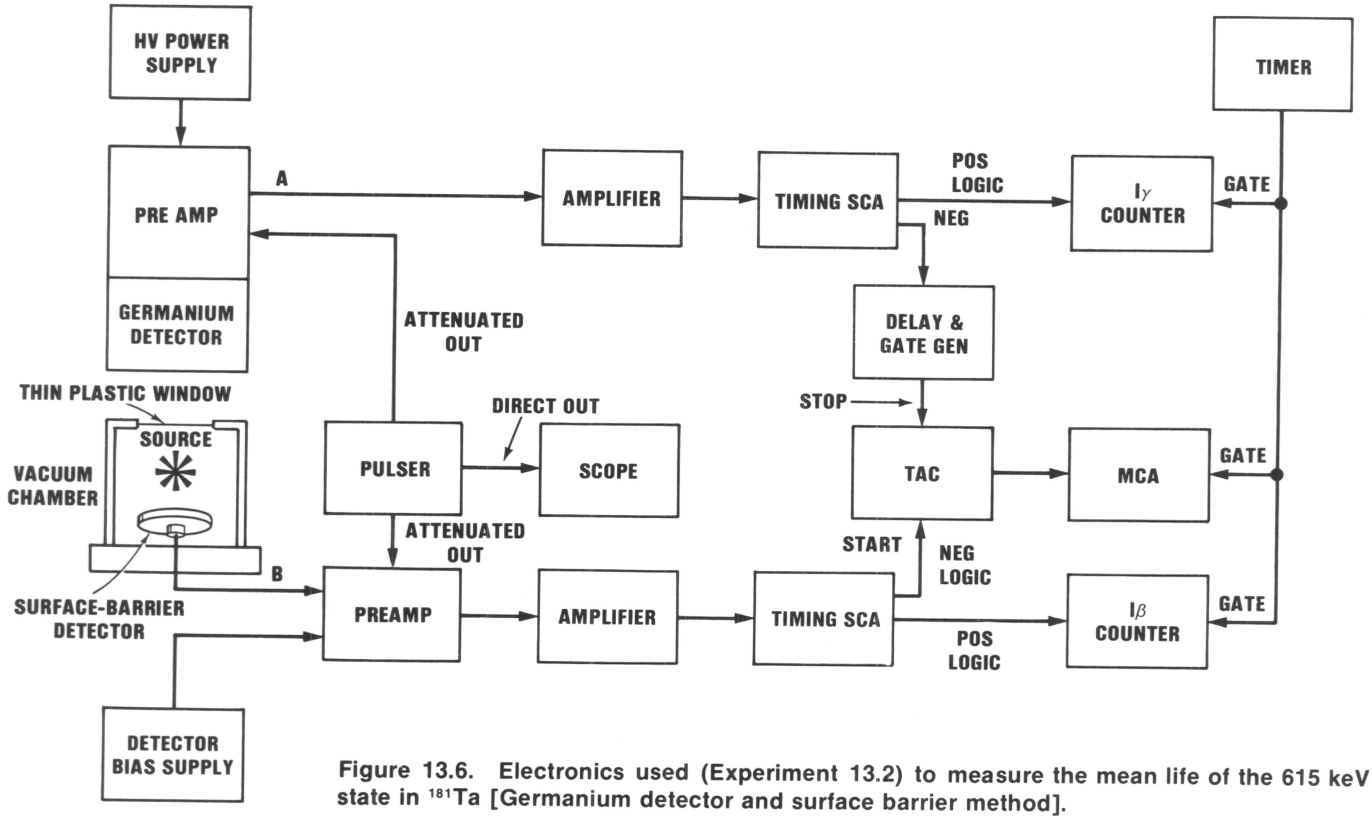

Figure 13.6. Electronics used (Experiment 13.2) to measure the mean life of the 615 keV state in ^{181}Ta [Germanium detector and surface barrier method].

EXPERIMENT 13.3

Mean Lifetime Measurement of the 14 keV State in ^{57}Fe with Two NaI(Tℓ) Detectors and a Time-to-Amplitude Converter (TAC)

Discussion

Figure 13.7 shows a NaI(Tℓ) pulse height spectrum of a ^{57}Co source. Shown also on the figure is the decay scheme of ^{57}Co. Most of the decays (99.8%) are by electron capture (EC) to the 136 keV ($^5/_2^-$) state in ^{57}Fe. The 136 keV state can decay directly to the ground state or cascade with a 122 keV gamma to the 14 keV ($^3/_2^-$) state and then to the ground state. The 122 keV gamma is shown as γ_1 in the figure and the 14 keV group is γ_2. Figure 13.8 shows a high resolution germanium spectrum of this isotope with the 122 and 136 keV lines resolved. Figure 13.9 shows a high resolution Si(Li) spectrum of the ^{57}Co source. The strong Kα_1 and Kβ_1 lines are from (EC) and the 14.39 keV gamma from the ($^3/_2^-$) first excited state in ^{57}Fe are clearly seen in the spectrum. In this experiment we will use the 122 keV (γ_1) to start the TAC and the 14 keV (γ_2) to stop the timing sequence. Our data will thus yield the **Mean Life** (98 ns) of the 14.39 keV ($^3/_2^-$) level in ^{57}Fe.

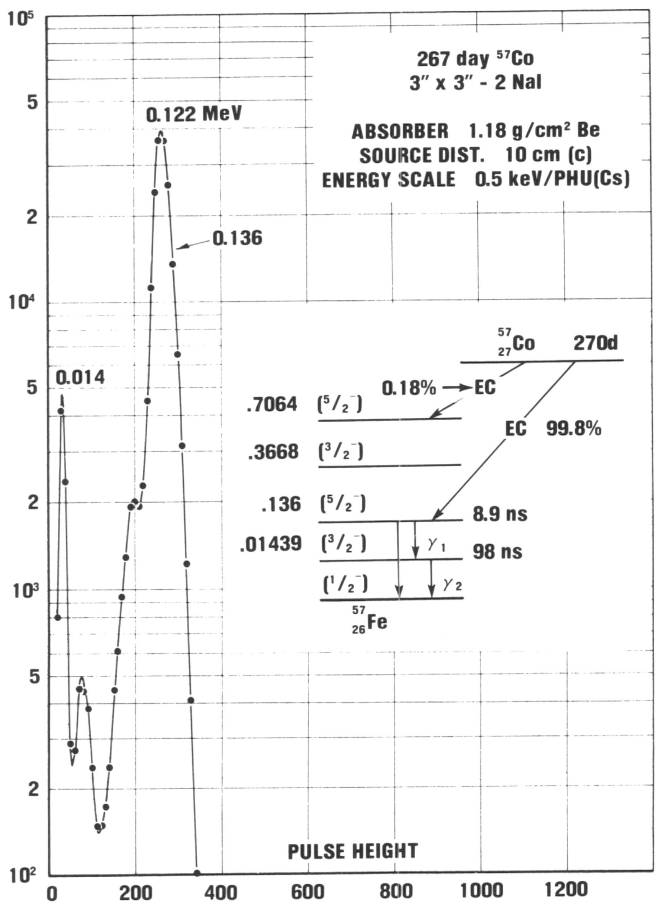

Figure 13.7. NaI(Tℓ) pulse height spectrum of a ^{57}Co source. Shown also on the figure is the decay scheme of ^{57}Co to levels in ^{57}Fe..

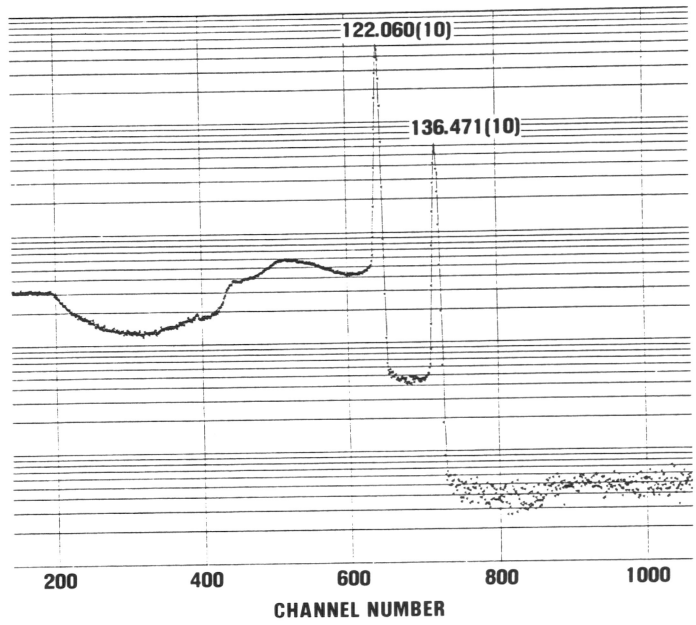

Figure 13.8. Germanium spectrum of ^{57}Co showing the resolved 136.471 and 122.060 lines.

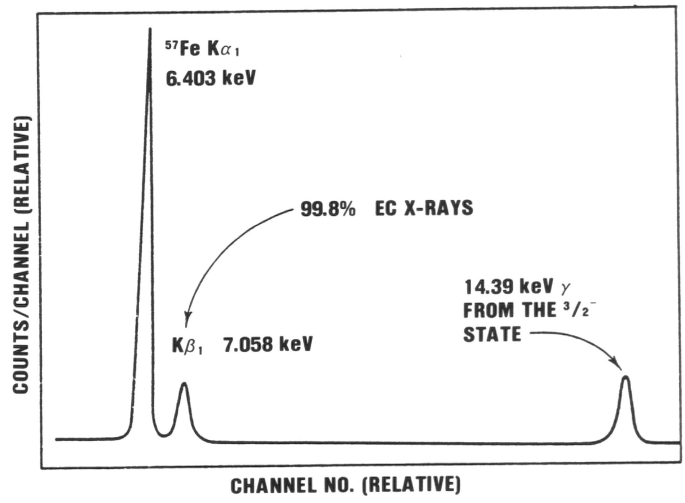

Figure 13.9. High resolution Si(Li) pulse height spectrum of a ^{57}Co source.

Experimental Procedure

1. Set up the electronics as shown in fig. 13.10. Set the high voltage supplies to their recommended values. Place the ^{57}Co source about 3 cm from each NaI(Tℓ) detector. **Note:** The TAC receives its start pulse from the top detector (γ_1). Adjust the gain of amplifier #1 so that the 122 keV gammas show an output of 4 volts. The output of amplifier #1, if fed into an MCA, should resemble fig. 13.7. Use the electronics schematic in fig. 11.11 to set the ΔE window of SCA #1 so that it brackets the 122

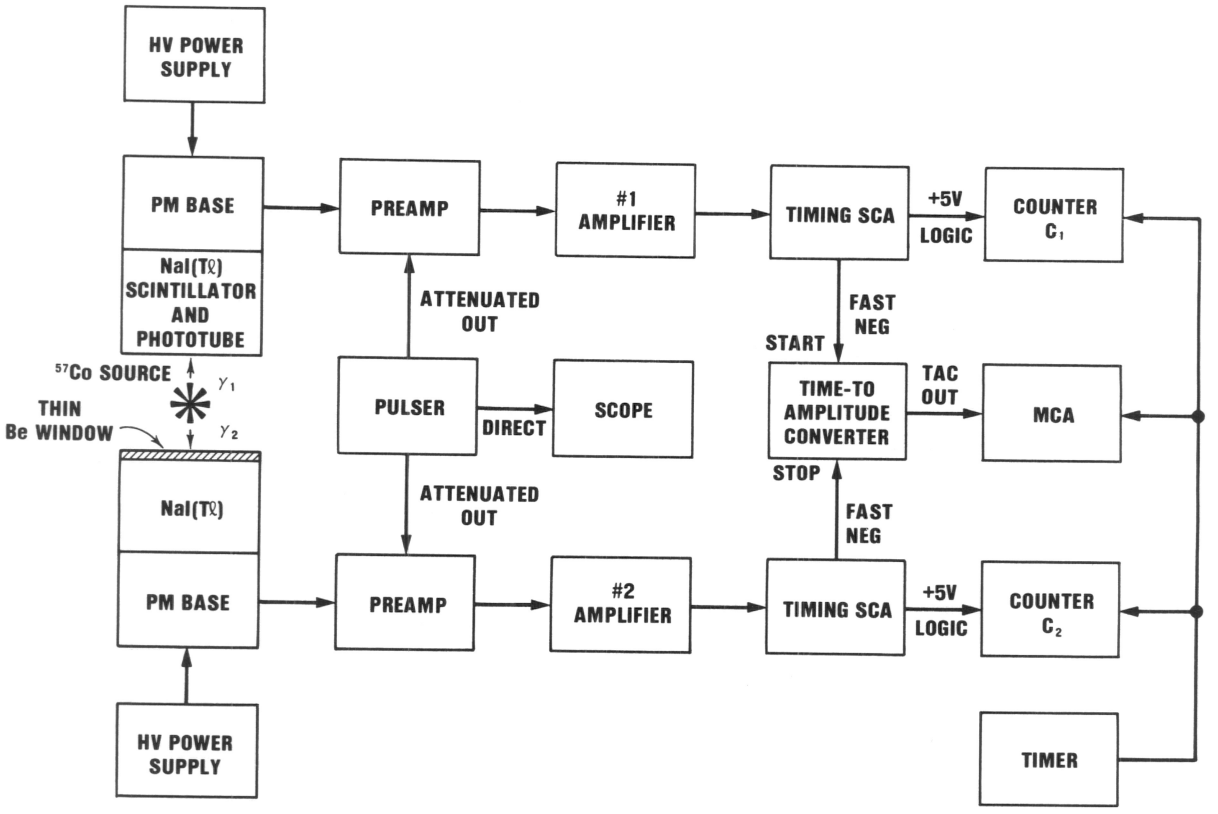

Figure 13.10. Electronics for measuring the mean life of the 14.39 keV state in ^{57}Fe (Experiment 13.3). The detectors used are a thin window NaI(Tℓ) for the 14 keV gamma and a 3" x 3" NaI(Tℓ) for the 122 keV start pulse.

keV line (fig. 13.7). When the window has been set, return the electronics to the configuration shown in fig. 13.10.

2. On the stop side, adjust the gain of the amplifier so that the 14 keV output is about 4 volts. Use the electronics in fig. 11.11 to set the ΔE window so that it brackets the 14 keV peak shown in fig. 13.11. After the gain and SCA #2 are set, return the electronics to the configuration shown in fig. 13.10. Remove the source and turn on the pulse generator.

3. Set the TAC on 200 nsec full scale time range. Set SCA #1 at minimum delay and SCA #2 at 150 nsec. The TAC output should occur in about channel 500 of the 1000 channel MCA. If it does not, adjust the delays in the SCA's so that it is stored about mid scale on the MCA.

4. Make a delay vs pulse height curve for the TAC. Plot the data and determine the time per channel for this 200 nsec range. Turn off the pulse generator and place the ^{57}Co source between the detectors.

5. Set the timer for a time of 600 sec and start the system counting.

Exercise Make a plot similar to fig. 13.5 for the data that was taken above. From fig. 13.7 the accepted value for the lifetime of the 14.39 keV state is 98 nsec. How well did you do?

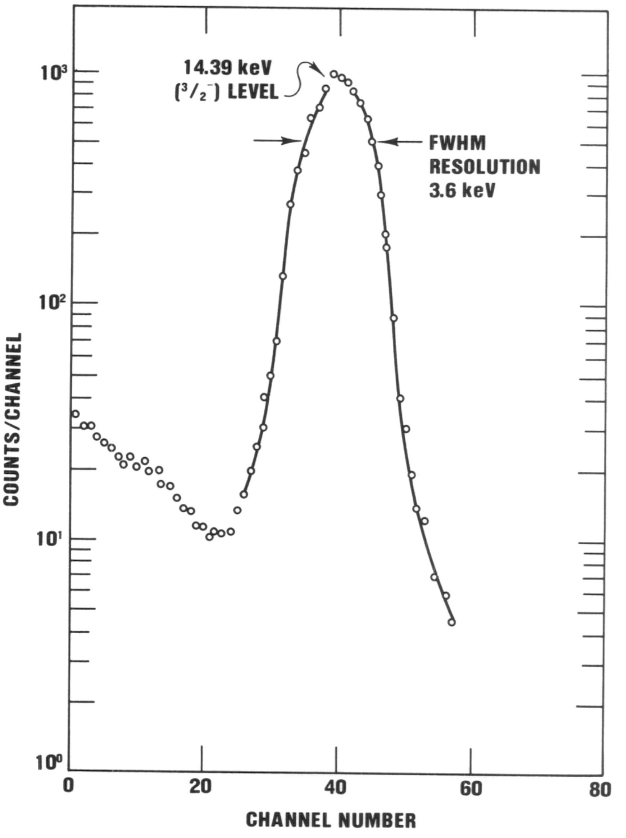

Figure 13.11. Beryllium window NaI(Tℓ) spectrum of the 14.39 keV gammas from a ^{57}Co source.

EXPERIMENT 13.4

Mean Lifetime Measurement of the 14 keV State in ^{57}Fe, Measured with Germanium and Si(Li) Detectors and a TAC

Experimental Procedure

1. Set up the electronics as shown in fig. 13.12. Place the source about 2 cm from each detector and turn on the high voltage supplies. Use the techniques learned in Experiment 11 (fig. 11.11) to set the window of SCA #1 on the 122 keV peak (see fig. 13.8). Use the same technique to set SCA #2 on the 14 keV peak of the Si(Li) detector (see fig. 13.9). The gains and ΔE windows for SCA's #1 and #2 are now set for the experiment. We must now set the timing.

2. Turn off the high voltage supplies and turn on the pulse generator. Set the delay on SCA #1 at minimum and SCA #2 at 150 nsec. Set the TAC for 200 nsec full scale. Make a time vs pulse height calibration for the TAC for at least 10 delay settings (SCA #2) between 150 and 20 nsec. Plot the data and determine the time per channel for the TAC. Turn off the pulser.

3. Accumulate a spectrum in the MCA for a time period of at least 600 sec or longer, if necessary, to get reasonable statistics.

Exercise Plot the data in an appropriate form similar to fig. 13.5. With this fancy electronic arrangement the mean life should be close to the accepted value of 98 nsec.

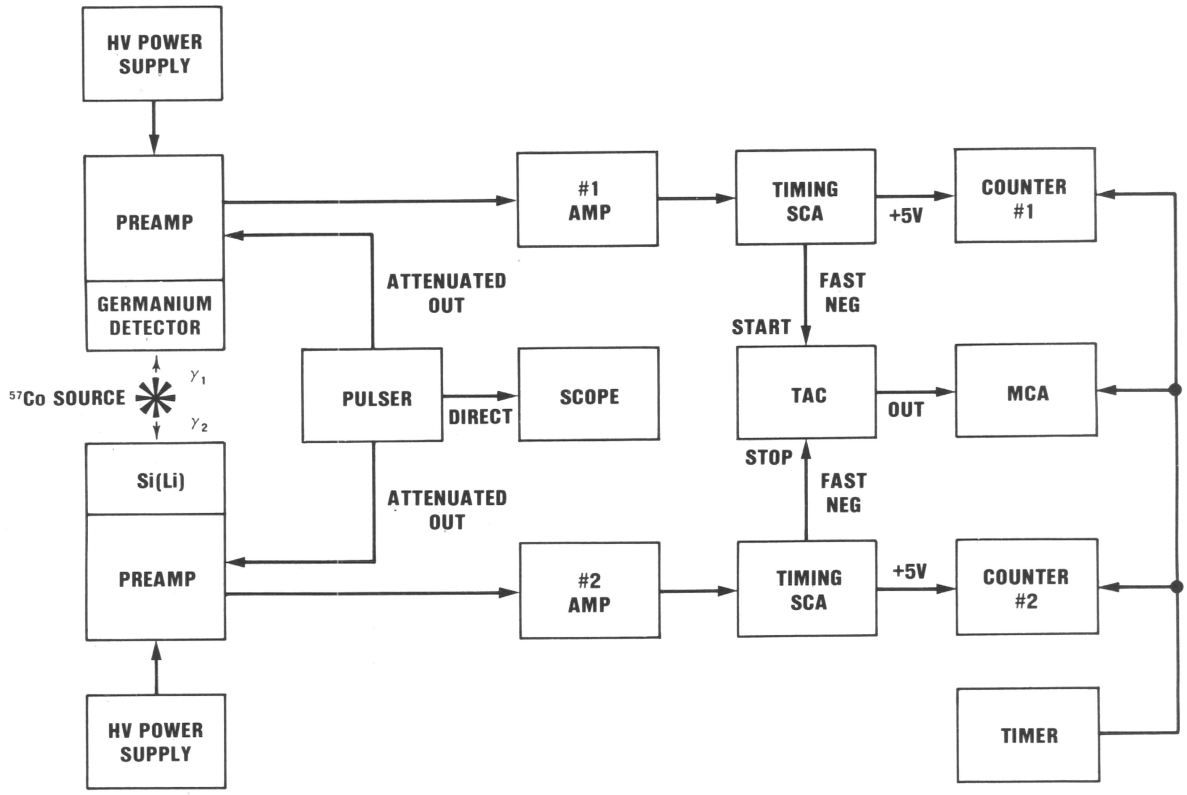

Figure 13.12. Electronics for measuring the mean life of the 14.39 keV state in ^{57}Fe. This set up uses a Germanium detector to start the TAC and a Si(Li) to stop the timing sequence.

REFERENCES FOR *EXPERIMENT 13*

1. K. Seigbahn, *Alpha, Beta and Gamma Spectroscopy*, North Holland Publishing Co., Amsterdam.

2. C. M. Lederer and V. S. Shirley, Eds., *Table of Isotopes*, 7th Edition, John Wiley and Sons, Inc., New York (1978).

3. A. C. Melissinos, *Experiments in Modern Physics*, Academic Press, New York (1966).

4. H. A. Enge, *Introduction to Nuclear Physics*, Addison-Wesley (1966).

5. B. L. Cohen, *Concepts of Nuclear Physics*, McGraw-Hill, New York (1971).

6. R. D. Evans, *The Atomic Nucleus*, McGraw-Hill, New York (1955).

7. P. Quittner, *Gamma Ray Spectroscopy*, Halsted Press, New York (1972).

8. J. B. Marion and P. C. Young, *Tables of Nuclear Reaction Graphs*, John Wiley and Sons, New York (1968).

9. C. E. Crouthamel, *Applied Gamma-Ray Spectrometry*, Pergammon, New York (1960).

10. G. F. Knolls, *Radiation Detection and Measurement*, John Wiley and Sons, New York (1979).

EXPERIMENT 14

Angular Correlation

Scope

In this experiment, we will study the sequential nature of the two gammas from ^{60}Co by the Multipurpose Coincidence Circuit Method and with a Linear Gate. This study of the decay scheme will be followed by a measurement of the directional angular correlation of ^{60}Co by two "state of the art" techniques. In the first method, the γ-γ angular correlation will be measured with two NaI(Tℓ) detectors and a Time-to-Amplitude Converter (TAC). The second method is like the first in every respect except two high resolution germanium detectors are used instead of NaI(Tℓ).

Discussion

We have used the *Table of Isotopes* as a reference at the end of most of the experiments in this manual. Clearly this reference contains more information about decay schemes of nuclei than any other. In this experiment, we are going to learn that a definite relationship exists in some cascading gamma isotopes that will tell us something about the nuclear spins of the levels that are involved in the decay. The spin of a state is associated with the angular momentum of the state. In a nuclear reaction, for example, the spin and parity of the states that are involved in the reaction will often determine the cross section or probability of the reaction in a certain direction relative to the incident beam direction. In any case, many of the spins that are listed in the *Table of the Isotopes* have been determined by directional γ-γ angular correlation which is exactly what we are going to do in this experiment. The measurements outlined in this experiment are intended as an exercise for a nuclear physics class, *however, the same equipment can be used for publishable research for many isotopes that have not been studied.* This equipment consists of: a precision angular correlation table, NaI(Tℓ) or germanium detectors and the electronics shown in the block diagrams in the angular correlation experiments. The cost is not prohibitive and some of the equipment is probably already available in your nuclear laboratory.

Theory

Figure 14.1 shows a pulse height spectrum of the decay of ^{60}Co. Shown also in the figure is the decay scheme of ^{60}Co. The 0.319 MeV β particle decays to the 2.507 MeV 4^+ state of the ^{60}Ni nucleus. This state decays by an E2 (γ_1) gamma to the 2^+ (9.7×10^{-12} sec mean life) state and then to the ground state. If the mean life of the 1.3325 MeV state is short enough, there can be a definite correlation between the direction of γ_2 relative to γ_1. The reason for this is that if the mean life of the state is short enough, some of the alignment that it might have had as a result of being formed by γ_1 emission might be maintained in the direction of γ_2. This is certainly the case for γ_1 and γ_2 in ^{60}Co. There is a 17% deviation from an isotropic distribution which is quite easy to measure in the laboratory. This correlation function is measured by fixing one detector relative to the decaying nucleus, requiring a coincidence between γ_1 and γ_2, and measuring the coincidence counting rate as a function of the angle between the two detectors. A more complete theoretical treatment of the correlation function is given in refs. 1, 2 and 7. For ^{60}Co:

$$W(\theta) = 1 + a_2 \cos^2\theta + a_4 \cos^4\theta + \ldots + a_{2L} \cos^{2L}\theta \qquad (1)$$

where $a_2 = 0.125$, $a_4 = 0.0417$, all other terms can be ignored

Figure 14.7 shows a plot of this theoretical function for θ = 90 degrees to 180 degrees in 10° increments.

The coefficients a_2 and a_4 are functions of the spins of the initial (4^+), intermediate (2^+), and final (0^+) states. The highest power of $\cos\theta$ in eq. (1) is determined by the condition 2L which must be equal to or less than $2I_1$, $2I_2$, or 2J whichever is smaller. In this example I_1 and I_2 are the multipolarities of γ_1 and γ_2 (both are E2) and J is the spin of the intermediate level (2^+ for the 1.3225 MeV state).

In our case, $2I_1 = 4$, $2I_2 = 4$, and $2J = 4$ and therefore the angular correlation function would contain only up to the $\cos^4\theta$ term. In order to see how this works, let us assume that we didn't know the spin of J but knew all of the other terms in our selection rules. The only acceptable values for the spin J of the 1.3325 MeV state are 0, 1, and 2. A spin of (0) would give no correlation but would yield an isotropic distribution. A spin of (1) would give:

$$W(\theta) = 1 + a_2 \cos^2\theta \qquad (2)$$

which is not what we experimentally observe. The only acceptable spin of this level is therefore (2) which is the correct value. Gamma angular correlation measurements thus give us information on the multipolarities of the two gammas that are involved, which helps in the assignments of the spins of nuclear levels. It is one of the most powerful nuclear techniques and, as you will see, the experiments are not difficult to do.

EXPERIMENT 14.1

Verification of the Gamma-Gamma Coincidence for ^{60}Co Using a Multipurpose Coincidence Circuit

Discussion

Figure 14.1 shows a pulse height spectrum of ^{60}Co which was measured with a NaI(Tℓ) detector. Shown also on the figure is the partial decay scheme for the isotope. ^{60}Co decays by the emission of a 0.319 MeV β to the 2.507 MeV level in ^{60}Ni. This level promptly gamma decays by E2 gamma radiation to the 2^+, 1.3325 MeV level. This gives us the 1.17 MeV gamma that is measured in the spectrum. The 1.3325 MeV state decays by E2 gamma emission directly to the ground state of ^{60}Ni. This 1.3325 MeV gamma decays with a mean life of 0.7×10^{-12} sec which is prompt as far as we are concerned. In fig. 14.3, if γ_1 is directed towards the top detector, then it is approximately true that γ_2 can go off in any direction. This means that a small number of them will strike the bottom detector and be counted. Therefore, there is a definite coincidence rate that will occur between the two detectors. (We will see in a later experiment that γ_2 actually varies from an isotropic distribution by about 17%, but for our present purpose it is essentially iso-

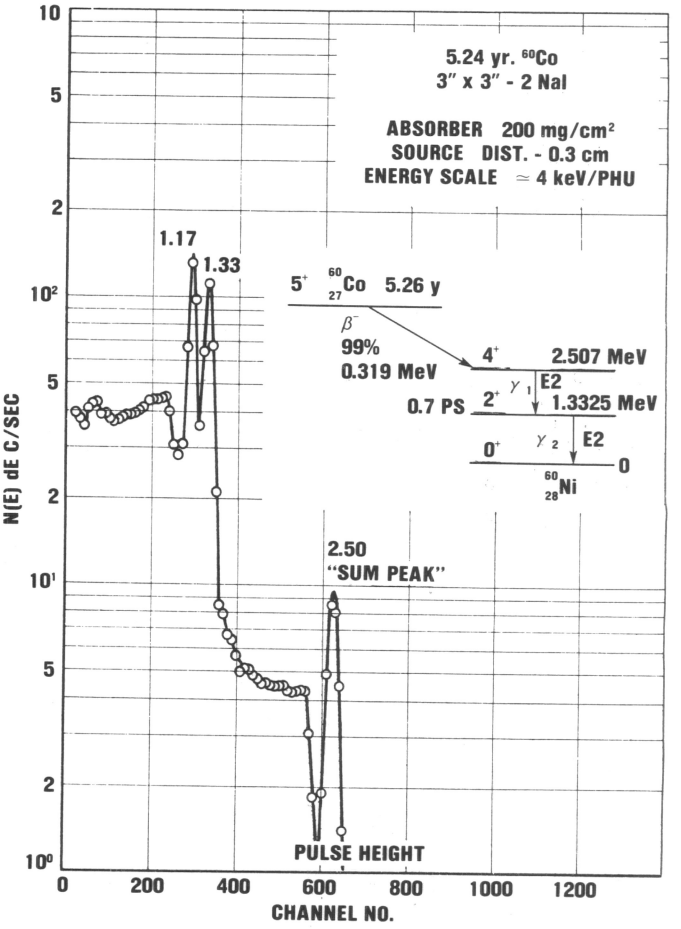

Figure 14.1. NaI(Tℓ) pulse height spectrum of ^{60}Co with a diagram showing the decay scheme.

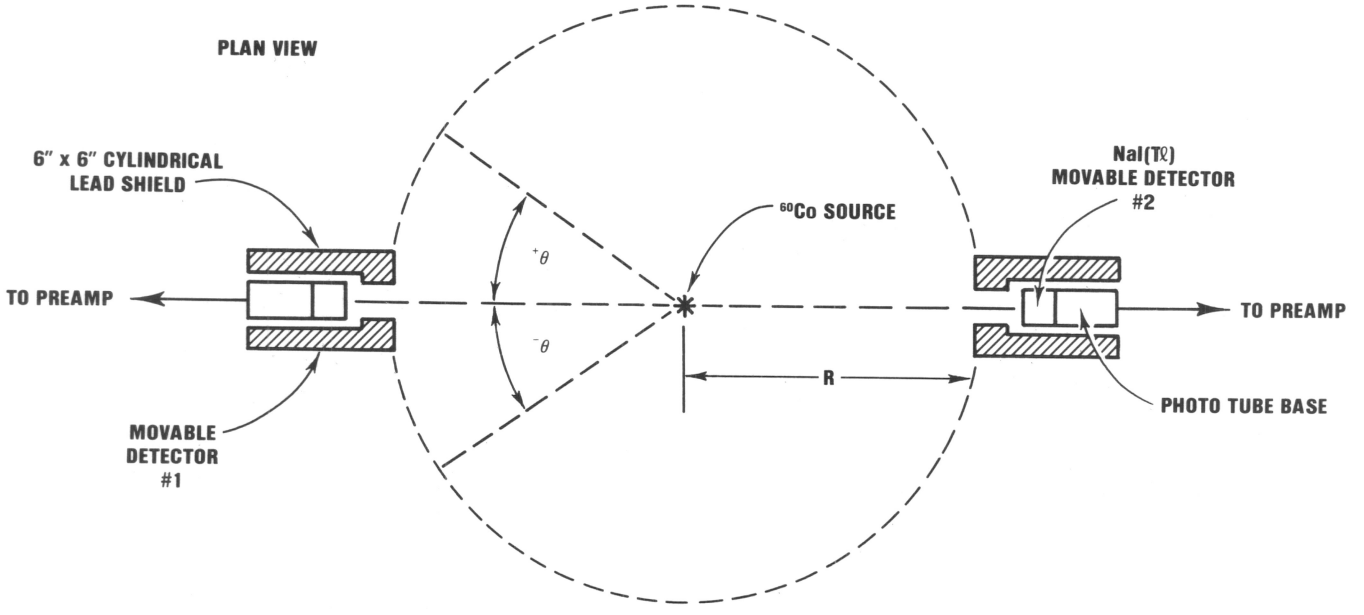

Figure 14.2. Plan view of the gamma-gamma directional angular correlation table with two rotating shields.

tropic.) In fig. 14.1, the sum peak at 2.50 MeV is a graphic illustration that if γ_1 goes up, γ_2 can go in any direction. In this case γ_2 goes in the same direction as γ_1 and the NaI(Tℓ) detector sees γ_1 and γ_2 at the same time. The detector sums the two pulses and gives an output equal to the sum 2.50 MeV. In this experiment, we will set the top SCA (#1) on the photopeak γ_1 and the bottom SCA (#2) on γ_2 (see fig. 14.3). We will then experimentally verify that the number of coincidences that are recorded agrees theoretically with a decay scheme consistent with that of fig. 14.1.

Scope

The purpose of this experiment is to verify that the 1.17 MeV and 1.33 MeV gammas are in coincidence in the decay of ^{60}Co.

Experimental Procedure

Note: In describing this experiment, we are going to assume that Experiments 11, 12, and 13 have already been done by the student, or, at least, carefully read and understood.

Figure 14.2 shows a schematic view of the angular correlation table that will be used for this experiment. The heavy lead shields with their NaI(Tℓ) detectors can both be moved independently. The angles θ can be precisely set to within $\pm$ 0.10 degree. The distance (R) from the source to either detector can be changed to accommodate sources of a wide range of activities up to 20 μCi.

1. Place the ^{60}Co source in its holder in the center of the angular correlation table. The detectors should be 180 degrees apart and at a distance (R) which will give reasonable counting rates (500-1000 cps) for the experiment. Set up the electronics as shown in fig. 14.3. Our first task will be to set SCA #1 so that its ΔE window brackets γ_1 (1.17 MeV in fig. 14.1). In order to do this, temporarily disconnect the +5V logic output from SCA #1 and feed it into the gate input of the MCA (or PCA) as shown in fig. 14.4. Take the output of amplifier #1 and feed it into the input of the MCA.

2. Set the high voltage at its recommended value and raise the gain of amplifier #1 until the 1.33 MeV line is about 4V amplitude as observed with the oscilloscope. Set SCA #1 in the integral mode with the lower level at 50/1000. The delay amplifier should be set on 3 μsec. If the amplifier has been set at a peaking time of 1 μsec, use the bipolar output, as we have done in all of the previous coincidence experiments. The spectrum in the MCA should be like fig. 14.1. While observing the spectrum in the MCA, raise the lower level to the Compton valley just below the 1.17 MeV peak. Switch the SCA to the ASYM window mode and adjust the window width so that it brackets the 1.17 MeV peak. Detector #1 is now set to count only γ_1.

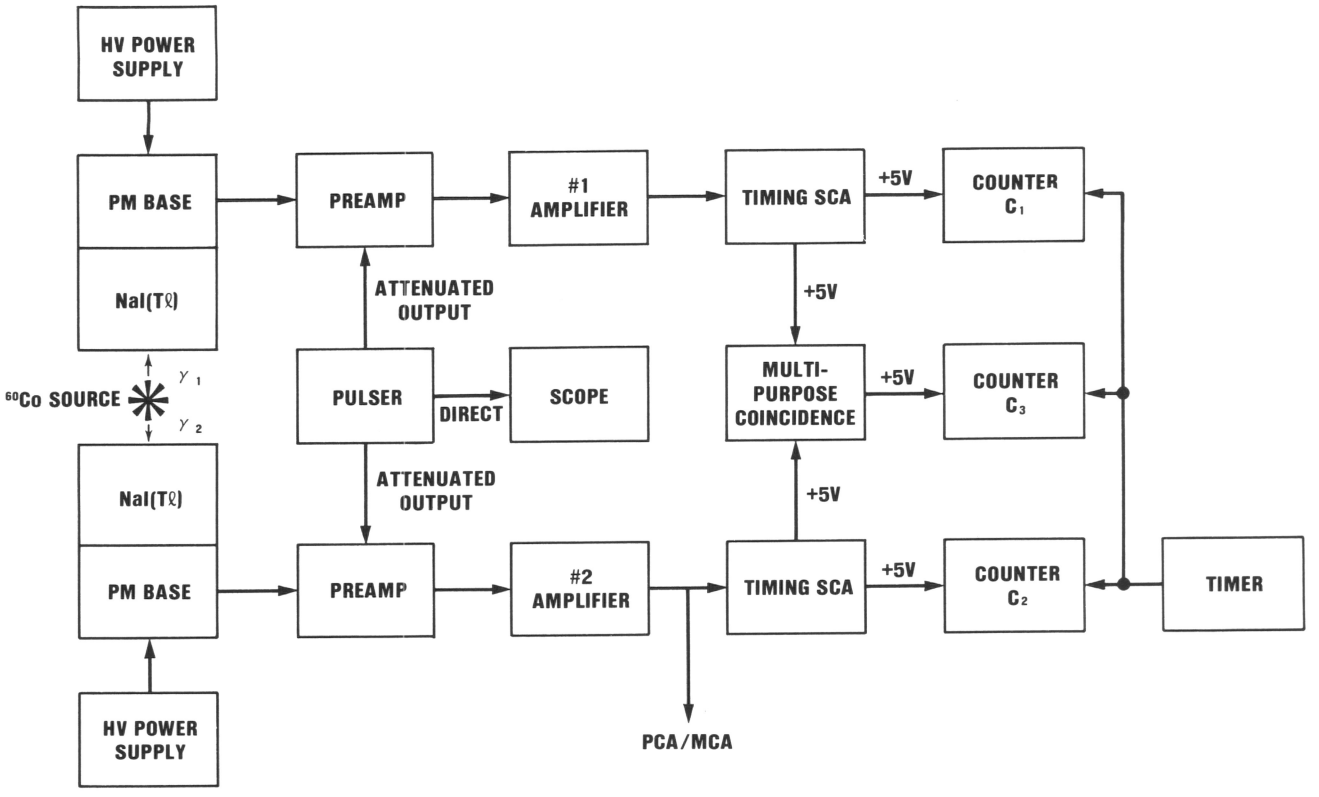

Figure 14.3. Electronics for verification of the gamma-gamma coincidence for ^{60}Co using a multipurpose coincidence circuit.

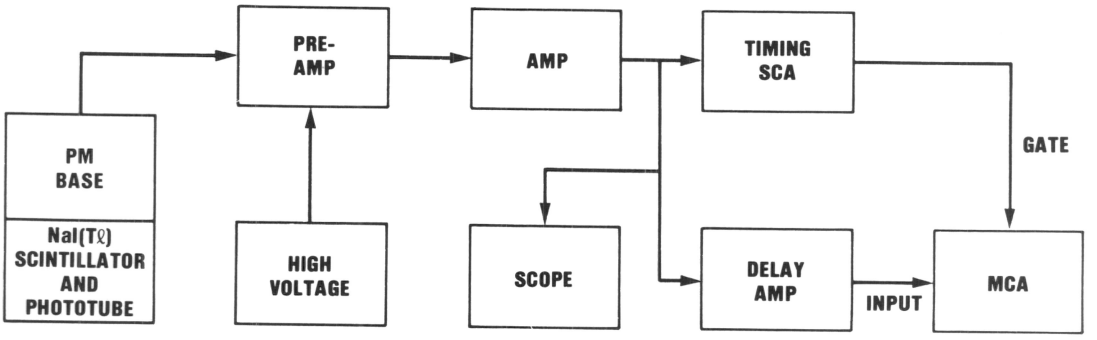

Figure 14.4. Electronics for setting the lower level threshold and ΔE windows for a single channel analyzer.

3. Use the same experimental procedure to set the SCA #2 so that it brackets gamma #2 (1.33 MeV). When this has been completed, connect the electronics as in fig. 14.3 and remove the ^{60}Co source.

4. Turn on the pulse generator and set the multipurpose coincidence unit as follows:

Resolving time 100 nsec; A and B in coincidence mode; C, D, and E out; use the G output to counter #3. Set the delays of SCA's #1 and #2 so that counter C_3 has a counting rate of 60 Hz. C_1 and C_2 should also record a 60 Hz rate. Turn off the pulser and place the ^{60}Co source in its holder.

5. Reset counters C_1, C_2, and C_3 and count for a time period of 300 sec or longer, if necessary, to get about 5000 counts in C_1 and C_2. Record all counter readings.

Exercise If the geometry is the same, the counting rate in C_1 should be slightly greater than the rate in C_2. The reason for this is that the intrinsic peak efficiency for 1.17 MeV is slightly greater than it is for 1.33 MeV. The coincidence rate should be approximately $A_d/4\pi R^2$ times the rate in either C_1 or C_2. Calculate this number and see how it compares to C_3.

It is interesting to note that the ratio of Σ for the 2.50 MeV sum peak (fig. 14.1) to the Σ for individual peaks in the spectrum should be approximately the ratio of coincidence counts in C_3 to either side counter. By now you should be convinced that γ_1 and γ_2 are coincident events which was the object of this first experiment.

EXPERIMENT 14.2

Verification of the γ-γ Cascade in the Decay of ^{60}Co (Linear Gate Method)

Experimental Procedure

1. Set up the electronics as shown in fig. 14.5. Use the procedures in Experiment 14.1 steps **1**, **2**, and **3** to set the window of SCA #1 on the 1.17 MeV peak.

2. Adjust the gain of amplifier #2 so that the 1.33 MeV pulses are about 4V amplitude as observed with the oscilloscope. Set the delay amplifier at 3 μsec.

3. Remove the ^{60}Co source and turn on the pulse generator. Adjust the delay of SCA #1 to minimum. Set the timer for 300 sec and start it. The counting rates in C_1, C_2, and Σ/t in the MCA should all be 60 Hz. Turn off the pulser and place the source in its holder.

4. Clear all counters and the MCA; set the timer for 600 sec, and run. The spectrum that is observed in the MCA should be almost exclusively the 1.33 MeV peak. The 1.17 MeV peak has been gated out by the coincidence requirement.

Exercise Determine Σ-β/t for the 1.33 MeV peak in the MCA. How does this compare with the number of coincidence counts (C_3) in the last experiment? Can you see that these numbers are giving you the same information?

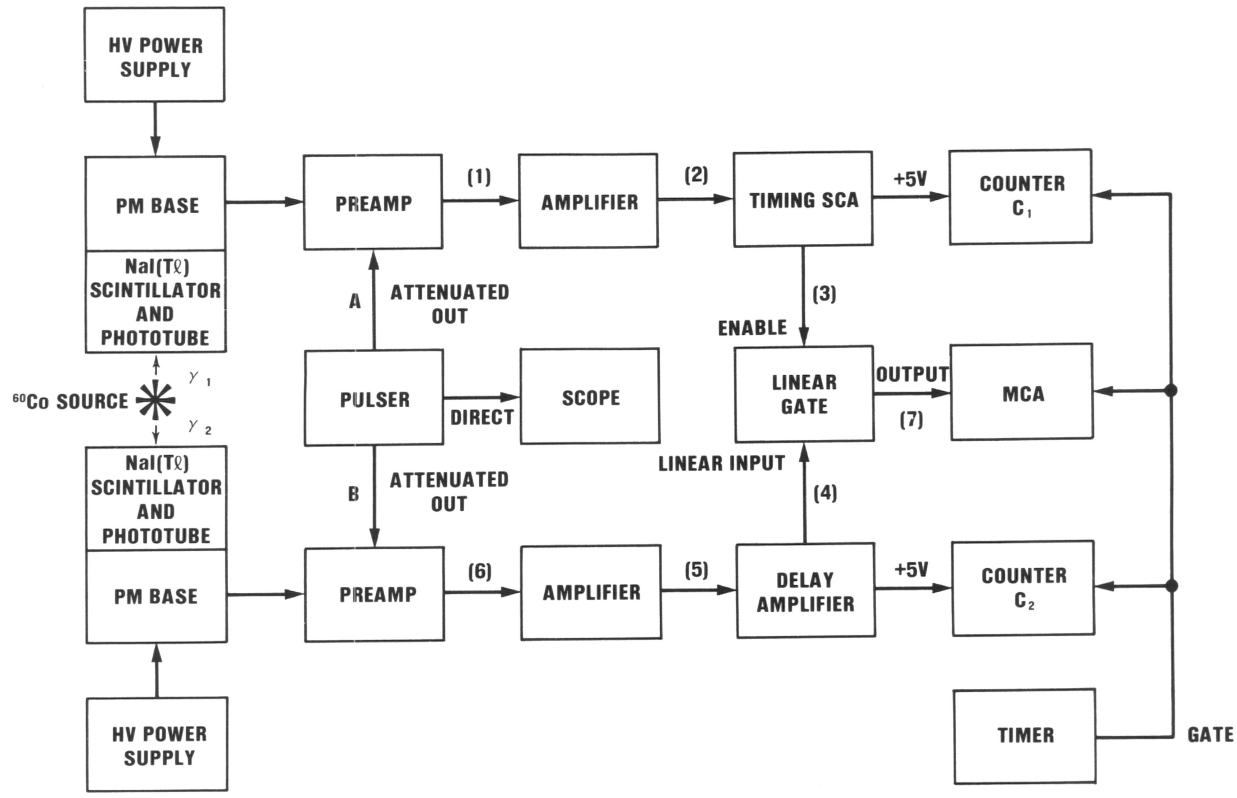

Figure 14.5. Electronics for the verification of the cascade of the delay of ^{60}Co (Linear Gate method).

EXPERIMENT 14.3

Gamma-Gamma Angular Correlation of ^{60}Co with Two NaI(Tℓ) Detectors Using Time-to-Amplitude Converter (TAC) Method

Experimental Procedure

1. Set up the electronics as shown in fig. 14.6. The first part of this procedure is the same as Experiment 14.1, steps **1**, **2**, and **3**. Follow these steps and set SCA #1 to bracket the 1.17 MeV peak and SCA #2 to bracket the 1.33 MeV peak.

2. Set the TAC on the 100 nsec full scale time range. Adjust the delays in the SCAs so that there is a 4V amplitude output from the TAC. This corresponds to coincidences between γ_1 and γ_2 at θ = 180 degrees.

3. We can now make a delay versus pulse height curve for the TAC. Change the delay in SCA #2 by 10 nsec and record ΔC, the channel shift in the MCA. Continue changing the delay and recording the channel position on the peak in the MCA until enough values are obtained to plot a curve of delay versus pulse height. This procedure was carefully outlined in Experiment 11.3. From the delay versus pulse height curve, determine the number of nsec/channel and ΔT, the FWHM of the TAC output.

4. Set the timer for 300 sec; clear all counters and the MCA and run. Calculate Σ-β/t for the TAC. These numbers should agree with those of Experiments 14.1 and 14.2. Record them in Table 14.1 as the entries for θ = 180 degrees.

5. For this angular correlation experiment, it is perhaps best to fix one of the detectors and rotate the other one so that the angles in data Table 14.1 are observed. Rotate the movable detector and count for 300 sec. Record all numbers in the data table and change θ to 100 degrees. Run for a time of 300 sec and record. Repeat for the other angles in Table 14.3.

Exercise In order to calculate the true coincidence rate, we will have to calculate the N_A, the accidental rate. N_A is given by:

$$N_A = 2\,(\delta T)\,N_1\,N_2$$

where δT is the FWHM of the TAC output and N_1, N_2 are the counts recorded in counters #1 and #2 for Table 14.1. The experimental value for W (θ) is then given by:

$$W(\theta)_{Exp} = W_1(\theta) - N_A$$

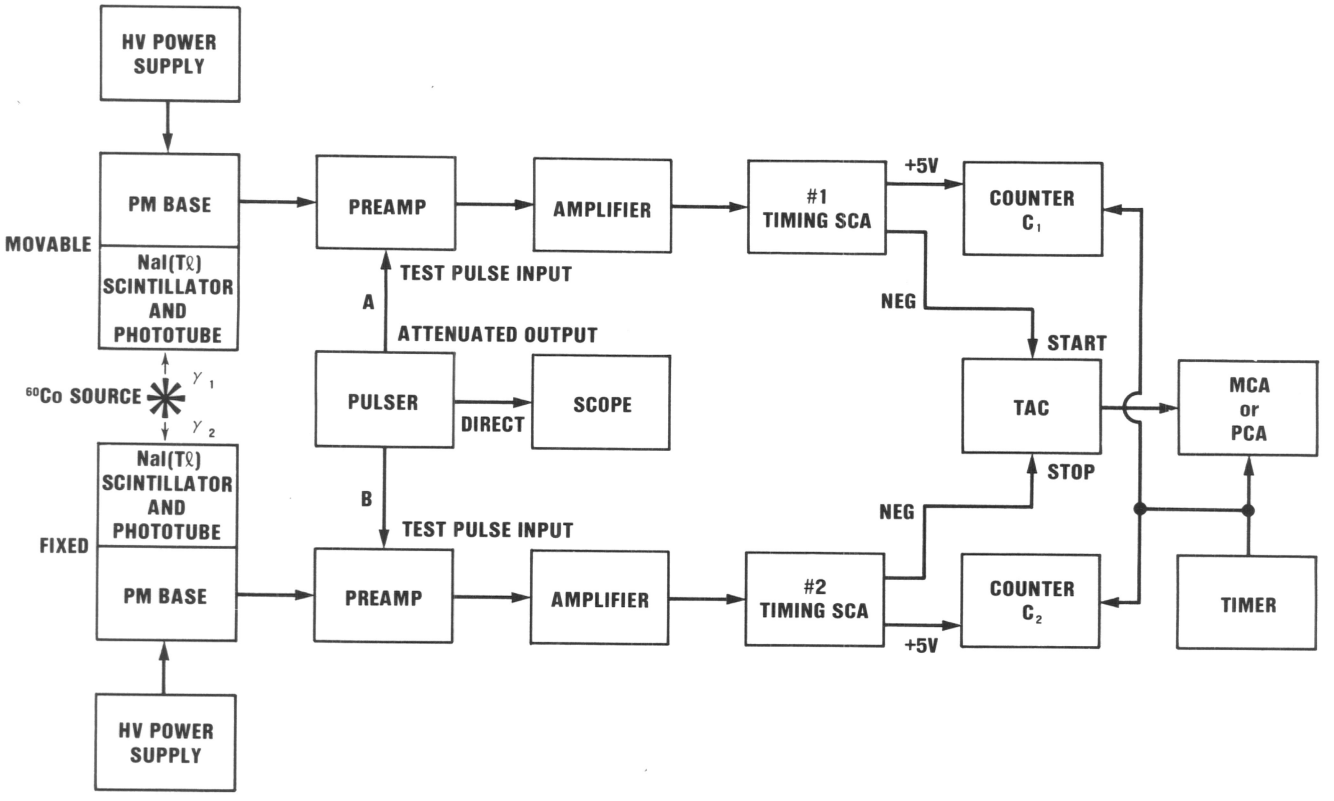

Figure 14.6. Electronics for measuring the angular correlation of ^{60}Co with two NaI(Tℓ) detectors [Time-to-Amplitude Counter (TAC) method].

calculate $W(\theta)_{Exp}$ for all of the angles listed in Table 14.1 and fill in the table.

For comparing the experimental values with theory, it is more convenient to define $G(\theta)_{Exp}$:

$$G(\theta)_{Exp} = \frac{W(\theta)_{Exp}}{W(90°)_{Exp}}$$

calculate the $G(\theta)_{Exp}$ values and enter them in your data table. Notice $G(\theta)_{Th}$ has the same numerical value as $W(\theta)_{Th}$ since $W(90°)_{Th} = 1$.

Plot a curve of $G(\theta)_{Th}$ versus θ and put your experimental points on the curve. Figure 14.7 shows a plot of some typical experimental data for this experiment.

Table 14.1 Data for the Angular Correlation Measurement of ^{60}Co

Run No.	(θ) (deg)	$W(\theta)$ Theory	$W_1(\theta)$ Exp	N_1 cts/s	N_2 cts/s	$W(\theta)$ Exp	$G(\theta)$ Exp
1	90	1.00000					
2	100	1.00381					
3	110	1.01519					
4	120	1.03385					
5	130	1.05876					
6	140	1.08770					
7	150	1.11719					
8	160	1.14287					
9	170	1.16042					
10	180	1.16667					

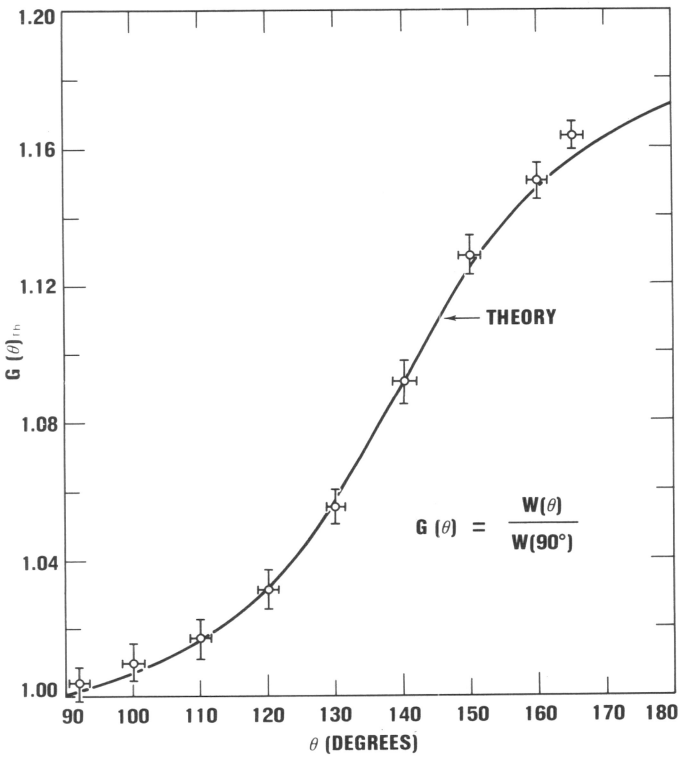

Figure 14.7. Theoretical angular correlation function for ^{60}Co with experimentally measured data points.

EXPERIMENT 14.4

Gamma-Gamma Angular Correlation of ^{60}Co with Two Germanium Detectors [Time-to-Amplitude Converter (TAC) Method]

Experimental Procedure

Note: The angular correlation table that has been designed for this germanium coincidence experiment has provisions for one fixed horizontal germanium detector and a rotating germanium detector which is also of the horizontal dipstick variety.

1. Set up the electronics as shown in fig. 14.8. Use the Linear Gate Method (fig. 14.4) to adjust the gains of both amplifiers so that the 1.33 MeV peak is being stored in the upper quarter of the MCA. Figure 14.9 shows a typical spectrum of ^{60}Co taken with a high resolution germanium detector.

2. The rest of this procedure and the exercise is exactly the same as those used for Experiment 14.3. Plot your results as shown in fig. 14.7. If the windows and timing have been carefully set, the experimental points should show excellent agreement with the theory since there is no better way to do this experiment than with the set up in fig. 14.8.

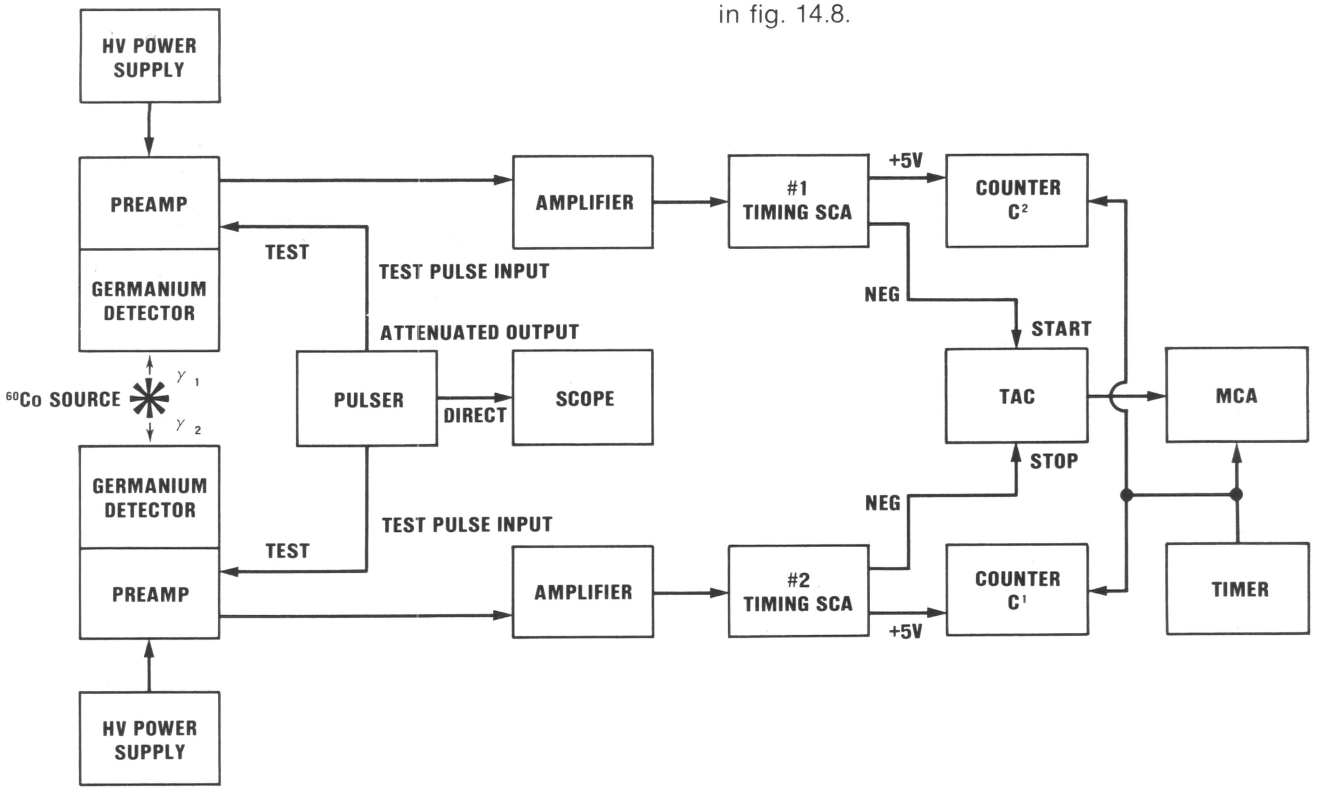

Figure 14.8. Electronics for measuring the angular correlation of ^{60}Co with two germanium detectors [Time-to-Amplitude Converter (TAC) method].

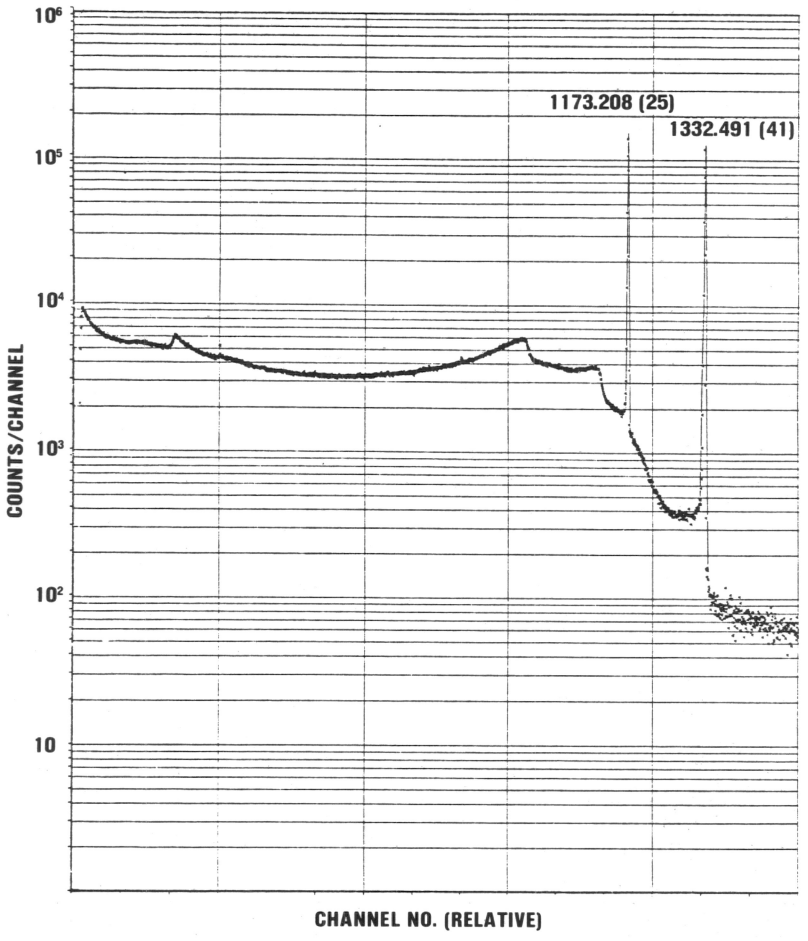

Figure 14.9. Pulse height spectrum of ^{60}Co taken with a high resolution germanium detector.

REFERENCES FOR *EXPERIMENT 14*

1. K. Seigbahn, *Alpha, Beta and Gamma Spectroscopy*, North Holland Publishing Co., Amsterdam. Pages 997-1198 (1965).

2. A. C. Melissinos, *Experiments in Modern Physics*, Academic Press, New York (1966).

3. R. D. Evans, *The Atomic Nucleus*, McGraw-Hill, New York (1955).

4. C. E. Crouthamel, *Applied Gamma-Ray Spectrometry*. Pergammon, New York (1960).

5. M. E. Rose, *Phys. Rev.*, Vol. 91, p 610 (1953).

6. A. L. Stanford, Jr., W. K. River, Jr., *Rev., Sci., Instr.*, Vol. 30, p 719 (1959).

7. L. C. Biedenharn and M. E. Rose, *Reviews of Modern Physics*, Vol. 25, p 729 (1953).

8. F. T. Avignone and G. D. Frey, *Rev. Sci., Instr., Vol. 40, p 1365 (1969).*

9. D. C. Camp and A. L. Van Lehn, Nuc. Instr. and Meth., Vol. 76, p 192 (1969).

10. G. F. Knolls, *Radiation Detection and Measurement*, John Wiley and Sons, New York (1979).

11. J. B. Marion and P. C. Young, *Tables of Nuclear Reaction Graphs*, John Wiley and Sons, New York (1968).

12. C. M. Lederer and V. S. Shirley, Eds., *Table of Isotopes*, 7th Edition, John Wiley and Sons, Inc., New York (1978).

EXPERIMENT 15

Neutron Activation Analysis

Discussion

Neutron Activation Analysis (NAA) was begun in the late 1930's. Since then it has become a very powerful analytic tool that is widely used in such fields as: medicine, geology, chemistry, metallurgy, the petroleum and semiconductor industries, and a host of others. Basically, the process is quite simple. A sample of the element to be studied is placed in a flux of neutrons from a neutron source or a reactor. The sample absorbs neutrons and becomes radioactive. We count the activity and determine what the sample is and, with care, how much of it is there.

In this experiment we are going to study the absorption of two kinds of neutrons, fast and thermal. The first few experiments treat thermal neutron absorption; therefore, this first part of the discussion will be concerned with these reactions. Later we will treat the fast neutron *reactions*.

Thermal Neutron Absorption — Neutrons are uncharged particles; therefore, they are not inhibited by the Coulomb forces of the nucleus. Thermal neutrons have an average energy of 0.035 eV. These neutrons have a high probability for interaction with matter termed (cross-section). If we place a sample (X) in a high flux of these neutrons, it will absorb neutrons in the following reaction:

$$ {}^{A}_{Z}X + n \rightarrow {}^{A+1}_{Z}X + \gamma \qquad (1) $$

$$ {}^{A+1}_{Z}X \rightarrow \beta + {}^{A+1}_{Z+1}Y + \gamma\text{'s} \qquad (2) $$

(In general the γ's that are seen from excited states in ${}^{A+1}_{Z+1}Y$ give all of the information that we need to know about the sample)

where X is the element of atomic weight A and Y is the new element formed in the β decay of ${}^{A+1}_{Z}X$.

The prompt γ is not measured in the experiment as it is absorbed in the activation chamber. An example of this reaction is:

$$ {}^{51}_{23}V + n \rightarrow {}^{52}_{23}V \rightarrow \beta + {}^{52}_{24}Cr \qquad (3) $$

The decay scheme of ^{52}V is shown in fig. 15.1 along with the pulse height spectrum of the gammas that come from the 1.43 MeV level in ^{52}Cr. By counting the 1.43 MeV gammas from ^{52}V, we can determine rather precisely the number of atoms of ^{51}V that were irradiated in the thermal neutron chamber. Figure 15.2 gives us an overview

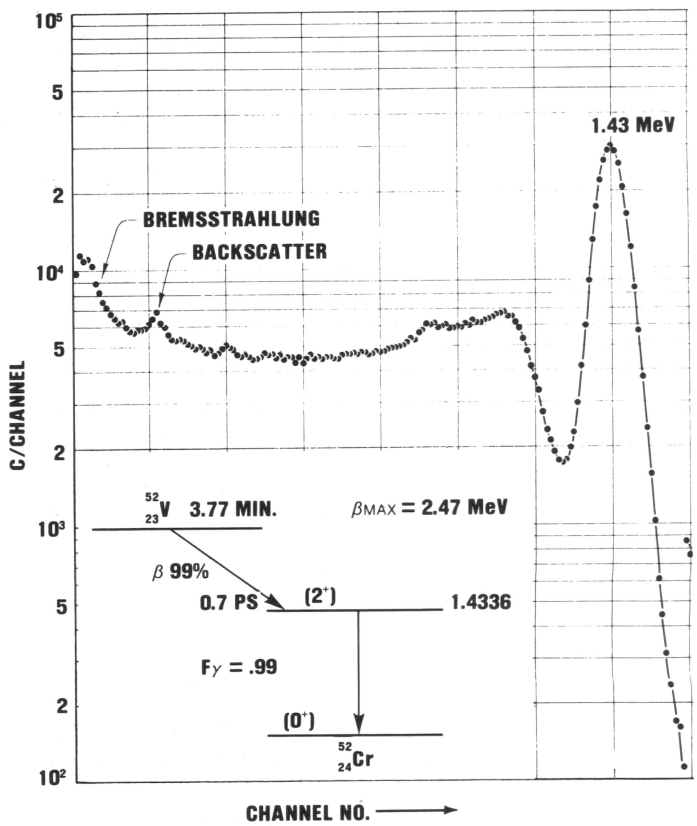

Figure 15.1. Pulse height spectrum of ^{52}V showing β decay to the 1.43 MeV 2^+ level in ^{52}Cr.

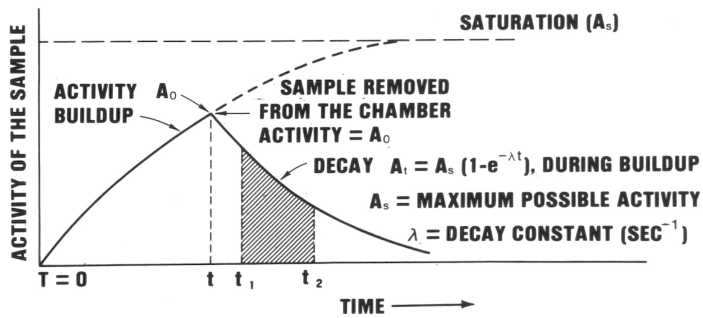

Figure 15.2. Buildup and decay of a sample during and after activation.

of the production of radioactive atoms during buildup and the subsequent decay when the sample is removed from the activation chamber. In this figure, we are assuming that the element to be studied is placed in the thermal neutron flux ϕ (n/cm^2·sec) at t = 0 and left in the chamber for a time (t). During the time (t), the number of

radioactive atoms and hence the activity of the sample will increase according to the equation:

$$A_t = A_s\ (1\text{-}e^{-\lambda t}) \qquad (4)$$

where

A_t = The activity at time (t)
A_s = The activity at saturation
λ = Decay constant

In eq. (4) A_t is the activity of the sample at any time (t) during buildup. (A_s) is the so-called saturation factor. If, for example, we are irradiating a ^{51}V sample ($T_{1/2}$ = 3.77 minutes), the activity would build up to some maximum value (A_s) and, at that point, the atoms of ^{52}V would be decaying as fast as we are making new ones; therefore, the activity can't get any higher than this limit. If we left the sample in for a long time, the activity build up portion of fig. 15.2 would approach A_s as shown in the dashed line in accordance to eq. (4). The activity never reaches A_s because we terminate the irradiation at time (t) in the figure. Recalling that $\lambda = .693/T_{1/2}$, it is easy to plug into eq. (4) and see that if we leave the sample in the activation chamber for two half lives, A_t/A_s is about 75%. Therefore, we have reached 75% of the saturation activity A_s. After the sample has been irradiated for a time (t), we terminate the irradiation and remove the sample from the irradiation chamber, take it to the NaI(Tℓ) or germanium detectors. The sample activity has decreased while we transferred it. This time (t_1) is called the "wait time." The reason for this name is that in some cases we purposely wait for short-lived activities in a complex sample to die out before we count the element of interest to us. In any case, we will see that the following equations will automatically take care of this wait time (t_1) for us. If we place a sample in the chamber and activate for a time (t), the activity (A_0) in fig. 15.2 is given by:

$$A_0 = \frac{\sigma m N_1 \phi a S}{W} \qquad (5)$$

where

σ = the cross section for the reaction in cm^2
m = mass of the whole sample in grams
N_1 = Avogradros number, 6.023×10^{23} atoms/g atomic weight
ϕ = The neutron flux, neutrons/$cm^2 \cdot sec$
a = The fraction of the target element in the sample. (In our example, ^{51}V is 99.76% of all vanadium. Therefore, if we were to irradiate a piece of bulk vanadium for the experiment, a = 0.9976)
S = The saturation factor ($1\text{-}e^{-\lambda t}$) eq. (4).
W = The atomic weight of the element being studied

After the sample is activated, we transfer it with a wait time (t_1) and count it for a time (t_2). The number of counts N_d that we would record in the detector is the shaded area in fig. 15.2. N_d is given by:

$$N_d = N_0\ (e^{-\lambda t_1} - e^{-\lambda t_3}) \qquad (6)$$

where

N_0 = The number of radioactive atoms present at the time the irradiation is terminated.
t_3 = $t_1 + t_2$ t_1 is the wait time; t_2 is the time for which the sample is being counted with the analyzer. Typically, we might wait for 60 sec and count for 300 sec; t_3 = 360 for this example.

Let us again assume that ^{51}V (fig. 15.1) was our original sample; therefore, ^{52}V is the activity that is being counted. If we sum under the photopeak (see experiment #2) with an analyzer time t_2, the actual number of disintegrations counted is given by:

$$N_d = \frac{\Sigma - \beta}{\epsilon_p\ G\ F\gamma} \qquad (7)$$

where

$\Sigma\text{-}\beta$ = Sum under the photopeak
ϵ_p = The intrinsic peak efficiency of the NaI(Tℓ) detector.
$F\gamma$ = The fraction of gammas in the decay scheme that lead to the 1.43 MeV 2^+ level in ^{52}Cr (this number is .99 for our example).
G = $A_d/4\pi R^2$, A_d = area of the detector and R is the distance from the sample to the detector.

Eqs. (6) and (7) are the theoretical and experimental values for N_d. If we equate them together, we have:

$$N_0 = \left(\frac{\Sigma\text{-}\beta}{\epsilon_p\ F\gamma\ G}\right)\left(\frac{1}{e^{-\lambda t_1} - e^{-\lambda t_3}}\right) = \frac{A_0}{\lambda} \qquad (8)$$

since $A_0 = \lambda\ N_0$ by definition.

Now equating (5) and (8) together gives:

$$\lambda \left(\frac{\Sigma\text{-}\beta}{\epsilon_p\ F\gamma\ G}\right)\left(\frac{1}{e^{-\lambda t_1} - e^{-\lambda t_3}}\right) = \frac{\sigma m N_1 \phi a S}{W} \qquad (9)$$

As a student exercise, we usually know everything in eq. (9) except one unknown. For example, we may be asked to determine σ, the neutron cross section. Everything in eq. (9) is known or can be measured except σ in this case. Therefore, we solve eq. (9) for σ and plug in all of the quantities to calculate the cross section. Scientists who activate samples to determine unknown or trace elements in the sample would be solving eq. (9) for m (the mass of the unknown). For example, if a geologist wanted to find out how much vanadium there was in a certain rock, he or she would solve eq. (9) for m.

The Activation Chamber: Howitzer

The activation chamber, or neutron howitzer, that is used for this experiment is a cubical chamber 3 ft on a side. The chamber contains paraffin which is a good neutron thermalization agent. The neutron source which is typically a 2 Ci source of Am-Be is loaded into the chamber from an entry port in the top. Provisions are made to lock the source in the chamber after it has been loaded. In this manner, it is virtually impossible for students to be exposed to the source. After the experiment has been completed, the instructor can use the procedures outlined by the Am-Be source manufacturer to return the source to its storage container. If proper health physics procedures are followed, there can be no question that these neutron activation experiments are safe. A large number of universities have been doing these experiments for as long as 30 years without any problems with these sources. Certainly, once a university is set up to do these experiments, the students will agree that they are among the best in the undergraduate curriculum.

The samples to be irradiated are placed in small inert plastic containers called "Rabbits." These "Rabbits" are then placed in loading tubes that are pushed to the center of the howitzer through four loading ports on the side of the chamber. The neutrons from the source are produced by the following reaction:

$$^{9}Be + {}^{4}He \rightarrow {}^{1}n + {}^{12}C + Q \ (Q \sim 5 \text{ MeV}) \qquad (10)$$

In the Am-Be source, alphas from the ^{241}Am (see Experiment 3) interact with ^{9}Be in the source to produce the neutrons. Since the alphas from ^{241}Am are 5.476 MeV and the Q value for the reaction is of the order of 5 MeV, we would expect the neutron spectrum to extend out to 10 MeV which is indeed the case. Figure 15.3 shows the neutron spectrum from a Pu-Be neutron source which looks quite similar to what is measured for Am-Be.

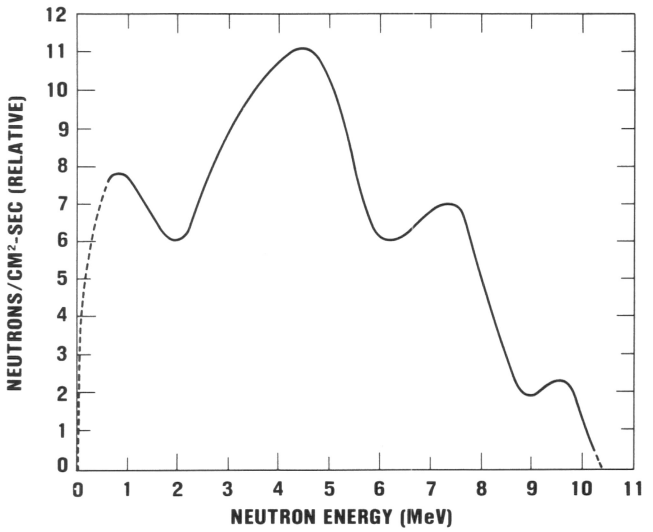

Figure 15.3. Flux of fast neutrons from a Pu-Be neutron source.

These fast neutrons are thermalized primarily by scattering from the hydrogen nuclei in the paraffin. When a neutron scatters from hydrogen, on the average, it loses half of its energy. Therefore, after 25 scatterings, the neutron energy is down to $1/2^{25} = 1/3.4 \times 10^{7}$ of its initial value, or, for our case, thermal energies. The thermal flux ϕ in eq. (9) is the number of these thermal neutrons that bombard each cm^2 of the target each second.

EXPERIMENT 15.1

Measurement of the Saturation Factor for Thermal Neutron Activation Analysis

Discussion

Figure 15.2 shows the buildup of radioactive atoms in a sample during irradiation and its decay when the sample is removed from the activation chamber. In this experiment, we are going to explore that portion of the curve that is associated with the buildup of the activity. The sample kit that is used for this experiment contains 12 each 2 g samples of vanadium. We will irradiate these samples for increasing amounts of time and watch the activity build up. Each new sample will be irradiated for its specified time and then immediately transferred to the counting station and counted. In other words, the wait time is zero in eq. (6). This allows us to experimentally measure eq. (4).

$$A_t = A_s \ (1-e^{-\lambda t})$$

Experimental Procedure

1. Set up the electronics as shown in fig. 15.4. A 256 channel MCA is adequate. With standard sources of ^{137}Cs, ^{65}Zn, and ^{60}Co, calibrate the system so that 2 MeV corresponds to channel 200. This calibration procedure was outlined in Experiment 2.

2. Take the first 2 g vanadium sample and activate it in one of the ports of the irradiation chamber for 2 minutes. Transfer it as fast as you can to the counting station and analyze it for 100 sec counting time. Record the (Σ-β/t) for the 1.4336 MeV gamma (see fig. 15.1) in Table 15.1.

3. Repeat this measurement on a fresh 2 g vanadium samples for the other activation times in Table 15.1 and record the corresponding (Σ-β/t) values for each activation. It should be noted that there are four activation

Table 15.1 Experimental Data for Determining the Saturation Factor for the $^{51}V(n,\gamma)^{52}V$ Reaction

(1) Run No.	(2) Activation Time (min)	(3) $\frac{A_t}{A_s}$ (theory)	(4) $\left(\frac{\Sigma - \beta}{t}\right)$	(5) $K_1 \left(\frac{\Sigma - \beta}{t}\right)$	% Diff $\frac{(3) - (5)}{(3)} \times 100\%$
1	2				
2	4				
3	6				
4	8				
5	7				
6	12				
7	14				
8	16				
9	18				
10	20				

ports in the activation chamber. All four ports give an identical flux of neutrons. Therefore, some of the longer activation times in Table 15.1 can be run simultaneously with shorter runs in a different port.

Exercise From eq. (4), calculate A_t/A_s for each of the times listed in Table 15.1 and fill in column (3). We will now determine K_1, the normalization constant. We will do this for the 4 minute run by equating column (3) to column (5).

$$\frac{A_t}{A_s} \text{ (Theory)} = K_1 \frac{\Sigma-\beta}{t} = (1-e^{-\lambda t}) \qquad (11)$$

Use t = 4 min (240 sec) and calculate the constant K_1. Now multiply all of the entries in column (4) by K_1 and fill in column (5). On a piece of linear graph paper, plot column (3) $(1-e^{-\lambda t})$ as a function of the irradiation times. The curve should look like the activity build up part of fig. 15.2 including the dashed line. Now put the normalized experimental points on the curve with error bars of ±8%. Your results should be similar to fig. 15.5.

EXPERIMENT 15.2

Measurement of the Thermal Neutron Flux (ϕ) in the Activation Chamber

Discussion

The $^{27}Al(n, \gamma)^{28}Al$ reaction is ideally suited for the measurement of ϕ, the neutron flux ($n/cm^2 \cdot s$), in the activation chamber. The decay of the ^{28}Al activity that results from the thermal neutron absorption of ^{27}Al is shown in fig. 15.6. The decay of the ^{28}Al (3^+) activity is by a 2.86

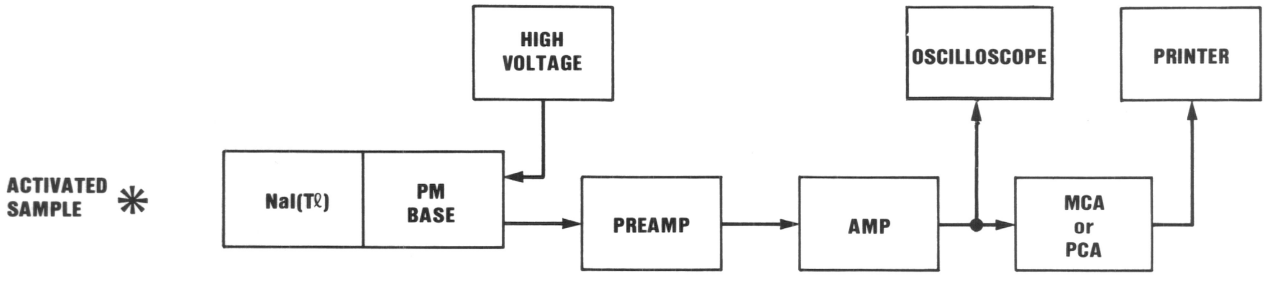

Figure 15.4. Electronics for neutron activation analysis with a NaI(Tℓ) detector.

MeV β to the (2^+) 1.78 MeV state of ^{28}Si. Since all of the decays are to this 1.78 MeV level, Fγ (eqs. 7 and 8) = 1. The thermal cross section for $^{27}Al(n,\gamma)^{28}Al$ is 0.21 x $10^{-24}cm^2$.

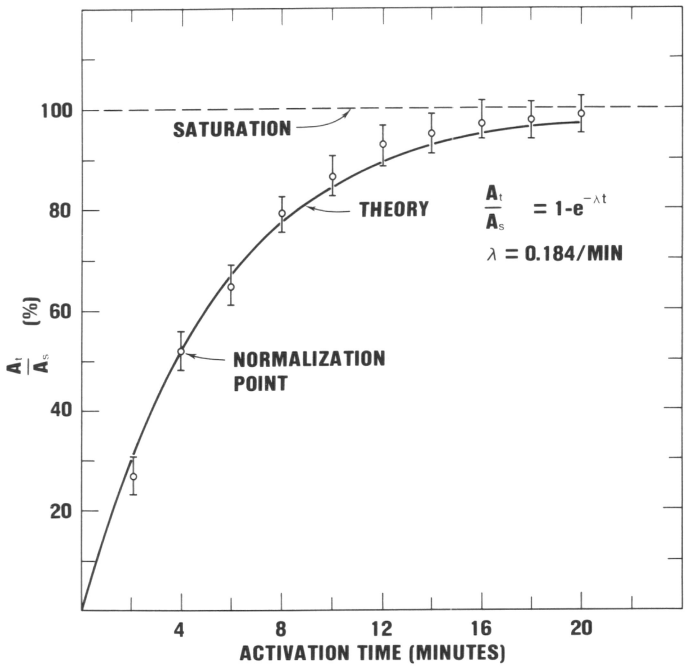

Figure 15.5. Theoretical curve for the saturation factor $^{51}V(n,\gamma)^{52}V$, $T_{1/2}$ = 3.77 min. Shown also on the curve, are the experimental points that have been normalized to the theory at t = 4 min.

Experimental Procedure

1. Set up the electronics as shown in fig. 15.4. Calibrate the system so that 2 MeV corresponds to channel 200.

2. Obtain a 3 g sample of aluminum from the instructor and irradiate it in the chamber for a time of 6 min. Transfer the sample to the activation chamber. After a wait time of one minute [t_1 = 1 minute, eq. (8)], count the sample for an analyzer live time of 3 minutes [$t_3 = t_1 + 3 = 4$ min in eq. (8)].

3. Use the integrate function of the analyzer to determine the sum under the 1.78 MeV peak. This value is (Σ-β) in eqs. (8) and (9).

4. Obtain the second 3 g sample from the instructor and repeat steps **1-3** above for this new sample.

Exercise The object of this exercise is to solve eq. (9) for ϕ. The following values of the variables in eq. (9) have thus far been determined:

m = 3 g
ϵ_p = See fig. 2.14 in Experiment 2 for the size NaI(Tℓ) crystal that is being used.
Fγ = 1
G = $A_d/4\pi R^2$, A_d in cm^2, R in cm
S = $(1\text{-}e^{-\lambda t})$ t = 6 min, λ = 0.30 min^{-1}
t_1 = 1 min.
t_3 = 4 min.

Note: Since λ is in reciprocal minutes, the flux ϕ will have units of $n/cm^2 \cdot min$ in eq. (9).

Repeat this calculation for your second sample, everything should be the same in eq. (9) except (Σ-β).

Determine ϕ average for the two measurements and calculate average in $n/cm^2 \cdot sec$ (these units will be more convenient for the next experiment). Record this average value of ϕ for further reference.

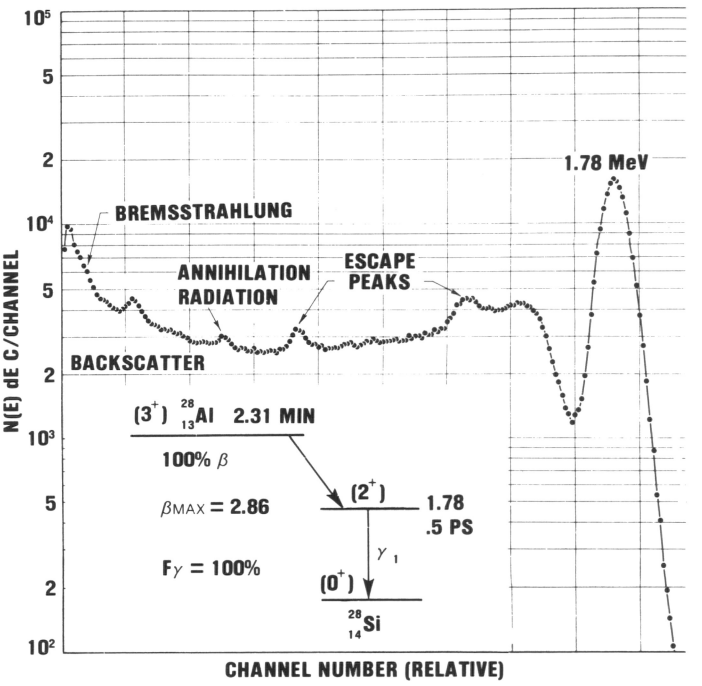

Figure 15.6. NaI(Tℓ) pulse height spectrum of the 2.31 minute ^{28}Al activity.

EXPERIMENT 15.3

Determination of the Thermal Neutron Cross Section for the $^{74}Ge(n,\gamma)^{75}Ge$ [NaI(Tℓ) Spectroscopy]

Discussion

In this experiment, we are going to take the flux that was calculated in the last experiment and calculate $\sigma(n,\gamma)$, the thermal neutron cross section for the reaction. We will start by telling you the answer, σ = 0.6 x $10^{-24}cm^2$. Let's see how close we can come to this answer.

Experimental Procedure

1. Set up the electronics as shown in fig. 15.4. Calibrate the system so that the 266 keV peak from ^{75}Ge (see fig. 15.7) falls in channel 266.

2. Obtain a 3 g sample of germanium metal from the instructor. **Note:** 36.7% of all germanium is ^{74}Ge therefore (a) in eq. (5) is 0.367. Activate the sample for 200 min. The student should start this activation before class actually begins.

3. Transfer the sample to the counting station and wait for 1 min (t_1 = 1 min) before counting. Count for a clock time of 30 minutes.

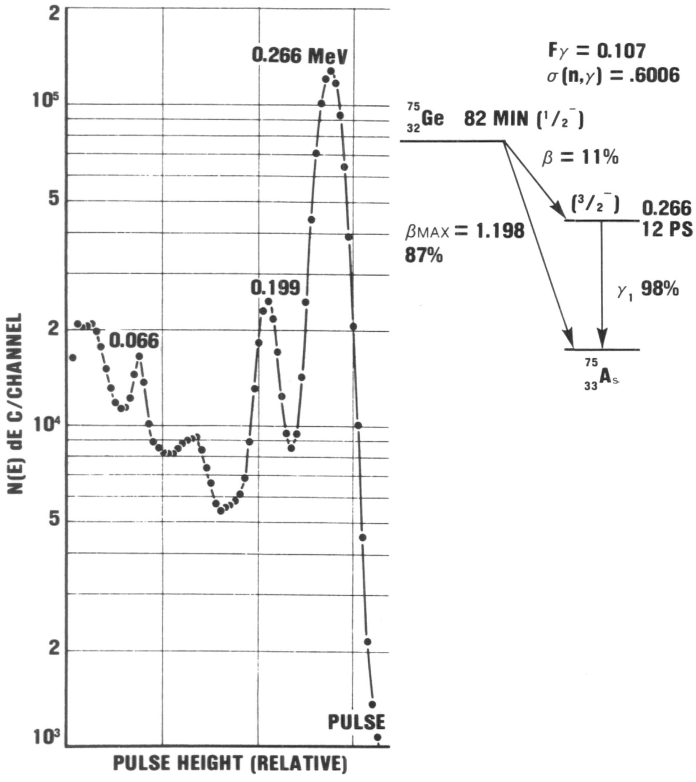

Figure 15.7. NaI(Tℓ) pulse height spectrum of the 82 minute ^{75}Ge activity.

4. Determine (Σ-β) for the 0.266 MeV peak. Record this value.

Exercise Solve eq. (9) for σ and fill in the values of the parameters as we did for the last experiment. ϵ_p can be obtained from fig. 2.14. How does your measured value of σ compare to the answer (0.6×10^{-24}cm^2)? Table 15.2 contains a list of other suggested samples that will work well for this experiment. The instructor may wish to have you verify σ for another one of the samples on the table. Remember, when possible, it is always a good idea to activate a sample for two half lives. This will give a saturation factor of 75% maximum. The last column on Table 15.2 (Relative Sensitivity) indicates the ability to detect small quantities of the element. A small number in this column means thermal neutron activation analysis is a sensitive technique for that element.

EXPERIMENT 15.4

Determination of the Thermal Neutron Cross Section for $^{51}V(n,\gamma)^{52}V$ by High Resolution Gamma Spectroscopy (Germanium Detector)

Experimental Procedure

1. Set up the electronics as shown in fig. 15.4 except a high resolution germanium detector is used instead of the NaI(Tℓ) detector. Calibrate the system so that the 1434 keV gamma from ^{52}V will fall in approximately channel 2000. Figure 15.8 shows a typical germanium pulse height spectrum for ^{52}V.

2. Obtain one of the 2 g vanadium samples from the instructor and irradiate it for a time period of 8 minutes. Transfer it to your high resolution germanium counting station. Use a wait time of 1 minute, and count for 5 minutes. From the MCA obtain Σ-β for the 1434.047 keV peak.

3. Obtain a second 2 g vanadium sample from the instructor and repeat steps (**1**) and (**2**) for this new sample. Average the two values of Σ-β and record in your data table.

Exercise As in the previous experiments, we will use eq. (9) to calculate σ for the $^{51}V(n,\gamma)^{52}V$ reaction. The value of ϕ (n/cm^2 · sec) will either be given by the instructor or the results in Experiment 15.2 can be used.

The value of ϵ_p was probably determined for your detector in Experiment 6. If you don't have a value of ϵ_p, the procedures outlined in Experiment number 6 can be used to measure your intrinsic peak efficiency. The value of σ listed in table 15.2 for this reaction is 5.1×10^{-24}cm^2. How well did you do?

Table 15.2 Recommended Targets for Thermal Neutron Activation Analysis

Element	% Abundance	σ	Produce Nuclide	$T_{1/2}$	Gamma Energy (keV)	Relative Sensitivity
Na-23	100	530mb	Na-24	15h	2754	1.5
Al-27	100	215mb	A1-28	2.32m	1779	1.0
Ti-50	5.34	140mb	Ti-51	5.79m	320	18.0
V-51	99.76	5.1b	V-52	3.75m	1434	0.07
Mn-55	100	13b	Mn-56	2.58h	847	0.015
Co-59	100	36b	Co-60M	10.5m	59	0.23
Ga-71	39.6	150mb	Ga-72	14.1h	834	0.32
As-75	100	4.30b	As-76	26.4h	559	0.32
In-115	95.77	210b	In-116M	53.7m	1293	0.006
I-127	100	6.7b	I-128	25m	443	0.30
Cs-133	100	2.6b	Cs-134M	2.9h	127	0.40
Sm-152	26.7	210b	Sm-153	46.8h	103	0.07
Eu-151	47.8	3.78b	Eu-152M	9.3h	963	0.08
Dy-164	28.2	2100b	Dy-165	2.32h	95	0.01
Ho-165	100	3.45b	Ho-166	26.8h	81	0.20
Er-170	14.9	6.0b	Er-171	7.52h	308	0.36
Lu-175	97.4	21b	Lu-176M	3.7h	88	0.20
Re-187	62.5	2.0b	Re-188	16.7h	155	0.07
Au-197	100	98b	Au-198	64.7h	412	0.027

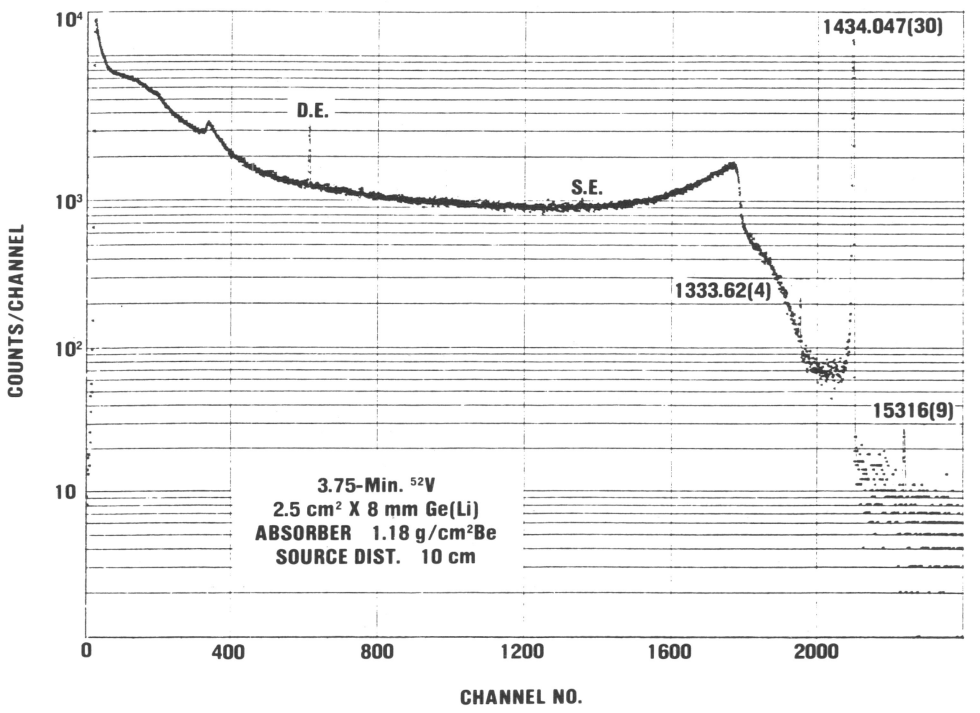

Figure 15.8. High resolution germanium gamma spectrum of ^{52}V.

EXPERIMENT 15.5

Fast Neutron Activation Analysis

Discussion

Figure 15.3 shows a typical spectrum of neutrons from a Pu-Be neutron source. The spectrum that would be seen from the Am-Be source used in this experiment is similar to fig. 15.3. The most common fast neutron experiments that are studied are as follows:

$$A(n,p)B^* \quad (12)$$

$$A(n,2n)B \quad (13)$$

$$A(n,\alpha)B \quad (14)$$

Of these three, only the (n,p) reactions are practical for our study since most of the (n,α) and (n,2n) reactions have neutron threshold values that are above E_n = 10 MeV which is higher than our source will produce. Table 15.3 shows a listing of the (n,p) reactions that can easily be done with our source. We have chosen the $^{52}Cr(n,p)^{52}V$ reaction to study, since we have already measured the ^{52}V isotope by the $^{51}V(n,\gamma)^{52}V$ reaction and many of the experimental parameters will be the same.

Caution: This experiment requires the special *Fast Neutron Activation Chamber* which has been designed for these (n,p) reactions. This chamber is quite different from the Thermal Neutron Activation Chamber that was used in the previous experiments. In fact, this chamber is designed to minimize thermalization of neutrons. The source should be loaded into the chamber by the instructor and locked in place. The chamber is shielded and can be safely used by the students once the source is loaded.

Experimental Procedure

1. Set up the electronics as shown in fig. 15.4. If available, you may wish to use a high resolution germanium detector instead of the NaI(Tℓ) shown in the figure.

2. Obtain a 3 g chromium sample and irradiate it in the *Fast Neutron Activation Chamber* for a time period of 15 minutes.

3. Transfer the sample to the counting station and use a wait time of 1 minute before counting. Count for 5 minutes. Determine Σ-β for the 1.43 MeV gamma [see fig.

Table 15.3 Common Fast Neutron Reactions that can be Studied with an Isotopic Neutron Source

Element	Reaction	Average Cross Section (σ), in mb	Half-Life	Radiation Emitted
Magnesium	$^{24}Mg(n,p)^{24}Na$	1.1	15.0 hr	β^-, γ
Aluminum	$^{27}Al(n,\alpha)^{24}Na$	0.57	15.0 hr	β^-, γ
Titanium	$^{46}Ti(n,p)^{46}Sc$	9.0	85 day	β^-, γ
	$^{47}Ti(n,p)^{47}Sc$	15	3.43 day	β^-, γ
	$^{48}Ti(n,p)^{48}Sc$	0.25	1.83 day	β^-, γ
Manganese	$^{55}Mn(n,2n)^{54}Mn$	0.18	314 day	Ec, γ
Iron	$^{54}Fe(n,p)^{54}Mn$	65	314 day	Ec, γ
Nickel	$^{58}Ni(n,p)^{58}Co$	90	72.0 day	Ec, γ
Copper	$^{63}Cu(n,\alpha)^{60}Co$	0.42	5.27 yr	β^-, γ
Zinc	$^{64}Zn(n,p)^{64}Cu$	25	12.82 hr	β^-, β^+, γ
Molybdenum	$^{92}Mo(n,p)^{92}Nb$	6.0	10.1 day	Ec, γ
Sulfur	$^{32}S(n,p)^{32}P$	65	14.3 day	β^-
Phosphorus	$^{31}P(n,p)^{31}S$	100	2.62 sec	β^+, γ
Chromium	$^{52}Cr(n,p)^{52}V$	80	3.76 min	β^-, γ
Sodium	$^{23}Na(n,p)^{23}Ne$	34	40.2 sec	β^-, γ
Silicon	$^{28}Si(n,p)^{28}Al$	250	2.3 min	β^-, γ
Vanadium	$^{51}V(n,p)^{51}Ti$	27	5.8 min	β^-, γ

15.1 NaI(Tℓ) or 15.8 if a high resolution germanium gamma detector is used].

4. Obtain the second 3 g sample of chromium from the instructor and repeat steps **1-3** for the second sample. Average the values of Σ-β and record them in your data table.

Exercise Use the eq. (9) to calculate ϕ, the number of fast n/cm^2·s. The % abundance of ^{52}Cr is 83.76%. The ^{52}Cr(n,p)^{52}V cross section is 80 millibarns. Everything else in eq. (9) is known or can be measured. How does your number for ϕ (fast) compare to ϕ (thermal) used in the previous experiments for the same source?

REFERENCES FOR *EXPERIMENT 15*

1. The Handbook of Chemistry and Physics "A Ready Reference Book of Chemical and Physical Data," Edited by Robert C. Weast. Available from the CRC Press 18901 Cranwood Parkway, Cleveland, Ohio 44128. (This book contains one of the most complete listings of Thermal Neutron Cross Sections, and Gamma Intensity Ratios for Isotopes. Table 15.2 was taken from this reference.)

2. R. C. Koch, *Activation Analysis Handbook*, Academic Press, New York (1960).

3. K. S. Vorres, "Neutron Activation Experiments in Radiochemistry," *J. Chem. Ed.* **37**, 391 (1960).

4. D. Taylor, *Neutron Irradiation and Activation Analysis*, Van Nostrand, Princeton, New Jersey (1964).

5. G. I. Gleason, *Isotopic Neutron Source Experiments*, **ORAU-102** (1967). Available from Oak Ridge Associated Universities, P.O.Box 117, Oak Ridge, Tennessee 37831.

6. S. S. Brar and D. M. Nelson, *Modern Trends in Neutron Activation Analysis*, National Bureau of Standards, Special Publication 312, (1969). Available from the National Technical Information Service, Springfield, Virginia.

7. D. Gray, *et al.*, "Determination of Trace Element Labels in Atmospheric Pollutants by Instrumental Neutron Activation Analysis," *IEEE Trans. Nucl. Sci.* **NS-19**(1), 194 (1972).

8. J. M. A. Lenihan and S. J. Thomson, Eds., *Activation Analysis—Principles and Applications*, Academic Press (1965).

9. C. M. Lederer and V. S. Shirley, Eds., *Table of Isotopes*, 7th Edition, John Wiley and Sons, Inc., New York (1978).

10. W. S. Lyon, *A Guide to Activation Analysis*, D. Van Nostrand Co., Inc., New York (1964).

EXPERIMENT 16

Time-of-Flight Measurements in Nuclear Spectroscopy

Scope

In this experiment, we will study the modern electronic techniques that can be used to measure the flight times of alpha particles and gammas for a given flight path. In the first few sections of the experiment, alpha particle time-of-flight spectroscopy will be studied. Alpha particles from a ^{231}Pa radioactive source will be allowed to pass through a thin ΔE detector, travel over a fixed path length, and finally stopped in an E detector. In this experiment, the pulses in the ΔE and E detectors will be summed to show that the sum of the energy deposited in the two detectors yields the original alpha spectrum. In the next experiment, the ΔE detector will be used to start a Time-to-Amplitude Converter and the E detector will provide a stop pulse. From the measured flight time and flight path, the velocity of the alpha particle will be determined. Finally, the energy loss of alphas in thin foils will be measured by this time-of-flight technique.

For the gamma time-of-flight experiment, we will use a 10 μCi ^{22}Na source to provide annihilation radiation for the start and stop signals for the TAC. As you should recall from the gamma angular correlation experiment, these two annihilation quanta leave the source with an angular separation of 180 degrees. Pulses from two fast-plastic scintillators will be processed and used to start and stop the Time-to-Amplitude Converter. The flight path between the two detectors will be changed and the corresponding flight time difference recorded. From these data, a very precise value of the velocity of the gamma photons (light) will be measured.

EXPERIMENT 16.1

Alpha Particle Time-of-Flight Spectroscopy: Setting up the System and Measuring the Sum of E Plus ΔE for ^{231}Pa Alphas

Discussion

Figure 16.1 shows a schematic of the apparatus that will be used for this alpha particle time-of-flight experiment. The vacuum chamber is designed in such a manner that the distance between the two detectors can be changed externally, without opening the vacuum system. Figure 16.2 shows the electronic arrangement that will be used for the experiment. Figure 16.3 shows a silicon surface barrier detector pulse height sum spectrum of the alphas from ^{231}Pa. The source has alphas that range in energy from 4.72 MeV to 7.36 MeV. It is an ideal source for this experiment since it has this 7.36 MeV alpha in its decay scheme.

The 7.36 MeV alpha particles from the source pass through the ΔE detector because it is only 27 μ meters thick. As they pass through, they will produce a pulse in the ΔE detector which is proportional to the energy lost in the detector. If δE is the energy lost in the ΔE detector, the energy of the alphas that emerge from the ΔE detector is given by:

$$E_1 = E_0 - \delta E \qquad (1)$$

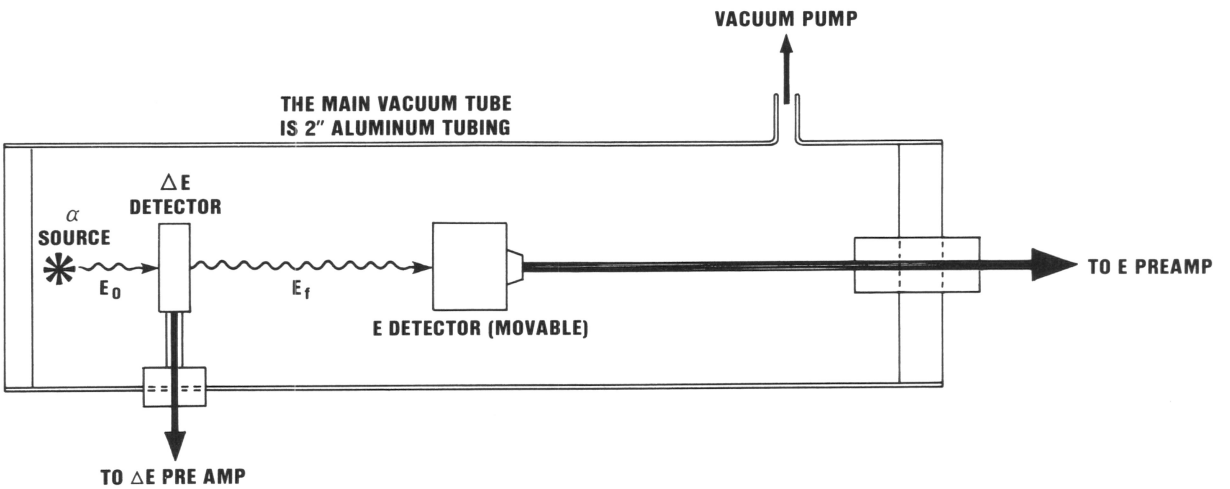

Figure 16.1. Alpha particle time-of-flight apparatus.

where E_0 is the initial energy of the alpha group being considered and δE is the energy loss of that particular alpha particle. In this first experiment (see fig. 16.2), we are going to take the linear pulses out of the ΔE and E amplifiers and add them together in a *sum amplifier* to show that the original spectrum can be reconstructed in parts (see fig. 16.3).

Experimental Procedure

1. Place the ^{231}Pa source in the alpha particle time-of-flight chamber. Adjust the ΔE and E detectors so that the flight path is 1 cm between the detectors. Evacuate the chamber and apply the recommended bias voltage to both detectors.

2. Set up the electronics as shown in fig. 16.2. **Note:** We are going to use the unipolar (linear) outputs of both the E and ΔE timing amplifiers for this part of the experiment. These unipolar outputs are fed into the *Dual Sum and Invert Amplifier*. Set this sum amplifier in the *Summing, Non Inverting* mode. The output of this amplifier is then fed into an MCA. In this mode of operation, the sum amplifier sums the ΔE and E pulses and feeds this sum into the MCA. If the gains of the ΔE and E amplifier are the same, the output of the sum amplifier, in theory, should give the original alpha spectrum.

3. We must first adjust the gain of the E amplifier so that the alpha pulses from the source will produce pulses in the MCA with the proper pulse height. Disconnect the ΔE input to the sum amplifier. Under these conditions the sum amplifier will simply pass the pulses from the E amplifier straight through to the MCA since there are no ΔE pulses to sum with them. Adjust the gain of the E amplifier so that the maximum pulse height seen is of the order of 3 volts. These pulses correspond to 7.36 MeV alphas from the ^{231}Pa source (see fig. 16.4) that have lost some energy in the ΔE detector. The gain of the E amplifier is now set properly for the experiment.

4. It is not possible to set the gain of the ΔE amplifier by using the alpha source since the alphas only lose a small amount of energy in the ΔE detector; therefore, the output pulses can't be normalized to a known reference. We can, however, set this ΔE amplifier gain equal to the E amplifier gain by using the pulse generator. Turn on the pulse generator and adjust the normalization switches and pulse height of the pulser until the output pulses from the E amplifier are 2 volts in amplitude. Record the position of the pulser peak in the MCA. Define this centroid to be C_1. We can now set the gain of the ΔE amplifier. Reconnect the ΔE input to the sum amplifier and disconnect the E input. Adjust the gain of the ΔE ampli-

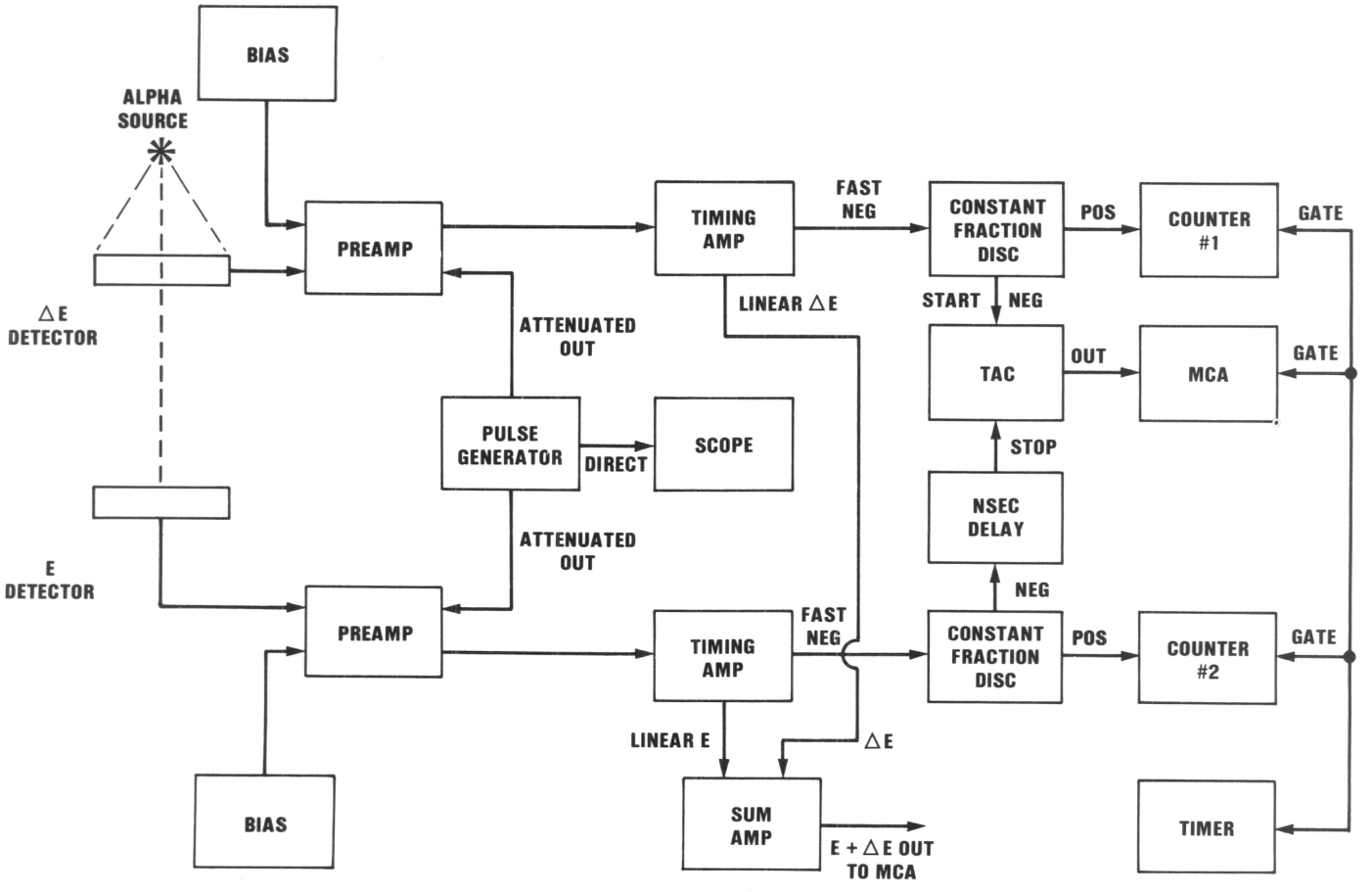

Figure 16.2. Electronics for the alpha particle time-of-flight measurement.

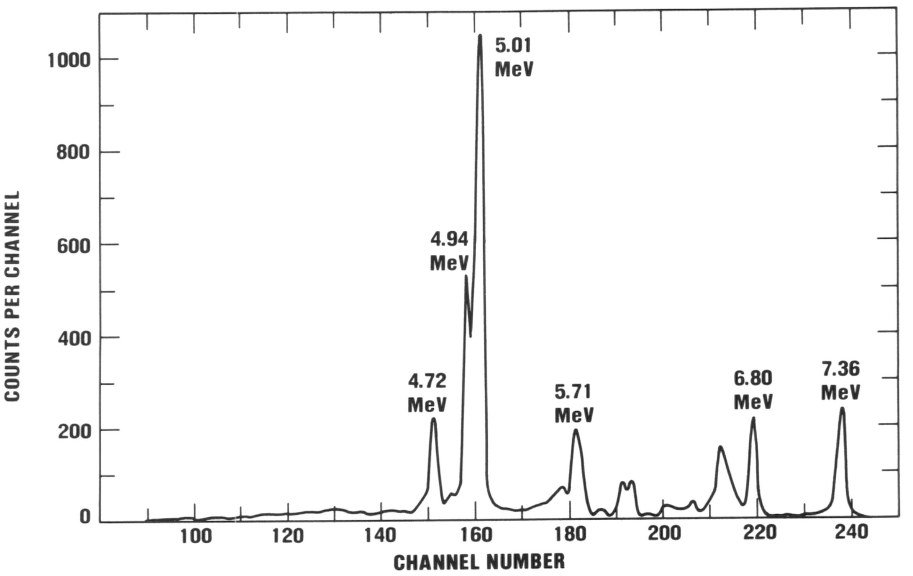

Figure 16.3. ΔE + E pulse height spectrum for ^{231}Pa.

fier so that the output pulses are 2 volts in amplitude and are being stored again in channel C_1. The amplifier gains are now set to the same value. Reconnect the E input to the sum amplifier.

5. Turn off the pulse generator and accumulate a sum amplifier spectrum from the alpha source for a time long enough to obtain reasonable statistics in the peaks of interest.

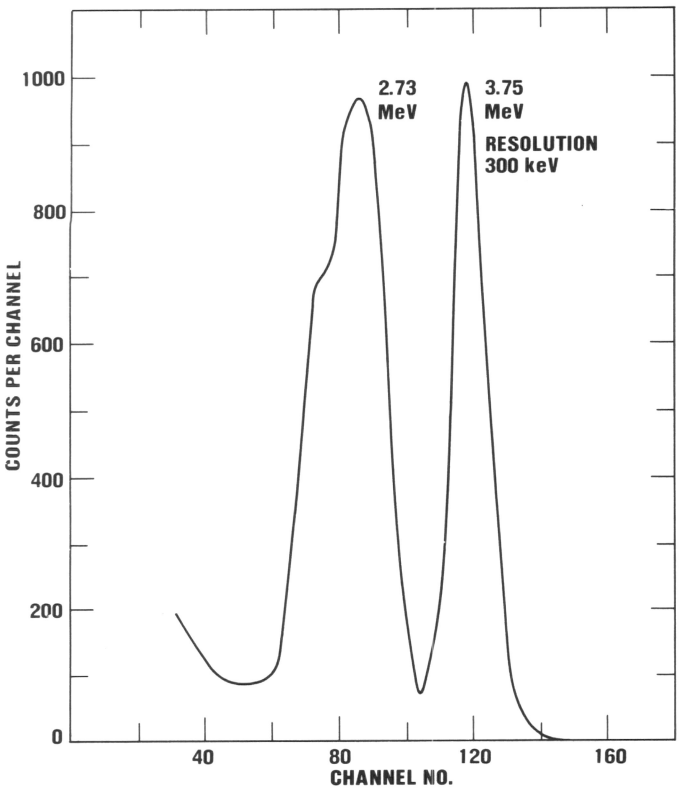

Figure 16.4. This pulse height spectrum represents the linear output of the E amplifier. The peak on the right corresponds to 7.36 MeV alphas that have lost 3.61 MeV in the ΔE detector.

6. Disconnect the ΔE input and accumulate an E spectrum similar to fig. 16.4. Record the position of the high energy peak.

Exercise Figure 16.3 shows a E + ΔE sum spectrum from the ^{231}Pa source which is similar to the one that you should measure. Use the known peaks in the spectrum to make a calibration curve. From your calibration curve, calculate the keV/ch and determine the resolution for all of the single peaks in the ^{231}Pa spectrum. Determine the energy of the high energy group in the E spectrum alone (your fig. 16.4). Use Table 16.1 to calculate the thickness of the ΔE detector.

EXPERIMENT 16.2

Time-of-Flight Measurement of the 7.36 MeV Alpha Group in ^{231}Pa

Experimental Procedure

1. Place the ^{231}Pa source in the time-of-flight chamber. Adjust the distance between the detectors for 1.65 cm. Evacuate the chamber and apply the proper bias voltage to both detectors. Set up the electronics as shown in fig. 16.2. **Note:** In this experiment, we are going to use the negative logic output pulses from the Fast/Slow Timing Amplifiers. The ΔE (start) side goes into a constant fraction discriminator and then directly into the TAC. The E negative logic output is fed through a constant fraction discriminator, then a nanosecond (nsec) delay box and finally into the stop side of the TAC.

2. Set the nsec delay box on 10 nsec delay. Set the TAC on the 50 nsec full scale range. Adjust the gain of each

Table 16.1. Stopping Power and Range of Alpha Particles in Silicon (Taken from Reference 1)

Energy MeV	Range g/cm²	Stopping Power MeV cm²/g
4.00	4.26 E (—03)	6.98 E (02)
4.20	4.55 E (—03)	6.78 E (02)
4.40	4.85 E (—03)	6.60 E (02)
4.60	5.15 E (—03)	6.42 E (02)
4.80	5.46 E (—03)	6.25 E (02)
5.00	5.78 E (—03)	6.10 E (02)
5.50	6.62 E (—03)	5.75 E (02)
6.00	7.51 E (—03)	5.43 E (02)
6.50	8.45 E (—03)	5.16 E (02)
7.00	9.44 E (—03)	4.91 E (02)
7.50	1.05 E (—02)	4.69 E (02)
8.00	1.15 E (—02)	4.49 E (02)

In the above table, 4.26 E (—03) means $4.26 \times 10^{+3}$, etc.

timing amplifier and the lower level of the CF discriminator so that the output negative logic pulses from the constant fraction discriminators represent only the 7.36 MeV alpha group.

3. Accumulate a spectrum in the MCA (512 channels full scale). This peak corresponds to the flight time of the alpha particle plus the 10 nsec delay in the nsec delay box. Record the position of the peak. Change the delay by 8 nsec and observe the new channel position of the peak. Continue changing the delay, and recording the corresponding channel number for all of the delay values in Table 16.2.

Table 16.2. Delay vs Pulse Height Calibration for the Time-to-Amplitude Converter (TAC)

(1) Run No.	(2) Delay nsec	(3) Channel number	(4) FWHM channels	(5) Time Resolution nsec
1	10			
2	14			
3	18			
4	22			
5	30			
6	36			
7	42			
8	48			

4. From the time spectra in the MCA, record the number of channels for the FWHM of each peak. For many MCA's or PCA's, there are programs that can be used to accurately determine these FWHM's. Plot a delay vs pulse height curve from the data in Table 16.2. Calculate the slope of the curve in nsec/ch. Multiply this number by the number of channels in the FWHM to obtain column (5) in Table 16.2 which is the *Time Resolution* for this alpha particle time-of-flight experiment. Figure 16.5 shows a delay vs pulse height curve which is similar to one that you should plot from the data in Table 16.2.

5. Return the nsec delay to 10 nsec. Increase the flight path to 5 cm and record the new peak position of the TAC output in the MCA. Calculate the channel shift (ΔC) and the corresponding (ΔT) for this ΔC. Repeat for the other flight path values in Table 16.3 and fill in the table. As the flight path gets longer, we will have to increase the MCA accumulate time to compensate for the $1/R^2$ change in counting rate. The sum in counter #2 should agree fairly well with Σ-β for the MCA since it is simply counting the stop pulses.

Exercise Figure 16.5 shows some typical TAC spectra for this experiment that was measured as a function of flight path. In all cases the time resolution was at least 2.7 nsec. Shown also on the figure is a pulser peak with 0.5 nsec resolution.

In Table 16.3, the velocity ($\Delta S/\Delta T$) can be calculated by taking any combination of the change in flight path ΔS divided by the corresponding ΔT. In other words, Run No. 3 had a flight path of 10 cm and Run No. 6 was for a flight path of 25 cm, ΔS, therefore, for this pair is 15 cm. The corresponding difference in flight times can be found by subtracting the entries in column (6). Calculate the average velocity of the alpha particles by using as many of these pairs of data as you wish. Use the techniques learned in Experiment #3 (Alpha Spectroscopy) to calibrate the E detector for energy and assign the energy of this transmitted group. **Note:** In fig. 16.4, the 7.36 MeV alpha group had an energy of 3.75 MeV after going through the ΔE detector. The answers for this transmitted energy should agree with the time-of-flight technique and the alpha spectroscopy measurements.

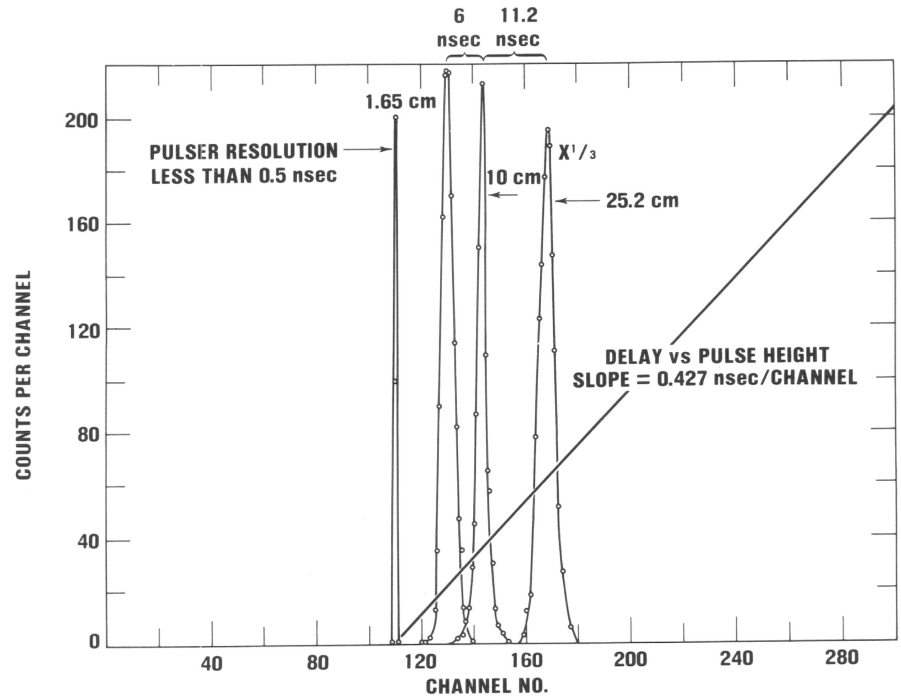

Figure 16.5. Time-to-Amplitude Converter (TAC) pulse height spectra and calibration for the alpha particle time-of-flight experiment.

Table 16.3. Timing Data for the Alpha Particle Time-of-Flight Experiment (The nsec delay box is fixed at 10 nsec)

(1) Run No.	(2) Flight Path	(3) Flight Path Change ΔS	(4) TAC Centroid	(5) Channel Shift (ΔC)	(6) Time Shift (δT)	(7) Velocity ΔS/δT
1	1.65	0		0	0	
2	5.00					
3	10.0					
4	15.0					
5	20.0					
6	25.0					

EXPERIMENT 16.3

(dE/dx) Measurement of Alphas in Copper by Time-of-Flight Spectroscopy

Discussion

This experiment is very similar to Experiment 16.2. We will separate the ΔE and E detectors by 10 cm and measure a time-of-flight spectrum for this flight path. It is assumed that we have already measured the energy of the transmitted alphas from the last experiment. Figure 16.4 shows the transmitted energy to be 3.75 MeV. Your value will depend on the thickness of the ΔE detector that you used for the experiment. Keeping this same flight path, a thin copper foil will be placed over the ΔE detector. The energy loss in the copper foil will give a new transmitted velocity; therefore, a shift in the TAC output. From the measured time shift and the known flight path, the new velocity can be calculated; therefore, the new energy. The measured energy loss will then be compared to the theoretical values which can be calculated from the data in Table 16.4.

Experimental Procedure

1. Separate the detectors by 10 cm and obtain a pulse height spectrum from the TAC as we did in the last

Table 16.4. Stopping Power and Range of Alpha Particles in Copper (Taken from Reference 1)

Energy MeV	Range g/cm²	Stopping Power MeV cm²/g
1.0	1.69 E (—03)	7.42 E (02)
1.2	1.95 E (—03)	7.19 E (02)
1.4	2.22 E (—03)	6.93 E (02)
1.6	2.50 E (—03)	6.67 E (02)
1.8	2.80 E (—03)	6.43 E (02)
2.0	3.10 E (—03)	6.21 E (02)
2.4	3.75 E (—03)	5.81 E (02)
2.6	4.10 E (—03)	5.63 E (02)
2.8	4.46 E (—03)	5.47 E (02)
3.0	4.82 E (—03)	5.31 E (02)
3.2	5.20 E (—03)	5.16 E (02)
3.4	5.58 E (—03)	5.03 E (02)
3.6	5.98 E (—03)	4.90 E (02)
3.8	6.39 E (—03)	4.78 E (02)
4.0	6.81 E (—03)	4.66 E (02)
4.2	7.24 E (—03)	4.56 E (02)
4.6	8.13 E (—03)	4.36 E (02)
4.8	8.59 E (—03)	4.26 E (02)
5.0	9.06 E (—03)	4.17 E (02)
5.5	1.03 E (—02)	3.69 E (02)
6.0	1.16 E (—02)	3.78 E (02)
6.5	1.29 E (—02)	3.62 E (02)
7.0	1.43 E (—02)	3.47 E (02)
7.5	1.58 E (—02)	3.34 E (02)

In the above table, 1.69 E (—03) means $1.69 \times 10^{+3}$, etc.

experiment. Record the channel number of the peak. This corresponds to Run No. 1 (zero foil thickness) in Table 16.5.

2. Turn down the bias voltages; open the chamber and place the 1.3×10^{-3} g/cm² foil over the ΔE detector. Evacuate the chamber; return the bias voltages to their values and accumulate a spectrum in the MCA for a period of time long enough to obtain reasonable statistics in the spectrum. Record the channel shift and calculate the new velocity and measured ΔE for the alpha particles.

3. Remove the 1.3×10^{-3} g/cm² copper foil and replace it with the next thickness and so forth. Fill in the recorded data and calculations as in step (**2**).

Exercise In calculating the new transmitted velocity for Table 16.5, the flight path is 10 cm and the flight times can be determined from the TAC output. The measured energy loss that is calculated for column (6) should have units of MeV. Table 16.4 and the methods used in Experiment 4 can be used to determine the theoretical energy loss for column (7). You should also calculate the percent difference between the ΔE (measured) and ΔE (theory) for each foil thickness.

EXPERIMENT 16.4

Gamma Ray Time-of-Flight Spectroscopy

Discussion

The electronics that will be used for this experiment are shown in fig. 16.6. As you will recall from the angular correlation experiment, ^{22}Na is a positron emitting isotope. We will count one of the annihilation quanta (γ_1) in a fixed detector and the other (γ_2) in a detector that can be moved on a straight line away from (γ_1) always keeping $\theta = 180$ degrees. We will start by placing the detectors 0.1 m apart and accumulating a time-to-amplitude spectrum for this flight path. Next, the movable detector will be moved to a distance of 1.10 m and the increase in flight time will be measured with the TAC. The gamma velocity will be calculated from the data. Additional flight paths will be used and an average value of (c) will be determined.

Experimental Procedure

1. Set up the electronics as shown in fig. 16.6. Place the detectors 0.10 m apart with the ^{22}Na source between the two detectors. The fast plastic scintillators represent the best method of collecting fast rise time pulses for this experiment. Set the high voltage of each phototube so that the input pulse to the constant fraction discriminators is at least -0.50 volts.

2. If you wish, the output of each phototube can be studied with a pre-amp, amp, and MCA. We have shown this connection with a dashed line on the bottom phototube. Figure 16.7 shows a pulse height spectrum which is similar to what would be seen from either detector. **Note:** There is no photopeak for either the 0.511 or 1.274 MeV peaks. As you will recall, the photoelectric interaction goes as Z^5 and, for a plastic scintillator, this term is negligible. Once you have looked at a spectrum similar to fig. 16.7 for each phototube, you may return to the basic schematic and the time calibration problem.

Table 16.5. (dE/dx) by Time-of-Flight Spectroscopy

(1) Run No.	(2) Copper Foil Thickness g/cm²	(3) Peak Shift ΔC	(4) Time Shift ΔT	(5) Velocity ΔS/ΔT	(6) Measured Energy Loss ΔE	(7) Energy Loss Theory
1	0.0	0.00	0.00			
2	1.3×10^{-3}					
3	1.5×10^{-3}					
4	1.7×10^{-3}					
5	2.0×10^{-3}					
6	2.25×10^{-3}					
7	2.50×10^{-3}					

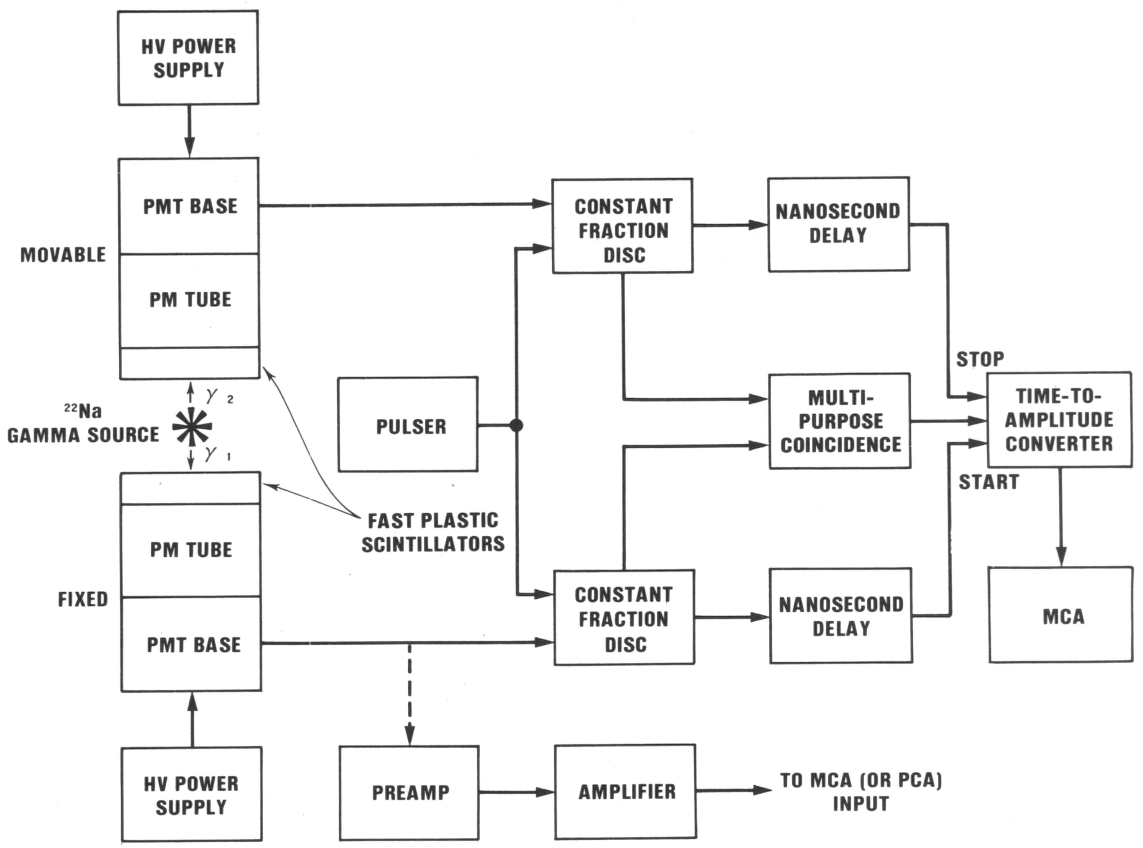

Figure 16.6. Electronics for gamma-ray time-of-flight spectroscopy.

3. Set the constant fraction discriminators in the CF mode with the lower level set at 50/1000; use the negative outputs to the nsec delay boxes. The positive output pulses are fed into the A & B inputs to the Multipurpose Coincidence Circuit. The other switches C, D, and E should be set on out. Use the positive output pulse of the coincidence circuit into the gate of the TAC. Set the resolving time of the coincidence unit on 100 nsec and coincidence requirements on 2.

4. Set the movable nsec delay on 10 nsec and the fixed one on zero. Set the TAC on 50 nsec resolving time in the coincidence mode.

5. Accumulate a time spectrum in the MCA. The TAC output spectrum should show a sharp peak in the lower quarter of the MCA. If this is not the case, change the delays in either nsec delay box until the spectrum is seen. Let's assume your TAC output is as it should be in the

lower quarter of the analyzer. You can now make a time per channel calibration for the MCA.

6. Increase the delay in the stop side of the TAC by 4 nsec and record the new peak position. Continue for enough delay settings to plot a delay vs pulse height curve. Determine the nsec/ch slope of the curve and the time resolution of the system. Return the delay to the values that gave us an output in the lower quarter of the MCA.

7. Move the movable detector by a $\Delta L = 1$ m additional flight path. Accumulate a spectrum for a period of time long enough to get reasonable statistics in the peak. Calculate the corresponding ΔT for this ΔL. Calculate (c) the velocity of light.

Repeat for distances of 2 m, 3 m, and 4 m and calculate the corresponding velocities of the gammas. **Note:** The accumulate times will have to be increased to compensate for the $1/R^2$ fall off in intensity.

Exercise Calculate the average gamma velocity from all of the above measurements and compare it to $3x\ 10^8$m/s. Isn't it amazing what modern day electronics will do?

REFERENCES FOR *EXPERIMENT 16*

1. C. F. Williamson, J. P. Boujot, and J. Picard, *Tables of Range and Stopping Power of Chemical Elements for Charged Particles of Energy 0.5 to 500 MeV*, **CEQ-R-3042** (1966). Available from Clearinghouse for Federal Scientific and Technical Information, Springfield, Virginia.

2. J. F. Janni, *Calculations of Energy Loss, Range, Pathlength, Straggling, Multiple Scattering, and the Probability of Inelastic Nuclear Collisions for 0.1- to 100-MeV Protons*, **AFWL-TR-65-150** (AD-643837), (1966). Available from Clearinghouse for Federal Scientific and Technical Information, Springfield, Virginia.

3. J. L. Duggan, W. D. Adams, and L. S. Anthony, "Charged-Particle Detector Experiments for the Modern Physics Laboratory," *Am. J. Phys.* **35**(7), 631 (1967).

4. J. B. Marion and F. C. Young, *Nuclear Reaction Analysis*, John Wiley and Sons, New York (1968).

5. J. F. Ziegler, *The Stopping Power and Ranges of Ions in Matter*, Pergammon Press, New York (1977).

6. L. C. Northcliffe and R. F. Schilling, *Nuclear Data Tables* **A7**, 233 (1970).

7. T. J. Paulus, R. D. McKnight, and T. L. Mayhugh, "Experimental Characterization of the Timing Properties of Detector Preamplifier System for Charged Particle Detectors Using a Laser Pulser," *IEEE Trans. Nucl. Sci.* **NS-24**(1), 335 (1977).

8. G. J. Wozniak, *et. al.* "Time-Walk Characteristics of an Improved Constant-Fraction Discriminator," *Nucl. Instrum. Methods* **180**, 509-519 (1981).

9. M. Moszynski and B. Bengtson, "Status of Timing with Plastic Scintillation Detectors," *Nucl. Instrum. Methods* **158** 1-31 (1979).

10. S. Sanyal, *et. al.*, "Sub-Nanosecond Timing Studies with Plastic Scintillation Detectors," *Nucl. Instrum. Methods* **136**, 157 (1976).

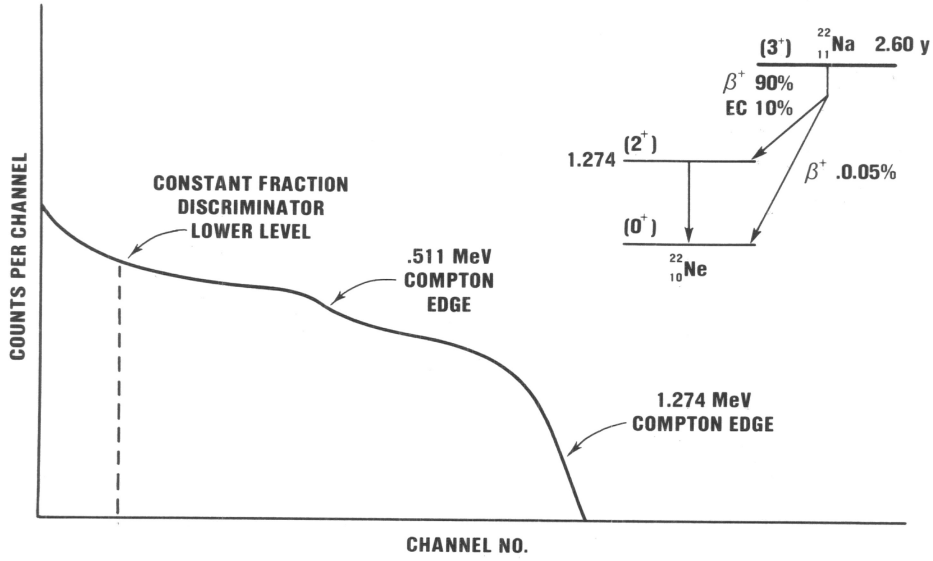

Figure 16.7. Plastic scintillator output for a ^{22}Na source (for these low Z scintillators the photopeak is almost nonexistent).

EXPERIMENT 17

X-Ray Measurements and X-Ray Fluorescence Using a Gas Filled Proportional Counter

Scope

In this experiment we are going to study the properties of the gas filled proportional counter. In the first part of the experiment, a calibration will be made with known radioactive sources. From the slope of the calibration curve, the energy per unit channel will be measured and the resolution of the counter determined. Next, the proportional counter will be used to study the photoelectric absorption of low energy photons in thin foils. Finally, an excitation source and the proportional counter will be used to study x-ray fluorescence from a variety of samples.

Discussion

In experiments 7 and 8, we measured low energy photons with Si(Li) and germanium detectors. These detectors were seen to have excellent resolution and fairly high efficiency for low energy photons. If they have a drawback, it is primarily cost, but also the fact that they have to be cooled to liquid nitrogen temperatures must be considered. As we will see in this experiment, the gas filled proportional counter can also be used to detect low energy photons. These detectors are rather inexpensive and, as we will see, their resolution is adequate for many experiments.

In appearance, the proportional counter is similar to the Geiger-Mueller tube that we studied in experiment number 1. The entrance window (see fig. 17.1) is usually a thin piece of beryllium metal either on the end or the side of the tube. In our case, these tubes are the end window variety that is vacuum mounted on the bottom of the Proportional Counter Chamber. The chamber is made in such a manner that an x-ray-fluorescence source can also be safety mounted in the bottom of the chamber to excite samples that are rotated in place from an external control. Figure 17.2 shows the various regions of operation of a gas filled tube. In experiment number 1, we have already studied the Geiger Region. As you will recall, in this region, the voltage on the tube is high enough that any ionizing event that enters the sensitive region will cause the detector to avalanche; therefore, give an output pulse. In this G-M region, however, no information is provided by the detector in regard to the energy of the ionizing particle. In the proportional region, the gas amplification of the tube is such that the output pulse height scales with the incident photon energy. Figure 17.3 shows the efficiency of a proportional counter that has 5 cm of gas above atmospheric pressure. As you will recall, at these low energies, the photoelectric effect is the most pronounced interaction and its probability is proportional to Z^5. Therefore, a (^{54}Xe) filled tube is more efficient, in general, than one with (^{18}Ar).

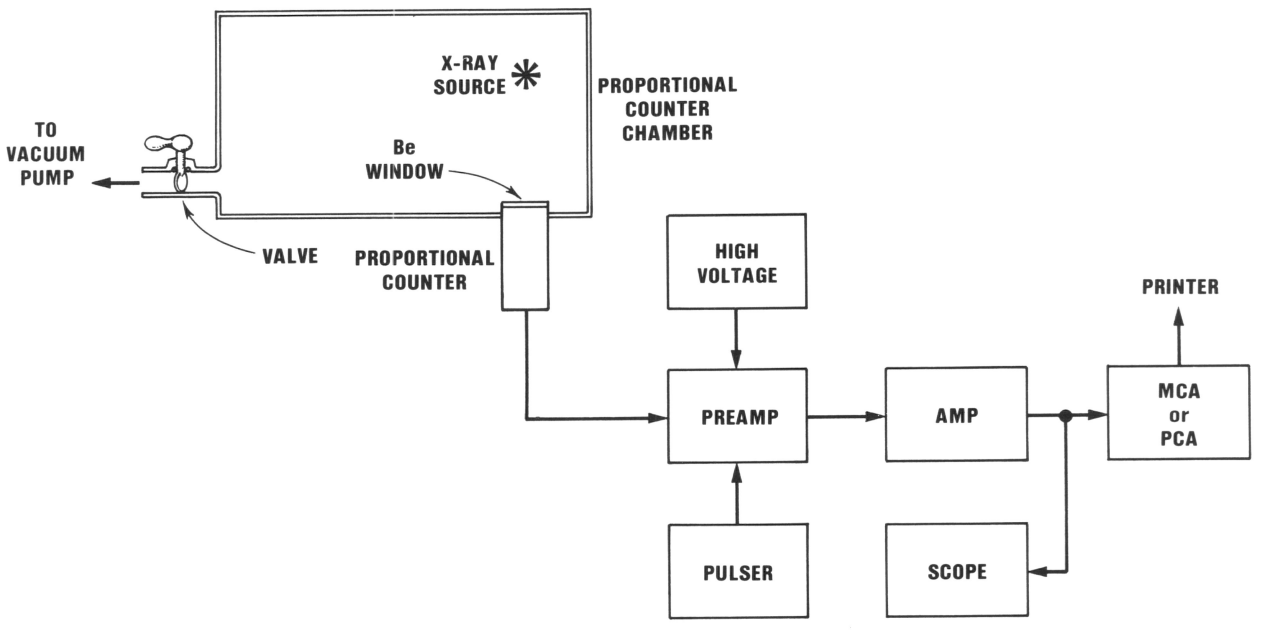

Figure 17.1. Proportional counter chamber and electronics for low energy x-ray measurements.

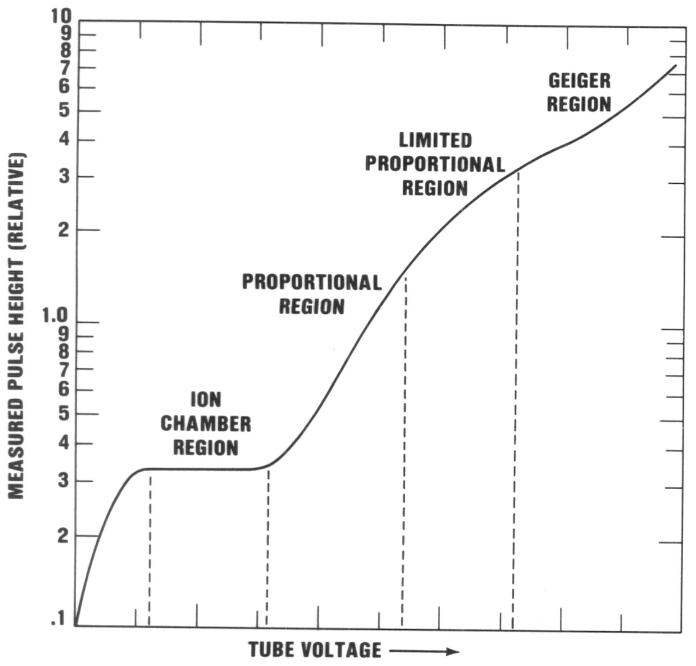

Figure 17.2. Output pulse height versus tube voltage for a proportional counter.

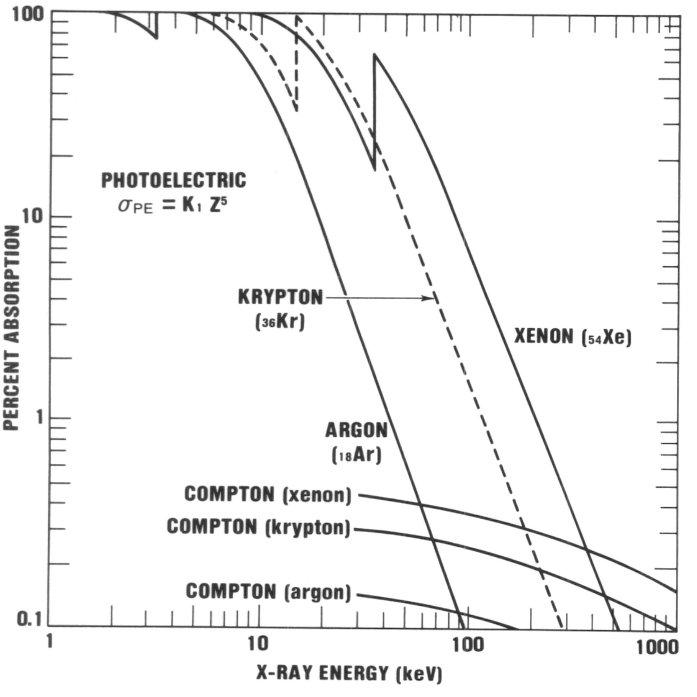

Figure 17.3. Relative absorption of various proportional counter gases for low energy x-rays (Taken from Reference 1) .

EXPERIMENT 17.1

Energy Calibration of the Proportional Counter

Experimental Procedure

1. Set up the electronics as shown in fig. 17.1. Place the ^{57}Co source in the source holder at its position in the proportional counter chamber. It is not necessary to evacuate the chamber for sources whose photon energy is greater than 5 keV. Set the high voltage at the value recommended for the detector. Adjust the gain of the amplifier so that the pulses from the 14.43 keV photon are about 3V in amplitude. Use 512 channels on the MCA and accumulate a spectrum. Figure 17.4 shows a typical spectrum of ^{57}Co with a proportional counter. Table 17.1 shows a 7.06 keV Kβ for the ^{57}Co source that does not appear on fig. 17.4. We simply have not shown it in the figure. Please recall it is only about 15% of the 6.4 keV peak and hence not very pronounced in the spectrum. Record the channel numbers for the 6.4 and 14.4 keV peaks.

2. Remove the ^{57}Co source and replace it with a ^{65}Zn source. Record the position of the 8.04 keV peak. Repeat for the ^{109}Cd source. From the positions of the peaks and the energies listed in Table 17.1, make a calibration curve for the detector.

3. After you have made the calibration curve, place the ^{241}Am source in the chamber and store a spectrum for a period of time long enough to see the peaks of interest. Try to identify the major peaks in the spectrum from your measured energies and Table 17.1. Figure 17.5 shows a typical ^{241}Am spectrum that was taken with a xenon filled proportional counter. The Pt Lα_1 and Lβ_1 lines in the spectrum are produced from alpha particle x-ray fluorescence of the platinum blank that served as a backing for the electrodeposited ^{241}Am source.

EXPERIMENT 17.2

Mass Absorption Coefficient Measurement for 8.04 keV Photons in Copper

Experimental Procedure

1. Use the same calibration as in Experiment 17.1. Place the ^{65}Zn source in the chamber. Place the foils for the first four runs (see Table 17.2) in the foil wheel of the chamber. **Note:** The copper foils that you use for this experiment may differ in thickness from those in Table 17.2. You should construct a new Table 17.2 with your exact foil thicknesses in column (2).

PROPORTIONAL COUNTER X-RAY SPECTRUM FROM ^{57}Co

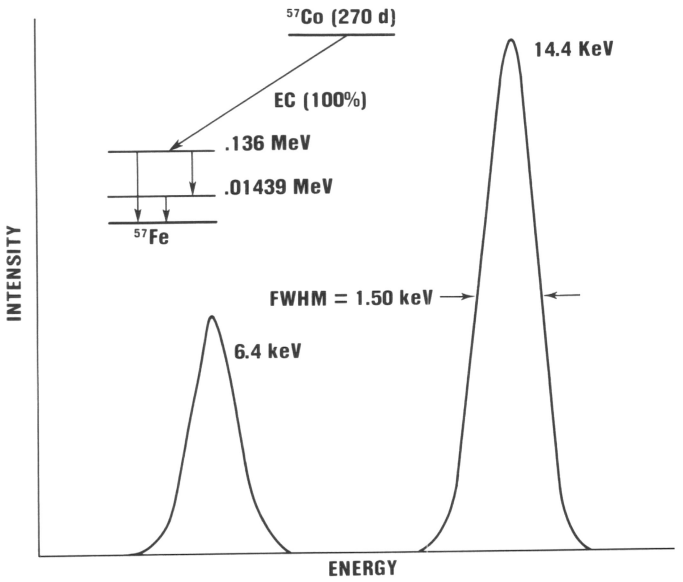

Figure 17.4. Typical pulse height spectrum of the low energy photons from ^{57}Co. Note: ^{57}Co also has 122 and 136 keV gammas but the proportional counter is not every efficient for these higher energy gammas; therefore, they are not seen in the spectrum.

Table 17.2 Data for Linear Asborption Coefficient Measurement, 8.05 keV Photons in Copper

(1) Run No.	(2) Absorber Thickness mg/cm^2	(3) $\left(\frac{\Sigma - \beta}{t}\right)$ Counts/s
1	0.00	
2	6.50	
3	11.10	
4	16.70	
5	21.20	
6	26.10	
7	33.00	
8	36.90	
9	39.80	
10	42.70	

Table 17.1 Low Energy X-Ray Calibration Sources for Thin Window Proportional Counter Experiments

Nuclide	Energy of X-Rays and Low-Energy Gamma (keV)	Energy of High-Energy Gamma (keV)	Intensity Ratio X/γ
^{54}Mn	5.414 (Kα) 5.946 (Kβ)	834.8	0.2514 (±0.5%) Kα + Kβ
^{57}Co	6.40 (Kα) 7.06 (Kβ) 14.43 (γ)	122.1	0.5727 (±2.0%) 0.7861 (±2.9%) 0.112 (±1.8%)
^{65}Zn	8.04 (Kα) 8.9 (Kβ)	1115.5	0.6596 (±0.8%) 0.0911 (±2.0%)
^{241}Am	11.89 N_pL_l 13.90 $N_pL\alpha$ 17.8 $N_pL\beta$ 20.8 $N_pL\gamma$ 26.35 γ	59.5	0.022 0.375 0.512 0.138 0.07
^{85}Sr	13.38 (Kα) 15.0 (Kβ)	514.0	0.5020 (±0.65%) 0.0880 (±1.4%)
^{88}Y	14.12 (Kα) 15.85 (Kβ)	898.0	0.5491 (±1.2%) 0.0989 (±1.9%)
^{109}Cd	22.10 (Kα) 25.0 (Kβ)	88.0	22.02 (±4.9%) 4.68 (±5.0%)
^{113}Sn	24.14 (Kα) 27.4 (Kβ)	391.7	1.219 (±3.5%) 0.267 (±3.6%)
^{137}Cs	32.1 (Kα) 36.6 (Kβ)	661.6	0.0666 (±3.0%) 0.0159 (±3.1%)
^{139}Ce	33.29 (Kα) 38.0 (Kβ)	165.9	0.808 (±11%) 0.195 (±11%)
^{198}Au	70.15 (Kα) 80.7 (Kβ)	411.8	0.0229 (±2.3%) 0.00635 (±2.4%)
^{203}Hg	72.11 (Kα) 83.0 (Kβ)	279.2	0.1247 (±2.1%) 0.0348 (±2.3%)

2. Take a spectrum for run number 1 (no foil) for a period of time long enough to obtain reasonable statistics in the 8.05 keV peak. Record (Σ-β/t) in your table. Repeat this measurement for the other foils listed in your Table 17.2.

Exercise Make a plot of (Σ-β/t) versus foil thickness on semilog paper. Figure 17.6 shows a typical set of experimental data for this experiment. Calculate the Half Value Layer (HVL) and σ, the cross-section for the interaction of these photons with copper. The value of σ_T = 51.5 cm^2/g is the theoretical cross section that is accepted in the literature. How well does your measured value compare to the theory?

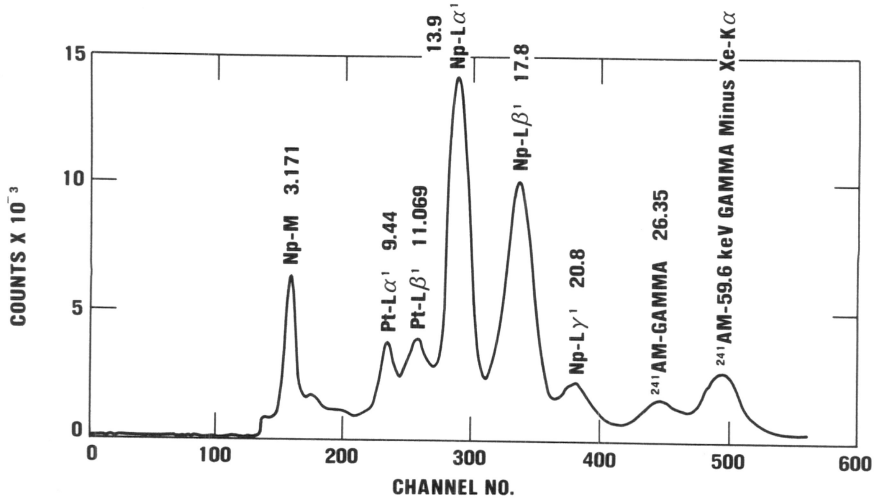

Figure 17.5. Proportional counter pulse height spectrum of an electrodeposited ^{241}Am source. See Table 17.1 for intensity ratios (This spectrum was taken from Reference 13).

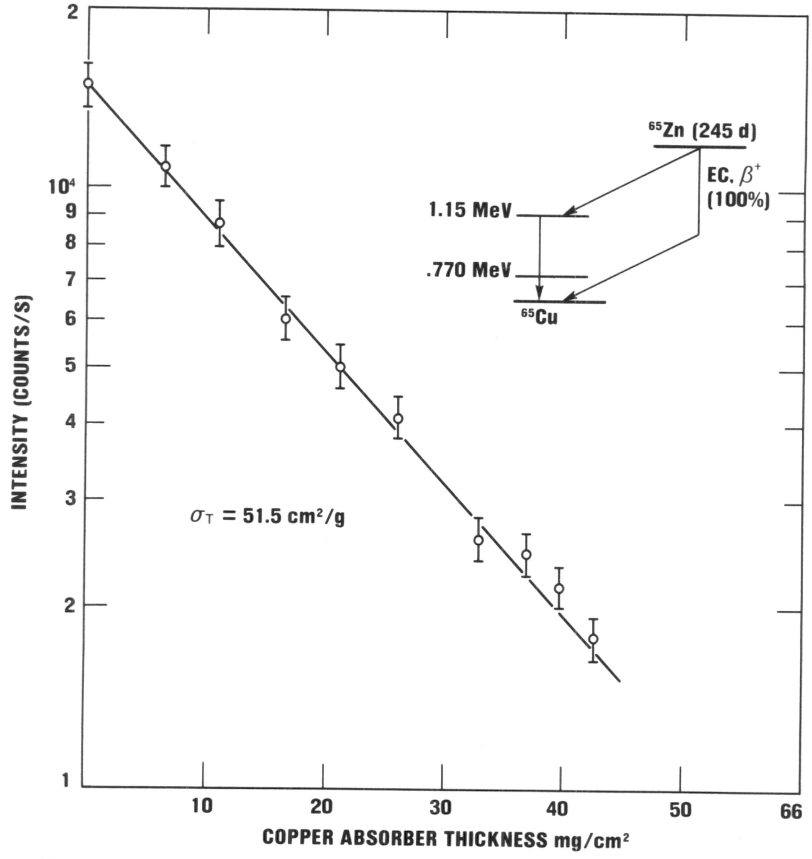

Figure 17.6. Linear absorption of 8.05 keV x-rays through copper.

EXPERIMENT 17.3

Mass Absorption Coefficient Measurement for 22.1 keV Photons in Silver

Experimental Procedure

1. The energy calibration used in the last experiment will also be used in this measurement. Place the ^{109}Cd source in the chamber and the three thinnest silver foils from Table 17.3 in the chamber.

2. Accumulate a spectrum with "no foil" for a period of time long enough to get good statistics in the 22.1 keV peak. Repeat for the other silver foils listed in your Table 17.3 and fill in the table.

Exercise Plot a curve similar to fig. 17.7 and determine the HVL and σ as in Experiment 17.2.

Table 17.3 Data for Linear Asborption Coefficient Measurement, 22.1 keV Photons from ^{109}Cd through Silver

(1) Run No.	(2) Absorber Thickness mg/cm^2	(3) $\frac{\Sigma - \beta}{t}$ Counts/s
1	0.0	
2	11.3	
3	21.6	
4	33.0	
5	45.2	
6	55.0	
7	69.8	
8	89.0	
9	105.4	
10	123.1	

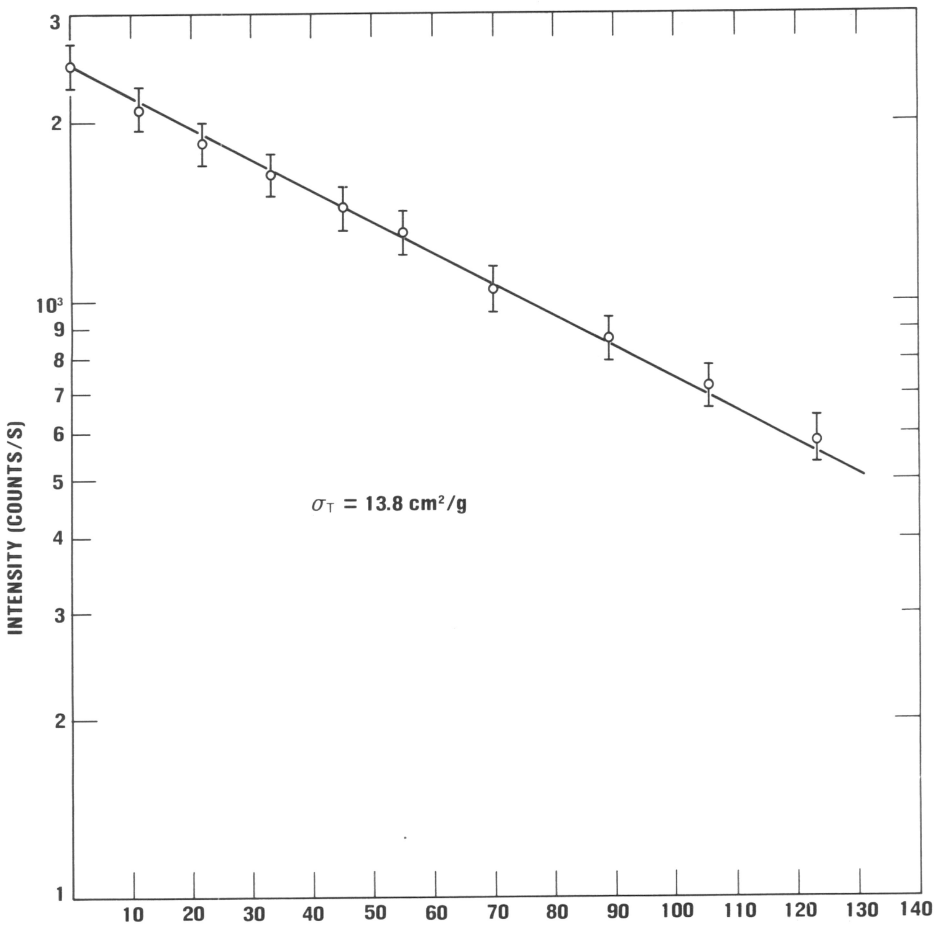

Figure 17.7. Linear absorption coefficient of 22.1 keV x-ray through silver.

EXPERIMENT 17.4

X-Ray Fluorescence Using a Gas Filled Proportional Counter and a Specially Designed Fluorescence Chamber

Discussion

Figure 17.8 shows the experimental arrangement that will be used for this experiment. The ring geometry source actually is positioned in the bottom of the proportional counter chamber. These excitation sources are usually between 25-100 mCi; therefore, good health physics procedures should be used at all times. Once the source is loaded in the chamber, it can be safely used for the experiment. The samples that are to be fluoresced are loaded through the top of the chamber. The source, sample, and detector geometry are designed to maximize the sensitivity of the system. In terms of the excitation energy that is to be used for a given sample, the vacancy production cross-section is the driving force. Figure 17.9 shows a plot of the vacancy production cross-section for copper as a function of the incident photon excitation energy. If you will carefully look at the figure, it can be seen that the maximum probability of creating a K-shell vacancy for copper is with a photon that has an energy equal to the binding energy of the K electron (8.98 keV). From a practical stand point, it is best to have an incident photon that has an energy of at least 1 keV higher than (K_{ab}), the K shell binding energy. The reason for this is that in collecting a spectrum of the sample, the elastic scattering of photons from the sample are always present in the spectrum and they will interfere with the K-x-rays that are being measured. For example, in copper the K x-rays have an energy of 8.04 keV. Therefore, the ideal source would be photons of about 10 keV. The proportional counter would then be able to resolve between x-rays from the source and the sample; therefore, we could determine the copper concentration in the sample. Table 17.4 shows the most common excitation sources and the primary photons that are given off by the sources. Therefore, if we were trying to study the x-ray fluorescence of copper, the 14.43 keV photon from ^{57}Co would probably be the best choice of an excitation source. We have shown, with an arrow, where this 14.43 keV excitation would occur on the copper vacancy production curve (fig. 17.9). It can be seen from the figure that ^{57}Co is probably a fairly good source to use if our problem is to find copper in a sample. Figure 17.10 shows a pulse height spectrum for manganese. From what has been said, the 6.403 keV line from ^{57}Co would do a good job of exciting this sample, as is evidenced from the spectrum.

Experimental Procedure

1. The instructor will load the excitation source (for our example ^{57}Co) in the chamber. The samples that we will fluoresce are copper, germanium, iron, and manganese. Load these samples in the chamber in the four excitation positions. Pump the chamber out and apply the recommended voltage to the proportional counter.

2. The gain of the amplifier and calibration will be the same as for all of the previous sections of this experiment. Rotate the manganese sample to the excitation position and accumulate a spectrum for a period of time long enough to get reasonable statistics in the Kα peak (see fig. 17.10). Determine (Σ-β/t) and the centroid of the peak. Record these in a data table.

3. Repeat steps **1** and **2** for the copper, germanium and iron samples and record (Σ-β/t) and the centroids of the peaks in your data table.

4. Obtain the K or L shell unknowns from the instructor and fluoresce them. Record (Σ-β/t) and the centroids of the observed peaks.

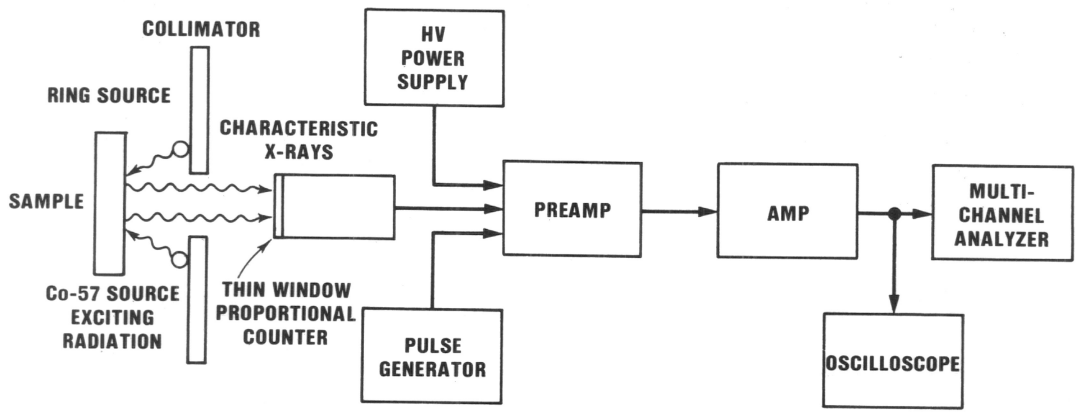

Figure 17.8. Experimental arrangement for x-ray fluorescence using the proportional counter chamber.

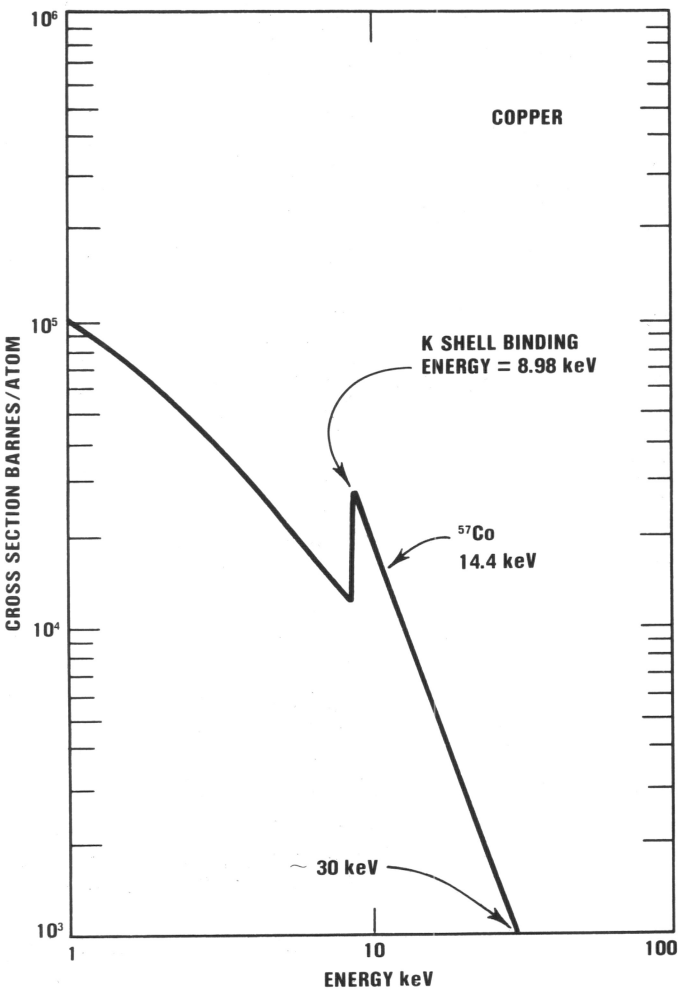

Figure 17.9. **Vacancy production cross section for copper as a function of photon excitation energy.**

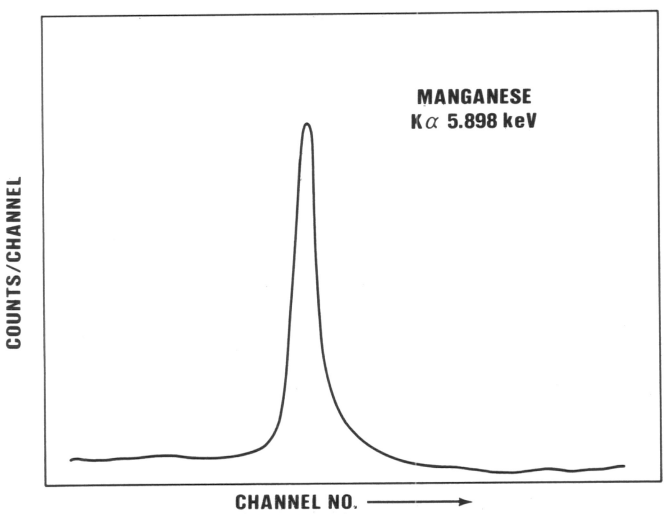

Figure 17.10. X-ray fluorescence of the Mn K lines with a ^{57}Co excitation source.

Exercise From your calibration curve determine the energies of the K lines from Mn, Fe, Cu, and Ge. How do these compare to the theoretical K energies listed in the Critical Absorption and Emission X-ray table in Appendix B? Calculate the % difference between your value and theoretical energy. From the calibration curve, determine the energies of the peaks in the unknowns. What are they, and how far did you miss their exact energies? Figure 17.11 shows a silver spectrum that might have been used as an unknown. From the (Σ-β/t) values collected for each sample, you can assign a relative sensitivity figure for each sample.

The identification of an unknown by analyzing the x-ray energies of the sample by XRF is one of the most accurate techniques in modern analytic procedures. Rarely does a student miss an unknown.

Table 17.4 Recommended Excitation Sources for X-Ray Fluorescence Measurements. With the Proportional Counter Chamber used for this Experiment, These Sources are in Ring Geometry (See Fig. 17.8)

Source	Excitation Photons (keV)	Half Life	Recommended Activity mCi
^{55}Fe	Mn Kα 5.898 Mn Kβ 6.490	2.60Y	25-100
^{57}Co	Fe Kα 6.403 Fe Kβ 7.057 14.43	270d	50-100
^{109}Cd	Ag Kα 22.162 Ag Kβ 13.945	453d	25-100
^{241}Am	Np Lα 13.945 Np Lβ 17.740 Np Lγ 20.774 26.35 59.5	458Y	25-100

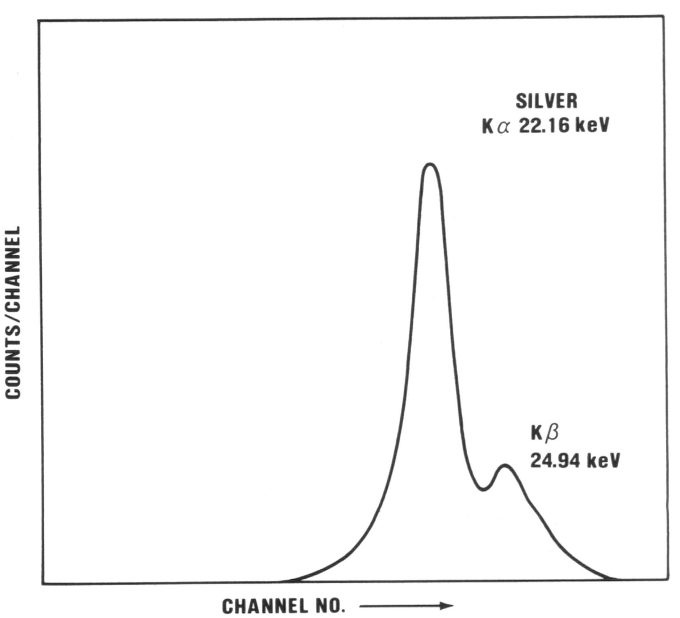

Figure 17.11. X-ray fluorescence of silver K lines with a ^{57}Co source. The measurement was made with a Xenon filled proportional counter.

REFERENCES FOR *EXPERIMENT 17*

1. D. West, *Progress in Nuclear Physics*, Vol. 3, Academic Press, New York (1953).

2. G. F. Knoll, *Radiation Detection and Measurement*, John Wiley and Sons, New York (1979).

3. K. Siegbahn, Ed., *Alpha, Beta and Gamma Spectroscopy*, North Holland Publishing Co., Amsterdam (1968).

4. C. M. Lederer and V. S. Shirley, Eds., *Table of Isotopes*, 7th Edition, John Wiley and Sons, Inc., New York (1978).

5. V. Arena, *Ionizing Radiation and Life*, The C. V. Mosby Co., Missouri (1971).

6. *Radiological Health Handbook*, U.S. Dept. of Health, Education, and Welfare, PHS Publication 2016. Available from National Technical Information Services, U.S. Dept. of Commerce, Springfield, Virginia.

7. W. Mann and S. Garfinkel, *Radioactivity and Its Measurement*, Van Nostrand-Reinhold, New York (1966).

8. G. D. Chase and J. L. Rabinowitz, *Principles of Radioisotope Methodology*, 3rd Edition, Burgess Publishing Co., Minnesota (1967).

9. R. W. Hendriks, *Nucl. Instrum. Methods* **102**, 309 (1972).

10. M. W. Charles and B. A. Cooke, *Nucl. Instrum. Methods* **88**, 317 (1970).

11. R. Gott and M. W. Charles, *Nucl. Instrum. Methods* **72**, 157 (1969).

12. B. E. Fischer, *Nucl. Instrum. Methods* **141**, 173 (1977).

13. J. L. Duggan, F. D. McDaniel, and J. G. Hehn, Advanced Experiments in Nuclear Science. National Science Foundation Project in *Nuclear Science Education*, published by North Texas State University Press 1978.

EXPERIMENT 18

Trace Element Measurements Using X-Ray Fluorescence and Neutron Activation Analysis: Applications in Environmental, Biological, and Geological Studies

Scope

In this experiment, we will use X-Ray Fluorescence and Thermal Neutron Activation Analysis to measure trace element concentrations in a wide variety of samples. In the first few sections of the experiment, we will study *Source Excited X-Ray Fluorescence*. This will be followed by a rather complete section on x-ray fluorescence measurements that are induced by x-rays from a specially designed *x-ray tube and fluorescence chamber*. Finally, several trace measurements will be presented using Neutron Activation Analysis. All of the sections in this experiment are suitable for advanced undergraduate projects or senior research projects. Many of the experiments in this section can be made more advanced and the results actually published in the open literature.

Discussion

X-Ray Fluorescence (XRF) and Neutron Activation Analysis (NAA) are two nuclear techniques that have wide applicability in trace element studies. We have studied both of these techniques in earlier experiments in this manual. The purpose of this experiment is to show how these techniques can be used in a wide variety of disciplines to analyze samples. In environmental studies, the best examples of the use of these techniques are air and water pollution, analysis and soil sample studies. XRF will be treated in the first few sections of this experiment; therefore, we start by discussing its applicability to other disciplines.

As we have mentioned before, there are two ways to do XRF: source excitation and x-ray tube excitation. Figure 18.1 shows the experimental arrangement that is used for the source excited experiments. The chamber that is used for these experiments has four sample positions. The samples are loaded in the chamber and then it is evacuated. The samples are usually powdered or dried onto filter paper, but they can be liquid or a solid piece of material. The various excitation sources that can be used were given in Table 17.4. The samples that are to be analyzed can be environmental, biological, geological, etc. Figure 18.2 shows an air pollution filter sample that was excited by a ^{109}Cd source. The sample was collected with a standard air sampler that is recommended for this experiment. Figure 18.3 shows an ^{55}Fe XRF spectrum of water from a commercial water treatment plant.

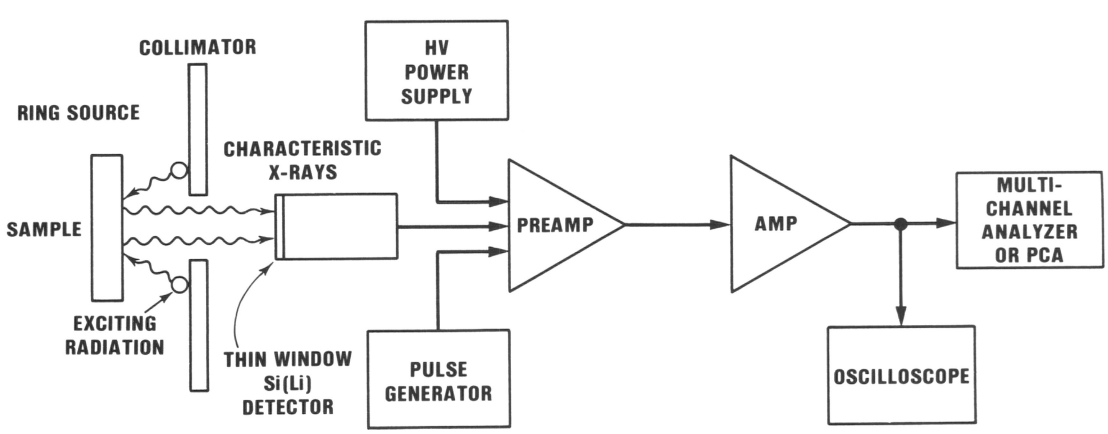

Figure 18.1. Experimental arrangement for source excited X-Ray Fluorescence (XRF) using a high resolution Si(Li) detector. It is not shown in this figure but the Si(Li) detector is vacuum sealed to the bottom of the excitation chamber that is used for these experiments.

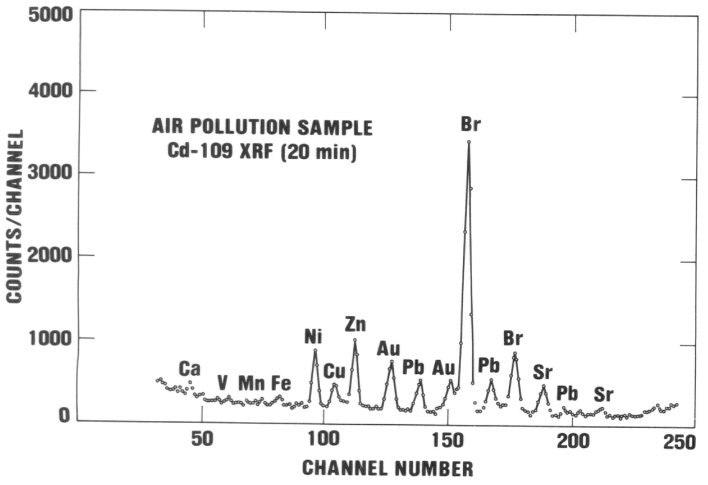

Figure 18.2. Tube excited x-ray flourescence spectrum of an air pollution filter sample that was excited with a ^{109}Cd source for 20 minutes.

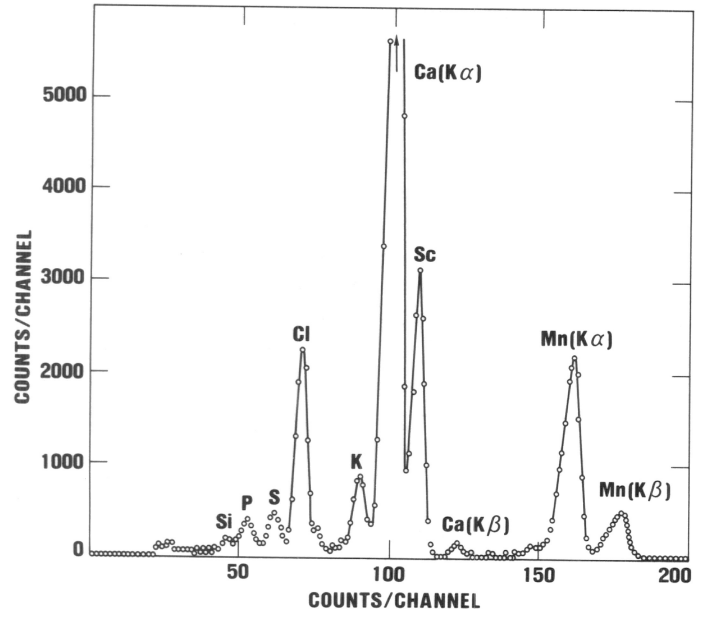

Figure 18.3. ^{55}Fe x-ray fluorescence of the effluent water from a commercial water treatment plant. The water samples were dried onto filter paper before being fluoresced.

Figure 18.4 shows the spectrum of a cigarette ash that was uniformly distributed on a piece of filter paper and then fluoresced with an ^{55}Fe source. In biology, there are numerous applications in which XRF can be used. Figure 18.5 shows a urine sample that was dried on a piece of filter paper and fluoresced with a ^{109}Cd source. From what has been shown above, it is quite obvious that source excited XRF has wide applicability as an analytic technique.

For science departments that are interested in sensitivities that are higher than those that can be obtained with a source, an x-ray tube excitation system should be considered. The additional sensitivity of the tube excited

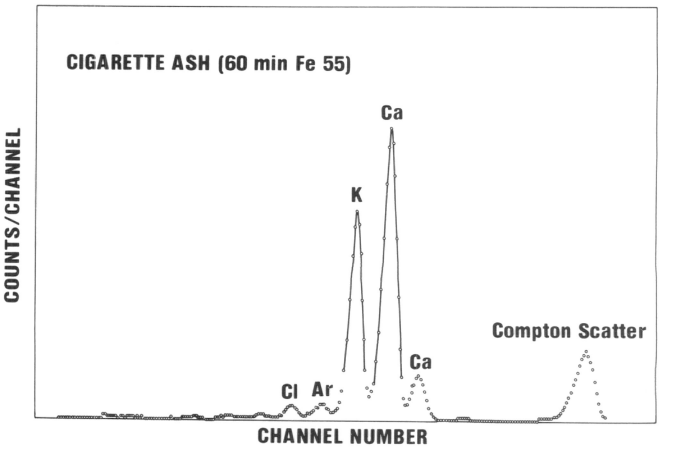

Figure 18.4. ^{55}Fe excitation of an ordinary cigarette ash showing the Ca, K, and Cl concentrations. The argon peak is present because of the small concentration of Ar in air. This peak could be eliminated by making the measurement under vacuum conditions.

system can be justified quite easily if one looks at the number of exciting photons per unit time for a tube and a source; for example,

$$100 \text{ mCi source gives } 3.7 \times 10^{9} \text{ photons/sec} \quad (1)$$

$$100\ \mu \text{ amp current tube give } 1 \times 10^{12} \text{ photon/sec} \quad (2)$$

An additional advantage of the tube comes from the fact that, in theory at least, one can set the accelerating voltage for the tube or choose the x-ray tube target to maximize the sensitivity of the system. In earlier experiments, these arguments were presented in regard to the yield, absorption edge and incident photon energy. The student should go back and read these experiments.

For an unfiltered x-ray tube the Bremsstrahlung and characteristic x-rays from the target are both effective in

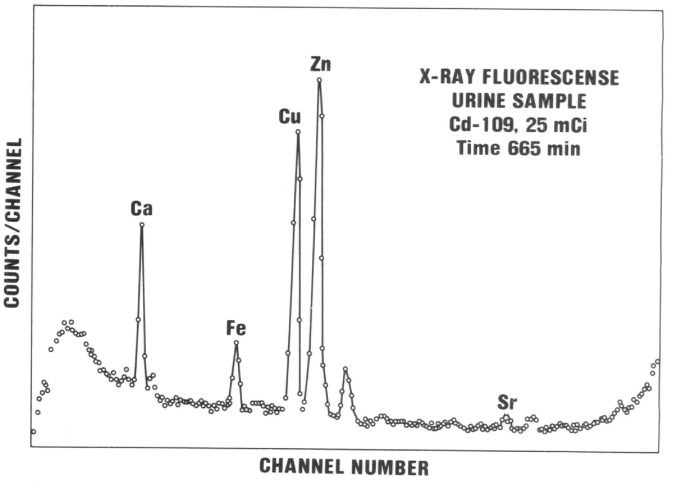

Figure 18.5. Pulse height spectrum of dried urine sample that was fluoresced with ^{109}Cd.

fluorescing the target. Figure 18.6 shows what the spectrum looks like for a molybdenum x-ray tube and an accelerating voltage of 50 keV. In many cases filtering is desirable. For example, if one was studying rubidium (K_{ab} = 15.20 keV) the tube used in fig. 18.6 would be ideal from almost every aspect.

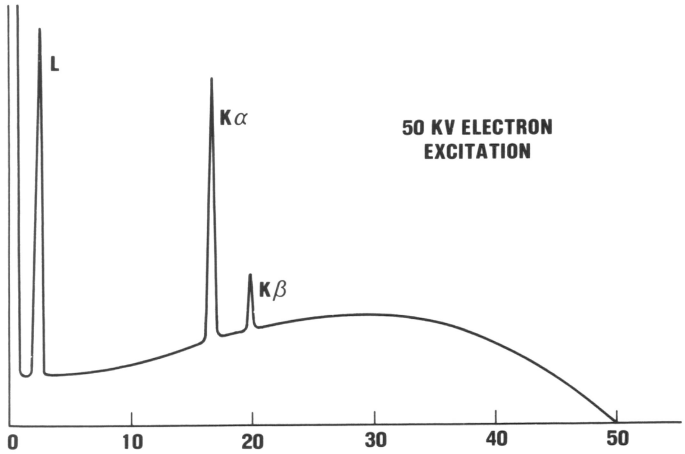

Figure 18.6. Typical unfiltered spectrum for a molybdenum target x-ray tube.

Once a science department has made an investment in one of these systems, the applications are almost unlimited. For example, fig. 18.7 shows a pulse height spectrum of freeze dried blood in which the lead concentration was being studied. Figure 18.8 shows a pulse height spectrum of swordfish in which the Hg content of the meat was being analyzed to determine possible pollution problems in that area of the sea. Other examples of the wide applicability of this technique will be shown later in this experiment.

In the last section of this experiment, we will treat Neutron Activation Analysis (NAA) as it applies to trace analysis. The thermal neutrons that are used for this experiment can be provided by the Am-Be source discussed earlier, a nuclear reactor, or a ^{252}Cf source. Universities that do not have either a reactor or a ^{252}Cf source can usually arrange to have samples irradiated at facilities that have these sources of neutrons. Figure 18.9 shows a pulse height spectrum of a dried water pollution sample that was produced by ^{252}Cf neutron activation. As we mentioned in earlier experiments, the best way to do quantitative analysis is to compare the element of interest to a known standard. In other words, if we wished to determine the amount of sodium in the water pollution sample shown in fig. 18.9, a sodium standard could be irradiated in the neutron flux under the same conditions as the pollution sample. Therefore, a simple ratio of the sodium peaks will give the amount of sodium in the unknown environmental sample. In this experiment we will see that for many elements NAA is one of the most sensitive analytic techniques that can be used.

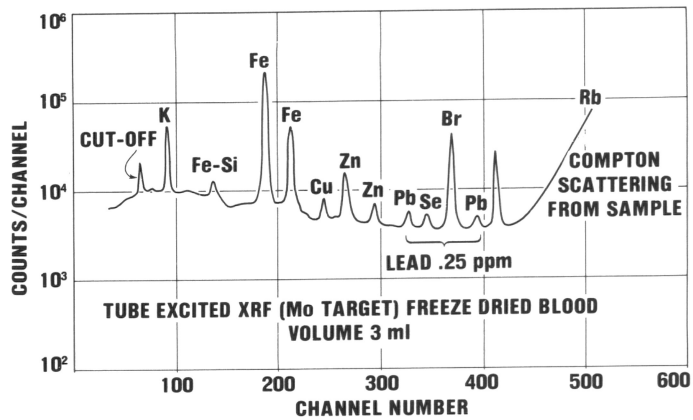

Figure 18.7. Tube excited pulse height spectrum of freeze dried blood taken to analyze the correlation of lead concentration and disease. (This spectrum was provided by Lawrence Berkeley Laboratory)

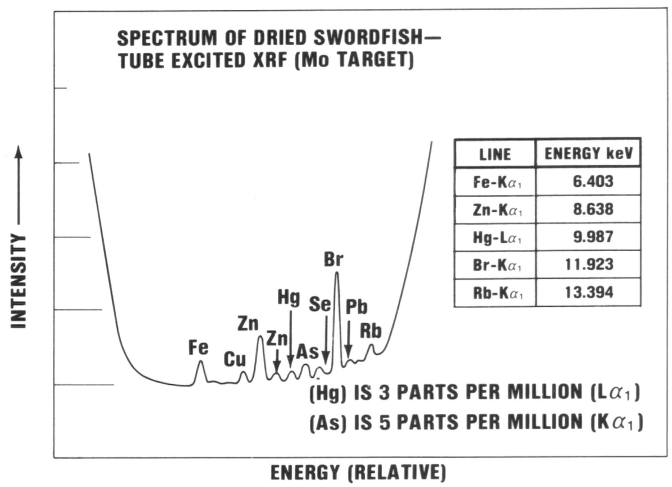

Figure 18.8. Tube excited pulse height spectrum of dried swordfish taken to analyze the meat for mercury contamination. (This spectrum was provided by Lawrence Berkeley Laboratory)

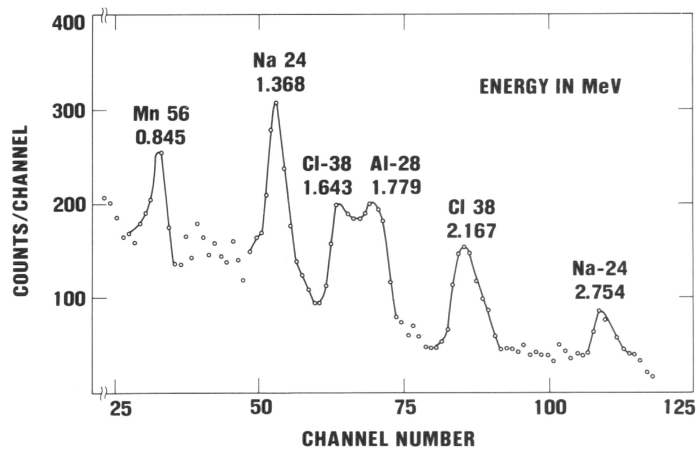

Figure 18.9. Neutron activated pulse height spectrum of a dried water pollution sample that was activated with a ^{252}Cf neutron source.

EXPERIMENT 18.1

Source Excited X-Ray Fluorescence in Environmental, Biological, and Geological Samples

Experimental Procedure

1. Set up the electronics as shown in fig. 18.1. Use 1024 channels of the MCA and calibrate it so that 25 keV is full scale. This will give a slope to the calibration curve of 25 eV per channel.

2. The instructor will load the excitation source in the chamber. Place the first four samples that you wish to study in the XRF activation chamber and evacuate. These samples can be from a wide variety of materials. Fluoresce the first sample for a period of time long enough to get reasonable statistics in the peaks of interest.

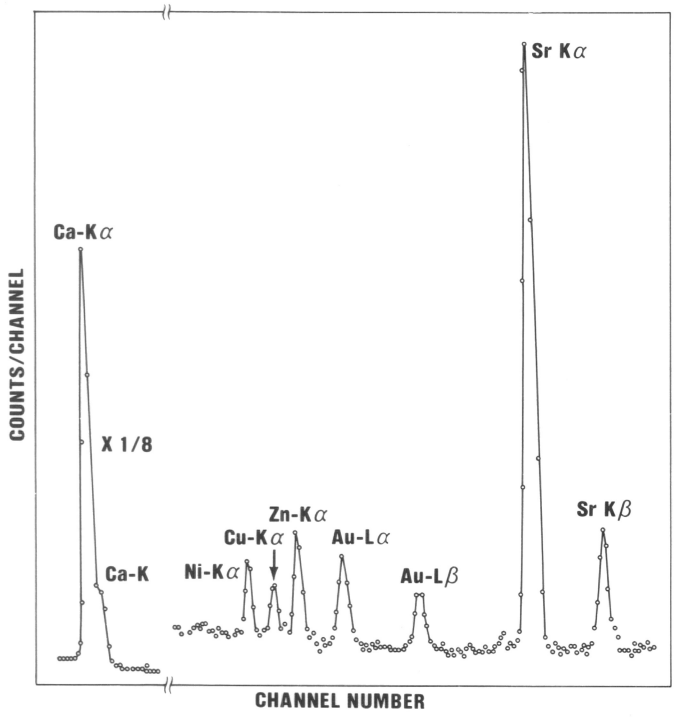

Figure 18.10. X-ray fluorescence spectrum of household water pipe scale. The excitation source was ^{109}Cd.

3. If the materials being fluoresced are thin samples, the quantitative analysis of the results can also be easily obtained. For example, fig. 18.10 shows a spectrum of household water pipe scale that was powdered and spread out on a piece of filter paper as a thin sample. The amount of Sr in the sample can be determined by fluorescing a Sr standard under the same conditions. The standards that can be provided for this experiment have been assigned their values based on a direct comparison

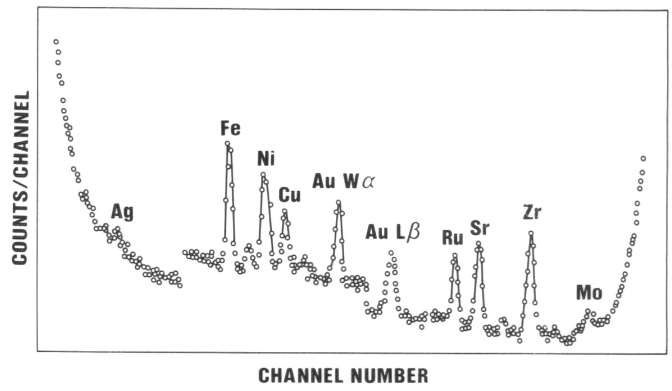

Figure 18.11. ^{109}Cd x-ray fluorescence spectrum of a National Bureau of Standards ore sample. (Note, the concentrations of all of the elements in this standard are known.)

to a National Bureau of Standards sample of that particular element which has been calibrated to a high degree of accuracy. Figure 18.11 shows a ^{109}Cd excited NBS ore sample. This sample can be used to quantify other results since the concentrations of the observed elements are very well known for this specimen. Figure 18.12 shows a ^{109}Cd excited spectrum of an ordinary postage stamp. Figure 18.13 is a spectrum of volcanic ash that was excited with an ^{55}Fe source. The Mn Kα and Kβ peaks in the spectrum are produced by the elastic scattering of the source x-rays. The Ti, Ca, K, Si, and Al peaks are from the sample. As was mentioned above, once this source excited system is in operation, samples in a wide variety of disciplines can be analyzed both qualitatively and quantitatively.

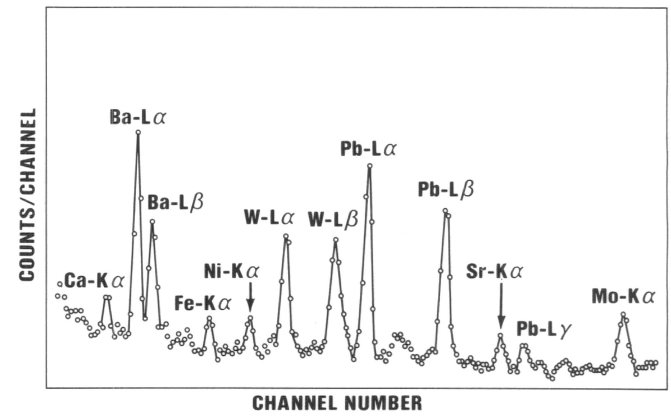

Figure 18.12. ^{109}Cd x-ray fluorescence spectrum of a postage stamp showing the trace elements in the ink and paper.

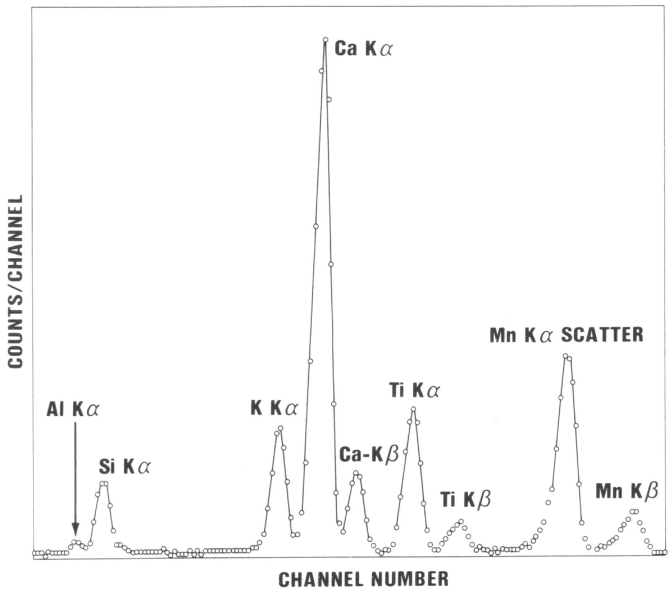

Figure 18.13. ^{55}Fe x-ray fluorescence spectrum of volcanic ash.

EXPERIMENT 18.2

Tube Excited X-Ray Fluorescence Analysis

Experimental Procedure

1. Use the calibration procedure that was outlined in the instruction manual to calibrate the system so that x-rays up to 20 keV can be measured.

2. Load the first ten air pollution filter samples in the chamber and evacuate. Fluoresce each sample for a period of time long enough to obtain reasonable statistics in the peaks of interest.

3. Use the data processor and *instrument software to* obtain the concentrations of each element of interest in the samples. Calculate the number of $\mu g/cm^2$ of the various elements in the sample. Figure 18.14 shows typical results of an air pollution filter. Figure 18.15 shows a powdered camellia leaf with various concentrations of the trace elements present in the leaf. As we mentioned

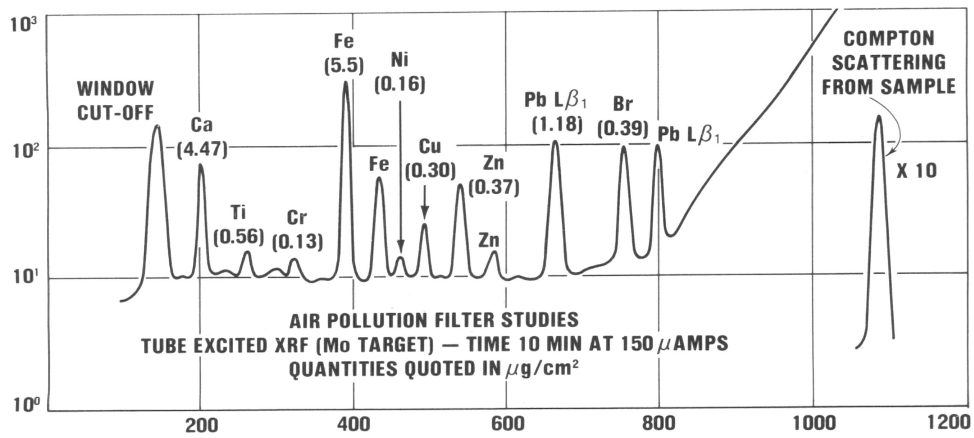

Figure 18.14. Tube excited pulse height spectrum of an air pollution filter sample. (This spectrum was provided by Lawrence Berkeley Laboratory)

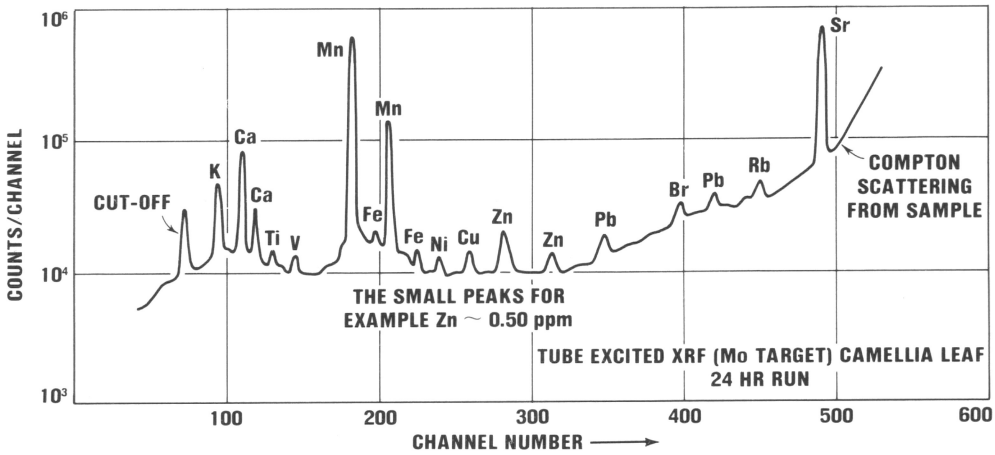

Figure 18.15. Tube excited pulse height spectrum of a camellia leaf. (This spectrum was provided by Lawrence Berkeley Laboratory)

before, and as in the case of source excited XRF, once this tube excitation apparatus has been installed, there is really no limit to the kinds of samples that can be analyzed with it. These experiments represent the best applications of nuclear techniques being applied directly to help solve scientific problems.

EXPERIMENT 18.3

Trace Element Studies by Neutron Activation Analysis

Experimental Procedure

1. Set up the electronics as shown in fig. 15.4 if you wish to use a NaI(Tℓ) detector for the experiment. If a germanium detector is to be used, the electronics are the same except for the detector.

2. Use ^{60}Co, ^{137}Cs, and ^{65}Zn sources to calibrate the system so that full scale is 1.5 MeV. For the NaI(Tℓ) system 512 channels are adequate for the MCA. If you are using a germanium detector 2000 or 4000 channels should be used.

3. Activate the sample for an appropriate length of time. This time was discussed somewhat in detail in the NAA experiment (No. 15). It depends on the half lives of the elements of interest in the sample and the flux ϕ of the neutron source. All of these points and the selected "wait time" were discussed in experiment 15.

4. Count the sample for a period of time long enough to obtain reasonable statistics in the peaks of interest in the spectrum. Use the NAA reference material and eq. (1) through (9) in experiment 15 to determine what elements are present and their concentrations. Figure 18.6 shows a germanium pulse height spectrum of an NBS ore sample that clearly shows Mn and W lines. This sample is an excellent one to check the qualitative and quantitative accuracy of your system since the concentrations of the two trace elements are known to a high degree of accuracy. As in the case of X-ray Fluorescence, Neutron Activation Analysis is a nuclear analytic technique that can be used for a variety of trace element studies.

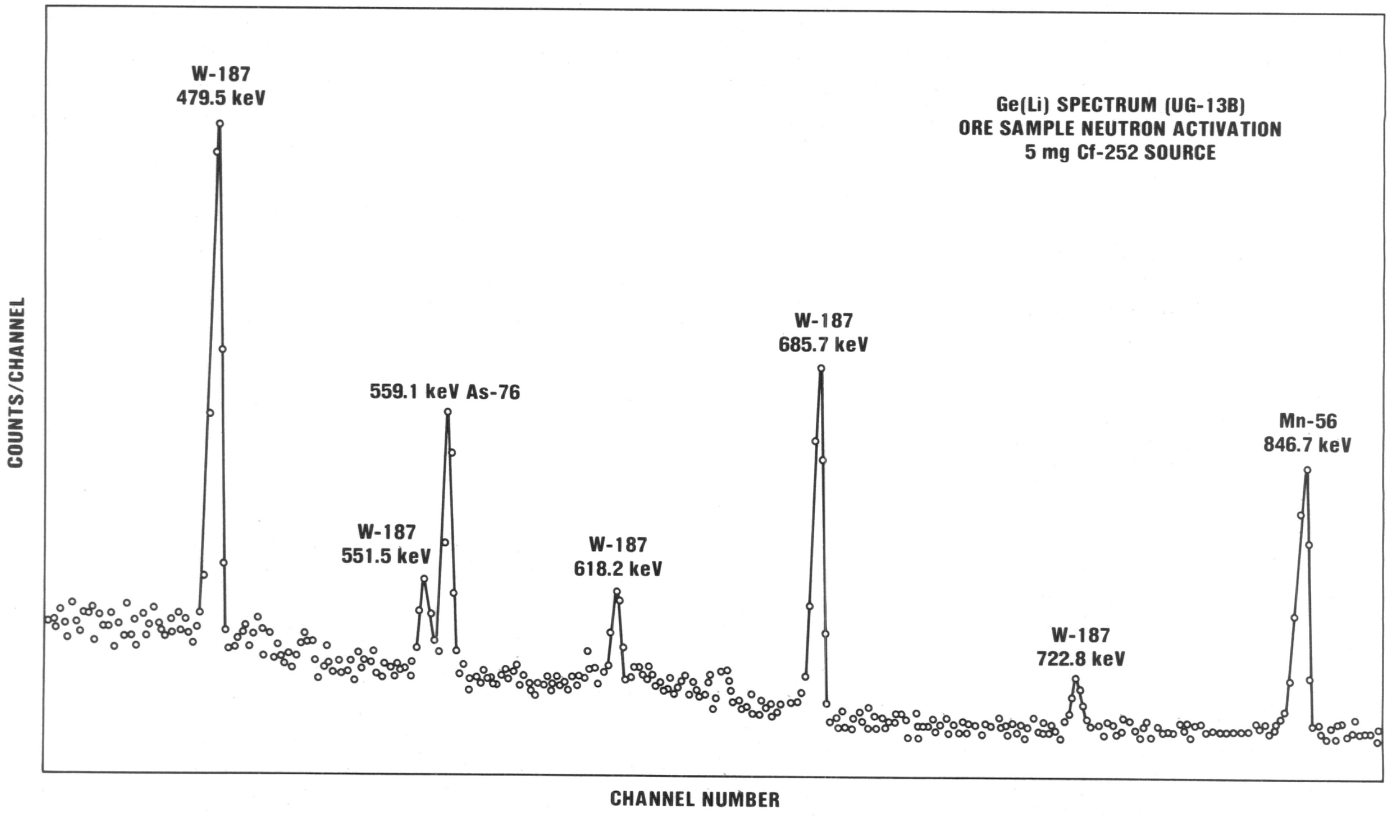

Figure 18.16. Neutron activated germanium pulse height spectrum of a National Bureau of Standards ore sample. (The elemental concentrations in this sample are well known.)

REFERENCES FOR *EXPERIMENT 18*

1. G. F. Knoll, *Radiation Detection and Measurement*, John Wiley and Sons, New York (1979).

2. K. Siegbahn, Ed., *Alpha, Beta and Gamma Spectroscopy*, North Holland Publishing Co., Amsterdam (1968).

3. C. M. Lederer and V. S. Shirley, Eds., *Table of Isotopes*, 7th Edition, John Wiley and Sons, Inc., New York (1978).

4. *Radiological Health Handbook*, U.S. Dept. of Health, Education, and Welfare, PHS Publication 2016. Available from National Technical Information Services, U.S. Dept. of Commerce, Springfield, Virginia.

5. W. Mann and S. Garfinkel, *Radioactivity and Its Measurement*, Van Nostrand-Reinhold, New York (1966).

6. J. L. Duggan, F. D. McDaniel, and J. G. Hehn, Advanced Experiments in Nuclear Science. National Science Foundation Project in *Nuclear Science Education*, published by North Texas State University Press 1978.

7. J. M. Jaklevic and F. S. Goulding, "Semiconductor Detector X-Ray Fluorescence Spectrometry Applied to Environmental and Biological Analysis, *IEEE Trans. Nucl. Sci.* **NS-19** (1972).

8. R. Dams, J. A. Robins, K. A. Rahn, and J. W. Winchester, "Non-Destructive Neutron Analysis of Air Pollution Particles," *Anal. Chem.* **42**, 861-867 (1970).

9. W. H. Zoller and G. E. Gordon, "Instrumental Neutron Activation Analysis of Atmospheric Pollutants Utilizing Ge(Li) Gamma-Ray Detectors," *Anal. Chem.* **42**, (1970).

10. J. V. Lagerwesff and A. W. Spech, "Contamination of Roadside Soil and Vegetation with Cadmium, Nickel, Lead, and Zinc," *Environ. Sci. and Tech.* **4**, 583 (1970).

11. D. Gray *et. al.*, "Determination of Trace Element Labels in Atmospheric Pollutants by Instrumental Neutron Activation Analysis," *IEEE Trans. Nucl. Sci.* **NS-19**(1), 194 (1972).

12. J. W. Nelson *et. al.*, Report of the Workshop on Nuclear Techniques for Environmental Trace Element Information Relative to Energy Production and Consumption (1974). National Technical Information Services, Dept. of Commerce, Springfield, Virginia.

13. R. D. Giaugue and J. M. Jaklevic, "Rapid Quantitative Analysis of Air Pollution Particles," available as Report No. LBL-204 from Lawrence Berkeley Laboratory, Berkeley, California.

EXPERIMENT 19

Experiments in Health Physics and Radiation Protection

Scope

It was mentioned in the introductory section of this manual that good health physics practices should be used when radioisotopes are being studied in the laboratory. In this experiment we are going to study a few of the basic problems of radiation protection.

Discussion

In the eighteen experiments that precede this one, various radioactive sources are studied. For the most part these are α, β, γ-ray and neutron sources. A short description and some relative hazard information will be given in regard to each of these sources. This information has been taken from various Department of Energy tabulations in regard to radiation safety.

Alpha Radiation

Alpha particles, which lose energy rapidly in any medium because of their relatively high specific ionization, can be stopped by very thin absorbing materials. A few sheets of paper or thin (less than 1/64 in.) aluminum foils will absorb alphas from emitting sources. The most energetic alphas will travel only a few centimeters in air. The outer layer of skin (about 7 mg/cm^2) on our body will absorb α particles up to about 7.5 MeV. Since this is dead tissue, no harmful effect is produced upon the body. Therefore, α radiation is not considered an *external* exposure problem.

Beta Radiation

The processes by which β particles lose energy in absorbers are similar to those for alphas. However, an additional process must be considered in dealing with β absorption. This is the process whereby electromagnetic radiation, called bremsstrahlung, is produced.

A β particle has a very small mass and one-half the value of the charge on an α particle. So, for a given energy, a β particle will have a much greater velocity than an α particle. As a result of these and other factors, the β particle has a lower specific ionization which means that its penetration in any absorber will be much greater than that of an α particle.

A 1-MeV β particle will travel about 10 feet in air. In order to penetrate the dead layer of skin, a β particle must have an energy of about 70 keV. Beta radiation is considered a slight *external* hazard.

The thickness and choice of material for shielding from beta radiation depends upon: (1) stopping the most energetic β's, and (2) bremsstrahlung.

The shielding thickness which is necessary to stop β particles of a given energy will decrease with increasing density. For example, about 0.1 inch of aluminum (ρ = 2.7 gm/cm^3) will stop 1.5 MeV beta, whereas only about 0.024 inches of lead (ρ = 11.3 gm/cc) is needed for the same purpose.

However, the production of bremsstrahlung increases with increasing atomic number of absorber. A β source with E_{max} = 1 MeV will lose about 3% of its energy as bremsstrahlung when lead (Z = 82) is the absorber. If aluminum (Z = 13) is the absorber, the fraction is about 0.4%. Therefore, low-Z absorbers such as aluminum, plastics (Lucite), or even glass are effective β shields. We will study the shielding effect for aluminum in Experiment 19.9.

Radiation Production — Bremsstrahlung

In addition to that energy lost in ionization and excitation by an electron in passing through matter, some energy may be given up in the form of x-rays produced in the substance as a result of interactions between high-speed electrons and nuclei of the absorbing substance. The x-ray spectrum which is obtained in these interactions is called bremsstrahlung (literally, braking radiation). The interactions leading to the production of bremsstrahlung are inefficient for electron energies below 1 MeV. As the energy increases above 1 MeV, the production of x-rays becomes increasingly greater.

When a charged particle is either accelerated or decelerated in an electric field, electromagnetic radiation may be given off. If an electron passes close to an atom while traversing a substance, the charge Z on the nucleus will exert a force on the electron. This will cause its path to be bent. During this acceleration, the electron may radiate energy of any amount from zero up to its total kinetic energy E_k. The total bremsstrahlung per atom is roughly proportional to $(Z/m)^2$, where Z is the atomic number of the absorbing matter and m is the mass of the charged particle. Because of a $1/R^2$ dependence, the amount of bremsstrahlung is almost completely negligible for all particles except electrons.

The beta particle is not as great an internal hazard as is the alpha particle. A beta will have much greater range in tissue, but the specific ionization will be less than that of alpha. Not as much energy is given up in a small volume of tissue as by an alpha. Thus, it will not be as effective in causing damage.

Gamma and X Radiation

Gamma rays do not lose energy continuously, in traversing a medium, as will α or β particles. As a result, γ rays are much more penetrating than α or β radiation. Gamma radiation is attenuated in matter by : (1) the photoelectric effect, (2) Compton effect, and (3) pair production.

As we mentioned earlier, X rays almost always interact by the photoelectric effect. Most of the gamma sources used in this manual are less than 10 μCi. These sources, in general, do not present a radiation hazard without a shield. Sources greater than 1 mCi, however, are called high intensity sources. For these high intensity sources, X and γ rays are of most concern as potential external hazards. These rays have great ranges in air and other substances, and may present a significant hazard (for high intensity sources) at fairly large distances from a source. In most cases shielding is needed to insure that no hazard exists. The shield which is required is much greater than for either alpha or beta radiation. Also, scattered rays from a source may contribute to the hazard, that is, a shield may provide good protection in one direction, but scattered rays from this shield may cause a hazard to exist in another area. Any cracks or breaks in an otherwise adequate shield may lead to streaming or beams of radiation.

X and γ radiation are not as great an internal hazard as are alpha or beta radiation. As is the case with beta radiation, the long range of gamma in tissue means that less energy will be given up in a small volume of tissue. A photon will give up energy only when it interacts. It does not produce a continuous path of ionization as do alpha and beta particles. For this reason, a small organ in the body will receive less damage from a gamma source than an equal alpha or beta source.

Neutrons

Neutrons, like gammas, are a highly penetrating form of radiation. They possess no charge and, therefore, are unaffected by the electric fields of atoms in the traversed medium.

Neutron attenuation is accomplished mainly through elastic and inelastic collisions which reduce the energy of the neutrons until they are absorbed in the medium. In many cases, penetrating γ rays are produced as a result of neutron absorption.

Along with gamma rays, neutrons are of most concern as potential external hazards. Since neutrons possess no charge, they travel great distances in air and other substances. Thus, it is more difficult to provide shielding for neutrons than for alpha or beta particles. As for gamma rays, scattered neutrons can add to the hazard.

The neutron source used in this manual is a 1 Ci Am-Be source. The instructor should transfer it to the activation chamber with a long pair of tongs or other means suggested by the source manufacturer. Once the source is in the chamber, it can be used by the students. Very little exposure will be received by the student during the experiment. As we mentioned earlier, universities all over the world have been safely doing these neutron activation experiments for over 20 years.

EXPERIMENT 19.1

A Study of the Efficiency of a GM Counter for Gammas and Betas

Experimental Procedure

1. Set up the GM system (Fig. 19.1) as we did for experiment number 1. (Note: A GM radiation survey meter may also be used for this experiment). Adjust the voltage of the G.M. tube to its operating value.

2. Place the 1 μCi ^{137}Cs source on the *second shelf* and count for 1 minute. Record this value in Table 19.1 as Beta and Gamma (trial 1) and record the average cts/min.

3. Place a 1/8 inch piece of aluminum on shelf (between the source and the detector) number 1. This thickness of aluminum is greater than the range of the 514 keV beta from ^{137}Cs but will not appreciably attenu-

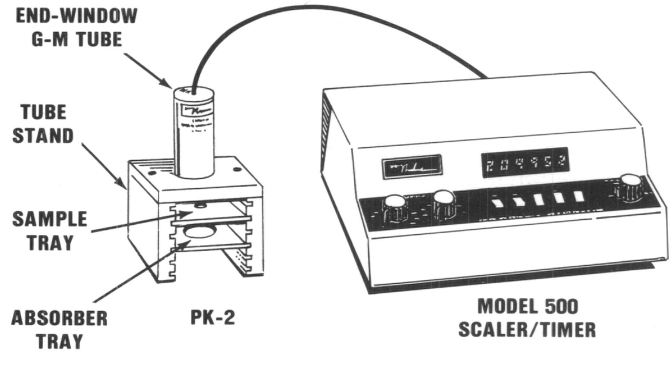

Figure 19.1. Electronics for GM counting.

Table 19.1 GM Relative Efficiency Data

Radiation	Cts/Min (Trial 1)	Cts/Min (Trial 2)	Cts/Min (AV)
Beta and Gamma			
Gamma Only			
Beta Only			

ate the 662 keV gammas from the source. (See the decay scheme fig. 19.2) Make two independent 60 second measurements with this beta shield in place. Record the average in Table 19.1 as gamma only.

Exercise A Subtract the *Gammas only* from the *Beta and Gamma* count to get the actual number of Betas and record. Since the GM tube is nearly 100% efficient for betas, this number represents the number of betas that impinge on the window of the GM tube. How does this number compare to the theoretical number that you calculate from the ^{137}Cs source activity and the geometry?

Exercise B *Relative Efficiency of GM Tube for Gammas.* This number is calculated by taking the ratio of gammas counted to the theoretical number that impinge on the face of the tube. From this experiment the student should gain some familiarity with beta absorbers and GM efficiencies. The portable GM counter or survey meter is one of the basic instruments used in Health Physics monitoring.

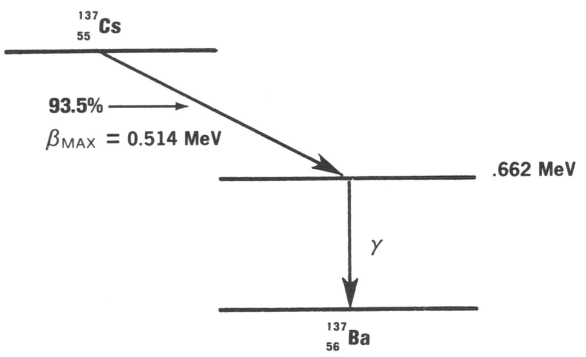

Figure 19.2. Decay scheme for ^{137}Cs (simplified).

EXPERIMENT 19.2

Beta Backscattering as a Function of Atomic Number

Discussion

When you are trying to measure a beta emitting source, the environmental surroundings are important. For example, let's assume that at a reactor site some beta activity has spilled on a steel pipe. The measurement that was made with a portable GM counter would have to be corrected for beta backscattering for Iron. This experiment is designed to give the student an overview of this backscattering phenomena and how it can affect the observed counting rate from the source.

Experimental Procedure

1. Use the same GM electronics (fig. 19.1) that was employed in the last experiment. (If you wish, a portable GM counter or survey meter may also be used).

2. Place the ^{204}Tl source (see fig. 19.3 for its decay scheme) on the third shelf of the GM assembly. Count for 60 seconds and record in Table 19.2 as (NONE).

3. Place the aluminum backscattering sheet from the backscatter kit (see Table 19.2) in contact with the source to enhance backscattering. Count for 60 seconds and record in Table 19.2. Repeat for the other materials in the kit and fill in the rest of the Table.

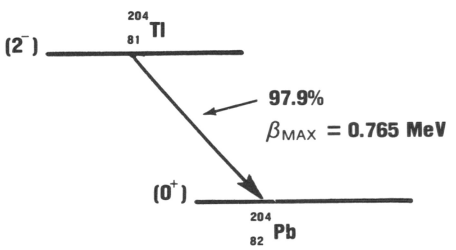

Figure 19.3. Beta decay scheme for ^{204}Tl.

Table 19.2 Data for Beta Backscattering Analysis

Run No.	Backscattering Material	Atomic Number	Cts/Min (Gross)	Backscattering Factor
1	None			
2	Aluminum			
3	Iron			
4	Copper			
5	Cadmium			
6	Molybdenum			
7	Tungsten			
8	Lead			

Exercise A From the known activity of the ^{204}Tl source and the fact that the GM counter is almost 100% efficient for a pure beta source, calculate the counts/minute that you would expect for the geometrical set up being used. How does your answer compare to the measurement made with no backscatter?

Exercise B The Backscattering Factor (BF) is defined to be the ratio of counts/minute with a scatterer, divided by the counts/minute without a scattering medium. Calculate this value for each of the measurements and fill in Table 19.2. Calculate the percent backscattering from your data and plot this value (y axis) as a function of the atomic number of the backscattering material. Figure 19.4 shows a plot of some typical experimental data.

EXPERIMENT 19.3

The 1/R² Relationship for An Intense Gamma Source

Experimental Procedure

Caution: The sources used for this experiment are, in general, ^{137}Cs with activities from 20 μCi to 10 mCi. The instructor should use tongs to place the source in its proper position. The measurements that are made close to the source, 50 cm and 100 cm, should be made as rapidly as possible to minimize exposure to the student. (After all, this is a Health Physics Experiment).

1. The instructor will place the ^{137}Cs source in its proper position for the experiment. A 1/8 inch piece of aluminum should be placed between the source and the detector to shield out the beta.

2. The best instrument to use for this experiment is a GM assembly such as fig. 19.1. A NaI(Tℓ) scintillation system can also be used.

3. The GM detector should always be arranged such that the gammas enter the detector perpendicular to the window. Place the detector 50 cm from the source and count for 60 seconds. Record your uncorrected counting rate in Table 19.3.

4. Move the GM detector to a distance of 100 cm and count for a long enough period of time to obtain a good statistical counting rate. Repeat for the other distances in Table 19.3.

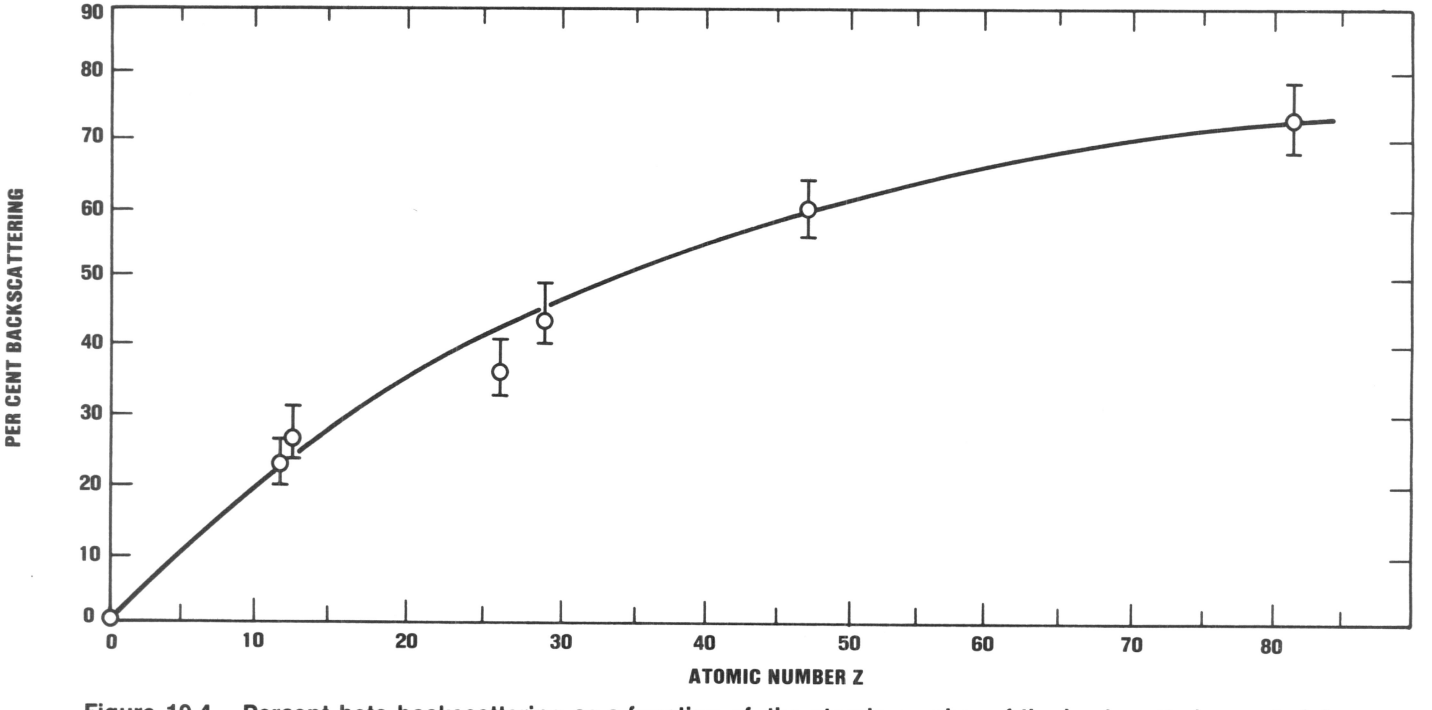

Figure 19.4. Percent beta backscattering as a function of the atomic number of the backscattering material.

Table 19.3 Data for $1/R^2$ Determination of an Intense Gamma Source

Run No.	Distance (cm)	Counting Rate Cts/Min (uncorrected)	Counting Rate Cts/Min (corrected)
1	50		
2	100		
3	150		
4	200		
5	250		
6	300		
7	350		
8	400		

5. After these measurements are made, the instructor will remove the source. Take a background count for a period of time long enough to get good statistics. Correct the counting rates and record them in Table 19.3. If this GM tube has a known resolving time, you can also include this correction (see Experiment #1).

Exercise On linear paper, plot counting rate (corrected) on the y axis versus $1/R^2$. Because of air scattering, this relationship will deviate from a straight line. Does the deviation seem reasonable?

In this experiment we placed a 1/8" piece of Aluminum between the source and the detector to shield out the high energy betas from the source. Table 19.4 shows the maximum Range of betas in air. From this table, it can be seen that the maximum Range of betas from the ^{137}Cs source is slightly greater than 150 cm. If we had not used the aluminum beta shield, our measurements at 50 cm, and possibly 150 cm, would be in error because of the Range of the betas in air.

Figure 19.5 shows the Range of betas in other common shielding material.

As we will see in the next experiment, gammas or electromagnetic radiation is much more penetrating and, in general, high atomic number (Z) shields are desirable. Figure 19.6 shows the Half Value Layers (HVL) of some of the above materials for gammas.

Table 19.4 Range of Beta Particles in Air

Energy (Million of Electron Volts)	Maximum Range of Beta Rays in Air (Meters)
0.01	0.0022
0.02	0.0072
0.03	0.015
0.04	0.024
0.05	0.037
0.06	0.050
0.07	0.064
0.08	0.080
0.09	0.095
0.10	0.11
0.15	0.21
0.2	0.36
0.3	0.65
0.4	1.0
0.6	1.8
0.8	2.8
1.0	3.7
1.5	6.1
2.0	8.4
3.0	13.0
4.0	16.0
5.0	19.0

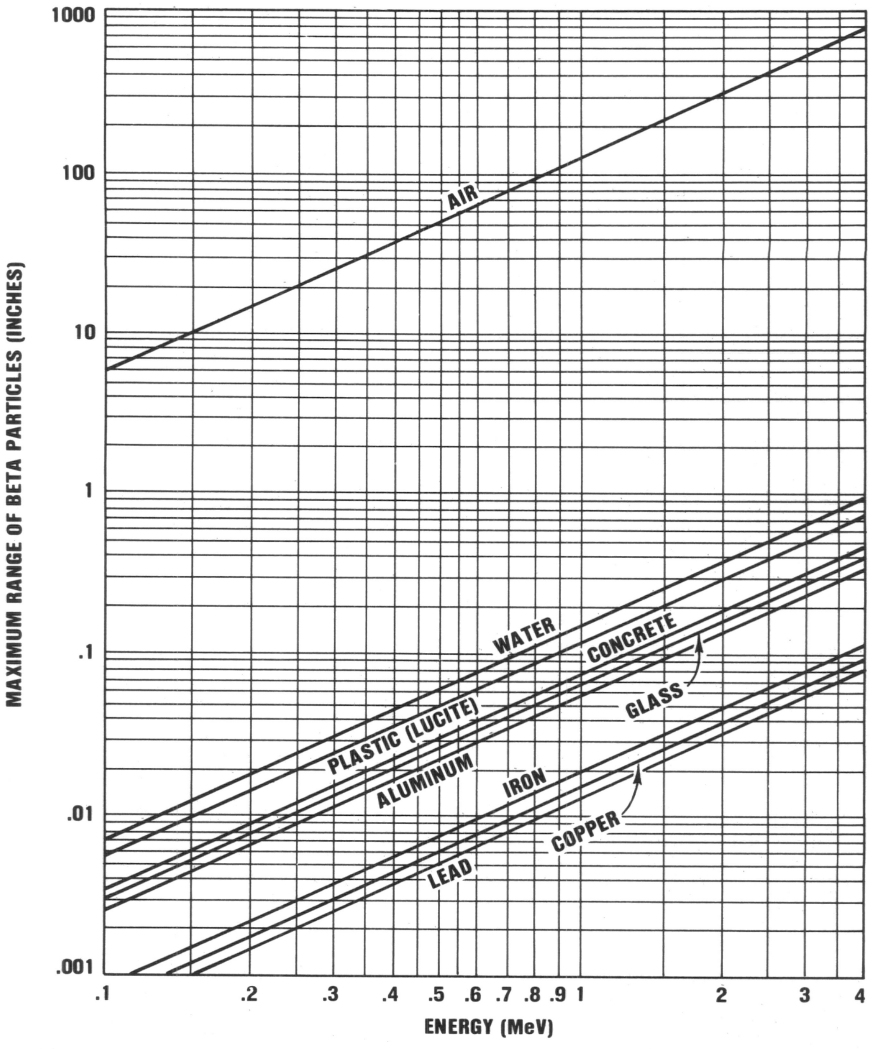

Figure 19.5. Beta ranges in common shielding materials and air. (Taken from the NBS Radiological Health Handbook, now out of print.)

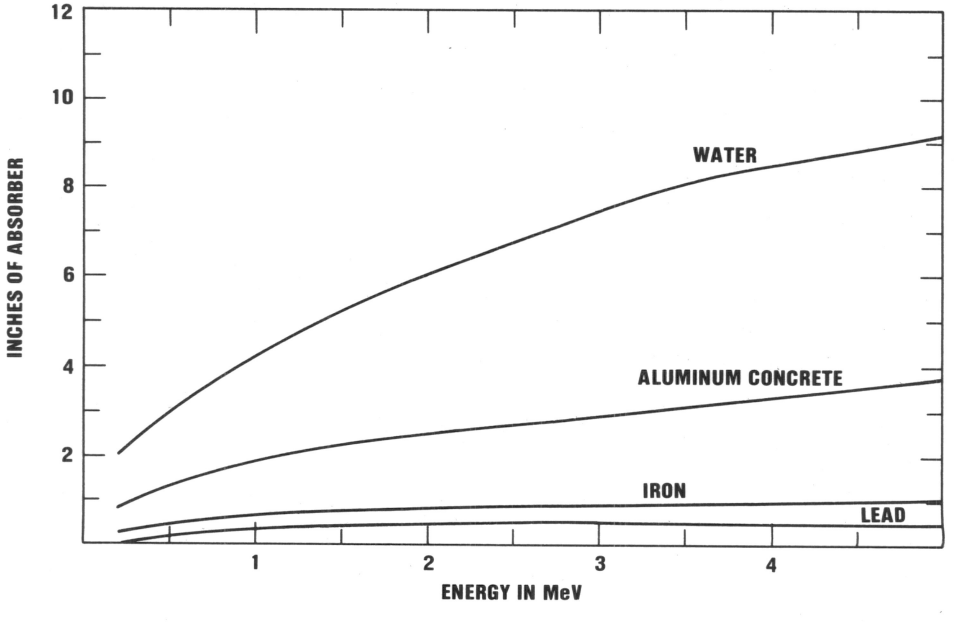

Figure 19.6. Half Value Layers (HVL) for various shielding material for gammas or x-rays.

EXPERIMENT 19.4

The Analysis of Gamma Shielding Material

Discussion

In various places in this manual, the attenuation of gammas and x-rays have been discussed. Photons interact in matter by: Photoelectric, Compton, and Pair Production. In lead (see fig. 19.7), for example, the Photoelectric and Compton or Scattering cross sections are roughly equal at 400 keV. This indicates that below 400 keV the Photoelectric effect clearly dominates. At 4 MeV, the Compton and Pair Production cross sections are equal. This means that the Compton interaction is the most pronounced effect between 400 keV and 4 keV. Of course, Pair Production clearly dominates above 4 MeV. The total Attenuation Coefficient or cross-section is, for the most part, the sum of the three individual cross-sections. It is also shown in fig. 19.7. The peak in the Photoelectric cross-section at 88 keV is there because this is the value of the K shell electron binding energy for lead. Remember, the Photoelectric Interaction is a quantum type collision between the incident photon and a tightly bound electron in the medium. Photons lower in energy than 88 keV (this quantity is called K_{ab} in Appendix B) do not have enough energy to remove the K shell electron. The Photoelectric effect must therefore occur with an L shell electron. The probability of this happening is about 20% of the K-shell cross-section; therefore, the dip in the curve at 88 keV. There is another depression in the curve at around 15 keV which is the corresponding L shell binding energy for Lead.

The analytic expressions for the various cross-sections will reveal how these values change with energy, mass (M) and atomic number (Z) of the absorbing medium. These expressions are given by:

Photoelectric Cross Section (σ_{PE})

$$\sigma_{PE} \propto 1.07 \times 10^{-32} Z^5 f \left(\frac{0.51}{E\gamma}\right)^{7/2} \text{ (All energies)} \quad (1)$$

$$\text{where } f = 0.1 + 0.3 \text{ Log}_{10}\left(\frac{E\gamma}{E_k}\right) \text{ when } \left(\frac{E\gamma}{E_k}\right) < 1000 \quad (2)$$

$$f = 1 \text{ if } \left(\frac{E\gamma}{E_k}\right) > 1$$

where $E\gamma$ is the photon energy in MeV, and E_k is the binding energy in MeV of the K shell electron in the medium.

Therefore, for photon energies less than 100 keV, the photoelectron cross section may be approximated:

$$\sigma_{PE} \propto \left(\frac{Z^5}{E\gamma^{7/2}}\right) \text{(Photon energies less than 100 keV)} \quad (3)$$

Equation (3) is also approximately correct for the whole photoelectric realm. Remember, from what was said above, σ_{PE} is the dominant interaction mechanism for photon energies below 400 keV. We certainly saw this in experiment No. 2 when the NaI(Tℓ) spectra were analyzed.

The Compton Cross Section (σ_c)

$$\sigma_c \propto \sigma_c \text{ Log}_{10}\left(\frac{E\gamma}{m_oc^2}\right) + .475 \quad (4)$$

where m_oc^2 = .511 MeV and $E\gamma$ values are in MeV and

$$0.1 < \frac{E\gamma}{m_oc^2} < 10$$

σ_o = The Classical Thompson Scattering Cross Section (see Experiment 9).

Since σ_o depends on the number of scattering electrons in the sample, it can be shown that:

$$\sigma_c \propto Z/M \text{ (Where M is the mass of the absorbing atom)} \quad (5)$$

In summarizing, the Compton Interaction is the dominant interaction mechanism for photons between 400 keV and 4 MeV and is proportional to Z/A.

Pair Production Cross Section (σ_{PAIR})

$$\sigma_{PAIR} \propto \text{Ln}\left(\frac{2E\gamma}{m_oc^2}\right) - K_1$$

Remember the Pair Production cross-section is zero for photon energies less than 2 m_oc^2 (1.02 MeV). It is, however, the dominant interaction mechanism for photons greater than 4 MeV in energy.

In this experiment, we are going to test the above equations by measuring the attenuation of gammas in various shielding materials that are found in the *shielding absorber kit set.* These materials are: Aluminum (Z=13), Iron (Z=26), Cadmium (Z=48), Tungsten (Z=74), and Lead (Z=82).

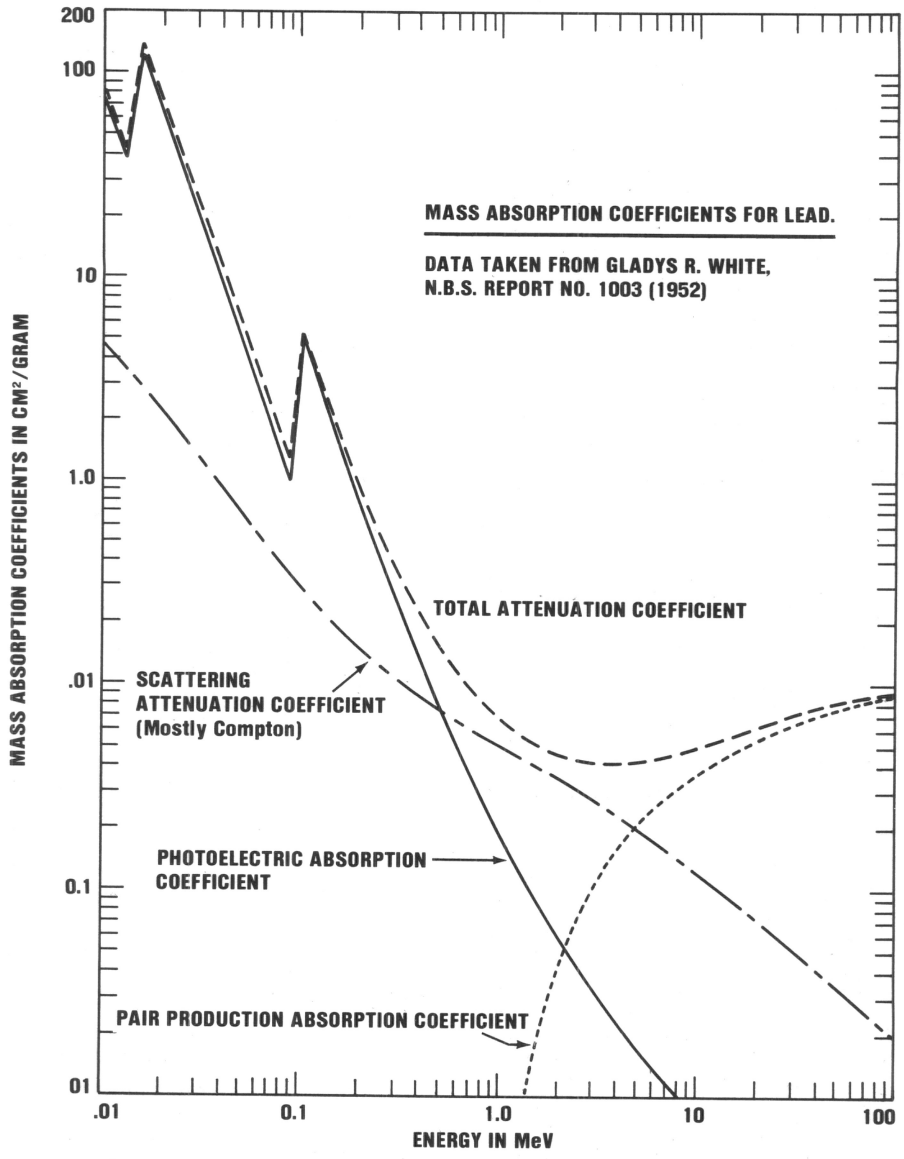

Figure 19.7. Mass absorption coefficient (cross-section) for photons in lead. (Taken from the NBS Radiological Health Handbook, now out of print.)

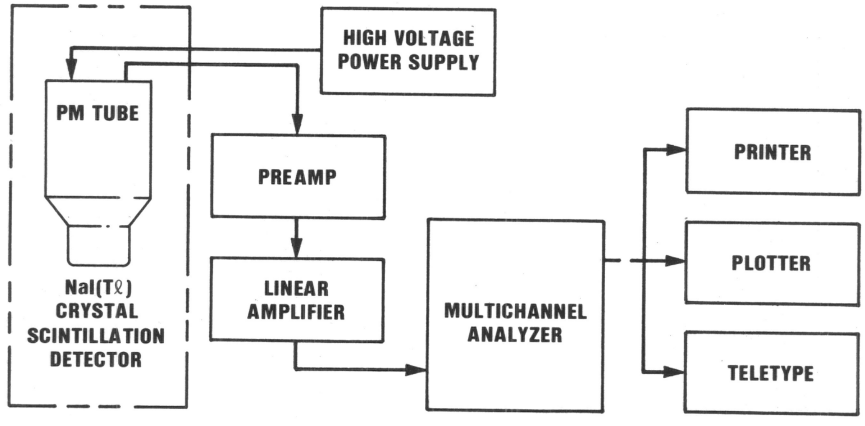

Figure 19.8. Components of a typical gamma spectrometry system (printer, plotter and teletype are optional).

Experimental Procedure

1. Set up the NaI(Tℓ) Scintillation Spectrometer as shown in fig. 19.8. Calibrate the system from zero to 2 MeV (see Experiment 2 for details).

2. Place a 1 μCi ^{137}Cs source on the last shelf of the assembly. Count for a long enough time to get an integrated count (the total spectrum) of 10,000 counts. Calculate the number of cts/sec. Place the thinnest lead absorber between the source and the detector and count long enough for good statistics and calculate the number of cts/sec.

3. Continue for enough lead thicknesses to plot an attenuation curve for lead. Remember, for the thicker absorbers, the counting time will have to be increased for good statistics.

4. Continue these measurements for all of the other absorbers in the kit. Plot attenuation curves for each of the five elements in the kit.

5. Remove the 1 μCi ^{137}Cs source and replace it with a ^{57}Co source of 1 μCi. Remember, the primary gamma energy for ^{57}Co is 122 keV. This energy is in the region where the Photoelectric Effect is dominant. Repeat all of the measurements made above with this ^{57}Co source. Make plots of cts/sec (y axis) as a function of g/cm^2 of the absorber for each of the samples as you did for lead.

Exercise A For the ^{137}Cs source measurements, calculate the half value layer and the mass absorption coefficient (see Experiment 2) for each sample. How do your results compare to fig. 19.7?

Exercise B For the ^{57}Co measurements, calculate the mass absorption coefficient for each element. Since the photon energy is 122 keV, this absorption coefficient or cross-section should be proportional to Z^5. Make a plot of σ_{TOTAL} (y axis) versus Z^5 for the five elements studied. Do your results agree with the theory?

EXPERIMENT 19.5
Radon Counting

Discussion

In recent years, because of Health Physics concerns, the detection and measurement of Radon gas in the home has become a major topic in the United States and other countries containing uranium deposits.

Radon is a radioactive gas produced in the decay chain of natural uranium, which is readily absorbed by activated charcoal. In the course of its decay (see fig. 19.9), Radium B (Lead-214) and Radium C (Bismuth-214) are produced which can be easily detected using conventional gamma-ray spectroscopy. Figure 19.10 shows a NaI(Tℓ) spectrum of the gammas from the decay of Radon-222.

The Nucleus has been involved in the measurement of Radon for many years and has supplied numerous systems to research and commercial testing laboratories for this application. Recent systems are based on the popular Personal Computer Analyzer which converts an IBM-PC or compatible into a full feature multichannel analyzer to perform gamma-ray spectroscopy. Your own NaI(Tℓ) Spectrometer can also be used for the indicated measurements.

Canisters containing a known amount of activated charcoal are exposed to room air and absorb radon over a period of 2-4 days. The canisters are then counted with a NaI(Tℓ) Spectrometer. The gamma spectrometer used to measure the Lead-214 in the canister normally consists of 3" x 3" NaI(Tℓ) scintillation detector housed in a 2" thick lead shield, coupled to a multichannel analyzer. The shield is used to improve sensitivity by reducing natural background radiation.

For accurate results, many correction factors must be applied. These include the amount of moisture absorbed by the charcoal, the exposure time, and the decay of the sample before measurement. (See for example, EPA Report No. 520/5-87-005 which is available from the Nucleus along with other literature and brochures on how to count Radon-222.) To facilitate routine measurement of numerous samples, the Nucleus has developed a software program that runs on the IBM-PC, in conjunction with the Personal Computer Analyzer, and applies all of these required corrections.

Complete single and multiple detector systems are also available from The Nucleus, together with custom low background lead shields. These shields feature ring construction for disassembly and transportation and contain roll-tops for easy sample loading.

These experiments are really quite simple to do. If you wish to do them, write The Nucleus for their brochures on Radon Counting. This literature will provide all of the information needed to make accurate measurements and provide the necessary corrections to produce results that reveal the actual Radon level in the area being tested.

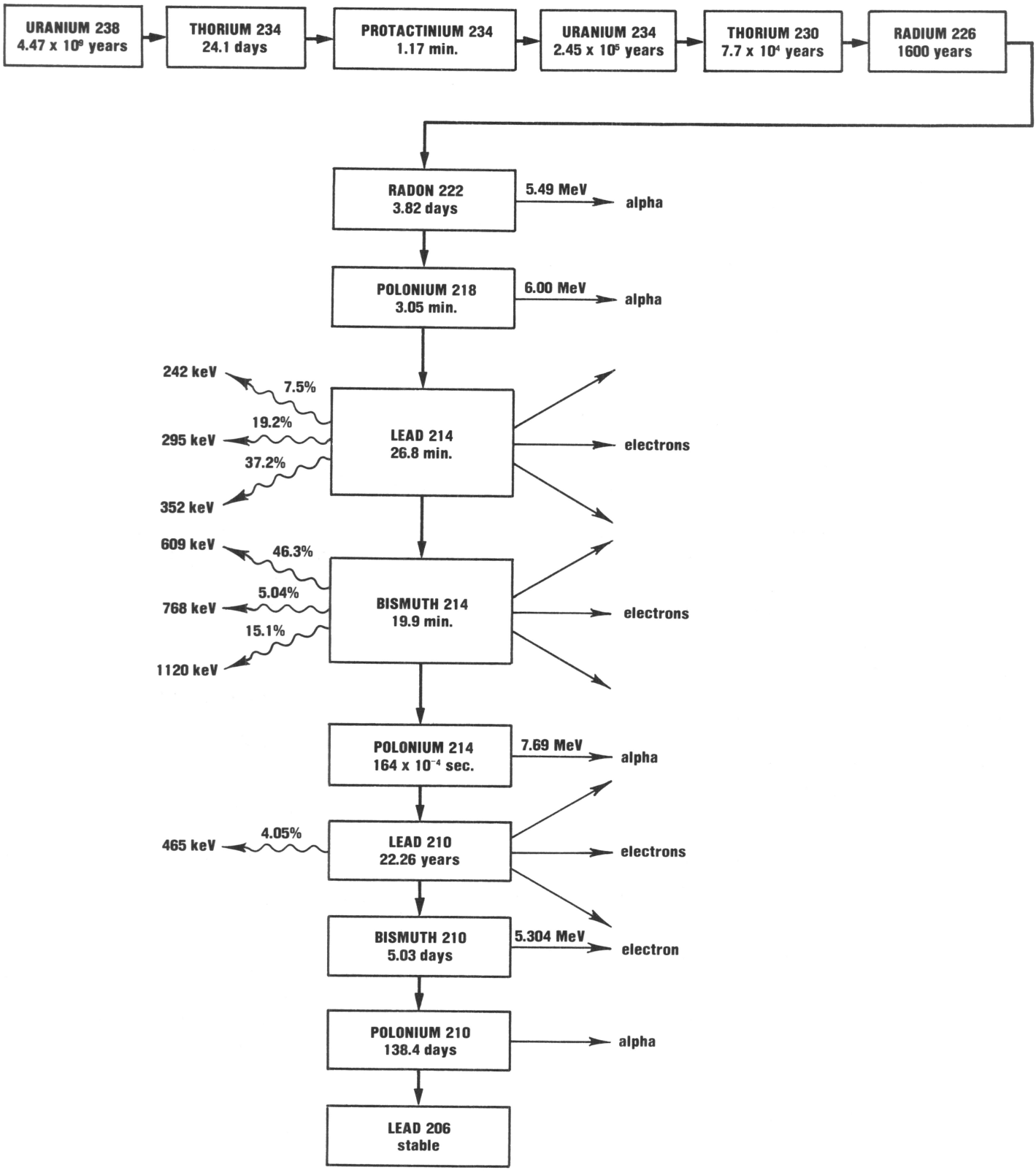

Figure 19.9. Decay scheme of ^{238}U which produces radon- 222. The decay of radon-222 gives lead-214 and bismuth 214 which are easily measured with a NaI(Tℓ) spectrometer.

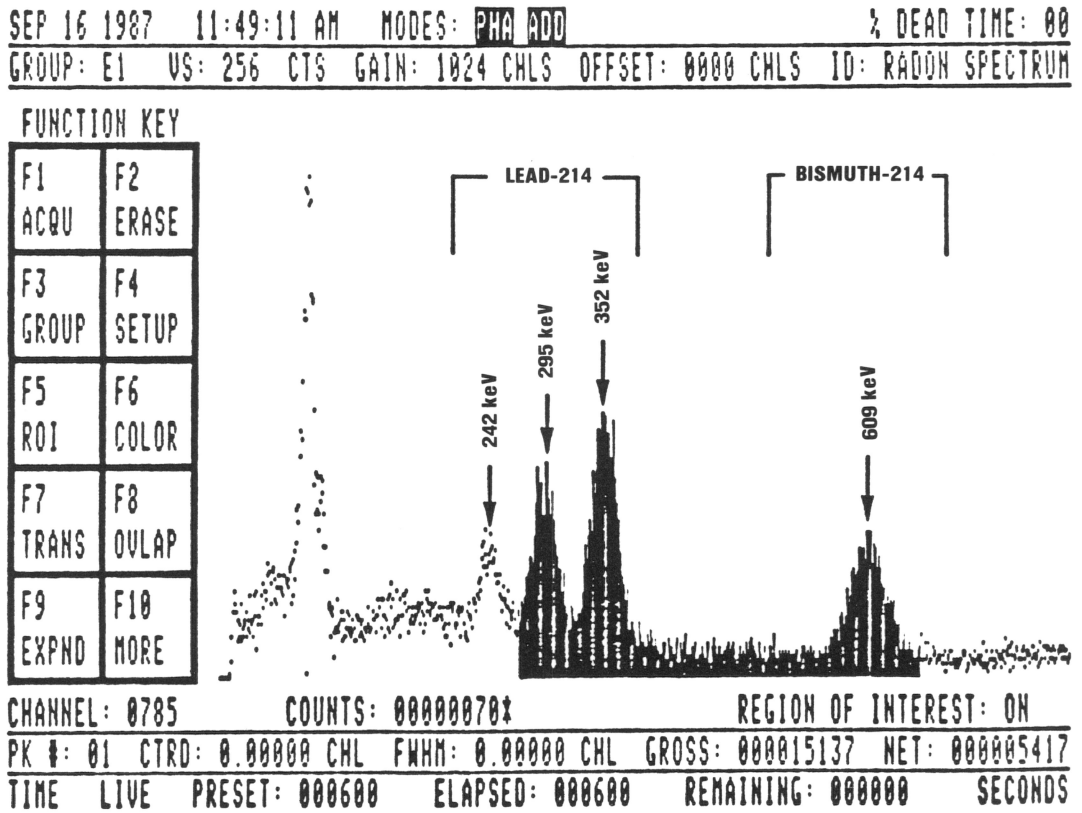
SEP 16 1987 11:49:11 AM MODES: PHA ADD % DEAD TIME: 00
GROUP: E1 VS: 256 CTS GAIN: 1024 CHLS OFFSET: 0000 CHLS ID: RADON SPECTRUM
FUNCTION KEY
F1 ACQU
F2 ERASE
F3 GROUP
F4 SETUP
F5 ROI
F6 COLOR
F7 TRANS
F8 OVLAP
F9 EXPND
F10 MORE
LEAD-214
BISMUTH-214
242 keV
295 keV
352 keV
609 keV
CHANNEL: 0785 COUNTS: 00000070 REGION OF INTEREST: ON
PK #: 01 CTRD: 0.00000 CHL FWHM: 0.00000 CHL GROSS: 000015137 NET: 000005417
TIME LIVE PRESET: 000600 ELAPSED: 000600 REMAINING: 000000 SECONDS

Figure 19.10. NaI(Tℓ) spectrum from ^{222}Ra showing ^{214}Pb and ^{214}Bi gammas from the decay.

Experimental Procedure

1. Set up the NaI(Tℓ) Spectrometer shown in fig. 19.8. Calibrate with known radioactive sources from 0-1 MeV.

2. The charcoal canisters (available from The Nucleus) have previously been placed in the area to be studied and left for several days.

3. The canisters are then counted with the geometry indicated in the literature that is obtained from The Nucleus for your spectrometer.

4. The ^{214}Pb and ^{214}Bi peaks are summed (see fig. 19.10) to obtain the critical photopeak data.

5. Corrections for water vapor, geometry, absorption, etc. are made as outlined in the literature.

Results

After all the corrections are made, a very accurate assay of the number of picocuries/l of ^{222}Ra can be established for each canister studied.

EXPERIMENT 19.6

Low Level Alpha, Beta, and Gamma Counting

Discussion

These Low Level counting systems are usually used to count samples of an environmental nature. Examples are: airborne particulate collection on filter paper, evaporated water residue, food, and soil samples. In the past several years, there has been an increased awareness in the low level activities mentioned above, primarily because of the Chernoble accident. The *Low Level* counting systems that are described in this experiment can give a university science department one of the best opportunities to enter into a meaningful research program. The students that do experiments with these systems will not only learn about "state of the art" Low Level counting, but they will also learn some facts about radiation in our environment.

Theory of Operation

For a low level counting system to be effective, it must possess a low background environment and a high efficiency detector system. A low background environment is achieved in the counting chamber by an effective lead shield and electronically eliminating cosmic ray problems with a guard detector. High counting efficiency is provided by optimizing the counting geometry of the

environmental sample with respect to the proportional counter detector and by providing "state of the art" electronics for processing pulses from the detectors to give a maximum signal-to-noise ratio. Figure 19.11 shows a block diagram of the electronics that are used for the *Low Level* counting system. Basically, alpha and beta pulses from the sample are counted with an ultra thin window, gas flow proportional counter. If a cosmic ray happens to come along, the system is automatically shut off until that disturbance has passed. This is accomplished by the guard proportional counter which is 99% efficient for detecting cosmic radiation. This is the only way to effectively eliminate the cosmic ray background. For example, the cosmic ray background 50 meters underground is still appreciable. The lead shield that is used in the system is for reducing background associated with the natural radioactive background in the environment where the detector is being used.

In Experiment 17 the proportional counter was used to detect low energy x-rays. The basic ideas for detecting alphas and betas are the same as for x-ray photons. When an alpha or beta enters the gas proportional counter, the gas is ionized by removal of one or more electrons from a number of gas molecules.

The collection of these electrons at the anode gives the pulse that is proportional to the energy of the incident charged particle. This charge is converted to a voltage signal by the capacitor shown in fig. 19.12 which is amplified by the electronics shown in fig. 19.11. As you will recall from Experiment 17, the pulse height that is produced is dependent on the operating voltage of the counter. Figure 19.13 shows a plot of output pulse height versus tube voltage for a typical proportional counter.

It should be remembered that for this experiment, the proportional counter voltage must be operated in the proportional region of the curve. If we examine this region more closely for incident alphas and betas a plot of counts above the discriminator level versus voltage is

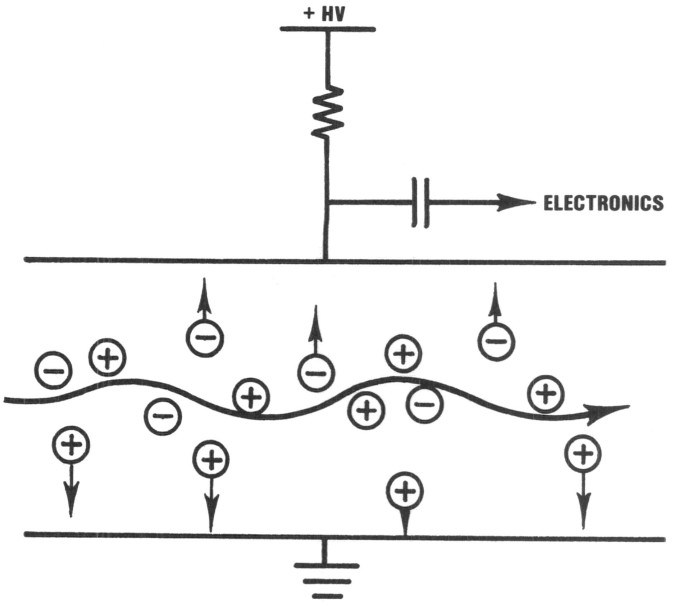

Figure 19.12. A gas filled proportional counter with a charged particle entering from the left. Electrons are attracted to the positive anode while the heavy positive charges are accelerated to the cathode.

helpful. Figure 19.14 shows this curve for a typical low level proportional counter output.

Shown also on the figure is the suggested voltage operating range for detecting both alphas and betas. If the detector output (at its operating voltage) is fed out of the amplifier in fig. 19.11 into a multichannel analyzer or PCA, the output spectrum will be as shown in fig. 19.15.

If we wish to count alphas only, it is easy to set an upper level discriminator on the spectrum as shown in the figure.

The exact experimental procedure that is used for this experiment is dependent on the *Low Level* counting system that is used. Tennelec can provide these systems

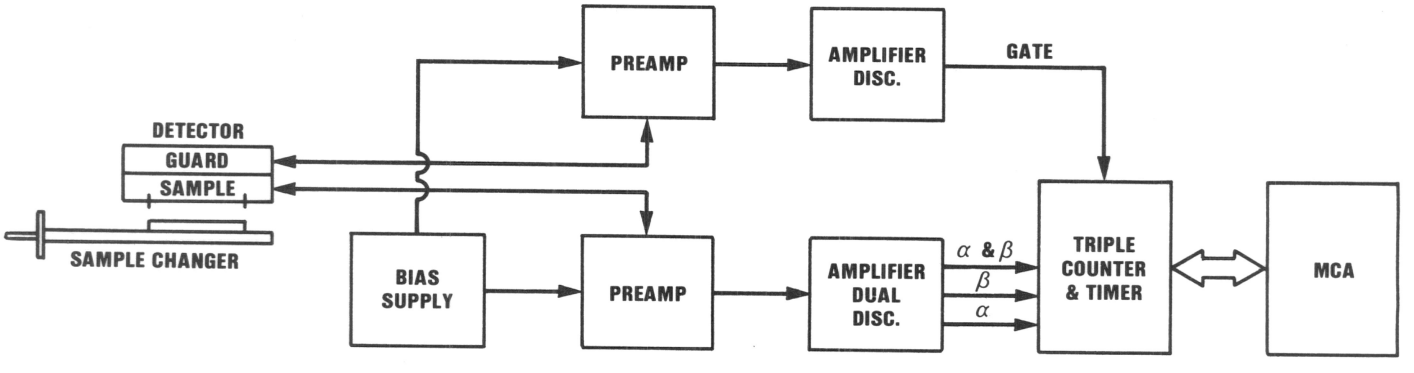

Figure 19.11. Block diagram for Tennelec low level alpha, beta counting system.

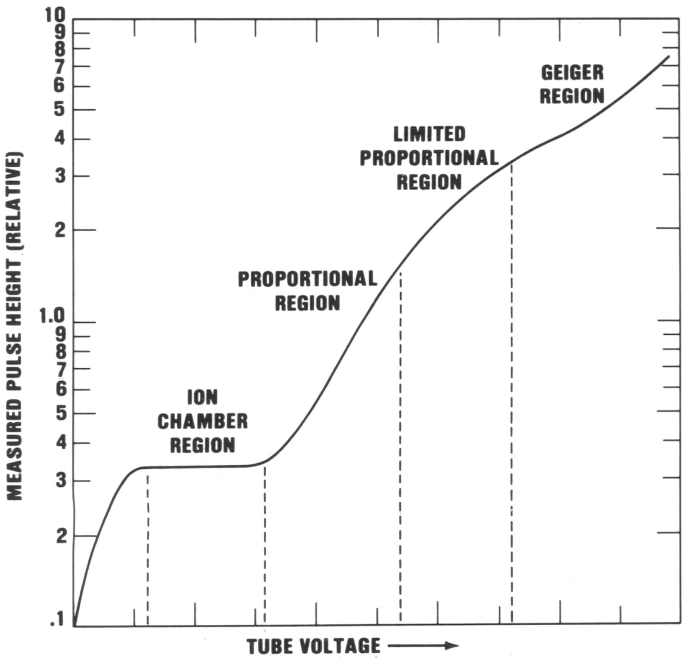

Figure 19.13. Output pulse height versus tube voltage for a proportional counter.

from a range of fully automatic, to manual operation. The instructor for this laboratory experiment will carefully go over the features of the system that is being used for the measurements outlined in this experiment.

Experimental Procedure

1. The block diagram that is used for this experiment is shown in fig. 19.11. The output of the sample amplifier for the first part of this experiment is fed directly into the MCA. Place the standard alpha source, provided by the instructor, in the chamber and adjust the amplifier gains to the values recommended by the instructor.

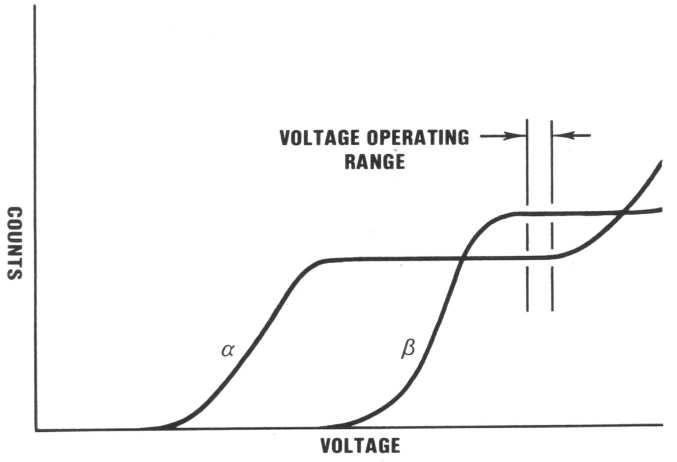

Figure 19.14. Response curve for alphas and betas for a typical gas flow proportional counter.

2. Adjust the voltage on the sample detector while observing the display in the MCA. An alpha spectrum similar to fig. 19.15 should be observed. **Note:** The betas will not be there, but a broad alpha peak should be observed in the upper channels of the MCA. If a plotter is available, the spectrum should be plotted for later use.

3. Remove the standard alpha source and replace it with the standard beta source that is provided by the instructor. The output of this source should be similar to the beta portion of the spectrum in fig. 19.15. Plot this spectrum.

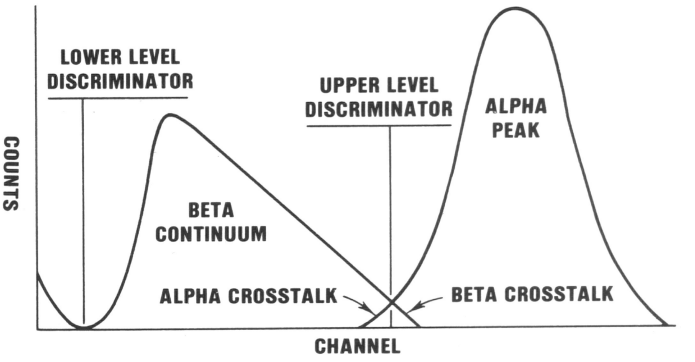

Figure 19.15. Typical gas flow proportional counter output spectrum for an alpha plus beta source.

4. From the two spectra, decide where the upper level discriminator should be set for counting alphas only. The sample detector is now ready to count the environmental samples.

5. Whether you count alphas only, alphas plus betas, or betas only depends on the samples that are being counted. The instructor will provide you with the environmental samples and give instructions for counting.

Summary

After the student has done this experiment, he will have a great appreciation for the versatility of this instrument for low level environmental radiation measurements. As we pointed out earlier, these instruments can be used for "state of the art" research in the study of environmental radiation research.

REFERENCES FOR *EXPERIMENT 19*

1. Chase, G., Rituper, S., & Sulcoski, J. W., *Experiments in Nuclear Science*, Burgess Press 1964 (Available from the Nucleus).

2. G. D. Chase and J. L. Rabinowitz, *Principles of Radioisotope Methodology*, 3rd Edition, Burgess Publishing Co., Minnesota (1967).

3. C. M. Lederer and V. S. Shirley, Eds., *Table of Isotopes*, 7th Edition, John Wiley and Sons, Inc., New York (1978).

4. *Radiological Health Handbook*, U.S. Dept. of Health, Education, and Welfare, PHS Publication 2016. Available from National Technical Information Service, U. S. Dept. of Commerce, Springfield, Virginia.

5. E. W. Emergy, *Geiger-Mueller and Procurement Counters in Radiation Dosimetry*, II, F. H. Attix and W. C. Roesch, Eds., Academic Press, New York (1966).

6. G. F. Knoll, *Radiation Detection and Measurement*, John Wiley and Sons, New York (1979).

7. H. L. Andrews, *Radiation Biophysics*, Prentice-Hall, New Jersey (1974).

8. V. Arena, *Ionizing Radiation and Life*, The C. V. Mosby Co., Missouri (1971).

9. C. E. Crouthamel, *Applied Gamma Ray Spectrometry*, Pergamon Press, New York (1960).

EXPERIMENT 20

Fundamental Nuclear Electronics

Introduction

This manual is composed, for the most part of basic nuclear science experiments. About 20 years ago the nuclear science electronics design community decided to standardize nuclear instrumentation. This standardization correlated, in part, with the introduction of the transistor, in amplifier circuits. As a result of eliminating vacuum tubes, circuits could be designed with much less power consumption. The idea was then presented that it was not necessary to have a separate power supply for each electronic device since a single bin with a built-in power supply would power several modules. This modular concept revolutionized the nuclear counting industry. The electronic power supply and bin was standardized as were the modules that were used with the bins. What all of this means to the student trying to perform the experiments in this manual is that nuclear electronics configurations are now quite simple to understand. This experiment is designed to study some of the basic modules that are used in nuclear counting experiments. These electronic measurements are usually not part of a nuclear science course but they are simple, easy to do, and the student will find that all of the other experiments are understandable, once the basic electronic modules are studied.

Linear and Logic Signals, Amplifiers and Modules

For the most part, there are two different kinds of output pulses from nuclear modules. These are called *linear* and *logic* pulses.

Most of us are familiar with linear devices. For example, a musical amplifier delivers an output whose amplitude is proportional to the signal from its pre-amp. In other words, the output is related in a linear fashion to the input. The gain of an amplifier gives the ratio of output signal voltage height to input height. For a typical counting arrangement the real gain of the amplifier might be x 1000. Therefore, an input pulse from the pre-amp of 1 x 10^{-3} volts would be delivered as a 1 volt pulse out of the amplifier. The coarse gain knob on an amplifier is a measure of the relative gain of the amplifier. For example, the amplifer might have coarse gain settings of times 1, 2, 4, and 8. The times (2) setting is twice the gain of the time (1) value, etc. The fine gain knob is a vernier that further divides the coarse setting.

Nuclear amplifiers in general will accept a negative or positive input pulse from the pre-amp. This option is selected on the front panel of the amp. The output of the amplifier can be either Unipolar or Bipolar. The output maximum voltage is usually 10V. Figure 20.1 shows these two output pulse shapes from a Tennelec amplifier.

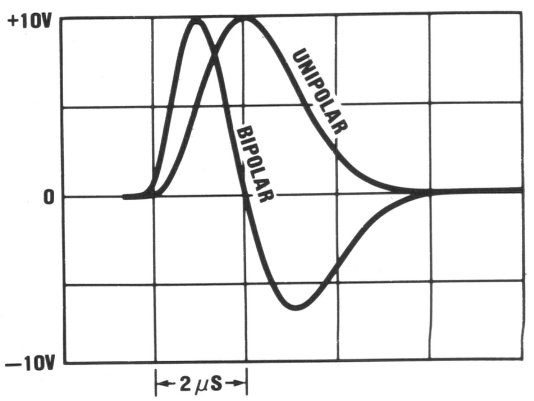

Figure 20.1. Typical output pulse shapes of a nuclear amplifier.

In general, the Unipolar output provides better energy resolution, whereas the Bipolar output is used for timing experiments and high count rate applications. Other common examples of linear modules are time-to-amplitude-converters (TAC), and Linear Gates. These and other linear modules are discussed in the experiments where they are used.

The other type of output mentioned above is the *Logic* output. Certain modules are called Logic modules. For example, an integral discriminator is a *Logic* module. The discriminator is designed to give an output +5V logic pulse if the input pulses are greater than the discriminator level. In other words, a logic module is a (yes)-(no) device. The electronic conditions for the input pulse are set and, if the conditions are satisfied, the module generates a +5 volt logic pulse. If the input pulse fails to meet these criterion, the module does nothing. An important point to remember is that the *Logic* output pulses are constant in amplitude. They do not vary in size as do the outputs of linear devices. In general, *Logic* modules will produce either a +5 volt pulse, as mentioned above, or a fast negative pulse of slightly less than one volt. Most of the experiments in this manual will use the +5 volt pulse. The fast negative *Logic* pulse is used for fast timing experiments such as the gamma ray time-of-flight experiment in this manual. Other common *Logic* modules are: single channel analyzers and coincidence circuits. These modules are discussed in the experiments in which they are used.

EXPERIMENT 20.1

The Pulse Generator

Discussion

The pulse generator or pulser is an electronic module designed to simulate the output signal from a nuclear particle detector. The repetition rate of the pulser is normally 50 or 60 Hz depending on the line frequency. The amplitude of the pulses generated can be varied from 0 to 10V open circuit or 0-5 volts terminated into 50 ohms. Figure 20.2 shows a typical negative pulser output pulse.

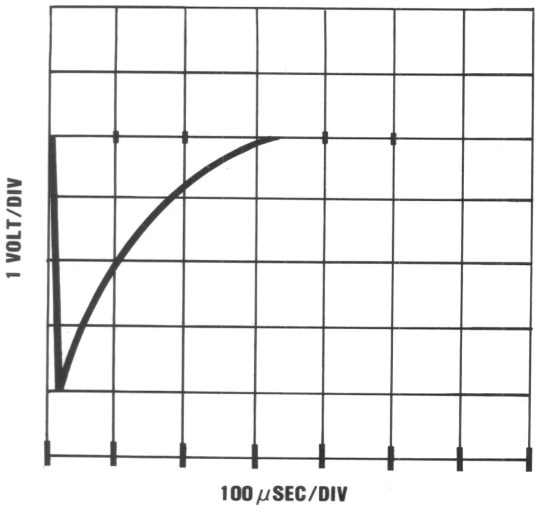

Figure 20.2. Typical negative output from a pulse generator.

The risetime (10% to 90%) of the pulse is equal 5 nsec and the fall time is approximately 300 μsec. This fall time depends on the output termination.

The *polarity* of the output pulse can be selected on the front panel of the pulser. As we will see, nuclear particle detectors and preamplifiers can have both positive and negative outputs, depending upon design.

The *amplitude* (called Pulse Height) of the pulse is controlled from the front panel by a ten turn potentiometer. Each turn has 100 small divisions on the dial, therefore there are a total of 1000 divisions. A setting on this pulse height dial of 500/1000 divisions would therefore correspond to 50% of the maximum setting. As was mentioned above the voltage output of the pulser would then be 5 volts in an open circuit.

The amplitude of the output pulse can also be adjusted by the *Normalization* (NORM) potentiometer. This Normalization potentiometer, which is a screwdriver adjustment, will allow the experimenter to vary the given output of the pulse height by up to x2. In general, this will allow the student to calibrate the pulse generator directly in the desired units of energy.

Nuclear measurements in this manual range from 3 keV x-rays up to 100 MeV fission Fragments. The corresponding outputs of detectors have similar variations. In order to accommodate this wide variation in pulse height, the pulse generator is supplied with attenuation switches (two position toggle switches) which attenuate (ATTEN) the output by factors of 2, 2, 5, 10 and 10. This gives a maximum attenuation of 1400 which is an adequate range for all of the experiments in this manual.

For timing and coincidence purposes the pulse generator also has a *direct output*. This output is constant in amplitude and is designed to be used to coincidence gate oscilloscopes and other timing functions.

In this experiment we are going to study the basic properties of the pulse generator. This will be done by feeding the (ATTEN) output of the pulser into a pre-amp which in turn is fed into an amplifier. The output of the amplifier will also be studied as a function of the various parameters of the pulse generator.

Experimental Procedure

1. Set up the electronics as shown in fig. 20.3. The dashed line in the diagram means this will be used later. All connections should be made with 50 Ω cable and BNC connectors. The (ATTEN) output of the pulse generator should be connected to the test pulse input of the pre-amp.

2. Set the Pulse Height of the pulser dial fully clockwise (1000/1000) div. With a small screwdriver, turn the *Norm* dial fully clockwise. Throw all attenuation switches to the out position except x2. Set the polarity of the pulser at negative. This also turns on the pulse generator. The pre-amp should be a non-inverting variety for this experiment.

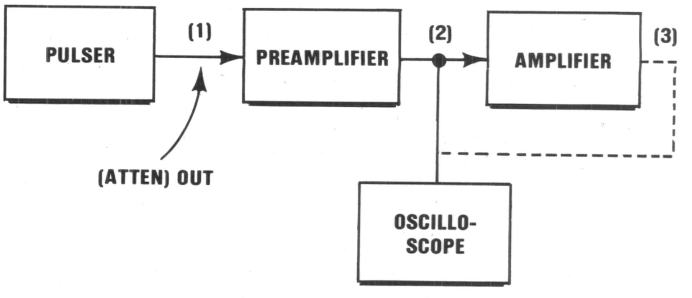

Figure 20.3. Basic electronics for evaluating the parameters of the pulse generator.

3. Trigger the oscilloscope and observe the output of the pre-amp. The output should show a 50 or 60 Hz (depending on line frequency) pulse similar to fig. 20.2. Most pre-amps do not appreciably change the shape or amplitude of the pulse being observed. In other words,

the output at position (1) in fig. 20.3 would look very similar to that at (2). Record this voltage amplitude value in Table 20.1 as Run No. 1.

4. Adjust the Pulse Height dial to 800/1000 and record the corresponding voltage amplitude in the table. Repeat for the other pulse height settings in Table 20.1.

5. Return the Pulse Height setting to 1000/1000. Throw in a x10 attenuation switch and you should observe a x10 attenuation of the voltage amplitude.

Table 20.1 Pulse Generator Linearity Test

Run No.	Pulse-Height Dial Settings	Voltage Amplitude (Oscilloscope)
1	1000/1000	
2	800/1000	
3	600/1000	
4	400/1000	
5	200/1000	

6. With the Pulse Height dial at 1000/1000 and only the x2 attenuator in, adjust the Normalize potentiometer and watch the output pulse amplitude change. Use various combinations of attenuators and the Normalize dial and observe the output.

7. Switch the polarity of the pulser to positive and re-trigger the oscilloscope for a positive pulse. Your output pulse should be similar to the other observations only positive.

Exercise *On linear graph paper make a plot of Pulse Height Dial Setting (y axis) as a function of voltage amplitude (Table 20.1). A very straight line should be observed if all the measurements have been carefully made.*

EXPERIMENT 20.2

A Study of Basic Amplifier Parameters

1. Set up the electronics as shown in fig. 20.3 only this time use the dashed line configuration. With this configuration, the output of the amplifier is being observed with the oscilloscope.

2. Amplifier Parameters: Coarse gain in the middle of its range, fine gain at full scale, input polarity negative. If there is a time constant switch on the amplifier, set it at 1 μsec. Use the unipolar output.

3. Set the polarity of the pulser at negative.

4. Adjust the pulser pulse height dial and attenuation switches until a +4 volt unipolar pulse is observed out of the amplifier. Figure 20.1 (Unipolar) shows a 10 volt pulse similar to what should be observed.

5. Decrease the fine gain control on the amplifier while observing the output. The shape of the pulse will not change but its amplitude will decrease linearly as the fine gain is decreased.

6. Use various combinations of the fine and coarse gains to produce outputs of 2, 3, 5, 7 and 8 volts.

7. With the gain set such that there is an output amplifier voltage of 8 volts, decrease the pulse height dial on the pulse generator. The output of the amplifier will decrease in a linear manner. You can also change the attenuation switches on the pulser and see the corresponding changes in the amplifier output.

8. Set the pulser pulse height dial at 1000/1000 and adjust the amplifier gain so that the amplifier output is 8 volts. Record this value in Table 20.2. Repeat for the other pulser pulse height settings in Table 20.2.

Table 20.2 Linearity Check of the Pulse Generator and Amplifier

Run No.	Pulser Pulse Height Dial Setting	Amplifier Output
1	1000/1000	8 volts
2	800/1000	
3	600/1000	
4	400/1000	
5	200/1000	

Exercise On linear graph paper plot pulse height setting as a function of output amplifier voltage from Table 20.2.

A Study of the Single Channel Analyzer

Discussion

The Single Channel Analyzer (SCA) is a logic module that is used to inspect the output pulses of the amplifier. It has two basic modes of operation. These are the integral mode and the window mode. In the integral mode, the SCA will produce an output logic pulse if its input from the amplifier has an amplitude greater than the lower level dial setting on the SCA. The lower level dial is a 1000 division potentiometer that sets the value of the lower level up to 10 volts. In other words, a lower level setting of 200/1000 corresponds to a lower level of 2 volts. In this configuration, the SCA acts like an integral discriminator and will produce an output logic pulse anytime its input is greater than 2 volts.

The other common mode of the SCA is the *window* or ΔE mode (called the asymmetrical ΔE mode). In this mode the SCA will generate a pulse when the output of the amplifier is at least as great as the lower level (called E) but not greater than $E + \Delta E$. The ΔE or window potentiometer is a ten turn (1000 division) dial. In this asymmetric window mode, the ΔE dial has a range of from 0 to 1 volt. A window setting of 100/1000 would therefore correspond to a 0.1 volt window. The instrument is designed in such a manner that the window (ΔE) rides above the lower level setting. In other words with the lower level (E dial) set at 400/1000 (this corresponds to 4.0 volts) and the window (ΔE) set at 200/100 (this corresponds to 0.2 volts), the single channel will deliver output logic pulses any time the amplifier output is between 4.0V and 4.2V.

EXPERIMENT 20.3

The Integral Mode of the Single Channel Analyzer

Experimental Procedure

1. Set up the electronics as shown in fig. 20.4. With the oscilloscope connected to the output of the amplifier, adjust the pulser and amplifier gains so that the output of the amplifier is a +4 volt pulse at the Unipolar output.

2. Set the SCA in the integral mode. Adjust the lower level to 1.0 volts (100/1000). Turn on the counter and a counting rate of 50 or 60 Hz should be observed (50 or 60 Hz depends on the line frequency). Set the timer for a time greater than 1000 seconds because several measurements will be made while the system is counting.

3. Now slowly raise the E dial while watching the counter. When the E dial just exceeds 400/1000, the counter should stop counting.

4. Now raise the amplifier voltage to 5 volts and again increase the E dial setting. At a value just over 500/1000 the counter will stop.

5. Now continue this experiment for the amplifier settings in Table 20.3 and record in the table the Lower Level values at which the counter stops.

Exercise On linear graph paper make a plot of amplifier voltage (y axis) as a function of lower level setting. If you have done everything correctly, your data should show a straight line.

Table 20.3 Integral Mode Evaluation Data

Run No.	Amplifier Output Voltage	Lower Level at which Counting Stops
1	2.5	
2	3.5	
3	4.5	
4	5.5	
5	6.5	

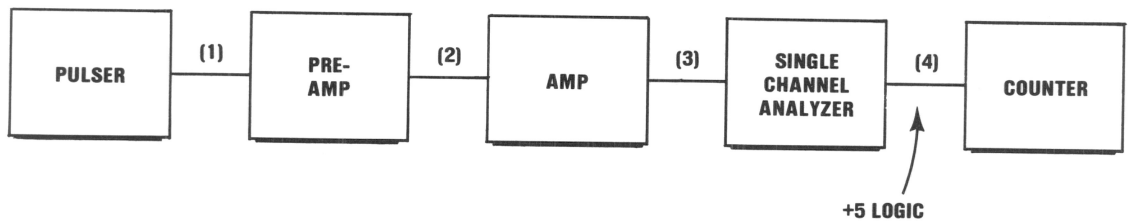

Figure 20.4. Simple electronic configuration to study the Single Channel Analyzer.

EXPERIMENT 20.4

The Differential or Window Mode of the Single Channel Analyzer

Experimental Procedure

1. The experimental set up for this experiment is exactly the same as that for *Experiment 20.3* except the SCA is switched to the Asymmetric Window Mode (ΔE). Set the window at ΔE = 0.1V (100/1000). Set the Lower Level at zero.

2. Adjust the output pulses of the amplifier for 4.0 volts. Set the counter for 1000 seconds. Now slowly raise the Lower Level while watching the counter. The counter should start counting at an E level of 3.9 volts and stop at 4.0 volts.

3. Now raise the gain of the amplifier so that the output is 5.0V. The counter should stop counting. Raise the upper level dial and at a setting of 4.9 volts the counter should start counting. It will stop again at 5.0 volts.

4. Repeat these measurements for the amplifier voltage values in Table 20.4. Record the upper level values at which the counter starts counting in column (2) and stops in (3).

5. Increase the ΔE window to 0.3V (300/1000) and repeat all of the data taken in Table 20.4 with this new ΔE setting.

Table 20.4 Data Table for Differential Mode (E) Evaluation

Run No.	Amplifier Output Voltage (1)	Lower Level Start Counting (2)	Lower Level Stop Counting (3)
1	6.5		
2	5.5		
3	4.5		
4	3.5		
5	2.5		

Exercise For all of the data taken in Procedure 4, make a plot of amplifier output voltage (y axis) as a function of the E + ΔE. Where E is the lower level setting, at which counting starts (2), and ΔE is the voltage of the window. Repeat this plot for your second data table where ΔE = 0.3V.

REFERENCES FOR *EXPERIMENT 20*

1. K. Siegbahn, Ed., *Alpha-, Beta-, and Gamma-Ray Spectroscopy* **1** and **2**, North Holland Publishing Co., Amsterdam (1965).

2. *Radiological Health Handbook*, U.S. Dept. of Health, Education, and Welfare, PHS Publication 2016. Available from National Technical Information Service, U.S. Dept. of Commerce, Springfield, Virginia.

3. G. F. Knoll, *Radiation Detection and Measurement*, John Wiley and Sons, New York (1979).

4. V. Arena, *Ionizing Radiation and Life*, The C. V. Mosby Co., St. Louis, Missouri (1971).

5. P. Quittner, *Gamma Ray Spectroscopy*, Halsted Press, New York (1972).

6. A. C. Melissinos, *Experiments in Modern Physics*, Academic Press, New York (1966).

7. W. Mann and S. Garfinkel, *Radioactivity and Its Measurement*, Van Nostrand-Reinhold, New York (1966).

8. H. L. Andrews, *Radiation Biophysics*, Prentice-Hall, Englewood Cliffs, New Jersey (1974).

9. V. Acosta, C. L. Cowan, and B. J. Graham, *Essentials of Modern Physics*, Harper and Row, New York (1973).

10. A. H. Wapstra, et al., *Nuclear Spectroscopy Tables*, North Holland Publishing Co., Amsterdam (1959).

APPENDIX A

Gamma Spectra and Nuclide Identification Library

Complied by
GEOFFREY GLEASON

Oak Ridge Associated Universities
Professional Training Programs
Manpower, Education, Research, and Training Division

4th Edition
January 1984

Oak Ridge, TN USA

PREFACE

This catalog contains an abbreviated listing of nuclides, gamma rays and spectra frequently encountered in radiation measurements. The nuclides selected have importance in the following categories:

(1) Neutron activation analysis
(2) Commercial availability
(3) Use as a standard
(4) Use in medicine
(5) Naturally occurring nuclides
(6) Fission Product (Fallout)

Only the most prominent gamma rays for each of the listed nuclides are given. All energies are expressed in keV.

The catalog consists of three parts:

Part I is a nuclide index. It is intended for use where information is needed on a specific nuclide. The elements are listed alphabetically for convenience. Under each element are listed the mass numbers of the nuclides included in the catalog and their respective "keys" gammas. More complete information can then be obtained by locating the designated "key" gamma in Part II.

Part II is intended for use in identifying nuclides from gamma energies observed in a spectrum.

Column 1 includes all gamma rays listed in the table in descending order of energy.

Column 4 lists a "key" gamma ray selected as being most characteristic of that nuclide, usually one of the most intense. More complete information on the nuclide, including absolute gamma intensities, can be found by locating the "key" gamma in column 1. For convenience, the "key" gammas in column 1 are bracketed. Gamma intensities expressed as a percent are indicated in parenthesis. The values cited represent the "best" available from the references attached, in the judgement of the authors. In many cases, the selections were influenced by measurements made at Oak Ridge Associated Universities.

Column 5, 6 and 7 list associated gammas, if any, that will be useful for confirmation of the identification. Under the "key" gamma, the most complete listing of associated gammas is found.

Column 8 list parent (P) or daughter (D) products with their associated "key" gammas, if any.

REFERENCES

1. Blachot, J., et al. *Gamma Ray and Half-Life Data for the Fission Products,* Academic Press Inc., Atomic Data and Nuclear Data Tables 20, pp. 241-310, 1977.

2. Dyer, F. F., et al. *RSIC Data Library Collection,* Oak Ridge National Laboratory, Union Carbide Corporation for the U.S.D.O.E., Radiation Shielding Information Center No. DLC-19, 1967.

3. Filby, R. H., et al. *Gamma Ray Energy Tables for Neutron Activation Analysis,* Washington State University, Nuclear Radiation Center, Pullman, Washington, WSUNRC-97(2), 1970.

4. Heath, R. L. *Gamma Ray Spectrum Catalogue,* Aeroject Nuclear Co., Idaho Operations Office, U.S.A.E.C., AT(10-1)-1375, 1974.

5. Heath, R. L. *Scintillation Spectrometry Gamma Ray Spectrum Catalog,* Phillips Petroleum Co., Idaho Operations Office, U.S.A.E.C., IDO-16880, 1964.

6. Kocher, D. C. *Radioactive Decay Data Tables,* Technical Information Center, U. S. Department of Energy, Oak Ridge, Tennessee, 1981.

7. Martin, M. J. *Nuclear Decay Data for Selected Radionuclides,* Oak Ridge National Laboratory, Union Carbide Corp., for E.R.D.A., ORNL-5114 Contract No. W-7405-eng-26, 1976.

8. *Radiological Health Handbook*, U. S. Government Printing Office, Washington, D. C., 1970.

9. Wakat, M. A. *Nuclear Data Tables,* Academic Press, Inc., Savannah River Laboratory, E. I. du Pont de Nemours & Co., Aiken, South Carolina, U.S.A.E.C., AT(07-2)-1, 1971.

I. NUCLIDE INDEX

INDEX

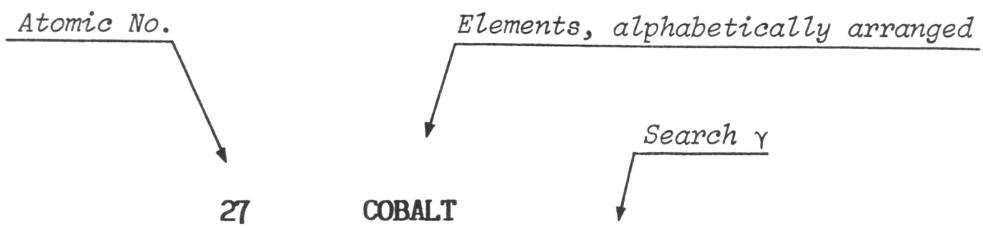

27	COBALT		
		56	[846.8]
		57	[122.1]
		58	[810.8]
		60	[1332.5]
		60m	[58.6]
29	COPPER		
		64	
		67	

NO.-SYMB.	ELEMENT MASS NO.	KEY GAMMA
89-Ac	ACTINIUM	
	228	[911.1]
13-Al	ALUMINUM	
	26	[1808.7]
	28	[1778.9]
95-Am	AMERICIUM	
	241	[59.5]
51-Sb	ANTIMONY	
	122	[564.0]
	124	[602.7]
	125	[427.9]
18-Ar	ARGON	
	41	[1293.6]
33-As	ARSENIC	
	74	[595.9]
	76	[559.1]
	77	[239.0]
56-Ba	BARIUM	
	131	[496.3]
	133	[356.0]
	137m	[661.6]
	139	[165.9]
	140	[537.3]
4-Be	BERYLLIUM	
	7	[477.6]
83-Bi	BISMUTH	
	207	[569.7]
	212	[727.2]
	214	[609.3]
35-Br	BROMINE	
	80	[616.2]
	80m	[37.0]
	82	[776.5]
48-Cd	CADMIUM	
	109	[88.0]
	111m	[245.4]
	115	[527.8]
20-Ca	CALCIUM	
	7	[1297.1]
	49	[3084.4]
58-Ce	CERIUM	
	139	[165.8]
	141	[145.4]
	143	[293.2]
	144	[133.5]
55-Cs	CESIUM	
	134	[795.8]
	134m	[127.4]
	137	[661.6]
	138	[1435.8]
17-Cl	CHLORINE	
	38	[2167.5]
24-Cr	CHROMIUM	
	51	[320.1]
27-Co	COBALT	
	56	[846.8]
	57	[122.1]
	58	[810.8]
	60	[1332.5]
	60m	[58.6]
29-Cu	COPPER	
	64	[1345.8]
	66	[1039.2]
	67	[184.6]
66-Dy	DYSPROSIUM	
	165	[94.7]
	165m	[108.2]
68-Er	ERBIUM	
	171	[308.3]
63-Eu	EUROPIUM	
	152	[1408.0]
	152m	[841.6]
	154	[123.1]
	155	[86.5]
9-Fl	FLUORINE	
	20	[1633.5]
64-Gd	GADOLINIUM	
	153	[97.4]
	159	[363.5]

NO.-SYMB.	ELEMENT MASS NO.	KEY GAMMA
31-Ga	**GALLIUM**	
	67	[93.3]
	68	[1077.4]
	72	[834.0]
32-Ge	**GERMANIUM**	
	75	[264.6]
	77	[264.4]
79-Au	**GOLD**	
	195	[98.9]
	198	[411.8]
	199	[158.4]
72-Hf	**HAFNIUM**	
	175	[343.6]
	180m	[332.3]
	181	[482.0]
67-Ho	**HOLMIUM**	
	166	[80.6]
49-In	**INDIUM**	
	111	[245.4]
	113m	[391.7]
	114m	[190.3]
	115m	[336.3]
	116m	[1097.3]
53-I	**IODINE**	
	125	[35.5]
	128	[442.9]
	129	[39.6]
	130	[536.1]
	131	[364.5]
	132	[667.7]
	135	[1260.4]
77-Ir	**IRIDIUM**	
	192	[316.5]
	194	[328.5]
26-Fe	**IRON**	
	52	[168.7]
	59	[1099.2]
36-Kr	**KRYPTON**	
	85	[514.0]
	85m	[151.2]
	88	[2392.0]
57-La	**LANTHANUM**	
	140	[1596.1]

NO.-SYMB.	ELEMENT MASS NO.	KEY GAMMA
71-Lu	**LUTETIUM**	
	176m	[88.3]
	177	[208.4]
82-Pb	**LEAD**	
	210	[46.5]
	212	[238.6]
	214	[351.9]
12-Mg	**MAGNESIUM**	
	27	[843.8]
	28	[1342.2]
25-Mn	**MANGANESE**	
	52	[1434.0]
	54	[834.8]
	56	[846.8]
80-Hg	**MERCURY**	
	197	[77.4]
	197m	[133.9]
	203	[279.2]
42-Mo	**MOLYBDENUM**	
	99	[739.5]
	101	[191.9]
60-Nd	**NEODYMIUM**	
	147	[91.1]
	149	[211.3]
	151	[116.8]
93-Np	**NEPTUNIUM**	
	239	[106.1]
28-Ni	**NICKEL**	
	65	[1481.8]
41-Nb	**NIOBIUM**	
	94	[871.1]
	95	[765.8]
	97	[657.9]
	97m	[743.4]
7-N	**NITROGEN**	
	16	[6129.2]
76-Os	**OSMIUM**	
	191	[129.4]
46-Pd	**PALLADIUM**	
	109	[88.0]

NO.-SYMB.	ELEMENT MASS NO.	KEY GAMMA
78-Pt	PLATINUM	
	195m	[98.9]
	199	[542.9]
19-K	POTASSIUM	
	40	[1460.8]
	42	[1524.7]
	43	[372.8]
59-Pr	PRASEODYMIUM	
	142	[1575.8]
	144	[696.5]
61-Pm	PROMETHIUM	
	149	[285.9]
	151	[340.1]
91-Pa	PROTACTINIUM	
	233	[312.0]
	234m	[1001.0]
88-Ra	RADIUM	
	224	[241.0]
	226	[186.2]
75-Re	RHENIUM	
	188	[155.0]
45-Rh	RHODIUM	
	104m	[51.4]
	105	[318.9]
37-Rb	RUBIDIUM	
	86	[1076.6]
	88	[1836.0]
44-Ru	RUTHENIUM	
	97	[215.7]
	103	[497.1]
	105	[724.5]
62-Sm	SAMARIUM	
	153	[103.2]
	155	[104.3]
21-Sc	SCANDIUM	
	44	[1157.0]
	46	[889.3]
	46m	[142.5]
	47	[159.4]
	48	[1312.1]
34-Se	SELENIUM	
	75	[264.7]

NO.-SYMB.	ELEMENT MASS NO.	KEY GAMMA
47-Ag	SILVER	
	108	[633.0]
	108m	[722.9]
	110m	[657.7]
	111	[342.2]
11-Na	SODIUM	
	22	[1274.5]
	24	[2754.0]
38-Sr	STRONTIUM	
	85	[514.0]
	85m	[231.7]
	87m	[388.5]
	91	[1024.3]
	92	[1384.0]
16-S	SULFUR	
	37	[3103.8]
73-Ta	TANTALUM	
	182	[1221.4]
43-Tc	TECHNETIUM	
	99m	[140.5]
	101	[306.8]
52-Te	TELLURIUM	
	123m	[159.0]
	129	[459.6]
	131	[149.7]
	131m	[773.7]
	132	[228.2]
65-Tb	TERBIUM	
	160	[879.4]
81-Tl	THALLIUM	
	201	[167.4]
	208	[2614.7]
90-Th	THORIUM	
	233	[86.5]
	234	[92.6]
69-Tm	THULIUM	
	170	[84.3]
50-Sn	TIN	
	113	[255.1]
	123m	[160.3]
	125	[1066.6]
	125m	[331.9]

NO.-SYMB.	ELEMENT MASS NO.	KEY GAMMA		NO.-SYMB.	ELEMENT MASS NO.	KEY GAMMA
22-Ti	**TITANIUM**					
	44	[78.3]				
	51	[320.1]				
74-W	**TUNGSTEN**					
	187	[685.8]				
92-U	**URANIUM**					
	235	[185.7]				
	239	[74.7]				
23-V	**VANADIUM**					
	48	[983.5]				
	52	[1434.0]				
54-Xe	**XENON**					
	133	[81.0]				
	135	[249.8]				
	135m	[526.6]				
70-Yb	**YTTERBIUM**					
	169	[198.0]				
	175	[396.3]				
39-Y	**YTTRIUM**					
	88	[1836.0]				
	90m	[202.5]				
	91m	[555.6]				
	92	[934.4]				
30-Zn	**ZINC**					
	65	[1115.5]				
	69m	[438.6]				
40-Zr	**ZIRCONIUM**					
	95	[756.7]				
	97	[507.6]				

II. SEARCH GAMMAS FOR NUCLIDE IDENTIFICATION

SEARCH	NUCLIDE	HALF-LIFE	KEY GAMMA	ASSOCIATED GAMMAS			P OR D
7115.2	N-16	7.10s	6129.2				
[6129.2]	N-16	7.10s	6129.2(69)	7115.2(5.0)			
4071.9	Ca-49	8.72m	3084.4				
3253.4	Co-56	78.8d	846.8	1238.3	2598.4	1771.3	
[3103.8]	S-37	5.06m	3103.8(100)				
[3084.4]	Ca-49	8.72m	3084.4(91)	4071.9(8.0)			
[2754.0]	Na-24	15.0h	2754.0(100)	1368.6(100)			
2677.9	Rb-88	17.8m	1836.0	898.0			
[2614.7]	Tl-208	3.05m	2614.7(100)*	583.1(84)	510.8(22)	860.4(12)	D. Th-228
2598.4	Co-56	78.8d	846.8	1238.3	1771.3	1037.9	
2507.8	Ga-72	14.1h	834.0	2201.7	629.9	894.2	
2490.9	Ga-72	14.1h	834.0	2201.7	629.9	2507.8	
[2392.0]	Kr-88	2.84h	2392.0(35)	196.1(26) 1529.8(11)	2195.9(13)	834.7(13)	
2201.7	Ga-72	14.1h	834.0	629.9	2507.8	894.2	
2195.9	Kr-88	2.84h	2392.0	196.1	834.7	1529.8	
2185.7	Pr-144	17.3m	696.5				
[2167.5]	Cl-38	37.2m	2167.5(44)	1642.4(33)			
2113.0	Mn-56	2.58h	846.8	1810.7			
2112.3	In-116m	54.2m	1097.3	1293.5	417.0	818.7	
2091.0	Sb-124	60.2d	602.7	1691.0	722.8	645.9	
2034.8	Co-56	78.8d	846.8	1238.3	2598.4	1771.3	
2032.0	Mo-101	14.6m	191.9	590.8	1012.5	505.9	
2002.0	Sn-125	9.64d	1066.6	1088.9	915.7	822.6	
1883.1	Ga-68	68.0m	1077.4	511.0			
1861.0	Ga-72	14.1h	834.0	2201.7	629.9	2507.8	

*Multiply each intensity by 0.36 when assaying Th-228

SEARCH	NUCLIDE	HALF-LIFE	KEY GAMMA	ASSOCIATED GAMMAS			P OR D
[1836.0]	Rb-88	17.8m	1836.0(22)	898.0(14)	2677.9(2.0)		
[1836.0]	Y-88	107d	1836.0(99)	898.0(93)			
1810.7	Mn-56	2.58h	846.8	2113.0			
[1808.7]	Al-26	7.4E5y	1808.7(100)	1129.6(2.5)	511.0(163)		
[1778.9]	Al-28	2.24m	1778.9(100)				D. Mg-28 [1342.2]
1771.3	Co-56	78.8d	846.8	1238.3	2598.4	1037.9	
1770.2	Bi-207	33.4y	569.7	1063.6			
1764.5	Bi-214	19.9m	609.3	1120.3	1238.1	768.4	
1750.5	Zr-97	16.9h	507.6	1148.0	355.4	1362.7	
1691.0	Sb-124	60.2d	602.7	722.8	645.9	2091.0	
1642.4	Cl-38	37.2m	2167.5				
[1633.5]	F-20	11.4s	1633.5(100)				
1596.7	Ga-72	14.1h	834.0	2201.7	629.9	2507.8	
[1596.1]	La-140	40.2h	1596.1(96)	487.0(45) 925.2(7.1)	815.8(23) 867.8(5.6)	328.8(21)	D. Ba-140 [537.3]
1581.9	Ho-166	26.8h	80.6	1379.4			
[1575.8]	Pr-142	19.1h	1575.8(3.7)				
1529.8	Kr-88	2.84h	2392.0	196.1	2195.9	834.7	
[1524.7]	K-42	12.4h	1524.7(18)	312.7(0.3)			
1507.6	In-116m	54.2m	1097.3	1293.5	417.0	2112.3	
1505.0	Ag-110m	250d	657.7	884.7	937.5	1384.3	
1499.4	Sc-44	3.93h	1157.0	511.0			
[1481.8]	Ni-65	2.52h	1481.8(24)	1115.5(15)	366.3(5)		
[1474.8]	Br-82	35.5h	776.5	554.3	619.1	698.3	
1464.0	Ga-72	14.1h	834.0	2201.7	629.9	2507.8	
[1460.8]	K-40	1.3E9y	1460.8(11)				

SEARCH	NUCLIDE	HALF-LIFE	KEY GAMMA	ASSOCIATED GAMMAS			P OR D
[1435.8]	Cs-138	32.2m	1435.8(76)	462.8(31) 546.8(10)	1009.7(30)	2218.0(15)	
[1434.0]	V-52	3.75m	1434.0(100)				
[1434.0]	Mn-52	5.59d	1434.0(100)	935.5(94) 511.0(59)	744.2(90)	1333.6(5.1)	D. Fe-52 [168.7]
1420.5	Ba-139	83.1m	165.9				
[1408.0]	Eu-152	13.5y	1408.0(21)	121.8(28) 1112.0(13) 244.7(7.5)	344.3(27) 778.9(13)	964.0(15) 1085.8(10)	
1405.4	Y-92	3.54d	934.4	560.8	448.5		
1398.6	I-132	2.30h	667.7	772.6	954.6	522.6	
1389.0	Eu-152m	9.32h	841.6	963.3	121.8	344.3	
1384.3	Ag-110m	250d	657.7	884.7	937.5	763.9	
[1384.0]	Sr-92	2.71h	1384.0(90)	953.3(3.6)	241.5(3.0)		
1379.4	Ho-166	26.8h	80.6	1581.9			
1368.6	Na-24	15.0h	2754.0				
1368.2	Sb-124	60.2d	602.7	1691.0	722.8	645.9	
1362.7	Zr-97	16.9h	507.6	1148.0	355.4	1750.5	
[1345.8]	Cu-64	12.7h	1345.8(0.5)	511.0(36)			
[1342.2]	Mg-28	20.9h	1342.2(53)	30.6(66)	941.5(38)	400.7(37)	P. Al-28 [1778.9]
1333.6	Mn-52	5.59d	1434.0	935.5	744.2	511.0	
[1332.5]	Co-60	5.27y	1332.5(100)	1173.2(100)			
1317.5	Br-82	35.3h	776.5	554.3	619.1	698.8	
1314.7	Eu-152m	9.32h	841.6	963.3	121.8	344.3	
[1312.1]	Sc-48	43.7h	1312.1(100)	983.5(100)	1037.5(98)	175.4(7.5)	
1312.1	V-48	16.0d	983.5	944.1	511.0		
[1297.1]	Ca-47	4.54d	1297.1(75)	807.9(6.9)	489.2(6.7)		P. Sc-47 [159.4]
[1293.6]	Ar-41	1.83h	1293.6(99)				
1293.5	In-116m	54.2m	1097.3	417.0	2112.3	818.7	

SEARCH	NUCLIDE	HALF-LIFE	KEY GAMMA	ASSOCIATED GAMMAS			P OR D
1291.6	Fe-59	44.6d	1099.2	192.3			
1274.5	Eu-154	8.6y	123.1	723.3	1004.8	873.2	
[1274.5]	Na-22	2.60y	1274.5(100)	511.0(180)			
1271.9	Tb-160	72.3d	879.4	298.6	966.1	1177.9	
[1260.4]	I-135	6.61h	1260.4(29)	1131.6(18)	1038.7(7.9)	P. Xe-135 [249.8]	P.Xe-135m [526.6]
1256.9	Sb-122	2.70d	564.0	692.8	1140.2		
1238.3	Co-56	78.8d	846.8	2598.4	1771.3	1037.9	
1238.1	Bi-214	19.9m	609.3	1764.5	1120.3	768.4	
1230.9	Ta-182	115d	1221.4	67.8	1121.3	1189.1	
[1221.4]	Ta-182	115d	1221.4(27)	67.8(42) 100.1(14)	1121.3(35) 1230.9(12)	1189.1(16) 222.1(7.6)	
1216.0	As-76	26.3h	559.1	657.0			
1206.6	Te-131m	30.0h	773.7	852.2	793.8	1125.5	
1189.1	Ta-182	115d	1221.4	67.8	1121.3	100.1	
1180.9	Nd-151	12.4m	116.8	255.7	175.1	139.0	
1177.9	Tb-160	72.3d	879.4	298.6	966.1	86.8	
1173.2	Co-60	5.27y	1332.5				
1157.5	I-130	12.4h	536.1	668.5	739.5	418.0	
[1157.0]	Sc-44	3.93h	1157.0(100)	1499.4(0.9)	511.0(189)		D. Ti-44 [78.3]
1148.0	Zr-97	16.9h	507.6	355.4	1750.5	1362.7	
1147.0	Te-131	25.0m	149.7	452.3	492.7	602.0	
1140.2	Sb-122	2.70d	564.0	692.8	1256.9		
1131.6	I-135	6.61h	1260.4	1038.7			
1129.6	Al-26	7.4E5y	1808.7	511.0			
1125.5	Te-131m	30.0h	773.7	852.2	793.8	1206.6	
1121.3	Ta-182	115d	1221.4	67.8	1189.1	100.1	

SEARCH	NUCLIDE	HALF-LIFE	KEY GAMMA	ASSOCIATED GAMMAS			P OR D
1120.5	Sc-46	83.8d	889.3				
1120.3	Bi-214	19.9m	609.3	1764.5	1238.1	768.4	
1115.5	Ni-65	2.52h	1481.8	366.3			
[1115.5]	Zn-65	244d	1115.5(51)	511.0(2.8)			
1112.0	Eu-152	13.5y	1408.0	121.8	344.3	964.0	
[1099.2]	Fe-59	44.6d	1099.2(56)	1291.6(43)	192.3(3.1)		
[1097.3]	In-116m	54.2m	1097.3(56)	1293.5(84) 818.7(12)	417.0(28) 1507.6(10)	2112.3(16)	
1088.9	Sn-125	9.64d	1066.6	915.7	822.6	2002.0	
1085.8	Eu-152	13.5y	1408.0	121.8	344.3	964.0	
1085.2	Ge-77	11.3h	264.4	211.0	215.5	416.3	
1083.8	Te-129	69.6m	459.6	487.4	278.4	250.6	
[1077.4]	Ga-68	68.0m	1077.4(3.3)	1883.1(0.1)	511.0(178)		
[1076.6]	Rb-86	18.7d	1076.6(8.8)				
[1066.6]	Sn-125	9.64d	1066.6(8.5)	1088.9(4.0) 2002.0(2.1)	915.7(3.8) 469.9(1.3)	822.6(3.8)	P. Sb-125 [427.9]
1063.6	Bi-207	33.4y	569.7	1770.2			
1050.7	Ga-72	14.1h	834.0	2201.7	629.9	2507.8	
1044.0	Br-82	35.3h	776.5	554.3	619.1	698.3	
[1039.2]	Cu-66	5.10m	1039.2(9.0)				
1038.7	I-135	6.61h	1260.4	1131.6			
1037.9	Co-56	78.8d	846.8	1238.3	2598.4	1771.3	
1037.5	Sc-48	43.7h	1312.1	983.5	175.4		
1024.5	Nb-97	72.1m	657.9				
[1024.3]	Sr-91	9.48h	1024.3(33)	749.8(23)	652.9(11)		P. Y-91m [555.6]
1014.4	Mg-27	9.46m	843.8				

SEARCH	NUCLIDE	HALF-LIFE	KEY GAMMA	ASSOCIATED GAMMAS			P OR D
1012.5	Mo-101	14.6m	191.9	590.8	505.9	2032.0	
1009.7	Cs-138	32.2m	1435.8	462.8	2218.0	546.8	
1004.8	Eu-154	8.6y	123.1	1274.5	723.3	873.2	
[1001.0]	Pa-234m	1.17m	1001.0(0.9)	766.4(0.2)			D. Th-234 [92.6]
997.3	Te-131	25.0m	149.7	452.3	1147.0	492.7	
996.3	Eu-154	8.6y	123.1	1274.5	723.3	1004.8	
983.5	Sc-48	43.7h	1312.1	1037.5	175.4		
[983.5]	V-48	16.0d	983.5(100)	1312.1(98)	944.1(7.8)	511.0(100)	
969.4	I-128	25.0m	442.9	526.6			
969.1	Ac-228	6.13h	911.1	338.3	794.7	463.0	
966.1	Tb-160	72.3d	879.4	298.6	1177.9	86.8	
964.0	Eu-152	13.5y	1408.0	121.8	344.3	1112.0	
963.3	Eu-152m	9.32h	841.6	121.8	344.3	1314.7	
962.3	Tb-160	72.3d	879.4	298.6	966.1	1177.9	
954.6	I-132	2.30h	667.7	772.6	522.6	630.2	
953.3	Sr-92	2.71h	1384.0	241.5			
944.1	V-48	16.0d	983.5	1312.1	511.0		
941.5	Mg-28	20.9h	1342.2	30.6	400.7		
937.5	Ag-110m	250d	657.7	884.7	1384.3	763.9	
935.5	Mn-52	5.59d	1434.0	744.2	1333.6	511.0	
[934.4]	Y-92	3.54h	934.4(14)	1405.4(4.8)	561.1(2.4)	448.5(2.3)	
928.6	Ti-51	5.75m	320.1	608.6			
925.2	La-140	40.2h	1596.1	487.0	815.8	328.8	
915.7	Sn-125	9.64d	1066.6	1088.9	822.6	2002.0	
[911.1]	Ac-228	6.13h	911.1(28)	969.1(17) 463.0(4.5)	338.3(11)	794.7(4.6)	D. Th-232

SEARCH	NUCLIDE	HALF-LIFE	KEY GAMMA	ASSOCIATED GAMMAS			P OR D
898.0	Rb-88	17.8m	1836.0	2677.9			
898.0	Y-88	107d	1836.0				
894.2	Ga-72	14.1h	834.0	2201.7	629.9	2507.8	
[889.3]	Sc-46	83.8d	889.3(100)	1120.5(100)			
884.7	Ag-110m	250d	657.7	937.5	1384.3	763.9	
[879.4]	Tb-160	72.3d	879.4(29)	298.6(27) 86.8(14) 197.0(4.9)	966.1(25) 962.3(9.0)	1177.9(15) 1271.9(7.0)	
873.2	Eu-154	8.6y	123.1	1274.5	723.3	1004.8	
[871.1]	Nb-94	2.0E4y	871.1(100)	702.6(100)			
867.8	La-140	40.2h	1596.1	487.0	815.8	328.8	
860.4	Tl-208	3.05m	2614.7	583.1	510.8		
852.2	Te-131m	30.0h	773.7	793.8	1125.5	1206.6	
[846.8]	Co-56	78.8d	846.8(100)	1238.3(67) 1037.9(14) 511.0(40)	2598.4(17) 3253.4(7.8)	1771.3(16) 2034.8(7.8)	
[846.8]	Mn-56	2.58h	846.8(99)	1810.7(27)	2113.0(14)		
[843.8]	Mg-27	9.46m	843.8(72)	1014.4(28)			
[841.6]	Eu-152m	9.32h	841.6(13)	963.3(12) 1314.7(1.0)	121.8(7.4) 1389.0(0.9)	344.3(2.5)	
[834.8]	Mn-54	313d	834.8(100)				
834.7	Kr-88	2.84h	2392.0	196.1	2195.9	1529.8	
[834.0]	Ga-72	14.1h	834.0(96)	2201.7(26) 894.2(9.9) 600.9(5.6) 1464.0(3.6)	629.9(25) 2490.9(7.5) 1861.0(5.2)	2507.8(13) 1050.7(6.9) 1596.7(4.2)	
827.8	Br-82	35.3h	776.5	554.3	619.1	698.3	
822.8	Te-131m	30.0h	773.7	852.2	793.8	1125.5	
822.6	Sn-125	9.64d	1066.6	1088.9	915.7	2002.0	
818.7	In-116m	54.2m	1097.3	1293.5	417.0	2112.3	

SEARCH	NUCLIDE	HALF-LIFE	KEY GAMMA	ASSOCIATED GAMMAS			P OR D
818.0	Ag-110m	250d	657.7	884.7	937.5	1384.3	
815.8	La-140	40.2h	1596.1	487.0	328.8	925.2	
812.3	I-132	2.30h	667.7	772.6	954.6	522.6	
[810.8]	Co-58	70.8d	810.8(99)	511.0(30)			
807.9	Ca-47	4.54d	1297.1	489.2			
801.9	Cs-134	2.06y	795.8	604.7	569.3	563.3	
[795.8]	Cs-134	2.06y	795.8(85)	604.7(98) 563.2(8.4)	569.3(15)	801.9(8.7)	
794.7	Ac-228	6.13h	911.1	969.1	338.3	463.0	
793.8	Te-131m	30.0h	773.7	852.2	1125.5	1206.6	
782.5	Te-131m	30.0h	773.7	852.2	793.8	1125.5	
778.9	Eu-152	13.5y	1408.0	121.8	344.3	964.0	
778.0	Mo-99	66.0h	739.5	181.1	140.5	366.4	
[776.5]	Br-82	35.3h	776.5(83)	554.3(71) 1317.5(27) 1474.8(17)	619.1(43) 1044.0(27)	698.3(28) 827.8(24)	
[773.7]	Te-131m	30.0h	773.7(38)	852.2(21) 1206.6(9.8) 782.5(7.8) 822.8(6.1) 452.3(1.5)	793.8(14) 334.3(9.6) 240.9(7.6) 149.7(5.1)	1125.5(11) 102.1(7.9) 200.7(7.6) 665.1(4.4)	P. I-131 [364.5]
772.9	W-187	23.8h	685.8	479.5	72.1	134.2	
772.6	I-132	2.30h	667.7	954.6	522.6	630.2	
768.4	Bi-214	19.9m	609.3	1764.5	1120.3	1238.1	
[765.8]	Nb-95	35.1d	765.8(100)				D. Zr-95 [756.7]
763.9	Ag-110m	250d	657.7	884.7	937.5	1384.3	
[756.7]	Zr-95	64.0d	756.7(55)	724.2(44)			P. Nb-95 [765.8]
749.8	Sr-91	9.48h	1024.3	652.9			
744.2	Mn-52	5.59d	1434.0	935.5	744.2	1333.6	

SEARCH	NUCLIDE	HALF-LIFE	KEY GAMMA	ASSOCIATED GAMMAS			P OR D
[743.4]	Nb-97m	60.0s	743.4(98)				D. Zr-97 [507.6]
[739.5]	Mo-99	66.0h	739.5(13)	181.1(6.2) 366.4(1.4)	778.0(4.5)	140.5(3.8)	P. Tc-99m [140.5]
739.5	I-130	12.4h	536.1	668.5	418.0	1157.5	
[727.2]	Bi-212	60.6m	727.2(12)				
725.2	In-114m	49.5d	190.3	558.4			
[724.5]	Ru-105	4.43h	724.5(49)	469.4(18) 262.9(7.2)	676.4(17)	316.5(12)	P.Rh-105 [318.9]
724.2	Zr-95	64.0d	756.7				
723.3	Eu-154	8.6y	123.1	1274.5	1004.8	873.2	
722.9	I-131	8.04d	364.5	637.0	284.3		
[722.9]	Ag-108m	127y	722.9(91)	614.4(91)	433.9(90)	79.2(7.1)	
722.8	Sb-124	60.2d	602.7	1691.0	645.9	2091.0	
722.0	Ce-143	33.0h	293.2	57.4	664.6		
717.8	Pm-151	28.4h	340.1	167.8	275.2	445.7	
715.3	Dy-165	2.33h	94.7	361.7	633.4		
706.7	Ag-110m	250d	657.7	884.7	937.5	1384.3	
702.6	Nb-94	2.0E4y	871.1				
698.3	Br-82	35.3h	776.5	554.3	619.1	1044.0	
[696.5]	Pr-144	17.3m	696.5(1.5)	2185.7(0.8)			D. Ce-144 [133.5]
692.8	Sb-122	2.70d	564.0	1140.2	1256.9		
[685.8]	W-187	23.8h	685.8(29)	479.5(23) 618.4(6.7)	72.1(12) 551.5(5.4)	134.2(9.5) 772.9(4.4)	
677.6	Ag-110m	250d	657.7	884.7	937.5	1384.3	
676.3	Ru-105	4.43h	724.5	469.4	316.5	262.9	
675.9	Au-198	2.69d	411.8				
671.6	I-132	2.30h	667.7	772.6	954.6	522.6	

SEARCH	NUCLIDE	HALF-LIFE	KEY GAMMA	ASSOCIATED GAMMAS			P OR D
669.8	Th-233	22.3m	86.5	459.2			
668.5	I-130	12.4h	536.1	739.5	418.0	1157.5	
[667.7]	I-132	2.30h	667.7(99)	772.6(76) 630.2(14) 671.6(5.2)	954.6(18) 1398.6(7.1) 505.9(5.0)	522.6(16) 812.3(5.6)	
665.8	Br-80	17.6m	616.2	511.0			
665.1	Te-131m	30.0h	773.7	852.2	793.8	1125.5	
664.6	Ce-143	33.0h	293.2	57.4	722.0		
[661.6]	Cs-137	30.2y	661.6(85)				P. Ba-137m [661.6]
[661.6]	Ba-137m	2.55m	661.6(90)				D. Cs-137 [661.6]
[657.9]	Nb-97	72.1m	657.9(98)	1024.5(1.1)			D. Nb-97m [743.4]
[657.7]	Ag-110m	250d	657.7(95)	884.7(73) 763.9(22) 677.6(11)	937.5(34) 706.7(17) 818.0(7.3)	1384.3(24) 1505.0(13)	
657.0	As-76	26.3h	559.1	1216.0			
654.8	Nd-149	1.73h	211.3	114.3	270.2	423.6	
652.9	Sr-91	9.48h	1024.3	749.8			
645.9	Sb-124	60.2d	602.7	1691.0	722.8	2091.0	
637.0	I-131	8.04d	364.5	284.3	722.9		
635.9	Sb-125	2.77y	427.9	600.6	463.4	176.3	
634.8	As-74	17.8d	595.9	511.0			
633.4	Dy-165	2.33h	94.7	361.7	715.3		
633.0	Re-188	17.0h	155.0				
[633.0]	Ag-108	2.37m	633.0(1.7)	433.9(0.5)	618.9(0.3)		
631.8	Ge-77	11.3h	264.4	211.0	215.5	416.3	
630.2	I-132	2.30h	667.7	772.6	954.6	522.6	
629.9	Ga-72	14.1h	834.0	2201.7	2507.8	894.2	
619.1	Br-82	35.3h	776.5	554.3	698.3	1044.0	

SEARCH	NUCLIDE	HALF-LIFE	KEY GAMMA	ASSOCIATED GAMMAS			P OR D
618.9	Ag-108	2.37m	633.0	433.9			
618.4	W-187	23.8h	685.8	479.5	72.1	134.2	
617.5	K-43	22.6h	372.8	593.4	396.9		
[616.2]	Br-80	17.6m	616.2(6.6)	665.8(1.1)	511.0(4.4)		
614.4	Ag-108m	127y	722.9	433.9	79.2		
612.5	Ir-192	74.2d	316.5	468.1	308.5	296.0	
610.3	Ru-103	39.4d	497.1				
[609.3]	Bi-214	19.9m	609.3(46)	1764.5(16) 768.4(5.0)	1120.3(15)	1238.1(6.0)	D. Ra-226 [186.2]
608.6	Ti-51	5.75m	320.1	928.6			
606.6	Sb-125	2.77y	427.9	600.6	635.9	463.4	
604.9	Ir-192	74.2d	316.5	468.1	308.5	296.0	
604.7	Cs-134	2.06y	795.8	801.9	569.3	563.2	
[602.7]	Sb-124	60.2d	602.7(98)	1691.0(49) 2091.0(5.7)	722.8(11) 1368.2(2.5)	645.9(7.3)	
602.0	Te-131	25.0m	149.7	452.3	1147.0	492.7	
600.9	Ga-72	14.1h	834.0	2201.7	629.9	2507.8	
600.6	Sb-125	2.77y	427.9	635.9	463.4	176.3	
[595.9]	As-74	17.8d	595.9(60)	634.8(15)	511.0(59)		
593.4	K-43	22.6h	372.8	617.5	396.9		
590.8	Mo-101	14.6m	191.9	1012.5	505.9	2032.0	
588.6	Ir-192	74.2d	316.5	468.1	308.5	296.0.	
583.1	Tl-208	3.05m	2614.7	510.8	860.4		
[569.7]	Bi-207	33.4y	569.7(98)	1063.6(75)	1770.2(6.8)		
569.3	Cs-134	2.06y	795.8	604.7	801.9	563.2	
[564.0]	Sb-122	2.70d	564.0(71)	692.8(3.7)	1256.9(0.8)	1140.2(0.8)	

SEARCH	NUCLIDE	HALF-LIFE	KEY GAMMA	ASSOCIATED GAMMAS			P OR D
563.2	Cs-134	2.06y	795.8	604.7	801.9	569.3	
561.1	Y-92	3.54h	934.4	1405.4	448.5		
[559.1]	As-76	26.3h	559.1(45)	657.0(6.1)	1216.0(3.8)		
558.4	In-114m	49.5d	190.3	725.2			
558.0	Ge-77	11.3h	264.4	211.0	215.5	416.3	
555.8	Rh-104m	4.34m	51.4	97.1	77.5		
[555.6]	Y-91m	49.7m	555.6(95)				D. Sr-91 [1024.3]
554.3	Br-82	35.3h	776.5	619.1	698.3	1044.0	
551.5	W-187	23.8h	685.8	479.5	72.1	134.2	
546.8	Cs-138	32.2m	1435.8	462.8	1009.7	2218.0	
545.1	Tc-101	14.2m	306.8	127.2	184.1		
[542.9]	Pt-199	30.0m	542.9(11)	493.3(3.6) 246.4(1.5)	317.0(3.4)	185.6(2.2)	P. Au-199 [158.4]
540.5	Nd-149	1.73h	211.3	114.3	270.2	423.6	
[537.3]	Ba-140	12.8d	537.3(24)	30.0(14) 423.7(3.2)	162.9(6.7)	304.8(4.5)	P. La-140 [1596.1]
[536.1]	I-130	12.4h	536.1(99)	668.5(96) 1157.5(11)	739.5(82)	418.0(34)	
531.0	Nd-147	11.0d	91.1	319.4			
[527.8]	Cd-115	53.5h	527.8(27)	492.3(7.7)	260.9(1.8)	231.4(0.8)	P.In-115m [336.3]
[526.6]	Xe-135m	15.4m	526.6(81)				D. I-135 [1260.4]
526.6	I-128	25.0m	442.9	969.4			
522.6	I-132	2.30h	667.7	772.6	954.6	630.2	
520.7	As-77	38.8h	239.0				
515.5	Dy-165m	1.26m	108.2				
[514.0]	Kr-85	10.7y	514.0(0.4)				
[514.0]	Sr-85	64.9d	514.0(99)				

SEARCH	NUCLIDE	HALF-LIFE	KEY GAMMA	ASSOCIATED GAMMAS			P OR D
511.0	Annihilation Radiation						
510.8	Tl-208	3.05m	2614.7	583.8	860.4		
[507.6]	Zr-97	16.9h	507.6(5.3)	1148.0(2.6) 1362.7(1.4)	355.4(2.3)	1750.5(1.4)	P. Nb-97m [743.4]
505.9	Mo-101	14.6m	191.9	590.8	1012.5	2032.0	
505.9	I-132	2.30h	667.7	772.6	954.6	522.6	
500.7	Hf-180m	5.50h	332.3	215.2	443.2	57.4	
[497.1]	Ru-103	39.4d	497.1(89)	610.3(5.6)			
[496.3]	Ba-131	11.8d	496.3(47)	123.8(29)	216.1(20)	373.2(14)	
493.3	Pt-199	30.0m	542.9	317.0	185.6	246.4	
492.7	Te-131	25.0m	149.7	452.3	1147.0	602.0	
492.3	Cd-115	53.5h	527.8	260.9	231.4		
489.2	Ca-47	4.54d	1297.1	807.9			
487.4	Te-129	69.6m	459.6	1083.8	278.4	250.6	
487.0	La-140	40.2h	1596.1	815.8	328.8	925.2	
484.6	Ir-192	74.2d	316.5	468.1	308.5	296.0	
[482.0]	Hf-181	42.4d	482.0(83)	133.0(42)	345.9(17)	136.3(5.2)	
479.5	W-187	23.8h	685.8	72.1	134.2	618.4	
479.5	Y-90m	3.19h	202.5				
[477.6]	Be-7	53.4d	477.6(10)				
469.9	Sn-125	9.64d	1066.6	1088.9	915.7	822.6	
469.4	Ru-105	4.43h	724.5	676.4	316.5	262.9	
468.1	Ir-192	74.2d	316.5	308.4	296.0	604.9	
463.4	Sb-125	2.77y	427.9	600.6	635.9	463.4	
463.0	Ac-228	6.13h	911.1	969.1	338.3	794.7	
462.8	Cs-138	32.2m	1435.8	1009.7	2218.0	546.8	

SEARCH	NUCLIDE	HALF-LIFE	KEY GAMMA	ASSOCIATED GAMMAS			P OR D
[459.6]	Te-129	69.6m	459.6(7.1)	487.4(1.3) 250.6(0.4)	1083.8(0.5)	278.4(0.5)	P. I-129 [39.6]
459.2	Th-233	22.3m	86.5	669.8			
452.3	Te-131	25.0m	149.7	1147.0	492.7	602.0	
452.3	Te-131m	30.0h	773.7	852.2	793.8	1125.5	
448.5	Y-92	3.54d	934.4	1405.4	561.1		
445.7	Pm-151	28.4h	340.1	167.8	275.2	717.8	
443.2	Hf-180m	5.50h	332.3	215.2	57.4	93.3	
[442.9]	I-128	25.0m	442.9(14)	526.6(1.4)	969.4(0.4)		
[438.6]	Zn-69m	13.8h	438.6(95)				
433.9	Ag-108m	127y	722.9	614.4	79.2		
433.9	Ag-108	2.37m	633.0	618.9			
[427.9]	Sb-125	2.77y	427.9(30)	600.6(18) 176.3(6.9)	635.9(11) 606.6(5.0)	463.4(10) 35.5(4.1)	D. Sn-125 [1066.6]
423.7	Ba-140	12.8d	537.3	30.0	162.9	304.8	
423.6	Nd-149	1.73h	211.3	114.3	270.2	540.5	
418.0	I-130	12.4h	536.1	668.5	739.5	1157.5	
417.0	In-116m	54.2m	1097.3	1293.5	2112.3		
416.3	Ge-77	11.3h	264.4	211.0	215.5	558.0	
[411.8]	Au-198	2.69d	411.8(95)	675.9(1.1)			
400.7	Mg-28	20.9h	1342.2	30.6	941.5		
400.6	Se-75	120d	264.7	136.0	279.5	121.1	
396.9	K-43	22.6h	372.8	617.5	593.4		
[396.3]	Yb-175	4.19d	396.3(6.5)	282.5(3.0)	113.5(1.9)		
393.5	Ga-67	3.26d	93.3	184.6	300.2	209.0	
[391.7]	In-113m	1.66h	391.7(65)				D. Sn-113 [255.1]

SEARCH	NUCLIDE	HALF-LIFE	KEY GAMMA	ASSOCIATED GAMMAS			P OR D
[388.5]	Sr-87m	2.81h	388.5(82)				
383.9	Ba-133	10.5y	356.0	81.0	302.8	276.4	
373.2	Ba-131	11.8d	496.3	123.8	216.1		
[372.8]	K-43	22.6h	372.8(87)	617.5(81)	593.4(11)	396.9(11)	
367.4	Ge-77	11.3h	264.4	211.0	215.5	416.3	
366.4	Mo-99	66.0h	739.5	181.1	778.0	140.5	
366.3	Ni-65	2.52h	1481.8	1115.5			
[364.5]	I-131	8.04d	364.5(81)	637.0(7.3)	284.3(6.0)	722.9(1.8)	D. Te-131m [773.7]
[363.5]	Gd-159	18.6h	363.5(11)	58.0(1.8)	348.2(0.2)		
361.7	Dy-165	2.33h	94.7	633.4	715.3		
[356.0]	Ba-133	10.5y	356.0(62)	81.0(33) 276.4(6.9)	302.8(19)	383.9(8.7)	
355.4	Zr-97	16.9h	507.6	1148.0	1750.5	1362.7	
[351.9]	Pb-214	26.8m	351.9(37)	295.2(19)	242.0(7.5)		D. Ra-226 [186.2]
348.2	Gd-159	18.6h	363.5	58.0			
345.9	Hf-181	42.4d	482.0	133.0	136.3		
344.3	Eu-152	13.5y	1408.0	121.8	964.0	1112.0	
344.3	Eu-152m	9.32h	841.6	963.3	121.8	1314.7	
[343.6]	Hf-175	70.0d	343.6(85)	89.6(3.4)			
[342.2]	Ag-111	7.45d	342.2(6.7)	245.4(1.2)			
340.5	Pa-233	27.0d	312.0	300.1			
[340.1]	Pm-151	28.4h	340.1(23)	167.8(8.8) 445.7(4.1)	275.2(7.2) 177.2(3.9)	717.8(4.1)	D. Nd-151 [116.8]
338.3	Ac-228	6.13h	911.1	969.1	794.7	463.0	
[336.3]	In-115m	4.36h	336.3(48)				D. Cd-115 [527.8]
334.3	Te-131m	30.0h	773.7	852.2	793.8	1125.5	

SEARCH	NUCLIDE	HALF-LIFE	KEY GAMMA	ASSOCIATED GAMMAS			P OR D
[332.3]	Hf-180m	5.50h	332.3(94)	443.2(82) 93.3(17)	215.2(82) 500.7(13)	57.4(48)	
[331.9]	Sn-125m	9.52m	331.9(100)				
328.8	La-140	40.2h	1596.1	487.0	815.8	925.2	
[328.5]	Ir-194	19.2h	328.5(13)	293.5(2.6)			
324.5	Ru-97	69.5h	215.7				
[320.1]	Cr-51	27.7d	320.1(9.8)				
[320.1]	Ti-51	5.75m	320.1(93)	928.6(6.9)	608.6(1.1)		
319.4	Nd-147	11.0d	91.1	531.0			
[318.9]	Rh-105	35.4h	318.9(20)	306.3(5.1)			D. Ru-105 [724.5]
317.0	Pt-199	30.0m	542.9	493.3	185.6	246.4	
316.5	Ru-105	4.43h	724.5	469.4	676.4	262.9	
[316.5]	Ir-192	74.2d	316.5(83)	468.1(48) 604.9(8.2) 205.8(3.3)	308.5(30) 612.5(5.3) 484.6(3.2)	296.0(29) 588.6(4.6)	
312.7	K-42	12.4h	1524.7				
[312.0]	Pa-233	27.0d	312.0(39)	300.1(6.6)	340.5(4.5)		D. Th-233 [86.5]
308.4	Ir-192	74.2d	316.5	468.1	296.0	604.9	
[308.3]	Er-171	7.52h	308.3(63)	295.9(28)	111.6(21)	124.0(9.1)	
307.7	Yb-169	32.0d	198.0	63.1	177.2	109.8	
[306.8]	Tc-101	14.2m	306.8(90)	545.1(6.0)	127.2(2.8)	184.1(1.6)	D. Mo-101 [191.9]
306.3	Rh-105	35.4h	318.9				
304.9	Kr-85m	4.48h	151.2				
304.8	Ba-140	12.8d	537.3	30.0	162.8	423.7	
302.8	Ba-133	10.5y	356.0	81.0	383.9	276.4	
300.2	Ga-67	3.26d	93.3	184.6	393.5	209.0	
300.2	Cu-67	61.9h	184.6	93.3	91.3		
300.1	Pa-233	27.0d	312.0	340.5			

SEARCH	NUCLIDE	HALF-LIFE	KEY GAMMA	ASSOCIATED GAMMAS			P OR D
300.1	Pb-212	10.6h	238.6				
298.6	Tb-160	72.3d	879.4	966.1	1177.9	86.8	
296.0	Ir-192	74.2d	316.5	468.1	308.5	604.9	
295.9	Er-171	7.52h	308.3	111.6	124.0		
295.2	Pb-214	26.8m	351.9	242.0			
293.5	Ir-194	19.2h	328.5				
[293.2]	Ce-143	33.0h	293.2(42)	57.4(12)	664.6(5.2)	722.0(5.1)	
[285.9]	Pm-149	53.1h	285.9(3.1)				D. Nd-149 [211.3]
284.3	I-131	8.04d	364.5	637.0	722.9		
282.5	Yb-175	4.19d	396.3	113.5			
279.5	Se-75	120d	264.7	136.0	121.1	400.6	
[279.2]	Hg-203	46.6d	279.2(77)				
279.0	Hg-197m	23.8h	133.9				
278.4	Te-129	69.6m	459.6	487.4	1083.8	250.6	
277.6	Np-239	2.36d	106.1	228.2	209.8		
276.4	Ba-133	10.5y	356.0	81.0	302.8	383.9	
275.2	Pm-151	28.4h	340.1	167.8	717.8	445.7	
270.2	Nd-149	1.73h	211.3	114.3	423.6	540.5	
267.7	Nd-149	1.73h	211.3	114.3	270.2	423.6	
[264.7]	Se-75	120d	264.7(60)	136.0(57) 400.6(12)	279.5(25)	121.1(17)	
[264.6]	Ge-75	82.8m	264.6(11)	198.6(1.4)			
[264.4]	Ge-77	11.3h	264.4(54)	211.0(31) 558.0(16) 1085.2(6.0)	215.5(29) 367.4(14)	416.3(22) 631.8(6.9)	P. As-77 [239.0]
262.9	Ru-105	4.43h	724.5	469.4	676.4	316.5	
260.9	Cd-115	53.5h	527.8	492.3	231.4		

SEARCH	NUCLIDE	HALF-LIFE	KEY GAMMA	ASSOCIATED GAMMAS			P OR D
255.7	Nd-151	12.4m	116.8	1180.9	175.1	139.0	
[255.1]	Sn-113	115d	255.1(1.9)				P. In-113m [391.7]
250.6	Te-129	69.6m	459.6	487.4	1083.8	278.4	
[249.8]	Xe-135	9.11h	249.8(90)				D. I-135 [1260.4]
247.9	Eu-154	8.6y	123.1	1274.5	723.3	1004.8	
246.4	Pt-199	30.0m	542.9	493.3	317.0	185.6	
245.7	Sm-155	22.4m	104.3	141.4			
245.4	Ag-111	7.45d	342.2				
[245.4]	Cd-111m	48.6m	245.4(94)	150.8(30)			
[245.4]	In-111	2.83d	245.4(94)	171.2(91)			
244.7	Eu-152	13.5y	1408.0	121.8	344.3	964.0	
242.0	Pb-214	26.8m	351.9	295.2			
241.5	Sr-92	2.71h	1384.0	953.3			
[241.0]	Ra-224	3.62d	241.0(4.0)				
240.9	Te-131m	30.0h	773.7	852.2	793.8	1125.5	
[239.0]	As-77	38.8h	239.0(1.6)	520.7(0.6)			D. Ge-77 [264.4]
[238.6]	Pb-212	10.6h	238.6(45)	300.1(3.4)			
[231.7]	Sr-85m	67.7m	231.7(85)	151.2(12)			
231.4	Cd-115	53.5h	527.8	492.3	260.9		
228.2	Np-239	2.36d	106.1	277.6	209.8		
[228.2]	Te-132	78.2h	228.2(88)				
222.1	Ta-182	115d	1221.4	67.8	1121.3	1189.1	
216.1	Ba-131	11.8d	496.3	123.8	373.2		
[215.7]	Ru-97	69.6h	215.7(86)	324.5(11)			
215.5	Ge-77	11.3h	264.4	211.0	416.3	558.0	

SEARCH	NUCLIDE	HALF-LIFE	KEY GAMMA	ASSOCIATED GAMMAS			P OR D
215.2	Hf-180m	5.50h	332.3	443.2	57.4	93.3	
[211.3]	Nd-149	1.73h	211.3(27)	114.3(19) 540.5(7.7) 267.7(6.0)	270.2(11) 654.8(7.3)	423.6(9.4) 155.9(6.0)	P. Pm-149 [285.9]
211.0	Ge-77	11.3h	264.4	215.5	416.3	558.0	
209.8	Np-239	2.36d	106.1	277.6	228.2		
209.0	Ga-67	3.26d	93.3	184.6	300.2	393.5	
[208.4]	Lu-177	6.71d	208.4(11)	113.0(6.4)			
208.2	Au-199	3.14d	158.4				
205.8	Ir-192	74.2d	316.5	468.1	308.5	296.0	
205.3	U-235	7.04E5y	185.7	143.8	163.4		
[202.5]	Y-90m	3.19h	202.5(97)	479.5(91)			
200.7	Te-131m	30.0h	773.7	852.2	793.8	1125.5	
198.6	Ge-75	82.8m	264.6				
[198.0]	Yb-169	32.0d	198.0(35)	63.1(44) 130.5(11)	177.2(22) 307.7(10)	109.8(18)	
197.0	Tb-160	72.3d	879.4	298.6	966.1	1177.9	
196.1	Kr-88	2.84h	2392.0	2195.9	834.7	1529.8	
192.3	Fe-59	44.6d	1099.2	1291.6			
[191.9]	Mo-101	14.6m	191.9(19)	590.8(17) 2032.0(7.1)	1012.5(13)	505.9(12)	P. Tc-101 [306.8]
191.4	Hg-197	64.1h	77.4				
[190.3]	In-114m	49.5d	190.3(16)	725.2(4.5)	558.4(4.5)		
[186.2]	Ra-226	1600y	186.2(3.3)				
[185.7]	U-235	7.04E5y	185.7(54)	143.8(10)	205.3(4.7)	163.4(4.7)	
185.6	Pt-199	30.0m	542.9	493.3	317.0	246.4	
184.6	Ga-67	3.26d	93.3	300.2	393.5	209.0	
[184.6]	Cu-67	61.9h	184.6(48)	93.3(16)	91.3(7.0)	300.2(0.8)	

SEARCH	NUCLIDE	HALF-LIFE	KEY GAMMA	ASSOCIATED GAMMAS			P OR D
184.1	Tc-101	14.2m	306.8	545.1	127.2		
181.1	Mo-99	66.0h	739.5	778.0	140.5	366.4	
177.2	Pm-151	28.4h	340.1	167.8	275.2	717.8	
177.2	Yb-169	32.0d	198.0	63.1	109.8	130.5	
176.3	Sb-125	2.77y	427.9	600.6	635.9	463.4	
175.4	Sc-48	43.7h	1312.1	983.5	1037.5		
175.1	Nd-151	12.4m	116.8	255.7	1180.9	139.0	
171.2	In-111	2.83d	245.4				
[168.7]	Fe-52	8.28h	168.7(97)	511.0(112)			P. Mn-52 [1434.0]
167.8	Pm-151	28.4h	340.1	275.2	717.8	445.7	
[167.4]	Tl-201	73.1h	167.4(10)	135.3(2.6)			
[165.9]	Ba-139	83.1m	165.9(22)	1420.5(0.3)			
[165.8]	Ce-139	138d	165.8(80)				
163.4	U-235	7.04E5y	185.7	143.8	205.3		
162.9	Ba-140	12.8d	537.3	30.0	304.8	423.7	
[160.3]	Sn-123m	40.1m	160.3(100)				
[159.4]	Sc-47	3.42d	159.4(68)				D. Ca-47 [1297.1]
[159.0]	Te-123m	120d	159.0(84)				
[158.4]	Au-199	3.14d	158.4(37)	208.2(8.4)			D. Pt-199 [542.9]
155.9	Nd-149	1.73h	211.3	114.3	270.2	423.6	
[155.0]	Re-188	17.0h	155.0(15)	633.0(1.3)			
151.2	Sr-85m	67.7m	231.7				
[151.2]	Kr-85m	4.48h	151.2(75)	304.9(14)			
150.8	Cd-111m	48.6m	245.4				
149.7	Te-131m	30.0h	773.7	852.2	793.8	1125.5	

SEARCH	NUCLIDE	HALF-LIFE	KEY GAMMA	ASSOCIATED GAMMAS			P OR D
[149.7]	Te-131	25.0m	149.7(68)	452.3(18) 602.0(4.2)	1147.0(5.0) 997.3(3.4)	492.7(4.8)	P. I-131 [364.5]
[145.4]	Ce-141	32.5d	145.4(48)				
143.8	U-235	7.04E5y	185.7	205.3	163.4		
[142.5]	Sc-46m	18.7s	142.5(63)				
141.4	Sm-155	22.4m	104.3	245.7			
[140.5]	Tc-99m	6.02h	140.5(90)				D. Mo-99 [739.5]
140.5	Mo-99	66.0h	739.5	181.1	778.0	366.4	
139.0	Nd-151	12.4m	116.8	255.7	1180.9	175.1	
136.5	Co-57	271d	122.1	14.4			
136.3	Hf-181	42.4d	482.0	133.0	345.9		
136.0	Se-75	120d	264.7	279.5	121.1	400.6	
135.3	Tl-201	73.1h	167.4				
134.2	W-187	23.8h	685.8	479.5	72.1	618.4	
[133.9]	Hg-197m	23.8h	133.9(34)	279.0(5.0)			
[133.5]	Ce-144	284d	133.5(11)	80.1(1.6)			P. Pr-144 [696.5]
133.0	Hf-181	42.4d	482.0	345.9	136.3		
130.5	Yb-169	32.0d	198.0	63.1	177.2	109.8	
129.8	Pt-195m	4.02d	98.9				
129.8	Au-195	183d	98.9				
[129.4]	Os-191	15.4d	129.4(26)				
[127.4]	Cs-134m	2.90h	127.4(13)				
127.2	Tc-101	14.2m	306.8	545.1	184.1		
124.0	Er-171	7.52h	308.3	295.9	111.6		
123.8	Ba-131	11.8d	496.3	216.1	373.2		
[123.1]	Eu-154	8.6y	123.1(40)	1274.5(36) 873.2(12)	723.3(19) 996.3(11)	1004.8(18) 247.9(6.6)	

SEARCH	NUCLIDE	HALF-LIFE	KEY GAMMA	ASSOCIATED GAMMAS			P OR D
[122.1]	Co-57	271d	122.1(86)	136.5(11)	14.4(10)		
121.8	Eu-152	13.5y	1408.0	344.3	964.0	1112.0	
121.8	Eu-152m	9.32h	841.6	963.3	344.3	1314.7	
121.1	Se-75	120d	264.7	136.0	279.5	400.6	
[116.8]	Nd-151	12.4m	116.8(60)	255.7(26) 139.0(11)	1180.9(17)	175.1(11)	
114.3	Nd-149	1.73h	211.3	270.2	423.6	540.5	
113.5	Yb-175	4.19d	396.3	282.5			
113.0	Lu-177	6.71d	208.4				
111.6	Er-171	7.52h	308.3	295.9	124.0		
109.8	Yb-169	32.0d	198.0	63.1	177.2	130.5	
[108.2]	Dy-165m	1.26m	108.2(1.3)	515.5(0.7)			
[106.1]	Np-239	2.36d	106.1(23)	277.6(14)	228.2(11)	209.8(3.2)	
105.3	Eu-155	4.76y	86.5				
[104.3]	Sm-155	22.4m	104.3(75)	245.7(3.7)	141.4(2.0)		P. Eu-155 [86.5]
103.2	Gd-153	242d	97.4	69.7			
[103.2]	Sm-153	46.8h	103.2(28)	69.7(5.2)	97.4(0.7)		
102.1	Te-131m	30.0h	773.7	852.2	793.8	1125.5	
100.1	Ta-182	115d	1221.4	67.8	1121.3	1189.1	
[98.9]	Pt-195m	4.02d	98.9(11)	129.8(2.8)			
[98.9]	Au-195	183d	98.9(11)	129.8(0.8)			
[97.4]	Gd-153	242d	97.4(31)	103.2(22)	69.7(2.6)		
97.4	Sm-153	46.8h	103.2	69.7			
97.1	Rh-104m	4.34m	51.4	77.5	555.8		
[94.7]	Dy-165	2.33h	94.7(3.6)	361.7(0.8)	633.4(0.6)	715.3(0.5)	
93.3	Cu-67	61.9h	184.6	91.3	300.2		

SEARCH	NUCLIDE	HALF-LIFE	KEY GAMMA	ASSOCIATED GAMMAS			P OR D
93.3	Hf-180m	5.50h	332.3	215.2	443.2	57.4	
[93.3]	Ga-67	3.26d	93.3(38)	184.6(20) 209.0(2.2)	300.2(16)	393.5(4.5)	
[92.6]	Th-234	24.1d	92.6(5.6)	63.3(3.9)			D. U-238
91.3	Cu-67	61.9h	184.6	93.3	300.2		
[91.1]	Nd-147	11.0d	91.1(28)	531.0(13)	319.4(2.0)		
89.6	Hf-175	70.0d	343.6				
[88.3]	Lu-176m	3.69h	88.3(10)				
[88.0]	Cd-109	464d	88.0(3.7)				
[88.0]	Pd-109	13.4h	88.0(3.7)				
86.8	Tb-160	72.3d	879.4	298.6	966.1	1177.9	
[86.5]	Th-233	22.3m	86.5(2.7)	459.2(1.4)	669.8(0.7)		
[86.5]	Eu-155	4.76y	86.5(31)	105.3(20)			D. Sm-155 [104.3]
[84.3]	Tm-170	129d	84.3(3.2)				
81.0	Ba-133	10.5y	356.0	302.9	383.8	276.4	
[81.0]	Xe-133	5.25d	81.0(37)	79.6(0.2)			
[80.6]	Ho-166	26.8h	80.6(6.2)	1379.4(0.9)	1581.9(0.2)		
80.1	Ce-144	284d	133.5	696.5			
79.6	Xe-133	5.25d	81.0				
79.2	Ag-108m	127y	722.9	614.4	433.9		
[78.3]	Ti-44	47.3y	78.3(98)	67.9(92)			P. Sc-44 [1157.0]
77.5	Rh-104m	4.34m	51.4	97.1	555.8		
[77.4]	Hg-197	64.1h	77.4(19)	191.4(0.5)			
[74.7]	U-239	23.4m	74.7(49)	43.5(4.3)			
72.1	W-187	23.8h	685.8	479.5	134.2	618.4	
69.7	Gd-153	242d	97.4	103.2			

SEARCH	NUCLIDE	HALF-LIFE	KEY GAMMA	ASSOCIATED GAMMAS			P OR D
69.7	Sm-153	46.8h	103.2	97.4			
67.9	Ti-44	47.3y	78.3				
67.8	Ta-182	115d	1221.4	1121.3	1189.1	1001.1	
63.3	Th-234	24.1d	92.6				
63.1	Yb-169	32.0d	198.0	177.2	109.8	130.5	
[59.5]	Am-241	432y	59.5(36)	26.3(2.4)			
[58.6]	Co-60m	10.5m	58.6(2.0)				
58.0	Gd-159	18.6h	363.5	348.2			
57.4	Hf-180m	5.50h	332.3	215.2	443.2	93.3	
57.4	Ce-143	33.0h	293.2	664.6	722.0		
[51.4]	Rh-104m	4.34m	51.4(48)	97.1(3.0)	77.5(2.0)	555.8(2.0)	
[46.5]	Pb-210	22.3y	46.5(4.0)				
43.5	U-239	23.4m	74.7				
[39.6]	I-129	1.57E7y	39.6(7.5)				
[37.0]	Br-80m	4.42h	37.0(39)				
35.5	Sb-125	2.77y	427.9	600.6	635.9	463.4	
[35.5]	I-125	60.1d	35.5(6.5)				
30.6	Mg-28	20.9h	1342.2	941.5	400.7		
30.0	Ba-140	12.8d	537.3	162.9	304.8	423.7	
26.3	Am-241	432y	59.5				
14.4	Co-57	271d	122.1	136.5			

APPENDIX B

X-Ray Critical-Absorption and Emission Energies in keV

By S. FINE and C. F. HENDEE
Philips Laboratories
Irvington on Hudson, New York

Increased use of energy-proportional detectors for x rays has created a need for a table of energy values of K and L absorption and emission series.

The table presented here includes all elements. Most values were obtained by a conversion to keV of tabulated experimental wavelength values (1–3); some are from previous energy-value compilations (4,5). Where a choice existed, the value chosen was the one derived from later work. Certain values were determined by interpolation, using Moseley's law. (All this is annotated in footnotes.)

The conversion equations relating energy and wavelength used are (6)

$$E(\text{keV}) = (12.39644 \pm 0.00017)/\lambda(\text{Å})$$
$$= 12.39644/1.002020\ \lambda(\text{kX unit})$$

In computing values the number of places retained sufficed to maintain the uncertainty in the original source value. The values in the table have been listed uniformly to 1 eV. However, chemical form may shift absorption edges as much as 10–20 eV (4,5).

To discover computational errors a fit was made to Moseley's law. In general the values were consistent, however there were a few irregularities due to the deviation of some input values (1). These were retained in the body of the table but a set of values calculated to fit better are footnoted.

* * *

The authors wish to express their appreciation to W. Parrish for helpful suggestions and to H. Kasper for performing the computation in connection with this work.

BIBLIOGRAPHY

1. Y. Cauchois, H. Hulubei, "Tables de Constantes et Donnees Numeriques, I, Longueurs D'Onde des Emissions X et des Discontinuites D'Absorption X" (Hermann et Cie, Paris, France, 1947).
2. A. H. Compton and S. K. Allison, "X-Rays in Theory and Experiment" (D. Van Nostrand Co., Inc., New York, 1951).
3. C. E. Moore, "Atomic Energy Levels," NBS 467 (National Bureau of Standards, U.S. Department of Commerce, Washington, D.C., 1949).
4. Y. Cauchois, J. phys. radium **13**, 113 (1952).
5. R. D. Hill, E. L. Church, and J. W. Mihelich, Rev. Sci. Instr. **23**, 523 (1952).
6. J. W. M. DuMond, E. R. Cohen, Phys. Rev. **82**, 555 (1951).

X-Ray Critical-Absorption and Emission Energies in kev

Atomic Number	Element	K series					L series							
		K_{ab}	$K\beta_2$	$K\beta_1$	$K\alpha_1$	$K\alpha_2$	I_{1ab}	L_{IIab}	L_{IIIab}	$L\gamma_1$	$L\beta_2$	$L\beta_1$	$L\alpha_1$	$L\alpha_2$
1	Hydrogen	0.0136‡												
2	Helium	0.0246‡												
3	Lithium	0.055				0.052								
4	Beryllium	0.116§				0.110								
5	Boron	0.192†				0.185								
6	Carbon	0.283				0.282								
7	Nitrogen	0.399				0.392								
8	Oxygen	0.531				0.523								
9	Fluorine	0.687†				0.677								
10	Neon	0.874*				0.851§	0.048†	0.022†	0.022†					
11	Sodium	1.08*		1.067		1.041	0.055§	0.034§	0.034§					
12	Magnesium	1.303		1.297		1.254	0.063	0.050	0.049					
13	Aluminum	1.559		1.553	1.487	1.486	0.087	0.073**	0.072**					
14	Silicon	1.838		1.832	1.740	1.739	0.118*	0.099**	0.098**					
15	Phosphorus	2.142		2.136	2.015§	2.014§	0.153*	0.129§	0.128§					
16	Sulphur	2.470		2.464	2.308	2.306	0.193*	0.164**	0.163**					
17	Chlorine	2.819¶		2.815	2.622	2.621	0.238*	0.203§	0.202§					
18	Argon	3.203		3.192§	2.957	2.955	0.287*	0.247**	0.245**					
19	Potassium	3.607		3.589	3.313	3.310	0.341*	0.297**	0.294**					
20	Calcium	4.038		4.012	3.691	3.688	0.399*	0.352	0.349			0.344		0.341
21	Scandium	4.496		4.460	4.090	4.085	0.462*	0.411**	0.406**			0.399		0.395
22	Titanium	4.964		−4.931	4.510	4.504	0.530*	0.460**	0.454**			0.458		0.452
23	Vanadium	5.463		−5.427	4.952	4.944	0.604*	0.519**	0.512**			0.519		0.510
24	Chromium	5.988		−5.946	5.414	5.405	0.679*	0.583**	0.574**			0.581		0.571
25	Manganese	6.537		6.490	5.898	5.887	0.762*	0.650**	0.639**			0.647		0.636
26	Iron	7.111		7.057	6.403	6.390	0.849*	0.721**	0.708**			0.717		0.704
27	Cobalt	7.709		7.649	6.930	6.915	0.929*	0.794**	0.779**			0.790		0.775
28	Nickel	8.331	8.328	8.264	7.477	7.460	1.015*	0.871**	0.853**			0.866		0.849
29	Copper	8.980	8.976	8.904	8.047	8.027	1.100*	0.953	0.933			0.948		0.928
30	Zinc	9.660	9.657	9.571	8.638	8.615	1.200*	1.045	1.022			1.032		1.009
31	Gallium	10.368	10.365	10.263	9.251	9.234	1.30*	1.134**	1.117**			1.122		1.096
32	Germanium	11.103	11.100	10.981	9.885	9.854	1.42*	1.248**	1.217**			1.216		1.186
33	Arsenic	11.863	11.863	11.725	10.543	10.507	1.529	1.359	1.323			1.317		1.282
34	Selenium	12.652	12.651	12.495	11.221	11.181	1.652	1.473	1.434			1.419		1.379
35	Bromine	13.475	13.465	13.290	11.923	11.877	1.794§	1.599**	1.552**			1.526		1.480
36	Krypton	14.323	14.313	14.112	12.648	12.597	1.931§	1.727**	1.675**			1.638§		1.587**
37	Rubidium	15.201	15.184	14.960	13.394	13.335	2.067	1.866	1.806			1.752	1.694	1.692
38	Strontium	16.106	16.083	15.834	14.164	14.097	2.221	2.008	1.941			1.872	1.806	1.805
39	Yttrium	17.037	17.011	16.736	14.957	14.882	2.369	2.154	2.079			1.996	1.922	1.920
40	Zirconium	17.998	17.969	17.666	15.774	15.690	2.547	2.305	2.220	2.302	2.219	2.124	2.042	2.040

TENNELEC the Nucleus inc.

Atomic Number	Element	K series					L series							
		K_{ab}	$K\beta_2$	$K\beta_1$	$K\alpha_1$	$K\alpha_2$	L_{Iab}	L_{IIab}	L_{IIIab}	$L\gamma_1$	$L\beta_2$	$L\beta_1$	$L\alpha_1$	$L\alpha_2$
41	Niobium	18.987	18.951	18.621	16.614	16.520	2.706	2.467**	2.374	2.462	2.367	2.257	2.166	2.163
42	Molybdenum	20.002	19.964	19.607	17.478	17.373	2.884‡	2.627	2.523	2.623	2.518	2.395	2.293	2.290
43	Technetium	21.054§	21.012§	−20.585¶	18.410¶	18.328¶	3.054§	2.795§	2.677§	2.792§	2.674§	2.538§	2.424§	2.420§
44	Ruthenium	22.118	22.072	21.655	19.278	19.149	3.236§	2.966	2.837	2.964	2.836	2.683	2.558	2.554
45	Rhodium	23.224	23.169	22.721	20.214	20.072	3.419	3.145	3.002	3.144	3.001	2.834	2.696	2.692
46	Palladium	24.347	24.297	23.816	21.175	21.018	3.617	3.329	3.172	3.328	3.172	2.990	2.838	2.833
47	Silver	25.517	25.454	24.942	22.162	21.988	3.810	3.528	3.352	3.519	3.348	3.151	2.984	2.978
48	Cadmium	26.712	26.641	26.093	23.172	22.982	4.019	3.727	3.538	3.716	3.528	3.316	3.133	3.127
49	Indium	27.928	27.859	27.274	24.207	24.000	4.237	3.939	3.729	3.920	3.713	3.487	3.287	3.279
50	Tin	29.190	29.106	28.483	25.270	25.042	4.464	4.157	3.928	4.131	3.904	3.662	3.444	3.435
51	Antimony	30.486	30.387	29.723	26.357	26.109	4.697	4.381	4.132	4.347	4.100	3.843	3.605	3.595
52	Tellurium	31.809	31.698	30.993	27.471	27.200	4.938	4.613	4.341	4.570	4.301	4.029	3.769	3.758
53	Iodine	33.164	33.016	32.292	28.610	28.315	5.190	4.856	4.559	4.800	4.507	4.220	3.937	3.926
54	Xenon	34.579	34.446¶	33.644	29.802¶	29.485¶	5.452	5.104	4.782	5.036§	4.720§	4.422§	4.111§	4.098§
55	Cesium	35.959	35.819	34.984	30.970	30.623	5.720	5.358	5.011	5.280	4.936	4.620	4.286	4.272
56	Barium	37.410	37.255	36.376	32.191	31.815	5.995	5.623	5.247	5.531	5.156	4.828	4.467	4.451
57	Lanthanum	38.931	38.728	37.799	33.440	33.033	6.283	5.894	5.489	5.789	5.384	5.043	4.651	4.635
58	Cerium	40.449	40.231	39.255	34.717	34.276	6.561	6.165†	5.729	6.052	5.613	5.262	4.840	4.823
59	Praseodymium	41.998	41.772	40.746	36.023	35.548	6.846	6.443	5.968	6.322	5.850	5.489	5.034	5.014
60	Neodymium	43.571	43.298¶	42.269	37.359	36.845	7.144	6.727	6.215	6.602	6.090	5.722	5.230	5.208
61	Promethium	45.207§	44.955§	−43.945¶	38.649¶	38.160¶	7.448§	7.018§	6.466§	6.891§	6.336§	5.956	5.431	5.408§
62	Samarium	46.846	46.553¶	45.400	40.124	39.523	7.754	7.281¶	6.721	7.180	6.587	6.206	5.636	5.609
63	Europium	48.515	48.241	47.027	41.529	40.877	8.069	7.624	6.983	7.478	6.842	6.456	5.846	5.816
64	Gadolinium	50.229	49.961	48.718	42.983	42.280	8.393	7.940	7.252	7.788	7.102	6.714	6.059	6.027
65	Terbium	51.998	51.737	50.391	44.470	43.737	8.724	8.258	7.519	8.104	7.368	6.979	6.275	6.241
66	Dysprosium	53.789	53.491	52.178	45.985	45.193	9.083	8.621¶	7.850¶	8.418	7.638	7.249	6.495	6.457
67	Holmium	55.615	55.292**	53.934§	47.528	46.686	9.411	8.920	8.074	8.748	7.912	7.528	6.720	6.680
68	Erbium	57.483	57.088	55.690	49.099	48.205	9.776	9.263	8.364	9.089	8.188	7.810	6.948	6.904
69	Thulium	59.335¶	58.969**	57.576¶	50.730	49.762	10.144	9.628	8.652	9.424	8.472	8.103	7.181	7.135
70	Ytterbium	61.303	60.959	59.352	52.360	51.326	10.486	9.977	8.943	9.779	8.758	8.401	7.414	7.367
71	Lutecium	63.304	62.946	61.282	54.063	52.959	10.867	10.345	9.241	10.142	9.048	8.708	7.654	7.604
72	Hafnium	65.313	64.936	63.209	55.757	54.579	11.264	10.734	9.556	10.514	9.346	9.021	7.898	7.843
73	Tantalum	67.400	66.999	65.210	57.524	56.270	11.676	11.130	9.876	10.892	9.649	9.341	8.145	8.087
74	Tungsten	69.508	69.090	67.233	59.310	57.973	12.090	11.535	10.198	11.283	9.959	9.670	8.396	8.333
75	Rhenium	71.662	71.220	69.298	61.131	59.707	12.522	11.955	10.531	11.684	10.273	10.008	8.651	8.584
76	Osmium	73.860	73.393	71.404	62.991	61.477	12.965	12.383	10.869	12.094	10.596	10.354	8.910	8.840
77	Iridium	76.097	75.605	73.549	64.886	63.278	13.413	12.819	11.211	12.509	10.918	10.706	9.173	9.098
78	Platinum	78.379	77.866	75.736	66.820	65.111	13.873	13.268	11.559	12.939	11.249	11.069	9.441	9.360
79	Gold	80.713	80.165	77.968	68.794	66.980	14.353	13.733	11.919	13.379	11.582	11.439	9.711	9.625
80	Mercury	83.106	82.526	80.258	70.821	68.894	14.841	14.212	12.285	13.828	11.923	11.823	9.987	9.896
81	Thallium	85.517	84.904	82.558	72.860	70.820	15.346	14.697	12.657	14.288	12.268	12.210	10.266	10.170
82	Lead	88.001	87.343	84.922	74.957	72.794	15.870	15.207	13.044	14.762	12.620	12.611	10.549	10.448
83	Bismuth	90.521	89.833	87.335	77.097	74.805	16.393	15.716	13.424	15.244	12.977	13.021	10.836	10.729
84	Polonium	93.112	92.386	89.809	79.296	76.868	16.935	16.244	13.817	15.740	13.338	13.441	11.128	11.014
85	Astatine	95.740	94.976	92.319	81.525	78.956	17.490	16.784	14.215	16.248	13.705	13.873	11.424	11.304
86	Radon	98.418	97.616	94.877	83.800	81.080	18.058	17.337	14.618	16.768	14.077	14.316	11.724	11.597
87	Francium	101.147	100.305	97.483	86.119	83.243	18.638	17.904	15.028	17.301	14.459	14.770	12.029	11.894
88	Radium	103.927	103.048	100.136	88.485	85.446	19.233	18.481	15.442	17.845	14.839	15.233	12.338	12.194
89	Actinium	106.759	105.838	102.846	90.894	87.681	19.842	19.078	15.865	18.405	15.227	15.712	12.650	12.499
90	Thorium	109.630	108.671	105.592	93.334	89.942	20.460	19.688	16.296	18.977	15.620	16.200	12.966	12.808
91	Protactinium	112.581	111.575	108.408	95.851	92.271	21.102	20.311	16.731	19.559	16.022	16.700	13.291	13.120
92	Uranium	115.591	114.549	111.289	98.428	94.648	21.753	20.943	17.163	20.163	16.425	17.218	13.613	13.438
93	Neptunium	118.619	117.533	114.181	101.005	97.023	22.417	21.596	17.614	20.774	16.837	17.740	13.945	13.758
94	Plutonium	121.720	120.592	117.146	103.653	99.457	23.097	22.262	18.066	21.401	17.254	18.278	14.279	14.082
95	Americium	124.876	123.706	120.163	106.351	101.932	23.793	22.944	18.525	22.042	17.677	18.829	14.618	14.411
96	Curium	128.088	126.875	123.235	109.098	104.448	24.503	23.640	18.990	22.699	18.106	19.393	14.961	14.743
97	Berkelium	131.357	130.101	126.362	111.896	107.023	25.230	24.352	19.461	23.370	18.540	19.971	15.309	15.079
98	Californium	134.683	133.383	129.544	114.745	109.603	25.971	25.080	19.938	24.056	18.980	20.562	15.661	15.420
99		138.067	136.724	132.781	117.646	112.244	26.729	25.824	20.422	24.758	19.426	21.166	16.018	15.764
100		141.510	140.122	136.075	120.598	114.926	27.503	26.584	20.912	25.475	19.879	21.785	16.379	16.113

For $Z \leq 69$, values without symbols are derived from (*1*). Values prefixed with a − sign are $K\beta_{1,3}$.

For $Z \geq 70$, absorption-edge values are from (*4*) in the case of Z = 70–83, 88, 90, and 92; remaining absorption edges to Z = 100 are obtained from these by least-squares quadratic fitting. All emission values for $Z \geq 70$ are derived from the preceding absorption edges, and others based on (*4*), using the transition relations $K\alpha_1 = K_{ab} - L_{III}$, $K\alpha_2 = K_{ab} - L_{II}$, $K\beta_1 = K_{ab} - M_{III}$, etc.

* Obtained from R. D. Hill, E. L. Church, J. W. Mihelich (*5*). † Derived from Compton and Allison (*2*). ‡ Derived from C. E. Moore (*3*).

¶ Values derived from Cauchois and Hulubei (*1*) which deviate from the Moseley law. Better-fitting values are: Z = 17, K_{ab} = 2.826; Z = 43, $K\alpha_1$ = 18.370, $K\alpha_2$ = 18.250, $K\beta_1$ = 20.612; Z = 54, $K\alpha_1$ = 29.779, $K\alpha_2$ = 29.463, $K\beta_2$ = 34.398; Z = 60, $K\beta_2$ = 43.349; Z = 61, $K\alpha_1$ = 38.726, $K\alpha_2$ = 38.180, $K\beta_1$ = 43.811; Z = 62, $K\beta_2$ = 46.581, L_{II} = 7.312; Z = 66, L_{II} = 8.591, L_{III} = 7.790; Z = 69, K_{ab} = 59.382, $K\beta_1$ = 57.487.

§ Calculated by method of least squares. ** Calculated by transition relations.

the Nucleus INC.

TENNELEC

761 Emory Valley Road
Oak Ridge, TN 37830-2561 USA
Telephone (615) 482-4041
Tlx 557-482
Fax (615) 483-0406

Printed in USA
December 1988